PLANT DISEASE MANAGEMENT IN THE POST-GENOMIC ERA: FROM FUNCTIONAL GENOMICS TO GENOME EDITING

EDITED BY: Sabrina Sarrocco, Alfredo Herrera-Estrella and David B. Collinge

PUBLISHED IN: Frontiers in Microbiology and Frontiers in Plant Science

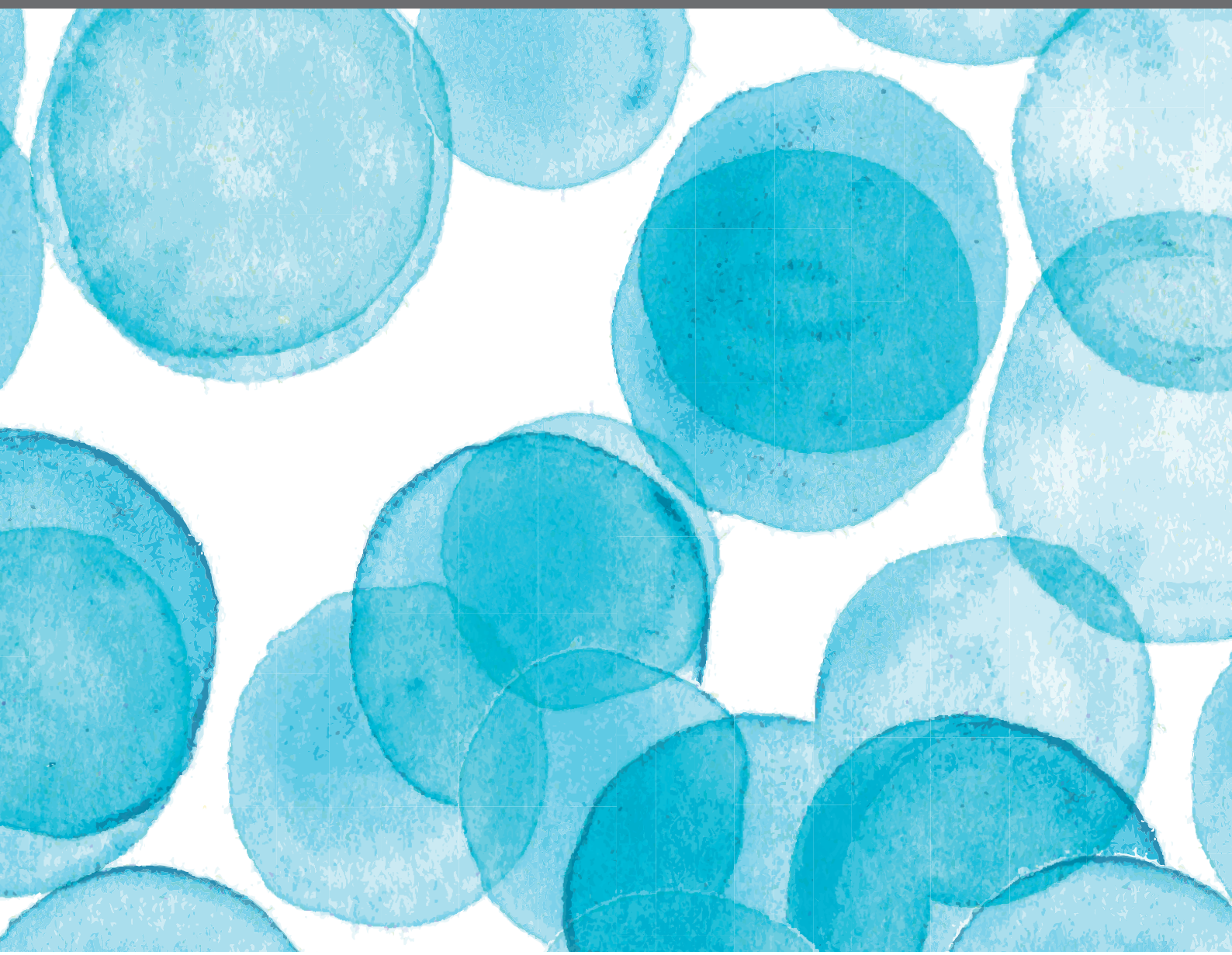

frontiers Research Topics

frontiers

ISSN 1664-8714
ISBN 978-2-88963-560-3
DOI 10.3389/978-2-88963-560-3

About Frontiers

Frontiers is more than just an open-access publisher of scholarly articles: it is a pioneering approach to the world of academia, radically improving the way scholarly research is managed. The grand vision of Frontiers is a world where all people have an equal opportunity to seek, share and generate knowledge. Frontiers provides immediate and permanent online open access to all its publications, but this alone is not enough to realize our grand goals.

Frontiers Journal Series

The Frontiers Journal Series is a multi-tier and interdisciplinary set of open-access, online journals, promising a paradigm shift from the current review, selection and dissemination processes in academic publishing. All Frontiers journals are driven by researchers for researchers; therefore, they constitute a service to the scholarly community. At the same time, the Frontiers Journal Series operates on a revolutionary invention, the tiered publishing system, initially addressing specific communities of scholars, and gradually climbing up to broader public understanding, thus serving the interests of the lay society, too.

Dedication to Quality

Each Frontiers article is a landmark of the highest quality, thanks to genuinely collaborative interactions between authors and review editors, who include some of the world's best academicians. Research must be certified by peers before entering a stream of knowledge that may eventually reach the public - and shape society; therefore, Frontiers only applies the most rigorous and unbiased reviews.
Frontiers revolutionizes research publishing by freely delivering the most outstanding research, evaluated with no bias from both the academic and social point of view. By applying the most advanced information technologies, Frontiers is catapulting scholarly publishing into a new generation.

What are Frontiers Research Topics?

Frontiers Research Topics are very popular trademarks of the Frontiers Journals Series: they are collections of at least ten articles, all centered on a particular subject. With their unique mix of varied contributions from Original Research to Review Articles, Frontiers Research Topics unify the most influential researchers, the latest key findings and historical advances in a hot research area! Find out more on how to host your own Frontiers Research Topic or contribute to one as an author by contacting the Frontiers Editorial Office: researchtopics@frontiersin.org

PLANT DISEASE MANAGEMENT IN THE POST-GENOMIC ERA: FROM FUNCTIONAL GENOMICS TO GENOME EDITING

Topic Editors:
Sabrina Sarrocco, University of Pisa, Italy
Alfredo Herrera-Estrella, Center for Research and Advanced Studies of the National Polytechnic Institute, Mexico
David B. Collinge, University of Copenhagen, Denmark

Citation: Sarrocco, S., Herrera-Estrella, A., Collinge, D. B., eds. (2020). Plant Disease Management in the Post-Genomic Era: From Functional Genomics to Genome Editing. Lausanne: Frontiers Media SA. doi: 10.3389/978-2-88963-560-3

Table of Contents

frontiers in Microbiology

EDITORIAL
published: 04 February 2020
doi: 10.3389/fmicb.2020.00107

Editorial: Plant Disease Management in the Post-genomic Era: From Functional Genomics to Genome Editing

Sabrina Sarrocco[1]*, *Alfredo Herrera-Estrella*[2]* and *David B. Collinge*[3]*

[1] Department of Agriculture, Food and Environment, University of Pisa, Pisa, Italy, [2] National Laboratory of Genomics for Biodiversity, Center for Research and Advanced Studies of the National Polytechnic Institute, Irapuato, Mexico, [3] Section for Microbial Ecology and Biotechnology, Department of Plant and Environmental Sciences and Copenhagen Plant Science Centre, University of Copenhagen, Copenhagen, Denmark

Keywords: disease management, NGS - next generation sequencing, food security, food safety, post-genomic era

Editorial on the Research Topic

Plant Disease Management in the Post-genomic Era: From Functional Genomics to Genome Editing

OPEN ACCESS

Edited by:
Brigitte Mauch-Mani, Université de Neuchâtel, Switzerland

Reviewed by:
Ivan Baccelli, Sede Secondaria Firenze, Italy

***Correspondence:**
Sabrina Sarrocco
sabrina.sarrocco@unipi.it
Alfredo Herrera-Estrella
alfredo.herrera@cinvestav.mx
David B. Collinge
dbc@plen.ku.dk

Specialty section:
This article was submitted to Plant Microbe Interactions, a section of the journal Frontiers in Microbiology

Received: *11 December 2019*
Accepted: *17 January 2020*
Published: *04 February 2020*

Citation:
Sarrocco S, Herrera-Estrella A and Collinge DB (2020) Editorial: Plant Disease Management in the Post-genomic Era: From Functional Genomics to Genome Editing. Front. Microbiol. 11:107. doi: 10.3389/fmicb.2020.00107

The growing world population requires an efficient management and control of diseases in crop production to guarantee both food security and safety (FAO, 2018; Sarrocco and Vannacci, 2018). The development of the so called NGS (Next Generation Sequencing) techniques has been positively welcomed as a new tool for understanding the nature of plant diseases, even if the potential for their use has not yet been fully discovered.

This Research Topic arises from the idea to give an updated and exhaustive overview of the exploitation of genome sequencing, genome comparison, transcriptomics, metagenomics, RNA based technologies, and genome editing strategies as a new frontier to contribute to plant disease management.

The knowledge of the complex relationship occurring among plants, pathogens, the environment and, eventually, beneficial organisms, is now increasing thanks to the ecological application of genomics (ecogenomics), both at single strain and at community level (Martin, 2014). Metagenomics and metatranscriptomics can be of help to describe the whole microbial community not only in terms of its ecology, but also to detect that fraction of the microbiome that, modulating the activity of plant pathogens in favor of the plant host, could be developed (as single isolate or in consortia) as biopesticides. Cobo-Díaz et al. used a concurrence culture-independent metabarcoding approach to characterize the microbial communities associated to the incidence and composition of *Fusarium* spp. on maize stalk and other bacterial and fungal genera, using co-occurrence network analysis. Such approach could be a useful tool as part of a screening strategy for novel antagonist candidates against toxigenic *Fusarium* spp..

The wide range of beneficial microorganisms does not only include those isolates directly interacting with harmful pathogens but also consists of endophytes that, thanks to their mutualistic relationship with the host, can increase plant tolerance to biotic and abiotic stress. Pereira et al. grouped into operational taxonomic units (OTU) ITS sequences amplified from culturable fungi associated to *Festuca rubra* subsp. *pruinosa* (FRP) roots thus demonstrating a set of seven species. These seem to be the components of the core mycobiome of FRP and include very promising candidates in the adaptation of FRP plants to salinity, a characteristic stress factor of their habitat. Indeed a *Diaporthe* strain could help ryegrass (*Lolium*) to adapt to high salinity. The genome of bacterial endophyte *Paraburkholderia phytofirmans* was extensively studied by Esmaeel et al., allowing the identification of all gene clusters which contribute to the adaptive mechanisms under different environmental conditions and explaining the high ecological competence of this

microorganism, able to promote plant growth and to induce resistance to abiotic and biotic stresses.

The number of fully-sequenced and released genomes is increasing rapidly. This genomics "revolution" gave an important contribution in plant pathology, rapidly increasing our knowledge of the molecular mechanisms underpinning pathogenesis, resistance and the mode of action of beneficial microorganisms (Klosterman et al., 2016). Firrao et al., through the analysis of Illumina sequence data-sets of 11 European and one non-European *Peudomonas syringae* pv. *actinidia* (Psa) genomes, gave a picture of the significant differences in the genome evolution of this bacterium before and after a clonal expansion, thus furnishing information of great value for epidemic management. In the same way, the genome-wide analysis of the plant pathogenic bacteria *Ralstonia solanacearum* and *Xantomonas oryzae* pv. *oryzae*, performed by Cho et al., and Doucouré et al., respectively, will have important effect in the sustainable deployment of broad-spectrum and durable resistance to these serious pathogens.

Broberg et al., by performing the re-sequencing of the genome of 52 isolates of the beneficial fungus *Clonostachys rosea*, made a genome-wide association study in conditions relevant for biocontrol activity, with particular attention to the cold tolerance of these fungi, an important implication for the management of plant diseases.

Also from the host-plant side, genomics and post-genomics techniques are actually giving wide opportunities to understand diseases and stress tolerance, as well as to design innovative control strategies, as overviewed by Leonetti et al. on chickpea. The contribution of plant proteomics is no less important for understanding mechanisms underlining resistance to common diseases, such as in the pathosystem *Fusarium oxysporum*/tomato, where defense gene response was phenotypically characterized by de Lamo et al..

During plant/microorganism interactions, plant colonization is governed by secreted effectors that can belong to the same families in the case both of harmful (phytopathogens) and beneficial (symbiontic) interactions. The role of effectors in the molecular chat occurring with *Trichoderma* isolates, as well as during arbuscular mycorrhizal (AM) symbiosis—that facilitates mineral nutrition and confers tolerance to biotic and abiotic stresses—was discussed by Ramirez-Valdespino et al. and Voß et al., respectively.

Progresses in genetic engineering created new opportunities in plant disease management. This is the case of RNA interference (RNAi) as well as genome editing technologies that, with a rapid progress, has become an important genetic tool to "*touch up*" the genome of host plants or pathogens, as well as of beneficial microorganisms (Collinge, 2018; Nødvig et al., 2018).

In filamentous fungi, as example, gene silencing mediated by RNAi, models important biological processes, including pathogenicity. Having previously demonstrated that it works (Koch et al., 2013). Gaffar et al. explored RNAi machinery in *Fusarium graminearum* for sexual-asexual reproduction, sensitivity to double-strand (ds)RNA and pathogenicity in order to develop RNAi-based plant protection strategies.

The CRISPR/Cas9 technology applied to plants was reviewed by Borrelli et al. as a tool to implement pathogen resistance, thus representing the natural consequence of years spent in deciphering and reading genomes. The possibility to edit and re-write fungal genomes described by Vicente Muñoz et al., is an additional possibility of controlling plant pathogens by creating new interesting biocontrol strains to be released in field thus avoiding the introduction of transgenes in the environment.

The availability of NGS and all the developing "omics" offer new tools for an environmentally and economically sustainable crop protection by improving our knowledge of the complex network, at cell, individual and ecosystem level, modulating plant diseases and by offering us new tools to rapidly react to new, emerging and re-emerging plant diseases in a fast changing environment.

AUTHOR CONTRIBUTIONS

All authors listed have made a substantial, direct and intellectual contribution to the work, and approved it for publication.

FUNDING

DC has received funding from the European Union's Horizon 2020 research and innovation programme under the Marie Sk-Curie grant agreement Nos. 674964 and 676480, respectively.

REFERENCES

Collinge, D. B. (2018). Transgenic crops and beyond: how can New Breeding Technologies contribute to the sustainable control of plant diseases? *Eur. J. Plant Pathol.* 152, 977–986. doi: 10.1007/s10658-018-1439-2

FAO, IFAD, UNICEF, WFP and WHO (2018). *The State of Food Security and Nutrition in the World 2018. Building Climate Resilience for Food Security and Nutrition*. Rome: FAO.

Klosterman, S. J., Rollins, J. R., Sudarshana, M. R., and Vinatzer, B. A. (2016). Disease management in the genomics era: summaries of focus issue papers. *Phytopathology* 106, 1068–1070. doi: 10.1094/PHYTO-07-16-0276-FI

Koch, A., Kumar, N., Weber, L., Keller, H., Imani, J., and Kogel, K.-H. (2013). Host-induced gene silencing of cytochrome P450 lanosterol C14α-demethylase–encoding genes confers strong resistance to *Fusarium* species. *Proc. Natl. Acad. Sci. U.S.A.* 110, 19324–19329. doi: 10.1073/pnas.1306373110

Martin, F. (ed.) (2014). *The Ecological Genomics of Fungi.* John Wiley and Sons Inc., 385.

Nødvig, C. S., Hoof, J. B., Kogle, M. E., Jarczynska, Z. D., Lehmbeck, J., Klitgaard, D. K., et al. (2018). Efficient oligonucleotide mediated CRISPR-Cas9 gene editing in Aspergilli. *Fung. Gen. Biol.* 115, 78–89. doi: 10.1016/j.fgb.2018.01.004

Sarrocco, S., and Vannacci, G. (2018). Preharvest application of beneficial fungi as a strategy to prevent postharvest mycotoxin contamination: a review. *Crop Prot.* 110, 160–170. doi: 10.1016/j.cropro.2017.11.013

Conflict of Interest: The authors declare that the research was conducted in the absence of any commercial or financial relationships that could be construed as a potential conflict of interest.

frontiers in Plant Science

REVIEW
published: 15 March 2018
doi: 10.3389/fpls.2018.00319

Viruses and Phytoparasitic Nematodes of *Cicer arietinum* L.: Biotechnological Approaches in Interaction Studies and for Sustainable Control

Paola Leonetti[1], *Gian Paolo Accotto*[2], *Moemen S. Hanafy*[3] *and Vitantonio Pantaleo*[1]*

[1] *Institute for Sustainable Plant Protection, Research Unit of Bari, National Research Council, Bari, Italy,* [2] *Institute for Sustainable Plant Protection, Research Unit of Turin, National Research Council, Turin, Italy,* [3] *Department of Plant Biotechnology, National Research Centre, Cairo, Egypt*

Cicer arietinum L. (chickpea) is the world's fourth most widely grown pulse. Chickpea seeds are a primary source of dietary protein for humans, and chickpea cultivation contributes to biological nitrogen fixation in the soil, given its symbiotic relationship with rhizobia. Therefore, chickpea cultivation plays a pivotal role in innovative sustainable models of agro-ecosystems inserted in crop rotation in arid and semi-arid environments for soil improvement and the reduction of chemical inputs. Indeed, the arid and semi-arid tropical zones of Africa and Asia have been primary areas of cultivation and diversification. Yet, nowadays, chickpea is gaining prominence in Canada, Australia, and South America where it constitutes a main ingredient in vegetarian and vegan diets. Viruses and plant parasitic nematodes (PPNs) have been considered to be of minor and local impact in primary areas of cultivation. However, the introduction of chickpea in new environments exposes the crop to these biotic stresses, compromising its yields. The adoption of high-throughput genomic technologies, including genome and transcriptome sequencing projects by the chickpea research community, has provided major insights into genome evolution as well as genomic architecture and domestication. This review summarizes the major viruses and PPNs that affect chickpea cultivation worldwide. We also present an overview of the current state of chickpea genomics. Accordingly, we explore the opportunities that genomics, post-genomics and novel editing biotechnologies are offering in order to understand chickpea diseases and stress tolerance and to design innovative control strategies.

Keywords: ***Cicer arietinum*** **L., plant viruses, plant parasitic nematodes, RNA silencing, viral metagenomics, plant transformation, genome editing**

OPEN ACCESS

Edited by:
Sabrina Sarrocco, Università degli Studi di Pisa, Italy

Reviewed by:
R. Varma Penmetsa, University of California, Davis, United States
Christophe Lacomme, Science and Advice for Scottish Agriculture (SASA), United Kingdom

***Correspondence:**
Vitantonio Pantaleo
vitantonio.pantaleo@cnr.it

Specialty section:
This article was submitted to Plant Microbe Interactions, a section of the journal Frontiers in Plant Science

Received: *15 November 2017*
Accepted: *27 February 2018*
Published: *15 March 2018*

Citation:
Leonetti P, Accotto GP, Hanafy MS and Pantaleo V (2018) Viruses and Phytoparasitic Nematodes of Cicer arietinum L.: Biotechnological Approaches in Interaction Studies and for Sustainable Control. Front. Plant Sci. 9:319. doi: 10.3389/fpls.2018.00319

CICER ARIETINUM L.: USES, ORIGIN, AND DISTRIBUTION

In many developing countries, grain legumes have gained much importance in view of acute shortages in the production of animal proteins and the prevalence of protein malnutrition. Conversely, they are a valid alternative as a source of protein for specific (vegetarian or vegan) or balanced diets worldwide, particularly in developed countries.

Legumes are able to fix atmospheric nitrogen, in association with bacteria, and play a central role in low-input and sustainable agricultural systems (Graham and Vance, 2003). With a global production of ca. 77×10^6 tons, grain legumes (also known as "pulses") rank third after cereals and oilseeds (FAO, 2014). The world production of chickpea in 2014 was more than 13×10^6 tons (FAO, 2014), making chickpea rank fourth among the pulses after soybean, peanut, and common bean. However, chickpea can be considered the most important crop at regional level, especially in semi-arid areas of the world and in Mediterranean regions (FAO, 2014). The genus *Cicer* L. includes 44 taxa, 9 annuals, and 35 perennials, and has a narrow genetic base, probably as a consequence of it being a monophyletic descendent from its wild progenitor *Cicer reticulatum,* grown in the Fertile Crescent region (the center of chickpea domestication and diversification) (Abbo et al., 2003). The most popularly known species is the cultivated *Cicer arietinum* L., with $2n = 2x = 16$ chromosomes and a genome size of ∼738 Mb (Varshney et al., 2013). Commercially, the cultivated chickpea varieties are grouped according to the plant's flowers pigmentation as well as size and color of seeds; i.e., *desi*-type (small-seeded) and *kabuli*-type (large-seeded). *Desi*-type accounts for about 85% of the world's production and is mainly grown in India, Pakistan, Iran, Afghanistan, and Ethiopia. *kabuli*-type, instead, is grown in the Middle East, India, Mexico, North and South America, Australia, Spain, and Italy. A third type is characterized by a medium-to-small size and cream-colored seed, and it is designated as "pea-shaped" (Upadhyaya et al., 2008). Seed color (black, red, or white, and their variations) is a key commercial characteristic, which is also associated with the content of phenylpropanoid pathway-derived bioactive secondary metabolites such as flavonoids, lignans, and isoflavones. In addition to seed coat color determination, these secondary products have potential medicinal properties (Sirtori, 2001), and varied and important functions in processes, such as UV protection, disease resistance, and nodulation (N_2 fixation) (Reinprecht et al., 2013).

The *ex-situ* collections of chickpea landraces and wild relatives are stored in 44 genebanks worldwide (Smýkal, 2015) and hold a combination of 98,313 accessions. The largest collections are conserved at the International Crops Research Institute for the Semi-Arid Tropics (ICRISAT) in India (20,140 accessions) and International Center for Agricultural Research in the Dry Areas (ICARDA) in Syria (13,818 accessions) (**Table 1**). Chickpea underwent a drastic loss of genetic diversity due to a series of bottlenecks unique to this crop, i.e., (i) reluctant cross-compatibility with wild species, (ii) difficulty in domestication, and (iii) winter-spring annual phenology (Abbo et al., 2003). Consequently, *C. arietinum* displays a lack of adaptive diversity for a range of biotic and abiotic stress. Susceptibility to viruses, pathogens and pests, sensitivity to environmental stress and poor cross-pollination are the main reasons for the limited diffusion and low production of chickpea.

VIRUSES AND VIRUS-LIKE ENTITIES HOSTED BY *C. ARIETINUM* L.

Several viruses have been isolated from naturally infected chickpea worldwide, but only a few cause diseases, which under specific environmental conditions can lead to significant economic loss (Bos et al., 1988; Kumar et al., 2008). The most relevant viruses reported to infect and induce disease in chickpea are: Alfalfa mosaic virus (AMV, *Alfamovirus, Bromoviridae*), Cucumber mosaic virus (CMV, *Cucumovirus*, *Bromoviridae*), Bean leafroll virus (BLRV) and Beet western yellows virus (BWYV) (both *Luteovirus, Luteoviridae)*, Pea enation mosaic virus complex (PEMV-1, *Enamovirus*, *Luteoviridae*) and (PEMV-2, *Umbravirus*), Chickpea stunt disease-associated virus (CpSDaV, genus unassigned, *Luteoviridae*), and a number of geminiviruses of the genus *Mastrevirus,* the most important being Chickpea chlorotic dwarf virus (CpCDV). Faba bean necrotic yellows virus (FBNYV, *Nanovirus*, *Nanoviridae*) has also been reported (Makkouk et al., 2012). **Table 2** contains a list of all the viruses to date associated with chickpea. **Figure 1** contains a schematic representations of life cycles and spread of two groups of plant viruses included in **Table 2** (i.e., with RNA or DNA genome).

In recent years, the most invasive chickpea virus has been CpCDV. This virus, first reported in India in 1993 (Horn et al., 1993), has recently spread in many countries and among several crops, including other leguminous species (faba bean, lentil, bean), some solanaceous (tomato, pepper) and cucurbits (squash, cucumber), as well as other unrelated species such as cotton, sugar beet, okra, and papaya (Manzoor et al., 2014; Fahmy et al., 2015; Kraberger et al., 2015; Ouattara et al., 2017). In a newly discovered disease of watermelon in Tunisia, causing fruit hardness, CpCDV has been found as the causal agent (Zaagueri et al., 2017a,b). CpCDV is known to be transmitted by leafhopper species of the genus *Orosius* in a persistent manner (Horn et al., 1994). Today, CpCDV has attained a very wide distribution, including the Indian subcontinent, the Middle East and North Africa. Being so polyphagous and having a very widespread vector, CpCDV is certainly an emerging pest that will most likely colonize new areas (and possibly hosts) in forthcoming years.

In the last two decades, chickpea cultivation has been exposed to viral infections in novel areas of cultivation, such as Australia, where a high incidence of disease due to outbreak of viruses has been detected. The Australian food and agriculture stakeholders are closely observing chickpea cultivations and claiming the need to develop strategies that can assist in avoiding future viral epidemics in chickpea and other pulse crops. The Australian Grains Research and Development Corporation (GRDC) (**Table 1**) is supporting surveys of chickpea viruses in Central and West Asia (Kumari et al., 2011). As a result, other geminiviruses similar to CpCDV (but not CpCDV) have been found (Thomas et al., 2010; Hadfield et al., 2012), though currently limited to Australia.

Some chickpea viruses have a recognized quarantine significance, as tested by the Germplasm Health Laboratory of ICRISAT and ICARDA (see the Crop Genebank Knowledge

TABLE 1 | Major "depositor institutes" conserving chickpea accessions.

Genebank and link	Acronym	Country	Accessions
International Crop Research Institute for the Semi-Arid Tropics http://www.icrisat.org	ICRISAT	India	20,140
International Center for Agricultural Research in the Dry Areas http://www.icarda.org	ICARDA	Syria	13,818
United States Department of Agriculture https://www.ars-grin.gov	USDA	USA	6,789
Aegean Agricultural Research Institute http://www.gfar.net	AARI	Turkey	2,075
Australian Temperate Field Crops Collection http://elibrary.grdc.com.au	GRDC	Australia	8,655
National Plant Gene Bank http://medomed.org	NPGB	Iran	5,700
Vavilov Institute of Plant Genetic Resources https://www.gbif.org	VIR	Russia	2,091
Institute for Agrobotany Tapi' oszele https://www.nebih.gov.hu	nèbih	Hungary	1,170
Mediterranean Germplasm Database http://ibbr.cnr.it/mgd/	MGR_IBBR_CNR	Italy	358

Base website: https://cropgenebank.sgrp.cgiar.org/index.php/management-mainmenu-433/stogs-mainmenu-238/chickpea/guidelines/viruses). They are: Pea seed-borne mosaic virus, Bean yellow mosaic virus (PSbMV and BYMV, respectively; *Potyvirus, Potyviridae*), AMV and CMV (**Table 2**). Although belonging to different families, these viruses are transmitted by aphids and are also seed-transmitted to variable degrees. This last feature is of paramount importance for international trade, because viruses can reach and invade new habitats by the long distance human transport of seeds. **Table 2** highlights the commercial sources of resistance against viruses, which to date are only two: PEMV-1 and PSbMV. For other viruses, no resistance has been described in the literature.

Recently, next-generation sequencing (NGS) approaches have opened the door to reconstructing viral populations in a high-throughput and cost-effective manner. Nowadays, NGS can be employed in environmental studies in the agro-ecosystem to either analyze known plant viruses by means of a reference-guided approach or to discover novel plant viruses using a *de novo*-based strategy (Massart et al., 2014).

Viral surveys using metagenomics in *C. arietinum* L. based on short (s)RNA analysis have been carried out in Apulia, Southern Italy, during the 2013–2017 time period. The surveys revealed that a large number of known viral species co-infect chickpea plants without causing any symptoms. Surprisingly, among the viruses found were Tomato mottle mosaic virus (ToMMV, *Tobamovirus, Virgaviridae*), which had not yet been observed in chickpea or reported in Europe, and one viroid referring to *Hop stunt viroid* (HSVd, *Hostuviroid, Pospiviroidae*) (Pirovano et al., 2014). In the same surveys, but in different plant samples, a high level of Turnip crinkle virus (TCV, *Carmovirus, Tombusviridae*) was found, though never reported before in chickpea (Ghasemzadeh et al., 2018). Worthy of note, viral metagenomics is showing that chickpea in open field is a highly permissive host for viruses and mixed infections are not uncommon. This means that most of the symptomatology that in the literature was ascribed to specific infections deserves further studies. In **Figure 2** some viral symptoms that could be unequivocally ascribed to infection by a single virus.

To date, other virus-like infectious agents, such as phytoplasmas, have been reported only in sporadic cases, i.e., Australia, Ethiopia, Oman, and Pakistan. In most cases, phytoplasmas were associated with yellowing, phyllody and little leaves. Generally, infectious phytoplasmas are recognized as members of the 16SrII peanut witches' broom group (Ghanekar et al., 1988; Saqib et al., 2005; Al-Saady et al., 2006; Akhtar et al., 2008).

PPNs ASSOCIATED WITH *C. ARIETINUM* L.

Diseases caused by soil-borne PPNs can generate significant yield losses in economically relevant crops (De Coninck et al., 2015). The estimation of plant parasitic nematodes (PPN) constrains to chickpea production was estimated in 14% (Castillo et al., 2008). PPNs are biotrophic (i.e., obligate parasites that are completely dependent on the host as the only source of nutrients) and polyphagous, because they can infect many different hosts among monocots and dicots. In the most representative PPNs families, root-lesion nematodes (*Pratylenchus* spp.), reniform nematodes (*Rotylenchus reniformis*), cyst-forming nematodes (CNs) (*Heterodera* spp.) and root-knot nematodes (RKNs) (*Meloidogyne* spp.) have been found pathogenic for chickpea and studies were carried out to characterized chickpea-nematode interactions, to describe geographical distributions, general symptoms even at histopathological levels (**Figures 3**, **4** and **Table 3**). The two PPNs largest groups most represented in the world's agro-ecosystem (Hussey, 1989) with interesting infections trategies and life cycles (**Figure 5**) are CNs and RKNs (**Figure 5**). Although three CN species of *Heterodera* have been found associated with chickpea worldwide (Castillo et al., 2008),

TABLE 2 | Viruses reported to infect chickpea.

Family	Virus	Type of transmission	Countries	Genetic resistance	Some References
Bromoviridae	Alfalfa mosaic virus (AMV, genus *Alfamovirus*)	Aphids (non-pers.), seeds, sap*	Iran	–	Kaiser and Danesh, 1971; Makkouk et al., 2003
	Cucumber mosaic virus (CMV, genus *Cucumovirus*)	Aphids (non-pers.), seeds, sap*	Iran, Morocco	–	Kaiser and Danesh, 1971; Ouizbouben and Fortass, 1997; Makkouk et al., 2003
Luteoviridae	Bean leafroll virus (BLRV, genus *Luteovirus*)	Aphid (pers.)	Azerbaijan, Iran, India, Turkey	–	Kaiser and Danesh, 1971
	Beet western yellows virus (BWYV, genus *Polerovirus*)	Aphids (pers.)	Azerbaijan, Iran	–	Makkouk et al., 2003; Mustafayev et al., 2011
	Soybean dwarf virus (SbDV, genus *Lutetovirus*)	Aphids	Iran, Syria	–	Makkouk et al., 2003; Kumari and Makkouk, 2007
	Chickpea chlorotic stunt virus (CpCSV, genus *Polerovirus*)	Aphids (pers.)	Ethiopia, Syria, Egypt, Eritrea, Iran, Morocco, Sudan	–	Abraham et al., 2006, 2009; Asaad et al., 2009; Banane et al., 2010
	Pea enation mosaic virus-1 (PEMV-1, genus *Enamovirus*)	Aphids (pers.), seeds, sap*	Canada, USA, Iran, Syria	yes	Makkouk et al., 2003
Potyviridae	Bean yellow mosaic virus (BYMV, genus *Potyvirus*)	Aphids (non-pers.), seeds, sap*	Iran, Algeria, Morocco	–	Makkouk et al., 2003
	Turnip mosaic virus (TuMV, genus Potyvirus)	Aphids (non-pers.), seeds, sap*	Australia	–	Schwinghamer et al., 2007
	Pea seed-borne mosaic virus (PSbMV, genus *Potyvirus*)	Aphid, seeds, sap*	Iran, Australia, Morocco, Algeria	yes	Ouizbouben and Fortass, 1997
Nanoviridae	Faba bean necrotic yellows virus (FBNYV, genus Nanovirus)	Aphids (pers.)	Jordan, Syria, Turkey, Lebanon, Iran, Egypt, Algeria	–	Yahia et al., 1997
Geminiviridae	Chickpea chlorotic dwarf virus (CpCDV, genus *Mastrevirus*)	Leafhoppers	India, Iran, Syria, Turkey	–	Horn et al., 1993; Makkouk et al., 2003
	Tobacco yellow dwarf virus (TYDV, genus *Geminiviridae*)	Leafhoppers	Australia	–	Thomas et al., 2010
Virgaviridae	Tomato mottle mosaic Virus (ToMMV, genus *Tobamovirus*)	Seeds, sap*	Italy	–	Pirovano et al., 2014
Tombusviridae	Turnip crinkle virus (TCV, genus *Carmovirus*)	Coleoptera, sap*	Italy	–	Ghasemzadeh et al., 2018
Pospiviroidae	Hop stunt viroid (HSVd, genus *Hostuviroid*)	Sap	Italy	–	Pirovano et al., 2014

*pers., persistent; *Mechanical infection by wounding using infectious sap as inoculum.*

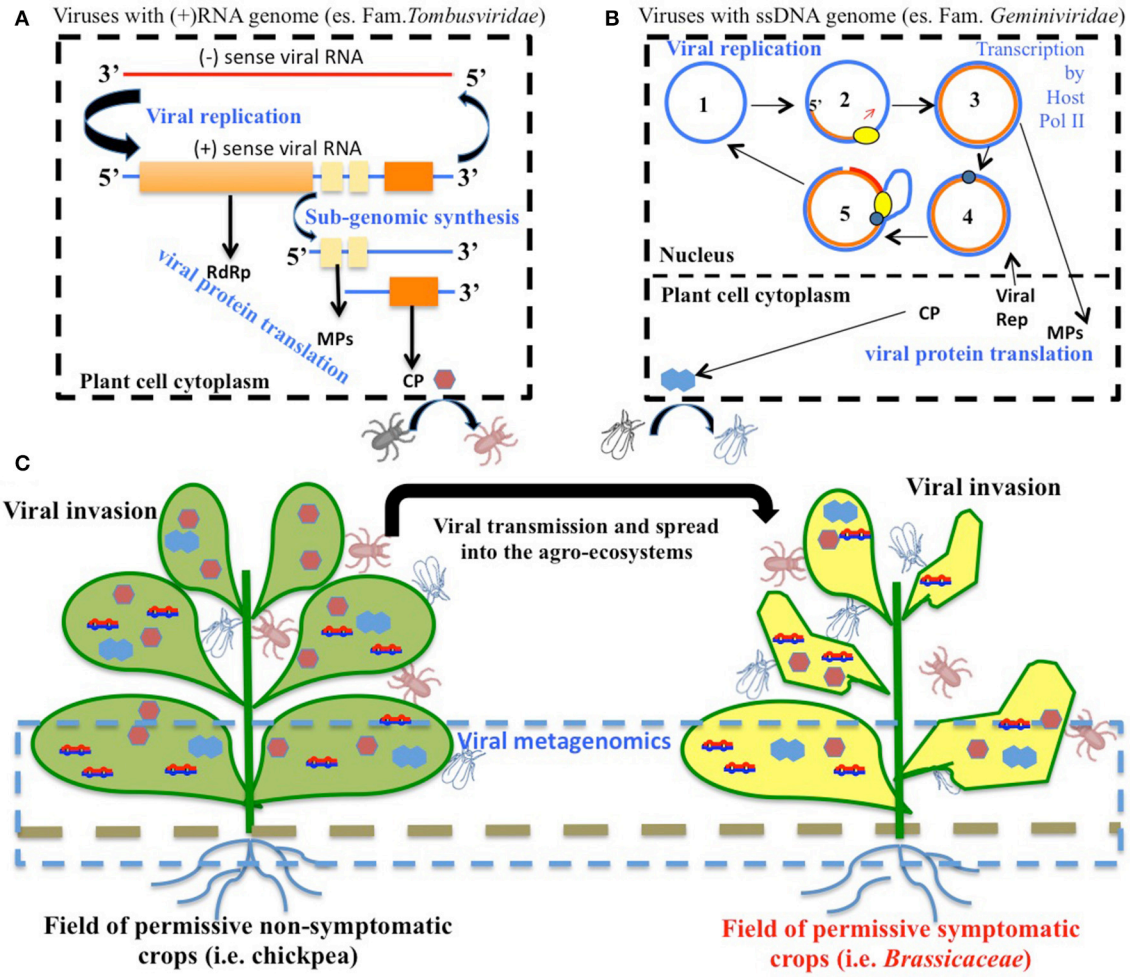

FIGURE 1 | Virus cycles in agro-ecosystems. **(A)** Schematic representation of replication cycles of *Turnip crinkle virus* (TCV) family *Tombusviridae*, genus *Carmovirus*), a virus that has been found associated to chickpea in open field. TCV has a positive (+) sense RNA genome that replicates (blue line). The viral RNA-dependent RNA polymerase (RdRp) amplifies the viral genome in the cytoplasm via negative (–) sense RNA template synthesis (red line). (+) RNA enters into the cellular translation machinery and codes for the RdRp. Moreover, movement proteins (MPs) and coat protein (CP) are the products of translation on viral sub-genomic RNAs. TCV genomic RNA can be encapsidated by the CP to form an icosahedral virion that can be then acquired by insects such as coleoptera. **(B)** Schematic representation of replication cycles of single stranded (ss) DNA viruses of the family *Geminiviridae*. Circular viral genomic ssDNA (1) functions as template for the synthesis of antisense ssDNA (orange line) due to the activity of host DNA-dependent DNA polymerase (yellow element) (2) to form a viral double stranded (ds)DNA intermediate (3). Viral dsDNA can be transcribed in the nucleus by the host DNA-dependent RNA polymerase PolII. Viral RNA transcripts are transferred to the cytoplasm, and enter into the translational machinery to release viral replicase (rep, blue element), MP and CP. One strand of the viral dsDNA can undergo cleavage by viral rep (4), thus allowing the access to the host DNA polymerase that extends the viral ssDNA and generates several copies of the circular genome (5). The ssDNA can be encapsidated and acquired by leafhopper vectors. **(C)** Chickpea is a permissive, non-symptomatic host for several viruses and it is often used in rotation with and/or in proximity to other crops for a sustainable agriculture. It therefore functions as a reservoir of virus inoculum that can be spread through insect vectors to other permissive crops that can show viral symptoms such as leaf yellowing, curling deformation and a general impact on the crop production. Metagenomics of nucleic acids of viral origin can be applied on either symptomatic or non-symptomatic plant tissues, as well as to other environmental samples (soil, insects) in order to explore viral entities associated to agro-ecosystems.

Heterodera ciceri (**Figure 4**) is the only nematode that can lead to significant economic loss. In semi-arid areas of cultivation, the eggs do not undergo dormancy but hatch in the presence of chickpea root diffusates (exudates), where there are suitable soil moisture and temperature conditions of at least 10°C. Chickpea is highly susceptible to damage by *H. ciceri* and, therefore, efforts have been dedicated to search for potential sources of resistance to transfer them into genotypes of commercial varieties. However, resistant accessions have been identified only in *C. bijugum*, *C. pinnatifidum,* and *C. reticulatum,* and were deposited in the ICARDA genebank (**Table 1**) (Malhotra et al., 2002). *Meloidogyne arenaria*, *Meloidogyne incognita* (**Figure 3**), and *Meloidogyne javanica* are the RKN species that cause damage to chickpea. All three are typically found in areas with warm climatic conditions, and attack chickpea especially in the Indian subcontinent. On the other hand, *Meloidogyne artiellia*

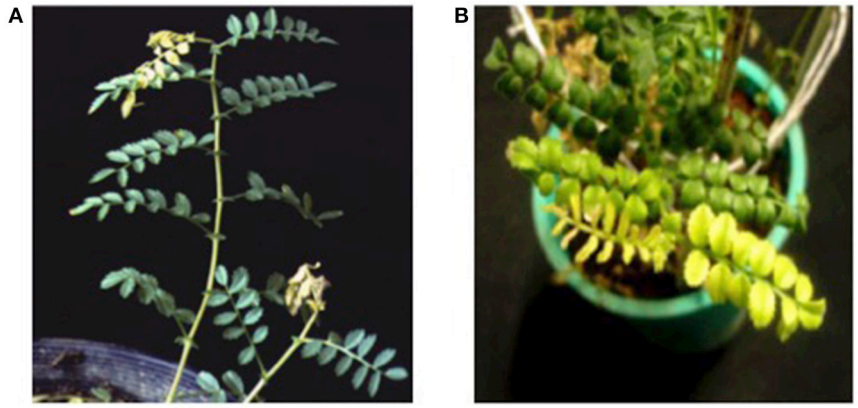

FIGURE 2 | Selected photos showing symptoms induced by viruses on chickpea plants. **(A)** Tip wilting induced by mechanical inoculation with TuMV (from Schwinghamer et al., 2007). **(B)** Symptoms of chlorotic stunt disease caused by CpCDV on chickpea (from Kanakala et al., 2013).

(**Figure 4**), being well-adapted to cool and wet conditions, is widely distributed in the Mediterranean region, including Italy (Castillo et al., 2008). Particularly *M. arenaria*, *M. incognita,* and *M. javanica* induce large galls in chickpea roots, whereas *M. artiellia* gives rise to very small galls surrounding the feeding sites (Vovlas et al., 2005) or no galls in the infected roots (**Table 3**). Ansari and co-authors (Ansari et al., 2004) screened more than 7,000 accessions of chickpea germplasm for resistance to *M. javanica* (Treub) Chitwood; four promising nematode-tolerant genotypes were found and conserved in the chickpea ICRISAT genebank (**Table 1**).

GENOMICS OF *C. ARIETINUM* L.: HOST RESPONSE TO PATHOGENS AND NEW APPLICATIONS OF BIOTECHNOLOGY

The chickpea genome has recently been released by two research groups (Jain et al., 2013; Varshney et al., 2013) and further analyzed (Parween et al., 2015; Thudi et al., 2016). The availability of a rich genomic platform of chickpea and its relatives, such as *C. reticulatum* (a source of interesting characteristics) (Gupta et al., 2017), provides insight into both genome diversity and domestication and therefore should be considered as a resource to improve chickpea resistance against biotic and abiotic stress.

One of the most recurrent themes in plant pathology research is the highly adaptable nature of pathogens, including viruses and nematodes. These organisms possess the ability to harness and modify cellular resources in order to coexist with the plant host. Current genomics in legumes make it possible to study specific layers of plant-pathogen interactions directly using crop plants, including chickpea. A phylogenetic analysis of legume species constructed with genome-wide, single-copy orthologous genes shows that the closest relative to chickpea is *Medicago truncatula,* and secondarily *Glycine max* (Zheng et al., 2016) (**Figure 6**). *M. truncatula* and *G. max* are widely considered as model legumes and, therefore, studies in chickpea could benefit from those carried out in the model relative species. The availability of a genomic platform of the chickpea, together with recent advances in understanding the mechanisms of immune responses to plant pathogens, presents interesting perspectives for attenuating the damage caused in chickpea by biotic stress. Below we highlight the promising main topics.

PLANT IMMUNE DEFENSE RESPONSE, EFFECTOR TARGETS, AND RNA SILENCING IN PATHOGEN ATTACK

Plants recognize pathogens and microbes through pathogen/microbe-associated molecular patterns (P/MAMPs). PAMPs are evolutionarily conserved molecules across kingdoms; in plants they carry out critical functions against several microbial attacks (Boutrot and Zipfel, 2017), including invasion of viruses, bacteria, fungi, and nematodes. For instance, it is widely accepted that the early stages of pathogen attack could be considered the key target step in plant defense strategies; this idea has also been recently extended to nematode parasitism (Holbein et al., 2016). PAMPs activate host defense responses (PAMP-triggered immunity or PTI) through a complex signaling cascade. Effectors should interfere with PTI responses, thereby leading to effector-triggered susceptibility (ETS). Manosalva and coauthors (Manosalva et al., 2015) showed that PPNs secrete conserved pheromones named "ascarosides," eliciting MAMP response in various plants, and are exclusively identified in the phylum Nematoda. In turn, microbial virulent pathogens are able to overcome plant defense mechanisms by secreting effectors into the host. An effector protein can also be the elicitor of effector-triggered immunity (ETI) (Mandadi and Scholthof, 2013). If this first defense system is defeated, then plant resistance initiates a second mechanism which is more amplified and faster than PTI and usually develops in a form of programmed cell death known as the hypersensitive response (HR), leading the infected host cell to apoptosis. In this second detection system level, plants are able to recognize pathogenic effectors through nucleotide-binding site leucine-rich repeat (NBS-LRR) proteins

FIGURE 3 | Symptoms of nematode infection on chickpea plants in field and greenhouse. **(A)** Symptoms of infection visible in the field on *C. arietinum*: plant reduced in crop yield with chlorotic, pale, and yellow leaves. **(B)** Greenhouse pot test: control plant (left) and *M. incognita* infected plant (right). **(C)** Root system of control (c) and *M. incognita* infected plants (+*n*). **(D)** Egg masses (em) generated by *M. incognita* mature female, in root galling tissue. **(E)** Newly formed cysts (cy) *of H. goettingiana*.

and are characterized by leucine-rich repeats (LRR) that give them binding specificity. In fact, among the largest gene families in plants deputed to play roles in response to a broad range of pests and pathogens is the *R*-gene family, which mainly includes NBS-LRR genes (Zheng et al., 2016). Chickpea contains at least 153 NBS-LRR homolog genes in eight chromosomes (Varshney et al., 2013). This number is considerably lower than the number of orthologs in other legume species (Jain et al., 2013). Once discovered in *M. truncatula* and *G. max*, the cascade regulation of NBS-LRRs triggered by micro (mi)RNAs of the miR2118/482 superfamily members has been associated with nodulation events (plant-rhizobium interactions) and not to better specified plant pathogen defense strategies (Zhai et al., 2011). The interaction between miRNA and *R*-genes might have long-term evolutionary benefits by buffering NBS-LRR levels to reduce the fitness cost of these genes (Zheng et al., 2016). More recently, NBS-LRR secondary siRNA cascade mechanisms have been revealed to spawn valuable layers of

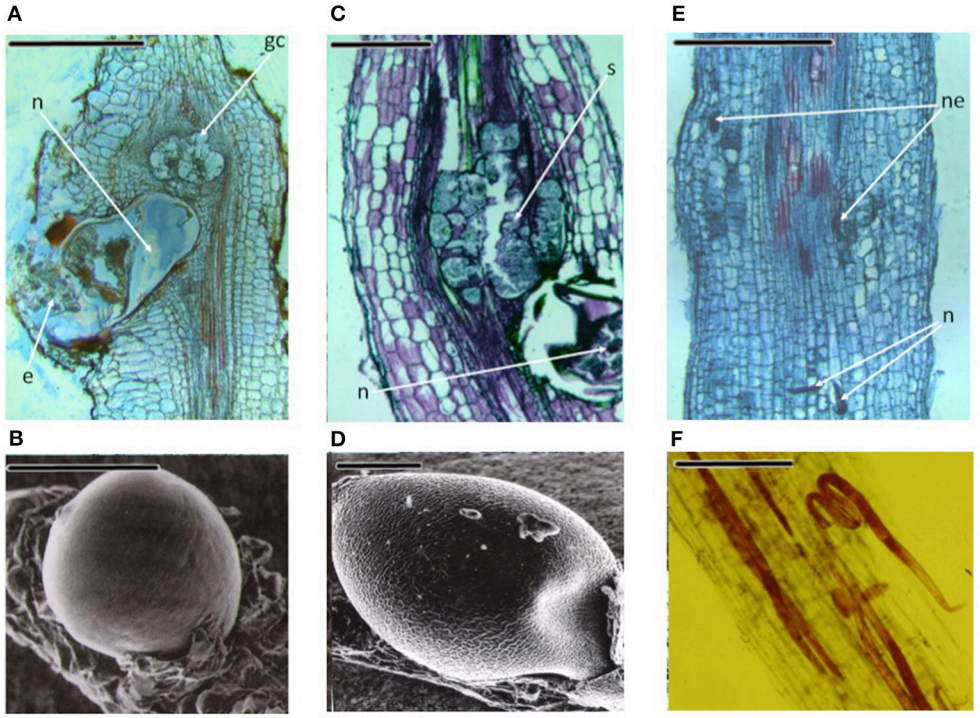

FIGURE 4 | Three important PPNs associated to chickpea roots. *Meloidogyne artiellia*: **(A)** Longitudinal root section showing anatomical alterations; **(B)** Scanning electron microscopy (SEM) photo of a female on the root. *Heterodera ciceri*: **(C)** The tissues disruption caused by the cyst nematode is shown in longitudinal root section; (D) SEM image of a mature female. *Pratylenchus thornei*: **(E)** Longitudinal section of the root showing lesions caused by the nematode; **(F)** Fuchsin-stained root cortex section, showing the migratory endoparasite. n, nematode; e, eggs; gc, giant cell; ne, necrotic tissues; s, syncytium. Scale bars: **(A,C,E)** = 500 μm; **(B,D,F)** = 200 μm (Source: Nicola Vovlas, CNR).

non-race-specific resistance against viral and bacterial pathogens (Shivaprasad et al., 2012) (**Figure 7**). This recently discovered plant strategy seems to be independent from either the NBS-LRR protein additive effect of expression or from the *R*-gene-to-pathogen gene interaction. In chickpea leaf/shoot/floral tissues, 22 nt-long miR2118 is fairly present and targets NBS-LRRs (Srivastava et al., 2015), and the secondary siRNA mechanism involved in cascade regulation of NBS-LRR is present as well. Importantly, NBS-LRR regulation can be subverted by plant viruses. RNA silencing in plants and insects can function as a defense mechanism against invading viruses, and viruses have evolved viral suppressors of RNA silencing (VSRs) to overcome the host defense (reviewed by Csorba et al., 2015). VSRs can act on various steps of the different silencing pathways and, thus, can have a profound impact on host endogenous RNA-silencing regulatory pathways, including the generation and function of plant endogenous siRNA, such as miRNAs and secondary siRNAs (**Figure 7**).

Chickpea seems to be a permissive host for many plant viruses that are considered capable of inducing pathogenesis in many plant species. All of the plant viruses families infecting chickpea (**Table 2**) are known to express VSRs, which, in turn, have been shown to subvert RNA silencing machinery. For instance, PEMV-1 expresses the P0 protein, which has been shown to destabilize AGO1 protein (Fusaro et al., 2012) and, therefore, could hinder the miR2118-triggered, NBS-LRR–mediated cascade mechanism of *R*-gene silencing at several stages (**Figure 7**). Similarly, but with a different mechanism, TCV P38 can alter AGO1 activity (Azevedo et al., 2010) (**Figure 7**). Tobamovirus replicase (i.e., P122/P126) is known to bind miRNA and siRNA, preventing their stabilization and incorporation into the RNA-induced silencing complex (Csorba et al., 2007; Vogler et al., 2007) (**Figure 7**). All these VSRs from viruses infecting chickpea can block downregulation of NBS-LRR and the downstream cascade mechanism, inducing overexpression of *R*-genes with a wider coverage against viral and other pathogens, despite the low number of *R*-genes in the chickpea genome.

Recently, it has become clear that silencing pathways also play an important role in other plant pathosystems, including the onset of nematode parasitism. Indeed, through a transgenic approach, it has been shown that VSRs can subvert host RNA silencing machinery and increase the susceptibility to nematode parasitism (Walsh et al., 2017).

RNA silencing approaches have also been exploited in plants to control PPNs, given that RNA silencing mechanisms are also conserved in nematodes (Fire et al., 1998). Double-stranded RNA (dsRNA) can be produced through engineered plants that have the ability to silence target genes in nematode body. The delivery of dsRNAs from plant to nematode occurs by the ingestion

TABLE 3 | Selection of PPNs, associated with chickpea (font: https://www.cabi.org).

Family	Species	Generic and characteristic symptoms	Countries	References
Meloidogynidae	*Meloidogyne incognita*, *Meloidogyne arenaria, Meloidogyne javanica*	Whole plant: early senescence; Leaves: abnormally colored and wilted Roots: galls, swollen and reduced root system	Indian Subcontinent	Ali and Sharma, 2003; Vovlas et al., 2005
	Meloidogyne artiellia	Root with small or absent galls and protruded adult female	Mediterranean Basin	Vovlas et al., 2005
Heteroderidae	*Heterodera goettingiana*	Whole plant: stunted Leaves: pale green at an early stage, later chlorotic. Reduced number of flowers and pods, small or no seeds Roots: poorly developed, lacking nitrogen-fixation nodules.	North Africa	Di Vito et al., 1994
	Heterodera ciceri	Soil infestation in small circular area that should extend to entire field. Eggs don't undergo dormancy.	Turkey, Syria	Greco et al., 1988; Castillo et al., 2008
Pratylenchidae	*Pratylenchus thornei*	Whole plant: dwarfing distributed in patches Leaves: chlorosis and reduction shoot weight Roots: necrotic streaks or lesions, soft rot of cortex	Australia, India, Mexico, North Africa, Spain	Castillo et al., 1996
	Pratylenchus penetrans	Whole plant: reduced crop yield Leaves: chlorotic (pale, yellowing) Roots: may be thin, and with a reduced number of lateral roots.	North Africa, Spain, Turkey	Di Vito et al., 1994
Hoplolaimidae	*Rotylenchus reniformis*	Whole plant: distorted Leaves: abnormal colors Stems: stunting or rosetting Roots: external feeding and reduced root system	India, Egypt, Ghana	Mahapatra and Pahdi, 1996

process and can trigger RNA interference (RNAi), resulting in the inactivation of targeted genes (Gheysen and Vanholme, 2007). Availability of a genomic platform of PPNs is a prerequisite to identify the nematode genes responsible for the interactions and run loss-of-function (Abad et al., 2008; Denver et al., 2016). This could lead, for example, to adopt strategies based on the manipulation of nematode-derived protein elicitor(s), molecules able to induce a PTI-like response (Mendy et al., 2017). The ETI defense response in plant-nematode interaction is relatively better investigated than PTI, and often involves an HR reaction due to the initiation of the two characteristic "feeding structures" induced in the root by sedentary endoparasitic nematodes (Goverse and Smant, 2014) (**Figure 5**). A noteworthy case is the HR that takes place in the induction of several individual "giant cells" in *Mi-1*-resistant tomato plants infected by RKN-infective second-stage juveniles (J2) (**Figure 5**). By contrast, the deterioration of the "*syncitium*" (composed of hundreds of fused root cells, induced by *H. glycines* in soybean genotypes harboring a natural resistance gene at the *Rgh1* locus, is not characterized by typical cell death. *Rgh1*-mediated resistance seems to involve the collapse of the feeding site by nuclear and cytoplasmic fragmentation.

Recently, a novel and unique mechanism of plant resistance has been discovered through mutation analysis, gene silencing and transgenic complementation in soybean–*H. glycines* interactions. Wu et al. (2016) have demonstrated that the single dominant *Rgh4* locus, which is a major quantitative trait locus encoding serine hydroxymethyltransferase (SHMT), confers resistance to CNs (Wu et al., 2016). SHMT is an enzyme that is ubiquitous in nature and structurally conserved across kingdoms. The resistant allele possesses two functional single nucleotide polymorphisms (SNPs, denoted as P130R and N358Y) compared to that of the sensitive allele, rhg4. These mutations affect the kinetic activity of SHMT, which could result in folate deficiency inside syncytia and a nutritional deficiency that starves the nematode. This is a novel plant defense strategy against roundworm that could readily be extended to other important crops. Preliminary exploration within the chickpea genome has confirmed the presence of at least two *shmt* loci (**Figure 8**). These findings will likely boost research to extend the use of SHMT resistance to chickpea by identifying the source of positive functional SNPs in ancient local varieties or, alternatively, to apply novel technologies such as genome editing of functional SNPs.

BIOTECHNOLOGY APPLICATIONS: CURRENT STATUS ON THE GENETIC TRANSFORMATION OF *CICER ARIETINUM* L.

The enhancement of tolerance to biotic and abiotic stress in chickpea can significantly increase its yield potential. However, due to the limited genetic pool, cross compatibility and lack of resistance sources to biotic constraints in the available germplasm the improvement of chickpea by means of conventional breeding faces serious limitations. Modern plant biotechnology tools offer several possibilities to finally overcome these limitations. The main objectives are (i) to enhance chickpea resistance to pests and other biotic and abiotic stress, and (ii) to achieve more

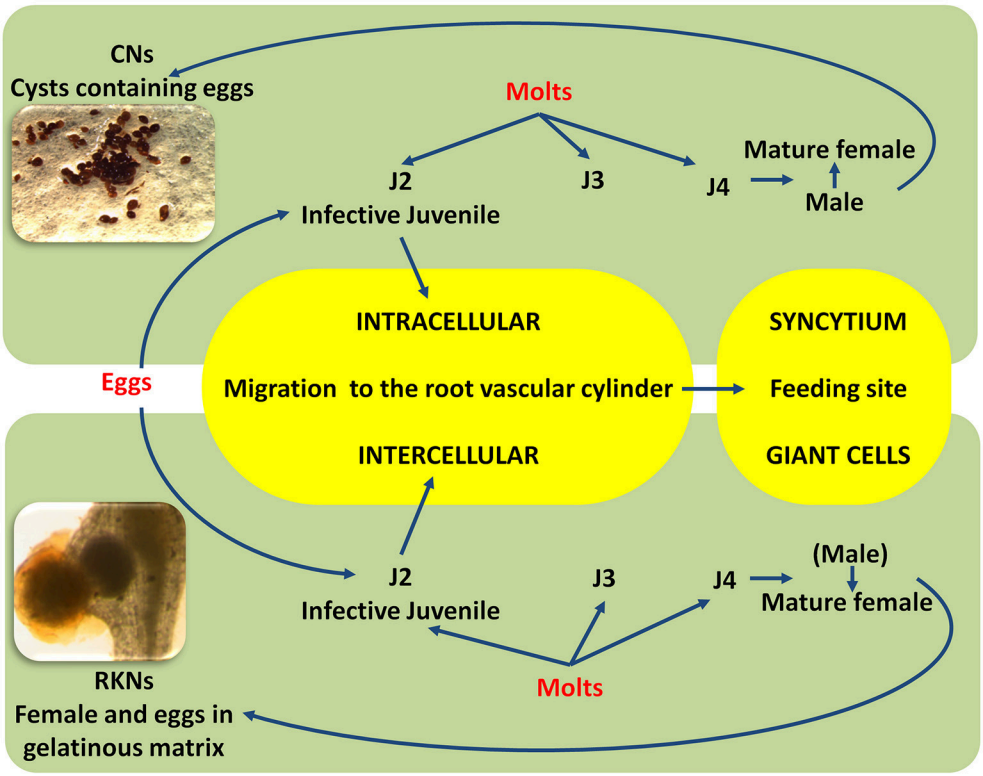

FIGURE 5 | Simplified life cycles of cyst nematodes (CNs) and root-knot (RKNs) nematodes. Larvae hatch from cysts or from egg masses; the first-stage juvenile molts inside the eggshell become an invasive second-stage juvenile (J2) adapted to penetrate the root using an intra, inter-cellular migration and to the establishment of the feeding site (Syncytium and Giant cell). The nematode has to change molts (J3, J4) to become a fully mature (male or female) adult. Parthenogenetic and amphimictic reproduction modalities are different between CNs and RKNs.

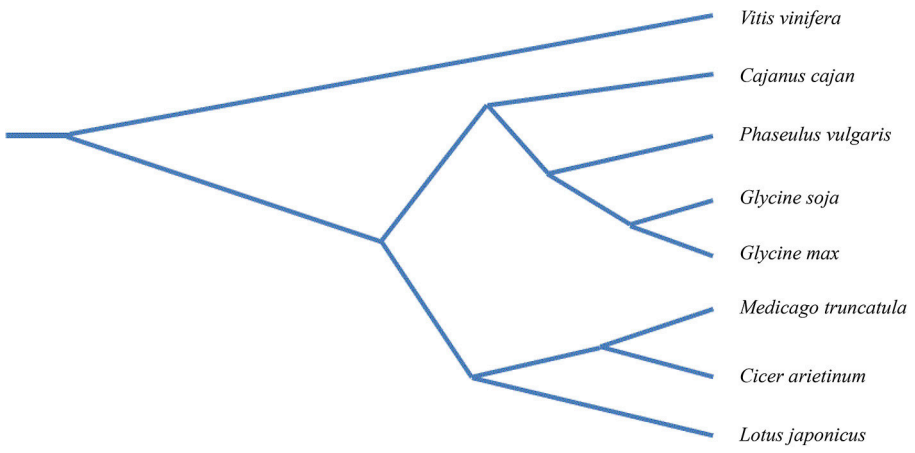

FIGURE 6 | Phylogenetic tree of seven legume species with *Vitis vinifera* as the out-group. The phylogenetic tree was constructed with a genome-wide single-copy orthologous genes of legume species i.e., *Glycine max*, (cultivated soybean), *Glycine soja* (wild soybean), *Medicago truncatula* (barrel clover), *Lotus japonicus* (bird's-foot trefoil), *Cajanus cajan* (Pigeonpea) *Cicer arietinum* (chickpea), *Phaseolus vulgaris* (common bean). Modified from Zheng et al. (2016).

sustainable food production in developing countries, such as in the semi-arid tropics where agrochemicals are inaccessible to low-income farmers (Sharma and Ortiz, 2000; Sharma et al., 2001). Most biotechnology approaches require skills and tools for manipulating the genome of a plant, either through transgenics or other means, and the process always includes plant transformation and regeneration steps. Chickpea, like other large-seed grain legumes such as faba bean, pigeonpea,

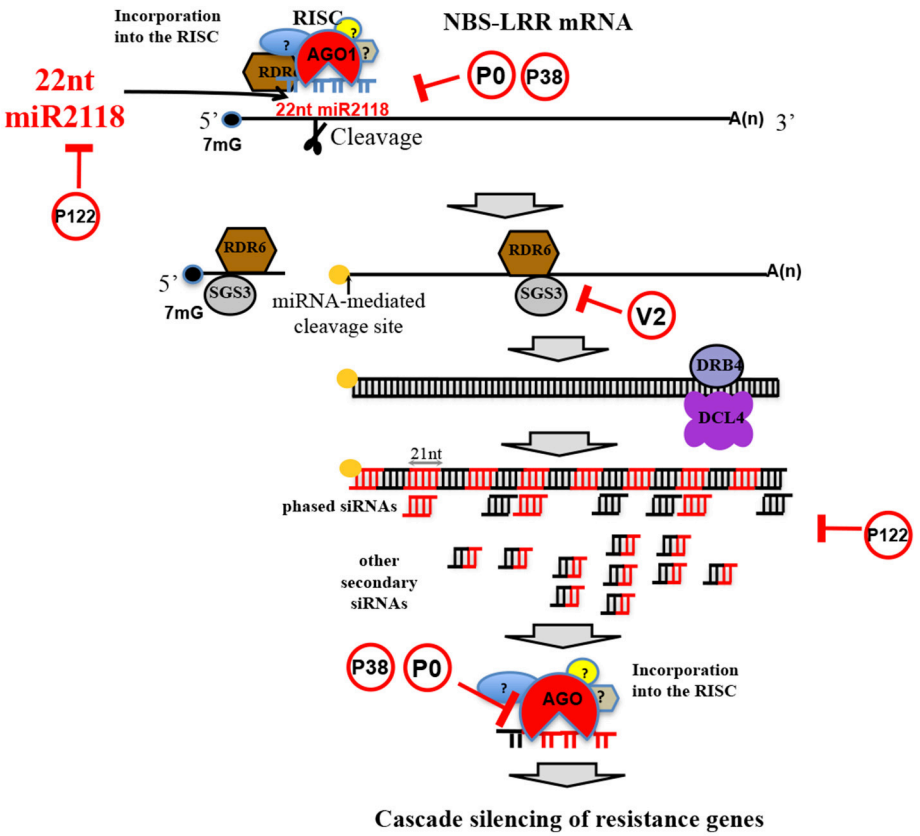

FIGURE 7 | NBS-LRR silencing cascade mechanism. Schematic representation of NBS-LRR silencing cascade mechanism triggered by miR2118 (a legume specific miRNAs discovered in soybean), highly conserved in *C. arietinum*. In red circles, viral silencing suppressors (Csorba et al., 2015) that can impair the cascade mechanism.

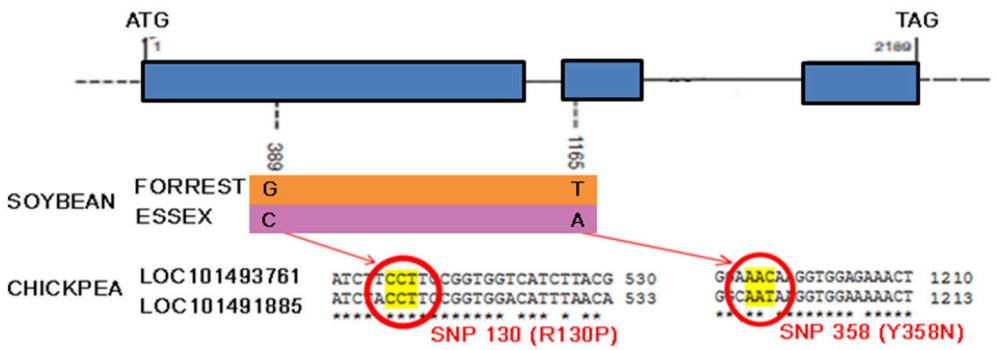

FIGURE 8 | Serine hydroxymethyltransferase gene model. Shmt model and polymorphism in resistant (Forrest) and susceptible (Essex) soybean cultivars and alignment of predicted chickpea shmt 1-like mRNA sequences (NCBI reference XM_004504310.1 and XM_004502186.1) showing the two functional SNPs positions.

and common bean, is considered to be "reluctant" to *in vitro* transformation and regeneration (Somers et al., 2003). Therefore, one critical point of chickpea productivity improvement remains the development of reliable genetic transformation techniques.

Plant genetic transformation is defined as the method for the delivery, integration, and expression of foreign genes into plant genomes (Atif et al., 2013). There are two main methods that enable delivery of the gene into the plant genome: (i) direct gene transfer (mediated by physical or chemical forces) and (ii) *Agrobacterium*-mediated genetic transformation, where *Agrobacterium tumefaciens* is used as a vehicle to introduce foreign genes into the plant genome.

In the case of the chickpea, many research efforts were undertaken to improve resistance against major biotic stress, such as pod borers (*Heliothis armigera* [Hub.]), aphids (*Aphis craccivora*), bruchids, fungal diseases (*Fusarium oxysporium/F.*

udum), and abiotic (drought and salinity) stress, as well as the nutritional quality by increasing the sulfur-containing amino acid content. The first transformation studies with chickpea were performed by Srinivasan et al. (1991) and Islam et al. (1994) using callus culture; shoot regeneration was not possible. Although these studies were unsuccessful due to poor regeneration, they showed the susceptibility of chickpea to infection with *A. tumefaciens* and proved its potential as a transformation vector for chickpea. Afterwards, generation of transgenic chickpea was reported with varying degrees of success. To our knowledge, however, the number of reports describing the successful production of transgenic chickpea using either *Agrobacterium*-mediated or particle bombardment transformation is still very limited (Mishra et al., 2012; Atif et al., 2013; Tripathi et al., 2013). **Table 4** summarizes chickpea transformation studies. Most of the first attempts on genetic transformation used the *Agrobacterium*-mediated method with few exceptions, where particle bombardment was employed (Tewari-Singh et al., 2004; Ganguly et al., 2014). Indurker et al. (2007) reported a successful transformation protocol (16% transformation frequency) using particle bombardment with gold particles as micro-carrier, in combination with helium pressure of 900 psi on epicotyl explants of the cultivars ICCC37 and PG-12. The construct was a pHS102 plasmid harboring the reporter gene *uidA*, neomycin phosphotransferase II (*nptII*) and insecticidal *cry1Ac*. Fontana and colleagues (Fontana et al., 1993) reported the first successful chickpea transformation protocol after transformation of embryonic axes with *A. tumefaciens*. The transferred genes were successfully inherited into subsequent generations. Molecular evidence for the transgenic nature was confirmed by studying the integration and expression of β-D-glucuronidase and *nptII* genes as well as the integration and expression of the transferred genes. Later, other reports described new protocols (Krishnamurthy et al., 2000; Polowick et al., 2004; Sarmah et al., 2004; Senthil et al., 2004; Sanyal et al., 2005) improved for their simplicity and relatively short time required to produce transgenic plants (T0) without the callus phase (4–6 months). From surveying the literature on chickpea transformation, it can be concluded that the average frequency of *Agrobacterium*-mediated transformation is 0.1–5.1%, which is very low compared to model plants such as *G. max* and *M. truncatula* (96 and 80%, respectively) (Iantcheva et al., 2001; Li et al., 2017). However, with the ICC10943 cultivar and using sonication-assisted, *Agrobacterium*-mediated transformation (SAAT) cases of transformation efficiency higher that 25% have been reported (Bhattacharjee et al., 2010; **Table 4**). Therefore a wider utilization of SAAT for chickpea transformation can be foreseen, which should be nonetheless tested on several other varieties.

PERSPECTIVES

The strong potential of genetic transformation techniques for crop improvement is unquestionable. The clustered regularly interspaced short palindromic repeat (CRISPR)-associated protein 9 (Cas9) DNA editing system has recently been developed as a new method for genome engineering. It is based on the type II CRISPR-associated immune system that protects bacteria against invading DNA viruses and/or plasmids (Jinek et al., 2012). Genome editing by CRISPR/Cas9 as well as other techniques, including zinc finger nucleases (ZFNs) and transcription activator-like effector nucleases (TALENs), have been applied to edit the genome in several plant species (Kim and Kim, 2014). The successful utilization of CRISPR/Cas9-directed genome editing in plant species has been reported and also includes the two relatives, i.e., the legume models *G. max* and *M. truncatula* (Li et al., 2015; Meng et al., 2017). CRISPR/Cas9 gene editing technology is currently revolutionizing genetic studies and crop improvement because it can be applied with high-throughput and at genome-scale (Yang et al., 2017). To our knowledge, no research effort has been made to implement this system in chickpea. The application of CRISP/Cas9 in chickpea genome editing will not only provide answers to basic biological questions but will also reduce public concern about transgenic plants, owing to its non-GMC nature. In most cases, Cas9 and guide (g)RNAs are delivered into plant cells by *Agrobacterium*-mediated T-DNA transformation or by physical means, such as PEG-mediated transformation of protoplasts or biolistic transformation of calluses. In the case of chickpea and other legumes, this approach could face limitations due to the difficulties of transformation and regeneration from callus. An alternative approach that could help to overcome these limitations is the identification and engineering of plant viruses as a tool for systemic gene editing in plants. Some successful examples are already available. Cabbage leaf curl virus, a geminivirus, is able to deliver gRNA and induce systemic gene mutations in plants (Yin et al., 2015). An RNA viral vector based on Tobacco rattle virus (TRV) has been demonstrated to serve as a vehicle to deliver genome-engineering reagents to all plant parts, including meristems. This provides a general method for easily recovering seeds with the desired modifications, obviating the need for transformation and/or tissue culture (Ali et al., 2015). More recently a legume virus, the Pea early-browning virus, has been demonstrated to be more efficient than TRV for these applications (Ali et al., 2017). An additional challenge would be the identification of the best DNA or RNA viruses able to fully infect chickpea to be engineered and used as viral vectors dedicated to genome editing.

Genome editing of chickpea may help improving specific characteristics of a crop with limited genetic pool and lack of resistance sources. An emblematic case would be the modification of functional SNPs in the SHMT gene (**Figure 8**) in order to confer resistance to nematodes or to modify miRNA target sites in NBS-LRR genes (**Figure 7**), ensuring the up-regulation of certain functional *R*-genes.

Perspectives for the improvement of chickpea should also take into account the genomic selection approach. It facilitates the rapid selection of superior genotypes and accelerates the breeding cycle and it has been applied with a large success in many other crops (Crossa et al., 2017).

Chickpea cultivations may constitute a reservoir of viral entities. Indeed, chickpea seems to be a permissive host for many viruses and viroids, thus ensuring their maintenance in

TABLE 4 | Genetic transformation studies in chickpea.

Transformation method	Cultivar	Explant type	Transferred genes	Transformation frequency %	References
Agrobacterium-mediated transformation	Local ecotype	EAx	*uid*A, *npt*II	4*	Fontana et al., 1993
	ICCV1, ICCV6 and desi (local) variety	EAx	*uid*A, *npt*II	e.g., ICCV-6: 1.96	Kar et al., 1996
	PG1, PG12, Chafa and Turkey	EAx	*uid*A, *npt*II	e.g., Turkey < 1.5	Krishnamurthy et al., 2000
	H-208, ICCL87322, K-850, Annigiri, and ICCV5	EAx	*uid*A, *bar*	5.1[§]	Senthil et al., 2004
	Semsen	Halved EAx attached to cotyledon	*nptII*, bean *αAI1*	0.72[¢]	Sarmah et al., 2004
	CDC Yuma	EAx	*uid*A, *npt*II	3.1^	Polowick et al., 2004
	C-235, BG-256, Pusa-362 and Pusa-372	Pre-conditioned CNs	*cry*1Ac, *npt*II	e.g., BG 256: 1.12	Sanyal et al., 2005
	K-850	EAx	*α-ai*, *uid*A, *npt*II	0.3	Ignacimuthu and Prakash, 2006
Sonication-assisted *Agrobacterium* mediated transformation (SAAT)	ICC10943 and ICC10386	Decapitated embryo	*uid*A, *hpt* II	ICC 10943: 26 ± 2, ICC 10386: 24 ± 3[Δ]	Pathak and Hamzah, 2008
	ICCV89314	Single cotyledon with half embryo	ASAL, *nptII*, *gusA*	0.066±0.003 (mean ± SE)	Chakraborti et al., 2009
	C-235, Annigiri and K-850	Wounded apical dome of shoot apex	*uid*A, *bar*	2.43	Singh et al., 2009
	C-235	EAx with half portions of both cotyledons	*pmi*	3	Patil et al., 2009
	C-235	AMEs	$P_5CSF_{129}A$, *npt* II, *uid*A	Not mentioned	Bhatnagar-Mathur et al., 2009
	Semsen, ICCV89314	Cotyledon with half EAx	*cry*2Aa, *npt*II	0.3	Acharjee et al., 2010
	Pusa-256, KWR-108, Pusa-1003 and local line (from market)	Cotyledon- and cotyledonary-node-derived-callus and EAx	*uid*A, *hpt*	e.g., KWR 108: 23.45	Bhattacharjee et al., 2010
	Annigeri	CNs	*P5CS*, *hpt*, *uid*A	Not mentioned	Ghanti et al., 2011
	P-362	CNs	*cry*1Ab, *cry*1Ac, *npt*II	2.77	Mehrotra et al., 2010
	C-235, BG-256, P-362 and P-372	Immature cotyledons, EAx	*uid*A, *npt*II	e.g., P 362: 2.08	Tripathi et al., 2013
	C-235	AMEs	DREB1A, *npt*II	Not mentioned	Anbazhagan et al., 2015
	DCP-923	EAx	fused *cry1*Ab/Ac, *hpt*	Not mentioned	Ganguly et al., 2014
	P-362	CNs explants	*nptII*, *uid*A, modified human α_1-PI, *cry1A*b, *cry1Ac*	Not mentioned	Yadav et al., 2017
	C-235	AMEs explants	*uid*A, *npt*II	1.2	Srivastava et al., 2017
Particle bombardment	ICCV1, ICCV6	EAx	*npt*II, *cry*1Ac	Not mentioned	Kar et al., 1997
	P-362, P-1042 and P-1043	Decapitated embryo	*pat, nptII*, *uid*A, *AK*	Not mentioned	Tewari-Singh et al., 2004
	Chaffa, PG12, ICCC37 and ICCC32	EAx, epicotyl and stem	*npt*II, *uid*A, *cry*1Ac	16±0.33[£]	Indurker et al., 2007

*EAx, embryonic axis; AMEs, Axillary meristem explants; CNs, Cotyledonary Nodes; uidA, β-Glucuronidase, commonly referred to as the gus gene; nptII, neomycin phospho transferase II; bar, Basta (bialaphos) resistance; αAI1, bean-α amylase inhibitor 1; pat, phosphinothricin-acetyltransferase; AK aspartate kinase; cry1Ac, insecticidal crystal toxins 1Ac; α-ai, α-amylase inhibitor; ASAL, Allium sativum leaf agglutinin; gusA, β-Glucuronidase; pmi, phosphomannose isomerase; $P_5CSF_{129}A$, D1- pyrroline-5-carboxylate synthetase $F_{129}A$; cry2Aa, insecticidal crystal toxins 2Aa; hpt, hygromycin phosphotransferase; P5CS, pyrroline-5-carboxylate; DREB1A, dehydration response element B1A; α_1-PI, modified human Alpha-1-proteinase inhibitor. *Number of whole plants transformed/initial number of embryos; [§]Number of confirmed independent lines/number of initial seeds; [¢]18 independently derived transgenic plants obtained from a total of 2,500 explants (explant that consisted of one cotyledon attached to half embryonic axis); ^7 separate experiments with the use of shoot elongation media (MS); [Δ]Obtained by dividing [100 times the number of confirmed transformed plants of independent lines (both PCR and Southern blot positive)] by the number of treated explants;[£]Epicotyl, average of three experiments with 150 explants each.*

agro-ecosystems: most of the hosted viruses are symptomless in chickpea, but pathogenic for other plant species. Viral metagenomics is currently the tool most indicated for surveys of virus-infected plants. In addition, metagenomics approaches can help to discover novel infectious entities and microbes either hosted by or associated to chickpea. This could help scientists better identify and describe the multi-trophic interactions that may influence nematode reproduction or plant-rhizobia interactions.

To modulate plant PPNs, several transgenic strategies have been used, such as (i) cloning of resistance genes from natural resources and transfer to other plant species; (ii) overexpression of different protease inhibitors; and (iii) suppression of nematode effectors in plants using RNAi (Ali et al., 2017). RNAi (Rosso et al., 2009; Banerjee et al., 2017) is worth exploring more in depth, particularly RNAi-based technology combined with peptide expression which disrupt nematode sensory activities (Fosu-Nyarko and Jones, 2015). Moreover, a number of CRISPR/Cas9 genome-editing protocols have been established in *Caenorhabditis elegans* (Friedland et al., 2013; Zamanian and Andersen, 2016). Genome manipulation with novel developments in this model organism, research, and advances in parasite genomics could open new doors to the biology of closely related nematode parasites during their interaction with legumes. A more in-depth understanding of the potentiality in biotechnologies for legume pest management will at least modernize chickpea breeding programs, targeting a greater impact on food and nutrition security, climate change adaptation and worldwide diffusion.

AUTHOR CONTRIBUTIONS

All the authors have contributed to the review with their proper specific expertise in plant science, plant pathology, and plant biotechnology.

ACKNOWLEDGMENTS

We thank CNR-IPSP (Italy)-NRC (Egypt) 2016-2017 Bilateral Project *Cicer arietinum* ancient varieties in Egypt: exploiting associated pathogens and modern defense strategies for supporting all the authors and SaveGraINPuglia project (PSR 2007-2013, Misura 214, 4a and PSR 2014-2020, Misura10.2.1) for supporting PL and VP. The authors are particularly grateful to Dr. Nicola Vovlas for the photos A and E in **Figure 3** and the photos in **Figure 4**.

REFERENCES

Abad, P., Gouzy, J., Aury, J. M., Castagnone-Sereno, P., Danchin, E. G., Deleury, E., et al. (2008). Genome sequence of the metazoan plant-parasitic nematode *Meloidogyne incognita*. *Nat. Biotechnol.* 26, 909–915. doi: 10.1038/nbt.1482

Abbo, S., Shtienberg, D., Lichtenzveig, J., Lev-Yadun, S., and Gopher, A. (2003). The chickpea, summer cropping, and a new model for pulse domestication in the ancient near east. *Q. Rev. Biol.* 78, 435–448. doi: 10.1086/378927

Abraham, A. D., Menzel, W., Lesemann, D. E., Varrelmann, M., and Vetten, H. J. (2006). Chickpea chlorotic stunt virus: a new polerovirus infecting cool-season food legumes in Ethiopia. *Phytopathology* 96, 437–446. doi: 10.1094/PHYTO-96-0437

Abraham, A. D., Menzel, W., Varrelmann, M., and Vetten, H. J. (2009). Molecular, serological and biological variation among chickpea chlorotic stunt virus isolates from five countries of North Africa and West Asia. *Arch. Virol.* 154, 791–799. doi: 10.1007/s00705-009-0374-0

Acharjee, S., Sarmah, B. K., Kumar, P. A., Olsen, K., Mahon, R., Moar, W. J., et al. (2010). Transgenic chickpeas (*Cicer arietinum* L.) expressing a sequence-modified cry2Aa gene. *Plant Sci.* 178, 333–339. doi: 10.1016/j.plantsci.2010.02.001

Akhtar, K. P., Shah, T. M., Atta, B. M., Dickinson, M., Jamil, F. F., Haq, M. A., et al. (2008). Natural occurrence of phytoplasma associated with chickpea phyllody disease in Pakistan – a new record. *Plant Pathol.* 57, 771. doi: 10.1111/j.1365-3059.2007.01800.x

Ali, S. S., and Sharma, S. B. (2003). Nematode survey of chickpea production areas in Rajasthan, India. *Nematol. Mediterr.* 31, 147–149. Available online at: http://journals.fcla.edu/nemamedi/article/view/86740/83656

Ali, Z., Abul-Faraj, A., Li, L., Ghosh, N., Piatek, M., Mahjoub, A., et al. (2015). Efficient virus-mediated genome editing in plants using the CRISPR/Cas9 system. *Mol. Plant* 8, 1288–1291. doi: 10.1016/j.molp.2015.02.011

Ali, Z., Eid, A., Ali, S., and Mahfouz, M. M. (2017). Pea early-browning virus-mediated genome editing via the CRISPR/Cas9 system in *Nicotiana benthamiana* and Arabidopsis. *Virus Res.* 244, 333–337. doi: 10.1016/j.virusres.2017.10.009

Al-Saady, N. A., Al-Subhi, A. M., Al-Nabhan, I. A., and Khan, A. (2006). First record of a Group 16SrII phytoplasma infecting chickpea in Oman. *Plant Dis.* 90, 273. doi: 10.1094/PD-90-0973C

Anbazhagan, K., Bhatnagar-Mathur, P., Vadez, V., Dumbala, S. R., Kishor, P. B., and Sharma, K. K. (2015). DREB1A overexpression in transgenic chickpea alters key traits influencing plant water budget across water regimes. *Plant Cell Rep.* 34, 199–210. doi: 10.1007/s00299-014-1699-z

Ansari, M. A., Patel, B. A., Mhase, N. L., Patel, D. J., Douaik, A., and Sharma, S. B. (2004). Tolerance of chickpea (*Cicer arietinum* L.) lines to root-knot nematode, *Meloidogyne javanica* (Treub) Chitwood. *Genet. Resour. Crop Evol.* 51, 1449–1453. doi: 10.1023/B:GRES.0000023460.26690.23

Asaad, N. Y., Kumari, S. G., Haj-Kassem, A. A., Shalaby, A. B. A., Al-Shaabi, S., and Malhotra, R. S. (2009). Detection and characterization of chickpea chlorotic stunt virus in Syria. *J. Phytopathol.* 157, 756–761. doi: 10.1111/j.1439-0434.2009.01574.x

Atif, R. M., Patat-Ochatt, R. M., Svabova, L., Ondrej, V., Klenoticova, H., Jacas, L., et al. (2013). "Gene transfer in legumes," in *Progress in Botany,* eds U. Lüttge, W. Beyschlag, D. Francis, and J. Cushman (Berlin; Heidelberg: Springer), 37–100.

Azevedo, J., Garcia, D., Pontier, D., Ohnesorge, S., Yu, A., Garcia, S., et al. (2010). Argonaute quenching and global changes in Dicer homeostasis caused by a pathogen-encoded GW repeat protein. *Genes Dev.* 24, 904–915. doi: 10.1101/gad.1908710

Banane, J. K., Vahdat, A., Menzel, W., and Vetten, H. J. (2010). Serological and molecular identification of Chickpea chlorotic stunt virus from chickpea in iran. *Plant Dis.* 94, 788. doi: 10.1094/PDIS-94-6-0788C

Banerjee, S., Banerjee, A., Gill, S. S., Gupta, O. P., Dahuja, A., Jain, P. K., et al. (2017). RNA interference: a novel source of resistance to combat plant parasitic nematodes. *Front. Plant Sci.* 8:834. doi: 10.3389/fpls.2017.00834

Bhatnagar-Mathur, P., Vadez, V., Devi, M. J., Lavanya, M., Vani, G., and Sharma, K. K. (2009). Genetic engineering of chickpea (*Cicer arietinum* L.) with the P5CSF129A gene for osmoregulation with implications on drought tolerance. *Mol. Breed.* 23, 591–606. doi: 10.1007/s11032-009-9258-y

Bhattacharjee, B., Mohan, M., and Nair, S. (2010). Transformation of chickpea: effect of genotype, explant, *Agrobacterium*-strain and composition of culture medium. *Biol. Plant.* 54, 21–32. doi: 10.1007/s10535-010-0004-4

Bos, L., Hampton, R. O., and Makkouk, K. M. (1988). "Viruses and virus diseases of pea, lentil, faba bean and chickpea," in *World Crops: Cool Season Food Legumes,* ed R. J. Summerfield (Dordrecht: Springer), 591–615.

Boutrot, F., and Zipfel, C. (2017). Function, discovery, and exploitation of plant pattern recognition receptors for broad-spectrum disease resistance. *Annu. Rev. Phytopathol.* 55, 257–286. doi: 10.1146/annurev-phyto-080614-120106

Castillo, P., Gomez-Barcina, A., and Jimenez-Diaz, R. M. (1996). Plant parasitic nematodes associated with chickpea in Southern Spain and effect of soil temperature on reproduction of *Pratylenchus thornei*. *Nematologica* 42, 211–219. doi: 10.1163/004325996X00057

Castillo, P., Navas-Cortés, J. A., Landa, B. B., Jiménez-Díaz, R. M., and Vovlas, N. (2008). Plant-parasitic nematodes attacking chickpea andtheir in planta interactions with rhizobia and phytopathogenic fungi. *Plant Dis.* 92, 840–853. doi: 10.1094/PDIS-92-6-0840

Chakraborti, D., Sarkar, A., Mondal, H. A., and Das, S. (2009). Tissue specific expression of potent insecticidal, *Allium sativum* leaf agglutinin (ASAL) in important pulse crop, chickpea (*Cicer arietinum* L.) to resist the phloem feeding *Aphis craccivora*. *Transgenic Res.* 18, 529–544. doi: 10.1007/s11248-009-9242-7

Crossa, J., Perez-Rodriguez, P., Cuevas, J., Montesinos-Lopez, O., Jarquin, D., De Los Campos, G., et al. (2017). Genomic selection in plant breeding: methods, models, and perspectives. *Trends Plant Sci.* 22, 961–975. doi: 10.1016/j.tplants.2017.08.011

Csorba, T., Bovi, A., Dalmay, T., and Burgyan, J. (2007). The p122 subunit of Tobacco Mosaic Virus replicase is a potent silencing suppressor and compromises both small interfering RNA- and microRNA-mediated pathways. *J. Virol.* 81, 11768–11780. doi: 10.1128/JVI.01230-07

Csorba, T., Kontra, L., and Burgyan, J. (2015). Viral silencing suppressors: tools forged to fine-tune host-pathogen coexistence. *Virology* 479–480, 85–103. doi: 10.1016/j.virol.2015.02.028

De Coninck, B., Timmermans, P., Vos, C., Cammue, B. P., and Kazan, K. (2015). What lies beneath: belowground defense strategies in plants. *Trends Plant Sci.* 20, 91–101. doi: 10.1016/j.tplants.2014.09.007

Denver, D. R., Brown, A. M., Howe, D. K., Peetz, A. B., and Zasada, I. A. (2016). Genome skimming: a rapid approach to gaining diverse biological insights into multicellular pathogens. *PLoS Pathog.* 12:e1005713. doi: 10.1371/journal.ppat.1005713

Di Vito, M., Greco, N., Oreste, G., Saxena, M. C., Singh, K. B., and Kusmenoglu, I. (1994). Plant parasitic nematodes of legumes in Turkey. *Nematol. Mediterr.* 22, 245–251.

Fahmy, I. F., Taha, O., and El-Ashry, A. N. (2015). First genome analysis and molecular characterization of Chickpea chlorotic dwarf virus Egyptian isolate infecting squash. *VirusDisease* 26, 33–41. doi: 10.1007/s13337-014-0246-4

FAO (2014). *Pulse Quantity Production*. Available online at: http://www.fao.org/faostat/en/

Fire, A., Xu, S., Montgomery, M. K., Kostas, S. A., Driver, S. E., and Mello, C. C. (1998). Potent and specific genetic interference by double-stranded RNA in *Caenorhabditis elegans*. *Nature* 391, 806–811. doi: 10.1038/35888

Fosu-Nyarko, J., and Jones, M. J. J. (2015). Application of biotechnology for nematode control in crop plants. *Adv. Bot. Res.* 73, 339–376. doi: 10.1016/bs.abr.2014.12.012

Fontana, G. S., Santini, L., Caretto, S., Frugis, G., and Mariotti, D. (1993). Genetic transformation in the grain legume *Cicer arietinum* L. (chickpea). *Plant Cell Rep.* 12, 194–198. doi: 10.1007/BF00237052

Friedland, A. E., Tzur, Y. B., Esvelt, K. M., Colaiacovo, M. P., Church, G. M., and Calarco, J. A. (2013). Heritable genome editing in *C. elegans* via a CRISPR-Cas9 system. *Nat Methods* 10, 741–743. doi: 10.1038/nmeth.2532

Fusaro, A. F., Correa, R. L., Nakasugi, K., Jackson, C., Kawchuk, L., Vaslin, M. F., et al. (2012). The Enamovirus P0 protein is a silencing suppressor which inhibits local and systemic RNA silencing through AGO1 degradation. *Virology* 426, 178–187. doi: 10.1016/j.virol.2012.01.026

Ganguly, M., Molla, K. A., Karmakar, S., Datta, K., and Datta, S. K. (2014). Development of pod borer-resistant transgenic chickpea using a pod-specific and a constitutive promoter-driven fused cry1Ab/Ac gene. *Theor. Appl. Genet.* 127, 2555–2565. doi: 10.1007/s00122-014-2397-5

Ghanekar, A. M., Manohar, S. K., Reddy, S. V., and Nene, Y. L. (1988). Association of a mycoplasma-like organism with chickpea phyllody. *Indian Phytopathol.* 41, 462–464.

Ghanti, K. K. S., Sujata, K. G., Vijay Kumar, B. M., Nataraja Karba, N., Reddy, K. J., Srinath Rao, M., et al. (2011). Heterologous expression of P5CS gene in chickpea enhances salt tolerance without affecting yield. *Biol. Plant.* 55, 634. doi: 10.1007/s10535-011-0161-0

Ghasemzadeh, A., Małgorzata Ter Haar, M., Shams-Bakhsh, M., Pirovano, W., and Pantaleo, V. (2018). Shannon entropy to evaluate substitution rate variation among viral nucleotide positions in datasets of viral siRNAs. *Methods Mol. Biol.* 1746. doi: 10.1007/978-1-4939-7683-6_15

Gheysen, G., and Vanholme, B. (2007). RNAi from plants to nematodes. *Trends Biotechnol.* 25, 89–92. doi: 10.1016/j.tibtech.2007.01.007

Goverse, A., and Smant, G. (2014). The activation and suppression of plant innate immunity by parasitic nematodes. *Annu. Rev. Phytopathol.* 52, 243–265. doi: 10.1146/annurev-phyto-102313-050118

Graham, P. H., and Vance, C. P. (2003). Legumes: importance and constraints to greater use. *Plant Physiol.* 131, 872–877. doi: 10.1104/pp.017004

Greco, N., Di Vito, M., Saxena, M. C., and Reddy, M. V. (1988). Effect of Heterodera cicero on yeld of chickpea and lentil and development of this nematode on chickpea in Syria. *Nematologica* 34, 98–114. doi: 10.1163/002825988X00099

Gupta, S., Nawaz, K., Parween, S., Roy, R., Sahu, K., Kumar Pole, A., et al. (2017). Draft genome sequence of *Cicer reticulatum* L., the wild progenitor of chickpea provides a resource for agronomic trait improvement. *DNA Res.* 24, 1–10. doi: 10.1093/dnares/dsw042

Hadfield, J., Thomas, J. E., Schwinghamer, M. W., Kraberger, S., Stainton, D., Dayaram, A., et al. (2012). Molecular characterisation of dicot-infecting mastreviruses from Australia. *Virus Res.* 166, 13–22. doi: 10.1016/j.virusres.2012.02.024

Holbein, J., Grundler, F. M., and Siddique, S. (2016). Plant basal resistance to nematodes: an update. *J. Exp. Bot.* 67, 2049–2061. doi: 10.1093/jxb/erw005

Horn, N. M., Reddy, S. V., and Reddy, R. D. V. (1994). Virus-vector relationships of chickpea chlorotic dwarf geminivirus and the leafhopper *Orosius orientalis* (Hemiptera: Cicadellidae). *Ann. Appl. Biol.* 124, 441–450. doi: 10.1111/j.1744-7348.1994.tb04149.x

Horn, N. M., Reddy, S. V., Roberts, I. M., and Reddy, R. D. V. (1993). Chickpea chlorotic dwarf virus, a new leafhopper-transmitted geminivirus of chickpea in India. *Ann. Appl. Biol.* 122, 467–479. doi: 10.1111/j.1744-7348.1993.tb04050.x

Hussey, R. S. (1989). Disease-inducing secretions of plant-parasitic nematodes. *Annu. Rev. Phytopathol.* 27, 127–141. doi: 10.1146/annurev.py.27.090189.001011

Iantcheva, A., Vlahova, M., Trinh, T. H., Brown, S. C., Slater, A., Elliott, M. C., et al. (2001). Assessment of polysomaty, embryo formation and regeneration in liquid media for various species of diploid annual Medicago. *Plant Sci.* 160, 621–627. doi: 10.1016/S0168-9452(00)00432-5

Ignacimuthu, S., and Prakash, S. (2006). *Agrobacterium*-mediated transformation of chickpea with alpha-amylase inhibitor gene for insect resistance. *J. Biosci.* 31, 339–345. doi: 10.1007/BF02704106

Indurker, S., Misra, H. S., and Eapen, S. (2007). Genetic transformation of chickpea (*Cicer arietinum* L.) with insecticidal crystal protein gene using particle gun bombardment. *Plant Cell Rep.* 26, 755–763. doi: 10.1007/s00299-006-0283-6

Islam, R., Malik, T., Husnain, T., and Riazuddin, S. (1994). Strain and cultivar specificity in the *Agrobacterium*-chickpea interaction. *Plant Cell Rep.* 13, 561–563. doi: 10.1007/BF00234511

Jain, M., Misra, G., Patel, R. K., Priya, P., Jhanwar, S., Khan, A. W., et al. (2013). A draft genome sequence of the pulse crop chickpea (*Cicer arietinum* L.). *Plant J.* 74, 715–729. doi: 10.1111/tpj.12173

Jinek, M., Chylinski, K., Fonfara, I., Hauer, M., Doudna, J. A., and Charpentier, E. (2012). A programmable dual-RNA-guided DNA endonuclease in adaptive bacterial immunity. *Science* 337, 816–821. doi: 10.1126/science.1225829

Kaiser, W. J., and Danesh, D. (1971). Biology of Four Viruses affecting *Cicer arietinum* in Iran. *Phytopathology* 61, 372–375. doi: 10.1094/Phyto-61-372

Kanakala, S., Verma, H. N., Vijay, P., Saxena, D. R., and Malathi, V. G. (2013). Response of chickpea genotypes to *Agrobacterium*-mediated delivery of Chickpea chlorotic dwarf virus (CpCDV) genome and identification of resistance source. *Appl. Microbiol. Biotechnol.* 97, 9491–9501. doi: 10.1007/s00253-013-5162-9

Kar, S., Basu, D., Das, S., Ramkrishnan, N. A., Mukherjee, P. P. N., and Sen, S. K. (1997). Expression of cryIA(c) gene of *Bacillus thuringiensis* in transgenic chickpea plants inhibits development of pod- borer (*Heliothis armigera*) larvae. *Transgenic Res.* 6, 177–185. doi: 10.1023/A:1018433922766

Kar, S., Johnson, T. M., Nayak, P., and Sen, S. K. (1996). Efficient transgenic plant regeneration through *Agrobacterium*-mediated transformation of Chickpea (*Cicer arietinum* L.). *Plant Cell Rep.* 16, 32–37. doi: 10.1007/BF01275444

Kim, H., and Kim, J. S. (2014). A guide to genome engineering with programmable nucleases. *Nat. Rev. Genet.* 15, 321–334. doi: 10.1038/nrg3686

Kraberger, S., Kumari, S. G., Hamed, A. A., Gronenborn, B., Thomas, J. E., Sharman, M., et al. (2015). Molecular diversity of Chickpea chlorotic dwarf virus in Sudan: high rates of intra-species recombination - a driving force in the emergence of new strains. *Infect. Genet. Evol.* 29, 203–215. doi: 10.1016/j.meegid.2014.11.024

Krishnamurthy, K. V., Suhasini, K., Sagare, A. P., Meixner, M., De Kathen, A., Pickardt, T., et al. (2000). *Agrobacterium* mediated transformation of chickpea (*Cicer arietinum* L.) embryo axes. *Plant Cell Rep.* 19, 235–240. doi: 10.1007/s002990050005

Kumar, P. L., Kumari, S. M. G., and Waliyar, F. (2008). "Virus diseases of Chickpea," in *Characterization, Diagnosis & Management of Plant Viruses, Vol. 3: Vegetable and Pulse Crops,* eds G. P. Rao, P. L. Kumar, and R. J. Holguín-Peña (Houston, TX: Studium Press LLC), 213–234.

Kumari, S. G., and Makkouk, K. M. (2007). "Virus diseases of faba bean (*Vicia faba* L.) in Asia and Africa," in *Plant Viruses* (Aleppo: Global Science Book), 93–95.

Kumari, S. G., Assad, N., Alnaasan, Y., Attar, N., and Van Leur, J. A. G. (2011). "Chickpea chlorotic stunt virus: host range, purification, serology and transmission characteristics and occurrence in Central and West Asia and North Africa (CWANA)," in *Fourth Conference of the International Working Group On Legume & Vegetable Viruses (IWGLVV)*, ed. Horticulture Australia. (Antequera).

Li, S., Cong, Y., Liu, Y., Wang, T., Shuai, Q., Chen, N., et al. (2017). Optimization of *Agrobacterium*-mediated transformation in soybean. *Front. Plant Sci.* 8:246. doi: 10.3389/fpls.2017.00246

Li, Z., Liu, Z. B., Xing, A., Moon, B. P., Koellhoffer, J. P., Huang, L., et al. (2015). Cas9-guide RNA directed genome editing in soybean. *Plant Physiol.* 169, 960–970. doi: 10.1104/pp.15.00783

Mahapatra, B. C., and Pahdi, N. N. (1996). Pathogenicity and control of *Rotylenchulus reniformis* on *Cicer arietinum*. *Nematol. Mediterr.* 14, 287–290.

Makkouk, K. M., Kumari, S. G., Shahraeen, N., Fazlali, Y., Farzadfar, S., Ghotbi, T., et al. (2003). Identification and seasonal variation of viral diseases of chickpea and lentil in Iran. *J. Plant Dis. Protect.* 110, 157–169. Available online at: https://www.cabdirect.org/cabdirect/abstract/20033060880

Makkouk, K., Pappu, H., and Kumari, S. G. (2012). Virus diseases of peas, beans, and faba bean in the Mediterranean region. *Adv. Virus Res.* 84, 367–402. doi: 10.1016/B978-0-12-394314-9.00011-7

Malhotra, R. S., Singh, K. B., Di Vito, M., Greco, N., and Saxena, M. C. (2002). Registration of ILC10765 and ILC 10766 chickpea germplasm lines resistant to cyst nematodes. *Crop Sci.* 42:1756. doi: 10.2135/cropsci2002.1756

Mandadi, K. K., and Scholthof, K. B. (2013). Plant immune responses against viruses: how does a virus cause disease? *Plant Cell* 25, 1489–1505. doi: 10.1105/tpc.113.111658

Manosalva, P., Manohar, M., Von Reuss, S. H., Chen, S., Koch, A., Kaplan, F., et al. (2015). Conserved nematode signalling molecules elicit plant defenses and pathogen resistance. *Nat. Commun.* 6, 7795. doi: 10.1038/ncomms8795

Manzoor, M. T., Ilyas, M., Shafiq, M., Haider, M. S., Shahid, A. A., and Briddon, R. W. (2014). A distinct strain of chickpea chlorotic dwarf virus (genus Mastrevirus, family Geminiviridae) identified in cotton plants affected by leaf curl disease. *Arch. Virol.* 159, 1217–1221. doi: 10.1007/s00705-013-1911-4

Massart, S., Olmos, A., Jijakli, H., and Candresse, T. (2014). Current impact and future directions of high throughput sequencing in plant virus diagnostics. *Virus Res.* 188, 90–96. doi: 10.1016/j.virusres.2014.03.029

Mehrotra, M., Singh, A. K., Sanyal, I., Altosaar, I., and Amla, D. V. (2010). Pyramiding of modified cry1Ab and cry1Ac genes of *Bacillus thuringiensis* in transgenic chickpea (*Cicer arietinum* L.) for improved resistance to pod borer insect *Helicoverpa armigera*. *Euphytica* 182, 87–102. doi: 10.1007/s10681-011-0501-3

Mendy, B., Wang'ombe, M. W., Radakovic, Z. S., Holbein, J., Ilyas, M., Chopra, D., et al. (2017). Arabidopsis leucine-rich repeat receptor-like kinase NILR1 is required for induction of innate immunity to parasitic nematodes. *PLoS Pathog.* 13:e1006284. doi: 10.1371/journal.ppat.1006284

Meng, Y., Hou, Y., Wang, H., Ji, R., Liu, B., Wen, J., et al. (2017). Targeted mutagenesis by CRISPR/Cas9 system in the model legume *Medicago truncatula*. *Plant Cell Rep.* 36, 371–374. doi: 10.1007/s00299-016-2069-9

Mishra, S., Sanyal, I., and Amla, D. V. (2012). Changes in protein pattern during different developmental stages of somatic embryos in chickpea. *Biol. Plant.* 56, 613–619. doi: 10.1007/s10535-012-0124-0

Mustafayev, E., Kumari, S. G., Attar, N., and Zeynal, A. (2011). Viruses infecting chickpea and lentil crops in Azerbaijan. *Austral. Plant Pathol.* 40, 611–620. doi: 10.1007/s13313-011-0094-2

Ouattara, A., Tiendrebeogo, F., Lefeuvre, P., Hoareau, M., Claverie, S., Traore, E. V., et al. (2017). New strains of chickpea chlorotic dwarf virus discovered on diseased papaya and tomato plants in Burkina Faso. *Arch. Virol.* 162, 1791–1794. doi: 10.1007/s00705-017-3262-z

Ouizbouben, A., and Fortass, M. (1997). Survey of chickpea for viruses in Morocco. *EPPO Bull.* 27, 249–254. doi: 10.1111/j.1365-2338.1997.tb00642.x

Parween, S., Nawaz, K., Roy, R., Pole, A. K., Venkata Suresh, B., Misra, G., et al. (2015). An advanced draft genome assembly of a desi type chickpea (*Cicer arietinum* L.). *Sci. Rep.* 5:12806. doi: 10.1038/srep12806

Pathak, M. R., and Hamzah, R. Y. (2008). An effective method of sonication-assisted *Agrobacterium*-mediated transformation of chickpeas. *Plant Cell Tissue Organ Cult.* 93, 65–71. doi: 10.1007/s11240-008-9344-6

Patil, G., Deokar, A., Jain, P. K., Thengane, R. J., and Srinivasan, R. (2009). Development of a phosphomannose isomerase-based *Agrobacterium*-mediated transformation system for chickpea (*Cicer arietinum* L.). *Plant Cell Rep.* 28, 1669–1676. doi: 10.1007/s00299-009-0766-3

Pirovano, W., Miozzi, L., Boetzer, M., and Pantaleo, V. (2014). Bioinformatics approaches for viral metagenomics in plants using short RNAs: model case of study and application to a *Cicer arietinum* population. *Front. Microbiol.* 5:790. doi: 10.3389/fmicb.2014.00790

Polowick, P. L., Baliski, D. S., and Mahon, J. D. (2004). *Agrobacterium tumefaciens*-mediated transformation of chickpea (*Cicer arietinum* L.): gene integration, expression and inheritance. *Plant Cell Rep.* 23, 485–491. doi: 10.1007/s00299-004-0857-0

Reinprecht, Y., Yadegari, Z., Perry, G. E., Siddiqua, M., Wright, L. C., McClean, P. E., et al. (2013). *In silico* comparison of genomic regions containing genes coding for enzymes and transcription factors for the phenylpropanoid pathway in *Phaseolus vulgaris* L. and *Glycine max* L. Merr. *Front. Plant Sci.* 4:317. doi: 10.3389/fpls.2013.00317

Rosso, M. N., Jones, J. T., and Abad, P. (2009). RNAi and functional genomics in plant parasitic nematodes. *Annu. Rev. Phytopathol.* 47, 207–232. doi: 10.1146/annurev.phyto.112408.132605

Sanyal, I., Singh, A. K., Kaushik, M., and Amla, D. V. (2005). *Agrobacterium*-mediated transformation of chickpea (*Cicer arietinum* L.) with *Bacillus thuringiensis* cry1Ac gene for resistance against pod borer insect *Helicoverpa armigera*. *Plant Sci.* 168, 1135–1146. doi: 10.1016/j.plantsci.2004.12.015

Saqib, M., Bayliss, K. L., Dell, B., Hardy Gest, J., and Jones, M. G. K. (2005). First record of a phytoplasma-associated disease of chickpea (*Cicer arietinum*) in Australia. *Austral. Plant Pathol.* 34, 425–426. doi: 10.1071/AP05047

Sarmah, B. K., Moore, A., Tate, W., Molvig, L., Morton, R. L., Rees, D. P., et al. (2004). Transgenic chickpea seeds expressing high levels of a bean α-amylase inhibitor. *Mol. Breed.* 24, 73–82. doi: 10.1023/B:MOLB.0000037996.01494.12

Schwinghamer, M. W., Thomas, J. E., Parry, J. N., Schilg, M. A., and Dann, E. K. (2007). First record of natural infection of chickpea by Turnip mosaic virus. *Australas. Plant Dis. Notes* 2, 41–43. doi: 10.1071/DN07020

Senthil, G., Williamson, B., Dinkins, R. D., and Ramsay, G. (2004). An efficient transformation system for chickpea (*Cicer arietinum* L.). *Plant Cell Rep.* 23, 297–303. doi: 10.1007/s00299-004-0854-3

Sharma, H. C., Sharma, K. K., Seetharama, N., and Ortiz, R. (2001). Genetic transformation of crop plants: risks and opportunities for the rural poor. *Curr. Sci.* 80, 1495–1508. Available online at: http://www.jstor.org/stable/24106285

Sharma, K. K., and Ortiz, R. (2000). Program for the application of genetic transformation for crop improvement in the semi-arid tropics. *In Vitro Cell. Dev. Biol. Plant* 36, 83–92. doi: 10.1007/s11627-000-0019-1

Shivaprasad, P. V., Chen, H. M., Patel, K., Bond, D. M., Santos, B. A., and Baulcombe, D. C. (2012). A microRNA superfamily regulates nucleotide binding site-leucine-rich repeats and other mRNAs. *Plant Cell* 24, 859–874. doi: 10.1105/tpc.111.095380

Singh, R. R., Cho-Vega, J. H., Davuluri, Y., Ma, S., Kasbidi, F., Milito, C., et al. (2009). Sonic hedgehog signaling pathway is activated in ALK-positive anaplastic large cell lymphoma. *Cancer Res.* 69, 2550–2558. doi: 10.1158/0008-5472.CAN-08-1808

Sirtori, C. R. (2001). Risks and benefits of soy phytoestrogens in cardiovascular diseases, cancer, climacteric symptoms and osteoporosis. *Drug Saf.* 24, 665–682. doi: 10.2165/00002018-200124090-00003

Smýkal, P., Coyne, C. J., Ambrose, M. J., l Maxted, N., Schaefer, H., Blair, M. W., et al. (2015). Legume crops phylogeny and genetic diversity for science and breeding. *Crit. Rev. Plant Sci.* 34, 43–104. doi: 10.1080/07352689.2014.897904

Somers, D. A., Samac, D. A., and Olhoft, P. M. (2003). Recent advances in legume transformation. *Plant Physiol.* 131, 892–899. doi: 10.1104/pp.102.017681

Srinivasan, R., Mohapatra, T., and Sharma, R. P. (1991). *Agrobacterium* mediated genetic transformation of chickpea, *Cicer arietinum* L. *Indian J. Exp. Biol.* 29, 758–761.

Srivastava, J., Datta, S., and Mishra, S. P. (2017). Development of an efficient *Agrobacterium* mediated transformation system for chickpea (*Cicer arietinum*). *Biol. Plant.* 72, 153–170. doi: 10.1515/biolog-2017-0015

Srivastava, S., Zheng, Y., Kudapa, H., Jagadeeswaran, G., Hivrale, V., Varshney, R. K., et al. (2015). High throughput sequencing of small RNA component of leaves and inflorescence revealed conserved and novel miRNAs as well as phasiRNA loci in chickpea. *Plant Sci.* 235, 46–57. doi: 10.1016/j.plantsci.2015.03.002

Tewari-Singh, N., Sen, J., Kiesecker, H., Reddy, V. S., Jacobsen, H. J., and Guha-Mukherjee, S. (2004). Use of a herbicide or lysine plus threonine for non-antibiotic selection of transgenic chickpea. *Plant Cell Rep.* 22, 576–583. doi: 10.1007/s00299-003-0730-6

Thomas, J. E., Parry, J. N., Schwinghamer, M. W., and Dann, E. K. (2010). Two novel mastreviruses from chickpea (*Cicer arietinum*) in Australia. *Arch. Virol.* 155, 1777–1788. doi: 10.1007/s00705-010-0763-4

Thudi, M., Chitikineni, A., Liu, X., He, W., Roorkiwal, M., Yang, W., et al. (2016). Recent breeding programs enhanced genetic diversity in both desi and kabuli varieties of chickpea (*Cicer arietinum* L.). *Sci. Rep.* 6:38636. doi: 10.1038/srep38636

Tripathi, L., Singh, A. K., Singh, S., Singh, R., Chaudhary, S., Sanya, I., et al. (2013). Optimization of regeneration and *Agrobacterium*-mediated transformation of immature cotyledons of chickpea (*Cicer arietinum* L.). *Plant Cell Tissue Organ Cult.* 113, 513–527. doi: 10.1007/s11240-013-0293-3

Upadhyaya, H. D., Dwivedi, S. L., Baum, M., Varshney, R. K., Udupa, S. M., Gowda, C. L., et al. (2008). Genetic structure, diversity, and allelic richness in composite collection and reference set in chickpea (*Cicer arietinum* L.). *BMC Plant Biol.* 8:106. doi: 10.1186/1471-2229-8-106

Varshney, R. K., Song, C., Saxena, R. K., Azam, S., Yu, S., Sharpe, A. G., et al. (2013). Draft genome sequence of chickpea (*Cicer arietinum*) provides a resource for trait improvement. *Nat. Biotechnol.* 31, 240–246. doi: 10.1038/nbt.2491

Vogler, H., Akbergenov, R., Shivaprasad, P. V., Dang, V., Fasler, M., Kwon, M. O., et al. (2007). sRNA modification associated with suppression of RNA silencing by tobamovirus replicase protein. *J. Virol.* 81, 10379–10388. doi: 10.1128/JVI.00727-07

Vovlas, N., Rapoport, H. F., Jimenez Diaz, R. M., and Castillo, P. (2005). Differences in feeding sites induced by root-knot nematodes, *Meloidogyne* spp., in chickpea. *Phytopathology* 95, 368–375. doi: 10.1094/PHYTO-95-0368

Walsh, E., Elmore, J. M., and Taylor, C. G. (2017). Root-knot nematode parasitism suppresses host RNA silencing. *Mol. Plant Microbe Interact.* 30, 295–300. doi: 10.1094/MPMI-08-16-0160-R

Wu, X. Y., Zhou, G. C., Chen, Y. X., Wu, P., Liu, L. W., Ma, F. F., et al. (2016). Soybean cyst nematode resistance emerged via artificial selection of duplicated serine hydroxymethyltransferase genes. *Front. Plant Sci.* 7:998. doi: 10.3389/fpls.2016.00998

Yadav, R., Mehrotra, M., Singh, A. K., Niranjan, A., Singh, R., Sanyal, I., et al. (2017). Improvement in *Agrobacterium*-mediated transformation of chickpea (*Cicer arietinum* L.) by the inhibition of polyphenolics released during wounding of cotyledonary node explants. *Protoplasma* 254, 253–269. doi: 10.1007/s00709-015-0940-0

Yahia, A. A., Ouada, M. A., Illoul, H., and Tair, M. I. (1997). First occurrence of bean yellow mosaic potyvirus on chickpea in Algeria. *EPPO Bull.* 27, 261–263. doi: 10.1111/j.1365-2338.1997.tb00645.x

Yang, N., Wang, R., and Zhao, Y. (2017). Revolutionize genetic studies and crop improvement with high-throughput and genome-scale CRISPR/Cas9 gene editing technology. *Mol. Plant* 10, 1141–1143. doi: 10.1016/j.molp.2017.08.001

Yin, K., Han, T., Liu, G., Chen, T., Wang, Y., Yu, A. Y., et al. (2015). A geminivirus-based guide RNA delivery system for CRISPR/Cas9 mediated plant genome editing. *Sci. Rep.* 5:14926. doi: 10.1038/srep14926

Zaagueri, T., Miozzi, L., Mnari-Hattab, M., Noris, E., Accotto, G. P., and Vaira, A. M. (2017a). Deep sequencing data and infectivity assays indicate that chickpea chlorotic dwarf virus is the etiological agent of the "hard fruit syndrome" of watermelon. *Viruses* 9:E311. doi: 10.3390/v9110311

Zaagueri, T., Mnari-Hattab, M., Zammouri, S., Hajlaoui, M. R., Accotto, G. P., and Vaira, A. M. (2017b). First report of chickpea chlorotic dwarf virus in watermelon (*Citrullus lanatus*) in Tunisia. *Plant Dis.* 101, 392. doi: 10.1094/PDIS-07-16-1028-PDN

Zamanian, M., and Andersen, E. C. (2016). Prospects and challenges of CRISPR/Cas genome editing for the study and control of neglected vector-borne nematode diseases. *FEBS J.* 283, 3204–3221. doi: 10.1111/febs.13781

Zhai, J., Jeong, D. H., De Paoli, E., Park, S., Rosen, B. D., Li, Y., et al. (2011). MicroRNAs as master regulators of the plant NB-LRR defense gene family via the production of phased, trans-acting siRNAs. *Genes Dev.* 25, 2540–2553. doi: 10.1101/gad.177527.111

Zheng, F., Wu, H., Zhang, R., Li, S., He, W., Wong, F. L., et al. (2016). Molecular phylogeny and dynamic evolution of disease resistance genes in the legume family. *BMC Genomics* 17:402. doi: 10.1186/s12864-016-2736-9

Conflict of Interest Statement: The authors declare that the research was conducted in the absence of any commercial or financial relationships that could be construed as a potential conflict of interest.

frontiers in Microbiology

ORIGINAL RESEARCH
published: 05 April 2018
doi: 10.3389/fmicb.2018.00656

Genomic Structural Variations Affecting Virulence During Clonal Expansion of *Pseudomonas syringae* pv. *actinidiae* Biovar 3 in Europe

Giuseppe Firrao[1,2]*, *Emanuela Torelli*[1†], *Cesare Polano*[1], *Patrizia Ferrante*[3], *Francesca Ferrini*[1], *Marta Martini*[1], *Simone Marcelletti*[3], *Marco Scortichini*[3]* and *Paolo Ermacora*[1]*

[1] Department of Agricultural, Food, Environmental and Animal Sciences, University of Udine, Udine, Italy, [2] Istituto Nazionale Biostrutture e Biosistemi, Rome, Italy, [3] Council for Agricultural Research and Analysis of Agricultural Economics (CREA), Research Centre for Olive, Fruit Trees and Citrus, Rome, Italy

OPEN ACCESS

Edited by:
Sabrina Sarrocco,
Università degli Studi di Pisa, Italy

Reviewed by:
Vittoria Catara,
Università degli Studi di Catania, Italy
Jason Sahl,
Northern Arizona University,
United States

***Correspondence:**
Giuseppe Firrao
giuseppe.firrao@uniud.it
Marco Scortichini
marco.scortichini@crea.gov.it
Paolo Ermacora
paolo.ermacora@uniud.it

†Present Address:
Emanuela Torelli,
ICOS Group, School of Computing Science, Centre for Bacterial Cell Biology, Newcastle University, Newcastle upon Tyne, United Kingdom

Specialty section:
This article was submitted to Plant Microbe Interactions, a section of the journal Frontiers in Microbiology

Received: 22 January 2018
Accepted: 20 March 2018
Published: 05 April 2018

Citation:
Firrao G, Torelli E, Polano C, Ferrante P, Ferrini F, Martini M, Marcelletti S, Scortichini M and Ermacora P (2018) Genomic Structural Variations Affecting Virulence During Clonal Expansion of Pseudomonas syringae pv. actinidiae Biovar 3 in Europe. Front. Microbiol. 9:656. doi: 10.3389/fmicb.2018.00656

Pseudomonas syringae pv. *actinidiae* (Psa) biovar 3 caused pandemic bacterial canker of *Actinidia chinensis* and *Actinidia deliciosa* since 2008. In Europe, the disease spread rapidly in the kiwifruit cultivation areas from a single introduction. In this study, we investigated the genomic diversity of Psa biovar 3 strains during the primary clonal expansion in Europe using single molecule real-time (SMRT), Illumina and Sanger sequencing technologies. We recorded evidences of frequent mobilization and loss of transposon Tn6212, large chromosome inversions, and ectopic integration of IS sequences (remarkably ISPsy31, ISPsy36, and ISPsy37). While no phenotype change associated with Tn6212 mobilization could be detected, strains CRAFRU 12.29 and CRAFRU 12.50 did not elicit the hypersensitivity response (HR) on tobacco and eggplant leaves and were limited in their growth in kiwifruit leaves due to insertion of ISPsy31 and ISPsy36 in the *hrpS* and *hrpR* genes, respectively, interrupting the *hrp* cluster. Both strains had been isolated from symptomatic plants, suggesting coexistence of variant strains with reduced virulence together with virulent strains in mixed populations. The structural differences caused by rearrangements of self-genetic elements within European and New Zealand strains were comparable in number and type to those occurring among the European strains, in contrast with the significant difference in terms of nucleotide polymorphisms. We hypothesize a relaxation, during clonal expansion, of the selection limiting the accumulation of deleterious mutations associated with genome structural variation due to transposition of mobile elements. This consideration may be relevant when evaluating strategies to be adopted for epidemics management.

Keywords: bacterial canker, genomic diversity, hypersensitivity response (HR), Illumina technology, single molecule real-time (SMRT) sequencing

INTRODUCTION

Pseudomonas syringae pv. *actinidiae* (Psa) is the causal agent of bacterial canker of green-fleshed (*Actinidia deliciosa*) and yellow-fleshed kiwifruit (*Actinidia chinensis*) (Scortichini et al., 2012). The pathogen was first isolated in Japan (Takikawa et al., 1989), where the disease was reported since 1984 and, subsequently, in Italy (Scortichini, 1994) and South Korea (Koh et al., 1994). In the years

2008–2011, sudden and repeated epidemics of bacterial canker developed firstly in central Italy (Balestra et al., 2009; Ferrante and Scortichini, 2009, 2010), and, subsequently, in all the other major areas of kiwifruit cultivation such as New Zealand (Everett et al., 2011), and Chile (EPPO, 2016). In Europe, the epidemics spread to Portugal, France, Spain, Switzerland, Germany, Slovenia and Greece (Abelleira et al., 2011; Dreo et al., 2014; Cunty et al., 2015b; Holeva et al., 2015; EPPO, 2016).

Genomic and genetic analyses have soon revealed that the Psa strains causing the 2008–2011 epidemics differed significantly from those previously found in Italy (Marcelletti et al., 2011) and that the first outbreaks of kiwifruit bacterial canker in Italy (Ferrante et al., 2015) were caused by a rapid and clonal expansion of the pathogen in the cultivated areas (Marcelletti and Scortichini, 2011). Then, the availability of strains isolated in China, the area of origin of many *Actinidia* spp., and the intensive use of Illumina sequencing of bacterial genomes (Mazzaglia et al., 2012; Butler et al., 2013; McCann et al., 2013, 2017) and VNTR analysis (Cesbron et al., 2015; Ciarroni et al., 2015; Cunty et al., 2015a) paved the way to the understanding of the epidemiology of this important disease.

At present, Psa is subdivided into four biovars, three of which with distinct phylogeographic structure. Strains belonging to biovar 1 produce phaseolotoxin and have been isolated in Japan and Italy before 2008. Strains of biovar 2 produce coronatine instead of phaseolotoxin and have been isolated only in South Korea. Strains belonging to biovar 3 produce neither phaseolotoxin nor coronatine and are responsible for the global outbreak of bacterial canker of kiwifruit in recent years. Strains of biovar 5 are found only in a limited local area of Japan (Saga Prefecture), they do not produce phaseolotoxin nor coronatine and are distinct but related to biovar 2 (Fujikawa and Sawada, 2016). A fifth clade, initially identified as Psa biovar 4, has been recently described as a new pathovar, *P.s.* pv. *actinidifoliorum* (Cunty et al., 2015b; Ferrante and Scortichini, 2015). Genome analysis performed so far is consistent with the hypothesis that all Psa biovars originated from a single natural source population and established subsequent outbreaks on cultivated kiwifruit. McCann et al. (2013) highlighted the overall clonal population structure with signatures of within-pathovar, intra-biovar recombination.

Psa biovar 3 is distinct from other biovars for the virulence and the sudden world-wide epidemic spread, that has unveiled major weakness of our kiwifruit cultivation system, while calling for efforts in the clarification of its dynamics in view of future prevention. Several genome-wide diversity studies revealed that epidemics in Europe, New Zealand and Chile of Psa biovar 3 originated from independent introductions of a single founder variant from China (Mazzaglia et al., 2012; Butler et al., 2013; McCann et al., 2013) which, however, is not deemed the center of origin of the biovar 3 (McCann et al., 2017).

In this work, we examined a sampling of the Psa population that originated in Europe from the putative single introduction that occurred in 2008. Through the analysis of Illumina sequence data-sets of 11 European and one non-European Psa genomes, and through the reconstruction and comparison of two complete genomes, a picture emerged that accounts for the significant differences in the modes of genome evolution of this bacterium before and after the clonal expansion associated with the pandemic. DNA mobilization due to transposable elements was a major cause of structural differences and, at least in one case, resulted in the disruption of genes relevant in pathogen-host interaction, with an effective reduction of strain virulence on kiwifruit.

MATERIALS AND METHODS

Strains and Sequencing

The strains investigated in this work and their genome data accessions are listed in **Table 1**.

Genomic DNA was extracted from 1 ml of 24 h old cultures grown in Nutrient Broth with agitation using a Wizard DNA purification kit (Promega Italia, Padova, Italy) following the manufacturer's instructions. DNA was measured and checked for quality using a NanoDrop spectrophotometer (NanoDrop products, Wilmington, DE, USA). Illumina libraries were prepared as described previously (Scortichini et al., 2013) and sent to the Istituto di Genomica Applicata (Udine, Italy) for sequencing on an Illumina Genome Analyser IIx (Illumina, USA). An average of 14 million single (50 nts) reads were obtained, filtered for quality using Prinseq (Schmieder and Edwards, 2011) and further processed. The sequence reads of strain 7286, obtained by Mazzaglia et al. (2012) were downloaded from the Sequence Read Archive (SRA accession SRX105337; https://www.ncbi.nlm.nih.gov/sra). The complete genome sequence of strain ICMP ICMP 18884 (Templeton et al., 2015) and ICMP 18708 (yet unpublished but made available by Poulter, R. T. M., Poulter, G. T. M., Stockwell, P. A., Lamont, I. L. and Butler, M. I.) were obtained from the NCBI nucleotide database and used as comparative reference for non-European strain.

Genomic DNA extracted from strains CRAFRU 12.29 and CRAFRU 14.08 was also sent for single molecule real-time (SMRT) sequencing to the University of Washington PacBio Sequencing Services. The genomes were then finished with Sanger sequencing using a primer walking approach on PCR fragments amplified from putatively adjacent contig ends, as resulted by scaffolding using ICMP 18708 as a reference; fragments were sent for sequencing to Genelab, Casaccia, Italy. Sequences were edited and manipulated using Seaview (Gouy et al., 2010) and Ugene (Okonechnikov et al., 2012).

Sequence Analysis

Preliminary read alignments and alignment manipulation were carried out using widely used tools such as BWA 0.5.5 (Li and Durbin, 2009), SAMtools 0.1.16 (Li et al., 2009) and PICARD tools (http://picard.sourceforge.net). SNP calling was carried out with the GATK package (McKenna et al., 2010); SNPs call was supported by a depth of coverage of at least 5 and a consensus of at least 95% of the aligned reads. Briefly, reads of each strain were preprocessed for quality using SGA [1], aligned on either CRAFRU 14.08 or ICMP 18884 chromosomes using BWA, indexed, sorted and reformatted using SAMtools, organized into reads-groups by PICARD tools; the resulting sam file was

TABLE 1 | Strains and sequences used in this work.

Strain name	Received as	Origin	Isolation year	Host plant	DNA sequence reference	HR on tobacco	HR on eggplant	Tn6212 integration	SRA database accession	GenBank accession
CRAFRU 14.08	Psa 354	Portugal	2010	*A. deliciosa* Summer	This work	+	+	–	SRR5273023	CP019730
CRAFRU 12.29	23b	Italy (Piemonte)	2011	*A. deliciosa* Hayward	This work	–	–	–	SRR5273025	CP019732
CRAFRU 14.25	our isolate	Italy (Latium)	2012	*A. chinensis* Hort16A	This work	+	+	+	SRR5273031	n.a.
CRAFRU 12.54	1616-291a	Italy (Piemonte)	2011	*A. deliciosa* Hayward	This work	+	+	+	SRR5273030	n.a.
CRAFRU 14.10	Psa 490	Italy (Calabria)	2010	*A. chinensis* Jintao	This work	+	+	+	SRR5273029	n.a.
CRAFRU 12.64	1616-231Aa	Italy (Piemonte)	2010	*A. chinensis* Jintao	This work	+	+	+	SRR5273028	n.a.
CRAFRU 10.29	4252 A,1	Italy (Emilia Romagna)	2009	*A. chinensis* Jintao	This work	+	+	+	SRR5273027	n.a.
CRAFRU 12.50	our isolate	Italy (Campania)	2011	*A. chinensis* Jintao	This work	–	–	–	SRR5273026	n.a.
CRAFRU 14.21	37.51	France	2011	*A. chinensis* Jintao	This work	+	+	–	SRR5273024	n.a.
CRAFRU 13.27	IVIA 3729.2	Spain	2011	*A. deliciosa* Hayward	This work	+	+	–	SRR5273022	n.a.
CRAFRU 8.43	our isolate	Italy (Latium)	2008	*A. chinensis* Hort16A	Marcelletti et al., 2011	+	+	+	n.a.	AFTG00000000
CRAFRU 13.04	ICMP 18884	New Zealand	2010	*A. deliciosa* Hayward	Templeton et al., 2015	n.i.[a]	n.i.	n.i.	SRR5273021	CP011972
ADDITIONAL SEQUENCES USED IN THIS WORK										
7286		Italy			Mazzaglia et al., 2012				SRR364082	
ICMP 18708, V13		New Zealand			Poulter et al., unpublished[b]				n.a.	CP012179

[a] *Not Investigated.*

[b] *Deposited as Poulter, R. T. M., Poulter, G. T. M., Stockwell, P. A., Lamont, I. L., and Butler, M. I. (unpublished).*

processed by GATK, and the output VCFs read by a bash script that checked each SNP for support and organized the results in a table for manual examination. Tablet (Milne et al., 2010) was used for the visualization of the alignments.

The genome assemblies for SMRT sequencing data were first generated using the hierarchical genome-assembly process (HGAP) [2], then Illumina reads were mapped and searched as described above for SNPs to identify incongruences; the alignments were then inspected with Tablet. For the genome of CRAFRU 14.08, the 4 gaps remaining were closed by Sanger sequencing using a primer walking approach. Once completed, the genomes were aligned with Mauve (Darling et al., 2004) and MUMmer (Delcher et al., 2002). The insertion thus identified were exported and annotated using Blast, the ISFinder database (Siguier et al., 2006), and the annotation service of Insertion Sequences (IS) provided by the ISsaga (Insertion Sequence semi-automatic genome annotation) engine (Varani et al., 2011).

Reads of several strains were aligned to the complete genome as described and visualized with IGV (Robinson et al., 2011), allowing the visual comparison of mapped reads densities. On the basis of the information gained by visual inspection, specific regions were selected for targeted assembly, that was carried out with Mapsembler2 ver. 2.2.4 (Peterlongo and Chikhi, 2011).

For reference based assemblies of relatively small DNA regions such as PAC_ICE2, and for the assembly of unmapped reads for gene discovery, the Illumina reads of the 12 European strains were processed with Edena (Hernandez et al., 2008). From the same datasets, full genomes were drafted with SPAdes (Bankevich et al., 2012) and scaffolded with Ragout (Kolmogorov et al., 2014) having the complete genome of CRAFRU 14.08 as a reference. Using Mauve and MUMmer the drafts were aligned to complete genomes, visualized and the polymorphic regions exported. Mobile elements and repeats were identified with Juxtaposer [3], the ISsaga engine, and the Tandem Repeats Finder program (http://tandem.bu.edu).

Structural variations were also searched using the split-read, (i.e., chimeric read) approach [4] with the aid of the program bbduck of the suite BBMap (*Bushnell* B. - sourceforge.net/projects/bbmap/).

The above listed tools were integrated with several *ad-hoc* Perl scripts into Bash scripts and run on Linux instances launched on the infrastructures of the DIAG (http://www.igs.umaryland.edu/resources/irc/) and CyVerse (Merchant et al., 2016) projects.

Plantlet Inoculations

To investigate whether or not Psa strains were impaired in their within plant colonization capabilities, micropropagated kiwifruit plantlets *A. chinensis* (cv. Soreli) at the stage of 6 leaves, provided by Azienda Agricola Fanna Giampaolo (Moimacco, Italy) were used for plantlet inoculation. Bacterial strains grown for 24 h in Nutrient Broth with agitation were washed twice and resuspended in 0.9% saline solution in concentration of 1–2 $\times$ 10^9 CFU/ml. Plantlets were cut from callus, dipped in the inoculum and transferred to a fresh medium. Control plants were dipped in sterile saline. Plantlets were inoculated in five repetitions per experiment. After 10 days the plantlets were collected, cut into two halves (about 3 cm from inoculation point), and DNA was extracted from each subsample according to standard protocols (Doyle and Doyle, 1990). The bacterial populations were quantified by qPCR according to published protocol (Gallelli et al., 2014). For statistical analysis, carried out with R (R Core Team, 2013), the median of three PCR reactions was used.

Leaf Inoculations

To compare the capability of strains to induce disease symptoms and to determine their growth *in planta*, *Actinidia chinensis* (cv. Dorì®) leaves were inoculated with the method described previously (Marcelletti et al., 2011). Leaf areas of approximately 1 cm in diameter were inoculated at the concentrations of 1–2 $\times$ 10^6 CFU/ml. For each experiment, 10 leaves were inoculated in four sites. Control plants were treated using solely sterile 0.85% NaCl. Two, 6, 15, and 22 days after inoculation, 10 leaf disks of about 0.5 cm of diameter were sampled and ground in 1 ml of sterile saline, then serial ten-fold dilutions were counted by colony growth onto nutrient agar supplemented with 3% of sucrose (NSA).

Hypersensitive responses were tested by infiltrating aqueous bacterial suspensions at 1–2 $\times$ 10^8 CFU/ml on fully expanded tobacco and eggplant leaves using a needless syringe. The development of typical hypersensitivity response was checked within 48 h after infiltration. Assays were repeated three times.

Other Wet Lab Methods

To determine the excised/integrated state of Tn6212, primers (Table S1) were designed on the inner and outer borders of the transposon. PCRs with primer pairs fX1/rX2; fX1/rX4, and fX3/rX4 were performed with the automated One Advanced thermocycler (EuroClone, Celbio, Milan, Italy) in 25 µl reactions containing 200 µM of each of the four dNTPs, 0.4 µM of each primer, 1.5 mM MgCl2, 0.625 units of GoTaq Flexi DNA Polymerase (Promega, Madison, WI, USA) and 1 µl of diluted bacterial DNA (5 ng/µl). The PCR program consisted of initial denaturation for 2 min at 94°C; 35 cycles of 1 min at 94°C, 45 s at 58°C, 1 min at 72°C; and a final extension for 8 min at 72°C.

PCR products were separated by electrophoresis in a 1% agarose gel, stained with ethidium bromide, and captured with a DigiDoc-It imaging system (UVP, Cambridge, United Kingdom).

RESULTS AND DISCUSSION

Differential Hypersensitive Response (HR) of Psa CRAFRU 12.29 and CRAFRU 12.50 Is due to Insertional Inactivation of the *hrp* Gene Cluster

Psa biovar 3 strains isolated in different regions of Europe were investigated to assess their phytopathogenic and genomic diversity. While most strains, as expected, induced HR in eggplant and tobacco leaves when infiltrated at concentrations of 1–2 $\times$ 10^8 CFU/ml, strains CRAFRU 12.50 and CRAFRU 12.29 failed in eliciting HR (not shown). Strains CRAFRU 12.50 and CRAFRU 12.29 were also compared with the reference strain CRAFRU 8.43 for their ability to colonize *A. chinensis*

leaves. Visual observations clearly revealed differences between CRAFRU 8.43 (HR+), that caused leaf spots, on one hand, and CRAFRU 12.29 (HR–) and CRAFRU 12.50 (HR–), on the other, that failed in inciting foliar symptoms. The estimate of bacterial concentration in leaves in the 22 days after inoculation, reported in **Figure 1**, showed that the population sizes of strain CRAFRU 12.29 and CRAFRU 12.50 did not increase during the assay time, while those of the virulent strain CRAFRU 8.43 peaked up to 100 times the inoculum. Thus, although the bacterial populations of HR– strains did not increase as much as the wild type, the bacteria remained detectable after 22 days. Further experiments carried out on micropropagated plantlets inoculated by dipping, revealed that the CRAFRU 12.29 cells move within the stem and were detectable by PCR in the stem segments above the point of inoculation 10 days after the dipping (results not shown).

In a preliminary SNPs analysis, based on Illumina sequencing data, only one nucleotide difference could be detected between the HR– strain CRAFRU 12.29 and the HR+ strain CRAFRU 14.08.

Hence, the genome sequences of strains CRAFRU 14.08 and CRAFRU 12.29 were completed by SMRT (Single Molecule, Real Time) and Sanger sequencing. The resulting finished chromosomes, as shown in the alignment of **Figure 2**, differ for several structural features.

First of all, CRAFRU 14.08 displays a large inversion of about half of the chromosome (3,637,997 nts) as compared to CRAFRU 12.29. The inversion occurred by recombination of the two identical copies of the gene encoding an integrating conjugative element protein of the PFL_4705 family, that are located, together with some other complete and incomplete copies, at position 1850000–1858000 and 5488000–5500000 in the chromosome of CRAFRU 12.29. Chromosome inversions have been reported to affect gene expression and occasionally the phenotype (Cui et al., 2012). However, whether or not the large genome inversion in CRAFRU 14.08 is associated with phenotype could not be determined in the present study.

The second major difference in strain CRAFRU 12.29 concerns a 1,700 bp integrative sequence, encoding an integrase and an IS3/IS911 transposase. This small integrative unit was inserted in the *hrpS* gene, within a transcriptional unit that spans several components of the type III secretion system, including the gene encoding harpin, *hrpZ* (**Figure 3**). Since, according to annotation and Blast searches, there are no other copies of *hrpZ* in the genome of Psa CRAFRU 12.29, the lack of expression of *hrpZ* may conceivably be the reason for the reduced virulence on kiwifruit and inability to elicit HR on eggplant and tobacco leaves. The phenotype is indeed reminiscent of previously characterized *hrpZ* deletion mutants (He et al., 1993).

The mobilization of IS3/IS911 elements has been already reported by Butler et al. (2013), who found that in the comparison of Pac_ICE1 from four New Zealand strains (ICMP 18708, ICMP18800, TP1, and 6.1) the presence of an IS element of the type IS3/IS911 in strain 6.1 was the only difference. They designated this small transposable element ISPsy31 at the IS Finder database (Siguier et al., 2006) and we will follow this nomenclature. As remarked by Butler et al. (2013), ISPsy31 is predicted to have two, partially overlapping reading frames associated with a 21 frame shift (the typical pattern found in IS3/IS911 type elements). Hence, although ISPsy31 encodes no functions other than those involved in its mobility, it may significantly impact the behavior of the pathogen in its interaction with the host.

There are many copies of ISPsy31 in the Psa genome. In strain CRAFRU 12.29 we counted 52 complete and five incomplete copies in the chromosome, and two complete copies in the plasmid. With the notable exception of the one interrupting *hrpS*, all other ISPsy31 copies are in corresponding positions in the chromosomes of strains CRAFRU 12.29 and CRAFRU 14.08.

On the other hand, strain CRAFRU 14.08 genome displays (position 5223542–5224799) the insertion of another IS element of the IS3/IS911 family, related to but well distinct from ISPsy31, and designated as ISPsy37 at the ISFinder database (Siguier et al., 2006). There are two copies of this transposon in CRAFRU 14.08, and only a single occurrence in CRAFRU 12.29.

Finally, one variation associated with variable number tandem repeats (VNTR) was also scored at positions 2787533–2786633 in CRAFRU 14.08, in additions to two unique SNPs (see below). Differences between the chromosomes of CRAFRU 14.08 and CRAFRU 12.29 are summarized in Table S2.

The finding that a small transposon insertion caused the loss of the ability to elicit the HR response in CRAFRU 12.29 prompted us to investigate whether or not the phenotype of the second HR– strain, CRAFRU 12.50, was associated to the same genomic event. To this end, we comparatively analyzed the ILLUMINA data-sets for discrepancies in reads coverage between the HR– and HR+ strains. Read coverage for the genome of the HR- strain CRAFRU 12.50 was similar to all HR+ strains in the locus of insertion of ISPsy31 in CRAFRU 12.29, but was markedly different from any other genome in a locus 1,273 nts upstream (Figure S1). Sorting the CRAFRU 12.50 reads using Mapsembler (Peterlongo and Chikhi, 2011) with sequence starters located on both sides of this locus (corresponding to position 1,473,520 in CRAFRU) we could extend the left side starter by 24 nts upstream and the right starter by 25 nts downstream, revealing the boundaries of a transposon tentatively identified as a copy of ISPsy36, inserted in the *hrpR* gene (**Figure 3B**).

Structural Diversity in the Chromosomes of the European Population of Psa Biovar 3

The availability of finished genomes of European Psa strains allowed to precisely map SNPs in additional 10 genomes (**Table 1**) of strains isolated in Europe, using Illumina data, as summarized in **Table 2** (to help following the results in this and the following sections, a tree based on distance among genomes of the Psa strains as deduced from SNPs and including all strains mentioned in this work has been included as Figure S2). According to SNP analysis, a single difference between the chromosomes of strains CRAFRU 14.08 and CRAFRU 12.29 was scored, at position 39328331 in CRAFRU 14.08. Comparison of the two finished chromosome sequences using MUMmer (Delcher et al., 2002) revealed an additional SNP at position 2736260; that position corresponds to a transposase gene that is present in several copies in the genome and therefore was

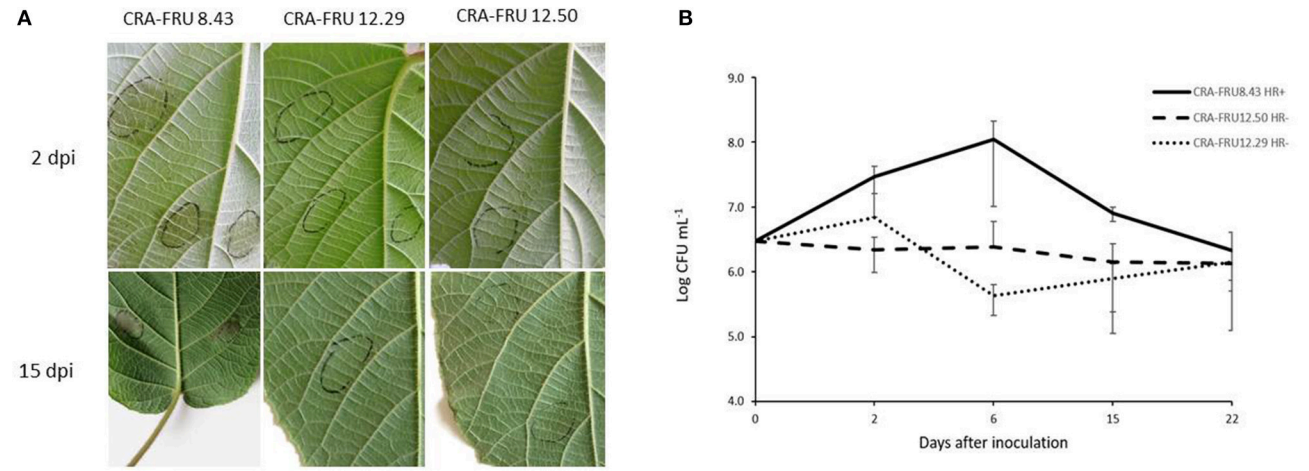

FIGURE 1 | (A) Symptoms on kiwifruit leaves 2 and 15 days post inoculation (dpi) with CRA-FRU 8.43, CRA-FRU 12.29, and CRA-FRU 12.50. **(B)** Population dynamics of Psa strains CRAFRU 8.43 (HR+), CRAFRU 12.29 (HR–), and CRAFRU12.50 (HR–) after inoculation of kiwifruit leaves.

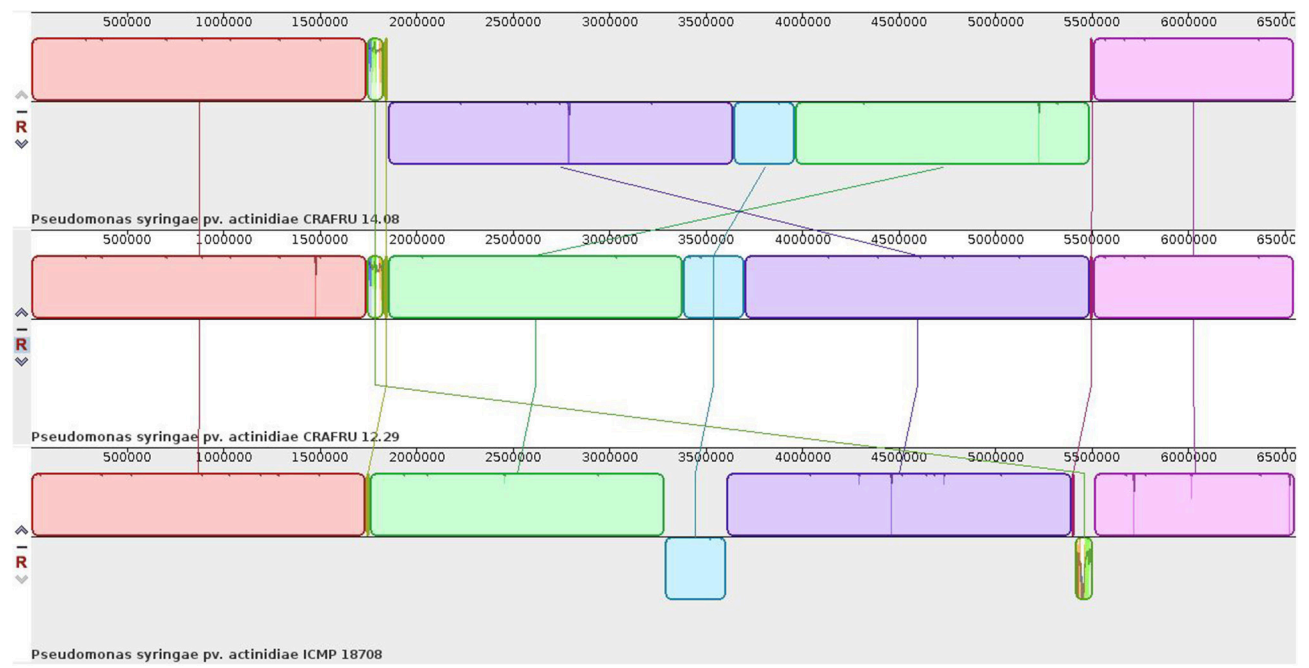

FIGURE 2 | Mauve alignment of the chromosomes of strains CRAFRU 14.08, CRAFRU 12.29, and ICMP 18708.

not detectable by read mapping (Table S2). In summary, the SNP comparison of the 12 European Psa genomes revealed that they differ from each other in 0 to 8 sites, on a total of 19 polymorphisms detected.

The SNP analysis reported here supports the assertion of Butler et al. (2013) that the clonal populations in New Zealand and Chile are undergoing divergence, but as yet the frequency of idiosyncratic SNPs is less than one per Mb. A similar rate was determined in this work for European strains, as it was also anticipated by Mazzaglia et al. (2012). However, these figures are significantly lower than those reported by McCann et al. (2013) who identified 28–70 polymorphisms among the four Italian strains included in their study. The explanation of this inconsistency may lay in the fact that for three out of the four strains compared by those Authors, they used the data from *de novo* draft assemblies deposited in the database by Marcelletti (Marcelletti et al., 2011), Butler (Butler et al., 2013), and Mazzaglia (Mazzaglia et al., 2012), respectively, and *de novo* assembly is much more error prone than the conservative read mapping method used in this work (Trivedi et al., 2014).

Mazzaglia et al. (2012) identified the presence, in the chromosome of Psa, of a divergent genomic island ∼100 kb

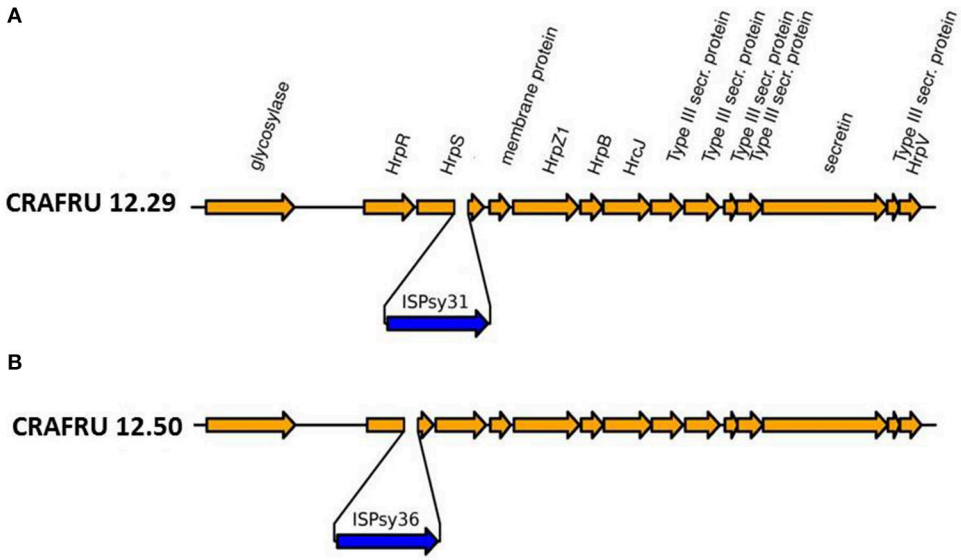

FIGURE 3 | Drawing of part of the *hrp* cluster of Psa, with the location of the insertion of **(A)** ISPsy31 in strain CRAFRU 12.29 and **(B)** ISPsy36 in strain CRAFRU 12.50.

TABLE 2 | SNPs identified among the strains used in this work by Illumina reads mapping. Position relative to the chromosome of CRAFRU 14.08.

Strain Position	CRAFRU 12.64	CRAFRU 10.29	CRAFRU 12.50	CRAFRU 12.29	CRAFRU 14.21	CRAFRU 14.08	#7286	CRAFRU 13.27	CRAFRU 8.43	CRAFRU 14.25	CRAFRU 12.54	CRAFRU 14.10
32022	G	G	G	G	G	G	G	G	C	G	G	G
1537885	C	T	C	C	C	C	C	C	C	T	C	C
1791521	G	G	G	G	G	G	C	G	G	G	G	G
1791522	G	G	G	G	G	G	C	G	G	G	G	G
2109838	C	C	C	C	C	C	C	C	T	C	C	C
2554115	G	G	A	G	G	G	G	G	G	G	G	G
3540152	A	T	A	A	A	A	A	A	A	A	A	A
3540154	C	T	C	C	C	C	C	C	C	C	C	C
3932833	C	C	C	T	C	C	C	C	C	C	C	C
4207959	C	C	C	C	C	C	C	C	C	C	T	C
4262863	G	G	T	G	G	G	G	G	G	G	G	G
5267844	C	A	C	C	C	C	C	C	C	C	C	C
5268734	C	C	C	C	C	C	A	C	C	C	C	C
5346399	A	T	T	T	T	T	T	T	T	T	T	T
5379834	C	C	C	C	A	C	C	C	C	C	C	C
5719829	G	G	G	G	G	G	G	G	T	G	G	G
5803673	C	C	C	C	C	C	G	C	C	C	C	C
6189845	C	C	T	C	C	C	C	C	C	C	C	C
6357274	C	C	T	C	C	C	C	C	C	C	C	C

long, similar to PPHGI-1, an integrative conjugative elements (ICE) described earlier in *P. syringae* pv. *phaseolicola* (Pitman et al., 2005), and also similar to PsyrGI-6, an ICE of *P. syringae* pv. *syringae* B728a (Feil et al., 2005). The genomic island was analyzed in more detail by Butler et al. (2013), who named Pac_ICE2 the type shared by European strains of Psa (in contrast with Pac_ICE1, for New Zealand strains, Pac_ICE3, for Chilean).

Butler et al. (2013) reported that the islands in ICMP 18708 (New Zealand), ICMP 18744 (Italy) and ICMP 19455 (Chile) were broadly syntenic, although the sequences shared by the ICEs were significantly divergent (∼85% identical). Two regions with high conservation were detected, corresponding to transposons named Tn6211 and Tn6212. While Tn6211 occupy distinct positions in each of the three ICE types, the second conserved region (bases 55201–71516 in Pac_ICE1 from ICMP 18708), designated Tn6212 and almost identical in all ICEs, was syntenic in the three ICE types.

Mapping of Illumina reads examined in this work revealed two distinct types of Pac_ICE2 among the 12 European Psa genomes. The Illumina reads from five strains (namely CRAFRU 12.50, CRAFRU 12.29, CRAFRU 14.21, CRAFRU 14.08, and CRAFRU 13.27) did not cover the about 16.3 kbp of Tn6212 (**Figure 4**). "Split reads" containing Tn6212 flanking sequences were also found suggesting that the transposon was excised.

PCR carried out with primers placed on the borders of Tn6212 (**Figure 4**) provided confirmation of the excision and loss of Tn6212 in the named five strains: with their DNA extracts as templates, both the PCRs with primers located on left end of Tn6212 and flanking region, and the PCRs with primers located on right end of Tn6212 and flanking region, failed to amplify a DNA fragment of the expected size. Conversely, PCRs with primers specific for the left and right flanking regions amplified a DNA fragment that was 686 bp in length, i.e., lacking the Tn6212 sequence. Unexpectedly, the DNA samples from the other strains were positive not only to PCRs designed to amplify the ends of Tn6212 and flanking regions, but also primed amplification of the 686 bp DNA fragment with primers specific for the left and right flanking regions.

Since the DNA samples were prepared from 24 h old liquid cultures started from single colonies, we hypothesize that Tn6212 may occur with high frequency *in vitro*, so that at the time of DNA extraction the sample contained a mixture of genomes with and without Tn6212 integration. A similar hypothesis may explain the incongruity of the results concerning strain CRAFRU 14.25, that showed reads coverage of the Tn6212 region but no amplification products with primers located on its ends. Since the sequencing was carried out more than 1 year before PCRs, we hypothesize that subculturing ultimately selected genomes missing Tn6212.

The evidence of optional and frequent excision of Tn6212 raised the question of its potential role in the interaction with the plant host, that could warrant its maintenance in the pathogen population over time and its detection in fresh strains.

Tn6212 has been reported to be the Psa specific part that distinguished ICEs of Psa and *Ps. syringae* pv. *phaseolicola* (Psp). McCann et al. (2013) pointed out the presence within the Tn6212 region of genes that may be implicated in the interaction with the plant host, such as those encoding a predicted enolase and various transporters, including an ortholog of DctT (a putative di- carboxylic acid transporter with N-terminus predicted to be targeted to the Type III Secretion System) and a methyl-accepting chemotaxis protein predicted to be involved in taxis toward malate.

In an attempt to detect differences in virulence and within-plant colonization of strains, we inoculated plantlets with strain CRAFRU 8.43 and CRAFRU 14.08 and, after 10 days incubation, estimated by qPCR the bacterial population in the point of inoculation ("bottom" in **Figure 5**) and in the stem segment 3 cm above ("Top" in **Figure 5**). Although the bacterial cell number estimated of CRAFRU 8.43 were higher, the detected difference was not statistically significant.

The optional excision of Tn6212 is the only significant variation in ICE2 among the 12 genomes examined. In fact, ICE2 resulted identical in all strains except for a single polymorphism in strain CRAFRU 10.29 at position 51525.

Furthermore, we examined the results of Illumina re-sequencing of all Psa strains with the aim of discovering new genes possibly acquired during clonal expansion. Following reads mapping on the complete genome of strain CRAFRU 12.29, we selected and assembled the Illumina reads that were not mapped. After filtering for Tn6212 (missing in the reference) sequences, we obtained in total 175 contigs for a total of 105,000 nts. The encoded amino acids sequences whose function could be recognized according to RAST annotation were exclusively phage associated proteins (Table S4). Hence, we could find no evidence

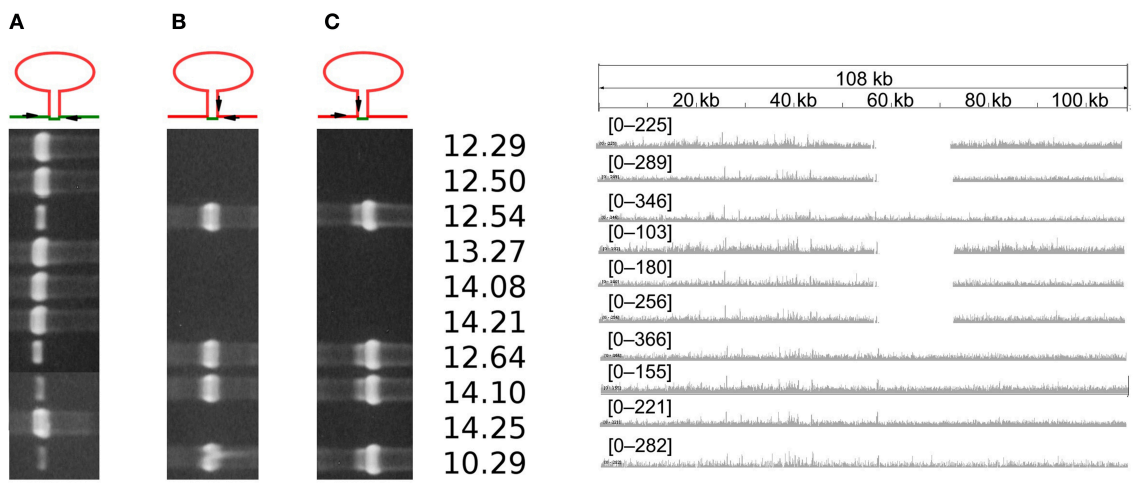

FIGURE 4 | Evidence of integration/excision of Tn6212. **(Left)** Agarose gels of PCR amplification products with (A) primers fX1/rX4 (686 bp) that amplify the chromosome region resulting from excision, (B) primers fX3/rX4 (739 bp) that amplify the downstream transposon junction, and (C) primers fX1/rX2 (933 bp) that amplify the upstream transposon junction, as indicated in the top scheme of PCR primers positions. **(Right)** Density of reads mapping on Tn6212 and flanking regions. The numbers indicate the CRAFRU strains.

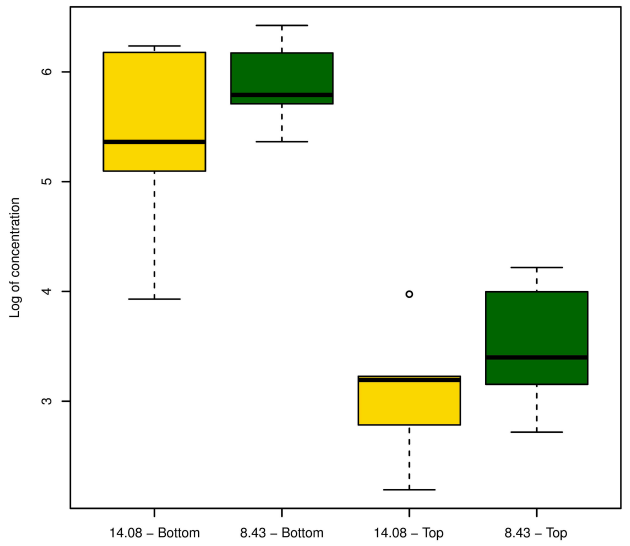

FIGURE 5 | Boxplot of the estimated bacterial population in the upper **(Top)** and lower **(Bottom)** part of the stem 10 days after inoculation with strains CRAFRU 8.43 and CRAFRU 14.08.

of gene gain in our sample of 12 European genomes, reveling a picture divergent from that described by Colombi et al. (2017) who showed the acquisition by strains isolated in New Zealand of exogenous integrative conjugative elements carrying copper resistance genes during clonal expansion.

To confirm that genome diversity in the European strains is mostly due to rearrangement of self-genetic elements, the Illumina dataset was used to investigate structural changes in the chromosomes of the collections of 10 European strains, with different approaches.

We mapped the Illumina reads from all strains on both the CRAFRU 12.29 and CRAFRU 14.08 chromosomes and visualized the alignments in the regions covering the structural changes that differentiate those chromosomes among themselves. As a result, we found that the ISPsy31 insertion in CRAFRU 12.29, as well as the ISPsy37 insertion and the large inversion in CRAFRU 14.08, and the ISPsy36 insertion in CRAFRU 12.50 were unique in the respective strain chromosomes and not shared by any other of the remaining European strains. We therefore focused on the detection of specific structural changes in the chromosomes of the other strains.

To this end, we prepared an inventory of the mobile elements that can be detected in the two complete chromosomes of European Psa, CRAFRU 12.29 and CRAFRU 14.08 (Figure S3), then mapped their ends on the assemblies of other strains to detect traces of transposon mobilization. By using this approach, we found contigs ending with sequences associated with mobile element borders that were not present in the reference chromosome. In particular, we found IS3 related sequences in unique positions in CRAFRU 12.64 and CRA 8.43, and an IS3 related sequence present in the same position in both CRAFRU 13.27 and CRAFRU 10.29.

The assemblies were also scaffolded using CRAFRU 12.29 genome as a reference and visualized, allowing the detection of an inversion around position 5508000 (CRAFRU 12.29 numbering) in strain CRAFRU 8.43.

Comparison of Chromosomes of European vs. New Zealand Psa Biovar 3 Strains

The comparison of the European strain CRAFRU 12.29 and the two complete genomes of New Zealand strains that were available from NCBI in October 2016, i.e., strains ICMP 18708 and ICMP 18884, showed substantial synteny of the chromosomes (**Figure 2**).

As previously noticed the sequences diverged largely in the ICE region, while divergence was much less in the rest of the genome. As it has already been reported for other strains (Butler et al., 2013) the ICE is inserted in a different lysine tRNA site in the genomes of European Psa strain CRAFRU 12.29 and in the New Zealand strain ICMP 18708/18884.

Excluding the ICE region, the chromosomes of the two New Zealand strains were identical to each other except for seven SNPs (including single nucleotide indels), according to the results of direct comparison using MUMmer (Delcher et al., 2002) and Mauve (Darling et al., 2004). Two of the indels occurred in homopolymer stretches and were not confirmed by our Illumina sequencing and reads mapping of strain ICMP 18884. Thus, the number of single nucleotide variations between the two New Zealand strains were similar to that occurring among the European strains. Conversely, 27 SNPs (including indels) and three sequence variations affecting multiple nucleotides were detected between the European Psa strain CRAFRU 12.29 and the New Zealand strain ICMP 18884 in the remaining (after exclusion of ICE) about 6 Mb of the chromosome (pos 1–5410820 and 5511674–6555571, strain ICMP 18708 numbering). This finding is in substantial agreement with the hypothesis that Psa strains originating the epidemics in Chile, New Zealand and Europe were independently invaded by Pac_ICE1/3, supporting the notion that this ICE may contain genetic elements that significantly affect the virulence of the pathogen.

In addition to SNPs, several genome rearrangement events distinguished the genome of the European Psa strain CRAFRU 12.29 and the New Zealand strains ICMP 18708/18884, as presented in Table S3. Major events include the insertion of a copy of a mobile selfish genetic element of the group named bacterial group II intron reverse transcriptase/maturase in CRAFRU 12.29 at positions 1023375–1025252. Proteins in this group have an N-terminal reverse transcriptase (RNA-directed DNA polymerase) domain (pfam00078) followed by an RNA-binding maturase domain (pfam08388). This mobile element is present in 14 copies in CRAFRU 12.29 and 13 copies in ICMP 18708/18884 genomes.

On the other hand, ICMP 18708 and ICMP 18884 are characterized by a similar event, the insertion of another distinct bacterial group II intron reverse transcriptase/maturase starting at position 5715260 and ending at position 5717133. Also this transcriptase/maturase is present in several identical copies in the Psa genomes, namely 14 copies in ICMP 18708

and 13 copies in CRAFRU 12.29, respectively. There are, in total, 54 protein annotated as bacterial group II intron reverse transcriptase/maturase in each of the two genomes in comparison. Another major difference between the two genomes concerns an insertion of two transposase genes at positions 3287490–3288700 in a DNA region that includes sequences encoding IS630 transposases, a phage invertase and related proteins that are associated with a 316 kb inversion in ICMP 18708/18884. Another IS630 insertion that is specific of ICMP 18708/18884 occurs in those genomes at position 6522179–6523356 (ICMP 18708 numbering). In ICMP 18708/18884 there are 61 complete and five incomplete IS630 transposases, while CRAFRU 12.29 displayed 59 complete and five incomplete copies of this gene. Two minor variations associated with repeats of variable lengths were also scored, one of which corresponding to the same repeat region that differentiated CRAFRU 14.08 from CRAFRU 12.29.

CONCLUSIONS

Mobile DNA elements contribute to bacterial evolution, as their ability to mobilize themselves and unrelated DNA in their proximity can lead to genome rearrangements that affect the microorganism phenotype (Bardaji et al., 2011). Their role in improving fitness and, potentially, pathogenicity and virulence of phytopathogenic bacteria is well established (Jackson et al., 2011). Many studies stressed the role of mobile DNA dependent gene gain in pathogen populations during epidemics, leading to the differentiation and development of more adapted clones (Holden et al., 2009; Mutreja et al., 2011; Santagati et al., 2012; Petrovska et al., 2016). Psa biovar 3 represents a relevant example of such a process, considering the primary role of mobile DNA mediated horizontal genetic transfer (particularly the gain of ICE) in its emergence as a pandemic pathogen of kiwifruit, according to several studies (Marcelletti et al., 2011; Butler et al., 2013; McCann et al., 2013, 2017).

However, Mobile DNA-induced mutations are often deleterious (Wu et al., 2015), and transposable elements have been regarded as a sort of genomic disease (Wagner, 2009). Loss of fitness due to the accumulation of deleterious mutations has been reported for small, obligate asexual populations, as these are incapable of reconstituting highly fit genotypes by recombination or back mutation (Lynch et al., 1993; Moran, 1996).

According to the results of a pangenomic study by Bolotin and Hershberg (2015), while non-clonal species diversify through a combination of changes to gene sequences (gene loss and gene gain), gene loss completely dominates as a source of genetic variation among clonal species, for which it needs to be taken into account as a potential dominant source of phenotypic variation. In the case of Psa biovar 3, we report here a relevant number (considering the small sample) of transposon mediated structural variations, occasionally impairing relevant phenotypic aspects of the interaction with the host, as occurred in the genome of strains CRAFRU 12.29 and CRAFRU 12.50 where a ISPsy31 insertion in the *hrpS* gene and a ISPsy36 insertion in the *hrpR* gene, respectively, disrupted the functionality of the TTSS. In all cases, structural variations implied rearrangement of self-genetic elements and not incorporation of external DNA.

There is a growing body of evidence supporting the hypothesis of two phases in the recent evolution of Psa biovar 3, with a landmark in the initiation of the worldwide pandemic in 2008. The SNP based comparisons (this work, McCann et al., 2017), as well as the evidence of independent invasions of ICE (Butler et al., 2013), suggest the preservation of within biovar diversity in the natural environment of the region of origin and during initial spread in China, before pandemic initiation. In this phase, acquisition of exogenous DNA through mobile DNA and selection for increased fitness were drivers of the evolution, promoting the emergence of adapted individuals. Also in this phase, recombination (intra- and inter-pathovar; McCann et al., 2013, 2017) and selection limited the proliferation of transposons and the deleterious mutations associated to DNA mobilization.

A new phase began with the introduction of adapted highly virulent strains from China into the kiwifruit cultivated areas in Europe, Chile and New Zealand. In Europe, Psa biovar 3 established and spread clonally in an ecological niche lacking competitive selection, such as that represented by the highly sensitive *A. chinensis* cv. Hort 16A. The results of this study show that the new phase was associated to an increase in the number of small transposons in the bacterial genome, with rearrangements leading to gene loss rather than to gain of functions by horizontal transfer. The data collected herein would suggest that clonal spread of the pathogen in a free ecological niche occurred with no access to the environmental gene pool, with diversification through rearrangement of self-genetic elements, and in the absence of the recombination-selection process that mitigates genome degeneration associated with transposon mobilization (Bast et al., 2016).

This suggestion is corroborated by the genome comparisons between European and New Zealand strain. According to the SNPs analysis presented in this and other papers (Mazzaglia et al., 2012; Butler et al., 2013), SNPs differences between the two geographically distinct groups of strains are one order of magnitude larger than within group SNPs differences, supporting the notion that the separation the European and New Zealand strains consistently predates the initiation of clonal expansion in Europe; conversely the mobile DNA associated structural differences are not larger between geographically distinct groups than within groups. This discrepancy, and the isolation of variant strains defective in virulence, are consistent with the view that the clonal expansion in the open niche of cultivated kiwifruit would be associated with genomic diversification through structural rearrangement with relaxation of the natural selection pressure against deleterious traits. This issue may be relevant for our understanding and management of epidemics.

Evidence of gene gain associated with the emergence of copper-resistant strains was recently reported by Colombi et al. (2017) for Psa in New Zealand, while we found no gene gain by European strains, variant strains resulting from rearrangement of self-genetic elements. The different outcomes of the surveys

may be related with differences in the environmental conditions, epidemic dynamics or disease management, such as timing of the disease spread on the territory, introduction of tolerant cultivars, use of containment measures directed to the reduction of the inoculum size (particularly copper treatments) or to the reduction of pathogen dispersal and the establishment of conducive conditions for the epidemics (pruning, girdling, cultivation under cover), prevalence of the crop in the region (Vanneste, 2017).

Modern strategies for the management of destructive epidemics, such as that caused by Psa biovar 3 on kiwifruit, may benefit from the awareness of their effect on short-term genome evolution and population structure of the pathogen. The results presented in this paper would suggest that strategies that do not promote recombination and preserve the clonal structure of the invasive microorganism may be associated with lower risk of developing variant strains with enhanced fitness or virulence.

AUTHOR CONTRIBUTIONS

GF, MS, and PE conceived the work, designed the experiments and wrote the paper. ET made the libraries. PF performed HR assays and leaf inoculations. FF carried out plantlets inoculation and quantitative PCRs. MM performed other wet lab methods. GF, CP, and SM analyzed the sequence data.

FUNDING

Financial support of this work was partially provided by the Region Friuli Venezia Giulia, Italy.

ACKNOWLEDGMENTS

The following colleagues are gratefully acknowledged for sharing their strains with us: G.M. Balestra, Tuscia University, Viterbo, Italy; C. Morone, Regione Piemonte, Servizio Fitosanitario regionale, Torino, Italy; M.M. Lopez, Instituto Valenciano de Investigaciones Agrarias, Moncada-Valencia, Spain; S. Poliakoff, ANSES, Angers, France. CyVerse, supported by the National Science Foundation under Award Numbers DBI-0735191 and DBI-1265383, and the Data Intensive Academic Grid (DIAG, sadly retired on Jan 2017), supported by the National Science Foundation under Grant No. 0959894 are acknowledged for providing computer resources. We are also grateful to Annalisa Polverari, University of Verona, Italy, for the critical reading and useful comments to the manuscript.

SUPPLEMENTARY MATERIAL

The Supplementary Material for this article can be found online at: https://www.frontiersin.org/articles/10.3389/fmicb.2018.00656/full#supplementary-material

REFERENCES

Abelleira, A., Lopez, M. M., Penalver, J., Aguin, O., Mansilla, J. P., Picoaga, A., et al. (2011). First report of bacterial canker of kiwifruit caused by *Pseudomonas syringae* pv. *actinidiae* in Spain. *Plant Dis.* 95, 1583–1583. doi: 10.1094/PDIS-06-11-0537

Balestra, G. M., Mazzaglia, A., Quattrucci, A., Renzi, M., and Rossetti, A. (2009). Occurrence of *Pseudomonas syringae* pv. *actinidiae* in Jin Tao kiwi plants in Italy. *Phytopathol. Mediterr.* 48, 299–301. doi: 10.14601/Phytopathol_Mediterr-2821

Bankevich, A., Nurk, S., Antipov, D., Gurevich, A. A., Dvorkin, M., Kulikov, A. S., et al. (2012). SPAdes: a new genome assembly algorithm and its applications to single-cell sequencing. *J. Comput. Biol.* 19, 455–477. doi: 10.1089/cmb.2012.0021

Bardaji, L., A-orga, M., Jackson, R. W., Martínez-Bilbao, A., Yanguas-Casás, N., and Murillo, J. (2011). Miniature transposable sequences are frequently mobilized in the bacterial plant pathogen *Pseudomonas syringae* pv. phaseolicola. *PLoS ONE* 6:e025773. doi: 10.1371/journal.pone.0025773

Bast, J., Schaefer, I., Schwander, T., Maraun, M., Scheu, S., and Kraaijeveld, K. (2016). No accumulation of transposable elements in asexual arthropods. *Mol. Biol. Evol.* 33, 697–706. doi: 10.1093/molbev/msv261

Bolotin, E., and Hershberg, R. (2015). Gene loss dominates as a source of genetic variation within clonal pathogenic bacterial species. *Genome Biol Evol.* 7, 2173–2187. doi: 10.1093/gbe/evv135

Butler, M. I., Stockwell, P. A., Black, M. A., Day, R. C., Lamont, I. L., and Poulter, R. T. M. (2013). *Pseudomonas syringae* pv. *actinidiae* from recent outbreaks of kiwifruit bacterial canker belong to different clones that originated in China. *PLoS ONE* 8:e57464. doi: 10.1371/journal.pone.0057464

Cesbron, S., Briand, M., Essakhi, S., Gironde, S., Boureau, T., Manceau, C., et al. (2015). Comparative genomics of pathogenic and nonpathogenic strains of *Xanthomonas arboricola* unveil molecular and evolutionary events linked to pathoadaptation. *Front. Plant Sci.* 6:1126. doi: 10.3389/fpls.2015.01126

Ciarroni, S., Gallipoli, L., Taratufolo, M. C., Butler, M. I., Poulter, R. T. M., Pourcel, C., et al. (2015). Development of a multiple loci variable number of tandem repeats analysis (MLVA) to unravel the intra-pathovar structure of *Pseudomonas syringae* pv. *actinidiae* populations worldwide. *PLoS ONE* 10:e0135310. doi: 10.1371/journal.pone.0135310

Colombi, E., Straub, C., Künzel, S., Templeton, M. D., McCann, H. C., and Rainey, P. B. (2017). Evolution of copper resistance in the kiwifruit pathogen *Pseudomonas syringae* pv. *actinidiae* through acquisition of integrative conjugative elements and plasmids. *Environ. Microbiol.* 19, 819–832. doi: 10.1111/1462-2920.13662

Cui, L., Neoh, H., Iwamoto, A., and Hiramatsu, K. (2012). Coordinated phenotype switching with large-scale chromosome flip-flop inversion observed in bacteria. *Proc. Natl. Acad. Sci. U.S.A.* 109, E1647–E1656. doi: 10.1073/pnas.1204307109

Cunty, A., Cesbron, S., Poliakoff, F., Jacques, M.-A., and Manceau, C. (2015a). Origin of the outbreak in France of *Pseudomonas syringae* pv. *actinidiae* Biovar 3, the causal agent of bacterial canker of kiwifruit, revealed by a multilocus variable-Number tandem-repeat analysis. *Appl. Environ. Microbiol.* 81, 6773–6789. doi: 10.1128/AEM.01688-15

Cunty, A., Poliakoff, F., Rivoal, C., Cesbron, S., Fischer-Le Saux, M., Lemaire, C., et al. (2015b). Characterization of *Pseudomonas syringae* pv. *actinidiae* (Psa) isolated from France and assignment of Psa biovar 4 to a de novo pathovar: *Pseudomonas syringae* pv. actinidifoliorum pv. nov. *Plant Pathol.* 64, 582–596. doi: 10.1111/ppa.12297

Darling, A. C. E., Mau, B., Blattner, F. R., and Perna, N. T. (2004). Mauve: multiple alignment of conserved genomic sequence with rearrangements. *Genome Res.* 14, 1394–1403. doi: 10.1101/gr.2289704

Delcher, A. L., Phillippy, A., Carlton, J., and Salzberg, S. L. (2002). Fast algorithms for large-scale genome alignment and comparison. *Nucleic Acids Res.* 30, 2478–2483. doi: 10.1093/nar/30.11.2478

Doyle, J. J., and Doyle, J. L. (1990). Isolation of plant DNA from fresh tissue. *Focus* 12, 13–15.

Dreo, T., Pirc, M., Ravnikar, M., Zezlina, I., Poliakoff, E., Rivoal, C., et al. (2014). First report of *Pseudomonas syringae* pv. *actinidiae*, the causal agent

of bacterial canker of kiwifruit in Slovenia. *Plant Dis*. 98, 1578–1578. doi: 10.1094/PDIS-05-14-0513-PDN

EPPO (2016). *EPPO Global Database*. Available online at: https://gd.eppo.int/taxon/PHLLAM/distribution (Accessed December 2, 2016).

Everett, K. R., Taylor, R. K., Romberg, R. K., Rees-George, J., Fullerton, R. A., Vanneste, J. L., et al. (2011). First report of *Pseudomonas syringae* pv. *actinidiae* causing kiwifruit bacterial canker in New Zealand. *Australas. Plant Dis. Notes* 6, 67–71. doi: 10.1007/s13314-011-0023-9

Feil, H., Feil, W. S., Chain, P., Larimer, F., Di Bartolo, G., Copeland, A., et al. (2005). Comparison of the complete genome sequences of *Pseudomonas syringae* pv. syringae B728a and pv. tomato DC3000. *Proc. Natl. Acad. Sci. U.S.A*. 102, 11064–11069. doi: 10.1073/pnas.0504930102

Ferrante, P., and Scortichini, M. (2009). Identification of *Pseudomonas syringae* pv. *actinidiae* as causal agent of bacterial canker of yellow kiwifruit *(Actinidia chinensis Planchon)* in central Italy. *J. Phytopathol*. 157, 768–770. doi: 10.1111/j.1439-0434.2009.01550.x

Ferrante, P., and Scortichini, M. (2010). Molecular and phenotypic features of *Pseudomonas syringae* pv. *actinidiae* isolated during recent epidemics of bacterial canker on yellow kiwifruit *(Actinidia chinensis)* in central Italy. *Plant Pathol*. 59, 954–962. doi: 10.1111/j.1365-3059.2010.02304.x

Ferrante, P., and Scortichini, M. (2015). Redefining the global populations of *Pseudomonas syringae* pv. *actinidiae* based on pathogenic, molecular and phenotypic characteristics. *Plant Pathol*. 64, 51–62. doi: 10.1111/ppa.12236

Ferrante, P., Takikawa, Y., and Scortichini, M. (2015). *Pseudomonas syringae* pv. *actinidiae* strains isolated from past and current epidemics to *Actinidia* spp. reveal a diverse population structure of the pathogen. *Eur. J. Plant Pathol*. 142, 677–689. doi: 10.1007/s10658-015-0643-6

Fujikawa, T., and Sawada, H. (2016). Genome analysis of the kiwifruit canker pathogen *Pseudomonas syringae* pv. *actinidiae* biovar 5. *Sci. Rep*. 6:21399. doi: 10.1038/srep21399

Gallelli, A., Talocci, S., Pilotti, M., and Loreti, S. (2014). Real- time and qualitative PCR for detecting *Pseudomonas syringae* pv. actinidiae isolates causing recent outbreaks of kiwifruit bacterial canker. *Plant Pathol*. 63, 264–276. doi: 10.1111/ppa.12082

Gouy, M., Guindon, S., and Gascuel, O. (2010). SeaView version 4: a multiplatform graphical user interface for sequence alignment and phylogenetic tree building. *Mol. Biol. Evol*. 27, 221–224. doi: 10.1093/molbev/msp259

He, S. Y., Huang, H. C., and Collmer, A. (1993). *Pseudomonas syringae* pv. syringae harpin Pss: a protein that is secreted via the Hrp pathway and elicits the hypersensitive response in plants. *Cell* 73, 1255–1266. doi: 10.1016/0092-8674(93)90354-S

Hernandez, D., François, P., Farinelli, L., Østerås, M., and Schrenzel, J. (2008). *De novo* bacterial genome sequencing: millions of very short reads assembled on a desktop computer. *Genome Res*. 18, 802–809. doi: 10.1101/gr.072033.107

Holden, M. T. G., Hauser, H., Sanders, M., Ngo, T. H., Cherevach, I., Cronin, A., et al. (2009). Rapid evolution of virulence and drug resistance in the emerging zoonotic pathogen Streptococcus suis. *PLoS ONE* 4:e6072. doi: 10.1371/journal.pone.0006072

Holeva, M. C., Glynos, P. E., and Karafla, C. D. (2015). First report of bacterial canker of kiwifruit caused by *Pseudomonas syringae* pv. *actinidiae* in Greece. *Plant Dis*. 99, 723–723. doi: 10.1094/PDIS-07-14-0738-PDN

Jackson, R. W., Vinatzer, B., Arnold, D. L., Dorus, S., and Murillo, J. (2011). The influence of the accessory genome on bacterial pathogen evolution. *Mob. Genet. Elements* 1, 55–65. doi: 10.4161/mge.1.1.16432

Koh, J. K., Cha, B. J., Chung, H. J., and Lee, D. H. (1994). Outbreak and spread of bacterial canker in kiwifruit. *Korean J. Plant Pathol*. 10, 68–72.

Kolmogorov, M., Raney, B., Paten, B., and Pham, S. (2014). Ragout-a reference-assisted assembly tool for bacterial genomes. *Bioinformatics* 30, i302– i309. doi: 10.1093/bioinformatics/btu280

Li, H., and Durbin, R. (2009). Fast and accurate short read alignment with Burrows-Wheeler transform. *Bioinformatics* 25, 1754–1760. doi: 10.1093/bioinformatics/btp324

Li, H., Handsaker, B., Wysoker, A., Fennell, T., Ruan, J., Homer, N., et al. (2009). The sequence alignment/map format and SAMtools. *Bioinformatics* 25, 2078–2079. doi: 10.1093/bioinformatics/btp352

Lynch, M., Butcher, D., Bürger, R., and Gabriel, W. (1993). The mutational meltdown in asexual populations. *J. Hered*. 84, 339–344. doi: 10.1093/oxfordjournals.jhered.a111354

Marcelletti, S., and Scortichini, M. (2011). Clonal outbreaks of bacterial canker caused by *Pseudomonas syringae* pv. *actinidiae* on *Actinidia chinensis* and *A. deliciosa* in Italy. *J. Plant Pathol*. 93, 479–483. Available online at: http://www.jstore.org/stable/41999021

Marcelletti, S., Ferrante, P., Petriccione, M., Firrao, G., and Scortichini, M. (2011). *Pseudomonas syringae* pv. *actinidiae* draft genomes comparison reveal strain-specific features involved in adaptation and virulence to *Actinidia* species. *PLoS ONE* 6:e27297. doi: 10.1371/journal.pone.0027297

Mazzaglia, A., Studholme, D. J., Taratufolo, M. C., Cai, R., Almeida, N. F., Goodman, T., et al. (2012). *Pseudomonas syringae* pv. *actinidiae* (PSA) isolates from recent bacterial canker of kiwifruit outbreaks belong to the same genetic lineage. *PLoS ONE* 7:e36518. doi: 10.1371/journal.pone.0036518

McCann, H. C., Li, L., Liu, Y., Li, D., Hui, P., Zhong, C., et al. (2017). Origin and evolution of a pandemic lineage of the kiwifruit pathogen *Pseudomonas syringae* pv. *actinidiae*. *Genome Biol. Evol*. 9, 932–944. doi: 10.1093/gbe/evx055

McCann, H. C., Rikkerink, E. H. A., Bertels, F., Fiers, M., Lu, A., Rees-George, J., et al. (2013). Genomic analysis of the Kiwifruit pathogen *Pseudomonas syringae* pv. *actinidiae* provides insight into the origins of an emergent plant disease. *PLoS Pathog*. 9:e1003503. doi: 10.1371/journal.ppat.1003503

McKenna, A., Hanna, M., Banks, E., Sivachenko, A., Cibulskis, K., Kernytsky, A., et al. (2010). The genome analysis toolkit: a mapreduce framework for analyzing next-generation DNA sequencing data. *Genome Res*. 20, 1297–1303. doi: 10.1101/gr.107524.110

Merchant, N., Lyons, E., Goff, S., Vaughn, M., Ware, D., Micklos, D., et al. (2016). The iPlant collaborative: cyberinfrastructure for enabling data to discovery for the life sciences. *PLOS Biol*. 14:e1002342. doi: 10.1371/journal.pbio.1002342

Milne, I., Bayer, M., Cardle, L., Shaw, P., Stephen, G., Wright, F., et al. (2010). Tablet-next generation sequence assembly visualization. *Bioinformatics* 26, 401–402. doi: 10.1093/bioinformatics/btp666

Moran, N. A. (1996). Accelerated evolution and Muller's rachet in endosymbiotic bacteria. *Proc. Natl. Acad. Sci. U.S.A*. 93, 2873–2878. doi: 10.1073/pnas.93.7.2873

Mutreja, A., Kim, D. W., Thomson, N. R., Connor, T. R., Lee, J. H., Kariuki, S., et al. (2011). Evidence for several waves of global transmission in the seventh cholera pandemic. *Nature* 477, 462–465. doi: 10.1038/nature10392

Okonechnikov, K., Golosova, O., and Fursov, M. (2012). Unipro UGENE: a unified bioinformatics toolkit. *Bioinformatics* 28, 1166–1167. doi: 10.1093/bioinformatics/bts091

Peterlongo, P., and Chikhi, R. (2011). *Mapsembler, Targeted Assembly of Larges Genomes on a Desktop Computer*. Research Report, RR-7565, INRIA, 17.

Petrovska, L., Mather, A. E., AbuOun, M., Branchu, P., Harris, S. R., Connor, T., et al. (2016). Microevolution of monophasic Salmonella Typhimurium during epidemic, United Kingdom, 2005–2010. *Emerg. Infect. Dis*. 22, 617–624. doi: 10.3201/eid2204.150531

Pitman, A. R., Jackson, R. W., Mansfield, J. W., Kaitell, V., Thwaites, R., and Arnold, D. L. (2005). Exposure to host resistance mechanisms drives evolution of bacterial virulence in plants. *Curr. Biol*. 15, 2230–2235. doi: 10.1016/j.cub0.2005.10.074

R Core Team (2013). *R: A Language and Environment for Statistical Computing*. Vienna: R Foundation for Statistical Computing. Available online at: http://www.R-project.org/

Robinson, J. T., Thorvaldsdóttir, H., Winckler, W., Guttman, M., Lander, E. S., Getz, G., et al. (2011). Integrative genomics viewer. *Nat. Biotechnol*. 29, 24–26. doi: 10.1038/nbt.1754

Santagati, M., Scillato, M., Patane, F., Aiello, C., and Stefani, S. (2012). Bacteriocin-producing oral streptococci and inhibition of respiratory pathogens. *FEMS Immunol. Med. Microbiol*. 65, 23–31. doi: 10.1111/j.1574-695X.2012.00928.x

Schmieder, R., and Edwards, R. (2011). Quality control and preprocessing of metagenomic datasets. *Bioinformatics* 27, 863–864. doi: 10.1093/bioinformatics/btr026

Scortichini, M. (1994). Occurrence of *Pseudomonas-syringae* pv *actinidiae* on kiwifruit in Italy. *Plant Pathol*. 43, 1035–1038. doi: 10.1111/j.1365-3059.1994.tb01654.x

Scortichini, M., Marcelletti, S., Ferrante, P., and Firrao, G. (2013). A genomic redefinition of *Pseudomonas avellanae* species. *PLoS ONE* 8:e75794. doi: 10.1371/journal.pone.0075794

Scortichini, M., Marcelletti, S., Ferrante, P., Petriccione, M., and Firrao, G. (2012). *Pseudomonas syringae* pv. *actinidiae*: a re-emerging,

multi-faceted, pandemic pathogen. *Mol. Plant Pathol.* 13, 631–640. doi: 10.1111/j.1364-3703.2012.00788.x

Siguier, P., Pérochon, J., Lestrade, L., Mahillon, J., and Chandler, M. (2006). ISfinder: the reference centre for bacterial insertion sequences. *Nucleic Acids Res.* 34(suppl_1), D32–D36. doi: 10.1093/nar/gkj014

Takikawa, Y., Serizawa, S., and Ichikawa, T. (1989). *Pseudomonas syringae* pv. *actinidiae* pv. nov. the causal bacterium of canker of kiwifruit in Japan. *Ann. Phytopathol. Soc. Jpn* 55, 437–444. doi: 10.3186/jjphytopath.55.437

Templeton, M. D., Warren, B. A., Andersen, M. T., Rikkerink, E. H. A., and Fineran, P. C. (2015). Complete DNA sequence of *Pseudomonas syringae* pv. *actinidiae,* the causal agent of kiwifruit canker disease. *Genome Announc.* 3:e01054-15. doi: 10.1128/genomeA.01054-15

Trivedi, U. H., Cézard, T., Bridgett, S., Montazam, A., Nichols, J., Blaxter, M., et al. (2014). Quality control of next-generation sequencing data without a reference. *Front Genet* 5:111. doi: 10.3389/fgene.2014.00111

Vanneste, J. L. (2017). The scientific, economic, and social impacts of the New Zealand outbreak of bacterial canker of kiwifruit (*Pseudomonas syringae* pv. *actinidiae). Annu. Rev. Phytopathol.* 55, 377–399. doi: 10.1146/annurev-phyto-080516-035530

Varani, A. M., Siguier, P., Gourbeyre, E., Charneau, V., and Chandler, M. (2011). ISsaga is an ensemble of web-based methods for high throughput identification and semi-automatic annotation of insertion sequences in prokaryotic genomes. *Genome Biol.* 12:R30. doi: 10.1186/gb-2011-12-3-r30

Wagner, A. (2009). Transposable elements as genomic diseases. *Mol. Biosyst.* 5, 32–35. doi: 10.1039/B814624C

Wu, Y., Aandahl, R. Z., and Tanaka, M. M. (2015). Dynamics of bacterial insertion sequences: can transposition bursts help the elements persist? *BMC Evol. Biol.* 15:288. doi: 10.1186/s12862-015-0560-5

Conflict of Interest Statement: The authors declare that the research was conducted in the absence of any commercial or financial relationships that could be construed as a potential conflict of interest.

frontiers in Microbiology

ORIGINAL RESEARCH
published: 06 August 2018
doi: 10.3389/fmicb.2018.01657

Functional and Genome Sequence-Driven Characterization of *tal* Effector Gene Repertoires Reveals Novel Variants With Altered Specificities in Closely Related Malian *Xanthomonas oryzae* pv. *oryzae* Strains

Hinda Doucouré[1,2], Alvaro L. Pérez-Quintero[1†], Ganna Reshetnyak[1], Cheick Tekete[1,2], Florence Auguy[1], Emilie Thomas[1], Ralf Koebnik[1], Boris Szurek[1], Ousmane Koita[2], Valérie Verdier[1] and Sébastien Cunnac[1]*

[1] IRD, Cirad, Université de Montpellier, IPME, Montpellier, France, [2] Laboratoire de Biologie Moléculaire Appliquée, Faculté des Sciences et Techniques, Université des Sciences Techniques et Technologiques de Bamako, Bamako, Mali

Rice bacterial leaf blight (BLB) is caused by *Xanthomonas oryzae* pv. *oryzae* (*Xoo*) which injects Transcription Activator-Like Effectors (TALEs) into the host cell to modulate the expression of target disease susceptibility genes. *Xoo* major-virulence TALEs universally target susceptibility genes of the SWEET sugar transporter family. TALE-unresponsive alleles of *OsSWEET* genes have been identified in the rice germplasm or created by genome editing and confer resistance to BLB. In recent years, BLB has become one of the major biotic constraints to rice cultivation in Mali. To inform the deployment of alternative sources of resistance in this country, rice lines carrying alleles of *OsSWEET14* unresponsive to either TalF (formerly Tal5) or TalC, two important TALEs previously identified in West African *Xoo*, were challenged with a panel of strains recently isolated in Mali and were found to remain susceptible to these isolates. The characterization of TALE repertoires revealed that *talF* and *talC* specific molecular markers were simultaneously present in all surveyed Malian strains, suggesting that the corresponding TALEs are broadly deployed by Malian *Xoo* to redundantly target the *OsSWEET14* gene promoter. Consistent with this, the capacity of most Malian *Xoo* to induce *OsSWEET14* was unaffected by either *talC*- or *talF*-unresponsive alleles of this gene. Long-read sequencing and assembly of eight Malian *Xoo* genomes confirmed the widespread occurrence of active TalF and TalC variants and provided a detailed insight into the diversity of TALE repertoires. All sequenced strains shared nine evolutionary related *tal* effector genes. Notably, a new TalF variant that is unable to induce *OsSWEET14* was identified. Furthermore, two distinct TalB variants were shown to have lost the ability to simultaneously induce two susceptibility genes as previously reported for the founding members of this group from strains MAI1 and BAI3. Yet, both new TalB variants retained

OPEN ACCESS

Edited by:
Sabrina Sarrocco, Università degli Studi di Pisa, Italy

Reviewed by:
Marco Scortichini, Consiglio per la Ricerca in Agricoltura e l'Analisi dell'Economia Agraria (CREA), Italy
Jianbin Su, University of Missouri, United States

***Correspondence:**
Sébastien Cunnac
sebastien.cunnac@ird.fr

†Present address:
Alvaro L. Pérez-Quintero, Institut de Biologie de l'Ecole Normale Supérieure, Centre National de la Recherche Scientifique, Paris, France

Specialty section:
This article was submitted to Plant Microbe Interactions, a section of the journal Frontiers in Microbiology

Received: *07 March 2018*
Accepted: *03 July 2018*
Published: *06 August 2018*

Citation:
Doucouré H, Pérez-Quintero AL, Reshetnyak G, Tekete C, Auguy F, Thomas E, Koebnik R, Szurek B, Koita O, Verdier V and Cunnac S (2018) Functional and Genome Sequence-Driven Characterization of tal Effector Gene Repertoires Reveals Novel Variants With Altered Specificities in Closely Related Malian Xanthomonas oryzae pv. oryzae Strains. Front. Microbiol. 9:1657. doi: 10.3389/fmicb.2018.01657

the ability to induce one or the other of the two susceptibility genes. These results reveal molecular and functional differences in *tal* repertoires and will be important for the sustainable deployment of broad-spectrum and durable resistance to BLB in West Africa.

Keywords: rice, *Xanthomonas oryzae*, bacterial leaf blight, TAL effector, Mali, disease resistance

INTRODUCTION

Genetic resistance is arguably the most sustainable strategy to control microbial diseases threatening crop production. However, effectiveness of resistance genes deployment in agricultural settings is contingent on a number of environmental and biological factors such as the spectrum of activity of the Resistance genes and the genetic diversity of pathogen populations, notably, with regards to the prevalence of resistance eliciting or suppressing factor(s) (Boyd et al., 2013; Brown, 2015).

Bacterial leaf blight (BLB) is a rice (*Oryza sativa*) foliar disease occurring in most rice growing regions. It has long been recognized in Asia as a serious yield limiting factors. BLB is considered as one of the three most important diseases of rice, causing yield reduction of 20–50% in extreme cases. *Xanthomonas oryzae* pv. *oryzae (Xoo)*, the gram negative bacteria responsible for BLB is a vascular pathogen that gains entry into plant tissues through hydathodes and wounds. *Xanthomonas oryzae* pv. *oryzicola (Xoc)* bacteria belong to another pathovar of the species and cause bacterial leaf streak (BLS) of rice, a disease less destructive than BLB but which is gaining in importance (Niño-Liu et al., 2006).

To successfully colonize its host and provoke significant disease symptoms, *Xoo* requires virulence proteins from the Transcription Activator-Like Effectors (TALEs) family. TALEs are injected into the host cell via the molecular syringe of the Type III Secretion System and subsequently localize to the nucleus where they molecularly mimic eukaryotic transcription factors and upregulate the expression of target genes. The central repeat region (CRR) of TALEs is responsible for recognition and binding to a specific target DNA sequence also termed effector binding element (EBE). The CRR domain is typically composed of 10–30 modular tandem repeats of 33–35 amino acids. The primary sequence of these repeats is highly conserved except at positions 12 and 13 which are referred to as repeat variable diresidue (RVD) (Boch and Bonas, 2010; Bogdanove et al., 2010). Structural insight into the features of TALE-DNA molecular complexes revealed that the CRR wraps around the DNA helix with the second residues of each RVDs interacting directly with a cognate nucleobase (Deng et al., 2012; Mak et al., 2012). The nature of each RVD determines affinity for a specific nucleotide in a linear fashion along the sequence of RVD in the TALE CRR and the target DNA sequence. The landmark elucidation of this TALE-DNA binding code (Boch et al., 2009; Moscou and Bogdanove, 2009) fostered the development of bioinformatic tools for the computational prediction of TALE target sequences (Moscou and Bogdanove, 2009; Doyle et al., 2012; Grau et al., 2013; Pérez-Quintero et al., 2013) and the design of artificial TALEs with tailored specificity (Boch et al., 2009; Morbitzer et al., 2010).

The functional interplay between TALEs and their rice gene targets is a major determinant of disease or resistance between *Xoo* strains and rice genotypes. When induction of a TALE target gene is demonstrated to make a positive contribution to disease outcome, this gene is termed a susceptibility gene. Documented BLB susceptibility host gene targets of TALEs include the transcription elongation factor *OsTFIIAγ1* and the b-ZIP transcription factor *OsTFX1* that were shown to be induced by TALE effectors from Philippine *Xoo* strains and have a mild effect on disease severity (White and Yang, 2009). In contrast, *OsSWEET* genes belonging to clade III of the family function as major susceptibility genes (Streubel et al., 2013). *SWEET* genes codes for membrane transporters with affinity for sugars and are primarily hypothesized to promote release of sucrose in the apoplast to provide a source of carbohydrate for bacterial multiplication (Bezrutczyk et al., 2018). *Xoo* strains do not monolithically target a single *OsSWEET* gene but rather have evolved TALEs inducing one of three *OsSWEET* clade III homologs: PthXo1 from the Philippine strain PXO99^{A} (Yang et al., 2006) targets Os*SWEET11* while PthXo2 from *Xoo* JXO1^{A} and MAFF311018 strains from Japan targets Os*SWEET13* (Zhou et al., 2015). Finally, in a remarkable example of convergent evolution, *OsSWEET14* stands out as being targeted by TALEs from geographically diverse and distantly related *Xoo* strains at the level of several distinct or overlapping EBEs in its promoter: AvrXa7 from strain PXO86 (Philippines) and PthXo3 from strain PXO61 (Philippines) (Antony et al., 2010) as well as Tal5 and TalC from African *Xoo* strains (Yu et al., 2011; Streubel et al., 2013). To date, the only African TALEs shown to target a clade III *OsSWEET* susceptibility gene are Tal5 from the Malian strain MAI1 and TalC from the Burkinabe strain BAI3. A *talC* mutant strain is unable to cause disease indicating that this effector is a major virulence TALE of the BAI3 strain (Yu et al., 2011; Streubel et al., 2013). To harmonize the nomenclature of African *Xoo* TALEs, Tal5 has been recently renamed TalF (Tran et al., 2018) and will be referred accordingly hereafter.

Resistance breeding is the only sustainable BLB control strategy in the field and more than 40 resistance loci have been characterized. With the notable exception of Pattern Recognition Receptors-encoding *Xa4*, *Xa21*, and *Xa23* genes, most BLB resistance systems described to date are based on the detection or the impairment of TALE activity (Zhang and Wang, 2013; Zuluaga et al., 2017) which further illustrates the critical status of this family of type III virulence effectors in the rice-*Xoo* evolutionary arms race. One type of host immunity relies on so-called 'executor' genes such as *Xa10*, *Xa23,* or *Xa27* that harbor a decoy TALE EBE in their promoter and act as triggers of a massive immune response upon infection attempts and promiscuous activation by a cognate TALE (Zhang et al., 2015).

Another recurring type of immunity originates from mutated alleles of gene promoters that confer a loss of TALE responsiveness to the corresponding *OsSWEET* susceptibility gene thereby hindering the establishment of proper bacterial growth conditions and preventing host tissues colonization (Hutin et al., 2015a). For example, the naturally occurring recessive resistance alleles *xa13* of *OsSWEET11* and *xa25* of *OsSWEET13* are, respectively, unresponsive to PthXo1 (Chu et al., 2006; Yang et al., 2006) and PthXo2 (Liu et al., 2011; Zhou et al., 2015) due to sequence polymorphism in the EBE recognized by the corresponding TALE. Recently, Hutin et al. (2015b) reported on *xa41(t)*, a resistance allele of *OsSWEET14* from the African wild rice species *O. barthii* that is also present in all examined cultivated varieties of the African *O. glaberrima* species. The *xa41(t)* promoter contains a 18 bp deletion spanning the AvrXa7 and TalF EBEs sequences and conferred resistance to half of the strains from a representative worldwide *Xoo* panel including six African strains from Burkina Faso, Niger, and Mali (Hutin et al., 2015b) which thus presumably rely solely on TalF for *OsSWEET14* activation.

Both the results of bioinformatic predictions of TALE target for strains with uncharacterized TALE repertoire (Pérez-Quintero et al., 2013; Grau et al., 2016; Quibod et al., 2016) and the consistent functional data on several *Xoo* TALE-*SWEET* pairs (Yang et al., 2006; Yu et al., 2011; Li et al., 2012; Zhou et al., 2015), support the view that this clade virtually act as universal BLB susceptibility genes. This and the existence of naturally occurring TALE-unresponsive *OsSWEET* resistance alleles in the rice germplasm hinted to a BLB resistance engineering strategy by genome editing of TALE EBEs in the promoter of *OsSWEET* genes. Pioneering work by Li et al. (2012) provided a proof of this concept by editing the AvrXa7 EBE upstream of *OsSWEET14* and conferring disease resistance to an Asian *Xoo* strain carrying this effector. A subsequent attempt to edit the TalF or the TalC EBE in the *OsSWEET14* promoter to create TALE-unresponsive resistance alleles tailored against African *Xoo* strains achieved immunity solely against those relying on TalF (Blanvillain-Baufumé et al., 2017). Intriguingly, the susceptibility of TalC-EBE edited lines to the TalC-relying strain BAI3 was unaffected even though none of the clade III *OsSWEET*, including *OsSWEET14*, was upregulated in these edited lines. This led to the conclusion that clade III *OsSWEET* induction is not an absolute requirement for BLB and that TalC also likely targets a genetically redundant susceptibility gene (Blanvillain-Baufumé et al., 2017).

In the past decade, rice has been recognized as a strategic crop and its cultivation has gained in importance in Africa. On this continent, BLB was first reported in Mali in 1979 and later found to occur in Senegal, Niger, Nigeria, Gabon, Mauritania, Benin, and Cameroon (Verdier et al., 2012). Probably due in part to surface extension and crop intensification, BLB is repeatedly observed in countries of the region, notably in Mali where rice pathologists have witnessed increased incidence and a marked susceptibility for local varieties in the field (Gonzalez et al., 2007; Sarra et al., 2010; Afolabi et al., 2015). Phylogenetic analysis of *Xoo* strains indicate that the African *Xoo* lineage is genetically distinct from the Asian one (Gonzalez et al., 2007; Poulin et al., 2015). It is noteworthy that among several distinguishing features, African *Xoo* strains harbor a reduced *tal* effector gene repertoire of nine elements (Gonzalez et al., 2007) compared to as much as 19 genes in Asian *Xoo* (Booher et al., 2015). Virulence profiling on nearly isogenic lines has clustered African strains isolated before 2007 into three races with Malian strains all belonging to race A3 which is incompatible on all lines of the IRBB panel, including the IR24 parental variety (Gonzalez et al., 2007). Recent work in our laboratories has expended our collection with ∼60 additional *Xoo* strains from Mali collected between 2009 and 2013. Virulence profiling on IRBB isogenic lines and Malian rice varieties as well as molecular typing indicated that these contemporary Malian *Xoo* isolates exhibit diversity both in terms of genetic content and virulence profiles as compared to strains isolated earlier. Many of these isolates define novel *Xoo* races and several of them are even able to overcome, at least partially, all tested sources of resistance (Tekete and Verdier, manuscript in preparation). Although, the TALE content of *Xoo* strains often underlies their pathogenicity, its variability among Malian strains remains unexplored. Until recently, our main insight into the nature of African *Xoo* TALEs came from the characterization of TalC and TalF. However, we used single molecule sequencing and functional assay to characterize the TALE repertoires of three African strains including MAI1 from Mali which redundantly activate *OsSWEET14* via both TalC and TalF (Tran et al., 2018). This work also identified TalB, a second major virulence TALE of African *Xoo* strains which remarkably targets two rice susceptibility genes, *OsTFX1* and *OsERF#123* (Tran et al., 2018).

Our objective is to provide farmers with broad BLB resistance to contemporary Malian *Xoo* strains. Recently described rice lines harboring either TalF- or TalC-unresponsive *OsSWEET14* promoter alleles were therefore challenged with Xoo but were found to be susceptible to all tested Malian isolates. To understand this lack of resistance, the *tal* gene repertoires of Malian strains were characterized. Active TalC appeared strictly conserved in Malian *Xoo* and, with one exception, consistently associated with an active version of the redundant TALE TalF. Comparative analysis of TALE repertoires additionally uncovered two variants of the TalB group that have lost the ability to induce one of the two documented targets of this group. Overall, Malian *Xoo* TALE groups members displayed an unexpected degree of variability raising the question of the functional significance of these differences in the interaction with rice.

RESULTS

OsSWEET14 Promoter Alleles Unresponsive to Single African TALEs Confer no Resistance to Malian *Xoo* Strains

Considering that TalF (previously Tal5) has been originally identified in a Malian strain (Streubel et al., 2013) and that an *O. barthii* accession containing the natural TalF-unresponsive allele *xa41(t)* is susceptible to strain MAI1 but resistant to three

other Malian strains (CFBP1951, MAI9, and MAI14) (Hutin et al., 2015b), *xa41(t)* could be an effective resistance allele to control BLB in Mali. We therefore sought to evaluate its efficiency against a larger set of contemporary Malian strains composed in majority of isolates collected between 2009 and 2013. For this, CG14, a cultivated *O. glaberrima* variety that harbors a functional *xa41(t)* (Hutin et al., 2015b) and the Azucena variety of *O. sativa*, acting as a susceptible positive control, were inoculated with 44 Malian strains (including MAI1, MAI9, MAI14 as references) using the standard leaf tip clipping assay. For each strain, the length of BLB lesions were measured 14 days post inoculation on both varieties and plotted in **Supplementary Figure S1**. Similar to the BAI3 control strain which relies on TalC rather that TalF for *OsSWEET14* induction (Yu et al., 2011; Tran et al., 2018), a large fraction of the Malian strains appeared equally proficient at causing symptoms on CG14 and Azucena. Only seven strains, including the PXO86 control which relies on the AvrXa7 TALE that is unable to induce *SWEET14* in *xa41(t)* (Hutin et al., 2015b), caused significant disease lesions on Azucena but were markedly less virulent on CG14 (average lesion length below 5 cm). This was thus an indication that *xa41(t)* is not broadly efficient against contemporary isolates.

Because this and previous experiments (Hutin et al., 2015b) with *xa41(t)*, could not use isogenic host rice backgrounds, interpretation on the causal role of *xa41(t)* on disease resistance can be confounded by other unrelated genetic factors. To unambiguously assess the contribution of a loss of TalF-responsiveness allele at *OsSWEET14* on resistance to Malian *Xoo*, we used the *OsSWEET14* promoter edited allele *sweet14-15*. It has been described previously and corresponds to a deletion of the entire AvrXa7 EBE and most (13 out of 19 bp) of the TalF EBE in a Kitaake cultivar (*O. sativa* ssp. *japonica*) parental background (Blanvillain-Baufumé et al., 2017). We also wanted to determine if a TalC-unresponsive *OsSWEET14* promoter edited allele could provide resistance to Malian *Xoo* and tested an homozygous line for the *sweet14-32* allele which has a large (16 out of 23 nt) deletion in the 3′ end of the TalC EBE (Blanvillain-Baufumé et al., 2017). Susceptibility assays of the edited lines and the parental Kitaake background were conducted with a restricted panel of Malian *Xoo* strains. As depicted in **Figure 1** and consistent with previous data, the BAI3 strain was equally virulent on the three rice genotypes. Similar to negative controls mock- or BAI3 *talC*-mutant-inoculated plants, the PXO86 control strain caused very short lesions, on *sweet14-15* plants as compared to wild type

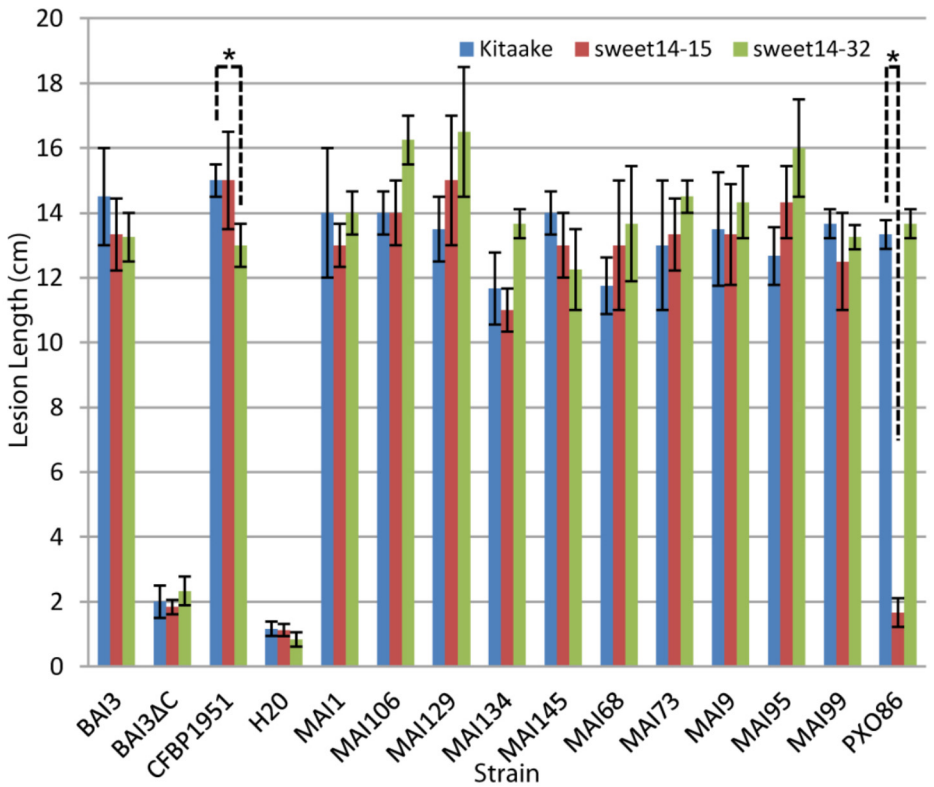

FIGURE 1 | The TalF (Tal5) or TalC EBE edited lines do not exhibit measurable resistance against Malian *Xoo* strains. Barplot of mean lesion length measured on Kitaake wild type, *sweet14-32* or *sweet14-15* homozygous individuals for the edited alleles of the *OsSWEET14* promoter TalC and TalF (Tal5) EBE, respectively. Leaves of 6-week-old plants were inoculated using the leaf-clipping method. Lesion length was measured 2 weeks after inoculation. Error bars represent standard deviation calculated from 3 to 4 replicate measurements. The 'BAI3ΔC' strain corresponds to the BAI3 *talC*$^{-}$ knockout derivative. For each strain, Welch two sample *t*-tests were performed to test if average lesion length in wild-type Kitaake plants is superior to lesion length in one of the two mutant *sweet14* lines. Significant comparisons with p-value ≤ 0.05 are highlighted in the plot with an asterisk. This experiment was repeated four times with similar results.

Kitaake. With the exception of CFBP1951 that caused slightly but significantly reduced lesions (p-value = 0.02473) on *sweet14-32* in this replicate of the experiment, Malian *Xoo* strains were similarly virulent on either of the *OsSWEET14* edited alleles than on the wild type control. We therefore conclude that none of the alleles conferred a strong resistance phenotype against any Malian *Xoo*. Altogether, these results demonstrate that not only TalC- but also TalF-unresponsive *OsSWEET14* alleles, either *xa41(t)* or *sweet14-15*, confer no or minor resistance against Malian *Xoo* strains. We further conclude that, in general, Malian strains do not rely solely on TalF for *SWEET* susceptibility gene induction.

tal RFLP-Haplotypes of Malian *Xoo* Strains Show a Limited Diversity and Include Both *talC* and *talF*

The conclusion that TalF is presumably not the only major TALE responsible for *SWEET* gene induction in Malian *Xoo* strains prompted us to explore the diversity of *tal* genes in our Malian strain collection. As a first step toward this goal, we conducted a preliminary screen of most of the Malian strains in our collection by Southern blotting with a PCR probe encompassing the 5′ part of the *talF* CDS on BamHI-digested genomic DNAs. As exemplified in **Figure 2A** on a restricted set of strains including those that were ultimately sequenced (see below), we detected a predominant haplotype of eight bands identical to the one obtained for our reference strain MAI1. Strain MAI68 defined a distinct haplotype differing at the level of the *talA*–*talB* band which migrated with a lower molecular weight. A third haplotype was also detected for strain MAI99 whose profile lacks the smallest *talI* band. Strain MAI134 defined a fourth haplotype with possibly an extra band beneath the *talC* one and the disappearance of the *talE* band. Importantly, the specific bands corresponding to *talC* and *talF* in strain MAI1 (Yu et al., 2011; Tran et al., 2018) were strictly conserved in all Malian strains examined, suggesting that these *tal* effector genes might be present in other Malian *Xoo* genomes as well.

In order to further ascertain the presence of a *talC* homolog in Malian strains, we designed a pair of PCR primers flanking a region in the 5′ portion of the coding sequence of *Xoo tal* genes that was found to be absent in the *talC* coding sequence (**Supplementary Figure S2**). As shown in **Figure 2B**, control PCRs with the BAI3 *talC* CDS cloned on a plasmid produced a band with a size consistent to the predicted 152 bp amplicon while using the cloned MAI1 *talF* CDS as a template yielded a band matching the size of the expected amplicon (224 bp). Additional control PCRs performed with the *talC*-containing strain BAI3 versus the Asian KACC10331 and PXO86 strains whose genomes are devoid of this gene revealed a ∼150 bp diagnostic band for the presence of *talC* in BAI3 only, thus verifying the specificity of this talC PCR marker. In the same experiment, we used it to also genotype a set of 24 genomic DNAs from Malian strains. Although the *talC* band had a weaker intensity, similar to PCR ran with BAI3 DNA as a template, we could repeatedly detect the *talC* diagnostic marker band for all tested Malian strains.

In conclusion, apart from three minor haplotypes observed only with single strains, Malian *tal* effector genes RFLP-profiles exhibit a low diversity with a major haplotype shared by most of the strains suggesting a limited divergence of TALE sequences

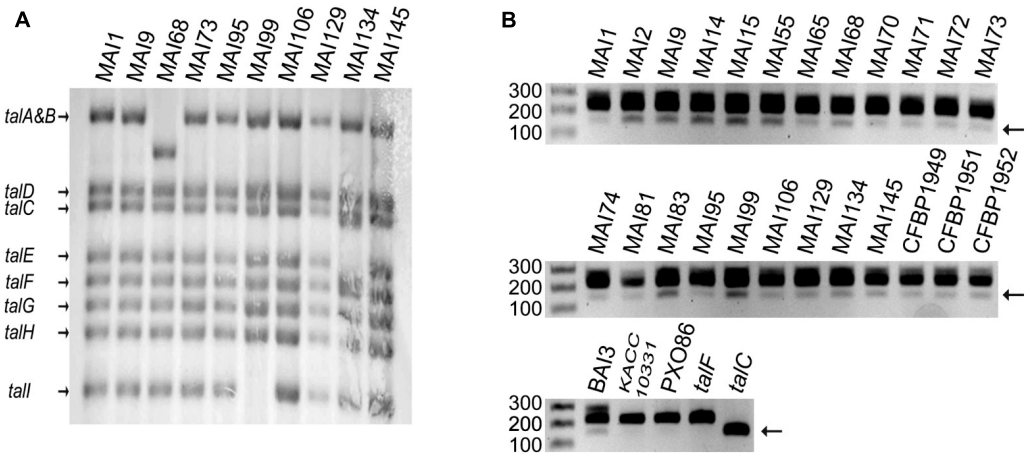

FIGURE 2 | A Survey of *tal* gene diversity in a set of Malian *Xoo* strains. **(A)** Genomic patterns of *tal* content as determined by Southern blot. The genomic DNAs were digested with BamHI prior to electrophoresis on a 1% agarose gel. Following transfer, bands corresponding to *tal* sequences were detected with a probe encompassing part of the N-terminal coding region of TalF from MAI1. The names of *tal* genes corresponding to MAI1 fragments are indicated on the left. **(B)** Detection of *talC* in Malian *Xoo* genomes. A portion of the N-terminal region of *tal* coding sequences was amplified by PCR with primers flanking a segment that is specifically deleted in *talC* and separated on a 1.5% agarose gel. Detection of a shorter 152 bp product as compared to the predominant ∼224 bp product is indicative of the presence of *talC*. Purified plasmid DNA containing *talF* or *talC* and genomic DNA from strains KACC10331 (Korea) and PXO86 (Philippines) or BAI3 (Burkina Faso) were used, respectively, as negative or positive controls. The single gel image was broken down into three subpanels for assembling the figure. For each of them, the first lane was loaded with a 100 bp Marker and the numbers on the left indicate fragment size in bp. Strain names are indicated on top of the blot and gel images.

across Malian *Xoo*. Furthermore, both *talF* and *talC* specific molecular markers were simultaneously detected in all surveyed Malian strains, suggesting that the corresponding TALEs are broadly deployed by Malian *Xoo* to redundantly target the *OsSWEET14* gene promoter.

Malian *Xoo* Strains Exhibit *OsSWEET14*-Inducing Activity That Is Unaffected by Single TalC or TalF EBE Disruption

In order to functionally corroborate the hypothesis that a majority of the Malian *Xoo* strains deploys TalC and TalF to redundantly induce the *OsSWEET14* gene, we examined the ability of a set of 12 Malian strains, including those profiled above for *tal* effector genes, to induce *OsSWEET14* following leaf infiltration of the TalC EBE-edited line *sweet14-32*, the TalF EBE-edited line *sweet14-15* or the wild type Kitaake background variety. The resulting real time RT-PCR data is summarized in **Figure 3**. First, for all strains the *OsSWEET14* expression ratio relative to water infiltrations in Kitaake was superior to the negative control BAI3ΔtalC mutant strain at significant statistical levels ($p < 0.05$), indicating that these strains express at least a TALE targeting this gene. Second, with the exception of the control PX086 strain which is unable to induce *OsSWEET14* in a *sweet14-15* background because the AvrXa7 EBE of this allele is edited, all Malian strains caused *OsSWEET14* induction at ratios significantly superior to the corresponding control BAI3ΔtalC mutant strain revealing that they possess TalF EBE-independent *OsSWEET14* inducing activity. Finally, when assayed on the TalC EBE-edited line *sweet14-32*, and consistent with previous reports (Blanvillain-Baufumé et al., 2017), BAI3 failed to induce expression of *OsSWEET14* above the corresponding control BAI3ΔtalC mutant. Likewise, MAI68 did not induce *OsSWEET14* expression above the BAI3ΔtalC mutant control indicating that similar to BAI3 (Yu et al., 2011), this strain exclusively relies on TalC EBE-dependant activity for *OsSWEET14* targeting. Albeit to a more varying extent than on other rice backgrounds, all other Malian strains produced *OsSWEET14* expression ratio that were superior to the negative control BAI3ΔtalC mutant strain at significant statistical levels ($p < 0.05$), indicating that these strains possess TalC EBE-independent *Os*SWEET14 inducing activity.

This data therefore demonstrate that all 12 Malian strains possess *OsSWEET14*-induction activity and that, with the exception of MAI68, this activity is insensitive to single TalF- or TalC-EBE disruption. On another hand, our previous genotyping

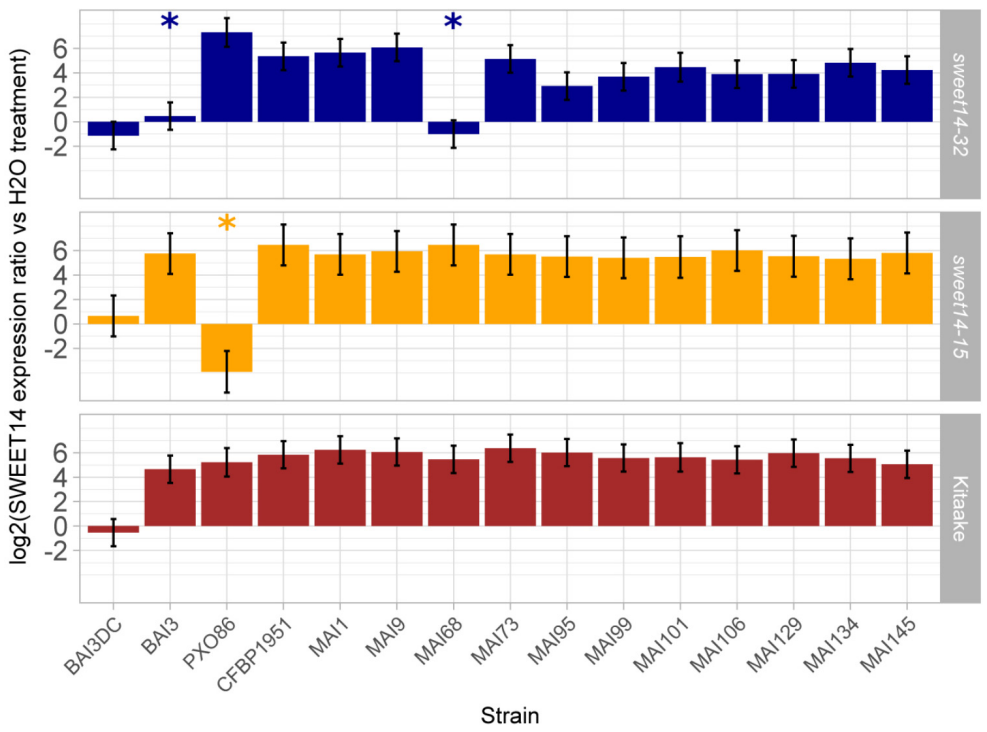

FIGURE 3 | Profiling Malian strains *OsSWEET14*-induction activities on EBE edited rice lines. Q-RT-PCR was conducted on rice RNA extracted from leaf samples 48 h after infiltration of the designated bacterial strains (BAI3DC refers to the *talC* mutant of BAI3). The barplot reports least-square means and standard errors computed from a mixed linear model of the $\log_2$-transformed SWEET14 induction ratio relative to water treatment of the corresponding rice line (174 observations from four independent experiments). Likelihood ratio tests demonstrated that the model explaining *OsSWEET14* induction ratio as a function of rice line and strain and including a random component performed better than a model incorporating fixed effects alone (L-ratio = 195.48; p-value < 0.00001). The null hypothesis that induction ratio is inferior or equal to the value of the negative control strain BAI3DC was systematically rejected (p-value < 0.05 with Sidak adjustment method) except for treatments designated with an asterisk.

data advocates for the simultaneous presence of the *talF* and *talC* genes in these genomes. Taken together, these observations suggest that most Malian *Xoo* exhibit internal redundancy in TALE repertoires for *OsSWEET14* gene induction, and that they presumably rely simultaneously on TalF and TalC TALEs for that purpose.

Whole Genome Sequencing of Eight Malian Strains

Single molecule, real-time (SMRT) sequencing (Pacific Biosciences) or 'PacBio' sequencing has been recently used for *X. oryzae* whole genome assembly and was shown to accurately and exhaustively reconstruct *tal* genomic sequences (Booher et al., 2015; Wilkins et al., 2015; Grau et al., 2016; Huguet-Tapia et al., 2016; Tran et al., 2018), surmounting the shortcomings of other NGS technologies to handle the repetitive nature of the CRR coding sequence. Available data on the genetic diversity of Malian *Xoo* strains is currently limited to MLVA typing (Poulin et al., 2015) and only one finished genome was sequenced (Tran et al., 2018). A more refined analysis of this genetic diversity, especially with regard to *tal* gene repertoires is critical to inform deployment of resistance genes and to design novel resistance by the creation of TALE unresponsive susceptibility genes alleles through EBE editing. We therefore performed *de novo* genome sequencing using the PacBio technology for selected Malian strains recently isolated (2010–2013) in the *Office du Niger* rice growing region with the aim of maximizing diversity in terms of virulence profile, genotype of the host of origin and *tal* haplotype. Hierarchical genome assembly of the PacBio data yielded a complete circular chromosomal sequence for all eight Malian strains with coverage above ∼130× (**Table 1**).

Next, to examine the position of these strains in the established phylogeny of *X. oryzae*, a set of core genome SNPs was obtained using the parsnp module of the Harvest suite for genome multiple alignments (Treangen et al., 2014). On average, the core genome amounted to 67% of a genome sequence and a set of 129,898 SNPs could be called from this alignment. The analysis included genomes from reference strains representative of each of the previously defined major *X. oryzae* clades (Gonzalez et al., 2007; Triplett et al., 2011; Hajri et al., 2012): Asian *Xoo*, Asian *Xoc*, African *Xoc*, the *X. campestris* pv. *leersiae* NCPPB4346 strain, a pathogen of southern cutgrass (Parkinson et al., 2009; Triplett et al., 2011) and African *Xoo*. Finally, the X11-5A US strain, belonging to a more distant clade (Triplett et al., 2011), was used as an outgroup for rooting the tree. Evolutionary relations were reconstructed using a maximum likelihood approach and the resulting best tree plotted on **Figure 4**. Consistent with the disease symptoms caused on rice and their sampling location, all eight newly sequenced Malian strains clustered within the African *Xoo* group (**Figure 4**). Interestingly, MAI134, the only strain isolated from tissues sampled from the perennial grass *O. longistaminata* (**Table 1**) branches out earlier and is the most divergent African *Xoo* in this dataset. The other seven genomes fall in a single group separate from the MAI1 reference and appear to be highly related with a number of polymorphic positions in pairwise comparisons of core SNPs haplotypes between strains of this group ranging only from 1 to 22 (**Supplementary Figure S3**). Accordingly, multiple genome alignment of the African *Xoo* sequences performed with Mauve (Darling et al., 2010) revealed a high degree of shared synteny and, with the exception of CFBP1947, as pointed out before (Tran et al., 2018), no major structural rearrangement (**Supplementary Figure S4**).

In conclusion, genomic analysis of the finished genomes obtained from eight Malian isolates confirms that they genetically belong to the African *Xoo* group and that, with the exception of MAI134, they form a highly related group.

Comparative Analysis of Malian Strains *tal* Effector Gene Repertoires

We then focused on the comparative analysis of *tal* effector gene repertoires to evaluate the nature and extent of TALE diversity in this set of genomes. To this end, the Malian genomes were searched for *tal* coding sequences (**Supplementary Table S1**). As before for strains MAI1, BAI3, and CFBP1947 (Tran et al., 2018), each was found to harbor nine *tal* genes that are highly syntenic (**Supplementary Figure S5**). These CDS were extracted and classified using the DisTAL module of the QueTAL suite that attempts to reconstruct evolutionary lineages based on the relatedness of the strings of unique repeat units amino acid sequences in the TALEs central region (Pérez-Quintero et al., 2015). The neighbor-joining tree obtained using DisTAL distances among African TALEs reproduced in **Figure 5A** indicates that TALEs from this new set of genomes belong to one of the nine African TALE groups previously defined by Tran et al. (2018). Furthermore, all genomes code for a single member of each group.

TABLE 1 | Origin and genomic features of the Malian strains selected for genome sequencing.

Strain	Region	Site	Year	Host	Genome size (bp)	Coverage	GB accession
MAI68	Office du Niger	Niono	2010	Huang Huazhon	4703782	213	CP019085
MAI73	Office du Niger	Niono	2012	Adny11	4703982	373	CP019086
MAI95	Office du Niger	Niono	2012	Adny11	4705038	155	CP019087
MAI99	Office du Niger	Niono	2012	Adny11	4698819	193	CP019088
MAI106	Office du Niger	Niono	2012	Adny11	4705454	374	CP019089
MAI129	Office du Niger	Bewani 1	2013	Adny11	4703963	169	CP019090
MAI134	Office du Niger	Kala 3	2013	*O. longistaminata*	4730142	263	CP019091
MAI145	Office du Niger	Kouroumari	2013	Kogoni91-1	4703977	136	CP019092

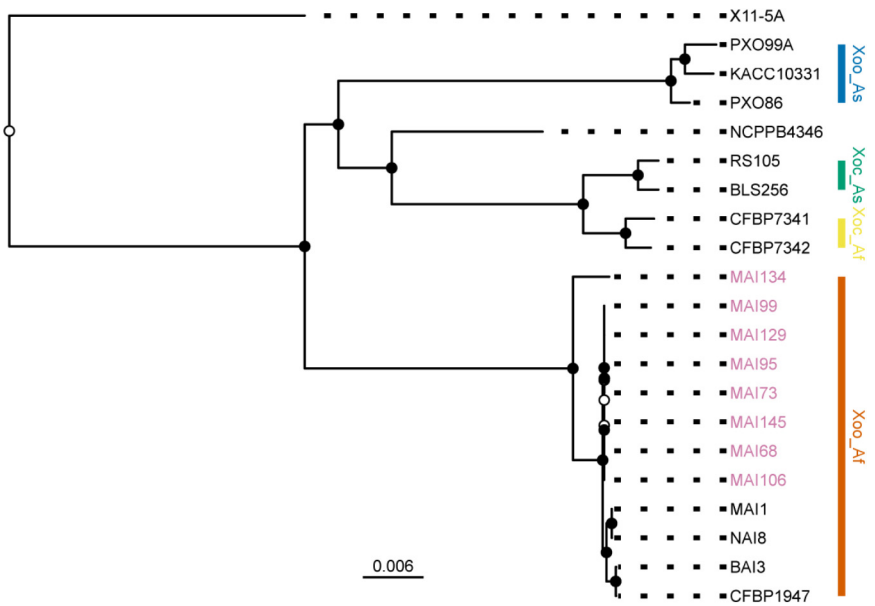

FIGURE 4 | Position of the sequenced Malian *Xoo* strains in the *X. oryzae* phylogeny. Plot of the RAxML tree obtained from a core genome SNPs alignment composed of the PacBio sequenced Malian strain haplotypes (pink strain labels) and reference strains representative of major genetic groups in the *X. oryzae* phylogeny. The *X. oryzae* X11-5A strain served as an outgroup for rooting the tree. The main clades are highlighted with a colored vertical bar. Abbreviations for the label of the clades are as follows: Xoo, *X. oryzae* pv. *oryzae*; Xoc, *X. oryzae* pv. *oryzicola*; As, Asia; Af, Africa. Internal nodes were colored in black when bootstrap support values were above 80. The scale bar at the bottom of the tree reflects branch length in mean number of nucleotide substitutions per site.

Thus, the newly sequenced Malian genomes do not reveal any unrelated TALE defining a new African group. However, the analysis of either RVD sequences (**Figure 5B**) or unique repeat units strings ('DisTAL sequences') (**Supplementary Figure S6**) similarity to measure intra-group diversity identified several new variants and yields some insight on *tal* repertoires variability across strains. As depicted in **Figure 5B**, when considering RVD sequences, new variants could be identified in our set of genomes in all but two TALE groups. For example, contemporary Malian strains encode a new variant of the TalD and TalG groups that were previously shown to be conserved across MAI1, BAI3, and CFBP1947 (Tran et al., 2018). Likewise, we found two new variants for the TalI and TalB groups. In contrast, despite a more comprehensive set of African genomes, the TalC and TalE groups remain strictly monomorphic at the RVD sequence level but polymorphic at the repeat sequences level (**Supplementary Figure S6**). Another observation, derived from the heatmap of **Figure 5B**, and mirroring the *tal* haplotypes shown in **Figure 2A**, is that strains MAI68, MAI99, and MAI134 exhibit distinct TALE RVD sequence variant profiles that are all different from the MAI1 reference. The five other strains displayed a Southern blot pattern identical to MAI1 (**Figure 2A**). Based on the analysis of their finished genome sequence, they share the same TALE RVD sequences content which is, however, distinct from MAI1 (**Figure 5B**).

In order to examine the differences in repeat array regions underlying each variant within individual TALE groups, we generated in **Supplementary Figure S7** multiple alignments of DisTAL sequences that allowed the insertion of gaps to maximize alignments (Pérez-Quintero, 2017). Two main type of variation seems to occur in these alignments. The TalA group for example (**Figure 5C**) but also the TalB (see below and **Figure 6B**), TalH and TalI groups (**Supplementary Figure S7**) harbor variants that may have arisen from the insertion/duplication or deletion of an internal block of several contiguous repeats in an ancestor variant. A second type of variation, that could be described as single repeat polymorphism, occurs pervasively in most African TALE groups but one of the most extreme examples is probably the TalG group (**Figure 5D**) where up to 12 positions out of 17 contain 2–3 unique repeat types that may (positions 3, 9, 11, 12, and 17), or may not, hold polymorphic RVDs. This repeat polymorphism splits TalG variants into two subgroups: one of them is composed of variants from all contemporary Malian strains while the other contains variants from the previously sequenced African *Xoo* genomes. Regardless of the type of variation, within an African TALE group, variants differences are often predicted to have marked repercussions on their respective set of rice target genes (**Supplementary Figure S8**). Indeed, for example, none of predicted rice gene targets for the TalG variant of contemporary Malian strains is shared with the ones predicted for the other variant.

In conclusion, within established evolutionary TALE groups, genome sequencing and comparative analysis identified several novel African TALE variants with distinct predicted target specificities. Two of them, namely TalC and TalE, were however, found to be invariant in terms of RVD sequence.

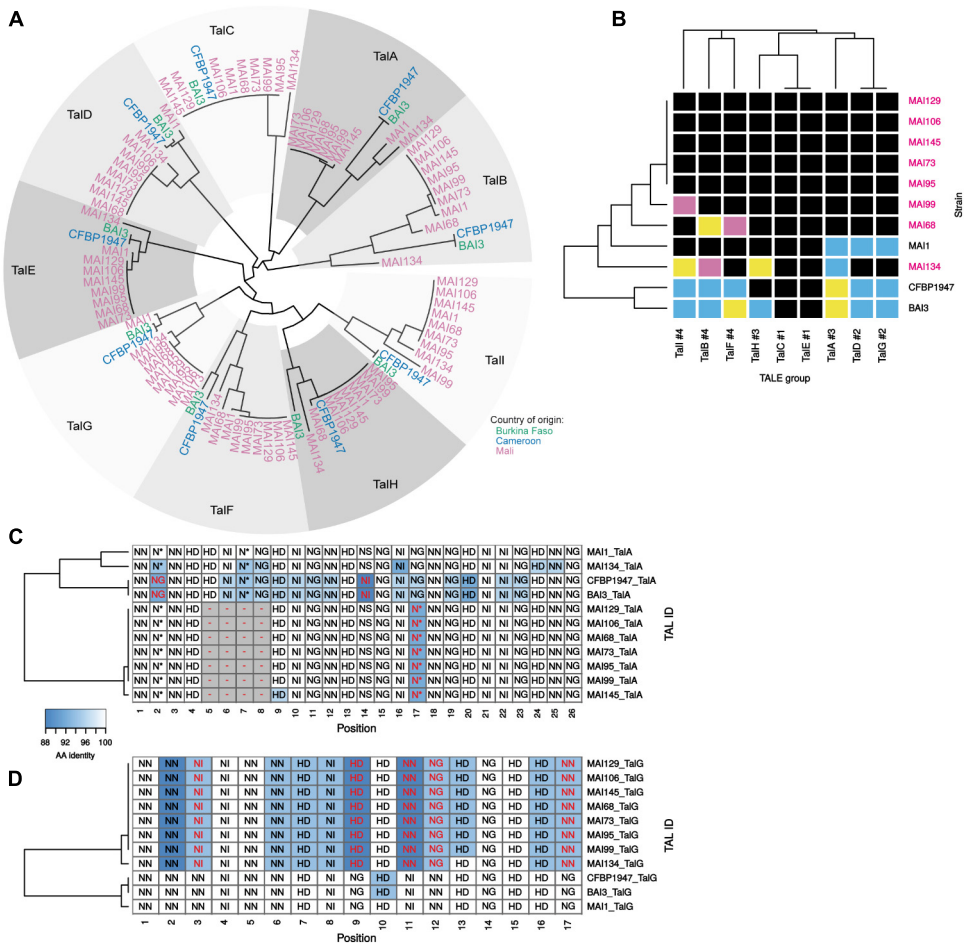

FIGURE 5 | *In silico* analysis of the diversity of *tal* genes content of Malian strains. **(A)** DisTAL neighbor-joining phylogenetic tree and group classification of *tal* genes. All detected *tal* genes in available complete genomes of African strain (colored tip labels) were assigned to one of the previously defined African TALE groups (Tran et al., 2018) (gray level colored sectors) based on their position in the tree topology. **(B)** Diversity of African *Xoo* strains TALE RVD sequence variants in each TALE group. Within each TALE group (columns) and across strains (rows), individual cell colors code for distinct TALE RVD sequence variants. The number following the pound sign in the label of the TALE groups designates the total number of unique variants found for this group in this genome set. Malian strains whose genome was determined in this work are labeled in pink. Multiple alignments of the African TALE central repeat regions based on DisTAL repeat unit sequences for the TalA **(C)** and TalG **(D)** groups. Cell coloring reflects amino-acid identity between each repeat and the MAI1 TALE repeat at this position that was used as a reference. Each cell is labeled with the RVD encoded by the corresponding repeat. RVDs that are different from the corresponding MAI1 reference at this position are colored in red font. Gaps introduced to maximize the alignment score are colored in gray.

RVD Sequence Polymorphism in the TalF and TalB Group Is Associated With Distinct Induction Patterns of the Corresponding Rice Target Genes

To explain *tal* typing and *OsSWEET14*-induction profile data, we proposed above that, similar to MAI1 (Tran et al., 2018), a majority of the Malian *Xoo* strains possess a version of both TalF and TalC, each being active on *OsSWEET14*. Our Malian *Xoo* genome sequences conclusively support this hypothesis: all TalC variants are strictly identical in terms of RVD sequence and, apart from MAI68, all Malian TalF variant RVD sequences are also identical (**Figure 5B** and **Supplementary Figure S7**). $TalF_{MAI68}$ appears to deviate from other members of the group only at the level of its last three repeats (**Supplementary Figure S7**). $TalF_{MAI68}$ may fail to induce *OsSWEET14* because it is unable to recognize its EBE. Consistent with this view, while *OsSWEET14* is the fifth best predicted target of $TalF_{MAI1}$, it only ranks at the 3906th position in Talvez EBE predictions (Pérez-Quintero et al., 2013) for $TalF_{MAI68}$ (see **Supplementary Figure S9**). In line with this, we examined the extent to which individual RVDs of active (MAI1) or inactive (BAI3) TalF variants are likely to recognize their cognate nucleotide along the DNA sequence of the TalF EBE in the *OsSWEET14* promoter (**Figure 6A**). $TalF_{BAI3}$ fail to recognize this target sequence possibly due to suboptimal pairing between positions 5 and 8 (Tran et al., 2018). Each of the last three polymorphic RVD (position 15–18) of $TalF_{MAI68}$, including the NN at position 17 which is present in place of the strong HD of $TalF_{MAI1}$, are predicted to be suboptimal for recognition of the cognate

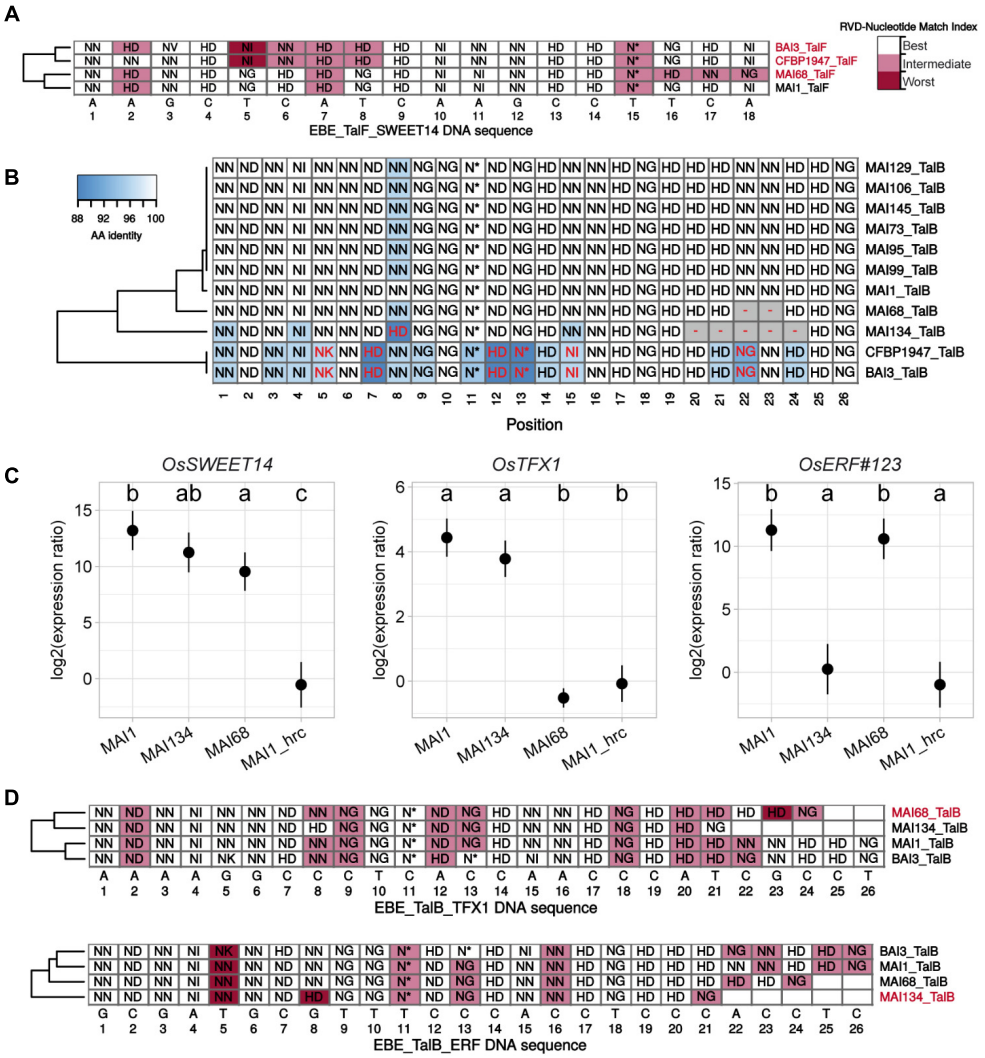

FIGURE 6 | RVD sequence variability in the TalF and TalB groups has functional consequences on target gene induction activity. **(A)** Plain multiple alignment of selected TalF group RVD sequences (no gap allowed) along the DNA sequence (position| nucleotide as column labels) of $TalF_{MAI1}$ predicted EBE on the promoter of *OsSWEET14* in the Nipponbare genome. A background color was assigned to each RVD based on the quality of the match between this RVD and the MAI1 TalF EBE nucleotide at this position. A RVD-nucleotide pair was classified in the 'Best' category if this nucleotide is the one with the best score in the RVD-nucleotide association matrix used by Talvez. It was assigned to the 'Worst' category if it corresponded to the worst score in the association matrix and in the 'Intermediate' category otherwise. TALE variants with labels colored in pink do not presumably recognize the corresponding EBE. **(B)** Multiple DisTAL repeat unit sequences alignments of the central repeat regions of TALEs from the TalB group. See the legend of **Figure 5** for details. **(C)** Target gene induction capacity of Malian strains MAI68 and MAI134 encoding TalB variants with repeat deletions. Q-RT-PCR was conducted on rice cultivar Kitaake total RNA extracted from leaf samples 48 h after infiltration of the designated bacterial strains. MAI1_hrc corresponds to the Type III Secretion System mutant derivative of MAI1. Average (points) and standard deviation (lines) of log_2-transformed target gene (plot label) induction ratios relative to water treatment were computed from three biological replicate samples. Means having identical letters on top of the plotting area are not significantly different based on a Tukey's HSD test ($a = 0.05$). This experiment was performed twice with similar results. **(D)** Plain multiple alignment of selected TalB group RVD sequences (no gap allowed) along the DNA sequence (position| nucleotide as column labels) of MAI1 TalF predicted EBE on the promoter of *OsTFX1* or *OsERF#123* in the Nipponbare genome. See the legend of **(A)** for details.

nucleotide, leaving a productive recognition scaffold of only 14 RVDs. Altogether, this suggests that MAI68 lacks TalF activity because the corresponding TALE variant is unable to bind the canonical EBE in the *OsSWEET14* promoter of the Nipponbare genome.

It has been recently discovered that the MAI1 and BAI3 variants of TalB are both able to simultaneously upregulate two rice susceptibility genes, *OsTFX1* and *OsERF#123* (Tran et al., 2018). Our genome sequences analysis reveals, however, that two strains, MAI68 and MAI134 encode shorter TalB group variants with a deletion of a block of, respectively, 2 and 5 repeats, in the C-terminal portion of the central domain (**Figure 6B** and **Supplementary Figure S7**). This prompted us to examine this additional TALE group with documented targets for altered induction activity of polymorphic variants. To this end, strains MAI68, MAI134, and MAI1, acting as a positive induction

control, were infiltrated into the leaf apoplast of Kitaake plant and tissues were sampled after 48 h. As shown in **Figure 6C**, induction of *OsTFX1*, *OsERF#123,* and *OsSWEET14*, as a control, was measured by qRT-PCR in total RNA extracted from theses samples. Consistent with data from **Figure 3**, all three strains induced *OsSWEET14* well above the background levels measured for the MAI1 Type III secretion minus mutant strain negative control. In contrast, *OsTFX1* and *OsERF#123* induction patterns proved to be different from *OsSWEET14*: while both genes were induced by the MAI1 positive control relative to the background levels defined by the MAI1 Type III secretion minus mutant values, MAI134 induced *OsTFX1* but not *OsERF#123* expression. The MAI68 strain had an opposite activity, inducing only *OsERF#123* but not *OsTFX1* expression (**Figure 6C**). This is a strong indication that these TalB variants have differentially lost the ability to recognize one of the documented targets of the group. We wondered if the inability to induce one of the two TalB susceptibility targets had an impact on the virulence of these strains on Kitaake. A Dunnet's test comparing mean lesion length obtained on Kitaake with MAI68 or MAI134 against the value obtained with MAI1 found no statistical difference (Adjusted p-values > 0.05) in data from three out of four of the replicate experiments performed for **Figure 1**. It therefore appears that in our experimental conditions, those strains have no reproducible virulence defect and behave as MAI1.

To understand why, in contrast to $TalB_{MAI1}$, $TalB_{MAI68}$, and $TalB_{MAI134}$ specifically fail to recognize the *OsTFX1* and *OsERF#123* EBEs, respectively, we first examined the results of Talvez predictions for these TALE-target pairs (**Supplementary Figure S9**). Consistent with target genes induction patterns, *OsTFX1* was absent from the list of the first 5000 best predictions of $TalB_{MAI68}$, likewise for *OsERF#123* with $TalB_{MAI134}$. Conversely, predictions scores for $TalB_{MAI68}$ on *OsTFX1* and $TalB_{MAI134}$ on *OsERF#123* where higher than the predictions scores for $TalB_{MAI1}$ on the corresponding targets. As above, we also inspected the expected fitness of individual RVD-nucleotide pairs alongside target DNA sequences (**Figure 6D**). For the *OsTFX1* EBE, $TalB_{MAI68}$ is shorter than active variants (24 versus 26 RVDs) and four of its last five RVD are suboptimal for recognition of the target nucleotides. Although $TalB_{MAI134}$ is even shorter (21 versus 26 RVDs), there is no such stretch of RVD-nucleotide mismatches and the substitution of NN at position 8 for a strong HD may compensate for a potential decrease in affinity of a shorter version. At the *OsERF#123* EBEs, it is possible that this substitution may in the case of the short $TalB_{MAI134}$ variant create a mismatch that disproportionately penalizes affinity for this DNA sequence.

In summary, comparative analysis of *tal* gene sequences assembled with the PacBio data identified variants in the TalF and TalB groups with modified rice gene target induction specificity relative to group founders in MAI1 and BAI3 strains. Intriguingly, the TalB group variants presumably remain functional but have lost the ability to induce one of the two documented susceptibility targets of TalB group founders without a detectable effect on virulence.

DISCUSSION

Bacterial leaf blight can represent a significant constraint to production in some rice growing areas of West Africa, notably in the irrigated perimeters of *Office du Niger* in Mali. A few resistance genes originally identified using Asian *Xoo* strains (Zhang and Wang, 2013) are also effective against West African strains (Gonzalez et al., 2007; Sarra et al., 2010) and could be readily deployed in breeding programs. To further expand the host genetic arsenal available to control BLB in Mali, this study initially aimed at assessing recently documented resistance alleles of the *OsSWEET14* susceptibility gene that loss responsiveness to the African TALE TalF for protection against Malian *Xoo* strains. Although *xa41(t)*, a *OsSWEET14* resistance allele identified in *O. barthii* and *O. glaberrima* African rice was previously shown to be effective against half of a worldwide diversity set of *Xoo* strains in a water-soaking assay after leaf infiltration (Hutin et al., 2015b), we unexpectedly found that most of the Malian strains isolated after 2009 were virulent on the CG14 accession bearing *xa41(t)* in leaf clipping assays (**Supplementary Figure S1**). In parallel, we tested the equivalent *sweet14-15* edited allele (Blanvillain-Baufumé et al., 2017) carrying also a lesion in the TalF EBE. Eleven Malian strains, including CFBP1951 and MAI9 that were previously shown to be controlled by the *xa41(t)* allele, were all as virulent on the *sweet14-15* genotype as on the parental Kitaake variety (**Figure 1**). In agreement with this, TalF is not the only TALE required for susceptibility gene induction by Malian strains because all Malian strains tested were able to up-regulate *OsSWEET14* in the TalF EBE edited line (**Figure 3**). We therefore propose that the resistance observed on rice accessions carrying *xa41(t)* against Malian strains is attributable to other unrelated resistance loci present in these genetic backgrounds. Furthermore, based on our data, TalF-unresponsive *OsSWEET14* alleles appear of limited practical value to control BLB caused by contemporary *Xoo* strains in Mali.

The lack of protective effect of TalF-unresponsive alleles is most probably due to the widespread if not the universal presence of an active *talC* gene in the genomes of contemporary Malian strains in addition to *talF*. Tran et al. (2018) recently discovered that the Malian *Xoo* strain MAI1 contains one active copy of both *talC* and *talF*. We further demonstrate that single EBE disrupted alleles of the *OsSWEET14* promoter still respond to MAI1 and to most of the 12 Malian *Xoo* tested (**Figure 3**). Moreover, *tal* haplotype characterization, PCR-based detection of *talC* sequences (**Figure 2**) and ultimately PacBio sequencing of eight *Xoo* strains (**Figure 5**) support the view that the Malian *Xoo* genetic diversity possess redundant TalF and TalC activities on *OsSWEET14*. Redundant targeting of the *SWEET* component of susceptibility is not unique to Malian *Xoo*. A significant proportion of tested Asian strains (∼40%) also adopted this strategy but implement it by targeting several (up to three) clade-III *OsSWEET* genes using a distinct TALE for each one of them (Parkinson et al., 2009). In principle, engineering TALE-unresponsive alleles for resistance against most Malian *Xoo* would require to edit both the TalC and TalF EBEs on the *OsSWEET14* promoter to abrogate induction of this susceptibility gene. Based on the phenotype of TalC EBE edited lines that

remain susceptible to the Burkinabe BAI3 (Blanvillain-Baufumé et al., 2017) and the Malian MAI68 (**Figure 1**) strains possessing TalC-activity only, one would, however, predict that a double edited *OsSWEET14* promoter unresponsive to Malian strains will not provide resistance. The failure to confer enhanced BLB resistance against the BAI3 strain despite unchanged clade-III *OsSWEET* expression has been hypothesized to originate from the presence of another genetically redundant TalC target of unknown nature (Blanvillain-Baufumé et al., 2017). Our results provide evidence that TalC is both widespread and highly conserved in Malian *Xoo*. It will therefore be critical to identify this redundant target if broad resistance against the African *Xoo* characterized to date is to be engineered utilizing genome editing technologies.

PacBio sequencing, assembly and analysis of eight finished *Xoo* Malian genomes provided valuable insight on the genetic diversity of contemporary *Xoo* strains in this country. The phylogenetic position of some of the contemporary Malian strains, namely, MAI73, MAI95, MAI99, and MAI106 was previously investigated using a MLVA scheme (Poulin et al., 2015). They were all shown to belong to a sub-cluster composed of Malian strains collected between 2010 and 2012 in *Office du Niger* and separated from another sub-cluster including MAI1 and composed of Malian strains isolated earlier. Our phylogenetic tree based on whole genome core SNP markers (**Figure 4**) also displays such a dichotomy between MAI1 and more recently collected strains which form a group of highly related genomes both in terms of DNA sequence identity and overall genome collinearity. Interestingly, *Xoo* MAI134 is the most divergent genome belonging to the African *Xoo* group and it clusters separately from the other Malian strains. To our knowledge, it is the first *Xoo* genome of a strain isolated from a wild rice species, in that case, *O. longistaminata*. The apparent divergence relative to other Malian genomes could be a consequence of a separate evolutionary path for specialization on this wild host. Sequencing the genome of additional *Xoo* strains isolated from wild rice would help address this question.

Our analysis of the finished Malian *Xoo* genomes extends previous foundational work on three African *Xoo* genomes from strains isolated in Cameroon, Burkina Faso, and Mali (Huguet-Tapia et al., 2016; Tran et al., 2018). We further characterized the nature and extent of the diversity of the genomic repertoires of *tal* effector gene homologs in a larger dataset. One interesting finding is that the new genomes also individually encodes nine TALEs each belonging to one of the nine previously defined groups of evolutionary related TALEs. Similar approaches identified in the order of 30 such groups or classes in Asian *Xoo* (Grau et al., 2016; Quibod et al., 2016). The limited number of TALE groups in African *Xoo* is intriguing. It could be due to incomplete sampling of this diversity but also probably reflects a narrower genetic basis of African *Xoo* populations mirroring the limited diversity of traditional African rice host genotypes (Vaughan et al., 2008). This restricted number of TALE groups may be somehow counter balanced by intra-group variability. Indeed, we describe new variants for all of the variable TALE groups and the TalD and TalG groups that were previously thought to be conserved in terms of RVD sequences (Tran et al., 2018) appear to be variable as well. The observed differences within TALE groups encompass repeat amino acid sequence polymorphism outside the RVD, polymorphic RVDs and insertion/deletion events of stretches of repeat units. As the number of *tal* sequences in databases is dramatically increasing the molecular mechanisms responsible for *tal* sequence variation are beginning to be deciphered and seem to include both point mutation and recombination between repeats (Erkes et al., 2017; Pérez-Quintero, 2017; Tran et al., 2018).

Long-read sequencing has made TALE diversity mining a straightforward task. As this diversity in *Xoo* populations is being increasingly recognized, new fundamental issues about TALEs biology and evolution are emerging. These questions will also be relevant for rice breeding because they may inform genetic disease resistance design and deployment strategies. In this regard, one of the most important challenges is to understand the significance of RVD sequence variability or conservation within TALE groups in terms of the underlying selective forces promoting this diversity. Does variability entails functional differences in host target gene sets providing a fitness benefit? Or, is this variability simply neutral with respect to susceptibility target specificity because of the tolerance to mismatches of the RVD-nucleotide recognition code? Variability within a TALE group could be a sign that diversifying selection is driving evolution of the corresponding genes. Two selective forces may promote diversification of TALE: escaping detection by a decoy *R* gene while potentially maintaining control over the cognate susceptibility gene target(s) or overcoming loss-of-TALE-responsiveness resistance alleles of susceptibility genes. While strict conservation of some TALE groups, such as TalC and TalE (**Figure 5B**), is generally understood as a clue that cognate host gene targets are important for susceptibility, because of strong purifying selection, it is also perhaps the sign that these variants are not engaged by TALE-dependant immune systems in the genetic pool of African *Xoo* hosts.

The case of the TalF group in African *Xoo* illustrates some of these considerations. $TalF_{BAI3}$ has previously been shown to be unable to recognize the *OsSWEET14* promoter in contrast to $TalF_{MAI1}$ (Tran et al., 2018). We identified a novel TalF variant from strain MAI68 that is also presumably unable to up-regulate this susceptibility gene. To integrate this observation with our current knowledge, we propose an evolutionary scenario whereby ancestral Malian strains were equipped with a functional $TalF_{MAI1}$-like TALE for *OsSWEET14* induction. However, the emergence of TALE-unresponsive *xa41(t)* resistance allele, which is present in all surveyed accessions of the domesticated *O. glaberrima* African species (Hutin et al., 2015b) must have exerted a strong selection pressure. Acquisition of *talC* lifted this barrier to colonization and resulted in the general spread of this effector gene in West African *Xoo* populations.

In this study, we also describe another case of target specificity shift for variants within the TalB group. The MAI1 and BAI3 founding members regulate two rice susceptibility genes, *OsTFX1* and *OsERF#123* (Tran et al., 2018). We discovered that strains MAI68 and MAI134 possess TalB variants with deletions of several repeats in the C-terminal region of the CRR and that they are incapable of inducing one of the two targets: *OsTFX1* for

$TalB_{MAI68}$ and *OsERF#123* for $TalB_{MAI134}$. Considering that these strains did not show reduced virulence relative to MAI1 in our assays (**Figure 1**), it is possible that these susceptibility targets are genetically redundant. Alternatively, unknown mechanisms may compensate the absence of induction of one of the susceptibility genes.

Using the RVD-nucleotide association code, we attempted to mechanistically explain the failure of some TalF and TalB variants to recognize cognate EBEs (**Figures 6A,D**). While formal demonstration of these hypotheses will require further experimental evidence, they are consistent with the concept of 'strong RVD' (Streubel et al., 2012) and with the influence of CRR repeat number on the effect of RVD-nucleotide mismatches on overall DNA affinity (Rinaldi et al., 2017). Ours results argues in favor of the idea that RVD sequence variability within TALE groups is not always neutral relative to the set of direct host gene target(s) and leads to distinct targets induction patterns by RVD polymorphic TALEs. However, at least for the TalB group, there are substantial differences between the BAI3 and the major Malian variant (**Figure 6B**) with, as yet, no detectable consequence. We observed that prediction scores for the TalB and TalF variants that have lost targeting specificity for a host gene are consistently lower than scores for the variants that are able to recognize that target. Examining the overlap of predicted target sets between variants revealed that for many of the variable African *Xoo* TALE groups predicted specificity also varies greatly (**Supplementary Figure S8**), indicating that if any, relevant targets may not be consistently induced by variants. Ultimately, systematic approaches to study the effect of TALE variants on functionally relevant target gene induction should yield crucial insight on these issues. Wilkins et al. (2015) have observed a conservation of the specificity for confirmed target(s) of a reference *Xoc* TALE when variants within that group differed by no more than six RVDs. Reminiscent of our findings regarding African *Xoo* TalB variants, another study reported on several *Xoc* TALE groups where different variants may have contrasted abilities to induce predicted targets (Erkes et al., 2017). In the future, relational databases such as daTALbase (Pérez-Quintero et al., 2017), that integrate massive TALE-centered 'omic' information should facilitate even more comprehensive inquiries, and help explore for example whether 'divergent' variants of a TALE group are predicted to gain the capacity to induce a polymorphic version of the target in another rice genome.

CONCLUSION

This work demonstrated that Malian *Xoo* populations circumvent unresponsive alleles of the susceptibility gene *OsSWEET14* by combining redundant *talF* and *talC* genes which makes this type of resistance unsuitable for control of BLB in the country. Genome sequence analysis further showed that most contemporary Malian strains are highly related but nevertheless harbor *tal* effector gene repertoires encoding polymorphic TALE groups that have contrasted abilities to induce documented susceptibility target genes, potentially underlying host adaptation at a small evolutionary scale.

MATERIALS AND METHODS

Bacterial Strains, Growth Conditions and DNA Isolation

The *Xoo* bacterial strains used in this study for leaf clipping and infiltration assays were as follows: wild-type PXO86 (Vera Cruz, 1989), BAI3 (Gonzalez et al., 2007), the BAI3 *talC*$^{-}$ knockout derivative (Yu et al., 2011), a MAI1 Type III Secretion System mutant and Malian *Xoo* strains (Poulin et al., 2015; Tekete and Verdier, manuscript in preparation). The isolates were maintained in 15% glycerol at −80°C. All *Xoo* strains were cultivated on PSA (10 g/liter peptone, 10 g/liter sucrose, 1 g/liter glutamic acid, 15 g/liter Bacto Agar) except BAI3ΔTalC that was grown on PSA supplemented with 50 μg/ml kanamycin. The isolates were incubated at 28°C for 48 h.

For DNA extraction of Malian *Xoo*, two loops of bacterial cultures grown on PSA were washed twice with sterilized water. The genomic DNA was extracted using either the Wizard genomic DNA purification kit (Promega) for Southern Blot assays, or with the DNeasy DNA extraction kit (Qiagen) for Pacific Biosciences single molecule real time sequencing following the manufacturers' instructions.

Leaf Clipping Assay

To evaluate the virulence of Malian *Xoo* strains, three lines of rice were used: Kitaake wild-type, *sweet14-32* (the TalC EBE edited line) and *sweet14-15* (the TalF and AvrXa7 EBEs edited line) described in Blanvillain-Baufumé et al. (2017). Plants were grown under greenhouse conditions under the following cycles of 12 h of light at 28°C and 80% relative humidity and 12 h of dark at 25°C and 70% RH. For inoculation, 2 days old *Xoo* cultures were resuspended in sterilized water and leaves of 6-week-old plants were cut with scissors previously dipped in bacterial suspensions at an OD600 = 0.2. The infected plants were kept in the green house for 14 days until disease symptoms were evaluated by measuring lesion length on leaves.

RNA Isolation and qRT-PCR

To assess the induction of the *OsSWEET14* gene, leaves of 3-week-old plants were infiltrated with a needleless syringe with sterilized water or bacterial suspensions at an OD600 adjusted to 0.5 in water. Segments of inoculated leaf were collected 48 h after inoculation. Samples were ground into powder using the Qiagen Tissue-Lyser system. Total RNA was extracted using Trizol reagent (Invitrogen) following the manufacturer's instructions. After TURBO DNase treatment (Ambion), 1 μg RNA was reverse transcribed into cDNA using SuperScript III (Invitrogen). Real-time PCR was carried on a Lightcycler 480 System (Roche) with primer pairs specific for *OsSWEET14*, *OsTFX1*, *OsERF#123* or *EF-1 alpha* (GenBank accession: GQ848072.1) as described before (Blanvillain-Baufumé et al., 2017; Tran et al., 2018). Gene expression was calculated using the $2^{-\Delta\Delta Ct}$ method with *EF-1 alpha* acting as a reference gene and the data from the water

inoculated leaves of the corresponding rice genotype as the reference condition.

Statistical Analysis

Statistical tests for mean comparisons were performed in R (R Core Team, 2010) using standard functions. The R package nlme (Pinheiro et al., 2017) was used to perform linear mixed-effects modeling of *OsSWEET14* expression with $\log_2$-transformed qRT-PCR values computed as the response variable. This transformation was necessary to ensure homogeneity. The dataset included one value for each 'strain' and 'rice line' factor combinations obtained from four independent replicates of the whole experiment. The fixed effects of the final model included the variables 'strain' and 'rice line' and their interaction term. The structure of the random component consisted of a random intercept and a random slope for the 'rice line' factor both conditioned on a 'replicate experiment ID' factor. The procedure for model selection and validation followed advices from Zuur et al. (2009). Visual inspection of residual plots did not reveal any major deviation from homoscedasticity or normality. For *post hoc* analysis on the linear mixed effect model, pairwise comparisons were performed on least-squares means computed using the R package lsmeans (Lenth, 2016).

Southern Blot Analysis

Genomic DNA of the Malian *Xoo* strains was digested by BamHI (New England Biolabs). The digested DNA was separated in 1% agarose gel at 50 Volt for 72 h at 4°C and transferred to a nylon membrane (Roche) overnight. A 560 bp fragment corresponding to the coding sequence of the N-terminal of TalF from MAI1 was used as a probe and PCR amplified using GCAGCTTCAGCGATCTGCTC and TCAGGGGGGCACCCGTCAGT primers. DIG-High prime DNA labeling and detection starter kit II (Roche) was applied for probe labeling, hybridization and detection procedures according to the manufacturer's instructions.

talC PCR Marker

To detect the presence of *talC* sequences in *Xoo*, a pair of primers (forward TCTGCGTGCAGCCGATGACCC and reverse CCACCAGTGCCTCGTGGTGCTG) was designed to anneal on sites flanking the deleted region (**Supplementary Figure S2**) and amplified a ∼152 bp fragment from *talC* and a ∼224 bp from typical *tal* sequences. PCR used the GoTaq DNA Polymerase (Promega) and thermal conditions were as follows: an initial denaturation at 95°C for 5 min, followed by 28 cycles of denaturation at 95°C for 30 s, annealing at 64°C for 30 s and extension at 72°C for 1 min, followed by a final extension at 72°C for 5 min. PCR amplicons were separated in 1.5% agarose gel at 100 V for 45 min.

Genome Sequencing and Assembly

The *X. oryzae* pv. *oryzae* genome sequences were obtained using the SMRT technology (Eid et al., 2009). 20 kb SMRTbell templates libraries were sequenced on a PacBio RS II instrument with the P6-C4 chemistry at the Icahn Institute for Genomics and Multiscale Biology (New York, NY, United States). For each strain, 1–2 SMRT cells were employed to generate sequencing data equivalent to more than 100× genome coverage. Genome assembly was performed with version 3 of the HGAP pipeline (Rank et al., 2013) using default parameters. Circularization of the HGAP contigs was performed with Circlator (Hunt et al., 2015). In some instances (MAI134, MAI95), it was necessary to iteratively trim the ends of the initial HGAP contig by 2 kb increments until Circlator successfully circularize the sequence. For strain MAI99, circularization was achieved with the minimus2 pipeline[1]. The absence of obvious structural anomaly was manually verified by inspecting the coverage plot of mapped reads on the SMRT View browser. Genome sequence finishing included several rounds of Quiver polishing (RS_Resequencing protocol) until the count of variant ceased to decrease in additional polishing rounds.

Polished sequenced were submitted to GenBank under the accession numbers indicated in **Table 1** and automatically annotated with the NCBI Prokaryotic Genome Annotation Pipeline. The displayed multiple- whole genome alignment was generated with progressiveMauve and visualized using Mauve 2.4.0 (Darling et al., 2010).

Phylogenetic Analysis

In addition to the Malian genome sequences determined in this study, the following reference genomes (with GB accession or Bioproject ID) where obtained from GenBank: *Xoo* MAI1 (PRJNA427174), *Xoo* CFBP1947 (NZ_CP013666), *Xoo*, BAI3 (PRJNA427174), *Xoo* NAI8 (NZ_AYSX01000001.1), *Xoo* PXO99A (NC_010717.2), *Xoo* PXO86 (NZ_CP007166.1), *Xoo* KACC10331 (AE013598.1), *Xoc* BLS256 (NC_017267.2), *Xoc* RS105 (NZ_CP011961.1), *Xoc* CFBP7341 (NZ_CP011959.1), *Xoc* CFBP7342 (NZ_CP007221.1), *X. campestris* NCPPB4346 (NZ_LHUK01000001.1), *X. oryzae* X11-5A (LHUJ01000001.1). The core genome SNPs matrix for strains under analysis was generated with the aligner module parsnp of the Harvest suite v1.1.2 (Treangen et al., 2014) enabling the -x flag to filter out SNPs in regions of recombination. Phylogeny reconstruction was conducted with RAxML version 8.2.9 (Stamatakis, 2014) using the following relevant parameters: '-V -T 5 -f -N 1000 -m ASC_GTRCATX –asc-corr = lewis.' For tree inference, RAxML was run in the rapid Bootstrap analysis and search for best-scoring ML tree mode with 1,000 bootstrap replicates and SNP ascertainment bias correction. The GTR model of nucleotide substitution without rate heterogeneity and invariant site was selected based on preliminary tests with jModeltest 2.1 (Darriba et al., 2012). Trees manipulation and display were performed using the R packages ape (Paradis et al., 2004) and ggtree (Yu et al., 2017).

TALE Analysis

Genomes were scanned for presence of TALE coding sequences. This was made using both a hidden a hidden Markov model built from sequences from TALE (Finn et al., 2015) as well as blast

[1]https://github.com/PacificBiosciences/Bioinformatics-Training/wiki/Circularizing-and-trimming

(Altschul et al., 1997). CRRs and RVD sequences were extracted using an in-house perl script that identified the first seven amino-acids for each repeat based on known repeat sequences as included in the QueTAL suite (Pérez-Quintero et al., 2015).

Alignments of coded TALE sequences were made using the program Arlem (Abouelhoda et al., 2010), as implemented in DisTAL as previously described (Pérez-Quintero et al., 2015), the program was modified to output alignment scores normalized by alignment length. DisTAL was also modified to output groups of TALEs and multiple alignments for each group. The modified version can be found at https://sourceforge.net/projects/tal-evolution-scripts/ and will be added to the QueTAL suite. Groups of TAL effectors were defined by cutting a DisTAL tree at a height equivalent to a score of 4.8 (roughly equivalent to 75% of the alignment consisting of highly similar repeats).

Heatmaps and alignment visualizations were created using the complexHeamap package[2]. For alignments showing color-coded repeat as those in **Figures 5**, **6B**, a vector of colors was generated based on positions and distances of unique repeats in a NJ tree, for this, the tree was cut at a height equivalent to 95% amino-acid identity, and unique colors were assigned to each resulting subgroups of repeats. Colors were assigned based on the position of each subgroup in a tree using the hue_pal function of the scales package[3]. All other figures were generated using the ggplot2 package[4].

AUTHOR CONTRIBUTIONS

HD, GR, FA, and ET performed the experiments. HD, AP-Q, GR, BS, RK, and SC analyzed the data. CT contributed materials. HD, OK, VV, and SC planned and designed the research. HD and SC wrote an initial version of the manuscript that was subsequently critically revised by all authors.

FUNDING

This work was funded by a Monsanto's Beachell-Borlaug International Scholars Program Ph.D. fellowship awarded to HD and a 'Chercheur d'Avenir' grant from the Region Languedoc-Roussillon attributed to SC. AP-Q and GR were supported by a doctoral fellowships awarded by the Erasmus Mundus Action 2 PANACEA, PRECIOSA program of the European Community and the MESR (Ministére de l'Enseignement Supérieur et de la Recherche), respectively. The authors are grateful to IRD for the financial support provided to the JEAI CoANA.

ACKNOWLEDGMENTS

We are grateful to Robert Sebra for his advices on PacBio sequencing. We also thank Jonathan M. Jacobs for generating and sharing the MAI1 T3SS mutant strain.

[2]https://bioconductor.org/packages/release/bioc/html/ComplexHeatmap.html

[3]https://cran.r-project.org/web/packages/scales/index.html

[4]https://cran.r-project.org/web/packages/ggplot2/index.html

SUPPLEMENTARY MATERIAL

The Supplementary Material for this article can be found online at: https://www.frontiersin.org/articles/10.3389/fmicb.2018.01657/full#supplementary-material

FIGURE S1 | Scatter plot of the virulence of Malian strains on *O. glaberrima* cv. CG14 bearing *xa41(t)* versus the susceptible reference line Azucena. Each strain is represented by a colored point whose position reflects mean lesion length obtained 14 days after leaf clipping inoculation of CG14 (*y*-axis) or Azucena (*x*-axis). Vertical and horizontal error bars correspond to the standard error of the mean on CG14 and Azucena, respectively. The color of the dots matches the year of isolation of the strain (see color key on the plot). This graph aggregates data obtained in the course of four independent experiments. Each strain has been tested in at least two independent experiment and the statistics were computed based on at least three replicate measurements.

FIGURE S2 | The *talC* gene contains a 69 nucleotides deletion in the coding sequence of the N-terminal domain. Alignment of MAI1 *tal* coding sequences. Numbers on the right refer to positions relative the fist nucleotide of the initiation codon. The binding sites for the primers used for PCR amplification are depicted by underlined regions of the *talC* sequence.

FIGURE S3 | Pairwise counts of polymorphic SNPs across *X. oryzae* genomes included in the phylogenetic analysis. Counts were obtained by applying the dist.dna function from the ape package with the value 'N' to the model parameter to pairs of genomes in the multiple SNP alignment file generated by parsnp and that included 129,898 SNPs. Rows and columns are in the same order than tips in the RAxML tree of **Figure 4**.

FIGURE S4 | Whole genomes alignment of African *Xoo* strains. Snapshot of the display generated by Mauve.

FIGURE S5 | Graphical view of the location of *tal* genes in sequenced genomes of Malian *Xoo* strains.

FIGURE S6 | Diversity of African *Xoo* strains TALE repeat units sequence variants found in each TALE group. Within each TALE group (columns) and across strains (rows), individual cell colors code for distinct repeat units sequence variants as defined by DisTAL. The number following the pound sign in the label of the TALE groups designates the total number of unique variants found for this group in this genome set.

FIGURE S7 | DisTALE alignments of African TALE groups variants. Each multiple-alignment corresponds to a TALE group. On the left, repeat sequences are aligned using the formalism of **Figure 5**. On the right the same alignments are colored and labeled based on strings of DisTALE unique repeat ID numbers.

FIGURE S8 | Fractions of shared predicted targets between TALEs of the same group. The 99 RVD sequences of African TALEs were used to predict the best 500 target EBEs with Talvez 3.1 in the promoterome of Nipponbare (sequences on both strands of the 500 bp upstream the annotated start codons of the MSU7 annotation). The resulting table was used to systematically compute the percentage of shared predicted targets between TALEs of the same group. This ratio was obtained by dividing the cardinality of the intersection of the set of unique gene targets predicted for the TALE variant in row and the set of unique gene targets predicted for the TALE variant in column by the cardinality of the set of unique gene targets predicted for the TALE variant in row. Note that the resulting matrix is not symmetric because some TALEs have several EBEs predicted on the promoter of the same gene.

FIGURE S9 | Talvez prediction results of selected TalB and TalF variants for previously documented targets of members of these TALE groups. **(A)** Network representation of predictions. Edge thickness and color encode Talvez prediction score values. Edges are labeled with the rank of the rice gene in Talvez predictions for the corresponding TALE variant. **(B)** Table representation of the corresponding Talvez predictions.

TABLE S1 | Positions of *tal* gene coding sequences in the genomes of African *Xoo* strains.

REFERENCES

Abouelhoda, M., El-Kalioby, M., and Giegerich, R. (2010). WAMI: a web server for the analysis of minisatellite maps. *BMC Evol. Biol.* 10:167. doi: 10.1186/1471-2148-10-167

Afolabi, O., Amoussa, R., Bilé, M., Oludare, A., Gbogbo, V., Poulin, L., et al. (2015). First report of bacterial leaf blight of rice caused by *Xanthomonas oryzae* pv. *oryzae* in Benin. *Plant Dis.* 100:515. doi: 10.1038/srep21423

Altschul, S. F., Madden, T. L., Schäffer, A. A., Zhang, J., Zhang, Z., Miller, W., et al. (1997). Gapped BLAST and PSI-BLAST: a new generation of protein database search programs. *Nucleic Acids Res.* 25, 3389–3402. doi: 10.1093/nar/25.17.3389

Antony, G., Zhou, J., Huang, S., Li, T., Liu, B., White, F., et al. (2010). Rice *xa13* recessive resistance to bacterial blight is defeated by induction of the disease susceptibility gene Os-*11N3*. *Plant Cell* 22, 3864–3876. doi: 10.1105/tpc.110.078964

Bezrutczyk, M., Yang, J., Eom, J. S., Prior, M., Sosso, D., Hartwig, T., et al. (2018). Sugar flux and signaling in plant-microbe interactions. *Plant J.* 93, 675–685. doi: 10.1111/tpj.13775

Blanvillain-Baufumé, S., Reschke, M., Solé, M., Auguy, F., Doucoure, H., Szurek, B., et al. (2017). Targeted promoter editing for rice resistance to *Xanthomonas oryzae* pv. *oryzae* reveals differential activities for SWEET14-inducing TAL effectors. *Plant Biotechnol. J.* 15, 306–317. doi: 10.1111/pbi.12613

Boch, J., and Bonas, U. (2010). *Xanthomonas* AvrBs3 family-type III effectors: discovery and function. *Annu. Rev. Phytopathol.* 48, 419–436. doi: 10.1146/annurev-phyto-080508-081936

Boch, J., Scholze, H., Schornack, S., Landgraf, A., Hahn, S., Kay, S., et al. (2009). Breaking the code of DNA binding specificity of TAL-type III effectors. *Science* 326, 1509–1512. doi: 10.1126/science.1178811

Bogdanove, A. J., Schornack, S., and Lahaye, T. (2010). TAL effectors: finding plant genes for disease and defense. *Curr. Opin. Plant Biol.* 13, 394–401. doi: 10.1016/j.pbi.2010.04.010

Booher, N. J., Carpenter, S. C. D., Sebra, R. P., Wang, L., Salzberg, S. L., Leach, J. E., et al. (2015). Single molecule real-time sequencing of *Xanthomonas oryzae* genomes reveals a dynamic structure and complex TAL (transcription activator-like) effector gene relationships. *Microb. Genomics* 1:e000032. doi: 10.1099/mgen.0.000032

Boyd, L. A., Ridout, C., O'Sullivan, D. M., Leach, J. E., and Leung, H. (2013). Plant–pathogen interactions: disease resistance in modern agriculture. *Trends Genet.* 29, 233–240. doi: 10.1016/j.tig.2012.10.011

Brown, J. K. M. (2015). Durable resistance of crops to disease: a Darwinian perspective. *Annu. Rev. Phytopathol.* 53, 513–539. doi: 10.1146/annurev-phyto-102313-045914

Chu, Z., Yuan, M., Yao, J., Ge, X., Yuan, B., Xu, C., et al. (2006). Promoter mutations of an essential gene for pollen development result in disease resistance in rice. *Genes Dev.* 20, 1250–1255. doi: 10.1101/gad.1416306

Darling, A. E., Mau, B., Perna, N. T., Batzoglou, S., and Zhong, Y. (2010). progressiveMauve: multiple genome alignment with gene gain, loss and rearrangement. *PLoS One* 5:e11147. doi: 10.1371/journal.pone.0011147

Darriba, D., Taboada, G. L., Doallo, R., and Posada, D. (2012). jModelTest 2: more models, new heuristics and parallel computing. *Nat. Methods* 9:772. doi: 10.1038/nmeth.2109

Deng, D., Yan, C., Pan, X., Mahfouz, M., Wang, J., Zhu, J.-K., et al. (2012). Structural basis for sequence-specific recognition of DNA by TAL effectors. *Science* 335, 720–723. doi: 10.1126/science.1215670

Doyle, E. L., Booher, N. J., Standage, D. S., Voytas, D. F., Brendel, V. P., VanDyk, J. K., et al. (2012). TAL Effector-Nucleotide Targeter (TALE-NT) 2.0: tools for TAL effector design and target prediction. *Nucleic Acids Res.* 40, W117–W122. doi: 10.1093/nar/gks608

Eid, J., Fehr, A., Gray, J., Luong, K., Lyle, J., Otto, G., et al. (2009). Real-time DNA sequencing from single polymerase molecules. *Science* 323, 133–138. doi: 10.1126/science.1162986

Erkes, A., Reschke, M., Boch, J., and Grau, J. (2017). Evolution of transcription activator-like effectors in *Xanthomonas oryzae*. *Genome Biol. Evol.* 9, 1599–1615. doi: 10.1093/gbe/evx108

Finn, R. D., Clements, J., Arndt, W., Miller, B. L., Wheeler, T. J., Schreiber, F., et al. (2015). HMMER web server: 2015 update. *Nucleic Acids Res.* 43, W30–W38. doi: 10.1093/nar/gkv397

Gonzalez, C., Szurek, B., Manceau, C., Mathieu, T., Séré, Y., and Verdier, V. (2007). Molecular and pathotypic characterization of new *Xanthomonas oryzae* strains from West Africa. *Mol. Plant Microbe Interact.* 20, 534–546. doi: 10.1094/MPMI-20-5-0534

Grau, J., Reschke, M., Erkes, A., Streubel, J., Morgan, R. D., Wilson, G. G., et al. (2016). AnnoTALE: bioinformatics tools for identification, annotation and nomenclature of TALEs from *Xanthomonas* genomic sequences. *Sci. Rep.* 6:21077. doi: 10.1038/srep21077

Grau, J., Wolf, A., Reschke, M., Bonas, U., Posch, S., and Boch, J. (2013). Computational predictions provide insights into the biology of TAL effector target sites. *PLoS Comput. Biol.* 9:e1002962. doi: 10.1371/journal.pcbi.1002962

Hajri, A., Brin, C., Zhao, S., David, P., Feng, J.-X., Koebnik, R., et al. (2012). Multilocus sequence analysis and type III effector repertoire mining provide new insights into the evolutionary history and virulence of *Xanthomonas oryzae*. *Mol. Plant Pathol.* 13, 288–302. doi: 10.1111/j.1364-3703.2011.00745.x

Huguet-Tapia, J. C., Peng, Z., Yang, B., Yin, Z., Liu, S., and White, F. F. (2016). Complete genome sequence of the African strain AXO1947 of *Xanthomonas oryzae* pv. *oryzae*. *Genome Announc.* 4:e1730-15. doi: 10.1128/genomeA.01730-15

Hunt, M., Silva, N., De, Otto, T. D., Parkhill, J., Keane, J. A., and Harris, S. R. (2015). Circlator: automated circularization of genome assemblies using long sequencing reads. *Genome Biol.* 16:294. doi: 10.1186/s13059-015-0849-0

Hutin, M., Pérez-Quintero, A. L., Lopez, C., and Szurek, B. (2015a). MorTAL Kombat: the story of defense against TAL effectors through loss-of-susceptibility. *Front. Plant Sci.* 6:535. doi: 10.3389/fpls.2015.00535

Hutin, M., Sabot, F., Ghesquière, A., Koebnik, R., and Szurek, B. (2015b). A knowledge-based molecular screen uncovers a broad spectrum *OsSWEET14* resistance allele to bacterial blight from wild rice. *Plant J.* 84, 694–703. doi: 10.1111/tpj.13042

Lenth, R. (2016). Least-squares means: the R package lsmeans. *J. Stat. Softw.* 69, 1–33. doi: 10.18637/jss.v069.i01

Li, T., Liu, B., Spalding, M. H., Weeks, D. P., and Yang, B. (2012). High-efficiency TALEN-based gene editing produces disease-resistant rice. *Nat. Biotechnol.* 30, 390–392. doi: 10.1038/nbt.2199

Liu, Q., Yuan, M., Zhou, Y., Li, X., Xiao, J., and Wang, S. (2011). A paralog of the MtN3/saliva family recessively confers race-specific resistance to *Xanthomonas oryzae* in rice. *Plant Cell Environ.* 34, 1958–1969. doi: 10.1111/j.1365-3040.2011.02391.x

Mak, A. N.-S., Bradley, P., Cernadas, R. A., Bogdanove, A. J., and Stoddard, B. L. (2012). The crystal structure of TAL effector PthXo1 bound to its DNA target. *Science* 335, 716–719. doi: 10.1126/science.1216211

Morbitzer, R., Römer, P., Boch, J., and Lahaye, T. (2010). Regulation of selected genome loci using de novo-engineered transcription activator-like effector (TALE)-type transcription factors. *Proc. Natl. Acad. Sci. U.S.A.* 107, 1–6. doi: 10.1073/pnas.1013133107

Moscou, M. J., and Bogdanove, A. J. (2009). A simple cipher governs DNA recognition by TAL effectors. *Science* 326:1501. doi: 10.1126/science.1178817

Niño-Liu, D. O., Ronald, P. C., and Bogdanove, A. J. (2006). *Xanthomonas oryzae* pathovars: model pathogens of a model crop. *Mol. Plant Pathol.* 7, 303–324. doi: 10.1111/j.1364-3703.2006.00344.x

Paradis, E., Claude, J., and Strimmer, K. (2004). APE: analyses of phylogenetics and evolution in R language. *Bioinformatics* 20, 289–290. doi: 10.1093/bioinformatics/btg412

Parkinson, N., Cowie, C., Heeney, J., and Stead, D. (2009). Phylogenetic structure of *Xanthomonas* determined by comparison of *gyrB* sequences. *Int. J. Syst. Evol. Microbiol.* 59, 264–274. doi: 10.1099/ijs.0.65825-0

Pérez-Quintero, A. L. (2017). *Bioinformatic Approaches to the Study of TAL Effector Evolution and Function*. Ph.D. thesis, Thèse de doctorat dirigée par Szurek, Boris Mécanismes des Interactions parasitaires pathogènes et symbiotiques, Montpellier. Available at: http://www.theses.fr/2017MONTT089/document

Pérez-Quintero, A. L., Lamy, L., Gordon, J. L., Escalon, A., Cunnac, S., Szurek, B., et al. (2015). QueTAL: a suite of tools to classify and compare TAL effectors functionally and phylogenetically. *Front. Plant Sci.* 6:545. doi: 10.3389/fpls.2015.00545

Pérez-Quintero, A. L., Lamy, L., Zarate, C. A., Cunnac, S., Doyle, E. L., Bogdanove, A. J., et al. (2017). daTALbase: a database for genomic and transcriptomic

data related to TAL effectors. *Mol. Plant Microbe Interact.* 31, 471–480. doi: 10.1094/MPMI-06-17-0153-FI

Pérez-Quintero, A. L., Rodriguez-R, L. M., Dereeper, A., López, C., Koebnik, R., Szurek, B., et al. (2013). An improved method for TAL effectors DNA-binding sites prediction reveals functional convergence in TAL repertoires of *Xanthomonas oryzae* strains. *PLoS One* 8:e68464. doi: 10.1371/journal.pone.0068464

Pinheiro, J., Bates, D., DebRoy, S., Sarkar, D., and R Core Team (2017). *nlme: Linear and Nonlinear Mixed Effects Models*. Available at: https://CRAN.R-project.org/package=nlme

Poulin, L., Grygiel, P., Magne, M., Gagnevin, L., Rodriguez-R, L. M., Forero Serna, N., et al. (2015). New multilocus variable-number tandem-repeat analysis tool for surveillance and local epidemiology of bacterial leaf blight and bacterial leaf streak of rice caused by *Xanthomonas oryzae*. *Appl. Environ. Microbiol.* 81, 688–698. doi: 10.1128/AEM.02768-14

Quibod, I. L., Perez-Quintero, A., Booher, N. J., Dossa, G. S., Grande, G., Szurek, B., et al. (2016). Effector diversification contributes to *Xanthomonas oryzae* pv. *oryzae* phenotypic adaptation in a semi-isolated environment. *Sci. Rep.* 6:34137. doi: 10.1038/srep34137

R Core Team (2010). *R: A Language and Environment for Statistical Computing*. Vienna: R Foundation for Statistical Computing.

Rank, D., Baybayan, P., Bettman, B., Bibillo, A., Bjornson, K., Chaudhuri, B., et al. (2013). Nonhybrid, finished microbial genome assemblies from long-read SMRT sequencing data. *Nat. Methods* 10, 563–569. doi: 10.1038/nmeth.2474

Rinaldi, F. C., Doyle, L. A., Stoddard, B. L., and Bogdanove, A. J. (2017). The effect of increasing numbers of repeats on TAL effector DNA binding specificity. *Nucleic Acids Res.* 45, 6960–6970. doi: 10.1093/nar/gkx342

Sarra, S., Diarra, L., Dembele, M. M., Coulibaly, M., and Séré, Y. (2010). "Characterization of bacterial leaf blight epidemic in the Office du Niger (Mali) and search for a sustainable resistance against the pathogen," in *Proceedings of The Second Africa Rice Congress*, Bamako. Available at: http://www.africarice.org/warda/arc.asp

Stamatakis, A. (2014). RAxML version 8: a tool for phylogenetic analysis and post-analysis of large phylogenies. *Bioinformatics* 30, 1312–1313. doi: 10.1093/bioinformatics/btu033

Streubel, J., Blücher, C., Landgraf, A., and Boch, J. (2012). TAL effector RVD specificities and efficiencies. *Nat. Biotechnol.* 30, 593–595. doi: 10.1038/nbt.2304

Streubel, J., Pesce, C., Hutin, M., Koebnik, R., Boch, J., and Szurek, B. (2013). Five phylogenetically close rice *SWEET* genes confer TAL effector-mediated susceptibility to *Xanthomonas oryzae* pv. *oryzae*. *New Phytol.* 200, 808–819. doi: 10.1111/nph.12411

Tran, T. T., Pérez-Quintero, A. L., Wonni, I., Carpenter, S. C. D., Yu, Y., Wang, L., et al. (2018). Functional analysis of African *Xanthomonas oryzae* pv. *oryzae* TALomes reveals a new susceptibility gene in bacterial leaf blight of rice. *PLoS Pathog.* 14:e1007092. doi: 10.1371/journal.ppat.1007092

Treangen, T. J., Ondov, B. D., Koren, S., and Phillippy, A. M. (2014). The Harvest suite for rapid core-genome alignment and visualization of thousands of intraspecific microbial genomes. *Genome Biol.* 15:524. doi: 10.1186/s13059-014-0524-x

Triplett, L. R., Hamilton, J. P., Buell, C. R., Tisserat, N. A., Verdier, V., Zink, F., et al. (2011). Genomic analysis of *Xanthomonas oryzae* isolates from rice grown in the United States reveals substantial divergence from known *X. oryzae* pathovars. *Appl. Environ. Microbiol.* 77, 3930–3937. doi: 10.1128/AEM.00028-11

Vaughan, D. A., Lu, B.-R., and Tomooka, N. (2008). The evolving story of rice evolution. *Plant Sci.* 174, 394–408. doi: 10.1016/j.plantsci.2008.01.016

Vera Cruz, C. (1989). "How variable is *Xanthomonas campestris* pv. *oryzae*?," in *Proceedings of the International Workshop: Bacterial Blight Rice* (Manila: International Rice Research Institute), 153–165.

Verdier, V., Vera Cruz, C., and Leach, J. E. (2012). Controlling rice bacterial blight in Africa: needs and prospects. *J. Biotechnol.* 159, 320–328. doi: 10.1016/j.jbiotec.2011.09.020

White, F. F., and Yang, B. (2009). Host and pathogen factors controlling the rice-*Xanthomonas oryzae* interaction. *Plant Physiol.* 150, 1677–1686. doi: 10.1104/pp.109.139360

Wilkins, K. E., Booher, N. J., Wang, L., and Bogdanove, A. J. (2015). TAL effectors and activation of predicted host targets distinguish Asian from African strains of the rice pathogen *Xanthomonas oryzae* pv. oryzicola while strict conservation suggests universal importance of five TAL effectors. *Front. Plant Sci.* 6:536. doi: 10.3389/fpls.2015.00536

Yang, B., Sugio, A., and White, F. F. (2006). *Os8N3* is a host disease-susceptibility gene for bacterial blight of rice. *Proc. Natl. Acad. Sci. U.S.A.* 103, 10503–10508. doi: 10.1073/pnas.0604088103

Yu, G., Smith, D. K., Zhu, H., Guan, Y., and Lam, T. T.-Y. (2017). ggtree: an r package for visualization and annotation of phylogenetic trees with their covariates and other associated data. *Methods Ecol. Evol.* 8, 28–36. doi: 10.1111/2041-210X.12628

Yu, Y., Streubel, J., Balzergue, S., Champion, A., Boch, J., Koebnik, R., et al. (2011). Colonization of rice leaf blades by an African strain of *Xanthomonas oryzae* pv. oryzae depends on a new TAL effector that induces the rice nodulin-3 *Os11N3* gene. *Mol. Plant Microbe Interact.* 24, 1102–1113. doi: 10.1094/MPMI-11-10-0254

Zhang, H., and Wang, S. (2013). Rice versus *Xanthomonas oryzae* pv. *oryzae*: a unique pathosystem. *Curr. Opin. Plant Biol.* 16, 188–195. doi: 10.1016/j.pbi.2013.02.008

Zhang, J., Yin, Z., and White, F. (2015). TAL effectors and the executor R genes. *Front. Plant Sci.* 6:641. doi: 10.3389/fpls.2015.00641

Zhou, J., Peng, Z., Long, J., Sosso, D., Liu, B., Eom, J.-S., et al. (2015). Gene targeting by the TAL effector PthXo2 reveals cryptic resistance gene for bacterial blight of rice. *Plant J.* 82, 632–643. doi: 10.1111/tpj.12838

Zuluaga, P., Szurek, B., Koebnik, R., Kroj, T., and Morel, J.-B. (2017). Effector mimics and integrated decoys, the never-ending arms race between rice and *Xanthomonas oryzae*. *Front. Plant Sci.* 8:431. doi: 10.3389/fpls.2017.00431

Zuur, A. F., Ieno, E. N., Walker, N. J., Saveliev, A. A., and Smith, G. M. (2009). *Mixed Effects Models and Extensions in Ecology with R*. New York, NY: Springer-Verlag. doi: 10.1007/978-0-387-87458-6

Conflict of Interest Statement: The authors declare that the research was conducted in the absence of any commercial or financial relationships that could be construed as a potential conflict of interest.

frontiers in Plant Science

REVIEW
published: 24 August 2018
doi: 10.3389/fpls.2018.01245

The Enhancement of Plant Disease Resistance Using CRISPR/Cas9 Technology

*Virginia M. G. Borrelli[1], Vittoria Brambilla[2], Peter Rogowsky[3], Adriano Marocco[1] and Alessandra Lanubile[1]**

[1] Department of Sustainable Crop Production, Università Cattolica del Sacro Cuore, Piacenza, Italy, [2] Department of Agricultural and Environmental Sciences – Production, Territory, Agroenergy, University of Milan, Milan, Italy, [3] Laboratoire Reproduction et Développement des Plantes, Université de Lyon, École Normale Supérieure de Lyon, Université Claude Bernard Lyon 1, Centre National de la Recherche Scientifique, Institut National de la Recherche Agronomique, Lyon, France

Genome editing technologies have progressed rapidly and become one of the most important genetic tools in the implementation of pathogen resistance in plants. Recent years have witnessed the emergence of site directed modification methods using meganucleases, zinc finger nucleases (ZFNs), transcription activator-like effector nucleases (TALENs), and clustered regularly interspaced short palindrome repeats (CRISPR)/CRISPR-associated protein 9 (Cas9). Recently, CRISPR/Cas9 has largely overtaken the other genome editing technologies due to the fact that it is easier to design and implement, has a higher success rate, and is more versatile and less expensive. This review focuses on the recent advances in plant protection using CRISPR/Cas9 technology in model plants and crops in response to viral, fungal and bacterial diseases. As regards the achievement of viral disease resistance, the main strategies employed in model species such as *Arabidopsis* and *Nicotiana benthamiana*, which include the integration of CRISPR-encoding sequences that target and interfere with the viral genome and the induction of a CRISPR-mediated targeted mutation in the host plant genome, will be discussed. Furthermore, as regards fungal and bacterial disease resistance, the strategies based on CRISPR/Cas9 targeted modification of susceptibility genes in crop species such as rice, tomato, wheat, and citrus will be reviewed. After spending years deciphering and reading genomes, researchers are now editing and rewriting them to develop crop plants resistant to specific pests and pathogens.

Keywords: CRISPR/Cas9, crop improvement, genome editing, disease resistance, virus, fungus, bacteria

OPEN ACCESS

Edited by:
Sabrina Sarrocco, Università degli Studi di Pisa, Italy

Reviewed by:
Kemal Kazan, Commonwealth Scientific and Industrial Research Organisation (CSIRO), Australia
Kaijun Zhao, Institute of Crop Sciences (CAAS), China

***Correspondence:**
Alessandra Lanubile
alessandra.lanubile@unicatt.it

Specialty section:
This article was submitted to Plant Microbe Interactions, a section of the journal Frontiers in Plant Science

Received: *11 June 2018*
Accepted: *06 August 2018*
Published: *24 August 2018*

Citation:
Borrelli VMG, Brambilla V, Rogowsky P, Marocco A and Lanubile A (2018) The Enhancement of Plant Disease Resistance Using CRISPR/Cas9 Technology. Front. Plant Sci. 9:1245. doi: 10.3389/fpls.2018.01245

INTRODUCTION

Plant breeding has been the most successful approach for developing new crop varieties since domestication occurred, making possible major advances in feeding the world and societal development. Crops are susceptible to a large set of pathogens including fungi, bacteria, and viruses, which cause important economic losses (FAO, 2017); the enhancement of plant resistance plays an important role in adjusting crop production to meet global population increases. Approaches to disease control that depend on resistant varieties and agrochemicals are usually

highly effective whenever they are deployed. However, due to the high evolutionary potential of many plant pathogens, novel genotypes no longer sensitive to the resistance gene or the phytosanitary product can rapidly emerge via mutation or recombination. When this happens, particular disease control approaches can rapidly be rendered ineffective as the novel genotypes increase in frequency through natural selection and quickly spread to other locations, causing failure of control over large geographic areas.

An understanding of interactions between plants and communities of bacteria, fungi, and other microorganisms has been a major area of investigation for many years. The advent of high-throughput molecular technologies has made a more complete inventory of the pathogens associated with particular crops possible, and provided insight into how these communities may be affected by environmental factors and the crop genotype. Disease involves a complex inter-play between a host plant and a pathogen, and the resistance/susceptibility response can involve several components. Natural and induced mutations may change the interaction and inhibit certain steps in the mechanism of infection (Boyd and O'Toole, 2012; Dracatos et al., 2018).

During pre-genomic years, traditional breeding programs were based on the identification of natural and induced mutant alleles for resistance, and their incorporation into elite genotypes through breeding techniques. These approaches were uncertain and imprecise, leading for instance to the transfer of large genome regions instead of just single gene insertions. Nevertheless, mutation breeding methods have been quite successful in improving disease resistance, and traditional plant breeding has been used to generate new crop varieties for decades. Numerous mutants have been developed through mutation induction, showing enhanced resistance to various diseases. Among the most widely known mutants are those induced at the mildew resistance locus (*MLO*) in barley for resistance to powdery mildew (Miklis et al., 2007), and mutations conferring resistance to several lettuce diseases (Christopoulou et al., 2015). The *mlo* mutant is interesting, as the allele has not broken down and has provided unprecedented resistance to mildew for two decades (Panstruga and Schulze-Lefert, 2002). This longevity is due to a gene knockout. In other cases where resistance to specific pathotypes is conferred by a specific host gene allele, mutagenesis needs to be deployed to provide more precise single nucleotide mutations in the target gene sequence.

The revolution driven by the availability of genome and transcriptome sequences offers a new start for plant breeding programs. Association genetics based on single nucleotide polymorphisms (SNPs) and other molecular markers are spreading in plant breeding, creating high throughput data fundamental for the identification of quantitative trait loci (QTL). Major QTL are employed in crops to provide quantitative resistance to pathogens, together with the use of major resistance (*R*) genes introduced into varieties with superior agronomic characteristics.

New breeding techniques (NBTs) are attracting attention in plant research and concern many different areas, such as developmental biology, abiotic stress tolerance or plant-pathogen resistance (Nelson et al., 2018). NBT include the most recent and powerful molecular approaches for precise genetic modifications of single or multiple gene targets. They employ site-directed nucleases to introduce double stranded breaks at predetermined sites in DNA. These breaks are repaired by different host cell repair mechanisms, resulting either in small insertions or deletions via near homologous end-joining (NHEJ) or micro-homology-mediated end-joining (MMEJ), or in a modified gene carrying predetermined nucleotide changes copied from a repair matrix via homologous recombination (HR). Meganucleases (MNs), zinc finger nucleases (ZFNs), transcription activator-like effector nucleases (TALENs), and clustered regularly interspaced short palindrome repeats (CRISPR)/CRISPR-associated protein 9 (Cas9) correspond to the four types of nucleases used in genome editing. The exponential increase in publications reporting the use of CRISPR/Cas9 illustrates the fact that this technology requires less know-how and financial means and has a higher success rate in gene modification compared to the other available nucleases. The application of CRISPR/Cas9 editing has become a powerful tool for future enhancement of agronomic traits in crops (Mohanta et al., 2017).

The objective of this review is to recall the main features of the CRISPR/Cas9 genome editing technique and discuss its application for the enhancement of pathogen resistance in model plants and important crops, with a focus on rice, wheat, and maize.

CRISPR/Cas9: ADVANCES, LIMITATIONS, AND NEW COMBINATIONS

CRISPR/Cas9 from *Streptococcus pyogenes* (SpCas9) has rapidly assumed an important role in different application areas of plant research and many other fields (Ding et al., 2018; Liu and Moschou, 2018). In the CRISPR/Cas9 system a single-guide RNA (sgRNA) can bind to Cas9 and target it to specific DNA sequences (**Figure 1**). The requirement of a protospacer adjacent motif (PAM) limits the possible target sequences in a gene of interest. This limitation is of minor importance if the aim is simply to inactivate a gene by targeted mutagenesis at any position. It has much more importance for genome editing aiming at the precise change of specific nucleotides in a gene. Consequently, major efforts are under way to find Cas9-like proteins with different PAM sequences or to engineer the original Cas9 from *S. pyogenes* to recognize other PAM sequences. For example, xCas9, an evolved version of SpCas9, has been shown to recognize a broad range of PAM sequences including NG, GAA, and GAT in mammalian cells (Hu et al., 2018). In plants, the most widely explored alternative to SpCas9 is Cpf1 from *Prevotella* and *Francisella* with the PAM sequence TTTV, where "V" is A, C, or G (Endo et al., 2016), and an illustrative diagram is shown in **Figure 1**. Cpf1 is also considerably smaller than Cas9, is capable of RNAse activity to process its guide RNA, and introduces

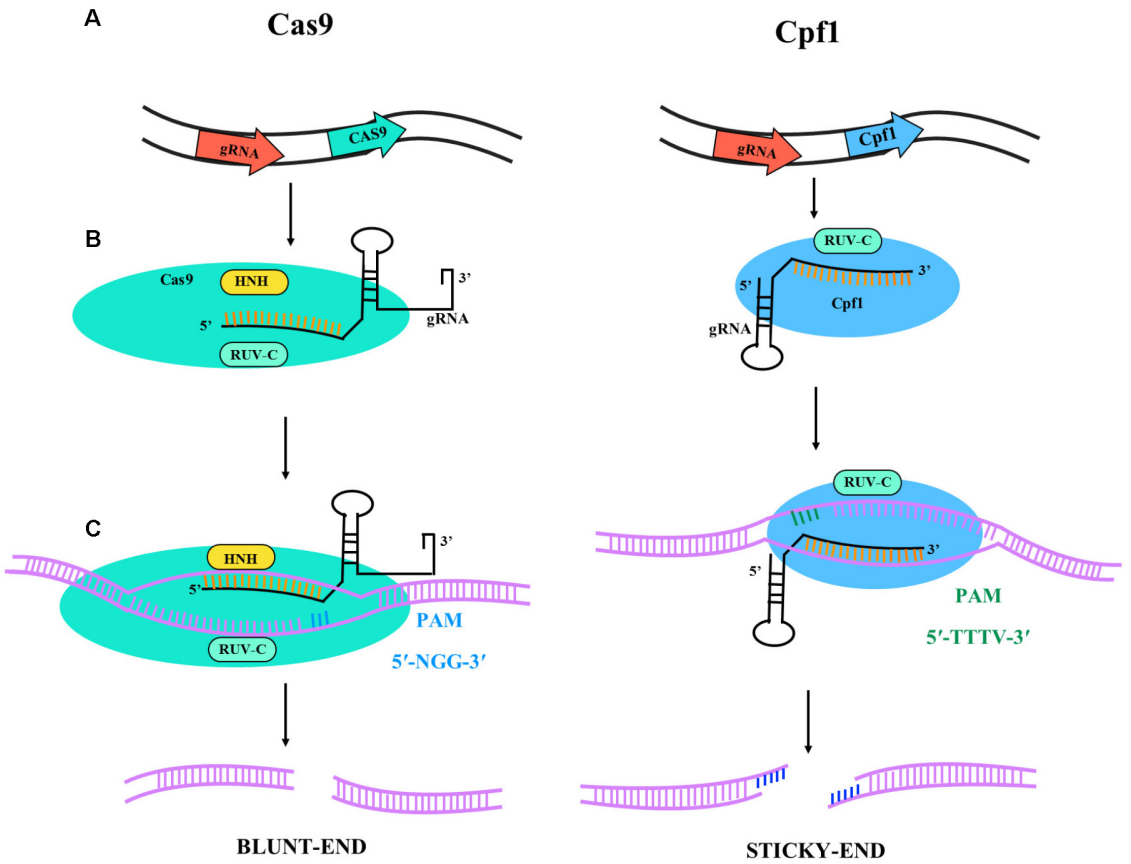

FIGURE 1 | Illustrative diagram of Cas9 and Cpf1 activities. The target specificity is given by the 17-20 nt located at the 5′ end of the sgRNA sequence. **(A)** Primary transcript and gRNA-nuclease (Cas9 or Cpf1) complex formation. The catalytic domains are RUV-C (light blue) and HNH (yellow) for Cas9 and RUV-C for Cpf1. The Cas9 is colored in light blue and the Cpf1 in dark blue; in black is represented the gRNA for gene targeting. **(B)** Gene target activity. Cas9 has 5′-NGG-3′ PAM sequence (blue bars) and Cpf1 has 5′-TTTV-3′ PAM sequence (green bars). **(C)** DNA ends after nuclease activity. Cas9 lead to blunt-end and Cpf1 to sticky-ends.

a staggered double break, which can be useful for enhancing homology-directed recombination and generating efficient gene insertion.

MULTIPLEX GENOME EDITING: WHEN DOES IT BECOME USEFUL?

The ease of multiplexing, i.e., the simultaneous targeting of several genes with a single molecular construct, is one of the major advantages of CRISPR/Cas9 technology with respect to MN, ZFN, or TALEN. For example, the simultaneous mutation of 14 different genes by a single construct has been demonstrated in *Arabidopsis* (Peterson et al., 2016). In crops, several multiplex genome editing (MGE) strategies were reported early on (Ma et al., 2014; Xing et al., 2014; Zhou et al., 2014; Xu et al., 2016), which were all based on a common strategy, i.e., the assembly of multiple gRNAs under the control of a U3 or U6 promoter into a single construct. In maize, the ISU Maize CRISPR platform (Char et al., 2017) permits the cloning of up to four gRNAs for multiplex gene targeting.

More recent multiplex systems exploit self-cleavage capacity of RNA molecules containing tRNA sequences. Constructs alternating sgRNA and tRNA sequences under the control of a single U3 or U6 promoter permit reduction of the size of the construct and limit the risk of silencing due to direct repetitions of promoter sequences. The use of such a strategy employing polycistronic tRNA-gRNA (PTG) to generate hereditable mutation in *TaLpx-1* and *TaMLO* genes has been reported in hexaploid wheat (Wang et al., 2018); the PTG system is described in **Figure 2**. Starting from a previous study on gene silencing of *TaLpx-1*, which encodes the wheat 9-lipoxygenase resistance gene to *Fusarium graminearum* (Nalam et al., 2015), the editing of homologs in wheat was tested. The PTG system containing gRNA activity was validated in wheat confirming gene editing efficacy and providing an effective tool for rapid trait pyramiding in breeding programs.

Recently, an alternative approach for MGEs based on PTG has been reported in rice, where crRNA transcription was obtained from introns inserted into Cpf1 and Cas9 sequences (Ding et al., 2018). Multiplex PTG/Cas9 systems can help with multigene family analysis, as reported for the closely related mitogen-activated protein kinase *MPK1* and *MPK6* in rice

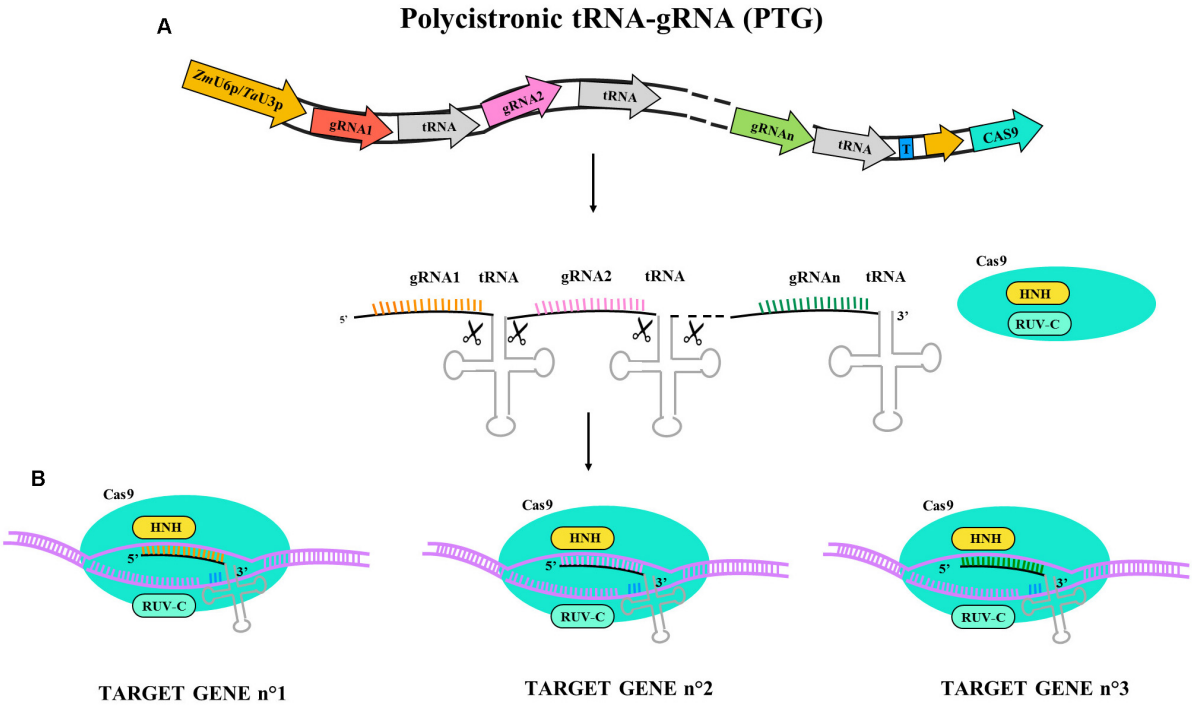

FIGURE 2 | Illustrative diagram of polycistronic tRNA-gRNA (PTG) gene construct and targeting activity for Cas9. PTG is composed of t-RNA-gRNA repeats and is upregulated by ZmU6 promoter or TaU3 promoter according the experimental design as different terminator region (T) are adopted. **(A)** PTG primary transcript. Endogenous endonuclease cuts the tRNA ends and let each tRNA-gRNA targeting the corresponding gene sequence. **(B)** In PTG system more sequence targets are available (n° gene targets) and the different gRNA are represented in different colors (orange, pink, and green).

(Minkenberg et al., 2017). 67% of all lines were double mutants for *MPK* genes with a high frequency of biallelic mutations on multiple target sites. The possibility of programming the PTG/Cas9 to delete chromosomal fragments could be adopted to remove genes and regulatory elements in order to produce transgene free plants.

OFF-TARGET MUTATIONS: FREQUENCY AND LIMITATIONS

High specificity is frequently put forward as a major argument in favor of CRISPR/Cas9 technology, for example in comparison to chemically or irradiation-induced mutagenesis. This raises the question of to what extent a gRNA targets only fully complementary genomic DNA sequences, and to what extent other genomic regions (off-target regions) can also be recognized and cleaved by the CRISPR/Cas9 tool, provoking potentially unwanted damage. Two types of off-target effects are evoked by scientists and regulatory agencies: (i) expected off-target in genome regions with high sequence similarity to the target and (ii) unexpected off-target in unrelated genome regions. The former is generally addressed by PCR amplification and sequencing of regions known to be similar to the target, the latter by whole genome sequencing (Feng et al., 2016).

Genome sequence information is necessary for the prediction of expected off-target effects. The search focuses on the 20 bp target sequence involved in base pairing with the gRNA but excludes the PAM 5′-NGG-3′. The PAM functions as a recognition site outside of the targeted element and does not give specificity for nuclease cleavage (Shah et al., 2013). Moreover, the CRISPR/Cas9 system accepts at least three mismatches in the 20 bp DNA target sequence. Most CRISPR/Cas9 design tools take this into account and propose only specific gRNA designs that do not bind theoretical off-target sites with more than 17 bp identity anywhere else in the genome. Such state-of-the art design is effortless if the gene is unique in the genome, but it becomes rather challenging if the gene has one or more paralogs. This also means that the design is generally easier for diploid genomes without recent duplications than for recently duplicated or polyploid genomes. *In silico* genome analysis of potential target sequences in dicots and monocots has confirmed that, as expected, larger genomes contain more PAMs and more potential targets (Bortesi et al., 2016). High specificity of between 87.3% and 94.3% was observed in relatively simple genomes of *Arabidopsis*, rice, tomato, and soybean, whereas maize, a recent allotetraploid with high levels of repetitive DNA, revealed only 29.5% specific targeting (Bortesi et al., 2016).

Analysis of expected off-target sites, with only one to several mismatches with the primary target, has revealed that the position of the mismatches in the sequence is significant. Mismatches in the seed sequence ("seed" is defined as the 12 bp close to the PAM) are generally not supported or poorly supported by the sgRNA/Cas9 complex (Tsai et al., 2015), causing

mutation less frequently at off-target sites, although in some cases mutations have been observed, as in barley (Lawrenson et al., 2015), soybean (Jacobs et al., 2015), and rice (Xie and Yang, 2013). Unwanted off-target mutations become more frequent when mismatches are located far from the seed region (Zhang et al., 2014).

To clarify the off-targeting issue in crops, recent investigations have screened progenies of CRISPR/Cas9 knockout in polyploid species. A study of CRISPR mutation frequency and mutation heritability of *TaGW2*, *TaLpx-1*, and *TaMLO* genes in the allohexaploid wheat was conducted (Wang et al., 2018). The results were different for the three genes: highly conserved for *TaGW2* (target sequence was specific for all three genomes), moderate for *TaLpx-1* (target sequence specific in two genomes), and low for *TaMLO*. The study showed the flexibility of CRISPR/Cas9 technology for implementing complex gene editing where the majority of genes have more than three homologous copies. Also, the gene editing process was investigated across generations: new mutant variants were recovered across multiple gene targets suggesting the transgenerational activity of CRISPR/Cas9 (Wang et al., 2018).

Another study on target accuracy and efficiency was performed in rice on paralogs *OsBEIIb* and *OSBEIIa* (Baysal et al., 2016). The study reveals the discrepancy in gRNA prediction and mutagenesis efficiency, confirming that gRNA with low predicted efficiency can achieve high mutation frequency even though the prediction suggested different targets with high mutagenesis scores. Empirical testing seems necessary in order to avoid putative gRNA inefficiency. Moreover, the authors also investigated off-target mutagenesis, reporting no mutation in the *OSBEIIa* paralog when only *OsBEIIb* was targeted, confirming the high accuracy of the strategy. CRISPR accuracy has been shown also in tomato (Čermák et al., 2015; Pan et al., 2016; Nekrasov et al., 2017).

To conclude, the CRISPR/Cas9 complex can bind with lower efficiency sequences with one to three mismatches. Therefore, expected off-target mutations do occur but can be avoided by rigorous design of the CRISPR/Cas9 tool. Unexpected off-target mutations do not occur at a frequency above the spontaneous mutation rate of plants.

PLANT TRANSFORMATIONS: CONVENTIONAL AND ALTERNATIVE TECHNIQUES

The bottleneck in the application of CRISPR/Cas9 technology to a wide range of crops is clearly the regeneration of fertile plants from the cells into which the CRISPR/Cas9 tool has been introduced (Altpeter et al., 2016). Consequently, the efficiency of the entire process remains very species- and genotype-dependent, meaning that in many crop species only a few lab varieties are accessible to CRISPR/Cas9 technology. Other important parameters are the quality of the design of the CRISPR/Cas9 tool and the method chosen for its introduction into the plant cell. As in conventional transgenesis, the introduction of the CRISPR/Cas9 tool can be achieved by the *Agrobacterium*-mediated and biolistic transformation of explants, or by direct transformation of protoplasts. The latter two systems have the advantage that not only can the DNA coding for Cas9 and the sgRNA be transferred, but this also applies for ribonucleoproteins (RNPs), i.e., an *in vitro* assembled complex of Cas9 protein with an sgRNA (Malnoy et al., 2016; Svitashev et al., 2016; Liang et al., 2017), or intermediate versions such as a DNA or RNA coding for Cas9 and an RNA representing the sgRNA (Svitashev et al., 2015; Zhang et al., 2016). In addition, both biolistics and direct DNA transfer permit an increase in the ratio of repair matrix DNA over DNA encoding Cas9 and sgRNA readily, thereby favoring HR over NHEJ/MMEJ.

In maize, ISU Maize CRISPR is a high efficiency public platform using *Agrobacterium*-mediated transformation (Char et al., 2017). The main genotypes used for immature embryo transformation are A188, A634, H99, W117 (Ishida et al., 2007), B104 and the hybrid Hi-II (Char et al., 2017). Private companies seem to prefer biolistic transformation to *Agrobacterium*-mediated transformation in the case of gene editing with donor template (Shi et al., 2017), particularly where multiple copies of donor template DNA molecules can be delivered (Svitashev et al., 2015). Even though both transformation processes have decent efficiencies nowadays, they remain limited to the above genotypes with poor agronomic traits. This limitation has recently been overcome by the overexpression of *Baby boom* (*Bbm*) and *Wuschel2* (*Wus2*) genes, which stimulated callus growth and increased the overall transformation frequency in maize, including in recalcitrant genotypes. Proof of concept has also been provided for enhanced transformation in sorghum (Lowe et al., 2016).

In rice, most genotypes can easily be transformed both via *Agrobacterium*-mediated transformation and by biolistic methods. In order to achieve CRISPR-mediated HR the DNA template is normally introduced via the biolistic method to increase its copy number in the host (Baysal et al., 2016). As for maize, but involving a higher number of studies, protoplast transient assay is becoming an efficient tool for testing CRISPR-target before starting the transformation of embryos or scutellum derived calli by *Agrobacterium* or particle bombardment (Gao et al., 2013; Jiang et al., 2013; Xie and Yang, 2013; Zhou et al., 2014; Lowder et al., 2015; Li et al., 2016; Luo et al., 2016; Wang et al., 2016). Regeneration of rice protoplasts is still very challenging, but important optimization efforts may render it feasible in the near future. In wheat, although very high *Agrobacterium*-mediated transformation efficiencies of up to 90% have been reported for specific wheat genetic backgrounds (Ishida et al., 2015a,b), particle bombardment has been more widely accepted as the standard method in wheat genetic transformation (Hakam et al., 2015; Wang et al., 2018). Remarkable success has been achieved by particle bombardment of both immature embryos and callus cells to obtain transient expression of the CRISPR/Cas9 DNA, and transgene-free homozygous mutant T0 plants have been generated in the absence of any selection (Zhang et al., 2016). Three studies have reported CRISPR mutagenesis in barley by using *Agrobacterium*-mediated transformation of immature embryos (Lawrenson et al., 2015; Holme et al., 2017;

Kapusi et al., 2017), while in Kapusi et al. (2017) a comparison with particle bombardment was carried out. Higher numbers of mutants were reported with the *Agrobacterium*-mediated compared to the biolistic transformation approach.

In conclusion, although preferences for certain delivery methods exist for certain species, efficiency is not only linked to the technique itself, but also to the know-how of a given lab as regards a given technique. Polyethylene glycol (PEG) or electroporation-mediated DNA transient expression in protoplasts have proven very useful for the evaluation of the efficiency of CRISPR/Cas9 designs (Malnoy et al., 2016). The importance of preliminary screens will certainly increase with the foreseeable shift from targeted mutagenesis to repair matrix based genome editing, which will increase the number of events to analyze due to lower efficiency. RNP technology has been established in plants and may help toward exemption from regulatory oversight, but its efficiency needs to be improved to make it a routine tool.

CRISPR/Cas-BASED STRATEGIES CONFERRING BIOTIC RESISTANCE

Biotic stresses including viral, fungal, and bacterial diseases are responsible for losses ranging from 20% to 40% of global agricultural productivity (Savary et al., 2012). Conferring host plant resistance to pathogens can reduce the impact of disease on crop development and yield, thereby addressing the challenge of feeding the world's growing population.

Advances in genome editing tools have opened new ways to achieve the improvement of resistance in crops. In recent years, the CRISPR/Cas system has been employed to respond to several agricultural challenges, including the achievement of improved biotic stress resistance (Arora and Narula, 2017). The application of CRISPR/Cas tools has mainly been explored against virus infection, followed by efforts to improve fungal and bacterial disease resistance. Recent studies demonstrating the power of the CRISPR/Cas technology in establishing resistance to these pathogen categories will be further discussed below.

Virus Resistance via CRISPR/Cas

Plant viruses are a serious threat to many economically important staple and specialty crops. Based on their genome nature, they are classified into six major groups: double-stranded DNA (dsDNA) viruses with no plant viruses in this group, single-stranded DNA (ssDNA), reverse-transcribing viruses, double-stranded RNA (dsRNA), negative sense single-stranded RNA (ssRNA−), and positive sense single-stranded RNA (ssRNA+) viruses (Roossinck et al., 2015). Most studies involving CRISPR-edited plants for virus resistance have targeted ssDNA geminivirus genomes (Ali et al., 2015, 2016; Baltes et al., 2015; Ji et al., 2015) (**Table 1**).

Geminiviridae is a large family of plant viruses causing worldwide crop losses among several important families, such as Cucurbitaceae, Euphorbiaceae, Solanaceae, Malvaceae, and Fabaceae (Zaidi et al., 2016). The virus genome is replicated through a rolling-circle amplification mechanism via a dsDNA replicative form, or by recombination-mediated replication (Hanley-Bowdoin et al., 2013). The most important genus of geminiviruses in economic terms is Begomovirus. Begomoviruses infect dicotyledonous plants via the sweet potato/tobacco/silverleaf whitefly (*Bemisia tabaci*) and are mainly found associated to the phloem of infected plants (Gilbertson et al., 2015). Their genome is organized in one (A, monopartite) or two (A and B, bipartite) components containing a common region of ∼220 bp (Fondong, 2013).

The first two studies focusing on resistance to geminiviruses, beet severe curly top virus (BSCTV) and bean yellow dwarf virus (BeYDV) in model plants *N. benthamiana* and *Arabidopsis* were reported by Baltes et al. (2015) and Ji et al. (2015) (**Table 1**). Ji et al. (2015) screened 43 candidate sgRNA/Cas9 target sites in coding and non-coding regions of the BSCTV genome. All the sgRNA/Cas9 constructs reduced virus accumulation in inoculated leaves at varying levels, but a greater resistance to virus infection was observed in *Nicotiana* and *Arabidopsis* plants showing the highest levels of expression of Cas9 and sgRNAs. Similar findings were described by Baltes et al. (2015), who employed 11 sgRNAs targeting Rep motifs, Rep-binding sites, hairpin, and the nonanucleotide sequence of BeYDV, and reported up to 87% reduction in the targeted viral load in *N. benthamiana*.

Two recent works have also employed a CRISPR/Cas9 approach for achieving resistance to begomoviruses (Ali et al., 2015, 2016) (**Table 1**). Both studies were based on the strategy of expressing the CRISPR/Cas9 system in the host cell nucleus to target and cleave the virus genome during replication. Ali et al. (2015) developed sgRNA molecules delivered via a tobacco rattle virus (TRV) vector into *N. benthamiana* plants stably overexpressing the Cas9 endonuclease. SgRNAs were specific for different tomato yellow leaf curl virus (TYLCV) coding and non-coding sequences, targeting the viral capsid protein (CP), the RCRII motif of the replication protein (Rep) and the intergenic region (IR). All sgRNAs were able to interfere with TYLCV genome sequences, but targeting the stem-loop invariant sequence contained in the IR caused a more significant reduction of viral replication and accumulation. The same CRISPR/Cas9 system was tested for targeting simultaneously the monopartite beet curly top virus (BCTV) and the bipartite Merremia mosaic virus (MeMV), geminiviruses that share the same stem-loop sequence in the IR. The results showed attenuated symptoms for both viruses, demonstrating that mixed infection immunity can be developed via a single sgRNA specific for conserved sequences of multiple viral strains.

Furthermore, Ali et al. (2016) analyzed not only the targeting efficiencies of the CRISPR/Cas9 tool but also the emergence of mutated viruses capable of replication and systemic movement. The CRISPR/Cas9 tool was designed to interfere with different coding and non-coding sequences of cotton leaf curl Kokhran virus (CLCuKoV), MeMV, and different severe and mild strains of TYLCV. The work revealed that when the sgRNA/Cas9 complex edited sites in the coding regions of all viruses, virus variants were generated capable of replicating and moving to escape the CRISPR/Cas9 machinery. Conversely, no novel variants were detected in *N. benthamiana* plants carrying sgRNAs addressing the IR sequences. Even though the NHEJ machinery

TABLE 1 | CRISPR/Cas9 applications for virus resistance.

Plant species	Virus	Target gene	Gene function	Strategy	Reference
Nicotiana benthamiana and *Arabidopsis thaliana*	BeYDV	CP, Rep, and IR	RCA mechanism	*Agrobacterium*-mediated transformation of leaves with Cas9/gRNA expression plasmid vectors	Ji et al., 2015
Nicotiana benthamiana	BSCTV	LIR and Rep/RepA	RCA mechanism	*Agrobacterium*-mediated transformation of leaves with Cas9/gRNA expression plasmid vectors	Baltes et al., 2015
Nicotiana benthamiana	TYLCV BCTV MeMV	CP, Rep and IR	RCA mechanism	*Agrobacterium*-mediated transformation of leaves with a TRV vector in Cas9 overexpressing plants	Ali et al., 2015
Nicotiana benthamiana	CLCuKoV MeMV TYLCV	CP, Rep, and IR	RCA mechanism	*Agrobacterium*-mediated transformation of leaves with a TRV vector in Cas9 overexpressing plants	Ali et al., 2016
Nicotiana benthamiana	TuMV	GFP1, GFP2, HC-Pro, CP	Replication mechanism	*Agrobacterium*-mediated transformation of leaves with a TRV vector in Cas13a overexpressing plants	Aman et al., 2018
Nicotiana benthamiana and *Arabidopsis thaliana*	CMV TMV	ORF1, 2, 3, CP and 3′UTR	Replication mechanism	*Agrobacterium*-mediated transformation of leaves with FnCas9/gRNA expression binary vectors Floral dipping for *Arabidopsis*	Zhang et al., 2018
Cucumis sativus	CVYV ZYMV PRSV-W	eIF4E	Host factor for RNA viruses translation	*Agrobacterium*-mediated transformation of cut cotyledons (without embryo) with Cas9/gRNA binary vectors	Chandrasekaran et al., 2016
Arabidopsis thaliana	TuMV	eIF(iso)4E	Host factor for RNA viruses translation	*Agrobacterium*-mediated transformation with Cas9/gRNA recombinant plasmid binary vectors (floral dipping)	Pyott et al., 2016
Oryza sativa L. *japonica*	RTSV	eIF4G	Host factor for RNA viruses translation	*Agrobacterium*-mediated transformation of immature embryos with Cas9/gRNA expression plasmid vectors	Macovei et al., 2018

BeYDV, bean yellow dwarf virus; BSCTV, beet severe curly top virus; TYLCV, tomato yellow leaf curl virus; BCTV, beet curly top virus; MeMV, Merremia mosaic virus; TRV, tobacco rattle virus; CLCuKoV, cotton leaf curl Kokhran virus; TuMV, turnip mosaic virus; CMV, cucumber mosaic virus; TMV, tobacco mosaic virus; CVYV, cucumber vein yellowing virus; ZYMV, zucchini yellow mosaic virus; PRSV-W, papaya ring spot mosaic virus-W; PVX, potato virus X; TCV, turnip crinkle virus; CMV, cucumber mosaic virus; RTSV, rice tungro spherical virus; CP, coat protein; Rep, replication association protein; IR, intergenic region; RCA, rolling-circle amplification; LIR, long intergenic region; GFP1, green fluorescent protein 1; GFP2, green fluorescent protein 2; HC-Pro, helper component proteinase silencing suppressor; ORF, open reading frame; UTR, untranslated terminal repeat; eIF4E, eukaryotic translation initiation factor 4E; eIF4G, eukaryotic translation initiation factor 4G.

repaired the double strand breaks caused by the Cas9 protein, the IR-repaired variants generated virus genomes unable to replicate, thus providing a better overall interference with the viral life cycle.

Protection against RNA viruses has seemed more difficult to achieve, since the classical SpCas9 from *Streptococcus pyogenes* only recognizes dsDNA. However, the search for and characterization of related nucleases has led to the discovery of enzymes that can bind to and cut RNA, such as FnCas9 from *Francisella novicida* or LwaCas13a from *Leptotrichia wadei*. A first report demonstrating resistance to RNA viruses (Zhang et al., 2018) (**Table 1**) expressed FnCas9 and RNA-targeting sgRNAs specific for cucumber mosaic virus (CMV) and tobacco mosaic virus (TMV) in *N. benthamiana* and *Arabidopsis* plants. Transgenic plants showed CMV and TMV accumulation reduced by 40–80% compared with control plants. Furthermore, the resistance obtained by expressing the sgRNA-FnCas9 system was quite stable and still active in the T6 generation. Importantly, Zhang et al. (2018) observed that the endonuclease activity of FnCas9 was not required for interference with the CMV genome, whereas its RNA-binding activity was essential, meaning that this particular application of FnCas9 can be considered as a CRISPR interference (CRISPRi) tool, similar to catalytically inactive SpCas9 proteins programmed to mitigate gene expression (Larson et al., 2013). The use of a catalytically inactive variant of FnCas9 has the advantage of limiting the onset of mutated viral variants capable of escaping CRISPR/Cas9. Moreover, in contrast with the previously described interference with geminivirus replication in the nucleus, no nuclear localization signal is necessary for FnCas9, which interferes with the RNA viruses in the cytoplasm.

Similar work has been carried out with Cas13a. Aman et al. (2018) exploited this RNA-guided ribonuclease to manipulate the turnip mosaic virus (TuMV) RNA genome (**Table 1**). Four different viral genomic regions were targeted: two targets in the green fluorescent protein (GFP) region, one in the helper component proteinase silencing suppressor (HC-Pro), and one in the coat protein (CP). The most efficient virus interference was observed with CRISPR RNA editing HC-Pro and GFP2 genes and resulted in a reduced replication and spread of TuMV in tobacco leaves. Furthermore, due to the innate ability of Cas13 to process pre-CRISPR RNA into functional CRISPR RNA, the multiplex targeting of several viral mRNA could be markedly improved through this alternative system (Aman et al., 2018).

All the systems aiming at protection against viruses described so far require the maintenance of a transgene for Cas9 and sgRNA in the genome of the crop plants, rendering them subject to genetically modified organism (GMO) regulation. A second strategy for the achievement of viral disease resistance consists in modifying plant genes that will generate virus resistance traits, to segregate the CRISPR/Cas9 tool and to release non-transgenic mutants in the field (Chandrasekaran et al., 2016; Pyott et al., 2016; Macovei et al., 2018) (**Table 1**). Plant host factors are required by RNA viruses to maintain their life cycle, including the eukaryotic translation initiation factors eIF4E, eIF(iso)4E and eIF4G (Sanfacon, 2015). Chandrasekaran et al. (2016) developed cucumber plants resistant to potyviruses by mutating independently two different sites of the host susceptibility gene *eIF4E* by CRISPR/Cas9. Non-transgenic Cucumis *eif4e* mutant plants were obtained by segregation of the CRISPR/Cas9 tool by three generations of backcrossing, making these plants safe for human consumption and for release into the environment, according to the authors. When challenged with viruses from the Potyviridae family, cucumber vein yellowing virus (CVYV), zucchini yellow mosaic virus (ZYMV), and papaya ring spot mosaic virus-W (PRSV-W), homozygous *eif4e* mutants showed immunity. Conversely, heterozygous knockout plants and non-mutant plants did not reveal any resistance to these viruses.

A similar editing approach was utilized by Pyott et al. (2016) in order to introduce site-specific mutations at the closely related *eIF(iso)4E* locus in *Arabidopsis* plants. Both 1 bp insertions and 1 bp deletions in *eIF(iso)4E* conferred complete resistance to the single-stranded RNA potyvirus (+ssRNA) TuMV and no off-target modification was detected in this study. Furthermore, homozygous T3 *eIF(iso)4E* mutants did not significantly differ in growth and development compared to wild-type plants.

Recently, Macovei et al. (2018) have developed new sources of resistance to rice tungro spherical virus (RTSV) through mutagenesis of *eIF4G* alleles in rice plants. The RTSV-resistant T_2 plants obtained did not show any detectable mutation in the off-target sites and were negative when tested for the presence of Cas9. Furthermore, after inoculation with RTSV, agronomic parameters such as plant height and grain yield were enhanced in the edited rice plants compared to their wild-type counterparts under glasshouse conditions.

The advantage of knocking out host susceptibility genes is that this is a relatively simple method that renders following the mutation easy. The loss of a host factor required for the viral life cycle is a form of recessive resistance that should be more durable than that of dominant *R* genes because viruses undergo a lower selective pressure, preventing their evolution to hinder host defense mechanisms. A possible disadvantage of the knockout strategy is that it may negatively influence plant vigor, supporting the selection of virus variants breaking the resistance, as already observed in nature (Abdul-Razzak et al., 2009). Pyott et al. (2016) and Macovei et al. (2018) did not observe any significant difference in growth defects between mutants and normal plants, although further investigations should be carried out in order to test the durability of this edited recessive resistance.

Resistance to Fungi Through CRISPR/Cas

Fungal pathogens are responsible for numerous diseases such as mildew, smut, rust, rot and many more. These diseases not only cause dramatic yield losses annually throughout the world but also compromise the quality of the harvested products. Moreover, mycotoxigenic fungi represent a serious concern due to the production of secondary metabolites known as mycotoxins, which cause severe health problems in humans and animals after exposure to contaminated food and feed. Several strategies have been evolved to enhance fungal resistance in plant species based on the current knowledge of molecular mechanisms implicated in plant-pathogen interaction. Potential candidate genes and gene

products involved in plant resistance against fungi have been described, and nowadays these are prime targets for editing through the CRISPR/Cas9 approach.

As previously partially discussed, *MLO* loci have been targeted by RNA-guided Cas9 endonuclease in three different plant species: bread wheat, tomato, and grapevine (Wang et al., 2014; Malnoy et al., 2016; Nekrasov et al., 2017) (**Table 2**). *MLO* encodes a protein with seven transmembrane domains localized in the plasma membrane and is ubiquitously present in monocots and dicots (Acevedo-Garcia et al., 2014). It had previously been reported that *MLO* were susceptibility (*S*) genes and that homozygous loss-of-function mutants had significantly increased resistance to powdery mildew in barley, *Arabidopsis* and tomato (Piffanelli et al., 2004; Consonni et al., 2006; Bai et al., 2008). Bread wheat plants mutated by CRISPR/Cas9 in one (*TaMLO-A1*) of the three *MLO* homeoalleles showed improved resistance to *Blumeria graminis* f. sp. tritici infection, a finding that once again demonstrated the important role of *TaMLO* genes in powdery mildew disease (Wang et al., 2014). In tomato, *SlMlo1*, previously identified as the most important of 16 *SlMlo* genes, was targeted at two sites and a deletion of 48 bp was obtained. The edited plants were self-pollinated in order to generate CRISPR/Cas cassette-free individuals. This new non-transgenic variety, "Tomelo," was fully resistant to *Oidium neolycopersici*. Furthermore, off-target analysis did not reveal any effect on the genomic regions outside the *SlMlo1* locus (Nekrasov et al., 2017). In grapevine, the molecular feasibility of *VvMLO7* knockout has been demonstrated through CRISPR/Cas9 RNP in protoplasts, but no plants have been regenerated (Malnoy et al., 2016). Parallel experiments with RNAi plants showed that the loss of *VvMLO7* reduced susceptibility to *Erysiphe necator* in grapevine (Pessina et al., 2016).

The RNP approach has also been used for editing *DIPM-1*, *DIPM-2*, and *DIPM-4* genes in apple protoplasts in order to confer resistance to fire blight disease (Malnoy et al., 2016). Again, only the molecular analysis attesting mutations has been carried out, not disease assay on regenerated plants. In perennial crops such as grapevine and apple, which take several years to flower, the transient introduction of genome editing tools in protoplasts is particularly interesting, since the segregation of stably integrated CRISPR/Cas9 cassettes by backcrosses would take a lot longer than in annual crops with generation times of only a few months. Secondly, the delivery of Cas9/sgRNA complex as RNP is a rapid approach, making possible the achievement of transformed protoplasts and the evaluation of sgRNA efficiency within 1 or 2 days. Thirdly, no foreign DNA is integrated into the genome and the Cas9/sgRNA complexes can be degraded rapidly during the cell culture regeneration process. Furthermore, even in transient approaches, the employment of plasmids can sometimes cause their undesired integration into the host genome, and the prolonged presence of CRISPR/Cas9 tools in the genome increases the risk of off-target mutations, while the CRISPR/Cas9 RNP shows improved on-target specificity. The drawback of this approach is the need to optimize plant regeneration protocols in order to apply this technology.

TABLE 2 | CRISPR/Cas9 applications for fungal resistance.

Plant species	Fungus	Target gene	Gene function	Strategy	Reference
Triticum aestivum	Powdery mildew (*Blumeria graminis* f. sp. *tritici*)	MLO-A1	Susceptibility (*S*) gene involved in powdery mildew disease	Particle bombardment of immature wheat embryos with Cas9/gRNA expression plasmid vectors	Wang et al., 2014
Solanum lycopersicum	Powdery mildew (*Oidium neolycopersici*)	MLO1	Major responsible for powdery mildew vulnerability	*Agrobacterium*-mediated transformation of cotyledons with Cas9/gRNA expression plasmid vectors	Nekrasov et al., 2017
Vitis vinifera	Powdery mildew (*Erysiphe necator*)	MLO-7	Susceptibility (*S*) gene involved in powdery mildew disease	PEG-mediated protoplast transformation with CRISPR ribonucleoproteins	Malnoy et al., 2016
Vitis vinifera	Gray mold (*Botrytis cinerea*)	WRKY52	Transcription factor involved in response to biotic stress	*Agrobacterium*-mediated transformation of proembryonal masses with Cas9/gRNA expression binary vectors	Wang et al., 2018
Theobroma cacao	Black pod disease (*Phytophthora tropicalis*)	NPR3	Regulator of the immune system	*Agrobacterium*-mediated transient transformation of stage C leaves with Cas9/gRNA expression binary vectors	Fister et al., 2018
Oryza sativa L. *japonica*	Rice blast disease (*Magnaporthe oryzae*)	SEC3A	Subunit of the exocyst complex	Protoplast transformation with Cas9/gRNA expression binary vectors	Ma et al., 2018
Oryza sativa L. *japonica*	Rice blast disease (*Magnaporthe oryzae*)	ERF922	Transcription factor implicated in multiple stress responses	*Agrobacterium*-mediated transformation of embryogenic calli with Cas9/gRNA expression binary vectors	Wang et al., 2016

MLO, MILDEW RESISTANT LOCUS; NPR3, non-expressor of pathogenesis-related 3; ERF922, ethylene responsive factor.

An example of the successful protection of grapevine by the CRISPR/Cas9 system is the *VvWRKY52* transcription factor, which was targeted by four gRNAs (Wang et al., 2018) (**Table 2**). About 21% of the transgenic plants showed biallelic mutations and were more resistant to *Botrytis cinerea* compared to the monoallelic mutants. No marked difference was observed in phenotype between wild-type and biallelic mutant plants, confirming the efficiency of the CRISPR/Cas9 strategy in woody plants with long reproductive cycles.

A further strategy to expedite genome editing application in slow generation tree crops is the employment of transient leaf transformation coupled to disease assays as demonstrated in *Theobroma cacao* (Fister et al., 2018) (**Table 2**). The authors reported for the first time the transient introduction of CRISPR/Cas9 components into cacao leaves targeting the *Non-Expressor of Pathogenesis-Related 3* (*NPR3*) gene, a suppressor of the immune system, and obtained leaves with increased resistance to *Phytophthora tropicalis*. This new system of *in vivo* mutagenesis in adult cacao trees is a fast and useful technique for validating sgRNA design and observing CRISPR mutagenized phenotypes. It encouraged the authors to regenerate genome-edited somatic embryos to validate the observed results at whole-plant level.

Plants resistant to rice blast disease were generated through CRISPR/Cas9 by disrupting *OsERF922* and *OsSEC3A* genes in rice (Wang et al., 2016; Ma et al., 2018) (**Table 2**). *Ossec3a* mutant plants disrupted in a putative subunit of a complex involved in exocytosis, revealed a pleiotropic phenotype including improved resistance against *Magnaporthe oryzae*, higher levels of salicylic acid (SA) content and up-regulation of pathogenesis- and SA-related genes, but also dwarf stature (Ma et al., 2018). In contrast, no alteration of a number of agronomic traits was observed in T1 and T2 transgene free plants mutated in the ethylene responsive factor (ERF)922, a transcription factor implicated in multiple stress responses. The mutant plants had a reduced number of blast lesions at both seedling and tillering stages (Wang et al., 2016). Overall, these results demonstrate the powerful and advantageous application of the CRISPR/Cas9 system for crop improvement as regards fungal disease resistance.

Resistance to Bacteria Through CRISPR/Cas

Among the bacterial species living on earth, just a few hundred are involved in crop damage, which often reveals multiple symptoms of disease (Schloss and Handelsman, 2004). Phytopathogenic bacteria are difficult to control, mainly because of undetected asymptomatic infections and the lack of suitable agrochemicals. Generally speaking, bacteriological plant control is based on prevention and exclusion of the pathogen by using genetic resistance, agronomic practices, and biocontrol agents (Kerr, 2016).

Phytopathogenic bacteria can be classified as crop specific, such as *Clavibacter michiganensis*, which is the causal agent of tomato bacterial ring rot; polyphagous specific, such as *Ralstonia solanacearum*, which causes disease in multiple monocot and dicot species; and "kingdom crosser," such as *Dickeya dadantii*, an entomo-phytopathogen, which can affect plants and animals.

Relatively few studies (**Table 3**) have been published on the application of the CRISPR/Cas system to counteract crop bacterial diseases. CRISPR/Cas9 mutagenesis of *OsSWEET13* has been performed in rice to achieve resistance to bacterial blight disease caused by γ-proteobacterium *Xanthomonas oryzae* pv. *oryzae* (Zhou et al., 2015). *OsSWEET13* is a susceptibility (*S*) gene encoding a sucrose transporter involved in plant-pathogen interaction. *X. oryzae* produces an effector protein, PthXo2, which induces *OsSWEET13* expression in the host and the consequent condition of susceptibility. In a previous work concerning *OsSWEET14* promoter mutagenesis adopting a TALEN approach, the disruption of this gene rendered the *X. oryzae* effector unable to bind *OsSWEET14* and ultimately resulted in disease resistance (Li et al., 2012). Similarly, Zhou et al. (2015) obtained a null mutation in *OsSWEET13* in order to better explore PthXo2-dependent disease susceptibility, and resultant mutants were resistant to bacterial blight. Further genome editing strategies for multiplexed recessive resistance using a combination of the major effectors and other resistance (*R*) genes will be the next step toward achieving bacterial blight resistance.

Two recent works have reported the employment of CRISPR/Cas9 with the aim of producing citrus plants resistant to citrus bacterial canker (CBC). CBC is caused by *Xanthomonas citri* subsp. *citri* (*Xcc*) and is the most widespread disease among commercial cultivars. In the first work, Jia et al. (2016) generated canker resistant mutants by editing the PthA4 effector binding elements in the promoter of the *Lateral Organ Boundaries 1* (*CsLOB1*) gene in Duncan grapefruit. Mutated lines showed a decrease in typical canker symptoms 4 days post inoculation with *Xcc*, and no further phenotypic alterations were detectable. Furthermore, no potential off-target mutations in other *LOB* family genes were found by PCR-sequencing. The second work, by Peng et al. (2017), confirmed the link between *CsLOB1* promoter activity and CBC disease susceptibility in Wanjincheng orange (*Citrus sinensis* Osbeck). The complete deletion of the EBE_{PthA4} sequence from both *CsLOB1* alleles induced resistance enhancement to CBC. Moreover, no alteration in plant development was observed after *CsLOB1* promoter modification. Additional efforts will be required to generate non-transgenic canker-resistant citrus varieties for facilitating their agronomic application in CBC prevention.

FUTURE PROSPECTS

In an era marked by political and societal pressure to reduce the use of pesticides, crop protection by genetic improvement provides a promising alternative with no obvious impact on human health or the environment. Genome editing is one of the genetic levers that can be adopted, and disease resistance is frequently cited as the most promising application of CRISPR/Cas9 technology in agriculture. There are three main

TABLE 3 | CRISPR/Cas9 applications for bacterial resistance.

Plant species	Fungus	Target gene	Gene function	Strategy	Reference
Oryza sativa	Bacterial blight (*Xanthomonas oryzae* pv. *oryzae*)	SWEET13	Sucrose transporter gene	*Agrobacterium*-mediated transformation of embryogenic callus with Cas9/gRNA expression plasmid vectors and TALEN	Li et al., 2012; Zhou et al., 2015
Citrus paradisi	Citrus canker (*Xanthomonas citri* subspecies *citric*)	LOB1	Susceptibility (S) gene promoting pathogen growth and pustule formation	*Agrobacterium*-mediated transformation of epicotyl with Cas9/gRNA expression plasmid vectors	Jia et al., 2016
Citrus sinensis Osbeck	Citrus canker (*Xanthomonas citri* subspecies *citric*)	LOB1	Susceptibility (S) gene promoting pathogen growth and pustule formation	*Agrobacterium*-mediated transformation of epicotyl with Cas9/gRNA expression plasmid vectors	Peng et al., 2017
Malus domestica	Fire blight (*Erwinia amylovora*)	DIPM-1 DIPM-2 DIPM-4	Susceptibility factor involved in fire blight disease	PEG-mediated protoplast transformation with CRISPR ribonucleoproteins	Malnoy et al., 2016

CsLOB1, Lateral Organ Boundaries 1; DIPM, DspE-interacting proteins of Malus.

reasons for this: firstly, scientific knowledge of the molecular mechanisms underlying numerous pathosystems is sufficiently advanced to enable the proposal of genes to be edited in order to achieve resistance. Secondly, disease resistance can frequently be achieved by the modification of a single gene, which is technically less challenging. This is similar to the modification of metabolic pathways, where the editing of a single gene can also have an all-or-nothing effect, but different from abiotic stress tolerance, where generally numerous genes have to be modified in a coordinated fashion to achieve incremental improvements. Thirdly, targeted mutagenesis, the only use of CRISPR/Cas9 technology at present mastered with respect to crops, is readily applicable to disease resistance, since the inactivation of susceptibility genes leads to protection. For other agriculturally interesting traits the achievement of positive effects by the loss-of-function of genes is a more delicate matter. However, acting as the spearhead of genome editing in crops also puts a certain responsibility on plant pathologists.

The first challenge is to demonstrate that the promises made by proofs of concept in confined environments can be maintained under field conditions. It is one thing to show that the population of a pathogen or the size of disease lesions is reduced in a greenhouse and another to protect a crop year after year under varying environmental conditions. Field tests are also necessary for correct evaluation of the agronomic fitness of the edited crops. Most of the genes inactivated by CRISPR/Cas9 technology in order to obtain disease resistance are likely to have roles in the physiology of the plant other than that linked to the life cycle of the pathogen. For example, triple knockouts of wheat *TaMLO* were not only resistant to powdery mildew but also showed leaf chlorosis (Wang et al., 2014), whereas EMS-induced triple mutants with non-conservative point mutations in *TaMLO* did not show obvious pleiotropic phenotypes (Acevedo-Garcia et al., 2017). Therefore, encouraging greenhouse observations of plant development or measurements of key parameters such as height, leaf area or grain weight absolutely must be confirmed under field conditions by multi-environmental yield trials in order to measure the relative importance of negative side effects. A final limitation of many published proofs of concept is that they involve lab varieties, which can easily be regenerated after the introduction of Cas9 and sgRNA, but which often have only a limited agronomic value. It remains to be shown that the phenotypic effects are maintained in elite lines under field conditions.

The second challenge is the durability of the disease resistances, and their agronomic management. This challenge needs to be dealt with seriously, in order to convince a public often hostile to this technology. Durability is not a specific aspect of resistance genes obtained by genome editing, and the answers are the same as for introgressed resistance genes discovered in the genetic variability of the species: (i) the stacking of several resistance genes, preferably with different modes of action, (ii) a focus on systems other than NBS-LRR receptor kinases known to break down rapidly, and (iii) good agronomic practices,

including, in particular, crop rotation and the concomitant use of biocontrol agents. An example of two independent CRISPR/Cas9-derived resistances against the same disease are the knockouts of *TaMLO* (Wang et al., 2014) and *TaEDR1* (Zhang et al., 2017), both conferring resistance to powdery mildew in wheat. Beyond the creation of novel alleles conferring protection, CRISPR/Cas9 technology can also be helpful in the stacking process itself. In contrast with the introgression of conventional resistance genes, the technology not only avoids genetic drag on neighboring regions with potentially negative impacts on agronomic performance, but also permits the simultaneous creation of multiple resistances in a single generation by multiplexing, i.e., the parallel use of several sgRNAs targeting different genes. Admittedly, multiplexing becomes more challenging with increasing ploidy levels, and in the above example in hexaploid wheat (A, B, and D genome), three *TaMLO* genes and three *TaEDR1* genes would need to be modified in parallel.

The third challenge is to overcome the present technical limitation regarding targeted mutagenesis and to implement true genome editing in crop plants. Targeted mutagenesis introduces random mutations (generally short insertions or deletions) at a predetermined site of a given gene, leading generally to loss-of-function, whereas true genome editing introduces predetermined base changes at one or several specific positions in a gene. For example, the elongation initiation factor 4E (eIF4E) is necessary for the translation of RNA into protein for both the host cell and single-stranded RNA viruses of the Potyviridae family. As described above, loss-of-function of eIF4E by targeted mutagenesis has been achieved in several model and crop species, consistently conferring resistance to potyviruses but also impacting the host plants to varying degrees. The specific modification of amino acids known to be important for the translation of viral but not host proteins would permit driving resistance to potyviruses without affecting plant physiology (Bastet et al., 2017). The expression of a transgene carrying a synthetic allele with six mutations in an *Arabidopsis eif4e* mutant validated the concept (Bastet et al., 2018), demonstrating indirectly the potential benefit of genome editing over targeted mutagenesis. However, at present true genome editing by HR is still hampered by very low efficiencies in plants, although it has recently become routine in many animal species. Continued efforts to improve its efficiency, for example by the use of *lig4* (Endo et al., 2016) or *polQ* mutations (Saito et al., 2017), or a copy number increase of the repair matrix by virus vectors (Čermák et al., 2015), are crucial to increasing the range of tools available to plant pathologists. Base editing, to date permitting C to T and A to G transitions in plants, is more limited in scope but has recently emerged as a readily available alternative for certain editing projects (Zhang et al., 2017; Hua et al., 2018).

The long term success of CRISPR/Cas9 technology in plant protection is dependent on new scientific knowledge. CRISPR/Cas9 technology can only be used if one knows which gene(s) to modify and which modification(s) to carry out in these genes in order to render plants resistant to disease. When pathogen resistance is achieved by the knock-out of one or several genes, inactivating mutations can easily be provoked by CRISPR-mediated specific DNA break and activation of the cell's error prone DNA repair, based on NHEJ. In this case, CRISPR can be used to target and inactivate a single gene or large gene families, both through single gRNA which matches several targets, or by multiplexing the system by introducing several gRNAs simultaneously. On the contrary, when specific allelic variants are involved in resistance, CRISPR-DNA break can be coupled with the less frequent cell repair mechanism based on HDR. The DNA template for HDR should be introduced into the cell together with the effector nuclease. This permits the introduction of a custom-designed sequence into the genome. The use of HDR, compared to NHEJ, can indefinitely expand the possibility of the type of mutations inserted by CRISPR, as any sequence can be inserted into a site of choice. Nevertheless, HDR is still technically challenging due to its low efficiency, the difficulty of having a selective marker and the lack of multiplexing protocols. These are aspects that will need to be improved if CRISPR applications are to expand in plant breeding. Despite the recent judgment of the Court of Justice of the European Union issued that organisms created using genome editing techniques are to be regulated as GMOs (Callaway, 2018), anyhow continuous efforts in plant pathology are necessary, in order to identify and characterize the genes involved in plant pathogen interactions. For example, the past decade was marked by the discovery of hundreds of effector molecules that are synthesized by different classes of pathogens and transferred into the host cell. A major challenge is to identify the host proteins targeted by these effectors and to characterize the underlying genes, which are one of many possible targets for future genome editing approaches. New knowledge does not necessarily have to stem from the crop species of interest. For example, the targeted mutagenesis of wheat *TaMLO* was based on knowledge of another crop, barley, where *Hvmlo* mutant varieties have provided good protection against powdery mildew that has not yet broken down, and the modification of *TaERF1* exploited knowledge from the model species *Arabidopsis*. These examples perfectly illustrate the added value of genome editing, which permits the enlargement of the gene pool of a crop species beyond all the available natural variability, by means of the transfer of knowledge acquired in other crops or model species.

AUTHOR CONTRIBUTIONS

VGB contributed by writing and editing the major part of the review. AL, AM, and PR organized and prepared some of the parts of this review. VB and PR critically revised the manuscript. AM and AL contributed to the design of the work's layout and were responsible for obtaining final approval from the other contributors.

FUNDING

VGB was supported by the Doctoral School on the Agro-Food System (Agrisystem) of Università Cattolica del Sacro Cuore (Italy). PR declares (i) a pending patent application involving CRISPR/Cas9 as one of many biotechnologies to obtain haploid

inducing maize lines, (ii) funding by the biotechnology company Meiogenix for research on targeting meiotic recombination to specific genome regions by CRISPR/Cas9 technology, and (iii) funding by the seed company Limagrain for research on haploid induction in maize.

ACKNOWLEDGMENTS

We acknowledge funding by the Investissement d'Avenir Program of the French National Agency of Research for the project GENIUS (ANR-11-BTBR-0001_GENIUS).

REFERENCES

Abdul-Razzak, A., Guiraud, T., Peypelut, M., Walter, J., Houvenaghel, M. C., Candresse, T., et al. (2009). Involvement of the cylindrical inclusion (CI) protein in the overcoming of an eIF4E- mediated resistance against *Lettuce mosaic* potyvirus. *Mol. Plant Pathol.* 10, 109–113. doi: 10.1111/j.1364-3703.2008.00513.x

Acevedo-Garcia, J., Kusch, S., and Panstruga, R. (2014). Magical mystery tour: MLO proteins in plant immunity and beyond. *New Phytol.* 204, 273–281. doi: 10.1111/nph.12889

Acevedo-Garcia, J., Spencer, D., Thieron, H., Reinstadler, A., Hammond Kosack, K., Phillips, A. L., et al. (2017). Mlo-based powdery mildew resistance in hexaploid bread wheat generated by a non-transgenic TILLING approach. *Plant Biotechnol. J.* 15, 367–378. doi: 10.1111/pbi.12631

Ali, Z., Abulfaraj, A., Idris, A., Ali, S., Tashkandi, M., and Mahfouz, M. M. (2015). CRISPR/Cas9-mediated viral interference in plants. *Genome Biol.* 16:238. doi: 10.1186/s13059-015-0799-6

Ali, Z., Ali, S., Tashkandi, M., Shan, S., Zaidi, A., and Mahfouz, M. M. (2016). CRISPR/Cas9-mediated immunity to geminiviruses: differential interference and evasion. *Sci. Rep.* 6:26912. doi: 10.1038/srep26912

Altpeter, F., Springer, N. M., Bartley, L. E., Blechl, A. E., Brutnell, T. P., Citovsky, V., et al. (2016). Advancing crop transformation in the era of genome editing. *Plant Cell* 28, 1510–1520. doi: 10.1105/tpc.16.00196

Aman, R., Ali, Z., Butt, H., Mahas, A., Aljedaani, F., Khan, M. Z., et al. (2018). RNA virus interference via CRISPR/Cas13a system in plants. *Genome Biol.* 19:1. doi: 10.1186/s13059-017-1381-1

Arora, L., and Narula, A. (2017). Gene editing and crop improvement using CRISPR-Cas9 system. *Front. Plant Sci.* 8:1932. doi: 10.3389/fpls.2017.01932

Bai, Y., Pavan, S., Zheng, Z., Zappel, N. F., Reinstädler, A., Lotti, C., et al. (2008). Naturally occurring broad-spectrum powdery mildew resistance in a central american tomato accession is caused by loss of Mlo function. *Mol. Plant Microbe Interact.* 21, 30–39. doi: 10.1094/MPMI-21-1-0030

Baltes, N. J., Hummel, A. W., Konecna, E., Cegan, R., Bruns, A. N., Bisaro, D. M., et al. (2015). Conferring resistance to geminiviruses with the CRISPR–Cas prokaryotic immune system. *Nat. Plants.* 1:15145. doi: 10.1038/nplants.2015.145

Bastet, A., Lederer, B., Giovinazzo, N., Arnoux, X., German-Retana, S., Reinbold, C., et al. (2018). Trans-species synthetic gene design allows resistance pyramiding and broad-spectrum engineering of virus resistance in plants. *Plant Biotechnol. J.* doi: 10.1111/pbi.12896 [Epub ahead of print].

Bastet, A., Robaglia, C., and Gallois, J. L. (2017). eIF4E resistance: natural variation should guide gene editing. *Trends Plant Sci.* 22, 411–419. doi: 10.1016/j.tplants.2017.01.008

Baysal, C., Bortesi, L., Zhu, C., Farré, G., Schillberg, S., and Christou, P. (2016). CRISPR/Cas9 activity in the rice OsBEIIb gene does not induce off-target effects in the closely related paralog OsBEIIa. *Mol. Breed.* 36:108. doi: 10.1007/s11032-016-0533-4

Bortesi, L., Zhu, C., Zischewski, J., Perez, L., Bassié, L., Nadi, R., et al. (2016). Patterns of CRISPR/Cas9 activity in plants, animals and microbes. *Plant Biotechnol. J.* 14, 2203–2216. doi: 10.1111/pbi.12634

Boyd, C. D., and O'Toole, G. A. (2012). Second messenger regulation of biofilm formation: breakthroughs in understanding c-di-GMP effector systems. *Annu. Rev. Cell Dev. Biol.* 28, 439–462. doi: 10.1146/annurev-cellbio-101011-155705

Callaway, E. (2018). CRISPR plants now subject to tough GM laws in European Union. *Nature* 560:16. doi: 10.1038/d41586-018-05814-6

Chandrasekaran, J., Brumin, M., Wolf, D., Leibman, D., Klap, C., Pearlsman, M., et al. (2016). Development of broad virus resistance in non-transgenic cucumber using CRISPR/Cas9 technology. *Mol. Plant Pathol.* 17, 1140–1153. doi: 10.1111/mpp.12375

Char, S. N., Neelakandan, A. K., Nahampun, H., Frame, B., Main, M., Spalding, M. H., et al. (2017). An Agrobacterium-delivered CRISPR/Cas9 system for high-frequency targeted mutagenesis in maize. *Plant Biotechnol. J.* 15, 257–268. doi: 10.1111/pbi.12611

Christopoulou, M., Reyes-Chin, W. S., Kozik, A., McHale, L. K., Truco, M. J., Wroblewski, T., et al. (2015). Genome-Wide architecture of disease resistance genes in lettuce. *G3 (Bethesda)* 5, 2655–2669. doi: 10.1534/g3.115.020818

Consonni, C., Humphry, M. E., Hartmann, H. A., Livaja, M., Durner, J., Westphal, L., et al. (2006). Conserved requirement for a plant host cell protein in powdery mildew pathogenesis. *Nat. Genet.* 38, 716–720. doi: 10.1038/ng1806

Čermák, T., Baltes, N. J., Čegan, R., Zhang, Y., and Voytas, D. F. (2015). High-frequency, precise modification of the tomato genome. *Genome Biol.* 16:32. doi: 10.1186/s13059-015-0796-9

Ding, D., Chen, K., Chen, Y., Li, H., and Xie, K. (2018). Engineering introns to express rna guides for Cas9- and Cpf1-mediated multiplex genome editing. *Mol. Plant* 11, 542–552. doi: 10.1016/j.molp.2018.02.005

Dracatos, P. M., Haghdoust, R., Singh, D., and Fraser, P. (2018). Exploring and exploiting the boundaries of host specificity using the cereal rust and mildew models. *New Phytol.* 218, 453–462. doi: 10.1111/nph.15044

Endo, A., Masafumi, M., Kayal, H., and Toki, S. (2016). Efficient targeted mutagenesis of rice and tobacco genomes using Cpf1 from Francisella novicida. *Sci. Rep.* 6:38169. doi: 10.1038/srep38169

FAO (2017). *The Future of Food and Agriculture – Trends and Challenges*. Rome: FAO.

Feng, C., Yuan, J., Wang, R., Liu, Y., Birchler, J. A., and Han, F. (2016). Efficient targeted genome modification in maize using CRISPR/Cas9 system. *J. Genet. Genomics* 43, 37–43. doi: 10.1016/j.jgg.2015.10.002

Fister, A. S., Landherr, L., Maximova, S. N., and Guiltinan, M. J. (2018). Transient expression of CRISPR/Cas9 machinery targeting TcNPR3 enhances defense response in *Theobroma cacao*. *Front. Plant Sci.* 9:268. doi: 10.3389/fpls.2018.00268

Fondong, V. N. (2013). Geminivirus protein structure and function. *Mol. Plant Pathol.* 14, 635–649. doi: 10.1111/mpp.12032

Gao, Z. Y., Zhao, S. C., He, W. M., Guo, L. B., Peng, Y. L., Wang, J. J., et al. (2013). Dissecting yield-associated loci in super hybrid rice by re- sequencing recombinant inbred lines and improving parental genome sequences. *Proc. Natl. Acad. Sci. U.S.A.* 110, 14492–14497. doi: 10.1073/pnas.1306579110

Gilbertson, R. L., Batuman, O., Webster, C. G., and Adkins, S. (2015). Role of the insect supervectors *Bemisia tabaci* and *Frankliniella occidentalis* in the emergence and global spread of plant viruses. *Annu. Rev. Virol.* 2, 67–93. doi: 10.1146/annurev-virology-031413-085410

Hakam, N., Vdupa, S. M., Robha, A., Ibriz, M., and Iraqi, D. (2015). Efficient callus induction and plantlets regeneration in bread wheat using immature and mature embryos. *Int. J. Biotechnol. Res.* 3, 1–9.

Hanley-Bowdoin, L., Bejarano, E. R., Robertson, D., and Mansoor, S. (2013). Geminiviruses: masters at redirecting and reprogramming plant processes. *Nat. Rev. Microbiol.* 11, 777–788. doi: 10.1038/nrmicro3117

Holme, I. B., Wendt, T., Humanes, J. G., Deleuran, L. C., Colby, G., Starker, C. G., et al. (2017). Evaluation of the mature grain phytase candidate HvPAPhy_a gene in barley (*Hordeum vulgare* L.) using CRISPR/Cas9 and TALENs. *Plant Mol. Biol.* 95, 111–121. doi: 10.1007/s11103-017-0640-6

Hu, J. H., Miller, S. M., Geurts, M. H., Tang, W., Chen, L., Sun, N., et al. (2018). Evolved Cas9 variants with broad PAM compatibility and high DNA specificity. *Nature* 556, 57–63. doi: 10.1038/nature26155

Hua, K., Tao, X., Yuan, F., Wang, D., and Zhu, J. K. (2018). Precise A·T to G·C base editing in the rice genome. *Mol. Plant* 11, 627–630. doi: 10.1016/j.molp.2018.02.007

Ishida, Y., Hiei, Y., and Komari, T. (2007). Agrobacterium-mediated transformation of maize. *Nat. Protoc.* 2, 16144–1621. doi: 10.1038/nprot.2007.241

Ishida, Y., Hiei, Y., and Komari, T. (2015a). "High efficiency wheat transformation mediated by *Agrobacterium tumefaciens*," in *Advances in Wheat Genetics: From Genome to Field*, eds Y. Ogihara, S. Takumi, and H. Handa (Tokyo: Springer), doi: 10.1007/978-4-431-55675-6_18

Ishida, Y., Tsunashima, M., Hiei, Y., and Komari, T. (2015b). Wheat (*Triticum aestivum* L.) transformation using immature embryos. *Methods Mol. Biol.* 1223, 189–198. doi: 10.1007/978-1-4939-1695-5_15

Jacobs, T. B., LaFayette, P. R., Schmitz, R. J., and Parrott, W. A. (2015). Targeted genome modifications in soybean with CRISPR/Cas9. *BMC Biotechnol.* 15:16. doi: 10.1186/s12896-015-0131-2

Ji, X., Zhang, H., Zhang, Y., Wang, Y., and Gao, C. (2015). Establishing a CRISPR–Cas-like immune system conferring DNA virus resistance in plants. *Nat. Plants* 1:15144. doi: 10.1038/nplants.2015.144

Jia, H., Orbovic, V., Jones, J. B., and Wang, N. (2016). Modification of the PthA4 effector binding elements in Type I CsLOB1 promoter using Cas9/sgRNA to produce transgenic *Duncan grapefruit* alleviating XccΔpthA4:dCsLOB1.3 infection. *Plant Biotechnol. J.* 14, 1291–1301. doi: 10.1111/pbi.12495

Jiang, L., Yu, X., Qi, X., Yu, Q., Deng, S., Bai, B., et al. (2013). Multigene engineering of starch biosynthesis in maize endosperm increases the total starch content and the proportion of amylose. *Transgenic Res.* 22, 1133–1142. doi: 10.1007/s11248-013-9717-4

Kapusi, E., Corcuera-Gómez, M., Melnik, S., and Stoger, E. (2017). Heritable genomic fragment deletions and small indels in the putative ENGase gene induced by CRISPR/Cas9 in barley. *Front. Plant Sci.* 8:540. doi: 10.3389/fpls.2017.00540

Kerr, A. (2016). Biological control of Crown Gall. *Australas. Plant Pathol.* 45, 15–18. doi: 10.1007/s13313-015-0389-9

Larson, M. H., Gilbert, L. A., Wang, X., Lim, W. A., Weissman, J. S., and Qi, L. S. (2013). CRISPR interference (CRISPRi) for sequence-specific control of gene expression. *Nat. Protoc.* 8, 2180–2196. doi: 10.1038/nprot.2013.132

Lawrenson, T., Shorinola, O., Stacey, N., Li, C., Østergaard, L., Patron, N., et al. (2015). Induction of targeted, heritable mutations in barley and *Brassica oleracea* using RNA-guided Cas9 nuclease. *Genome Biol.* 16:258. doi: 10.1186/s13059-015-0826-7

Li, Q., Zhang, D., Chen, M., Liang, W., Wei, J., Qi, Y., et al. (2016). Development of japonica photo-sensitive genic male sterile rice lines by editing carbon starved anther using CRISPR/Cas9. *J. Genet. Genomics* 43, 415–419. doi: 10.1016/j.jgg.2016.04.011

Li, T., Liu, B., Spalding, M. H., Weeks, D. P., and Yang, B. (2012). High-efficiency TALEN-based gene editing produces disease-resistant rice. *Nat. Biotechnol.* 30, 390–392. doi: 10.1038/nbt.2199

Liang, Z., Chen, K., Li, T., Zhang, Y., Wang, Y., Zhao, Q., et al. (2017). Efficient DNA-free genome editing of bread wheat using CRISPR/Cas9 ribonucleoprotein complexes. *Nat. Commun.* 8:14261. doi: 10.1038/ncomms14261

Liu, C., and Moschou, P. N. (2018). Phenotypic novelty by CRISPR in plants. *Dev. Biol.* 435, 170–175. doi: 10.1016/j.ydbio.2018.01.015

Lowder, L. G., Zhang, D., Baltes, N. J., Paul, J. W., and Tang, X. (2015). A CRISPR/Cas9 toolbox for multiplexed plant genome editing and transcriptional regulation. *Plant Physiol.* 169, 971–985. doi: 10.1104/pp.15.00636

Lowe, K., Wu, E., Wang, N., Hoerster, G., Hastings, C., Cho, M. J., et al. (2016). Morphogenic regulators Baby boom and Wuschel improve monocot transformation. *Plant Cell* 28, 1998–2015. doi: 10.1105/tpc.16.00124

Luo, M., Gilbert, B., and Ayliffe, M. (2016). Applications of CRISPR/Cas9 technology for targeted mutagenesis, gene replacement and stacking of genes in higher plants. *Plant Cell Rep.* 35, 1439–1450. doi: 10.1007/s00299-016-1989-8

Ma, J., Chen, J., Wang, M., Ren, Y., Wang, S., Lei, C., et al. (2018). Disruption of OsSEC3A increases the content of salicylic acid and induces plant defense responses in rice. *J. Exp. Bot.* 69, 1051–1064. doi: 10.1093/jxb/erx458

Ma, Y., Zhang, L., and Huang, X. (2014). Genome modification by CRISPR/Cas9. *FEBS J.* 281, 5186–5193. doi: 10.1111/febs.13110

Macovei, A., Sevilla, N. R., Cantos, C., Jonson, G. B., Slamet-Loedin, I., Cermak, T., et al. (2018). Novel alleles of rice eIF4G generated by CRISPR/Cas9-targeted mutagenesis confer resistance to Rice tungro spherical virus. *Plant Biotechnol. J.* doi: 10.1111/pbi.12927 [Epub ahead of print].

Malnoy, M., Viola, R., Jung, M. H., Koo, O. J., Kim, S., Kim, J. S., et al. (2016). DNA-free genetically edited grapevine and apple protoplast using CRISPR/Cas9 ribonucleoproteins. *Front. Plant Sci.* 7:1904. doi: 10.3389/fpls.2016.01904

Miklis, M., Consonni, C., Riyaz, A. B., Volker, L., Schulze-Lefert, P., and Panstruga, R. (2007). Barley MLO modulates actin-dependent and actin-independent antifungal defense pathways at the cell periphery. *Plant Physiol.* 144, 1132–1143. doi: 10.1104/pp.107.098897

Minkenberg, B., Xie, K., and Yang, Y. (2017). Discovery of rice essential genes by characterizing a CRISPR-edited mutation of closely related rice MAP kinase genes. *Plant J.* 89, 636–648. doi: 10.1111/tpj.13399

Mohanta, T. K., Bashir, T., Hashem, A., Allah, E., and Bae, H. (2017). Genome editing tools in plants. *Genes* 8:399. doi: 10.3390/genes8120399

Nalam, V. J., Alam, S., Keereetaweep, J., Venables, B., Burdan, D., Lee, H., et al. (2015). Facilitation of Fusarium graminearum infection by 9-Lipoxygenases in Arabidopsis and Wheat. *Mol. Plant Microbe Interact.* 28, 1142–1152. doi: 10.1094/MPMI-04-15-0096-R

Nekrasov, V., Wang, C., Win, J., Lanz, C., Weigel, D., and Kamoun, S. (2017). Rapid generation of a transgene-free powdery mildew resistant tomato by genome deletion. *Sci. Rep.* 7:482. doi: 10.1038/s41598-017-00578-x

Nelson, R., Wiesner-Hanks, T., Wisser, R., and Balint-Kurti, P. (2018). Navigating complexity to breed disease-resistant crops. *Nat. Rev. Genet.* 19, 21–33. doi: 10.1038/nrg.2017.82

Pan, C., Ye, L., Qin, L., Liu, X., He, Y., Wang, J., et al. (2016). CRISPR/Cas9-mediated efficient and heritable targeted mutagenesis in tomato plants in the first and later generations. *Sci. Rep.* 6:24765. doi: 10.1038/srep24765

Panstruga, R., and Schulze-Lefert, P. (2002). Live and let live: insights into powdery mildew disease and resistance. *Mol. Plant Pathol.* 3, 495–502. doi: 10.1046/j.1364-3703.2002.00145.x

Peng, A., Chen, S., Lei, T., Xu, L., He, Y., Wu, L., et al. (2017). Engineering canker-resistant plants through CRISPR/Cas9-targeted editing of the susceptibility gene CsLOB1 promoter in citrus. *Plant Biotechnol. J.* 15, 1509–1519. doi: 10.1111/pbi.12733

Pessina, S., Lenzi, L., Perazzolli, M., Campa, M., Dalla Costa, L., Urso, S., et al. (2016). Knockdown of MLO genes reduces susceptibility to powdery mildew in grapevine. *Hortic. Res.* 3:160616. doi: 10.1038/hortres.2016.16

Peterson, B. A., Haak, D. C., Nishimura, M. T., Teixeira, P. J., James, S. R., Dangl, J. L., et al. (2016). Genome-Wide assessment of efficiency and specificity in CRISPR/Cas9 mediated multiple site targeting in Arabidopsis. *PLoS One* 11:e0162169. doi: 10.1371/journal.pone.0162169

Piffanelli, P., Ramsay, L., Waugh, R., Benabdelmouna, A., D'Hont, A., Hollricher, K., et al. (2004). A barley cultivation-associated polymorphism conveys resistance to powdery mildew. *Nature* 430, 887–891. doi: 10.1038/nature02781

Pyott, D. E., Sheehan, E., and Molnar, A. (2016). Engineering of CRISPR/Cas9-mediated potyvirus resistance in transgene-free Arabidopsis plants. *Mol. Plant Pathol.* 4, 1–13. doi: 10.1111/mpp.12417

Roossinck, M. J., Martin, D. P., and Roumagnac, P. (2015). Plant virus metagenomics: advances in virus discovery. *Phytopathology.* 105, 716–727. doi: 10.1094/PHYTO-12-14-0356-RVW

Saito, S., Maeda, R., and Adachi, N. (2017). Dual loss of human POLQ and LIG4 abolishes random integration. *Nature Commun.* 8:16112. doi: 10.1038/ncomms16112

Sanfacon, H. (2015). Plant translation factors and virus resistance. *Viruses* 7, 3392–3419. doi: 10.3390/v7072778

Savary, S., Ficke, A., Aubertot, J. N., and Hollier, C. (2012). Crop losses due to diseases and their implications for global food production losses and food security. *Food Secur.* 4, 519–537. doi: 10.1007/s00203-017-1426-6

Schloss, P. D., and Handelsman, J. (2004). Status of the microbial census. *Microbiol. Mol. Biol. Rev.* 68, 686–691. doi: 10.1128/MMBR.68.4.686-691.2004

Shah, S. A., Erdmann, S., Mojica, F. J., Roger, A., and Garrett, R. A. (2013). Protospacer recognition motifs mixed identities and functional diversity. *RNA Biol.* 10, 891–899. doi: 10.4161/rna.23764

Shi, J., Gao, H., Wang, H., Lafitte, H. R., Archibald, R. L., Yang, M., et al. (2017). ARGOS8 variants generated by CRISPR-Cas9 improve maize grain yield under field drought stress conditions. *Plant Biotechnol. J.* 15, 207–216. doi: 10.1111/pbi.12603

Svitashev, S., Schwartz, C., Lenderts, B., Young, J. K., and Cigan, A. M. (2016). Genome editing in maize directed by CRISPR–Cas9 ribonucleoprotein complexes. *Nature Commun.* 7:13274. doi: 10.1038/ncomms13274

Svitashev, S., Young, J. K., Schwartz, C., Gao, H., Falco, S. C., and Cigan, A. M. (2015). Targeted mutagenesis, precise gene editing, and site-specific gene insertion in maize using Cas9 and guide RNA. *Plant Physiol.* 169, 931–945. doi: 10.1104/pp.15.00793

Tsai, M., Lu, Y., Liu, Y., Lien, H., Huang, C., Wu, J., et al. (2015). Modulation of p53 and met expression by krüppel-like factor 8 regulates zebrafish cerebellar development. *Dev. Neurobiol.* 75, 908–926. doi: 10.1002/dneu.22258

Wang, F., Wang, C., Liu, P., Lei, C., Hao, W., and Gao, Y. (2016). Enhanced rice blast resistance by CRISPR/Cas9-targeted mutagenesis of the ERF transcription factor gene OsERF922. *PLoS One* 11:e0154027. doi: 10.1371/journal.pone.0154027

Wang, W., Pan, Q., He, F., Akhunova, A., Chao, S., Trick, H., et al. (2018). Transgenerational CRISPR-Cas9 activity facilitates multiplex gene editing in allopolyploid wheat. *CRISPR J.* 1, 65–74. doi: 10.1089/crispr.2017.0010

Wang, Y., Cheng, X., Shan, Q., Zhang, Y., Liu, J., Gao, C., et al. (2014). Simultaneous editing of three homoeoalleles in hexaploid bread wheat confers heritable resistance to powdery mildew. *Nat. Biotechnol.* 32, 947–952. doi: 10.1038/nbt.2969

Xie, K., and Yang, Y. (2013). RNA-guided genome editing in plants using a CRISPR-Cas system. *Mol. Plant.* 6, 1975–1983. doi: 10.1093/mp/sst119

Xing, H. L., Dong, L., Wang, Z. P., Zhang, H. Y., Han, C. Y., Liu, B., et al. (2014). A CRISPR/Cas9 toolkit for multiplex genome editing in plants. *BMC Plant Biol.* 14:327. doi: 10.1186/s12870-014-0327-y

Xu, R., Yang, Y., Qin, R., Li, H., Qiu, C., Li, L., et al. (2016). Rapid improvement of grain weight via highly efficient CRISPR/Cas9-mediated multiplex genome editing in rice. *J. Genet. Genomics* 43, 529–532. doi: 10.1016/j.jgg.2016.07.003

Zaidi, S. S., Tashkandi, M., Mansoor, S., and Mahfouz, M. M. (2016). Engineering plant immunity: using CRISPR/Cas9 to generate virus resistance. *Front. Plant Sci.* 7:1673. doi: 10.3389/fpls.2016.01673

Zhang, F., Wen, Y., and Guo, X. (2014). CRISPR/Cas9 for genome editing: progress, implications and challenges. *Hum. Mol. Genet.* 23, 40–46. doi: 10.1093/hmg/ddu125

Zhang, Y., Bai, Y., Wu, G., Zou, S., Chen, Y., Gao, C., et al. (2017). Simultaneous modification of three homoeologs of TaEDR1 by genome editing enhances powdery mildew resistance in wheat. *Plant J.* 91, 714–724. doi: 10.1111/tpj.13599

Zhang, Y., Liang, Z., Zong, Y., Wang, Y., Liu, J., Chen, K., et al. (2016). Efficient and transgene-free genome editing in wheat through transient expression of CRISPR/Cas9 DNA or RNA. *Nat. Commun.* 7:12617. doi: 10.1038/ncomms12617

Zhang, Y. Z., Shi, M., and Holmes, E. C. (2018). Using metagenomics to characterize an expanding virosphere. *Cell* 172, 1168–1172. doi: 10.1016/j.cell.2018.02.043

Zhou, H., Liu, B., Weeks, D. P., Spalding, M. H., and Yang, B. (2014). Large chromosomal deletions and heritable small genetic changes induced by CRISPR/Cas9 in rice. *Nucleic Acids Res.* 42, 10903–10914. doi: 10.1093/nar/gku806

Zhou, J., Peng, Z., Long, J., Sosso, D., Liu, B., Eom, J. S., et al. (2015). Gene targeting by the TAL effector PthXo2 reveals cryptic resistance gene for bacterial blight of rice. *Plant J.* 82, 632–643. doi: 10.1111/tpj.12838

Conflict of Interest Statement: The authors declare that the research was conducted in the absence of any commercial or financial relationships that could be construed as a potential conflict of interest.

frontiers in Microbiology

REVIEW
published: 30 August 2018
doi: 10.3389/fmicb.2018.02093

Paraburkholderia phytofirmans PsJN-Plants Interaction: From Perception to the Induced Mechanisms

Qassim Esmaeel[1], Lidiane Miotto[1], Marine Rondeau[1], Valérie Leclère[2], Christophe Clément[1], Cédric Jacquard[1], Lisa Sanchez[1] and Essaid A. Barka[1]**

[1] *Unité de Résistance Induite et Bioprotection des Plantes EA 4707, SFR Condorcet FR CNRS 3417, University of Reims Champagne-Ardenne, Reims, France,* [2] *Univ. Lille, INRA, ISA, Univ. Artois, Univ. Littoral Côte d'Opale, EA 7394-ICV- Institut Charles Viollette, SFR Condorcet FR CNRS 3417, Lille, France*

The use of plant-associated bacteria has received many scientific and economic attention as an effective and alternative method to reduce the chemical pesticides use in agriculture. The genus *Burkholderia* includes at least 90 species including pathogenic strains, plant pathogens, as well as plant beneficial species as those related to *Paraburkholderia,* which has been reported to be associated with plants and exerts a positive effect on plant growth and fitness. *Paraburkholderia phytofirmans* PsJN, a beneficial endophyte able to colonize a wide range of plants, is an established model for plant-associated endophytic bacteria. Indeed, in addition to its plant growth promoting ability, it can also induce plant resistance against biotic as well as abiotic stresses. Here, we summarized an inventory of knowledge on PsJN-plant interaction, from the perception to the resistance mechanisms induced in the plant by a way of the atypical colonization mode of this endophyte. We also have carried out an extensive genome analysis to identify all gene clusters which contribute to the adaptive mechanisms under different environments and partly explaining the high ecological competence of *P. phytofirmans* PsJN.

Keywords: ***Paraburkholderia phytofirmans*** **PsJN, perception, PGPR, endophyte, biotic and abiotic stress**

OPEN ACCESS

Edited by:
Sabrina Sarrocco,
Università degli Studi di Pisa, Italy

Reviewed by:
Nikos Tzortzakis,
Cyprus University of Technology, Cyprus
Trevor Carlos Charles,
University of Waterloo, Canada

****Correspondence:***
Qassim Esmaeel
quassin.esmaeel@univ-reims.fr
Essaid A. Barka
ea.barka@univ-reims.fr

Specialty section:
This article was submitted to Plant Microbe Interactions, a section of the journal Frontiers in Microbiology

Received: *29 May 2018*
Accepted: *16 August 2018*
Published: *30 August 2018*

Citation:
Esmaeel Q, Miotto L, Rondeau M, Leclère V, Clément C, Jacquard C, Sanchez L and Barka EA (2018) Paraburkholderia phytofirmans PsJN-Plants Interaction: From Perception to the Induced Mechanisms. Front. Microbiol. 9:2093. doi: 10.3389/fmicb.2018.02093

INTRODUCTION

Historically, plant diseases have been controlled by the application of chemical pesticides, commonly leading to residual contamination and pathogen resistance (Couderchet, 2003). Therefore, the use of plant-associated bacteria has shown a great promise for controlling diseases and thereby reducing the use of agrochemicals in the agriculture (Pieterse et al., 2014). Plant growth-promoting bacteria (PGPB) are naturally associated with plant roots and confer positive effects to host plants (Shameer and Prasad, 2018). They can increase yield, improve plant growth, reduce pathogen infection, and enhance plants' tolerance to adverse environmental stresses (Compant et al., 2005a). Among PGPB, endophytes are defined as those bacteria able to colonize the internal tissue of the plant without causing negative effects or external symptoms of infection on their host (Compant et al., 2008). They can enter the plant *via* different sites including tissue wounds (Agarwal, 1987), stomata (Roos and Hattingh, 1983), penetration of root hairs (Huang, 1986) and secretion of cell wall degradative enzymes (Huang, 1986; Reinhold-Hurek et al., 2006).

Endophytes, some of which are belonged to the common soil bacteria, such as *Bacillus*, *Pseudomonas*, and *Burkholderia,* are applied to different plant species to promote their growth and control their diseases (Hardoim et al., 2015).

The high diverse genus *Burkholderia*, representing a group of approximately 90 species of Gram-negative β-proteobacteria (Sawana et al., 2014), has been isolated from different ecological niches including plants, soil, the atmosphere, water, fungi, animals and human (Ramette et al., 2005; Compant et al., 2008; Lackner et al., 2011; DeLeon-Rodriguez et al., 2013). Some members of *Burkholderia* have attracted a great deal of interest in biotechnology such as plant growth promotion, bioremediation, and biocontrol of plant diseases (Depoorter et al., 2016). Among *Burkholderia* strains, *Paraburkholderia phytofirmans* strain PsJN is a Gram-negative rod-shaped, non-sporulating and motile bacterium. This bacterium was first isolated from surface-sterilized onion roots infected with the mycorrhizal fungus *Glomus vesiculiferum* (Frommel et al., 1991a; Sessitsch et al., 2005). It has been recently classified as a member of *Paraburkholderia*, a group of formerly named *Burkholderia* species, mostly reported to be associated with plants and have biocontrol and bioremediation properties (Sawana et al., 2014; Eberl and Vandamme, 2016). *P. phytofirmans* PsJN has been reported as a prominent and efficient plant growth-promoting endophyte (Ait Barka et al., 2000) and a promising biological control agent against plant pathogens (Miotto-Vilanova et al., 2016).

Furthermore, *P. phytofirmans* PsJN employs different mechanisms to have a positive role in plant productivity. These mechanisms act either directly, by providing adequate plant nutrition, and producing plant hormones, or indirectly, by reducing susceptibility to diseases (Yang et al., 2009; Andreolli et al., 2016). The bacterium is also able to decrease the ethylene level in host plants through production of the 1-aminocyclopropane-1-carboxylate (ACC) deaminase enzyme (Glick et al., 2007). Moreover, it confers plants resistance against a broad spectrum of phytopathogens by the induction of plant-mediated resistance response in above ground parts of plants (Miotto-Vilanova et al., 2016). The strain also has been shown to induce tolerance toward different abiotic stresses including high temperature, cold, drought, and salinity (Bensalim et al., 1998; Ait Barka et al., 2006; Naveed et al., 2014a; Pinedo et al., 2015; Nafees et al., 2018). The complete genome sequences (8.2 Mb) of the plant endophyte *P. phytofirmans* PsJN, arranged in two chromosomes and one plasmid (121 kbp), was published by Weilharter et al. (2011). Previous comparative analysis of this strain revealed numerous biosynthetic gene clusters, secretion system, and metabolic potentials involved in endophytic behavior with diverse beneficial effects (Mitter et al., 2013; Ali et al., 2014). Compared to other PGPB, less information is available about the mechanisms attributing to biocontrol effect and endophyte lifestyle of *P. phytofirmans* PsJN, which is an established model for plant-associated endophytic bacteria. Here, together with previously published data, we summarize an inventory of knowledge on *P. phytofirmans* PsJN-plant interaction, from the perception to the resistance mechanisms associated with beneficial effects in plants. Gene clusters contribution to the adaptive mechanisms and beneficial effects on plant growth and biocontrol under different environments are also highlighted.

PERCEPTION OF *P. phytofirmans* PsJN

The interaction between endophytes and plants takes place in different areas including root and foliar surfaces as well as intercellular spaces of both root and foliar surfaces which are the first contact area for plant-associated microbes (Lindow and Brandl, 2003; Hardoim et al., 2015). A successful colonization of plant tissue by beneficial bacteria is influenced by the excretion of organic acids by their host plant (Kost et al., 2014). It has been reported that plant roots secrete a significant mixture of organic compounds known as exudates, which attract complex microbial populations present in the rhizosphere and initiate the first communication between host plants and endophytes (Kawasaki et al., 2016). The contribution of carbon sources in the recruitment of endophytic strain PsJN by host plants has been reported (Kost et al., 2014). Comparing to wild-type strain of PsJN, PsJNΔ*oxc* defective in oxalate assimilation was significantly impaired in colonization of both lupin and maize and the mutant population was also significantly reduced (Kost et al., 2014). Microbial quorum sensing molecules presented by acylated homoserine lactones (AHLs) have also been shown to act as targets for host recognition and are likely implicated in communication with host plants, and subsequently colonization process (Mathesius et al., 2003). It has been shown that N-AHLs from strain PsJN play a crucial role in the communication and colonization with plants as quorum sensing mutants of PsJN could no longer efficiently colonize and promote the growth of *Arabidopsis thaliana* as compared to the wild-type (Zúñiga et al., 2013). Moreover, endophytic bacteria move toward the plant roots, using chemotactic affinity for root exudates, and subsequently followed by adhesion to the plant root surfaces. The attachment of endophytes to the root surfaces can be enhanced through the production of cellulose or exopolysaccahrides (EPS) by bacteria (Kandel et al., 2017). Furthermore, genome mining of endophytic strain PsJN revealed that many gene clusters involved in motility, biofilm production, adhesion and genes encoding for chemotactic activity and siderophore synthesis may reflect the efficient plant colonization and endophytic lifestyle of this bacterium (Mitter et al., 2013; Ali et al., 2014).

In response to microbial perception, plants evolve different strategies to recognize and respond to microbial signal exposure (Pieterse et al., 2014). The recognition is firstly achieved *via* pattern recognition receptors (PRRs) known as pathogen- or microbe-associated molecular patterns (PAMPs or MAMPs) (Jones and Dangl, 2006). To defend themselves from potential invaders, plants use PAMP-triggered immunity (PTI) as the first line of the plant immune system. Therefore, endophytes have developed strategies to minimize the plant immunity by secretion of proteins called effectors that cross the first layer of defense and suppress the PTI signaling or avoid the recognition by the host. In addition, plants have a second layer of perception in which resistance receptors mediate the recognition of effectors compounds leading to effectors-triggered immunity (ETI) which

plays an essential role to control the pathogen progress (Pieterse et al., 2014).

Plant perception of endophytic strain PsJN begins after an exposure to bacterial signals such as flagellin leading to the plant response characterized by early and long-term responses in plant immunity and plant growth regulation and morphogenesis (Bordiec et al., 2011; Trdá et al., 2013). It has been shown that *P. phytofirmans* PsJN is perceived by grapevine cell suspensions and led to the production of a monophasic and transient burst of alkalinization during the first minute of the interaction (Bordiec et al., 2011). However, no significant accumulation of H_2O_2 neither cell death was observed in grapevine after *P. phytofirmans* PsJN challenge (Bordiec et al., 2011; Miotto-Vilanova et al., 2016). Plant phytohormones play a crucial role as key regulators in plant defense-signaling pathways (Pieterse et al., 2012). The expression levels of related defense genes after endophyte perception is a key point as endophytes are firstly known as potential invaders. Therefore, active interference with the plant immune responses is essential for the initiation of a compatible relationship with the host plant. In case of strain PsJN, the low level of induced defense genes in the grapevine may give insight into the ability of this strain to colonize the rhizoplane and to transfer into the entire tissue leading to the endophytic behavior of this bacterium (Bordiec et al., 2011). Moreover, the distribution of different secretion system gene clusters (**Figure 1**) in the PsJN genome might play a crucial role in the plant-*P. phytofirmans* PsJN interaction (Mitter et al., 2013).

P. phytofirmans PsJN COLONIZATION AND DISTRIBUTION WITHIN PLANT

Endophytes are defined as those bacteria that live in plant tissues and do not visibly harm the plant (Hardoim et al., 2015). Plant colonization by endophytes can occur either in intracellular or intercellular spaces in plant tissues. The colonization depends on the strain and different colonization routes and specific interactions have been described (James et al., 2002). Some endophytic bacteria are able to penetrate the endodermis, which represents an obstacle for colonization, and inhabits the internal plant compartment (Compant et al., 2010). One of the most frequently raised questions related to endophytic bacteria is how do they enter plant tissue?

In the early stages of colonization, *P. phytofirmans* PsJN moves toward the plant roots *via* chemotactic response to plant-released compounds (Kost et al., 2014). The secretion of root exudates by the plant initiates the first communication between endophytes and host plants (Kandel et al., 2017). Moreover, quorum sensing compounds produced by strain PsJN play an important role in host communication, and the subsequent colonization process (Zúñiga et al., 2017). The attachment of endophytes to the root surfaces is considered the first colonization step which is essential in getting access to the main entry points. The production of EPS by endophytes as well as the presence of bacterial flagella and cell surface polysaccharides may help the adhesion of endophytes onto the host roots and may facilitate the colonization process (Kandel et al., 2017). Depending on the strain, endophytes can get into plant tissues through wounds, stomata, and hydathodes, which are considered as the main entry sites (Hardoim et al., 2015). The emergence zone of secondary roots and injuries constitute also a natural opening allowing the entry of the endophytes inside the plant (Kandel et al., 2017). Moreover, some bacterial endophytes deploy a wide range of catabolic activities that allow them to break down different selections of organic compounds and modify the plant cell wall compositions (Preston, 2004; Taghavi et al., 2010).

The PsJN genome harbors a total of 41 putative plant polymer genes, encoding for putative hydrolytic enzymes (Mitter et al., 2013), which may help entry into the host plant through the distraction of the host. Among them, 14 genes represent glycoside hydrolyses (GH) that are involved in cell wall and sugar metabolism. *In silico* analysis of the PsJN genome also revealed the presence of genes involved in malonate metabolizing such as malonate decarboxylase which is important for symbiosis between endophytes and the plant (Kim, 2002). Genes related to cupin superfamily involved in the modification of plant cell wall carbohydrates (Dunwell et al., 2004) are also present in the PsJN genome. Furthermore, it has been reported that bacteria, mostly related to plant pathogens, produce different extracellular enzymes or cell wall degrading factors such as cellulases, hemicellulases, and endoglucanases which enable endophytes to penetrate plant cell wall and colonize the interspatial region between plant cells (Taghavi et al., 2010; Ali et al., 2014). In the course of a search of the PsJN genome, one gene cluster (**Figure 2A**) responsible for bacterial cellulose biosynthesis has been found in the chromosome 2 and gene encoding for endo 1, 4 glucanase was found as a part of the cluster. Beside the cluster for cellulose synthesis, another one involved in pectin degradation was also found (**Figure 2B**). The latter includes genes coding for polygalcturonate and galactarate dehydratase, which are involved in the degradation of pectin and could play a crucial role in colonizing the interspatial part between plant cells (Taghavi et al., 2010). In addition, the PsJN genome harbors ABC transporter genes involved in degradation of the cell wall.

Paraburkholderia phytofirmans PsJN establishes rhizosphere and endophytic colonization in different plants such as potato (Bensalim et al., 1998), switchgrass (Kim et al., 2012), tomato (Pillay and Nowak, 1997), *Arabidopsis* (Zúñiga et al., 2013), maize and lupin (Kost et al., 2014), and grapevine (Ait Barka et al., 2002). The bacterium colonizes the grapevine rhizoplane immediately after the inoculation and transmits to the root interior 3 h after inoculation and then systemically migrates from the rhizoplane to aerial tissues (Compant et al., 2005b). It has been shown that the highest level of bacterial populations on grapevine rhizoplane, and aerial parts achieved at 24 and 84 h after inoculation, respectively, and the colonization level in leaves was significantly greater than stem (Compant et al., 2005b). Compant et al. (2007) showed that strain PsJN colonizes the internal xylem vessels and the bacterium takes the advantage of holes between xylem to migrate and spread to grape inflorescence stakes, pedicels, and then to youngberries. Furthermore, Mitter et al. (2017) demonstrated that *P. phytofirmans* PsJN is able to colonize the seeds of monocot and dicot after the flowers

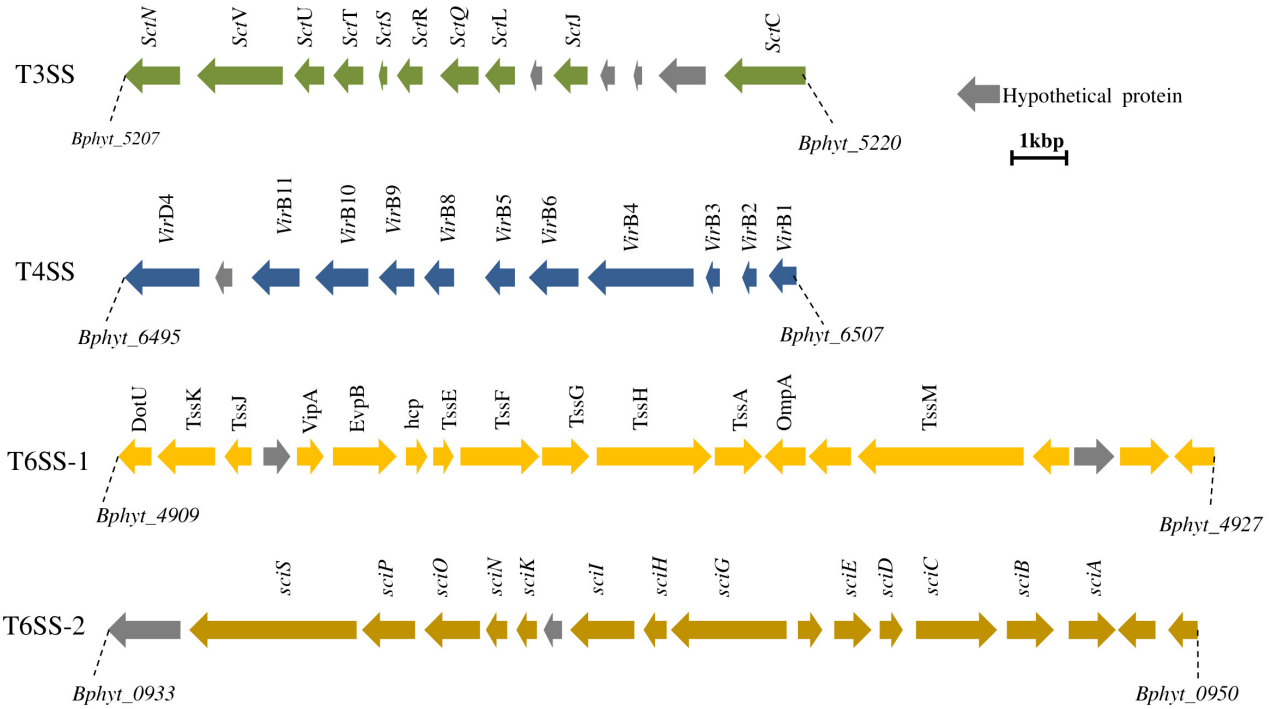

FIGURE 1 | Distribution of secretion systems in the genome of *Paraburkholderia phytofirmans* PsJN. T3SS and T4SS clusters are located in chromosome 2 (position 1396242–1383596 and 2785143–2797095, respectively). T6SS is represented by two clusters located on chromosomes 1 and 2 (position 1046459–1070567 and 1046459–1058642, respectively). Secretion systems in PsJN might inject effector proteins which cross the cell wall and might act on host plant to modulate plant signal transduction and elicit host defense responses.

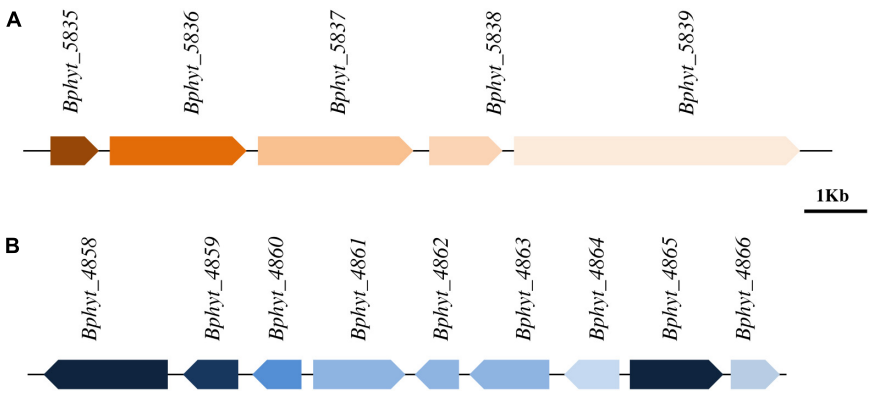

FIGURE 2 | Biosynthetic genes clusters located in chromosome 2 of *P. Phytofirmans* PsJN genome. **(A)** Cellulose biosynthesis gene cluster containing the gene encoding for degradation enzyme endoglucanase *Bphyt_5838* (position 2045332–2046513) which facilitates the penetration of cell wall of host plants **(B)** genes involved in pectin degradation including genes *Bphyt_ 4858* (position 978791–980806) encoding for polygalcturonate and *Bphyt_4865* (position 988328–989917) encoding for galactarate dehydratase.

were inoculated, and subsequently get transferred into the next generation of plants. In potato plantlets, strain PsJN was observed in the first epidermal layers of roots and in the xylem tissue of stem (Frommel et al., 1991a). In maize, under normal conditions, strain PsJN was observed in root and shoot interior and the maximum population density (CFU g^{-1} dry weight) reached 5.86×10^5 (rhizosphere), 5.44×10^5 (root interior), and 9.36×10^4 (shoot interior) (Naveed et al., 2014b). The ability of PsJN to produce EPS and form a biofilm as well as the presence of genes implicated in the biosynthesis of flagella, cellulose and genes encoding for chemotactic activity in the genome of PsJN may reflect the efficient endophytic colonization of the plant by this bacterium (Mitter et al., 2013; Ali et al., 2014). Moreover, the capacity of strain PsJN to colonize different plant hosts is probably due to large genome size (8.2 Mb), divided in two chromosomes and one plasmid (Weilharter et al., 2011).

P. phytofirmans STRAIN PsJN, A PLANT GROWTH PROMOTING RHIZOBACTERIA

Endophytes produce beneficial effects on the plant growth through several mechanisms. The mechanism can be either direct through the production/modulation of plant hormones (Pieterse et al., 2012), facilitating resource acquisition (Naveed et al., 2014a), or indirect by producing secondary metabolites (Esmaeel et al., 2017), and induction of systemic resistance (ISR) leading to more adaptability to different stress conditions (Pieterse et al., 2014). The endophytic *P. phytofirmans* strain PsJN is a highly efficient plant beneficial bacterium as it is able to promote the growth across a range of plant species including wheat (Naveed et al., 2014a), maize (Naveed et al., 2015), brassica (Nafees et al., 2018), grapevine (Compant et al., 2005b), switchgrass (Kim et al., 2012; Wang et al., 2015), *Arabidopsis* (Poupin et al., 2013; Zhao et al., 2016), tomato (Pillay and Nowak, 1997), lupin (Kost et al., 2014), watermelon and cantaloupe (Liu et al., 1995), potato (Frommel et al., 1991a), cucumber and sweet pepper (Nowak et al., 2004). The different beneficial effects of strain PsJN on different host plants are reported in **Table 1**. The mechanisms behind the observed positive effect are linked to the production of plant phytohormones, ACC deaminase, siderophores and other secondary metabolites which contribute as signaling molecules for better bacteria-plant communication leading to an efficient colonization of plant roots (Sun et al., 2009; Naveed et al., 2015).

1-Aminocyclopropane-1-Carboxylate Deaminase (ACC)

The ACC, produced by endophytic bacteria, is linked with an alleviation of plant stress as it contributes to lowering the ethylene level hence promoting the plant growth (Glick et al., 1998). Indeed, ACC prevents ethylene signaling by cleaving the ethylene precursor (ACC deaminase) to ammonia and 2-oxobutanoate. Moreover, the ACC deaminase-expressing bacteria were reported to enhance the plant growth under different biotic and abiotic stresses, including pathogen attack, drought, salinity, organic and inorganic contaminants (Glick, 2004). The plant growth promoting effect in tomato associated with the strain PsJN was suggested to be linked to the expression of ACC deaminase, which plays a crucial role to enhance the growth performance of tomato plants (Onofre-Lemus et al., 2009). Sun et al. (2009) showed that ACC produced by strain PsJN is involved in the colonization as the deletion mutant *P. phytofirmans* PsJN Δ*acd*S (*Bphyt_5397*) lost its ability to promote the elongation of the roots of canola seedlings.

Production of the Plant Growth Promoting Hormones Indole-3-Acetic Acid (IAA)

The production of IAA by endophytic bacteria has received a lot of attention due to its crucial role in each stage of the plant development (Pieterse et al., 2012). Complete genome analysis of strain PsJN revealed the presence of relevant genes involved in the indole-3-acetamide and the tryptophan side chain oxidase pathways (Weilharter et al., 2011). The production of IAA by PsJN was experimentally demonstrated with or without the addition of L-ryptophan (L-TRP), a precursor of auxins in plants (Naveed et al., 2015). Furthermore, this study demonstrated that the different plant growth parameters (plant height and biomass, photosynthesis, and chlorophyll content) of maize were significantly improved when applying PsJN inoculum supplemented with L-TRP. It has been previously shown that production of IAA by strain PsJN is likely involved in the efficient colonization of *Arabidopsis* (Zúñiga et al., 2013). The ability of strain PsJN to produce and degrade IAA as a sole carbon source gave an insight into the ability of this bacterium to resist under different stresses and lead to understand its friendly interaction with host plant (Donoso et al., 2017). Beside its role in the colonization, the IAA is also involved in the root proliferation (Zúñiga et al., 2013) and is considered as a signaling molecule in bacteria-plant interactions (Van Puyvelde et al., 2011).

Siderophore Production and Other Secondary Metabolites

Iron is essential for microorganisms due to its intervention in the synthesis of many essential components of the cell (Leclère et al., 2009). The availability of iron in the environment to living microbes is very low due to its poor solubility at neutral pH 7 (Andrews et al., 2003). Therefore, bacteria including endophytes have evolved several pathways including siderophore with high affinity to scavenge and transport iron from the environments (Loaces et al., 2011; Esmaeel et al., 2016a). Beside their ability to produce siderophores, some endophytes have membrane receptor proteins for the uptake of siderophores produced by other endophytes (Cornelis and Bodilis, 2009). The ability of endophytes to produce or capture siderophores, under iron stress condition, is one the most traits which provide iron to host plants (Johnson et al., 2013). It also contributes to protect host plant against phytopathogenic infection (Miethke and Marahiel, 2007), to activate the ISR (Van Loon et al., 2008), to facilitate the bacteria-plant interaction and is involved in the colonization of root, stem, and leaves (Compant et al., 2005a). The main mechanism of siderophore synthesis is achieved through modular megaenzymes called non-ribosomal peptides synthetases (NRPSs), and others are assembled by various enzymes known as NRPS independent siderophore (NIS) (Challis, 2005). NRPSs organized in modules, arranged in sets of primary domains including adenylation (A), thiolation (T), condensation (C), and thioesterase (TE) domains, which synthesize basic peptides. Moreover, secondary domains such as epimerization (E) are also contributing in the modifying peptides into more structurally complex peptides (Esmaeel et al., 2016b). The genome of *P. phytofirmans* PsJN was mined with the aim to screen all potentially produced secondary metabolites (SMs), especially those produced by NRPSs by following Florine workflow previously described (Esmaeel et al., 2016b) (**Figure 3A**). Genome analysis of PsJN revealed the presence of a siderophore gene cluster located in the chromosome 2 (*mba*A to *mba*N). This cluster includes two NRPS genes (*mba*A and *mba*B) as well as genes involved

TABLE 1 | Beneficial effects provided by the endophytic strain *Paraburkholderia phytofirmans* PsJN on different plants.

Crop	Benefit provided to the host plant	Reference
Grapevine	Growth enhancement, more secondary roots and leaf hairs.	Ait Barka et al., 2000; Compant et al., 2005b
	Increased shoot and root fresh and dry weight as well as the number of nodes.	
Maize	Increased shoot/root biomass, and leaf area.	Kost et al., 2014; Naveed et al., 2014b
	Increased leaf chlorophyll content, photosynthesis, and photochemical efficiency of PSII.	
Wheat	Better grain yield.	Naveed et al., 2014a
	Improvement of the ionic balance, antioxidant levels.	
	Increased nitrogen, phosphorus, potassium and protein concentration.	
Lupin	Degradation of plant-secreted oxalate and reduce the oxalate level which might reduce the infection potential of oxalate-producing phytopathogenic fungi or bacteria.	Kost et al., 2014
Watermelon	Root growth promotion and enhanced stem performance.	Liu et al., 1995
Switchgrass	Growth promotion.	Kim et al., 2012; Wang et al., 2015
	Increased shoot/root biomass, elongation of root, stem and leaf.	
	Early tillers and persistent growth vigor.	
	Improved the photosynthetic rates and greater water use efficiency.	
Tomato	Increased plant height, shoot/root biomass.	Frommel et al., 1991b; Pillay and Nowak, 1997; Sharma and Nowak, 1998; Nowak et al., 2004; Onofre-Lemus et al., 2009
	Greener leaves, shorter root system with more lateral roots and root hairs.	
Potato	Increased root number/dry weight, halum dry weight, stem length and node numbers.	Frommel et al., 1991a, 1993; Lazarovits and Nowak, 1997; Bensalim et al., 1998
	Induction of root branching and hair formation.	
	Increased chlorophyll and starch content, nutrient and water uptake.	
	Enhanced leaf hair formation, secondary root branching, and total plant lignin content Improved tuber number and weight, increased medium pH.	
	Enhanced tuber number and weight, earlier stolon formation.	
Arabidopsis	Stimulation of growth parameters (plant fresh weight, dry weight, number of root hairs and chlorophyll content)	Poupin et al., 2013; Zhao et al., 2016
	Enlarged stem cell size of pith and improved the essential metals, specifically iron, uptake and accumulation. Modulation of phytohormones.	
Cucumber	Inoculated seeds enhanced the early growth and promoted root growth and weight.	Nowak et al., 2004
Sweet pepper	Bacterized seedlings had higher initial vigor, higher root, and shoot fresh weight.	Nowak et al., 2004
Brassica	Optimized plant performance (height, root length, fresh and dry shoot biomass and root).	Nafees et al., 2018
	Improved the plant physiology parameters [photosynthetic rate, transpiration rate, stomatal conductance, chlorophyll contents (Chl), sub-stomatal CO_2 concentration (Ci), and water use efficiency] and antioxidant activity and reduced Cr uptake in Cr-contaminated soil.	
Cantaloupe	Reduced shoot growth and root length.	Liu et al., 1995
Canola	Root elongation.	Sun et al., 2009

in uptake and accessory genes (**Figure 3B**). The cluster also includes a gene (*mba*F) encoding for an extracytoplasmic sigma 70 factor involved in the regulation. Furthermore, the strain PsJN is also possesses 7 outer membranes ferric related siderophore receptors (TonB dependent), which are essentially required for strain PsJN to compete for iron through the uptake of siderophore-iron complexes produced by other microorganisms.

P. phytofirmans STRAIN PsJN, A PLANT DEFENDER

The high demand for agriculture crops is growing and is expected to keep on increasing for decades (Tilman et al., 2011). Under stress conditions, including biotic and abiotic, plants can be subjected to negative effects on the growth resulting in heavy losses. Therefore, improvement of plant tolerance to stress using plant-associated bacteria has arisen as an alternative strategy to enhance plant adaptation to different stress conditions (Shameer and Prasad, 2018). While most of the described endophytes protect the plant from biotic stresses, some are also able to defend their host plants against abiotic stresses. Among them, the endophytic strain PsJN that has been shown to improve tolerance toward high temperature, heavy metals (Nafees et al., 2018), cold, drought, and salinity stresses (Ait Barka et al., 2006; Naveed et al., 2014a; Pinedo et al., 2015) (**Table 2**). The role of strain PsJN on plants stress tolerance is discussed in the following subsections.

Plants Under Biotic Stress

Most of endophytic bacteria are well known for their capacity to produce secondary metabolites that have an inhibitory effect toward a wide range of phytopathogens. These metabolites

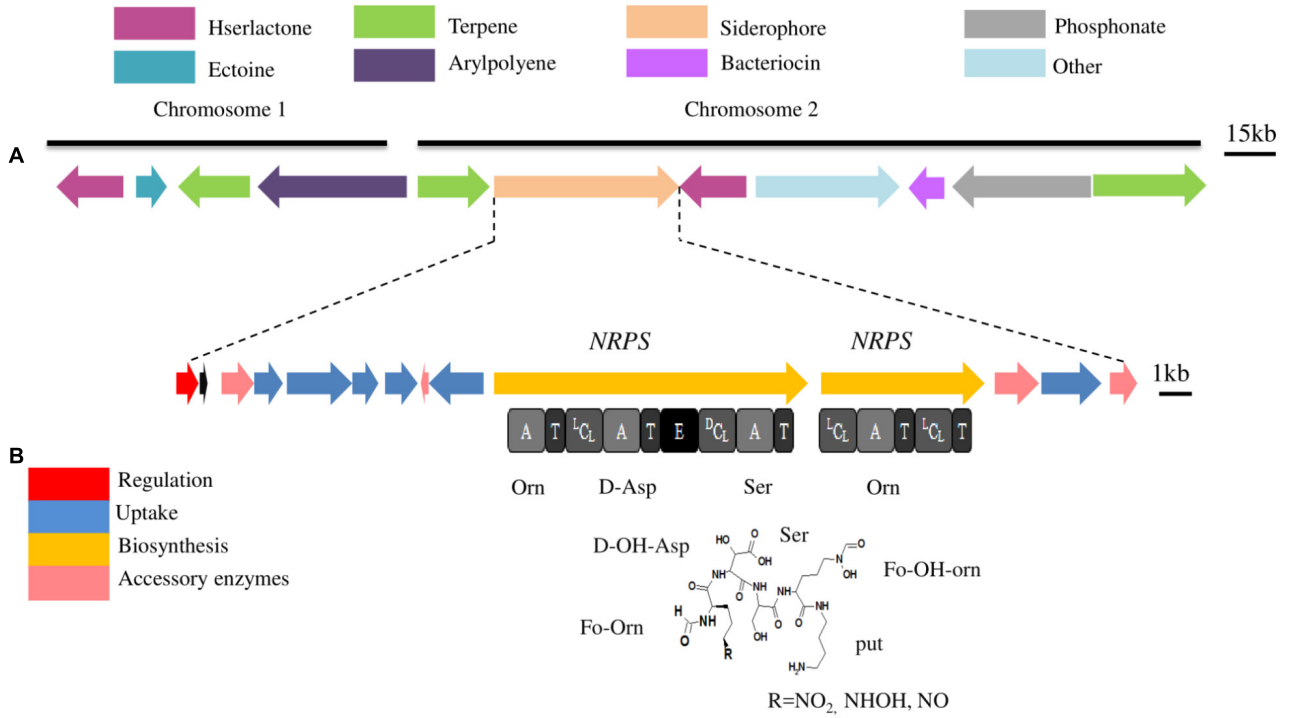

FIGURE 3 | (A) Secondary metabolite gene clusters predicted in the genome of *P. phytofirmans* PsJN. These gene clusters have been predicted using Florine workflow (Esmaeel et al., 2016b). Each color of gene clusters represents a different class of metabolites. Clusters were located in chromosomes 1 or 2 and some clusters are present in both chromosomes. **(B)** Siderophore gene cluster located in chromosomes 2. Gene implicated in the synthesis are represented by arrows. The domain organization of the NRPS genes is shown below arrows. A, Adenylation domain; $^{L}C_{L}$, condensation between 2 L-monomers; $^{D}C_{L}$, condensation between D-monomer and L-monomer; E, Epimerization domain; T, Thiolation domain. Predicted amino acid specificity is shown under each A domain, Asp, aspartic acid; Ser, serine; hfOrn, hydroxyformylornithine.

comprise polyketides, non-ribosomal peptides, terpenoids, alkaloids, steroids, flavonoids, 2-phenylethanol, and phenols (Taghavi et al., 2010; Hardoim et al., 2015; Esmaeel et al., 2017). Some of these compounds are important for protection and also play a significant role in mechanisms of signaling, defense, and genetic regulation of the interaction (Shameer and Prasad, 2018). *P. phytofirmans* PsJN has been reported as a remarkable biocontrol agent against *Botrytis cinerea* on grapevine (Ait Barka et al., 2000), *Fusarium oxysporum* and *Verticillium dahliae* on tomato (Frommel et al., 1991b; Sharma and Nowak, 1998), and *Pseudomonas syringae* on *Arabidopsis* (Su et al., 2017; Timmermann et al., 2017) (**Table 2**). Inoculation of the grapevine (*Vitis vinifera* L.) plantlets with PsJN induced their resistance against the pathogen *B. cinerea*, achieving a significant reduction of *Botrytis*-related necrosis (Ait Barka et al., 2000; Miotto-Vilanova et al., 2016). The mechanism behind the protection of *in vitro*- PsJN-bacterized plantlets against the mold disease can be explained through the direct inhibition of spore germination and disruption of the cellular membrane hence inducing mycelium cell death (Ait Barka et al., 2002; Miotto-Vilanova et al., 2016). Previous studies of plant-microbe interactions have discussed the ability of PGPB to trigger plant immune response and induce the systemic resistance (ISR) (Pieterse et al., 2014). Several factors have been identified to be responsible for ISR including flagella, antibiotic, *N*-acyl-homoserine lactones, lipopolysaccharides, salicylic acid (SA), jasmonic acid (JA), siderophores, and volatile compounds (Van Loon et al., 2008; Bordiec et al., 2011). Miotto-Vilanova et al. (2016) showed that strain PsJN-induced resistance against *Botrytis* is clarified through the induction of plant immunity response. When the bacterium is perceived by the plant cell, no significant induction of plant-related genes was observed. However, after the pathogen challenge, PsJN primed the expression of SA and JA related genes; modulated the level of leaf sugars and accumulated the stress-related metabolites including H_2O_2 and callose deposition (Miotto-Vilanova et al., 2016).

In tomato, bacterized plants challenged with *V. dahliae* caused a significant increase in plant height and biomass resulting in better performance of plant to withstand and reduce the severity of *Verticillium* wilt disease (Sharma and Nowak, 1998). Moreover, the combination of strain PsJN and *Serratia plymuthica* induced the resistance of tomato plants co-cultured with *Fusarium oxysporum* sp. *lycopersici* (Frommel et al., 1991b).

In *Arabidopsis*, the strain reduced disease severity and incidence of *Pseudomonas syringae* pv. *Tomato* DC3000 (Timmermann et al., 2017). In this study, strain PsJN-treated plants exhibited resistance to pathogen infection *via* the activation of plant signaling pathways including salicylic acid, jasmonate, and ethylene, leading to higher expression of plant defense-related genes. In the other hand, Su et al. (2017) showed

TABLE 2 | The proposed mechanism behind elevation in stress tolerance of different plants provided by the endophytic strain *P. phytofirmans* PsJN.

Stress conditions		Host	Mechanisms associated to the tolerance	Reference
Biotic stresses	*Botrytis cinerea*	Grapevine	Biofilm formation around *Botrytis.*	Ait Barka et al., 2000; Miotto-Vilanova et al., 2016
			Induced the expression of defense related genes (*PR1*, *PR2*, *PR5,* and *JAZ*).	
			Modulated the level of leaf carbohydrate and chlorophyll fluorescence.	
	Verticillium dahliae	Tomato	Reduced the severity of *Verticillium* wilt in tomato through induction of defense response.	Sharma and Nowak, 1998
			Improved the performance of plant which help plant to be more efficient to endure and reduce disease severity.	
	Fusarium oxysporum sp. *lycopersici*	Tomato	PsJN combined with *Serratia plymuthica* increased the resistance of tomato plants co-cultured with *Fusarium oxysporum* sp. *Lycopersici.*	Frommel et al., 1991b
	Pseudomonas syringae	*Arabidopsis*	Activation of plant defense-signaling pathways (salicylic acid, jasmonate, and ethylene).	Su et al., 2017; Timmermann et al., 2017
			Primed the expression of plant defense-related genes (PR1, PDF1.2).	
Abiotic stresses	High temperature	Potato	Induced the synthesis of tuberization factors, jasmonic acid which compensate abscissic acid (ABA).	Lazarovits and Nowak, 1997; Bensalim et al., 1998
			Induced morphological, physiological and cytological modifications represented by sturdier stem, larger leaves, more leaf hairs, more plastid numbers, more functional stomata leading to greater efficiency in controlling water loss.	
	Low temperature	Grapevine	Enhanced CO2 fixation and O2 evolution.	Ait Barka et al., 2006; Theocharis et al., 2011; Fernandez et al., 2012
			Accumulated the stress-related metabolites such as starch, proline, and phenolics and increased levels of soluble sugars (glucose, fructose, saccharose, M6P the precursor of mannose, raffinose, and maltose).	
			Enhanced the expression of antifreeze related genes (PR proteins), cold-specific transcription factor CBF4, stilbene synthase (STS), phenylalanine ammonia-lyase (PAL) and LOX genes.	
	Drought stress	Maize And wheat	Increased the leaf water content by 30%.	Naveed et al., 2014a,b
			Reduced leaf damage.	
			Improved the morphological and physiological (photosynthetic rate, water use efficiency and chlorophyll content) performance of plant.	
			Enhance water uptake.	
			Improved the ionic balance, antioxidant levels, and also increased the nitrogen, phosphorus, potassium and protein concentrations in the grains.	
	Salt stress	*Arabidopsis*	Accumulated less sodium within leaf tissues.	Pinedo et al., 2015; Ledger et al., 2016
			Accelerated the accumulation of proline, ROS scavenging, detoxification, and expression of abscisic acid signaling pathway, and down-regulated the expression of jasmonic acid biosynthesis related genes.	
			Regulated the expression of important ion-homeostasis related genes.	
			Production of ACC, auxin catabolism, *N*-acyl-homoserine-lactone production, and flagellin synthesis.	
	Heavy metal contaminated soil	Brassica	Stabilized chromium (Cr) levels in soil and reduced Cr uptake in Cr−contaminated soil.	Nafees et al., 2018

that PsJN, *in vitro*, did not exhibit direct antibacterial activity toward *P. syringae*. However, *in planta*, the presence of PsJN at the site of infection alleviates the pathogen growth during the early stage of infection. In addition, bacterized seeds limited the presence of the pathogen in the root system through priming the expression of plant defense-related genes.

Plants Under Abiotic Stress

Plants are exposed to different environmental stresses such as drought, heat, heavy metals, and salinity which have profound effects on plant growth and yield leading to significant reduction in crops production. Thus, the reduction of abiotic stresses using eco-friendly strategy is essentially important. One way to achieve the sustainable agriculture and reduce the loss is the application of beneficial bacteria, which provides better choice to improve the crop productivity and enhance the plant tolerance to different stresses. The use of *P. phytofirmans* strain PsJN to alleviate and induce tolerance toward different abiotic stresses in different crops (**Table 2**) has been reported, hence opening an effective and a promising strategy for sustainable agriculture.

Heat Stress

The high temperature is a serious problem affecting plant physiology and maturity leading to enormous crop losses. In the field, plant growth and quality are affected by different stresses including high temperature surrounding the plants. Since each species has an optimum range of temperature, temperatures exceeding this range would initiate a heat stress which is a primary factor imposing a drastic impact on plant growth resulting therefore in heavy losses (Hatfield et al., 2011). As a result of global climate change, the rate of high temperature is expected to keep on increasing in different parts of the world which negatively influences the yield. High temperature causes a reduction in roots and shoots development, a severe reduction in potato tuber number and fresh weight (Bensalim et al., 1998). Therefore, evolving low-cost strategies to enhance the plant tolerance to heat stress would help in overcoming the negative impact of climate change. The use of PGPB to improve the tolerance to elevated temperature has received a lot of attention as a promising method for sustainable agriculture. In potato, the effect of inoculation with strain PsJN on the plant growth at elevated temperature was reported (Bensalim et al., 1998). As compared to non-PsJN treated (control), *in vitro*-plantlet inoculated with strain PsJN showed a better performance in plant growth likely due to the development of more secondary roots (Frommel et al., 1991a) which lead to more water and nutrient availability. The ability of the PsJN strain to accumulate cytokinin content and increase medium pH in bacterized plantlets might also explain its significant role to modify the plant performance and consequently increase heat stress tolerance (Lazarovits and Nowak, 1997).

Low Temperature

Plant health can be subjected to different environmental stresses including low temperature which affects the geographical distribution of many plant species and causes significant impacts in the yield of the most valuable agricultural crops (Theocharis et al., 2012). Under low temperature, plants evolve several physiological and molecular changes to improve their tolerance to cold stress. This process is known as cold acclimation which includes different modifications such as accumulation of carbohydrates and osmolytes, the expression of stress-related genes, and specific proteins synthesis (Ruelland et al., 2009; Theocharis et al., 2012). The use of beneficial bacteria to enhance chilling resistance has been reported as a new solution to induce plant defense to cope toward cold stress (Yang et al., 2009; Theocharis et al., 2011).

The *P. phytofirmans* strain PsJN was shown to help plants to overcome chilling stress in the grapevine by inducing physiological and biochemical changes. PsJN-bacterized plantlets showed significant elevation of proline, phenolics, starch deposition, and the photosynthetic rate was also enhanced as compared to non-PsJN treated plantlets (Ait Barka et al., 2006). Furthermore, bacterized plantlets exhibited significant accumulation of compatible osmolytes which are involved in cold adaptation in plants (Theocharis et al., 2011). Moreover, Fernandez et al. (2012) demonstrated that grapevine-bacterized plantlets, upon exposure to low temperature, accumulated more concentrations of starch, raffinose, and mannose, and other soluble sugars, likely related to the stimulation of reactive oxygen species (ROS)-scavenging system by this bacterium (Theocharis et al., 2011). The PsJN-associated tolerance to low-temperature stress might also be related to enhanced expression of stress-related genes stilbene synthase and phenylalanine ammonia-lyase, involved in the synthesis of resveratrol and SA, respectively, known for their involvement in plant stress responses (Theocharis et al., 2011, 2012). Moreover, PsJN enhanced the expression of cold-specific transcription factor CBF4 and PR proteins, including acidic chitinases and a basic glucanase, both are well known for their involvement in grapevine resistance against pathogen attacks (Miotto-Vilanova et al., 2016) and cold stress (Griffith and Yaish, 2004).

Drought Stress

Drought is a major abiotic stress that limits the plant productivity. It affects plant growth and crop quality by reducing plant water availability leading to physiological and morphological changes such as leaf wilting, reduction in chlorophyll content, root elongation and production of ROS (Vurukonda et al., 2016). To cope with this stress, different solutions have been reported including the use of PGPB as a promising strategy to improve plant growth under water deficit conditions (Yang et al., 2009). The inoculation of plants with strain PsJN led to growth improvement, increased nutrient uptake and helped plants to be more tolerant to drought stress (Naveed et al., 2014a). In maize (*Zea mays* L.), under drought stress conditions, inoculation with strain PsJN resulted in more production of plant biomass and significantly improved the physiological traits in both varieties comparing to plant inoculated with *Enterobacter* sp. FD17 or non-inoculated plant (control) (Naveed et al., 2014b). In wheat (*Triticum aestivum* L.), under reduced irrigation, strain PsJN was effective to improve relative water content, chlorophyll content, antioxidant activities, and photosynthetic rate, and consequently improved crop yield and quality (Naveed et al., 2014a). The mechanism of drought-stress tolerance could be explained by the alteration of plant defense-related genes in the presence of strain PsJN (Sheibani-Tezerji et al., 2015).

Salt Stress

Salinity is a serious threat affecting the plant productivity worldwide (Gupta and Huang, 2014). It defines by the

accumulation of excessive amounts of sodium salts in the plant tissue. As a result of salinity stress, plant can be subjected to significant physiological disorder (s) leading to substantial loss in crop productivity and quality. The most drastically step of increased salinity is the ion imbalance resulting in high Na^+ concentration and consequently leading to deleterious effects on cell metabolism. Furthermore, accumulation of Na^+ at high concentration minimizes the plant's ability to take up K^+ ions, an essential macroelement for proper growth and development of plants (Gupta and Huang, 2014). It is involved in many plant processes such as protein synthesis, the activation of enzymes, cell metabolism, photosynthesis, and osmoregulation. Furthermore, for osmotic functions, most plants have preference for K^+ rather than Na^+ (Zhang et al., 2009). Therefore, under salinity stress, plants require sufficient amounts of K^+ ions that are captured by the root from the soil particles. The accumulation of Na^+ can be influenced by the presence of other elements. For example, the supplement of Ca^{2+} and Mg^{2+} was shown to have a protective

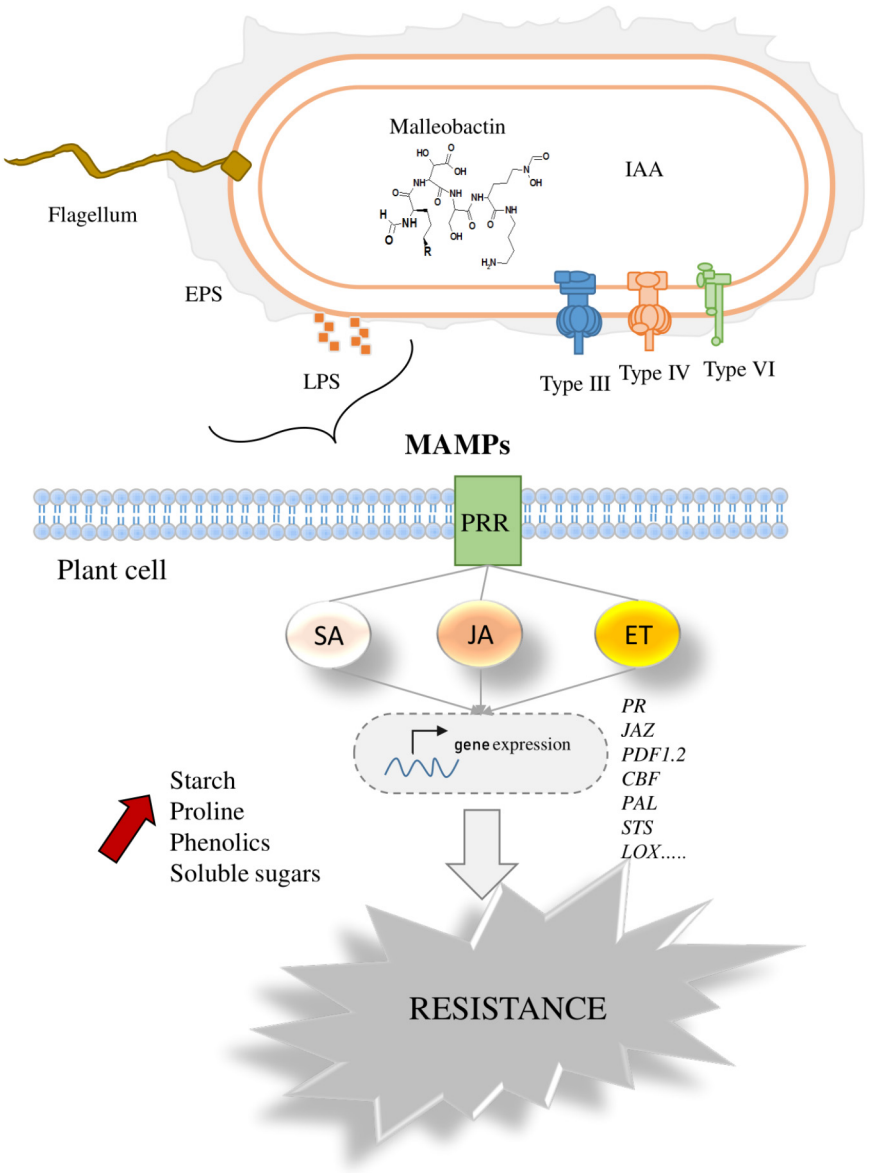

FIGURE 4 | Overview of plant perception of *P. phytofirmans* PsJN. The figure explains the range of signals produced by strain PsJN that can be perceived by host plant cell. These include flagellin, phytohormones, malleobactin, LPS, and effectors proteins, injected by secretion pathways. After exposure to bacterial signals, plant cell responses are characterized by early and long-term responses in plant immunity represented by the expression of plant defense-signaling networks and modulation the level of soluble sugars, starch, proline, and phenolic compounds. PR, pathogenesis-related proteins; JAZ, jasmonate; PDF1.2, plant defensin; PAL, phenylalanine ammonia lyase; STS, stilbene synthase; LOX, lipoxygenase; EPS, Exopolysaccahrides; IAA, indole-3-acetic acid; Type III, type III secretion system; Type IV, type IV secretion system; Type IV, type VI secretion system.

effect on salinity stress through the inhibition of Na+ transport (Zhang et al., 2009).

As a result of osmotic stress, different physiological disorders are generated including accumulation of ROS, reduced photosynthetic capability, increased ethylene, and reduction of root and shoot length (Zhang and Shi, 2013; Deinlein et al., 2014). Therefore, the improvement of plant salinity tolerance is urgently needed to cope the growing demand for crop production. The use of plant growth-promoting bacteria as a valuable strategy to promote the salt stress tolerance in plants have been reported (Han et al., 2014). Plants inoculated with beneficial bacteria were shown to increase their tolerance toward salinity stress by maintaining the K^+/Na^+ ratio and reducing the sodium salts in the cytoplasm (Zhang and Shi, 2013; Gupta and Huang, 2014).

In *A. thaliana*, upon exposure to salt stress, plants treated with *P. phytofirmans* strain PsJN displayed different salt-stress responses involved in ROS scavenging and ABA-dependent pathways (Pinedo et al., 2015). PsJN-Inoculated plants induced the expression of genes involved in ion homeostasis and one gene associated to JA biosynthesis was down regulated. The mechanism of salt-stress tolerance associated with PsJN could be explained by the priming effects of the strain and maintaining the expression of salt stress-related genes over time. Beneficial bacteria can also induce the tolerance by the secretion of exudates osmolytes which can act together with other osmolytes produced by plants to reduce the negative effects of salt stress and stimulate plant growth (Paul and Nair, 2008). The volatile compounds (VOCs) produced by PsJN were shown to play a crucial role in the plant growth promoting effect and tolerance to salinity stress. Exposure of *A. thaliana* to VOCs produced by PsJN induced the growth promotion and the salt-stress tolerance (Ledger et al., 2016).

CONCLUSION

Plants are exposed to different environmental stress conditions that reduce their productivity. While no real solutions are available to withstand abiotic stress, chemical pesticides are mainly applied to control plant pathogens and to enhanced crop yield and quality. However, negative impacts such as a development of resistance in pathogenic races are generated. Therefore, one strategy to minimize the use of synthetic fungicides is the application of beneficial microbes able to improve the plant health and enhance the plant defense against a broad range of phytopathogens.

In this review, the potential beneficial effects of *P. phytofirmans* strain PsJN on different host plants have been highlighted. The bacterization with the strain PsJN improved the growth parameters in different host plants and significantly reduced the negative impacts of biotic and abiotic stresses. Studies of plant-*P. phytofirmans* PsJN interaction have discussed different key signals implicated in plant perception of the bacterium and in the bacterial modulation of host metabolisms, which help to understand the observed positive effect of strain PsJN on host plants (**Figure 4**). Furthermore, the positive roles of strain PsJN in sustainable agriculture emphasized its promising applications to optimize crops performance and improved their tolerance to different environmental stress conditions.

Overall, beneficial effects associated with strain PsJN suggest using this bacterium as a model system in sustainable crop production. This will open new doors for improving plant health and reducing the global dependency on chemical pesticides.

On the other side, beneficial effects of plant-associated bacteria vary under artificial laboratory conditions, greenhouse, and field trials. The intended results under field trails are sometimes difficult due to the unpredicted environments as well as the climate variation which impact the effectiveness of plant associated bacteria. Furthermore, in the field, the survival and the viability of bacterial cell need to be more explored.

AUTHOR CONTRIBUTIONS

QE did the writing. QE and LS drew the graphs. LM and MR were partially involved in writing the review. VL, CC, CJ, LS, and EB revised the manuscript with contributions and discussion from all co-authors. All authors given their approval to the final version of the manuscript.

FUNDING

This work was supported by the University of Reims Champagne-Ardenne. The authors would like to thank European Union funding through the INTERREG V FWF (France Wallonie Flandre) a SmartBioControl project (BioScreen project).

REFERENCES

Agarwal, S. (1987). Tetrazolium reducing microorganisms inside the root of *Brassica* species. *Curr. Sci.* 56, 187–188.

Ait Barka, E., Belarbi, A., Hachet, C., Nowak, J., and Audran, J. C. (2000). Enhancement of *in vitro* growth and resistance to gray mould of *Vitis vinifera* co-cultured with plant growth-promoting rhizobacteria. *FEMS Microbiol. Lett.* 186, 91–95. doi: 10.1111/j.1574-6968.2000.tb09087.x

Ait Barka, E., Gognies, S., Nowak, J., Audran, J. C., and Belarbi, A. (2002). Inhibitory effect of endophyte bacteria on *Botrytis cinerea* and its influence to promote the grapevine growth. *Biol. Control* 24, 135–142. doi: 10.1016/S1049-9644(02)00034-8

Ait Barka, E., Nowak, J., and Clément, C. (2006). Enhancement of chilling resistance of inoculated grapevine plantlets with a plant growth-promoting rhizobacterium, *Burkholderia phytofirmans* strain PsJN. *Appl. Environ. Microbiol.* 72, 7246–7252. doi: 10.1128/aem.01047-06

Ali, S., Duan, J., Charles, T. C., and Glick, B. R. (2014). A bioinformatics approach to the determination of genes involved in endophytic behavior in *Burkholderia* spp. *J. Theor. Biol.* 343, 193–198. doi: 10.1016/j.jtbi.2013.10.007

Andreolli, M., Lampis, S., Zapparoli, G., Angelini, E., and Vallini, G. (2016). Diversity of bacterial endophytes in 3 and 15 year-old grapevines of *Vitis vinifera* cv. Corvina and their potential for plant growth promotion and phytopathogen control. *Microbiol. Res.* 183, 42–52. doi: 10.1016/j.micres.2015.11.009

Andrews, S. C., Robinson, A. K., and Rodríguez-Quiñones, F. (2003). Bacterial iron homeostasis. *FEMS Microbiol. Rev.* 27, 215–237. doi: 10.1016/S0168-6445(03)00055-X

Bensalim, S., Nowak, J., and Asiedu, S. K. (1998). A plant growth promoting rhizobacterium and temperature effects on performance of 18 clones of potato. *Am. J. Potato Res.* 75, 145–152. doi: 10.1007/BF02895849

Bordiec, S., Paquis, S., Lacroix, H., Dhondt, S., Ait Barka, E., Kauffmann, S., et al. (2011). Comparative analysis of defence responses induced by the endophytic plant growth-promoting rhizobacterium *Burkholderia phytofirmans* strain PsJN and the non-host bacterium *Pseudomonas syringae* pv. *pisi* in grapevine cell suspensions. *J. Exp. Bot.* 62, 595–603. doi: 10.1093/jxb/erq291

Challis, G. L. (2005). A widely distributed bacterial pathway for siderophore biosynthesis independent of nonribosomal peptide synthetases. *Chembiochem* 6, 601–611. doi: 10.1002/cbic.200400283

Compant, S., Clément, C., and Sessitsch, A. (2010). Plant growth-promoting bacteria in the rhizo-and endosphere of plants: their role, colonization, mechanisms involved and prospects for utilization. *Soil Biol. Biochem.* 42, 669–678. doi: 10.1016/j.soilbio.2009.11.024

Compant, S., Duffy, B., Nowak, J., Clément, C., and Barka, E. A. (2005a). Use of plant growth-promoting bacteria for biocontrol of plant diseases: principles, mechanisms of action, and future prospects. *Appl. Environ. Microbiol.* 71, 4951–4959. doi: 10.1128/aem.71.9.4951-4959.2005

Compant, S., Reiter, B., Sessitsch, A., Nowak, J., Clément, C., and Barka, E. A. (2005b). Endophytic colonization of *Vitis vinifera* L. by plant growth-promoting bacterium *Burkholderia* sp. strain PsJN. *Appl. Environ. Microbiol.* 71, 1685–1693. doi: 10.1128/AEM.71.4.1685-1693.2005

Compant, S., Kaplan, H., Sessitsch, A., Nowak, J., Ait Barka, E., and Clément, C. (2007). Endophytic colonization of *Vitis vinifera* L. by *Burkholderia phytofirmans* strain PsJN: from the rhizosphere to inflorescence tissues. *FEMS Microbiol. Ecol.* 63, 84–93. doi: 10.1111/j.1574-6941.2007.00410.x

Compant, S., Nowak, J., Coenye, T., Clément, C., and Ait Barka, E. (2008). Diversity and occurrence of *Burkholderia* spp. in the natural environment. *FEMS Microbiol. Rev.* 32, 607–626. doi: 10.1111/j.1574-6976.2008.00113.x

Cornelis, P., and Bodilis, J. (2009). A survey of tonb-dependent receptors in fluorescent *Pseudomonads*. *Environ. Microbiol. Rep.* 1, 256–262. doi: 10.1111/j.1758-2229.2009.00041.x

Couderchet, M. (2003). Benefits and problems of fungicide control of *Botrytis cinerea* in vineyards of Champagne. *Vitis* 42, 165–172.

Deinlein, U., Stephan, A. B., Horie, T., Luo, W., Xu, G., and Schroeder, J. I. (2014). Plant salt-tolerance mechanisms. *Trends Plant Sci.* 19, 371–379. doi: 10.1016/j.tplants.2014.02.001

DeLeon-Rodriguez, N., Lathem, T. L., Rodriguez-R, L. M., Barazesh, J. M., Anderson, B. E., Beyersdorf, A. J., et al. (2013). Microbiome of the upper troposphere: species composition and prevalence, effects of tropical storms, and atmospheric implications. *Proc. Natl. Acad. Sci. U.S.A.* 110, 2575–2580. doi: 10.1073/pnas.1212089110

Depoorter, E., Bull, M. J., Peeters, C., Coenye, T., Vandamme, P., and Mahenthiralingam, E. (2016). Burkholderia: an update on taxonomy and biotechnological potential as antibiotic producers. *Appl. Microbiol. Biotechnol.* 100, 5215–5229. doi: 10.1007/s00253-016-7520-x

Donoso, R., Leiva-Novoa, P., Zúñiga, A., Timmermann, T., Recabarren-Gajardo, G., and González, B. (2017). Biochemical and genetic bases of indole-3-acetic acid (auxin phytohormone) degradation by the plant-growth-promoting rhizobacterium *Paraburkholderia phytofirmans* PsJN. *Appl. Environ. Microbiol.* 83, e01991-16. doi: 10.1128/AEM.01991-16

Dunwell, J. M., Purvis, A., and Khuri, S. (2004). Cupins: the most functionally diverse protein superfamily? *Phytochemistry* 65, 7–17. doi: 10.1016/j.phytochem.2003.08.016

Eberl, L., and Vandamme, P. (2016). Members of the genus *Burkholderia*: good and bad guys. *F1000Res.* 5:1007. doi: 10.12688/f1000research.8221.1

Esmaeel, Q., Chevalier, M., Chataigné, G., Subashkumar, R., Jacques, P., and Leclère, V. (2016a). Nonribosomal peptide synthetase with a unique iterative-alternative-optional mechanism catalyzes amonabactin synthesis in *Aeromonas*. *Appl. Microbiol. Biotechnol.* 100, 8453–8463. doi: 10.1007/s00253-016-7773-4

Esmaeel, Q., Pupin, M., Kieu, N. P., Chataigné, G., Béchet, M., Deravel, J., et al. (2016b). *Burkholderia* genome mining for nonribosomal peptide synthetases reveals a great potential for novel siderophores and lipopeptides synthesis. *MicrobiologyOpen* 5, 512–526. doi: 10.1002/mbo3.347

Esmaeel, Q., Pupin, M., Jacques, P., and Leclère, V. (2017). Nonribosomal peptides and polyketides of *Burkholderia*: new compounds potentially implicated in biocontrol and pharmaceuticals. *Environ. Sci. Pollut. Res.* doi: 10.1007/s11356-017-9166-3 [Epub ahead of print].

Fernandez, O., Theocharis, A., Bordiec, S., Feil, R., Jacquens, L., Clément, C., et al. (2012). *Burkholderia phytofirmans* PsJN acclimates grapevine to cold by modulating carbohydrate metabolism. *Mol. Plant Microbe Interact.* 25, 496–504. doi: 10.1094/MPMI-09-11-0245

Frommel, M., Nowak, J., and Lazarovits, G. (1993). Treatment of potato tubers with a growth promoting *Pseudomonas* sp.: plant growth responses and bacterium distribution in the rhizosphere. *Plant Soil* 150, 51–60. doi: 10.1007/BF00779175

Frommel, M. I., Nowak, J., and Lazarovits, G. (1991a). Growth enhancement and developmental modifications of *in vitro* grown potato (*Solanum tuberosum* spp. *tuberosum*) as affected by a nonfluorescent *Pseudomonas* sp. *Plant Physiol.* 96, 928–936.

Frommel, M. I., Nowak, J., and Lazarovits, G. (1991b). Plant growth stimulation and biocontrol of *Fusarium* wilt by co-inoculation of tomato seeds with *Serratia plymuthica* and *Pseudomonas* sp. *Fitopatologia* 26, 66–73.

Glick, B. R. (2004). Bacterial ACC deaminase and the alleviation of plant stress. *Adv. Appl. Microbiol.* 56, 291–312. doi: 10.1016/S0065-2164(04)56009-4

Glick, B. R., Penrose, D. M., and Li, J. (1998). A model for the lowering of plant ethylene concentrations by plant growth-promoting bacteria. *J. Theor. Biol.* 190, 63–68. doi: 10.1006/jtbi.1997.0532

Glick, B. R., Todorovic, B., Czarny, J., Cheng, Z., Duan, J., and McConkey, B. (2007). Promotion of plant growth by bacterial ACC deaminase. *Crit. Rev. Plant Sci.* 26, 227–242. doi: 10.1080/07352680701572966

Griffith, M., and Yaish, M. W. F. (2004). Antifreeze proteins in overwintering plants: a tale of two activities. *Trends Plant Sci.* 9, 399–405. doi: 10.1016/j.tplants.2004.06.007

Gupta, B., and Huang, B. (2014). Mechanism of salinity tolerance in plants: physiological, biochemical, and molecular characterization. *Int. J. Genomics* 2014:701596. doi: 10.1155/2014/701596

Han, Q. Q., Lü, X. P., Bai, J. P., Qiao, Y., Paré, P. W., Wang, S. M., et al. (2014). Beneficial soil bacterium *Bacillus subtilis* (GB03) augments salt tolerance of white clover. *Front. Plant Sci.* 5:525. doi: 10.3389/fpls.2014.00525

Hardoim, P. R., Van Overbeek, L. S., Berg, G., Pirttilä, A. M., Compant, S., Campisano, A., et al. (2015). The hidden world within plants: ecological and evolutionary considerations for defining functioning of microbial endophytes. *Microbiol. Mol. Biol. Rev.* 79, 293–320. doi: 10.1128/MMBR.00050-14

Hatfield, J. L., Boote, K. J., Kimball, B., Ziska, L., Izaurralde, R. C., Ort, D., et al. (2011). Climate impacts on agriculture: implications for crop production. *Agron. J.* 103, 351–370. doi: 10.2134/agronj2010.0303

Huang, J.-S. (1986). Ultrastructure of bacterial penetration in plants. *Annu. Rev. Phytopathol.* 24, 141–157.

James, E. K., Gyaneshwar, P., Mathan, N., Barraquio, W. L., Reddy, P. M., Iannetta, P. P., et al. (2002). Infection and colonization of rice seedlings by the plant growth-promoting bacterium *Herbaspirillum seropedicae* Z67. *Biol. Plant Microbe Interact.* 15, 894–906. doi: 10.1094/MPMI.2002.15.9.894

Johnson, L. J., Koulman, A., Christensen, M., Lane, G. A., Fraser, K., Forester, N., et al. (2013). An extracellular siderophore is required to maintain the mutualistic interaction of *Epichloë festucae* with *Lolium perenne*. *PLoS Pathog.* 9:e1003332. doi: 10.1371/journal.ppat.1003332

Jones, J. D., and Dangl, J. L. (2006). The plant immune system. *Nature* 444, 323–329. doi: 10.1038/nature05286

Kandel, S. L., Joubert, P. M., and Doty, S. L. (2017). Bacterial endophyte colonization and distribution within plants. *Microorganisms* 5:E77. doi: 10.3390/microorganisms5040077

Kawasaki, A., Donn, S., Ryan, P. R., Mathesius, U., Devilla, R., Jones, A., et al. (2016). Microbiome and exudates of the root and rhizosphere of *Brachypodium distachyon*, a model for wheat. *PLoS One* 11:e0164533. doi: 10.1371/journal.pone.0164533

Kim, S., Lowman, S., Hou, G., Nowak, J., Flinn, B., and Mei, C. (2012). Growth promotion and colonization of switchgrass (*Panicum virgatum*) cv. Alamo by bacterial endophyte *Burkholderia phytofirmans* strain PsJN. *Biotechnol. Biofuels* 5:37. doi: 10.1186/1754-6834-5-37

Kim, Y.-S. (2002). Malonate metabolism: biochemistry, molecular biology, physiology, and industrial application. *J. Biochem. Mol. Biol.* 35, 443–451. doi: 10.5483/BMBRep.2002.35.5.443

Kost, T., Stopnisek, N., Agnoli, K., Eberl, L., and Weisskopf, L. (2014). Oxalotrophy, a widespread trait of plant-associated *Burkholderia* species, is involved in

successful root colonization of lupin and maize by *Burkholderia phytofirmans*. *Front. Microbiol.* 4:421. doi: 10.3389/fmicb.2013.00421

Lackner, G., Moebius, N., Partida-Martinez, L., and Hertweck, C. (2011). Complete genome sequence of *Burkholderia rhizoxinica*, an endosymbiont of *Rhizopus microsporus*. *J. Bacteriol.* 193, 783–784. doi: 10.1128/jb.01318-10

Lazarovits, G., and Nowak, J. (1997). Rhizobacteria for improvement of plant growth and establishment. *HortScience* 32, 188–192.

Leclère, V., Beaufort, S., Dessoy, S., Dehottay, P., and Jacques, P. (2009). Development of a biological test to evaluate the bioavailability of iron in culture media. *J. Appl. Microbiol.* 107, 1598–1605. doi: 10.1111/j.1365-2672.2009.04345.x

Ledger, T., Rojas, S., Timmermann, T., Pinedo, I., Poupin, M. J., Garrido, T., et al. (2016). Volatile-mediated effects predominate in *Paraburkholderia phytofirmans* growth promotion and salt stress tolerance of *Arabidopsis thaliana*. *Front. Microbiol.* 7:1838. doi: 10.3389/fmicb.2016.01838

Lindow, S. E., and Brandl, M. T. (2003). Microbiology of the phyllosphere. *Appl. Environ. Microbiol.* 69, 1875–1883. doi: 10.1128/aem.69.4.1875-1883.2003

Liu, Z., Pillay, V., and Nowak, J. (1995). *In vitro* culture of watermelon and cantaloupe with and without beneficial bacterium. *Acta Hortic.* 402, 58–60. doi: 10.17660/ActaHortic.1995.402.1

Loaces, I., Ferrando, L., and Scavino, A. F. (2011). Dynamics, diversity and function of endophytic siderophore-producing bacteria in rice. *Microb. Ecol.* 61, 606–618. doi: 10.1007/s00248-010-9780-9

Mathesius, U., Mulders, S., Gao, M., Teplitski, M., Caetano-Anollés, G., Rolfe, B. G., et al. (2003). Extensive and specific responses of a eukaryote to bacterial quorum-sensing signals. *Proc. Natl. Acad. Sci. U.S.A.* 100, 1444–1449. doi: 10.1073/pnas.262672599

Miethke, M., and Marahiel, M. A. (2007). Siderophore-based iron acquisition and pathogen control. *Microbiol. Mol. Biol. Rev.* 71, 413–451. doi: 10.1128/MMBR.00012-07

Miotto-Vilanova, L., Jacquard, C., Courteaux, B., Wortham, L., Michel, J., Clément, C., et al. (2016). *Burkholderia phytofirmans* PsJN confers grapevine resistance against *Botrytis cinerea* via a direct antimicrobial effect combined with a better resource mobilization. *Front. Plant Sci.* 7:1236. doi: 10.3389/fpls.2016.01236

Mitter, B., Petric, A., Shin, M. W., Chain, P. S. G., Hauberg-Lotte, L., Reinhold-Hurek, B., et al. (2013). Comparative genome analysis of *Burkholderia phytofirmans* PsJN reveals a wide spectrum of endophytic lifestyles based on interaction strategies with host plants. *Front. Plant Sci.* 4:120. doi: 10.3389/fpls.2013.00120

Mitter, B., Pfaffenbichler, N., Flavell, R., Compant, S., Antonielli, L., Petric, A., et al. (2017). A new approach to modify plant microbiomes and traits by introducing beneficial bacteria at flowering into progeny seeds. *Front. Microbiol.* 8:11. doi: 10.3389/fmicb.2017.00011

Nafees, M., Ali, S., Naveed, M., and Rizwan, M. (2018). Efficiency of biogas slurry and *Burkholderia phytofirmans* PsJN to improve growth, physiology, and antioxidant activity of *Brassica napus* L. in chromium-contaminated soil. *Environ. Sci. Pollut. Res.* 25, 6387–6397. doi: 10.1007/s11356-017-0924-z

Naveed, M., Hussain, M. B., Zahir, Z. A., Mitter, B., and Sessitsch, A. (2014a). Drought stress amelioration in wheat through inoculation with *Burkholderia phytofirmans* strain PsJN. *Plant Growth Regul.* 73, 121–131. doi: 10.1007/s10725-013-9874-8

Naveed, M., Mitter, B., Reichenauer, T. G., Wieczorek, K., and Sessitsch, A. (2014b). Increased drought stress resilience of maize through endophytic colonization by *Burkholderia phytofirmans* PsJN and *Enterobacter* sp. FD17. *Environ. Exp. Bot.* 97, 30–39. doi: 10.1016/j.envexpbot.2013.09.014

Naveed, M., Qureshi, M. A., Zahir, Z. A., Hussain, M. B., Sessitsch, A., and Mitter, B. (2015). L-Tryptophan-dependent biosynthesis of indole-3-acetic acid (IAA) improves plant growth and colonization of maize by *Burkholderia phytofirmans* PsJN. *Ann. Microbiol.* 65, 1381–1389. doi: 10.1007/s13213-014-0976-y

Nowak, J., Sharma, V., and A'Hearn, E. (2004). Endophyte enhancement of transplant performance in tomato, cucumber and sweet pepper. *Acta Hortic.* 631, 253–263.

Onofre-Lemus, J., Hernández-Lucas, I., Girard, L., and Caballero-Mellado, J. (2009). ACC (1-aminocyclopropane-1-carboxylate) deaminase activity, a widespread trait in *Burkholderia* species, and Its growth-promoting effect on tomato plants. *Appl. Environ. Microbiol.* 75, 6581–6590. doi: 10.1128/aem.01240-09

Paul, D., and Nair, S. (2008). Stress adaptations in a plant growth promoting rhizobacterium (PGPR) with increasing salinity in the coastal agricultural soils. *J. Basic Microbiol.* 48, 378–384. doi: 10.1002/jobm.200700365

Pieterse, C. M., Van der Does, D., Zamioudis, C., Leon-Reyes, A., and Van Wees, S. C. (2012). Hormonal modulation of plant immunity. *Annu. Rev. Cell Dev. Biol.* 28, 489–521. doi: 10.1146/annurev-cellbio-092910-154055

Pieterse, C. M., Zamioudis, C., Berendsen, R. L., Weller, D. M., Van Wees, S. C., and Bakker, P. A. (2014). Induced systemic resistance by beneficial microbes. *Annu. Rev. Phytopathol.* 52, 347–375. doi: 10.1146/annurev-phyto-082712-102340

Pillay, V., and Nowak, J. (1997). Inoculum density, temperature, and genotype effects on in vitro growth promotion and epiphytic and endophytic colonization of tomato (*Lycopersicon esculentum* L.) seedlings inoculated with a *Pseudomonad* bacterium. *Can. J. Microbiol.* 43, 354–361. doi: 10.1139/m97-049

Pinedo, I., Ledger, T., Greve, M., and Poupin, M. J. (2015). *Burkholderia phytofirmans* PsJN induces long-term metabolic and transcriptional changes involved in *Arabidopsis thaliana* salt tolerance. *Front. Plant Sci.* 6:466. doi: 10.3389/fpls.2015.00466

Poupin, M. J., Timmermann, T., Vega, A., Zuñiga, A., and González, B. (2013). Effects of the plant growth-promoting bacterium *Burkholderia phytofirmans* PsJN throughout the life cycle of *Arabidopsis thaliana*. *PLoS One* 8:e69435. doi: 10.1371/journal.pone.0069435

Preston, G. M. (2004). Plant perceptions of plant growth-promoting *Pseudomonas*. *Philos. Trans. R. Soc. Lond. B* 359, 907–918. doi: 10.1098/rstb.2003.1384

Ramette, A., LiPuma, J. J., and Tiedje, J. M. (2005). Species abundance and diversity of *Burkholderia cepacia* complex in the environment. *Appl. Environ. Microbiol.* 71, 1193–1201. doi: 10.1128/aem.71.3.1193-1201.2005

Reinhold-Hurek, B., Maes, T., Gemmer, S., Van Montagu, M., and Hurek, T. (2006). An endoglucanase is involved in Infection of rice roots by the not-cellulose-metabolizing endophyte *Azoarcus* sp. strain BH72. *Mol. Plant Microbe Interact.* 19, 181–188. doi: 10.1094/mpmi-19-0181

Roos, I. M., and Hattingh, M. (1983). Scanning electron microscopy of *Pseudomonas syringae* pv, morsprunorum on sweet cherry leaves. *J. Phytopathol.* 108, 18–25.

Ruelland, E., Vaultier, M.-N., Zachowski, A., and Hurry, V. (2009). Chapter 2 cold signalling and cold acclimation in plants. *Adv. Bot. Res.* 49, 35–150. doi: 10.1016/S0065-2296(08)00602-2

Sawana, A., Adeolu, M., and Gupta, R. S. (2014). Molecular signatures and phylogenomic analysis of the genus *Burkholderia*: proposal for division of this genus into the emended genus *Burkholderia* containing pathogenic organisms and a new genus Para*burkholderia* gen. nov. harboring environmental species. *Front. Genet.* 5:429. doi: 10.3389/fgene.2014.00429

Sessitsch, A., Coenye, T., Sturz, A. V., Vandamme, P., Barka, E. A., Salles, J. F., et al. (2005). *Burkholderia phytofirmans* sp. nov., a novel plant-associated bacterium with plant-beneficial properties. *Int. J. Syst. Evol. Microbiol.* 55, 1187–1192. doi: 10.1099/ijs.0.63149-0

Shameer, S., and Prasad, T. N. V. K. V. (2018). Plant growth promoting rhizobacteria for sustainable agricultural practices with special reference to biotic and abiotic stresses. *Plant Growth Regul.* 84, 603–615. doi: 10.1007/s10725-017-0365-1

Sharma, V. K., and Nowak, J. (1998). Enhancement of *verticillium* wilt resistance in tomato transplants by in vitro co-culture of seedlings with a plant growth promoting rhizobacterium (*Pseudomonas* sp. strain PsJN). *Can. J. Microbiol.* 44, 528–536. doi: 10.1139/w98-017

Sheibani-Tezerji, R., Rattei, T., Sessitsch, A., Trognitz, F., and Mitter, B. (2015). Transcriptome profiling of the endophyte *Burkholderia phytofirmans* PsJN indicates sensing of the plant environment and drought stress. *mBio* 6:e00621-15. doi: 10.1128/mBio.00621-15

Su, F., Villaume, S., Rabenoelina, F., Crouzet, J., Clément, C., Vaillant-Gaveau, N., et al. (2017). Different *Arabidopsis thaliana* photosynthetic and defense responses to hemibiotrophic pathogen induced by local or distal inoculation of *Burkholderia phytofirmans*. *Photosynth. Res.* 134, 201–214. doi: 10.1007/s11120-017-0435-2

Sun, Y., Cheng, Z., and Glick, B. R. (2009). The presence of a 1-aminocyclopropane-1-carboxylate (ACC) deaminase deletion mutation alters the physiology of the endophytic plant growth-promoting bacterium *Burkholderia phytofirmans* PsJN. *FEMS Microbiol. Lett.* 296, 131–136. doi: 10.1111/j.1574-6968.2009.01625.x

Taghavi, S., van der Lelie, D., Hoffman, A., Zhang, Y.-B., Walla, M. D., Vangronsveld, J., et al. (2010). Genome sequence of the plant growth promoting endophytic bacterium *Enterobacter* sp. 638. *PLoS Genet.* 6:e1000943. doi: 10.1371/journal.pgen.1000943

Theocharis, A., Bordiec, S., Fernandez, O., Paquis, S., Dhondt-Cordelier, S., Baillieul, F., et al. (2011). *Burkholderia phytofirmans* PsJN primes *Vitis vinifera* L. and confers a better tolerance to low nonfreezing temperatures. *Mol. Plant Microbe Interact.* 25, 241–249. doi: 10.1094/mpmi-05-11-0124

Theocharis, A., Clément, C., and Barka, E. A. (2012). Physiological and molecular changes in plants grown at low temperatures. *Planta* 235, 1091–1105. doi: 10.1007/s00425-012-1641-y

Tilman, D., Balzer, C., Hill, J., and Befort, B. L. (2011). Global food demand and the sustainable intensification of agriculture. *Proc. Natl. Acad. Sci. U.S.A.* 108, 20260–20264. doi: 10.1073/pnas.1116437108

Timmermann, T., Armijo, G., Donoso, R., Seguel, A., Holuigue, L., and González, B. (2017). *Paraburkholderia phytofirmans* PsJN protects *Arabidopsis thaliana* against a virulent strain of *Pseudomonas syringae* through the activation of induced resistance. *Mol. Plant Microbe Interact.* 30, 215–230. doi: 10.1094/mpmi-09-16-0192-r

Trdá, L., Fernandez, O., Boutrot, F., Héloir, M. C., Kelloniemi, J., Daire, X., et al. (2013). The grapevine flagellin receptor VvFLS2 differentially recognizes flagellin-derived epitopes from the endophytic growth-promoting bacterium *Burkholderia phytofirmans* and plant pathogenic bacteria. *New Phytol.* 201, 1371–1384. doi: 10.1111/nph.12592

Van Loon, L. C., Bakker, P. A., van der Heijdt, W. H., Wendehenne, D., and Pugin, A. (2008). Early responses of tobacco suspension cells to rhizobacterial elicitors of induced systemic resistance. *Mol. Plant Microbe Interact.* 21, 1609–1621. doi: 10.1094/MPMI-21-12-1609

Van Puyvelde, S., Cloots, L., Engelen, K., Das, F., Marchal, K., Vanderleyden, J., et al. (2011). Transcriptome analysis of the rhizosphere bacterium *Azospirillum brasilense* reveals an extensive auxin response. *Microb. Ecol.* 61, 723–728. doi: 10.1007/s00248-011-9819-6

Vurukonda, S. S., Vardharajula, S., Shrivastava, M., and SkZ, A. (2016). Enhancement of drought stress tolerance in crops by plant growth promoting rhizobacteria. *Microbiol. Res.* 184, 13–24. doi: 10.1016/j.micres.2015.12.003

Wang, B., Mei, C., and Seiler, J. R. (2015). Early growth promotion and leaf level physiology changes in *Burkholderia phytofirmans* strain PsJN inoculated switchgrass. *Plant Physiol. Biochem.* 86, 16–23. doi: 10.1016/j.plaphy.2014.11.008

Weilharter, A., Mitter, B., Shin, M. V., Chain, P. S. G., Nowak, J., and Sessitsch, A. (2011). Complete genome sequence of the plant growth-promoting endophyte *Burkholderia phytofirmans* strain PsJN. *J. Bacteriol.* 193, 3383–3384. doi: 10.1128/jb.05055-11

Yang, J., Kloepper, J. W., and Ryu, C.-M. (2009). Rhizosphere bacteria help plants tolerate abiotic stress. *Trends Plant Sci.* 14, 1–4. doi: 10.1016/j.tplants.2008.10.004

Zhang, J.-L., Flowers, T. J., and Wang, S.-M. (2009). Mechanisms of sodium uptake by roots of higher plants. *Plant Soil* 326:45. doi: 10.1007/s11104-009-0076-0

Zhang, J.-L., and Shi, H. (2013). Physiological and molecular mechanisms of plant salt tolerance. *Photosynth. Res.* 115, 1–22. doi: 10.1007/s11120-013-9813-6

Zhao, S., Wei, H., Lin, C.-Y., Zeng, Y., Tucker, M. P., Himmel, M. E., et al. (2016). *Burkholderia phytofirmans* inoculation-induced changes on the shoot cell anatomy and Iron accumulation reveal novel components of *Arabidopsis*-endophyte interaction that can benefit downstream biomass deconstruction. *Front. Plant Sci.* 7:24. doi: 10.3389/fpls.2016.00024

Zúñiga, A., Donoso, R. A., Ruiz, D., Ruz, G. A., and González, B. (2017). Quorum-sensing systems in the Plant growth-promoting bacterium *Paraburkholderia phytofirmans* PsJN exhibit cross-regulation and are Involved in biofilm formation. *Mol. Plant Microbe Interact.* 30, 557–565. doi: 10.1094/mpmi-01-17-0008-r

Zúñiga, A., Poupin, M. J., Donoso, R., Ledger, T., Guiliani, N., Gutiérrez, R. A., et al. (2013). Quorum sensing and indole-3-acetic acid degradation play a role in colonization and plant growth promotion of *Arabidopsis thaliana* by *Burkholderia phytofirmans* PsJN. *Biol. Plant Microbe Interact.* 26, 546–553. doi: 10.1094/MPMI-10-12-0241-R

Conflict of Interest Statement: The authors declare that the research was conducted in the absence of any commercial or financial relationships that could be construed as a potential conflict of interest.

frontiers in Microbiology

ORIGINAL RESEARCH
published: 04 September 2018
doi: 10.3389/fmicb.2018.02068

RiCRN1, a Crinkler Effector From the Arbuscular Mycorrhizal Fungus *Rhizophagus irregularis*, Functions in Arbuscule Development

*Stefanie Voß[1], Ruben Betz[1], Sven Heidt[1], Nicolas Corradi[2] and Natalia Requena[1]**

[1] Molecular Phytopathology, Botanical Institute, Karlsruhe Institute of Technology (KIT), Karlsruhe, Germany, [2] Department of Biology, Canadian Institute for Advanced Research, University of Ottawa, Ottawa, ON, Canada

Arbuscular mycorrhizal (AM) symbiosis is one of the most prominent and beneficial plant–microbe interactions that facilitates mineral nutrition and confers tolerance to biotic and abiotic stresses. AM fungi colonize the root cortex and develop specialized structures called arbuscules where the nutrient exchange takes place. Arbuscule development is a highly controlled and coordinated process requiring the involvement of many plant proteins recruited at that interface. In contrast, much less is known about the fungal proteins involved in this process. Here, we have identified an AM fungal effector that participates in this developmental step of the symbiosis. RiCRN1 is a crinkler (CRN) effector that belongs to a subfamily of secreted CRN proteins from *R. irregularis*. CRNs have been so far only functionally characterized in pathogenic microbes and shown to participate in processes controlling plant cell death and immunity. *RiCRN1* accumulates during symbiosis establishment parallel to *MtPT4*, the gene coding for an arbuscule-specific phosphate transporter. Expression in *Nicotiana benthamiana* leaves and in *Medicago truncatula* roots suggest that RiCRN1 is not involved in cell death processes. RiCRN1 dimerizes and localizes to nuclear bodies, suggesting that, similar to other CRNs, it functions in the plant nucleus. Downregulation of *RiCRN1* using host-induced gene silencing led to an impairment of the symbiosis in *M. truncatula* and to a reduction of *MtPT4*, while ectopic expression of *RiCRN1,* surprisingly, led to a drastic reduction in arbuscule size that correlated with a decrease not only in *MtPT4* but also in *MtBCP1,* a marker for initial stages of arbuscule development. Altogether, our results suggest that a tightly regulated expression in time and space of *RiCRN1* is critical for symbiosis progression and for the proper initiation of arbuscule development.

Keywords: effectors, crinkler (CRN) proteins, arbuscular mycorrhiza, plant symbioses, arbuscule

OPEN ACCESS

Edited by:
Alfredo Herrera-Estrella, Centro de Investigación y de Estudios Avanzados del Instituto Politécnico Nacional, Mexico

Reviewed by:
Luisa Lanfranco, Università degli Studi di Torino, Italy
Nuria Ferrol, Consejo Superior de Investigaciones Científicas (CSIC), Spain

****Correspondence:***
Natalia Requena
natalia.requena@kit.edu

Specialty section:
This article was submitted to Plant Microbe Interactions, a section of the journal Frontiers in Microbiology

Received: *06 July 2018*
Accepted: *13 August 2018*
Published: *04 September 2018*

Citation:
Voß S, Betz R, Heidt S, Corradi N and Requena N (2018) RiCRN1, a Crinkler Effector From the Arbuscular Mycorrhizal Fungus Rhizophagus irregularis, Functions in Arbuscule Development. Front. Microbiol. 9:2068. doi: 10.3389/fmicb.2018.02068

INTRODUCTION

Most microbial activity in soils is concentrated in the rhizosphere, the area in close vicinity to the root and influenced by the secretion of plant substances. The microbial activity of the rhizosphere and the balance between mutualistic and antagonistic microbial interactions ultimately determines plant health (Berendsen et al., 2012). Several rhizospheric microbes associate intimately with plant roots establishing long lasting relationships. Among those, the mutualistic arbuscular

mycorrhizal (AM) symbiosis is the most prominent microbial association of roots involving the majority of terrestrial plants (Smith and Smith, 2011). AM fungi belong to the subphylum Glomeromycotina, from the Mucoromycota phylum (Spatafora et al., 2016) and comprise many different genera and species all forming the same type of symbiotic association. AM fungal colonization is restricted to the epidermis and the cortex of the root but excluding the endodermis. After penetration of the epidermis, the AM fungus grows into the root cortex, inter- and intracellularly, but never invading the plant protoplast. In inner cells of the cortex, intracellular tree-like branched hyphae are formed called arbuscules that are key for the nutrient exchange with the plant (Luginbuehl and Oldroyd, 2017; MacLean et al., 2017). The establishment and functioning of the AM symbiosis is accompanied by an extensive and complex bidirectional signal exchange that redirects plant and fungal development (Lanfranco et al., 2018). Interestingly, signal exchange between AM fungi and their host plants starts prior physical contact as it has been shown by transcriptomic changes in host plants and in the fungi in response to diffusible signals (MacLean et al., 2017; Lanfranco et al., 2018), and likely continues throughout the whole duration of the symbiosis. The identification of fungal signals involved in AM symbiosis has been an active field of research in the last decade with the identification of chito- and lipochito-oligosaccharides as key molecules involved in this interkingdom communication (Maillet et al., 2011; Genre et al., 2013). Perception of these signals, and likely others not yet identified, leads to the activation of the common symbiosis signaling pathway (SYM pathway) that controls the accommodation of the fungus within the cortex (Luginbuehl and Oldroyd, 2017; MacLean et al., 2017). A totally different class of fungal signal molecules has been recently identified. AM fungi, similar to pathogenic microbes have been shown to contain effector molecules in their genetic repertoire (Kloppholz et al., 2011; Tisserant et al., 2013; Lin et al., 2014; Sedzielewska Toro and Brachmann, 2016; Kamel et al., 2017; Zeng et al., 2018). Although only few functional analyses have been carried out with AM fungal effectors (Kloppholz et al., 2011; Tsuzuki et al., 2016), it is proposed that these effector proteins might contribute to modulate the immune system of the plant and/or to facilitate the nutrient exchange as it is the case in plant-pathogenic fungi (Doehlemann et al., 2014). Thus, the *R. irregularis* SP7 (Secreted Protein 7) was shown to positively impact on the symbiosis, counteracting the function of the pathogenesis-related transcription factor MtERF19 (Kloppholz et al., 2011). Also, strigolactone induced secreted protein 1 (SIS1), another effector from *R. irregularis* was shown to be induced during symbiosis and upon strigolactone treatment. Its silencing via HIGS led to a suppression of colonization and formation of stunted arbuscules (Tsuzuki et al., 2016). But, it is also conceivable that some AM fungal effectors might contribute to the plant developmental changes required for symbiosis establishment.

Among the identified AM fungal effectors in the work of Lin et al. (2014), 42 sequences were identified with similarities to proteins belonging to the large pathogen associated crinkler (CRN) effector family, specifically to the highly conserved amino-terminal (N-terminal) LFLAK domain. Among these, some also harbor a signal peptide for secretion and other conserved CRN domains. CRNs were first described in phytopathogenic oomycetes such as *Phytophthora* spp., as a large family of effectors located, together with the RxLR effectors, in fast-evolving genomic regions (Torto et al., 2003; Haas et al., 2009; Raffaele et al., 2010; Schornack et al., 2010; Amaro et al., 2017). This gene family is also present in other oomycetes such as the legume pathogen *Aphanomyces euteiches* that, interestingly, lacks RxLR effectors in its genome (Gaulin et al., 2008, 2018; Amaro et al., 2017). CRNs are in fact, ubiquitously present in all plant pathogenic oomycetes analyzed (Adhikari et al., 2013; Shen et al., 2013), but surprisingly absent in the genome of animal pathogenic ones. It has been suggested that this is an indication of their involvement in facilitating plant susceptibility, as new transcriptomic data seems to indicate (Gaulin et al., 2018). Interestingly, CRNs are also found outside the oomycetes, in several fungi including the animal pathogenic chytrid *Batrachochytrium dendrobatidis* (Raffaele et al., 2010; Sun et al., 2011) as well as in other chytridiomycota (Farrer et al., 2017). Furthermore, recent data suggests that they might be more ubiquitously distributed than predicted, and present even in non-parasitic free-living eukaryotes including plants (Zhang et al., 2016).

Like RxLR effectors, CRN effectors are modular proteins. The N-terminus harbors the characteristic LFLAK domain, with the highly conserved LxLFLAK motif and a neighboring DWL domain, marking the end of the N-terminus with the highly conserved HVLxxP motif. The carboxy-terminal (C-terminal) region exhibits a large variety of domains and it has been suggested, that recombination between different clades drives CRN diversity (Haas et al., 2009). Extensive studies on the functional role of CRN proteins have been carried out in plant pathogenic oomycetes, where they have been described as effector proteins that enter the plant cell nucleus to exert their function (Schornack et al., 2010; van Damme et al., 2012; Stam et al., 2013b; Rajput et al., 2014, 2015; Mafurah et al., 2015; Song et al., 2015). Although initially CRN proteins were characterized as cell death inducing factors (Torto et al., 2003), many studies on this subject have proven even the opposite function (Liu et al., 2011; Shen et al., 2013; Rajput et al., 2014, 2015). Thus, for instance, PsCRN115 is able to suppress the cell death elicited by PsCRN63, although these two effectors are only different in four amino acids (Liu et al., 2011). Furthermore, it was shown that those two CRN proteins interact with plant catalases to regulate plant programmed cell death by modulating H_2O_2 homeostasis and thus overcoming host immunity (Zhang et al., 2015). Another CRN protein shown to suppress cell death is PsCRN161. This effector, in addition, enhances tolerance to salinity and drought stress, extending the role of CRNs to the protection of plants from biotic and abiotic stresses (Rajput et al., 2015). A very recent study has even shown that the virulence activity of the *Phytophthora capsici* CRN83_152 *in planta* is not related to its cell death inducing activity (Amaro et al., 2018). All these results suggest that CRN proteins could have other functions besides cell death induction.

While it has been shown that CRN translocation into plant cells is mediated by the LxLFLAK motif in the N-terminus

(Schornack et al., 2010), the effector function of CRN proteins within the plant is ascribed to their C-terminal region (Liu et al., 2011; van Damme et al., 2012; Stam et al., 2013b). Very few CRNs were predicted to contain domains with a putative function and for some of them this function has been proven. Thus, for instance, PiCRN8 C-terminus has homology to serine/threonine kinases and it was demonstrated to have an autophosphorylation activity essential for *P. infestans* virulence (van Damme et al., 2012). Similarly, the PsCRN108 from *P. sojae* contains a Helix hairpin Helix (HhH) motif suggesting that CRNs could modulate plant gene expression by targeting plant promoters. Indeed, in PsCRN108 this domain was responsible for inhibition of heat shock proteins expression by binding to their promoter and preventing the association of the corresponding heat shock transcription factor (Song et al., 2015). Also, the HhH-like endonuclease motif in AeCRN13 from the legume pathogen *A. euteiches* was shown to be essential for DNA binding *in planta*. CRN13 binding to DNA induces the DNA damage response eventually leading to cell death (Ramirez-Garces et al., 2016). Interestingly AeCRN13 is homolog to BdCRN13 from the animal pathogenic fungus *B. dendrobatidis*, and reciprocal expression in amphibians or plant cells induced aberrant cell development, suggesting a conserved mechanism of function for both effectors.

Haas et al. (2009) proposed a CRN classification in families grouped by the homology of their C-termini and new domains were proposed. However, no functions could be ascribed to those domains. In contrast, the new non-targeted analysis by Zhang et al. (2016) that extended the presence of CRNs to non-pathogenic organisms, allowed a re-classification of CRN proteins and a plethora of new functional domains were identified in their C-termini. These results have challenged our view of CRN proteins and will allow to propose new hypotheses regarding their evolution and function (Amaro et al., 2017).

In this work, we carried out the first characterization of a CRN protein from the AM fungus *R. irregularis*. We show that a subset of *R. irregularis* CRNs with a predicted signal peptide is expressed during plant colonization. From those, *RiCRN1* accumulates concomitantly to the arbuscule marker *MtPT4*. Localization of RiCRN1 was observed in nuclear bodies and silencing of the gene led to an impairment of fungal colonization. Most interestingly, ectopic expression of *RiCRN1* in *Medicago truncatula* showed a drastic arbuscule phenotype. Our data suggest a critical involvement of RiCRN1 proteins in the establishment of a functional symbiosis.

MATERIALS AND METHODS

Plant Material and Growth Conditions

Medicago truncatula Jemalong A17 plants were grown at 25°C in a growth chamber (Binder GmbH, Germany) with a 16-h light/8-h darkness period. To generate composite plants, *M. truncatula* roots were transformed with *Agrobacterium rhizogenes* ARquaI (Quandt et al., 1993) after the protocol of Boisson-Dernier et al. (2001) and cultivated on Fahraeus medium for 5 weeks. Successfully transformed roots were visually selected via constitutive expression of DsRED. Wild type roots were removed, and composite plants were cultivated one additional week on Fahraeus medium containing 400 mg/l Augmentin (AmoxiClav, Hikma Farmaceutical, Portugal). Plants were then transferred into 50 ml Falcon tubes containing a sand:gravel (1:4) mixture inoculated with *R. irregularis* DAOM 197198 that was previously propagated in monoaxenic culture with carrot roots (1 plate inoculum for 100 ml substrate). Plants were cultivated for 5 weeks and fertilized with a half strength low Pi (20 μM) Long Ashton nutrient solution (Hewitt, 1966) twice a week (5 ml). Wild type *M. truncatula* plants used for time course analyses were inoculated and grown under the same conditions.

Nicotiana benthamiana was used for transient expression of GFP fusion proteins in localization and necrosis analyses. Plants were grown in soil at 28°C in a growth chamber (CLF Plant Climatics, Germany), with a 16-h light/8-h darkness period.

Rhizophagus irregularis DAOM 197198 (Schenck and Smith, 1982) was cultivated in monaxenic culture as described before (Kuhn et al., 2010).

Bioinformatic Online Resources Used in This Study

Signal peptide prediction analyses for RiCRN protein candidates were carried out using SignalP3.0[1] and SignalP4.0[2] versions. All sequences that were predicted to contain a signal peptide in at least one of the servers were considered as putative secreted effectors. The presence of possible NLS in RiCRN candidates was predicted using PSORTII[3]. Alignments were performed with the ORF (full length, N-terminal, or C-terminal regions) of all RiCRNs using Clustal Omega[4] and visualized with Jalview[5]. N-terminal regions were defined as the amino acid sequence located in front of the characteristic HVLxxP motif as previously described in Haas et al. (2009). For analyses of consensus motifs, the respective aligned (ClustalO) sequences were used in WebLogo[6] to create consensus logos. For protein structure homology-modeling of RiCRN1 and PcCRN20, the Phyre2 web portal[7] was used implementing the intensive modeling mode option (Kelley et al., 2015). The structural models obtained were visualized and manually curated in UCSF Chimera by removing the low confident part of the proteins. Superimposed models were created using the integrated MatchMaker tool (Pettersen et al., 2004). Template structures used by Phyre2 were obtained directly from PDB[8].

The multiple sequence alignment of RiCRN1 and RiCRN10 with the CR-REase 5 family was manually performed using the same multiple sequence alignment created by Zhang et al. (2016).

[1] http://www.cbs.dtu.dk/services/SignalP-3.0/
[2] http://www.cbs.dtu.dk/services/SignalP/
[3] https://psort.hgc.jp/form2.html
[4] http://www.ebi.ac.uk/Tools/msa/clustalo/
[5] http://www.jalview.org/node/13
[6] http://weblogo.berkeley.edu
[7] http://www.sbg.bio.ic.ac.uk/phyre2/
[8] https://www.rcsb.org/

Generation of Constructs Used in This Study

For overexpression analyses in *M. truncatula* roots, the carboxy terminus of *RiCRN1* was amplified from cDNA (starting right after the HVLVEPP motif), subcloned into pENTR®/D-TOPO (Invitrogen by Thermo Fisher Scientific, Germany) and cloned into the destination vector 2xP35S-pKGW-RedRoot (Heck et al., 2016). For yeast two hybrid interaction studies, the ORF of *RiCRN2* (without signal peptide), *MtSR45*, *MtU1-70k*, and *RiCRN1* (without signal peptide) as well as the *RiCRN1* carboxy terminus were amplified from cDNA using restriction sites, subcloned into PCR®2.1 TOPO® (Invitrogen by Thermo Fisher Scientific, Germany) and cloned into the bait or prey vectors pGBKT7 or pGADT7 (Takara Clontech Bio Europe, France). *MtU2AF*^{35b} was isolated from a previous yeast two hybrid library screen (Kloppholz et al., 2011). For localization and necrosis analyses in *N. benthamiana*, the ORF of *RiCRN1*, with and without signal peptide, as well as the C-terminus alone, were amplified from cDNA and subcloned into pENTR®/D-TOPO (Invitrogen by Thermo Fisher Scientific, Germany). For localization studies, the constructs were cloned into the destination vector pCGFP-RR (Kuhn et al., 2010) and for necrosis assays, constructs were cloned into pK7FWG2 (Karimi et al., 2002). For co-localization studies, the carboxy terminus of *RiCRN1* was cloned into the vector pK7FWG2 (Karimi et al., 2002) and *MtSR45* was cloned into the vector pK7RWG2 (Limpens et al., 2005). Silencing of *RiCRN1* was carried out by host-induced gene silencing (HIGS) as described in Helber et al. (2011). Three RNAi constructs targeting the regions from −119 to +200 (RiCRN1.1), +52 to +353 (RiCRN1.2), and +209 to +514 (RiCRN1.3) with respect to the start codon ATG were amplified from cDNA, subcloned into pENTR®/D-TOPO (Invitrogen by Thermo Fisher Scientific, Germany) and then cloned into pK7GWIWG2D (Karimi et al., 2002). All primers used for cloning of the constructs described above, are listed in **Supplementary Table S2** and the three target sequences of *RiCRN1* HIGS constructs are listed in **Supplementary Table S3**.

Gene Expression Analyses

Total RNA extraction from *M. truncatula* roots was performed using the innuPREP RNA kit (Analytik Jena AG, Germany) and quantified using a DeNovix Ds-11+Spectrophotometer (DeNovix Inc., United States). cDNA synthesis was performed using the reverse transcriptase SuperScriptII (Invitrogen by Thermo Fisher Scientific, Germany) as described before (Kuhn et al., 2010). Quantitative real-time expression analyses were carried out using the MESA Green 231qPCR Master Mix Plus (Eurogentec, Germany) in a CFX Connect Real-Time PCR Detection System (Bio-Rad Laboratories GmbH, Germany). A total of 1 µl cDNA (1:5) was used per well as template with the following PCR protocol: 5 min 95°C, 15 s 95°C, 20 s 56°C, 30 s 72°C (40 cycles). Plant transcript levels and transcript levels of the translation elongation factor 1-alpha of *R. irregularis* (*RiTEF1α*, DQ282611) were normalized to the translation elongation factor 1-alpha of *M. truncatula* (*MtTEF1α*, Medtr6g021800) while fungal transcripts were normalized to *RiTEF1α*. Transcript levels of genes were determined in three technical replicates in each independent biological replicate. Numbers of biological replicates are indicated in the corresponding figure legends. All primers are listed in **Supplementary Table S2**.

Yeast Two Hybrid Interaction Studies

Direct protein–protein interactions were assayed by co-transforming the bait (pGBKT7) and prey (pGADT7) vectors in *Saccharomyces cerevisiae* AH109 (Takara Clontech Bio Europe, France). To verify successful transformation events, single colonies were plated in a dilution series, on yeast synthetic drop-out (SD) medium, lacking leucine, and tryptophan. Interaction was tested on SD medium deficient of leucine, tryptophan, histidine, and adenine. Yeast growth was validated after 5 days at 30°C.

Transient Expression of Proteins in *N. benthamiana*

For localization and necrosis assays *N. benthamiana* leaves were infiltrated with *A. tumefaciens* GV3101 or AGL1 strain, respectively, after the protocol of Voinnet et al. (2003). The bacterial suspension was infiltrated in leaves using a needleless syringe. For localization studies, the bacterial suspension was infiltrated into the whole leaf area, with a final optical density (OD_{600}) of 0.5 (adjusted with AS medium supplemented with 2% sucrose). Plants were cultivated at 21°C and confocal microscopy was performed 3 days after infiltration. For the necrosis assay, bacterial culture was infiltrated only in spots into the leaves, using an OD_{600} of 0.25 (adjusted with AS medium without sucrose). Plants were cultivated at 21°C and scoring of lesions was performed 7 days after infiltration. To verify protein integrity in *N. benthamiana* during necrosis analyses, a western blot was employed to detect RiCRN1:eGFP (81.3 kDa), RiCRN1ΔSP:eGFP (79.7 kDa), RiCRN-C:eGFP (78 kDa), eGFP:PcCRN20_624 (58.4 kDa), and eGFP:PcCRN1_719 (81.5 kDa) or free eGFP (26.9 kDa). *N. benthamiana* leaves expressing these constructs, as well as untransformed leaves, were ground to a fine powder in liquid nitrogen. Total protein extraction was performed using a GTEN extraction buffer [25 mM Tris–HCL (pH7.5), 150 mM NaCl, 1 mM EDTA, 10% Glycerol, 1X protease inhibitor cocktail (complete™, Roche), 10 mM DTT, 1 mM PMSF and 0.2% Nonidet P40]. Extracts were spun down, or filtrated (RiCRN1:eGFP) through Miracloth (Calbiochem, Germany) and supernatants/flow-through (RiCRN1:eGFP) was separated in SDS-PAGE (5% stacking-gel and 8% running-gel) and blotted on nitrocellulose membranes. Ponceau S staining (Sigma-Aldrich, Germany) was used to show transfer of the protein to the membrane. Immunodetection of GFP was carried out with an anti-GFP primary antibodies from rabbit (G1544, Sigma-Aldrich, Germany), in a 1:4000 dilution and a horseradish peroxidase coupled anti-rabbit secondary antibody from goat (A0545, Sigma-Aldrich, Germany) in a 1:8000 dilution. Chemiluminescence was detected with the ChemiSmart 5100 detector (Peqlab Biotechnology GmbH, Germany).

Phenotypical Analysis and Quantification of Mycorrhization

Fungal structures were immunostained with WGA-fluorescein as described in Rech et al. (2013) for phenotypical analysis and quantification of mycorrhization. Quantification of mycorrhizal structures was carried out according to Trouvelot et al. (1986). F% represents the frequency of mycorrhization, M% the intensity of colonization, A% the abundance of arbuscules, and I% the abundance of hyphae in the root system. For morphometrical analyses of arbuscule length and width, images were taken randomly from colonized roots. Measurements were done using the Fiji software[9] on $n \geq 200$ arbuscules.

Confocal Microscopy

Microscopical analyses were done using a Leica TCS SP5 (DM5000) confocal microscope with conventional PMT detectors and the color camera Leica DFC295 (Leica, Germany). WGA-fluorescein stained roots and eGFP in localization analyses were both excited with an argon laser at 488 nm. Emission was detected from 493 to 530 nm. In co-localization studies, mRFP was excited at 561 nm with a DPSS 561 laser and emission was detected from 566 to 670 nm. Images were processed using the Fiji software[9].

Statistical Analyses

All data shown represent the mean of several biological replicates indicated in each figure. Error bars represent SEM. Two-tailed Student's *t*-test was used for pairwise comparisons of qPCR data, quantified data of mycorrhizal colonization and comparison of morphometrical analysis of arbuscules. Significance is indicated by asterisks ($^{*}p < 0.05$; $^{**}p < 0.01$; $^{***}p < 0.001$). A one-way ANOVA with *post hoc* Tukey HSD Test was used to validate significance of expression between time points of the time-course. Different letters indicate significant difference in expression ($p < 0.05$). Values of *n* are indicated in the corresponding figure legends.

Data Availability

The CDS sequences of *RiCRN1* to *RiCRN8* and *RiCRN10* have been submitted to GenBank with the identification numbers: MH542411 to MH542419.

RESULTS AND DISCUSSION

R. irregularis Contains a Large Number of CRN-Like Proteins

Sequencing of the *R. irregularis* genome (Tisserant et al., 2013; Lin et al., 2014) showed the existence of several entries with similarities to genes coding for CRN proteins, that had been first identified in oomycetes and chytridiomycota (Haas et al., 2009; Raffaele et al., 2010). Surprisingly, the CRN sequences from *R. irregularis* identified in two different sequencing projects revealed major differences in number and in composition, indicating that perhaps the number of CRN-like sequences might be larger than the current assemblies suggest. Indeed, the analysis of two *R. irregularis* isolates (DAOM 197198 and C2) and of *G. diaphanus* (data not shown) showed the existence of many other putative CRN-like proteins lacking the LFLAK domain. Therefore, they were not ascribed as CRNs but the presence of several of the CRN C-terminal domains identified in Haas et al. (2009), such as DC or DN17, indicates that they might be *bona fide* CRN proteins. We decided therefore, to look at the different data sets publicly available (Tisserant et al., 2013; Lin et al., 2014; Chen et al., 2018) and make a global analysis of CRNs in the symbiotic AM fungus *R. irregularis*. The data sets used contained 82 and 42 sequences. Several of the genes are present in both but often not as complete sequences. Multiple ClustalO alignments showed the existence of clusters that corresponded to genes having similar amino- or carboxy-terminal domains (**Supplementary Figure 1** and **Supplementary Table S1**).

Interestingly, although very few of the CRN-like proteins from *R. irregularis* contained a signal peptide, most of them did not, and were accordingly not predicted as secreted proteins. This suggests that these proteins might exert their function within the fungal cytoplasm, or that they might be alternatively secreted. In agreement with this, in oomycetes only very few CRN proteins contain a signal peptide, and from the rest, several were predicted to contain other motifs that might serve for alternative secretion (Haas et al., 2009; Gaulin et al., 2018). We decided to first focus our attention to those *R. irregularis* CRN proteins having a predicted signal peptide and thus, more likely functioning as effectors outside the fungus. From all data sets analyzed, only nine CRN proteins were predicted as secreted according to SignalP 3.0 or SignalP 4.0. An alignment of these nine proteins using ClustalO clearly showed a highly conserved N-terminus and a more divergent C-terminus (**Supplementary Figure 2**). All amino termini contained, similar to the CRNs described in oomycetes, the LFLAK and the DWL domains, proposed as trafficking sequences for entering the plant cell (Schornack et al., 2010). Compared to the consensus N-terminus of *Phytophthora* spp. described in Haas et al. (2009), we could observe that in *R. irregularis*, the highly conserved LxLFLAK motif is modified to LxLWKV not only in the nine secreted CRN proteins but also in many other CRN sequences from both genome assemblies (**Figure 1A** and **Supplementary Table S1**). This is interesting, because deviations of the LxLFLAK motif have been also found in some oomycetes such as *Phythium* or *Aphanomyces*, and even more dissimilar in the chytridiomycete *B. dendrobatidis* (Cheung et al., 2008; Gaulin et al., 2008, 2018; Levesque et al., 2010; Links et al., 2011). The consensus logo of all these organisms for the LxLFLAK motif shows that only the LxL triade is fully conserved (**Figure 1B**). Interestingly, besides the LxLWKV motif, *R. irregularis* CRNs with signal peptide also contain two other amino acids stretches highly conserved in the LFLAK domain, and also present in the *Phytophthora* consensus sequence (AFPVxI and LKxxI). This is in marked contrast to the DWL domain, in which the conservation is mainly restricted to the conserved HVLxxP motif that in oomycetes has been defined as the amino acid stretch marking the end of the N-terminus (Haas et al., 2009). Given these

[9]http://fiji.sc/Fiji

commonalities and disparities, we wondered how the protein structure of RiCRN1, as a representative of the secreted AM CRNs, would correspond to PcCRN20, a CRN protein from *P. capsici*, known to elicit cell death in leaf tissue (Stam et al., 2013b). To assess this, three-dimensional models of RiCRN1 and PcCRN20 N-termini were created using the structure prediction server Phyre2 according to proteins of the β-GRASP (ubiquitin-like) domain superfamily (IPR012675) (**Figures 1C,D**). This is consistent with the predictions made by Zhang et al. (2016) that considered the N-termini of CRN proteins as header domains containing the ubiquitin-like fold. N-termini of RiCRN1 (amino acids 1–104) and PcCRN20 (amino acids 1–65) show high similarities in protein structure, with the exception of one extra loop in RiCRN1 located at the transition from the LFLAK to the DWL domain (**Figure 1C**).

The analysis of the C-termini of secreted *R. irregularis* CRN proteins showed that 6 of 9 contained at least one nuclear localization domain (NLS), in some cases more, like RiCRN10 that contained three (**Figure 2A**). This is similar to the presence of NLS in about 60% of oomycetes CRNs, and consistent with the nuclear localization observed for most CRN proteins analyzed (Haas et al., 2009; Schornack et al., 2009; Gaulin et al., 2018). Besides the NLS, three *R. irregularis* CRNs (RiCRN4, RiCRN5, and RiCRN10) were previously predicted to contain the DN17 domain (Lin et al., 2014) while RiCRN2 was shown to contain the DC domain (Tisserant et al., 2013; Lin et al., 2014; Chen et al., 2018). However, none of these two domains have a clearly ascribed function. In contrast, most of the secreted *R. irregularis* CRNs contained functional domains such as REases (Restriction Endonucleases 5, 6, and 8), NTPase4 and HhH domains (**Supplementary Table S1**) according to the prediction by Zhang et al. (2016).

Using a percentage of identity matrix for all predicted secreted *R. irregularis* CRNs, it could be observed that five of them (RiCRN1, RiCRN4, RiCRN5, RiCRN8, and RiCRN10) showed a high conservation in their C-terminus (**Figure 2B**). From those, three of them (RiCRN5, RiCRN8, and RiCRN10) were annotated as containing an REase5 domain, while RiCRN4 was, in contrast, predicted to contain an REase6 domain due to the presence of an extra amino acid stretch (Zhang et al., 2016). RiCRN8 is a shorter sequence than the rest and despite the high homology to RiCRN5 and RiCRN10, its potential REase5 domain is likely not detectable. RiCRN1 was not included in the analysis of Zhang et al. (2016). Therefore, in order to investigate whether RiCRN1 could also contain an REase5 domain, we aligned it with the sequences from the REase5 family used in the Zhang analysis. The results showed, that indeed, all critical amino acids, including those of the catalytic domain, are conserved in RiCRN1. Therefore, we hypothesize that this protein also contains an REase5 domain (**Figure 2C**).

CRN1 a Novel Effector Protein From *R. irregularis*

In order to investigate the role that predicted secreted CRN-like proteins might play in *R. irregularis* during the interaction with plants, we first analyzed their expression during symbiosis. From those nine CRN genes, several were not expressed at all or only at low levels in *M. truncatula* mycorrhizal roots (RiCRN3, RiCRN4, RiCRN6, RiCRN7, and RiCRN8). In contrast, RiCRN1, CRN2, CRN5, and CRN10 showed relatively high levels of expression *in planta* (**Supplementary Figure 3**). We could also detect a possible CRN-like pseudogene in this group, RiCRN3, that contains a premature stop codon and a predicted kinase domain not in frame, suggesting that some CRN-like proteins might be subjected to rapid evolution as it has been shown for *Phytophthora* (Haas et al., 2009).

The expression of *RiCRN1*, *2*, *5*, and *10* was further analyzed in a time-course manner in *M. truncatula* plants inoculated with *R. irregularis*. Plants were harvested at 2, 3, 4, and 5 weeks post inoculation (wpi) and the fungal colonization levels assessed by the expression of the fungal marker *RiTEF1α*. The level of functional symbiosis was determined by the expression of the phosphate transporter *MtPT4* which is a key marker for arbuscule-containing cells and its function directly relates to the symbiotic phosphate download that takes place at these structures (Harrison et al., 2002; Javot et al., 2007). The four CRN-like genes analyzed showed different patterns of expression with *RiCRN1* accumulating progressively during symbiosis (**Figure 3A**). A Pearson's correlation analysis with *MtPT4* showed that only *RiCRN1* had a moderate positive correlation to this marker, while it is difficult to predict a trend for the other three genes (**Figure 3B**). This is interesting because CRNs from *Phytophthora* have been shown to have differential patterns of expression during infection. Thus, for instance CRNs from *P. capsici* can be divided in two groups according to their expression patterns, with Class 1 upregulated in early and late stages of colonization and Class 2 with expression that gradually increases to peak in late stages (Stam et al., 2013a,b). In *Phytophthora*, a correlation with the presence of the DN17 C-terminal domain and an effector expression at later stages was observed (Stam et al., 2013a,b). However, RiCRN5 and RiCRN10, which presumably contain the DN17 domain and are highly similar to RiCRN1, do not show this expression trend. Thus, it seems unlikely that the presence of the DN17 is related to the timing of expression in AM fungi. CRN effectors have been so far only functionally analyzed in pathogenic organisms, therefore, and given its pattern of expression, we decided to investigate the function of RiCRN1 during the mycorrhizal symbiosis.

RiCRN1 Localizes to Nuclear Bodies

To date, all functionally characterized CRN effector proteins have been shown to localize to the nucleus when expressed *in planta* (Haas et al., 2009; Schornack et al., 2010; Stam et al., 2013a,b; Mafurah et al., 2015; Song et al., 2015; Zhang et al., 2015). Interestingly, distinct nuclear localization patterns could be observed for different CRN proteins, suggesting that they might not all perform the same function (Stam et al., 2013a,b). In order to analyze whether RiCRN1, that possesses two predicted NLS, also localizes to the cell nucleus and if yes to which region, the protein was tagged with GFP at its carboxy-terminus. Localization analyses were performed in *N. benthamiana* leaves. Three different versions of the protein were employed, the full-length (RiCRN1:eGFP),

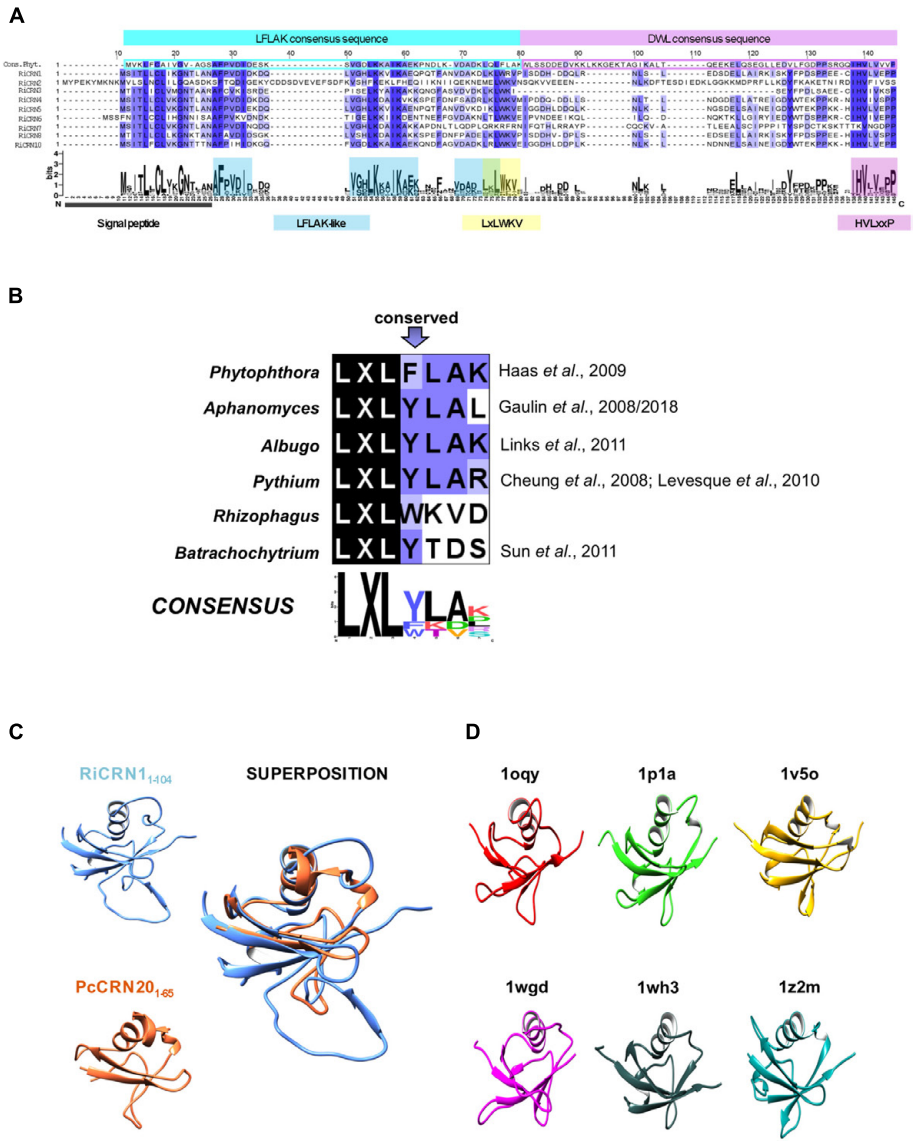

FIGURE 1 | Candidate CRN effectors from *R. irregularis* containing a predicted signal peptide. **(A)** Alignment of the N-terminal regions of RiCRN proteins containing a predicted SP (SignalP-3.0 or 4.0) with the consensus sequence of the *P. infestans* LFLAK and DWL domains (Haas et al., 2009). At the position of the *P. infestans* highly conserved LxLFLAK motif, a modified version (LxLWKV) is present in almost all *R. irregularis* sequences. Moreover, most RiCRNs show two additional conserved motifs (AFPVDI and VGLKxxIKA) within the *Phytophthora* LFLAK domain. Except for RiCRN7, all *R. irregularis* members harbor the characteristic HVLxxP motif, which marks the end of *Phytophthora* N-terminal CRN region. **(B)** Comparison of LxLFLAK-like motifs present in different organisms. This motif is highly conserved in oomycetes but less conserved in fungi. The LxL triade is conserved in all organisms. **(C)** Partial three-dimensional models of the N-terminal regions of RiCRN1 and PcCRN20_624 obtained from Phyre2 show the fold of the Ubiquitin-like superfamily and can be superimposed. Amino acids included in each model are indicated. **(D)** Protein structures from the 6 PDB templates used by Phyre2 to model the N-terminus of RiCRN1 are shown. The structures belong to the ubiquitin-like domains from the human ubiquitin-like DNA repair proteins hHR23a (1ogy) and hHR23B (1p1a), the mouse hypothetical 1700011N24Rik protein (1v5o), the human Herp protein (1wgd), the human 2′-5′-oligoadenylate synthetase-like (p59 OASL) protein (1wh3) and the human Interferon-Induced ubiquitin cross reactive protein ISG15 (1z2m).

the carboxy-terminus starting after the HVLxxP-like motif (RiCRN1-C:eGFP) and the full-length without secretion peptide (RiCRN1ΔSP:eGFP) (**Figure 4A**). Confocal microscopy analyses showed that RiCRN1 and RiCRN1-C were exclusively observed in nuclear bodies (**Figure 4B**). In contrast, expression of RiCRN1 without signal peptide but still containing the LFLAK-like domain (RiCRN1ΔSP:eGFP) showed cytoplasmic and nuclear localization, with variable patterns and only sometimes at nuclear bodies (**Figure 4C**). This suggests that the presence of the putative entry domain (LFLAK domain) might perturb protein localization. We hypothesize that RiCRN1 in the natural context localizes to nuclear bodies and that the C-terminus is responsible and sufficient for this localization. This is in line with results from oomycete CRNs that show that the C-terminus is sufficient to

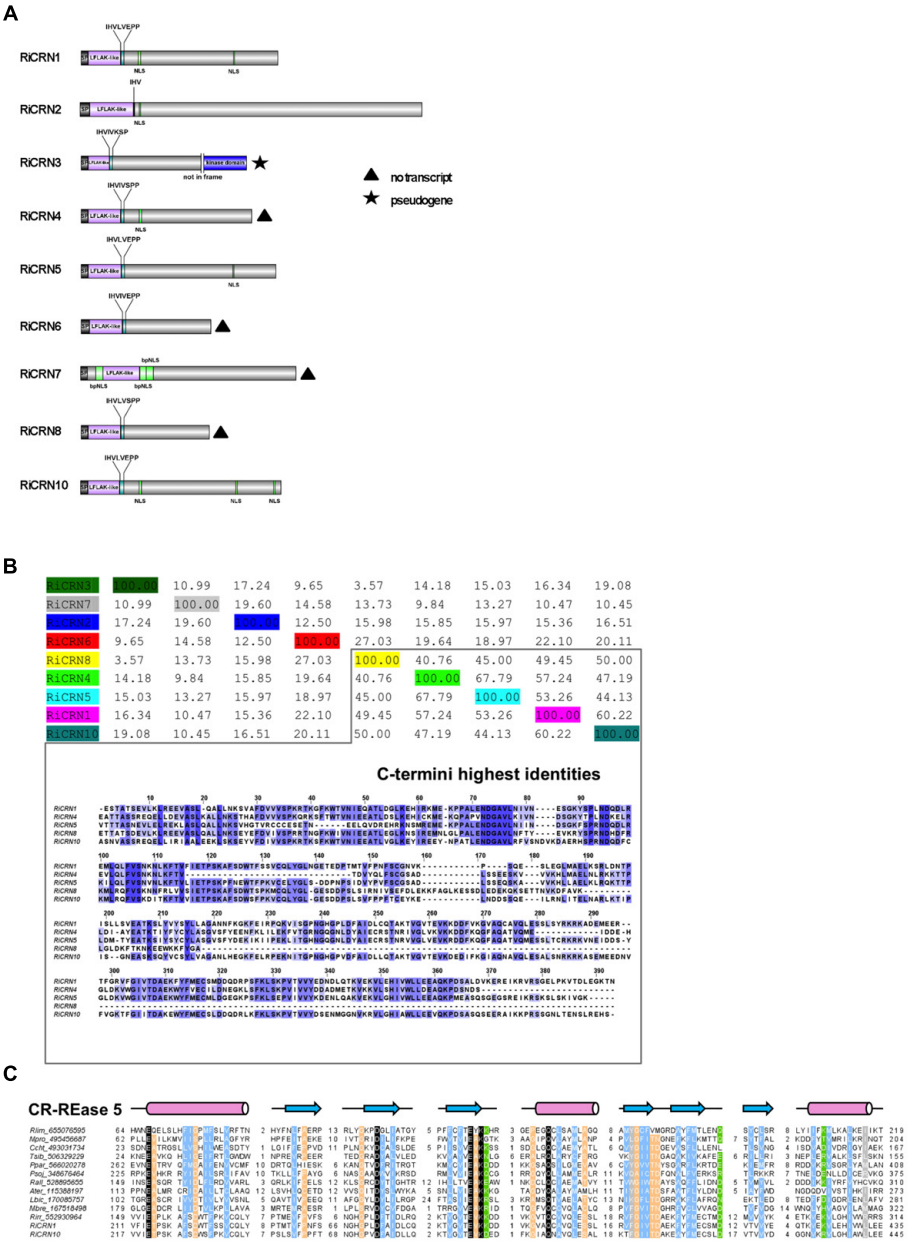

FIGURE 2 | Sequence features of *R. irregularis* CRNs with predicted signal peptide. **(A)** Protein organization of secreted *R. irregularis* CRNs. Besides the N-terminus that contains the signal peptide, the LFLAK-like and DWL domain, RiCRN proteins contain C-termini of different lengths, some of them harboring one or more predicted NLS motifs (PSORTII), sometimes as bipartite NLSs (bpNLS). Four RiCRN candidates (*RiCRN4*, *6*, *7*, and *8*) did not show expression during symbiosis and are marked with a black triangle (see **Supplementary Figure 3**). RiCRN3 is predicted to be a pseudogene because its transcript contains a premature stop codon that would prevent the translation of the kinase domain located at the end of the C-terminus. **(B)** Percentage identity matrix score (ClustalO) of the secreted RiCRN C-termini. Five of them show high protein identities (between 41 and 68%), while the others are less conserved. Alignment of the C-termini (ClustalO, identical amino acids are shown in blue) revealed highly conserved amino acid stretches, suggesting that they might belong to a common CRN subfamily. **(C)** Multiple sequence alignment of the CR-REase 5 family members used in Zhang et al. (2016) together with the RiCRN1 and RiCRN10 showed the presence of the conserved catalytic residues (in black) and the topology predicted for the CR-REase 5 family. Pink cylinders indicate α-helices and blue arrows indicate β-sheets. Sequence limits and missing residues between sequence blocks shown are indicated with numbers.

target the proper nuclear localization and for the induction of cell death (Schornack et al., 2010; Stam et al., 2013b). Our results also suggest that RiCRN1 is able to enter the plant cell on its own without the requirement of additional fungal proteins.

RiCRN1 Forms a Homodimer

Some CRN proteins have been shown to form homo and hetero-dimers and this process to be essential for their function at controlling plant immunity (Li et al., 2016). Thus,

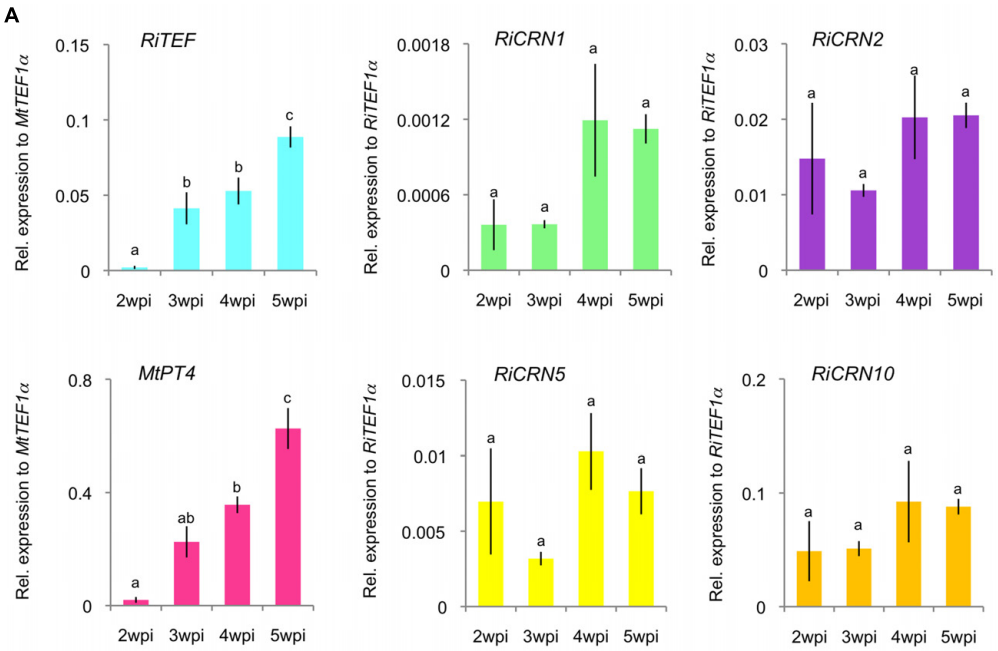

B

Pearson's Correlation

RiCRN1	$r = 0.56$
RiCRN2	$r = 0.36$
RiCRN5	$r = 0.21$
RiCRN10	$r = 0.38$

FIGURE 3 | Expression analysis of a subset of *R. irregularis* CRN effectors during symbiosis with *M. truncatula*. A time course experiment was carried out to analyze the expression of *RiCRN1, RiCRN2*, *RiCRN5*, and *RiCRN10* during symbiosis of *R. irregularis* with *M. truncatula*. **(A)** Expression of the *R. irregularis* elongation factor 1α (*RiTEF1*α), the phosphate transporter and arbuscule marker *MtPT4*, and the *R. irregularis* CRN effectors *CRN1*, *CRN2*, *CRN5*, and *CRN10* were analyzed at 2, 3, 4, and 5 weeks post inoculation (wpi). Expression is shown as relative expression to *M. truncatula* elongation factor 1α (*MtTEF1*α) for *MtPT4* and *RiTEF1*α or to *RiTEF1*α for *RiCRN1*, *RiCRN2*, *RiCRN5*, and *RiCRN10*. All four CRNs are expressed during the symbiosis, albeit with different patterns. Error bars represent SEM with $n = 3$ biological replicates for all time points. A one-way ANOVA with *post hoc* Tukey HSD test was used to validate significance of expression between time points. Different letters indicate significant difference in expression ($p < 0.05$). **(B)** A Pearson's correlation analysis was carried out between expression of *MtPT4* and the *R. irregularis CRN1*, *CRN2*, *CRN5*, and *CRN10*. *RiCRN1* is the only CRN gene showing a moderate correlation ($r \geq 0.50$) with the arbuscule marker *MtPT4*.

homodimerization of PsCRN63 was shown to be critical for suppressing immunity and induction of cell death. Interestingly, PsCRN63 can also heterodimerize with PsCRN115, which is only 4 amino acids different, as well as with two other dissimilar CRN proteins. PsCRN115 has an opposed function to PsCRN63 and suppresses host defenses (Liu et al., 2011). Thus, it is possible that homo- and heterodimerization processes among CRNs could be critical to control the output of effector functions in plants (Amaro et al., 2017). In order to investigate whether RiCRN1 could form homo- or heterodimers with a different type of CRN protein, yeast two hybrid analyses with RiCRN1 and RiCRN2 were carried out (**Figure 5A**). Interestingly, RiCRN1 expressed without signal peptide, and in contrast to RiCRN2, was able to dimerize. However, both proteins did not interact with each other. Noteworthy, RiCRN1-C was sufficient to confer homodimerization, suggesting that dimerization could be important for RiCRN1 function at nuclear bodies. Nuclear bodies are often occupied by splicing components such as U1-70K, U2AF^{35}b, or SR proteins and are then called speckles (Ali et al., 2008; Day et al., 2012). Therefore, in order to test whether RiCRN1 could be part of the splicing machinery, interaction assays with those splicing components were also analyzed by yeast two hybrid (**Figure 5A**). The results showed that RiCRN1 did not interact, at least directly, with any of those components. Furthermore, co-localization experiments with MtSR45 showed localization of the proteins in different nuclear bodies strongly excluding each other (**Figure 5B**). Altogether, it appears that RiCRN1 might play a role *in planta* as a dimer but functionally not related to splicing.

RiCRN1 Does Not Control Plant Cell Death

As mentioned above, CRN proteins were initially described as triggers for crinkling and necrosis phenotypes *in planta* (Torto et al., 2003). However, further functional analyses of this

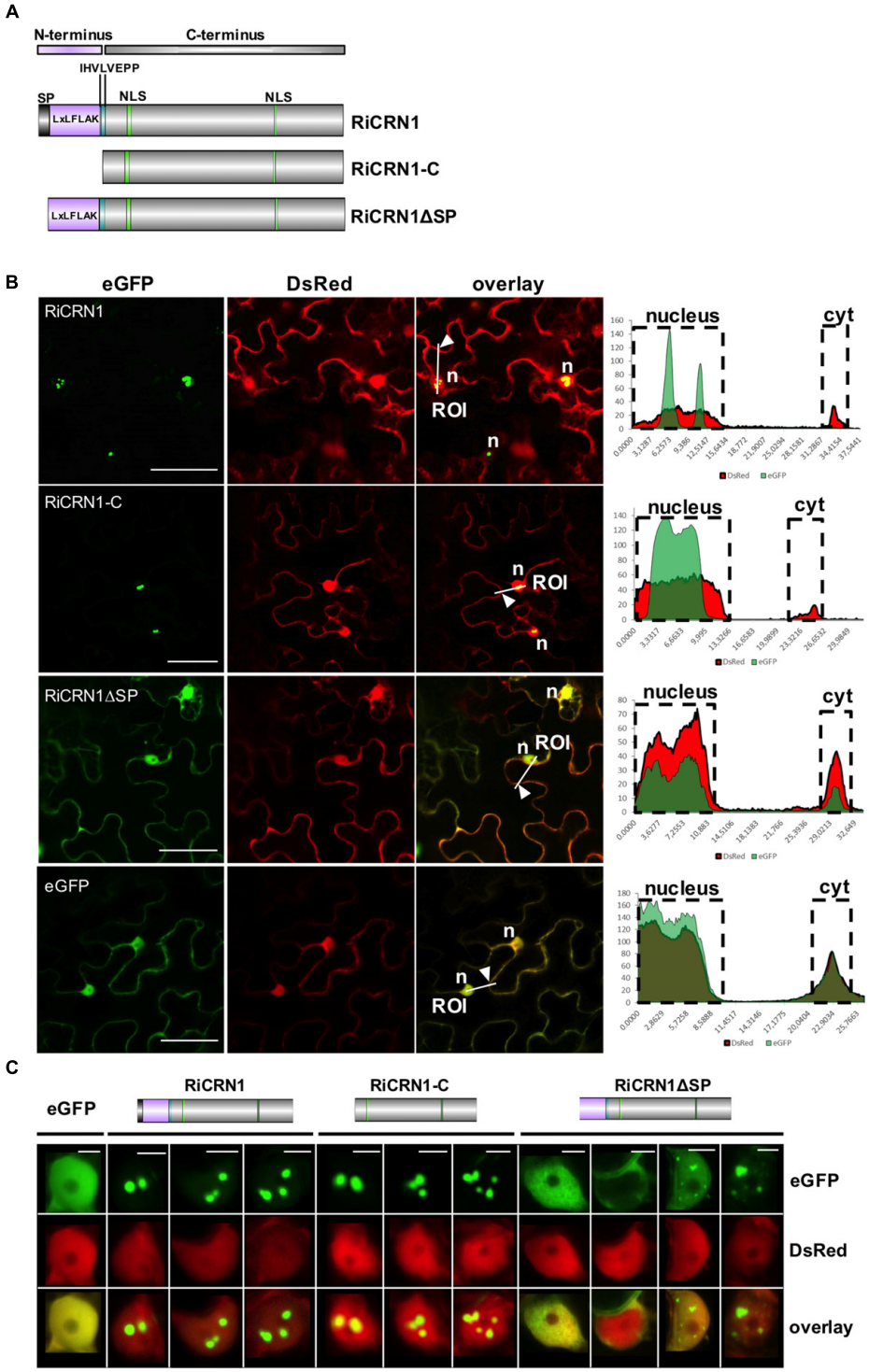

FIGURE 4 | RiCRN1 localizes to the plant nucleus. **(A)** Domain organization of RiCRN1 constructs employed for localization assays. **(B)** Confocal imaging shows localization of ectopically expressed RiCRN1 versions fused to eGFP in *N. benthamiana* epidermal cells. Free DsRed was co-expressed as control for transformation and labels the plant nucleus and cytoplasm. RiCRN1:eGFP and RiCRN1-C:eGFP localize to distinct nuclear foci. No or only a weak signal is visible in the cytoplasm. In contrast, RiCRN1 ΔSP:eGFP localizes to the cytoplasm and nucleus similar to free eGFP. Right panels show fluorescence intensity at specific transects marked in the overlay pictures. ROI indicates start of transection lines for fluorescent intensity measurements. White arrowheads indicate cytoplasmic areas. *n* = nucleus. Scale bar = 50 μm. **(C)** Representative localization pictures of the three RiCRN1 versions in nuclei. RiCRN1:eGFP as well as RiCRN1-C:eGFP localize to discrete nuclear foci, while RiCRN1 ΔSP:eGFP shows variable nuclear patterns: even nuclear distribution, localization in foci or absence from the nucleus. Scale bar = 5 μm.

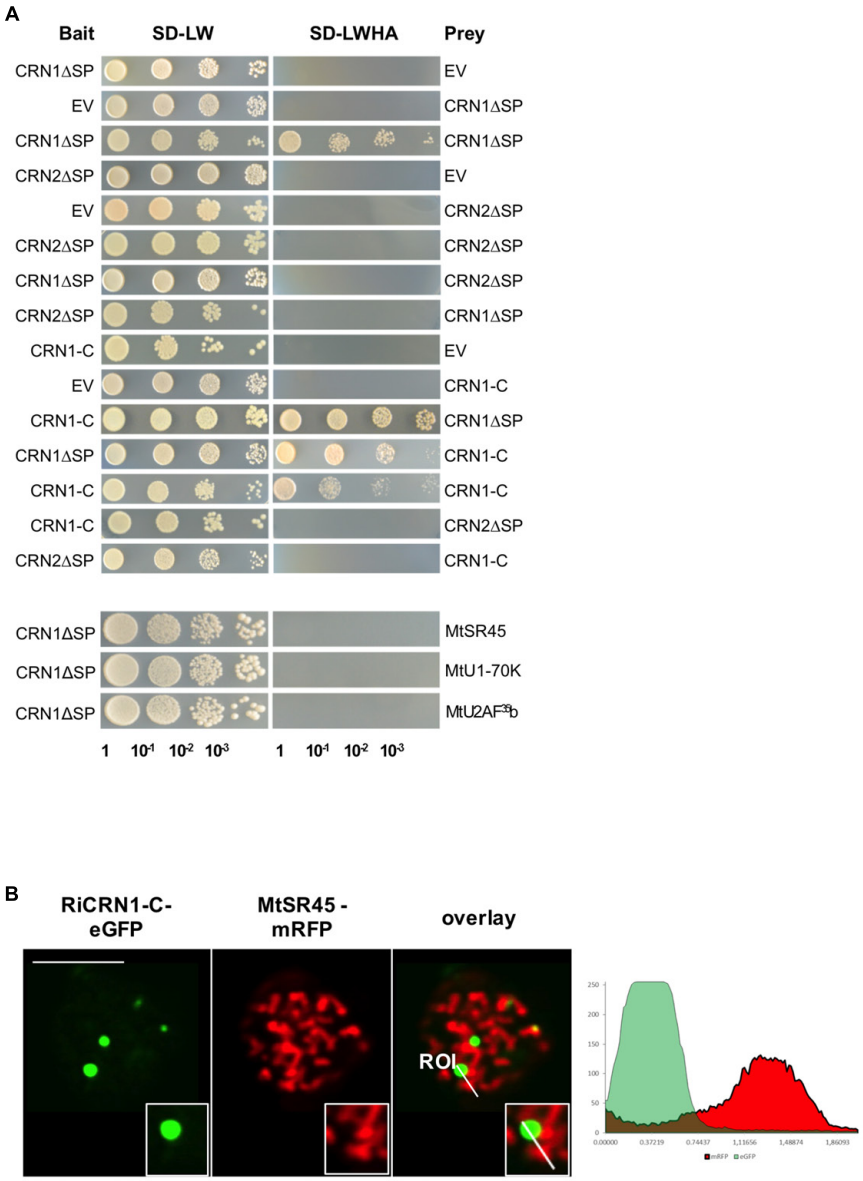

FIGURE 5 | RiCRN1 forms a homodimer but does not interact neither with RiCRN2 nor with several splicing factors. **(A)** A direct interaction assay was carried out using the Y2H system. RiCRN1 ΔSP was tested for interaction with itself, RiCRN2 ΔSP and the splicing factors MtSR45, MtU1-70K, and MtU2AF^{35}. In addition, RiCRN1-C was assayed for interaction with itself, RiCRN1 ΔSP and RiCRN2 ΔSP. Successful transformation was confirmed by growth on SD-LW medium in serial dilutions. Positive interaction was visualized on SD-LWHA medium. RiCRN1 is able to form a homodimer but does not interact with RiCRN2 ΔSP or any of the tested splicing factors. **(B)** A co-localization experiment was carried out in *N. benthamiana* leaves with ectopically expressed RiCRN1-C fused to eGFP and the splicing factor MtSR45 fused to mRFP. Confocal imaging shows localization of both fusion proteins in distinct nuclear foci, however, strongly excluding each other. Right panel shows fluorescence intensity at specific transects marked in the overlay pictures. ROI indicates start of transection lines for fluorescent intensity measurement. Scale bar = 10 μm.

large family showed that although some CRNs do induce necrosis, many others do not, and some of them rather function by preventing host cell death (Liu et al., 2011; Shen et al., 2013; Rajput et al., 2014, 2015). Thus, one of the functions ascribed to several CRNs is to be regulators of cell death (Amaro et al., 2017). In order to investigate the ability of RiCRN1 to induce cell death, we infiltrated *N. benthamiana* leaves with *Agrobacterium tumefaciens* carrying RiCRN1 fused to GFP expressed under the control of the CaMV 35 S promoter. The assay was performed either with the full-length sequence (RiCRN1:eGFP), the carboxy terminus (RiCRN1-C:eGFP) or with RiCRN1 ΔSP:eGFP lacking the signal peptide. As positive and negative controls, the *Phytophthora capsici* effectors PcCRN20_624 and PcCRN1_719 were used (Stam et al., 2013a,b), both also fused to GFP and under the control of the CaMV 35S promoter. The results showed

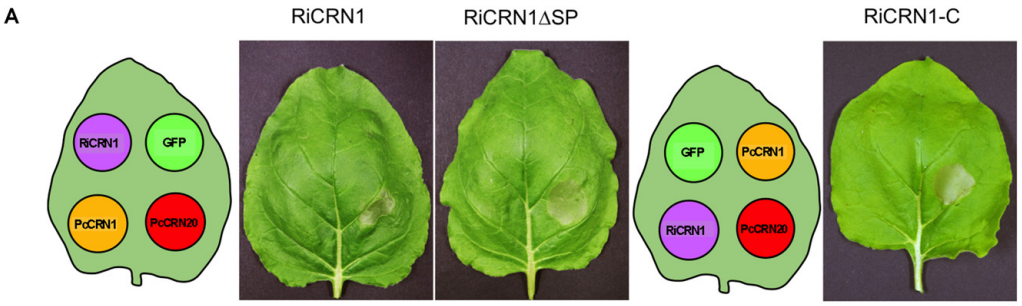

PcCRN20	PcCRN1	GFP	RiCRN1ΔSP	RiCRN1
30/36	0/36	2/36	0/36	0/36

PcCRN20	PcCRN1	GFP	RiCRN1-C
24/24	5/24	2/24	2/24

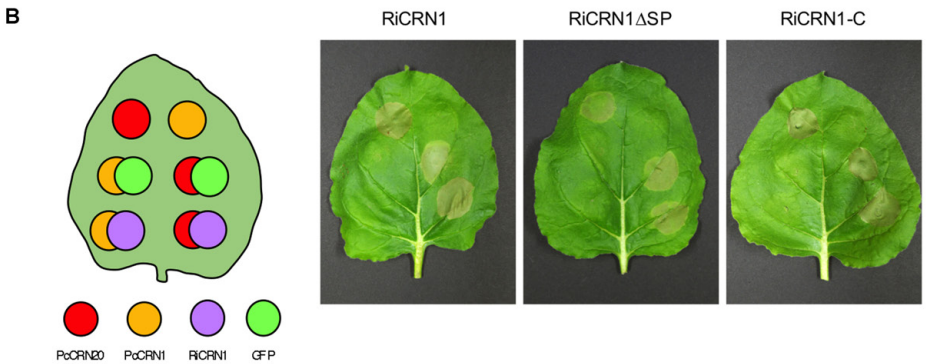

	PcCRN20	PcCRN1	GFP + PcCRN1	RiCRN1 + PcCRN1	GFP + PcCRN20	RiCRN1 + PcCRN20
RiCRN1	21/21	4/21	4/21	3/21	20/21	21/21
RiCRN1ΔSP	21/21	2/21	1/21	0/21	21/21	21/21
RiCRN1-C	21/21	4/21	2/21	4/21	20/21	21/21

FIGURE 6 | RiCRN1 does not control cell death in *N. benthamiana*. **(A)** To test a potential ability of cell death induction, a necrosis assay was carried out in *N. benthamiana*. For transient expression, leaves were infiltrated with *A. tumefaciens* carrying the constructs RiCRN1:eGFP, RiCRN1ΔSP:eGFP and RiCRN1-C:eGFP as well as PcCRN20_624 (positive control), PcCRN1_719 (negative control) and eGFP (negative control). Photographs were taken 7 days after infiltration. Quantification is shown as numbers of leaves displaying necrosis compared to the total amount of leaves assayed per construct. Infiltration sites of the three RiCRN1 versions show healthy leaf tissue with no induced cell death. **(B)** To assay a putative function of RiCRN1 as cell death inhibitor, the necrosis elicitor PcCRN20-624 was co-infiltrated with RiCRN1:eGFP, RiCRN1ΔSP:eGFP and RiCRN1-C:eGFP. Co-infiltration of PcCRN1_719 with the three RiCRN1 constructs as well as PcCRN20_624 with eGFP served as negative controls. Photographs were taken 7 days after infiltration. Quantification is shown as numbers of leaves displaying necrosis compared to the total amount of leaves assayed per construct. Cell death induced upon PsCRN20_624 was never inhibited by RiCRN1 versions.

that none of the RiCRN1 versions are able to induce cell death in *N. benthamiana* leaves, similar to the negative control PcCRN1_719 or to GFP. In contrast, leaf areas infiltrated with the positive control, the effector PcCRN20_624, clearly showed cell death symptoms (**Figure 6A** and **Supplementary Figure 4**). To test whether RiCRN1 could prevent the cell death elicited by PcCRN20_624, co-infiltration experiments were carried out. However, none of the RiCRN1 versions were able to decrease the number of cell death events elicited by PcCRN20_624 (**Figure 6B**). These results suggest that the function of RiCRN1 is not associated to cell death processes, at least in leaves. This is perhaps not surprising given that *R. irregularis* only colonizes roots and not leaves. However, expression of *RiCRN1* in *M. truncatula* roots (see below) or in *A. thaliana* plants (results not shown) does not induce cell death. Thus, it indicates that RiCRN1 function is not related to cell death but rather to the colonization process of the fungus, as the expression analysis suggests.

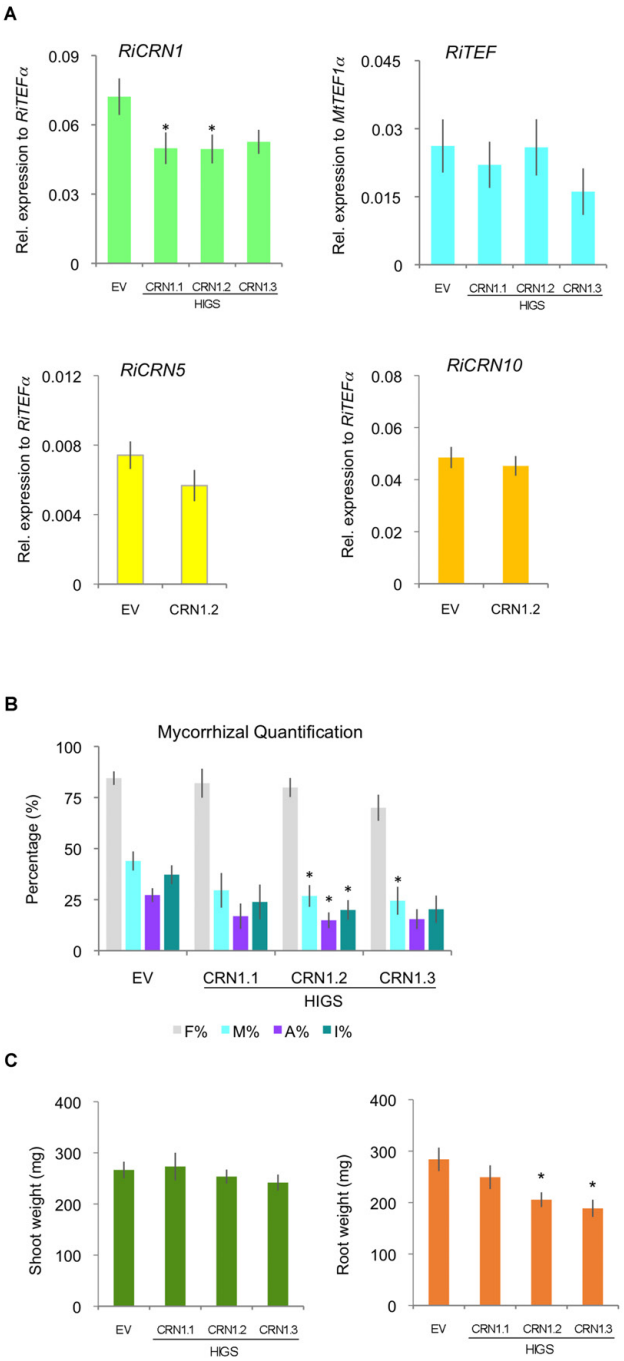

FIGURE 7 | Host-induced gene silencing of *RiCRN1* in mycorrhizal *M. truncatula* plants. **(A)** *M. truncatula* composite plants expressing three RNAi constructs targeting different regions of the gene *RiCRN1* (HIGS CRN1.1, CRN1.2, and CRN1.3) were inoculated with *R. irregularis*. Expression of *RiTEF1*α, *MtPT4* and the *R. irregularis* effectors *CRN1*, *CRN5*, and *CRN10* were analyzed at 5 wpi. Expression is shown as relative expression to *MtTEF1*α for *MtPT4* and *RiTEF1*α or to *RiTEF1*α for *RiCRN1*, *RiCRN5*, and *RiCRN10*. *RiCRN1* is downregulated compared to the EV control, significantly for constructs HIGS CRN1.1 and HIGS CRN1.2. In contrast, *RiCRN5* and *RiCRN10* as potential off-targets are not. The expression of the arbuscule marker *MtPT4* is reduced in plants expressing all three constructs, being significant for HIGS CRN1.2. Expression of *RiTEF1*α is not changed as compared to the EV control. Error bars represent SEM with $n = 9$ biological replicates for each condition. Student's *t*-test was used to validate significance of expression between the three different RNAi conditions and the EV control (*$p \leq 0.05$). **(B)** Mycorrhizal quantification was calculated after Trouvelot et al. (1986). Intensity of colonization (M%), arbuscule abundance (A%), and hyphal abundance (I%) in the root system are significantly reduced in HIGS CRN1.2 compared to the EV control. M% is also significantly reduced in HIGS CRN1.3. While frequency of colonization in the root system (F%) is constant in all conditions. Error bars represent SEM with $n = 9$ biological replicates for each condition. Student's *t*-test was used to validate significance of results comparing the different RNAi conditions with the EV plants (*$p \leq 0.05$). **(C)** Shoot and root fresh weight was also determined at 5 wpi. Compared to the EV control, none of the *RiCRN1* HIGS constructs seem to have an effect on shoot weight. In contrast, HIGS CRN1.2 and HIGS CRN1.3 induced a significant reduction in root biomass.

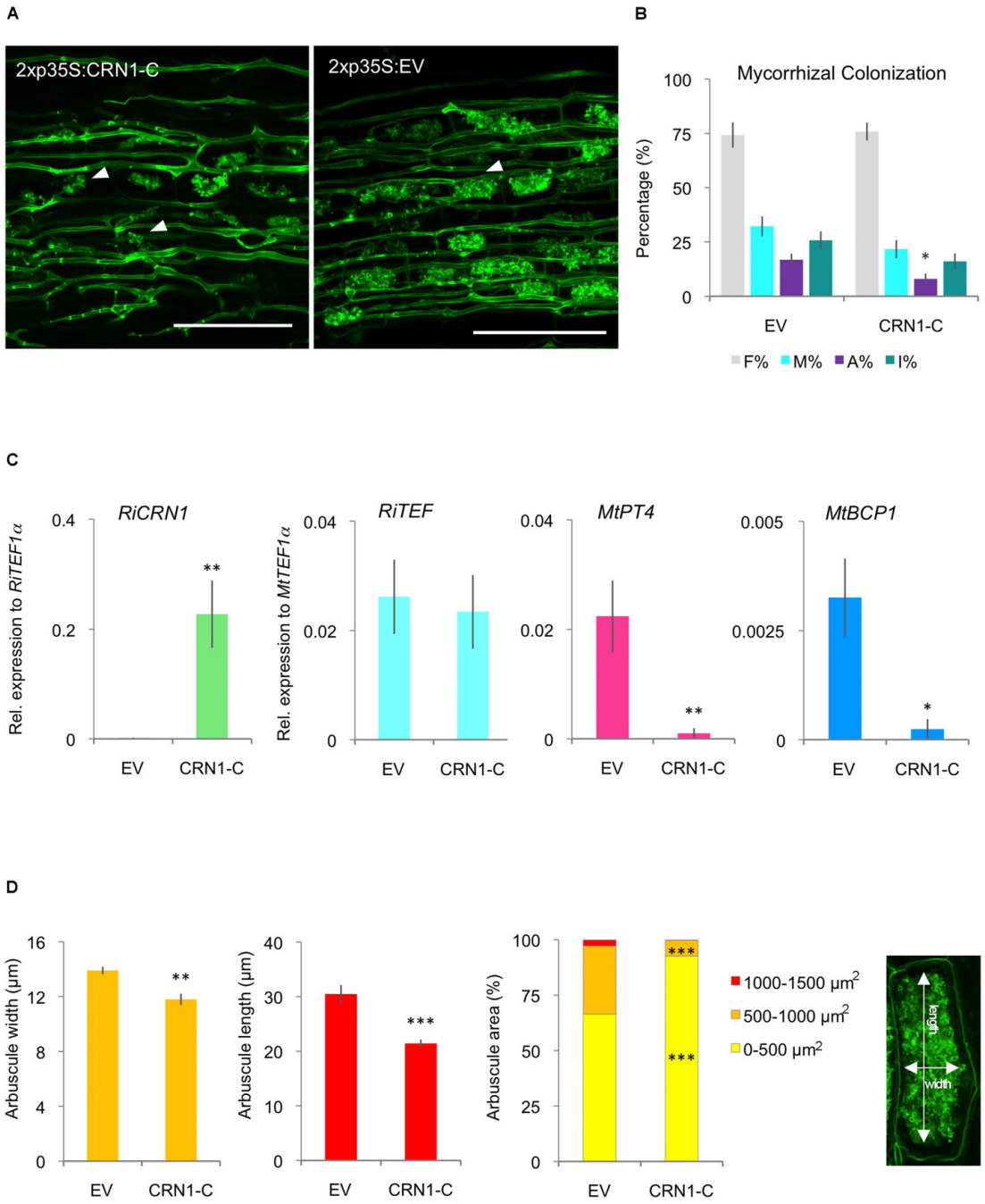

FIGURE 8 | Ectopic expression of *RiCRN1* in mycorrhizal *M. truncatula* plants. **(A)** *M. truncatula* composite plants expressing *RiCRN1-C* were inoculated with *R. irregularis*. Visualization of *R. irregularis* colonization at 5 wpi was carried out by wheat-germ agglutinin (WGA)-FITC immunostaining. Arrowheads indicate arbuscules in both conditions. Note the smaller arbuscule size in *RiCRN1-C* overexpressing plants. Scale bars represent 100 µm. **(B)** Mycorrhizal quantification was made after Trouvelot et al. (1986). A reduction of arbuscule abundance in the root system (A%) is significant compared to the EV control. Error bars represent SEM with $n = 6$ biological replicates for each condition. Student's *t*-test was used to calculate significance of results, comparing *RiCRN1-C* expressing with EV plants ($*p \leq 0.05$). **(C)** Expression of *RiTEF1*α, *MtPT4*, *MtBCP1*, and the *R. irregularis* effector *CRN1* were analyzed 5 wpi. Expression is shown as relative expression to *MtTEF1*α for *MtPT4*, *MtBCP1*, and *RiTEF1*α or to *RiTEF1*α for *RiCRN1*. Error bars represent SEM with $n = 6$ biological replicates for each condition. Student's *t*-test was used to calculate significance, comparing *RiCRN1* expressing with EV plants ($*p \leq 0.05$). **(D)** Arbuscule size and distribution in arbuscule populations of mycorrhizal *M. truncatula* roots 5 wpi. Arbuscules were measured in width and length as illustrated. Distribution of arbuscule size (area) within the root system is shown in percentage. Arbuscules were categorized based on area (0–500, 500–1000, and 1000–1500 µm^2). Data represent averages of $n = 6$ biological replicates. About 8–10 randomly selected infection sites were used to measure $n \geq 200$ arbuscules in each biological replicate. Error bars represent SEM. Student's *t*-test was used to calculate significance between *RiCRN1-C* and EV composite plants ($*p \leq 0.05$; $**p \leq 0.01$; $***p \leq 0.001$).

RiCRN1 Silencing by HIGS Leads to a Reduction in Mycorrhizal Colonization

In order to link the function of RiCRN1 to the colonization of the fungus and the establishment of the symbiosis, and given that AM fungi cannot be genetically manipulated, we attempted its inactivation using HIGS (Helber et al., 2011). There has been, as far as we know, few publications where CRN proteins were inactivated in other organisms, possibly given the difficulty to transform them. However, Liu et al. (2011) successfully silenced *PsCRN63* and *PsCRN115* in *P. sojae* and interestingly those silenced lines had a reduced virulence that correlated with a diminished ability to suppress cell death and defense responses. Also, silencing *PcCRN4* in *P. capsici* reduced the pathogen virulence and boosted the host defenses of the plant (Mafurah et al., 2015). To silence *RiCRN1*, three silencing constructs were employed that targeted different regions of the gene and nine transgenic plants were used per construct. Plants were then mycorrhized for 5 weeks. The results showed that two of the constructs did significantly downregulate the expression of *RiCRN1 in planta* (**Figure 7A**), albeit only ca. 30%, as compared to control plants transformed with an empty vector (EV). This is not surprising considering the mechanism of function of HIGS and the difficulties of obtaining fully downregulated fungal transcripts with this methodology. Nevertheless, the moderate downregulation led to a decrease in mycorrhizal intensity (M%) for two of the constructs and in one of them, HIGS-CRN1.2, also to a significant reduction in the number of arbuscules (A%) (**Figure 7B**). This correlated with a significantly lower expression of the arbuscule specific marker, the symbiotic plant phosphate transporter *MtPT4* (**Figure 7A**) in these silenced plants. In addition, mycorrhization of HIGS-CRN1 plants had an impact on root biomass, with a significant decrease observed in HIGS-CRN1.2 and HIGS-CRN1.3 plants (**Figure 7C**). Given that RiCRN1 is highly homologous to RiCRN5 and RiCRN10 that are also expressed *in planta*, we analyzed the off-target effects of the HIGS-CRN1.2 silencing construct on these two CRNs (**Figure 7A**). The results showed that HIGS-CRN1.2 did not silence *RiCRN5* or *RiCRN10*. Altogether, these data indicate that reduction of *RiCRN1* expression affects symbiosis progression and plant growth.

Ectopic Expression of *RiCRN1* Impacts on Arbuscule Development

To further get insights into the specific function of RiCRN1 during symbiosis, transgenic plants ectopically expressing the effector domain (RiCRN1-C) were created. It has been shown for some CRN effectors such as AeCRN13 from *A. euteiches* or PcCRN4 from *P. capsici*, that their expression *in planta* increases the susceptibility towards the pathogenic oomycete *Phytophthora capsici* (Mafurah et al., 2015; Ramirez-Garces et al., 2016). Thus, we hypothesized that the expression of *RiCRN1*, which increases concomitantly to the expression of *MtPT4*, could be related to a mechanism to facilitate the development of arbuscules. The expression of *RiCRN1-C* did not significantly modify plant growth nor produced browning symptoms that could indicate cell death induction (**Supplementary Figure 5**). This is different from the results observed in *M. truncatula* plants ectopically expressing *CRN13* from *A. euteiches* and *B. dendrobatidis,* that were abnormally developed (Ramirez-Garces et al., 2016). Also, expression of *RiCRN1-C* did not affect the mycorrhizal colonization levels (**Figures 8A,B**). However, in contrast to our prediction, the number of arbuscules was significantly reduced (**Figure 8B**). In agreement, overexpression of *RiCRN1-C* did not alter the *RiTEF1*α levels in roots but almost abolished the expression of the phosphate transporter *MtPT4* (**Figure 8C**). Because silencing of *RiCRN1* also impacted in arbuscule function, we wondered whether the negative effect of the ectopic expression of *RiCRN1* on arbuscule number was related to the development of new arbuscules. Thus, we also analyzed the expression of *MtBCP1,* a marker for arbuscule initiation (Gutjahr and Parniske, 2013), and similarly to *MtPT4*, its expression was much reduced in roots overexpressing *RiCRN1-C* (**Figure 8C**). These results suggest that RiCRN1 plays a specific role during arbuscule development. Morphometric analyses of arbuscules in *RiCRN1-C* overexpressing roots confirmed that hypothesis, showing that arbuscules were not only less but also significantly smaller than in control plants (**Figures 8A,D**). Furthermore, the size distribution of arbuscules between both treatments was significantly altered, with a much higher proportion of smaller arbuscules (0–500 μm^2) in RiCRN1-C roots and a reduction in larger arbuscules (**Figure 8D**). Thus, it appears that RiCRN1 rather plays a role in controlling arbuscule initiation, and that the amount of transcript together with the time and place of expression is critical for its proper function. Arbuscule development is a highly concerted process where many genes have to act in a coordinated manner (Gutjahr and Parniske, 2013; MacLean et al., 2017). In this scenario, *RiCRN1* accumulates during mycorrhiza establishment parallel to arbuscule development suggesting that it is mainly expressed in arbuscules, and that its targets might be located in plant cells that harbor them. In contrast, overexpression of *RiCRN1* is constitutive, high, and ubiquitous and therefore it might prevent the coordinated action on its plant targets.

CONCLUSION

Here, we show that AM fungi contain a repertoire of putative CRN effectors that besides the SP7-like proteins represent a new family of effectors characterized in an AM fungus. This is unique because although CRN effectors are widespread in plant-pathogenic oomycetes, they have never been described in a fungus interacting with plants. Most of the AM CRNs do not contain a signal peptide and thus, if they are secreted, the mechanisms of their unconventional secretion should be investigated. A small set of *R. irregularis* predicted CRNs contains a canonical signal peptide, and several of them accumulate during fungal development *in planta*. Here, we have functionally analyzed RiCRN1 and showed that it localizes in

nuclear bodies different from speckles, forms dimers and does not induce plant cell death. Its expression pattern and its effect during symbiosis suggest an involvement in arbuscule development. Thus, *RiCRN1* expression is necessary for symbiosis progression as shown by the silencing experiments, and its ectopic expression negatively impacts the initiation of arbuscule formation. However, given that several other similar CRNs exist and are expressed during symbiosis, more studies of the whole family and their plant targets will be required to fully understand the role of *R. irregularis* CRNs in the AM symbiosis.

AUTHOR CONTRIBUTIONS

SV and NR conceived the experiments and wrote the manuscript. SV, RB, and SH carried out all the experimental works. NC provided the initial sequence information.

FUNDING

We acknowledge the support by Deutsche Forschungsgemeinschaft and Open Access Publishing Fund of Karlsruhe Institute of Technology. SV holds a Ph.D. fellowship from the Baden-Württemberg Landesgraduiertenförderung.

ACKNOWLEDGMENTS

We thank E. Huitema and R. Stam for the *Phytophthora* effectors used in the necrosis assays.

SUPPLEMENTARY MATERIAL

The Supplementary Material for this article can be found online at: https://www.frontiersin.org/articles/10.3389/fmicb.2018.02068/full#supplementary-material

REFERENCES

Adhikari, B. N., Hamilton, J. P., Zerillo, M. M., Tisserat, N., Levesque, C. A., and Buell, C. R. (2013). Comparative genomics reveals insight into virulence strategies of plant pathogenic oomycetes. *PLoS One* 8:e75072. doi: 10.1371/journal.pone.0075072

Ali, G. S., Prasad, K. V., Hanumappa, M., and Reddy, A. S. (2008). Analyses of in vivo interaction and mobility of two spliceosomal proteins using FRAP and BiFC. *PLoS One* 3:e1953. doi: 10.1371/journal.pone.0001953

Amaro, T., Thilliez, G. J. A., McLeod, R. A., and Huitema, E. (2018). Random mutagenesis screen shows that *Phytophthora capsici* CRN83_152-mediated cell death is not required for its virulence function(s). *Mol. Plant Pathol.* 19, 1114–1126. doi: 10.1111/mpp.12590

Amaro, T. M., Thilliez, G. J., Motion, G. B., and Huitema, E. (2017). A perspective on CRN proteins in the genomics age: evolution, classification, delivery and function revisited. *Front. Plant Sci.* 8:99. doi: 10.3389/fpls.2017.00099

Berendsen, R. L., Pieterse, C. M., and Bakker, P. A. (2012). The rhizosphere microbiome and plant health. *Trends Plant Sci.* 17, 478–486. doi: 10.1016/j.tplants.2012.04.001

Boisson-Dernier, A., Chabaud, M., Garcia, F., Becard, G., Rosenberg, C., and Barker, D. G. (2001). *Agrobacterium rhizogenes*-transformed roots of *Medicago truncatula* for the study of nitrogen-fixing and endomycorrhizal symbiotic associations. *Mol. Plant Microbe Interact.* 14, 695–700. doi: 10.1094/MPMI.2001.14.6.695

Chen, E. C. H., Morin, E., Beaudet, D., Noel, J., Yildirir, G., Ndikumana, S., et al. (2018). High intraspecific genome diversity in the model arbuscular mycorrhizal symbiont *Rhizophagus irregularis*. *New Phytol.* doi: 10.1111/nph.14989 [Epub ahead of print].

Cheung, F., Win, J., Lang, J. M., Hamilton, J., Vuong, H., Leach, J. E., et al. (2008). Analysis of the *Pythium ultimum* transcriptome using Sanger and Pyrosequencing approaches. *BMC Genomics* 9:542. doi: 10.1186/1471-2164-9-542

Day, I. S., Golovkin, M., Palusa, S. G., Link, A., Ali, G. S., Thomas, J., et al. (2012). Interactions of SR45, an SR-like protein, with spliceosomal proteins and an intronic sequence: insights into regulated splicing. *Plant J.* 71, 936–947. doi: 10.1111/j.1365-313X.2012.05042.x

Doehlemann, G., Requena, N., Schaefer, P., Brunner, F., O'Connell, R., and Parker, J. E. (2014). Reprogramming of plant cells by filamentous plant-colonizing microbes. *New Phytol.* 204, 803–814.

Farrer, R. A., Martel, A., Verbrugghe, E., Abouelleil, A., Ducatelle, R., Longcore, J. E., et al. (2017). Genomic innovations linked to infection strategies across emerging pathogenic chytrid fungi. *Nat. Commun.* 8:14742. doi: 10.1038/ncomms14742

Gaulin, E., Madoui, M. A., Bottin, A., Jacquet, C., Mathe, C., Couloux, A., et al. (2008). Transcriptome of *Aphanomyces euteiches*: new oomycete putative pathogenicity factors and metabolic pathways. *PLoS One* 3:e1723. doi: 10.1371/journal.pone.0001723

Gaulin, E., Pel, M. J. C., Camborde, L., San-Clemente, H., Courbier, S., Dupouy, M. A., et al. (2018). Genomics analysis of *Aphanomyces* spp. identifies a new class of oomycete effector associated with host adaptation. *BMC Biol.* 16:43. doi: 10.1186/s12915-018-0508-5

Genre, A., Chabaud, M., Balzergue, C., Puech-Pages, V., Novero, M., Rey, T., et al. (2013). Short-chain chitin oligomers from arbuscular mycorrhizal fungi trigger nuclear $Ca2^{+}$ spiking in *Medicago truncatula* roots and their production is enhanced by strigolactone. *New Phytol.* 198, 190–202. doi: 10.1111/nph.12146

Gutjahr, C., and Parniske, M. (2013). Cell and developmental biology of arbuscular mycorrhiza symbiosis. *Annu. Rev. Cell Dev. Biol.* 29, 593–617. doi: 10.1146/annurev-cellbio-101512-122413

Haas, B. J., Kamoun, S., Zody, M. C., Jiang, R. H., Handsaker, R. E., Cano, L. M., et al. (2009). Genome sequence and analysis of the Irish potato famine pathogen *Phytophthora infestans*. *Nature* 461, 393–398. doi: 10.1038/nature08358

Harrison, M. J., Dewbre, G. R., and Liu, J. (2002). A phosphate transporter from *Medicago truncatula* involved in the acquisition of phosphate released by arbuscular mycorrhizal fungi. *Plant Cell* 14, 2413–2429.

Heck, C., Kuhn, H., Heidt, S., Walter, S., Rieger, N., and Requena, N. (2016). Symbiotic fungi control plant root cortex development through the novel GRAS transcription factor MIG1. *Curr. Biol.* 26, 2770–2778. doi: 10.1016/j.cub.2016.07.059

Helber, N., Wippel, K., Sauer, N., Schaarschmidt, S., Hause, B., and Requena, N. (2011). A versatile monosaccharide transporter that operates in the arbuscular mycorrhizal fungus *Glomus* sp is crucial for the symbiotic relationship with plants. *Plant Cell* 23, 3812–3823. doi: 10.1105/tpc.111.089813

Hewitt, E. J. (1966). *Sand and Water Culture Methods Used in the Study of Plant Nutrition*. London: Foreign and Commonwealth Office.

Javot, H., Penmetsa, R. V., Terzaghi, N., Cook, D. R., and Harrison, M. J. (2007). A *Medicago truncatula* phosphate transporter indispensable for the arbuscular mycorrhizal symbiosis. *Proc. Natl. Acad. Sci. U.S.A.* 104, 1720–1725. doi: 10.1073/pnas.0608136104

Kamel, L., Tang, N., Malbreil, M., San Clemente, H., Le Marquer, M., Roux, C., et al. (2017). The comparison of expressed candidate secreted proteins from two arbuscular mycorrhizal fungi unravels common and specific molecular tools to invade different host plants. *Front. Plant Sci.* 8:124. doi: 10.3389/fpls.2017.00124

Karimi, M., Inze, D., and Depicker, A. (2002). GATEWAY vectors for Agrobacterium-mediated plant transformation. *Trends Plant Sci.* 7, 193–195.

Kelley, L. A., Mezulis, S., Yates, C. M., Wass, M. N., and Sternberg, M. J. (2015). The Phyre2 web portal for protein modeling, prediction and analysis. *Nat. Protoc.* 10, 845–858. doi: 10.1038/nprot.2015.053

Kloppholz, S., Kuhn, H., and Requena, N. (2011). A secreted fungal effector of *Glomus intraradices* promotes symbiotic biotrophy. *Curr. Biol.* 21, 1204–1209. doi: 10.1016/j.cub.2011.06.044

Kuhn, H., Kuster, H., and Requena, N. (2010). Membrane steroid-binding protein 1 induced by a diffusible fungal signal is critical for mycorrhization in *Medicago truncatula*. *New Phytol.* 185, 716–733. doi: 10.1111/j.1469-8137.2009.03116.x

Lanfranco, L., Fiorilli, V., and Gutjahr, C. (2018). Partner communication and role of nutrients in the arbuscular mycorrhizal symbiosis. *New Phytol.* doi: 10.1111/nph.15230 [Epub ahead of print].

Levesque, C. A., Brouwer, H., Cano, L., Hamilton, J. P., Holt, C., Huitema, E., et al. (2010). Genome sequence of the necrotrophic plant pathogen *Pythium ultimum* reveals original pathogenicity mechanisms and effector repertoire. *Genome Biol.* 11:R73. doi: 10.1186/gb-2010-11-7-r73

Li, Q., Zhang, M., Shen, D., Liu, T., Chen, Y., Zhou, J. M., et al. (2016). A *Phytophthora sojae* effector PsCRN63 forms homo-/hetero-dimers to suppress plant immunity via an inverted association manner. *Sci. Rep.* 6:26951. doi: 10.1038/srep26951

Limpens, E., Mirabella, R., Fedorova, E., Franken, C., Franssen, H., Bisseling, T., et al. (2005). Formation of organelle-like N2-fixing symbiosomes in legume root nodules is controlled by DMI2. *Proc. Natl. Acad. Sci. U.S.A.* 102, 10375–10380.

Lin, K., Limpens, E., Zhang, Z., Ivanov, S., Saunders, D. G., Mu, D., et al. (2014). Single nucleus genome sequencing reveals high similarity among nuclei of an endomycorrhizal fungus. *PLoS Genet.* 10:e1004078. doi: 10.1371/journal.pgen.1004078

Links, M. G., Holub, E., Jiang, R. H., Sharpe, A. G., Hegedus, D., Beynon, E., et al. (2011). De novo sequence assembly of *Albugo candida* reveals a small genome relative to other biotrophic oomycetes. *BMC Genomics* 12:503. doi: 10.1186/1471-2164-12-503

Liu, T., Ye, W., Ru, Y., Yang, X., Gu, B., Tao, K., et al. (2011). Two host cytoplasmic effectors are required for pathogenesis of *Phytophthora sojae* by suppression of host defenses. *Plant Physiol.* 155, 490–501. doi: 10.1104/pp.110.166470

Luginbuehl, L. H., and Oldroyd, G. E. D. (2017). Understanding the arbuscule at the heart of endomycorrhizal symbioses in plants. *Curr. Biol.* 27, R952–R963. doi: 10.1016/j.cub.2017.06.042

MacLean, A. M., Bravo, A., and Harrison, M. J. (2017). Plant signaling and metabolic pathways enabling arbuscular mycorrhizal symbiosis. *Plant Cell* 29, 2319–2335. doi: 10.1105/tpc.17.00555

Mafurah, J. J., Ma, H., Zhang, M., Xu, J., He, F., Ye, T., et al. (2015). A virulence essential CRN effector of *Phytophthora capsici* suppresses host defense and induces cell death in plant nucleus. *PLoS One* 10:e0127965. doi: 10.1371/journal.pone.0127965

Maillet, F., Poinsot, V., Andre, O., Puech-Pages, V., Haouy, A., Gueunier, M., et al. (2011). Fungal lipochitooligosaccharide symbiotic signals in arbuscular mycorrhiza. *Nature* 469, 58–63. doi: 10.1038/nature09622

Pettersen, E. F., Goddard, T. D., Huang, C. C., Couch, G. S., Greenblatt, D. M., Meng, E. C., et al. (2004). UCSF Chimera–a visualization system for exploratory research and analysis. *J. Comput. Chem.* 25, 1605–1612. doi: 10.1002/jcc.20084

Quandt, H. J., Pühler, A., and Broer, I. (1993). Transgenic root nodules of *Vicia hirsuta*: a fast and efficient system for the study of gene expression in indeterminate-type nodules. *Mol. Plant Microbe Interact.* 6, 699–706.

Raffaele, S., Farrer, R. A., Cano, L. M., Studholme, D. J., MacLean, D., Thines, M., et al. (2010). Genome evolution following host jumps in the Irish potato famine pathogen lineage. *Science* 330, 1540–1543. doi: 10.1126/science.1193070

Rajput, N. A., Zhang, M., Ru, Y., Liu, T., Xu, J., Liu, L., et al. (2014). *Phytophthora sojae* effector PsCRN70 suppresses plant defenses in *Nicotiana benthamiana*. *PLoS One* 9:e98114. doi: 10.1371/journal.pone.0098114

Rajput, N. A., Zhang, M., Shen, D., Liu, T., Zhang, Q., Ru, Y., et al. (2015). Overexpression of a *Phytophthora* cytoplasmic CRN effector confers resistance to disease, salinity and drought in *Nicotiana benthamiana*. *Plant Cell Physiol.* 56, 2423–2435. doi: 10.1093/pcp/pcv164

Ramirez-Garces, D., Camborde, L., Pel, M. J., Jauneau, A., Martinez, Y., Neant, I., et al. (2016). CRN13 candidate effectors from plant and animal eukaryotic pathogens are DNA-binding proteins which trigger host DNA damage response. *New Phytol.* 210, 602–617. doi: 10.1111/nph.13774

Rech, S. S., Heidt, S., and Requena, N. (2013). A tandem Kunitz protease inhibitor (KPI106)-serine carboxypeptidase (SCP1) controls mycorrhiza establishment and arbuscule development in *Medicago truncatula*. *Plant J.* 75, 711–725. doi: 10.1111/tpj.12242

Schenck, N., and Smith, G. (1982). Additional new and unreported species of mycorrhizal fungi (Endogonaceae) from Florida. *Mycologia* 74, 77–92.

Schornack, S., Huitema, E., Cano, L. M., Bozkurt, T. O., Oliva, R., Van Damme, M., et al. (2009). Ten things to know about oomycete effectors. *Mol. Plant Pathol.* 10, 795–803. doi: 10.1111/j.1364-3703.2009.00593.x

Schornack, S., van Damme, M., Bozkurt, T. O., Cano, L. M., Smoker, M., Thines, M., et al. (2010). Ancient class of translocated oomycete effectors targets the host nucleus. *Proc. Natl. Acad. Sci. U.S.A.* 107, 17421–17426. doi: 10.1073/pnas.1008491107

Sedzielewska Toro, K., and Brachmann, A. (2016). The effector candidate repertoire of the arbuscular mycorrhizal fungus *Rhizophagus clarus*. *BMC Genomics* 17:101. doi: 10.1186/s12864-016-2422-y

Shen, D., Liu, T., Ye, W., Liu, L., Liu, P., Wu, Y., et al. (2013). Gene duplication and fragment recombination drive functional diversification of a superfamily of cytoplasmic effectors in *Phytophthora sojae*. *PLoS One* 8:e70036. doi: 10.1371/journal.pone.0070036

Smith, S. E., and Smith, F. A. (2011). Roles of arbuscular mycorrhizas in plant nutrition and growth: new paradigms from cellular to ecosystem scales. *Annu. Rev. Plant Biol.* 62, 227–250. doi: 10.1146/annurev-arplant-042110-103846

Song, T., Ma, Z., Shen, D., Li, Q., Li, W., Su, L., et al. (2015). An oomycete CRN effector reprograms expression of plant HSP genes by targeting their promoters. *PLoS Pathog.* 11:e1005348. doi: 10.1371/journal.ppat.1005348

Spatafora, J. W., Chang, Y., Benny, G. L., Lazarus, K., Smith, M. E., Berbee, M. L., et al. (2016). A phylum-level phylogenetic classification of zygomycete fungi based on genome-scale data. *Mycologia* 108, 1028–1046. doi: 10.3852/16-042

Stam, R., Howden, A. J., Delgado-Cerezo, M., Amaro, T. M. M. M., Motion, G. B., Pham, J., et al. (2013a). Characterization of cell death inducing *Phytophthora capsici* CRN effectors suggests diverse activities in the host nucleus. *Front. Plant Sci.* 4:387. doi: 10.3389/fpls.2013.00387

Stam, R., Jupe, J., Howden, A. J., Morris, J. A., Boevink, P. C., Hedley, P. E., et al. (2013b). Identification and characterisation CRN effectors in *Phytophthora capsici* shows modularity and functional diversity. *PLoS One* 8:e59517. doi: 10.1371/journal.pone.0059517

Sun, G., Yang, Z., Kosch, T., Summers, K., and Huang, J. (2011). Evidence for acquisition of virulence effectors in pathogenic chytrids. *BMC Evol. Biol.* 11:195. doi: 10.1186/1471-2148-11-195

Tisserant, E., Malbreil, M., Kuo, A., Kohler, A., Symeonidi, A., Balestrini, R., et al. (2013). Genome of an arbuscular mycorrhizal fungus provides insight into the oldest plant symbiosis. *Proc. Natl. Acad. Sci. U.S.A.* 110, 20117–20122. doi: 10.1073/pnas.1313452110

Torto, T. A., Li, S., Styer, A., Huitema, E., Testa, A., Gow, N. A., et al. (2003). EST mining and functional expression assays identify extracellular effector proteins from the plant pathogen *Phytophthora*. *Genome Res.* 13, 1675–1685. doi: 10.1101/gr.910003

Trouvelot, A., Kough, J., and Gianinazzi-Pearson, V. (1986). "Estimation of VA mycorrhizal infection levels. Research for methods having a functional significance," in *Physiological and Genetical Aspects of Mycorrhizae*, eds V. Gianinazzi-pearson and S. Gianinazzi (Paris: INRA Press), 223–232.

Tsuzuki, S., Handa, Y., Takeda, N., and Kawaguchi, M. (2016). Strigolactone-induced putative secreted protein 1 is required for the establishment of symbiosis by the arbuscular mycorrhizal fungus *Rhizophagus irregularis*. *Mol. Plant Microbe Interact.* 29, 277–286. doi: 10.1094/MPMI-10-15-0234-R

van Damme, M., Bozkurt, T. O., Cakir, C., Schornack, S., Sklenar, J., Jones, A. M., et al. (2012). The Irish potato famine pathogen *Phytophthora infestans* translocates the CRN8 kinase into host plant cells. *PLoS Pathog.* 8:e1002875. doi: 10.1371/journal.ppat.1002875

Voinnet, O., Rivas, S., Mestre, P., and Baulcombe, D. (2003). An enhanced transient expression system in plants based on suppression of gene silencing by the p19 protein of tomato bushy stunt virus. *Plant J.* 33, 949–956.

Zeng, T., Holmer, R., Hontelez, J., Te Lintel-Hekkert, B., Marufu, L., de Zeeuw, T., et al. (2018). Host- and stage-dependent secretome of the arbuscular mycorrhizal fungus *Rhizophagus irregularis*. *Plant J.* 94, 411–425. doi: 10.1111/tpj.13908

Zhang, D., Burroughs, A. M., Vidal, N. D., Iyer, L. M., and Aravind, L. (2016). Transposons to toxins: the provenance, architecture and diversification of a widespread class of eukaryotic effectors. *Nucleic Acids Res.* 44, 3513–3533. doi: 10.1093/nar/gkw221

Zhang, M., Li, Q., Liu, T., Liu, L., Shen, D., Zhu, Y., et al. (2015). Two cytoplasmic effectors of *Phytophthora sojae* regulate plant cell death via interactions with plant catalases. *Plant Physiol.* 167, 164–175. doi: 10.1104/pp.114.252437

Conflict of Interest Statement: The authors declare that the research was conducted in the absence of any commercial or financial relationships that could be construed as a potential conflict of interest.

frontiers in Microbiology

ORIGINAL RESEARCH
published: 22 November 2018
doi: 10.3389/fmicb.2018.02844

Out in the Cold: Identification of Genomic Regions Associated With Cold Tolerance in the Biocontrol Fungus *Clonostachys rosea* Through Genome-Wide Association Mapping

Martin Broberg[1]*, *Mukesh Dubey*[1], *Man-Hong Sun*[2], *Katarina Ihrmark*[1], *Hans-Josef Schroers*[3], *Shi-Dong Li*[2], *Dan Funck Jensen*[1], *Mikael Brandström Durling*[1] *and Magnus Karlsson*[1]

[1] Department of Forest Mycology and Plant Pathology, Swedish University of Agricultural Sciences, Uppsala, Sweden, [2] Key Laboratory of Integrated Pest Management in Crops, Ministry of Agriculture, Institute of Plant Protection, Chinese Academy of Agricultural Sciences, Beijing, China, [3] Agricultural Institute of Slovenia, Ljubljana, Slovenia

There is an increasing importance for using biocontrol agents in combating plant diseases sustainably and in the long term. As large scale genomic sequencing becomes economically viable, the impact of single nucleotide polymorphisms (SNPs) on biocontrol-associated phenotypes can be easily studied across entire genomes of fungal populations. Here, we improved a previously reported genome assembly of the biocontrol fungus *Clonostachys rosea* strain IK726 using the PacBio sequencing platform, which resulted in a total genome size of 70.7 Mbp and 21,246 predicted genes. We further performed whole-genome re-sequencing of 52 additional *C. rosea* strains isolated globally using Illumina sequencing technology, in order to perform genome-wide association studies in conditions relevant for biocontrol activity. One such condition is the ability to grow at lower temperatures commonly encountered in cryic or frigid soils in temperate regions, as these will be prevalent for protecting growing crops in temperate climates. Growth rates at 10°C on potato dextrose agar of the 53 sequenced strains of *C. rosea* were measured and ranged between 0.066 and 0.413 mm/day. Performing a genome wide association study, a total of 1,478 SNP markers were significantly associated with the trait and located in 227 scaffolds, within or close to (<1000 bp distance) 265 different genes. The predicted gene products included several chaperone proteins, membrane transporters, lipases, and proteins involved in chitin metabolism with possible roles in cold tolerance. The data reported in this study provides a foundation for future investigations into the genetic basis for cold tolerance in fungi, with important implications for biocontrol.

Keywords: biocontrol, *Clonostachys rosea*, comparative genomics, genome sequencing, GWAS

OPEN ACCESS

Edited by:
Sabrina Sarrocco,
Università degli Studi di Pisa, Italy

Reviewed by:
Richard Allen White III,
RAW Molecular Systems LLC,
United States
Kathryn Bushley,
University of Minnesota Twin Cities,
United States

***Correspondence:**
Martin Broberg
martin.broberg@slu.se

Specialty section:
This article was submitted to Plant Microbe Interactions, a section of the journal Frontiers in Microbiology

Received: *25 June 2018*
Accepted: *05 November 2018*
Published: *22 November 2018*

Citation:
Broberg M, Dubey M, Sun M-H, Ihrmark K, Schroers H-J, Li S-D, Jensen DF, Brandström Durling M and Karlsson M (2018) Out in the Cold: Identification of Genomic Regions Associated With Cold Tolerance in the Biocontrol Fungus Clonostachys rosea Through Genome-Wide Association Mapping. Front. Microbiol. 9:2844. doi: 10.3389/fmicb.2018.02844

INTRODUCTION

As the human global population grows and plant pathogens and pests increase and spread, sustainable agricultural production, and disease control increases in importance to ensure future food security (Syed Ab Rahman et al., 2018). Biological control agents (BCAs) demonstrate an environmentally sustainable and potent alternative to current industrial pesticide practices in agriculture, due to the risk chemicals may pose to human and animal health (Syed Ab Rahman et al., 2018). The mycoparasitic fungus *Clonostachys rosea* (Link: Fr.) Schroers, Samuels, Seifert & W. Gams, comb. nov. (Schroers et al., 1999) is a widely studied BCA, effective against several economically important fungal plant pathogens such as *Botrytis cinerea*, *Bipolaris sorokiniana*, *Fusarium* spp., and *Sclerotinia sclerotiorum* (Knudsen et al., 1995; Sutton et al., 1997; Teperi et al., 1998; Xue et al., 2009; Rodríguez et al., 2011). The sexual form (teleomorph) is described as *Bionectria ochroleuca* (Schw.) Schroers & Samuels, and certain strains readily produce sexual fruiting bodies (perithecia) in single culture indicating its homothallic mode of reproduction (Schroers et al., 1999). The biocontrol effect of *C. rosea* can be derived from its ability to directly parasitize plant pathogenic fungi, but also from exploitation competition for space and nutrients and from interference competition via antibiosis (Li et al., 2002; Rodríguez et al., 2011; Jensen et al., 2017).

Active growth in colder temperatures (below 15°C), is an important trait for a BCA to be effective in the field in temperate climates such as in the Nordic countries. This enables rapid colonization of seeds, wounds and other substrates for efficient exploitation competition, but is also important for maintaining high metabolic activity. This trait was originally one of the reasons for the selection of certain *C. rosea* strains as BCAs, e.g., for control of *F. culmorum* on wheat and barley at 15°C (Knudsen et al., 1995; Teperi et al., 1998). On the molecular level, mechanisms of cold tolerance in fungi partly overlap with other abiotic stress tolerances. Estimations suggest that approximately 85% of the biosphere is constantly subjected to temperatures of 5°C or lower (Li et al., 2012). Cold tolerance can be associated with changes in cell wall composition (carbohydrates, proteins and pigments), changes in lipid and osmolyte composition of cell membranes and the RNA translation and protein folding machinery (RNA helicases, trehalose, chaperone proteins), alcohol metabolism, transport proteins and mitochondria (Ellison et al., 2011; Blanc et al., 2012; Treseder and Lennon, 2015). Temperature such as cold has also been identified as a major environmental factor for organisms to adapt to, as it is one of the major environmental forces limiting life (D'Amico et al., 2002; Blanc et al., 2012; Li et al., 2012). Cold adaptation has been studied across free-living and plant-associated fungi to assess the temperature effects on adaptation, for example as a driving force for environmental colonization in plant-associated fungi and population divergence in fungi such as *Neurospora crassa* (Robinson, 2001; Ellison et al., 2011; Li et al., 2012). For fungi, cold tolerance may further be associated with osmotic stress tolerance, and spore survivability in low water, low nutrient conditions (Ruisi et al., 2007).

As genome sequencing has become cheaper and more user friendly, performing large-scale comparative genomics is now a standard practice for the identification of single nucleotide polymorphisms (SNPs), and determining their association with phenotypes of interest using genome-wide association studies (GWAS). The GWAS approach allows for statistical determination of SNPs of interests over a population of individuals with a shared evolutionary history. Previously, GWASs have been performed on fungal pathogens such as *Heterobasidion annosum*, *Zymoseptoria tritici*, *Parastagonospora nodorum,* and *Fusarium graminearum* (Dalman et al., 2013; Gao et al., 2016; Talas et al., 2016; Hartmann et al., 2017). However, as far as we are aware, no GWAS on fungal BCAs have been performed to date. The *C. rosea* strain IK726 genome was originally sequenced using short reads of the Illumina platform (Karlsson et al., 2015). However, the modern sequencing technology of the PacBio platform is allowing for more comprehensive and accurate genomics, by sequencing reads that are thousands to hundreds of thousands of base pairs (bp) in length instead of a few hundred bp (Roberts et al., 2013). This provides a very potent framework when combined with short read sequencing for assembling genomes (Schadt et al., 2010; Rhoads and Au, 2015; Chakraborty et al., 2016).

In this study, we evaluate the potential for performing GWAS in a fungal BCA. We present a re-sequenced genome of *C. rosea* IK726, combining the previously published genome scaffolds with long contigs gained from PacBio sequencing into a second, improved version of the genome, expanding the size from 58.3 to 70.7 Mbp and adding 6,497 predicted genes to a total of 21,246. In addition, we used Illumina technology to re-sequence the genomes of 52 additional *C. rosea* strains and performed a GWAS for growth rate in cold temperature (10°C). The analysis identified 1,478 SNP markers associated with the trait and certain genes located in the vicinity were predicted to encode several chaperone proteins, membrane transporters, lipases, and proteins involved in chitin metabolism with possible roles in cold tolerance. This genomic study updated the *C. rosea* IK726 genome, established a population genomic dataset for *C. rosea* and revealed important genomic regions for future studies of cold tolerance in this very promising BCA.

MATERIALS AND METHODS

Fungal Growth and Culture Conditions

Clonostachys rosea strains (**Supplementary Table 1**) were revived from glycerol stocks stored at −80°C, and maintained on potato dextrose agar (PDA; Oxoid, Cambridge, UK) at 25°C in darkness. Two growth rate assays were performed in triplicates for each strain by inoculating ½ strength PDA petri dishes with an agar plug with actively growing mycelium, followed by incubation at 10°C and 25°C, respectively, in darkness. Growth measurements of strains at 10°C were made by marking the edges of the fungal mycelium in four places in a square shape on the petri dish at 4 days and 28 days post inoculation. The mean change in millimeters between the 4-day and 28-day marks was measured and divided by 24 to provide data as mm growth per day. Growth measurements at 25°C were done in the same manner,

but measured from the edge of the inoculation agar plug to the mycelial front at 5 days post inoculation. Growth rate data at 10°C were analyzed by analysis of variance (ANOVA) using the Welch's test implemented in Minitab ver. 18 (Minitab Inc., State Collage, PA), while pairwise comparisons were made using the Games-Howell method at the 95% significance level. Growth rate data at 25°C were analyzed by ANOVA using a general linear model approach implemented in Minitab ver. 18 (Minitab Inc., State Collage, PA). Pairwise comparisons were made using the Fisher method at the 95% significance level. Linear regression analysis was performed by Pearson correlation in Minitab ver. 18 (Minitab Inc., State Collage, PA). Principle component analysis, using the R programming language, was performed in order to detect whether there was any correlation between geographical location of isolate origin and growth at 10°C.

For DNA extraction, strains were grown in 200 ml liquid Czapek-Dox medium (Sigma-Aldrich, Steinheim, Germany), Vogel's minimal medium (Vogel 1956) or malt extract (1.75 %) with peptone (0.25 %) medium at room temperature, shaking at 120 rpm. Cultures were harvested after 3–13 days, depending on growth rate, by snap freezing in liquid nitrogen, and then freeze-dried.

Genomic DNA Extraction and Sequencing

High-quality genomic DNA was extracted using CTAB/chloroform extraction for Illumina sequencing or Qiagen-tip 100 (Qiagen, Hilden, Germany) for PacBio sequencing (Menkis et al., 2015). Starting material for both protocols were freeze-dried mycelium ground with sand in a mortar and pestle. The CTAB/chloroform was scaled up to 50 ml falcon tubes with 10 ml CTAB-buffer and two to four rounds of chloroform extraction. Qiagen-tip 100 DNA extractions followed the Qiagen genomic DNA handbook with modifications of the yeast protocol. Instead of making spheroplasts, extraction started with adding G2 buffer to the ground mycelium and thereafter following the protocol. Regardless of protocol, at the precipitation step DNA was harvested with a glass hook and the remaining DNA was pelleted by centrifugation. For PacBio sequencing the harvested DNA was used, while for Illumina sequencing the harvested DNA was mostly used but the precipitated DNA was used in a few cases. DNA quality and concentrations were measured with Nanodrop (Thermo Fisher Scientific, Waltham, MA), Qubit dsDNA BR assay kit (Thermo Fisher Scientific, Waltham, MA) and agarose gel electrophoresis.

Base coverage of the *C. rosea* IK726 genome was generated using PacBio RSII Technology with an insert length of 20 kbp using standard library preparation kits. Base coverage of additional *C. rosea* genomes were generated using Illumina HiSeqX paired end sequencing with an insert length of 350 bp and read length of 150 bp using standard library preparation kits. The PacBio long reads were assembled into polished contigs using HGAP and the SMRT workflow (Chin et al., 2013).

Genome Assembly and Annotation, SNP Calling and Population Structure Analysis

The previously reported genome assembly of *C. rosea* IK726 (Karlsson et al., 2015) was combined with the polished contig output of the PacBio sequencing using quickmerge (Chakraborty et al., 2016). The PacBio contigs and the original assembly were compared using MUMmer ver. 3.23 (Delcher et al., 2003). The merged genome (version 2) was annotated using a pipeline described previously (Karlsson et al., 2015). For the additional 52 *C. rosea* strains, Illumina reads were aligned against the *C. rosea* IK726 ver. 2 genome using Bowtie 2 ver. 2.2.4 (Langmead and Salzberg, 2012). The alignments were further analyzed with SAMtools ver. 0.1.18 for filtering out PCR duplicates (Li et al., 2009). Variant calling was performed on filtered alignments using a combination of Freebayes ver. 1.0 and the bamaddrg script for adding read groups to binary alignment map (BAM) files (Garrison and Marth, 2012; Garrison, 2018). Population structure analysis was performed on the 53 isolates using Structure ver. 2.3.4 (Hubisz et al., 2009) using 8,000 randomly sampled SNPs across the population. Linkage disequilibrium (LD) was determined by using vcftools ver. 0.1.15, and to calculate r^2 using a 10 kbp window (Danecek et al., 2011).

Genome-Wide Association Study

The GWAS was performed using PLINK ver. 1.90 (Purcell et al., 2007), using the parameters—maf 0.1—hwe 1e-5 for SNP filtering. The SNPs were annotated using the ANNOVAR software (Wang et al., 2010). The resulting beta and beta standard deviation from the PLINK analysis were used as input to the R package ashr, for empirical Bayesian multiple hypothesis testing, for estimating local false sign rate (lfsr) for more appropriate significance estimation (Stephens, 2016). We used an lfsr of 0.05 as cut-off for significance. In addition, we used false discovery rate (FDR) correction for multiple testing as implemented in PLINK. Identification of conserved protein modules and features were made using the conserved domain database (CDD, Marchler-Bauer et al., 2017) and the transporter classification database (TCDB, Saier et al., 2016).

Chitin Synthase Phylogenetic Analysis

The amino acid sequences of the *C. rosea* chitin synthetases CRV2G00008512 and CRV2G00019295 were used to search GenBank at the National Center for Biotechnology Information (NCBI) for similar sequences using the BlastP algorithm. Amino acid sequence alignment was performed using MUSCLE (Edgar, 2004; Tamura et al., 2013), in the MEGA6 software. Phylogenetic analysis was performed using Maximum Likelihood methods implemented in MEGA6. Pairwise gap deletion was performed and the substitution model used was WAG with gamma distributed rates. Statistical support was performed using 1,000 bootstrapped resamplings of the tree.

Nucleotide Accession Numbers

Sequencing analysis files for all isolates in this study except *C. rosea* IK726 (deposited separately described by Karlsson et al., 2015) were deposited under the study accession number PRJEB26874 at the European Nucleotide Archive/European Molecular Biology Laboratory–European Bioinformatics Institute repository. PacBio sequencing files for the re-sequencing of *C. rosea* strain IK726, and the updated genome annotation were also deposited under ENA project PRJEB26874.

RESULTS

Growth Rates at 10°C and 25°C Differs Between *C. rosea* Strains

Growth rates of 53 *C. rosea* strains at 10°C were normally distributed, ranged from 0.066 to 0.413 mm/day (**Table 1**), and there were significant differences between strains ($P < 0.001$). The lowest growth rates were recorded for strains CBS 708.97, SHW-1-1, 1881, and IK726 originating from USA, China, Slovenia and Denmark, respectively. The highest growth rates were recorded for two strains from Slovenia (1832 and 1882) and strain CBS 188.33 from the Netherlands. No connection between growth rate and geographic origin was detected (**Supplementary Figure 1**). Growth rates at 25°C were normally distributed, ranged from 0.940 to 3.796 mm/day (**Table 1**), and there were significant differences between strains ($P < 0.001$). There was a weak correlation between growth rates at 10°C and 25°C ($r^2 = 0.178$, $P = 0.025$), indicating that the mechanisms for cold tolerance were distinct from the basis for high growth rate at ambient temperature. Therefore, the growth rate at 10°C for each strain was normalized by the growth rate at 25°C (**Table 1**) for the GWAS analysis, to enable identification of SNPs and genomic regions specifically contributing to higher growth rate at colder temperature.

PacBio Sequencing Results in an Improved Genome Assembly of *C. rosea* IK726

PacBio sequencing of the *C. rosea* IK726 genome resulted in 71.2 Mbp sequence data. The PacBio reads were subjected to error correction of the longest reads by subread filtering, mapping and *de novo* assembly of all reads into long polished contigs using HGAP ver 3.0 and the SMRT pipeline (Chin et al., 2013; Roberts et al., 2013). Combining the polished contigs of the PacBio sequencing with the previously reported Illumina-based genome of *C. rosea* IK726 (Karlsson et al., 2015), expanded the genome from 58.3 (ver. 1) to 70.7 (ver. 2) Mbp across 767 scaffolds (**Supplementary Table 2**). N50 increased from 790 kbp to 1.9 Mbp, and the gap length decreased from 924 to 207 kbp (**Supplementary Table 2**). Comparisons between ver. 1 and ver. 2 using MUMmer revealed a strong correlation between the longer PacBio contigs and the ver. 1 genome (**Supplementary Figure 2**). Several smaller PacBio contigs were left without a corresponding scaffold of the old version, demonstrating the superior coverage generated by PacBio. A total of 21,246 genes were predicted, although this number dropped to 17,508 when excluding exclusively *ab initio* predicted genes.

GWAS Identifies SNPs Associated With Growth Rate at 10°C

The 52 Illumina-sequenced genomes exhibited an average alignment percentage to the *C. rosea* genome ver. 2 of 91% (**Supplementary Table 1**). The genomes had an average of 2.6 Gbp of total reads with a Q value of ≥30, resulting in an average coverage of 35X. Initially, we used vcftools to extract a total of 1,898,673 SNPs. These were further filtered during the GWAS analysis with PLINK, filtering SNPs using a minor allele frequency cut-off of 10% and a Hardy-Weinberg statistic of 10^{-5}, leaving 63,726 SNPs. Based on 8,000 randomly sampled SNPs from the vcftool results, no population structure among the 53 strains was detected using the Structure software. The LD half decay distance was determined to 625 bp (**Figure 1**). Overall, the unfiltered SNPs were identified across 717 scaffolds (**Figure 2**, **Supplementary Table 3**).

Empirical Bayesian multiple hypothesis testing identified an association between 1,478 SNP markers and normalized growth rate at 10°C with an lfsr lower than 0.05 (**Supplementary Table 4**). These 1,478 SNPs were located on 227 different scaffolds (**Supplementary Table 4**). A single SNP (unitig_823:6016) was identified as associated with normalized growth rate at 10°C using FDR correction (**Supplementary Table 4**).

Gene Content in Genomic Regions Associated With Growth Rate at 10°C

Out of the 1,478 significantly cold growth associated SNP markers, 581 were located within or close (<1,000 bp) to 265 different genes, mostly predicted to encode proteins with unknown function (**Supplementary Table 4**). Out of these, 175 SNPs were located in exonic regions, 37 in intronic regions, 2 in splice sites, and 40 in the untranslated regions (UTRs) on the 3′ or 5′ ends. 145 of the 1,478 SNPs were highly significant according to the ashr analysis (lfsr $<10^{-10}$). The 20 most significant SNPs based on ashr are depicted in **Table 2**. The most common gene ontology categories were catalytic activity (GO:0003824), protein binding (GO:0005515), metabolic process (GO:0008152), oxidoreductase activity (GO:0016491), oxidation-reduction process (GO:0055114), ATP binding (GO:0005524), and zink ion binding (GO:0008270). The most highly associated SNP to growth rate at 10°C according to standard PLINK association ($P = 1.5^{*}10^{-7}$, FDR = 0.01) was located in gene CRV2G00015476. This gene was predicted to encode a beta lactam utilization protein, LamB. Nineteen SNPs were identified in an intergenic region between a gene for a predicted short-chain dehydrogenase (CRV2G00018099) and a gene for a predicted glutathione-dependent formaldehyde-activating enzyme (CRV2G000 18100).

Ten and eight SNPs, respectively, were identified close, exonic or within 1,000 bp up- or downstream, to two genes predicted to encode mitochondrial chaperone proteins (CRV2G00019610 and CRV2G00008672) (**Supplementary Table 4**). Two additional genes encoding heat shock protein (HSP) chaperones contained exonic SNPs; the small ATP-independent HSP chaperone CRV2G00019134 and the ATP-dependent HSP70 chaperone CRV2G00021296. Four SNPs were identified close, exonic, or within 500 bp upstream, to a gene for a predicted efflux membrane protein (CRV2G00021344). A more detailed analysis revealed that is was a major facilitator superfamily (MFS) transporter from the drug:H^+ antiporter-2 family (2.A.1.3), with the highest sequence similarity to members from the 2.A.1.3.33, 2.A.1.3.65, and 2.A.1.3.73 subfamilies that are implicated in drug, fungicide, or fungal secondary metabolite export. We also identified SNPs nearby (<700 bp) two additional genes putatively

TABLE 1 | Growth rates of *Clonostachys rosea* strains on PDA at 10°C and 25°C, and adjusted growth at 10°C.

Isolate	Cold growth mm/day	PDA growth mm/day	Cold rate/PDA rate	Origin
GG-1-2	0.201	0.940	0.214	Asia
2177	0.326	1.556	0.210	Europe
CBS 705.97	0.399	2.202	0.181	North America
JLB-7-1	0.347	1.923	0.181	Asia
IK216	0.326	1.811	0.180	Europe
2178	0.358	2.020	0.177	Europe
1832	0.410	2.416	0.170	Europe
2176	0.295	1.755	0.168	Europe
1316	0.326	2.022	0.161	Europe
IK371	0.309	2.035	0.152	Europe
B13	0.396	2.683	0.148	Oceania
1701	0.260	1.881	0.138	Europe
CBS 188.33	0.410	3.000	0.137	Europe
CBS 376.55	0.399	2.952	0.135	North America
CBS 193.94	0.372	2.850	0.130	South America
GL-1-1	0.313	2.474	0.126	Asia
1882	0.413	3.290	0.126	Europe
1829	0.194	1.550	0.125	Europe
1833	0.233	1.857	0.125	Europe
CBS 178.28	0.333	2.800	0.119	Europe
CBS 287.78	0.226	1.921	0.117	North America
CMI192798	0.344	2.930	0.117	Europe
GJS89-34	0.295	2.525	0.117	South America
CBS 154.27	0.326	2.828	0.115	North America
CBS 907.72E	0.351	3.061	0.115	Asia
CBS 907.72D	0.281	2.458	0.114	Asia
1884	0.208	1.856	0.112	Europe
CBS 100502	0.233	2.141	0.109	Europe
CBS 148.72	0.278	2.588	0.107	Europe
1827	0.174	1.627	0.107	Europe
SDT-5-1	0.208	1.985	0.105	Asia
CBS 421.87	0.285	2.825	0.101	Europe
CBS 222.93	0.219	2.210	0.099	South America
1830	0.215	2.175	0.099	Europe
SYP-4-2	0.191	1.971	0.097	Asia
1883	0.278	2.892	0.096	Europe
CBS 704.97	0.160	1.724	0.093	North America
NHH-61-2	0.188	2.074	0.090	Asia
STG-21-1	0.142	1.586	0.090	Asia
CBS 569.69	0.191	2.200	0.087	Europe
JXLS-1-1	0.267	3.240	0.083	Asia
CBS 649.8	0.194	2.383	0.082	Africa
SHW-1-1	0.122	1.561	0.078	Asia
IBT7519	0.194	2.531	0.077	Europe
CBS 100000	0.201	2.776	0.073	Oceania
NHH-48-2	0.174	2.426	0.072	Asia
CBS 907.72G	0.222	3.315	0.067	Asia
1885	0.174	2.700	0.064	Europe
CBS 706.97	0.184	2.969	0.062	North America
CBS 277.5	0.188	3.045	0.062	North America
1881	0.128	2.446	0.053	Europe
IK726	0.132	3.138	0.042	Europe
CBS 708.97	0.066	2.002	0.033	North America

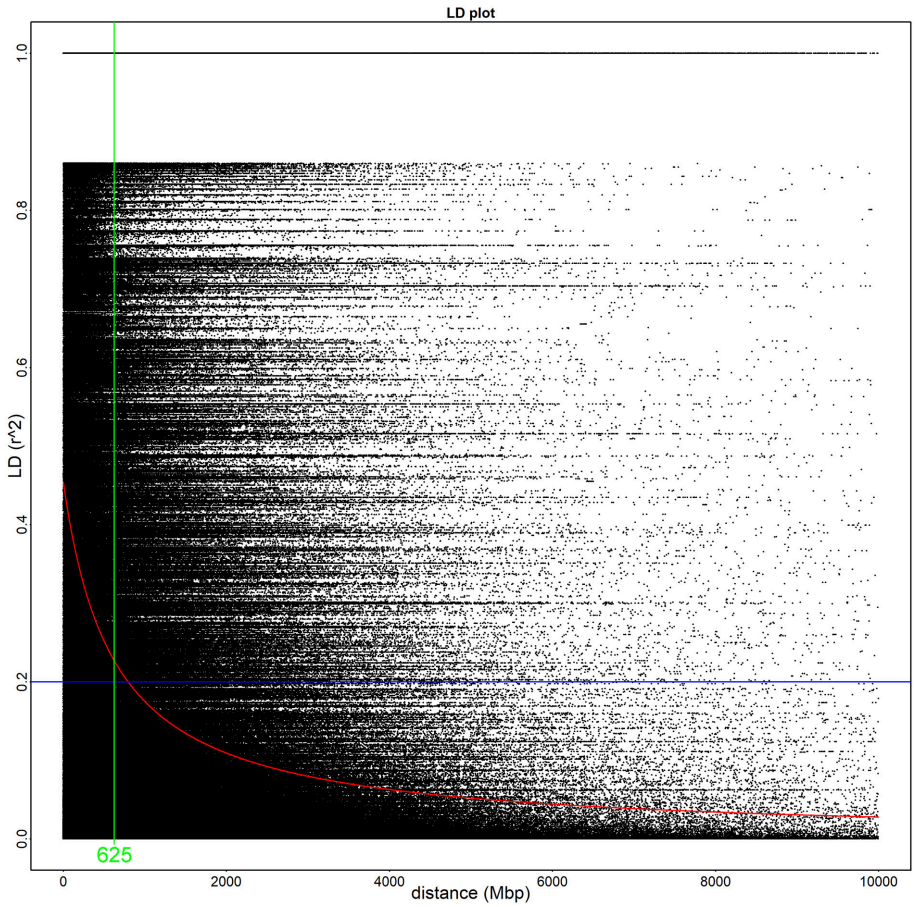

FIGURE 1 | The linkage disequilibrium half decay is 625 base pairs in this population of *Clonostachys rosea*. Linkage disequilibrium of all identified SNPs in a 10,000 base pair window. The green line demonstrates the linkage disequilibrium half decay mark, the blue line highlights an r^2 value of 0.2, and the red line describes the overall r^2 decay according to the Hill and Weir formula.

encoding MFS efflux pumps from the same drug:H+ antiporter-2 family (CRV2G00015724 and CRV2G00018834), also implicated in drug resistance. Other transport protein-encoding genes associated with significant SNPs were CRV2G00019382 and CRV2G00018067 encoding homologs of *Saccharomyces cerevisiae* FMP42, possibly associated with mitochondria.

We also identified two different genes encoding putative esterases/lipases (CRV2G00019392, CRV2G00021710) with three and one SNPs, respectively, exonic or within 600 bp downstream, significantly associated with growth rate at cold temperature. We detected seven SNPs close to or within three genes associated with chitin metabolism; CRV2G00008512, CRV2G00019295 (chitin synthases), and CRV2G00019292 (the *chiA4* chitinase). Additionally, we identified CRV2G00012293 (chitinase domain containing protein) with a significantly cold growth associated SNP at a distance of 2794 bp (**Table 2**). A sequence analysis of CRV2G00008512 and CRV2G00019295 showed that they displayed similarity with chitin synthases from other *Sordariomycete* fungi (**Supplementary Table 5**). A phylogenetic analysis further revealed that CRV2G00019295 clustered together with chitin synthase 1 from *N. crassa*, while CRV2G00008512 was more distantly related with chitin synthases from other Sordariomycetes (**Figure 3**). Besides the two previously mentioned mitochondrial chaperone protein genes and the FMP42 transporters, additional genes in close proximity with significant SNPs were predicted to encode proteins related to mitochondrial functioning; CRV2G00021544 putatively encoding a mitochondrial kinase activator of the bc1 complex required for the biosynthesis of Coenzyme Q and CRV2G00019380 similar to a mitochondrial aminolevulinate synthase involved in heme biosynthesis (**Supplementary Table 5**). We also detected three SNPs associated (one 6578 bp upstream, two in the 5′ UTR region) with CRV2G00020684, and one SNP associated with CRV2T00007803 (exonic), associated with frequency clock protein (FRQ) encoding gene in *C. rosea* (**Supplementary Table 4**, **Table 2**).

DISCUSSION

Fungi exhibit several advantages for applying GWA analysis such as small genomes, a haploid life stage and production of high numbers of clonal propagules that can be used for repeated

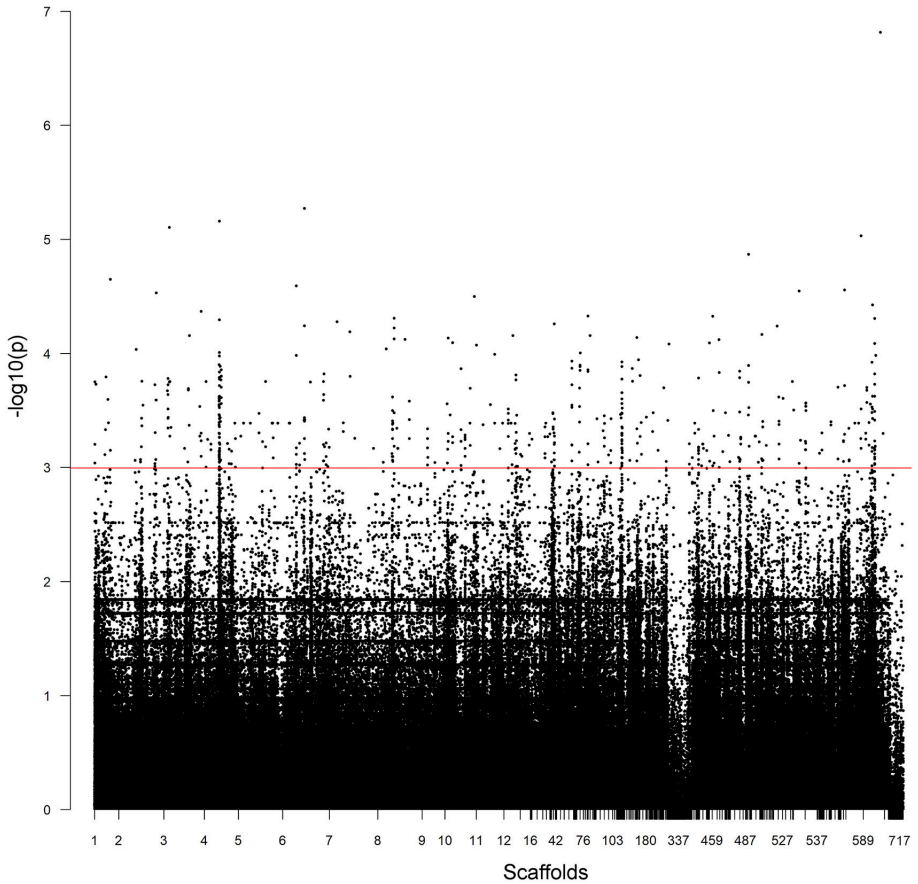

FIGURE 2 | Unfiltered SNPs in *Clonostachys rosea* across all scaffolds, numbered as described in **Supplementary Table 3**. Manhattan plots of the scaffold positions and *P*-values of cold growth for all SNPs across the all scaffolds. The red line indicates a *P*-value of 0.05-$\log_{10}$.

phenotypic assessments. Especially the possibility to genotype haploid individuals by sequencing makes GWAS particularly powerful, since the phenotype is the results of a single haplotype and not a result of two haplotypes as in the diploid case where heterozygosity can confound the signal. Despite these advantages, GWA analyses have not yet been utilized to study the genetic basis for biocontrol traits in fungal BCAs. In this study, we therefore set out to establish *C. rosea* as a population genomic model system for BCA fungi and to evaluate its usefulness for GWAS.

A high-quality reference genome with few gaps is an important aspect for a successful GWAS. The PacBio sequencing platform has been shown to improve older assemblies, primarily for eukaryotic organisms, by reconciling the long reads with older second generation short read sequencers (Chakraborty et al., 2016; Jayakumar and Sakakibara, 2017). Combining PacBio polished contigs with Illumina-based sequences substantially increased N50 and decreased gaps in the *C. rosea* ver. 2 genome. It also increased the total genome size to 70.7 Mbp, which is considerably larger than the genomes of other hypocrealean mycoparasitic species (Karlsson et al., 2018) such as *Trichoderma* spp. (31.7–39.0 Mbp, Kubicek et al., 2011; Studholme et al., 2013; Xie et al., 2014), *Tolypocladium ophioglossoides* (31.2 Mbp, Quandt et al., 2015) and *Escovopsis weberi* (29.5 Mbp, de Man et al., 2016). The draft genome of the closely related species *C. chloroleuca* (Moreira et al., 2016) is 55.4 Mbp (Sun et al., 2015), although this was based on Illumina-technology only and therefore comparable to the *C. rosea* ver. 1 genome of 58.3 Mbp (Karlsson et al., 2015). The large genomes of *Clonostachys* spp. is however comparable to certain related *Fusarium* spp., such as *F. solani* (51.1 Mbp, Coleman et al., 2009) and *F. oxysporum* (61.4 Mbp, Ma et al., 2010). The *C. rosea* ver. 2 genome was predicted to contain 21,246 genes that were 6,978 more than ver. 1 (Karlsson et al., 2015). However, 3,738 of these genes were solely predicted through *ab initio* methods and some of these may represent artifacts, suggesting that the total gene number in *C. rosea* is between 17,508 and 21,246.

We further established a population genomic dataset by sequencing the genomes of 52 different *C. rosea* strains. The high coverage of the Illumina-based genomes and the high sequence similarity with the strain IK726 ver. 2 genome indicate high quality of the generated genomes. Previous fungal GWASs have

TABLE 2 | Top 20 highest significance SNPs reported to be associated with growth rate at 10°C in ashr analysis.

SNP	lfsr	Location	Location	Annotation	NCBI Conserved domain search
unitig_630:6733	0.00	intergenic	CRV2G00019736(dist = 3623)	Protein of unknown function	No conserved domains identified
unitig_878:353	0.00	intergenic	NONE	.	.
unitig_760:385	0.00	intergenic	CRV2G00020684(dist = 6578)	Similar to FRQ Frequency clock protein	FRQ domain
unitig_47:563	0.00	intergenic	NONE	.	.
unitig_47:602	0.00	intergenic	NONE	.	.
unitig_793:2158	0.00	intergenic	CRV2G00016485(dist = 1475)	Protein of unknown function	No conserved domains identified
unitig_793:2167	0.00	intergenic	CRV2G00016485(dist = 1484)	Protein of unknown function	No conserved domains identified
unitig_298:2434	0.00	intergenic	NONE	.	.
unitig_298:2460	0.00	intergenic	NONE	.	.
unitig_280:2479	0.00	intergenic	NONE	.	.
unitig_345:10970	0.00	intergenic	CRV2G00021787(dist = 1241)	Protein of unknown function	FN3-like domain
unitig_246:11272	0.00	exonic	CRV2G00021642	Similar to fmpE Nonribosomal peptide synthetase	AFD class I superfamily, alpha am amid superfamily
unitig_640:12334	0.00	exonic	CRV2G00022020	Protein of unknown function	Fungal_TF_MHR, GAL4, DNA pol3 gamma3 superfamily
unitig_640:12340	0.00	exonic	CRV2G00022020	Protein of unknown function	Fungal_TF_MHR, GAL4, DNA pol3 gamma3 superfamily
unitig_818:85374	0.00	intergenic	CRV2G00017605(dist = 1606)	Mitochondrial chaperone BCS1-B	UhpC superfamily
unitig_601:93320	0.00	intergenic	CRV2G00019351(dist = 7767)	Protein of unknown function	Fasciclin domain
unitig_643:109199	0.00	intergenic	CRV2G00019327(dist = 50251)	Similar to betA Oxygen-dependent choline dehydrogenase	Choline dehydrogenase
unitig_697:153157	0.00	upstream	CRV2G00018410(dist = 872)	Protein of unknown function	No conserved domains identified
unitig_823:628705	0.00	intergenic	CRV2G00015724(dist = 3408)	Similar to FUS6 Efflux pump FUS6	TRI12 Superfamily
scf_014:970797	0.00	intergenic	CRV2G00012293(dist = 2794)	Protein of unknown function	GH18 chitinase-like superfamily

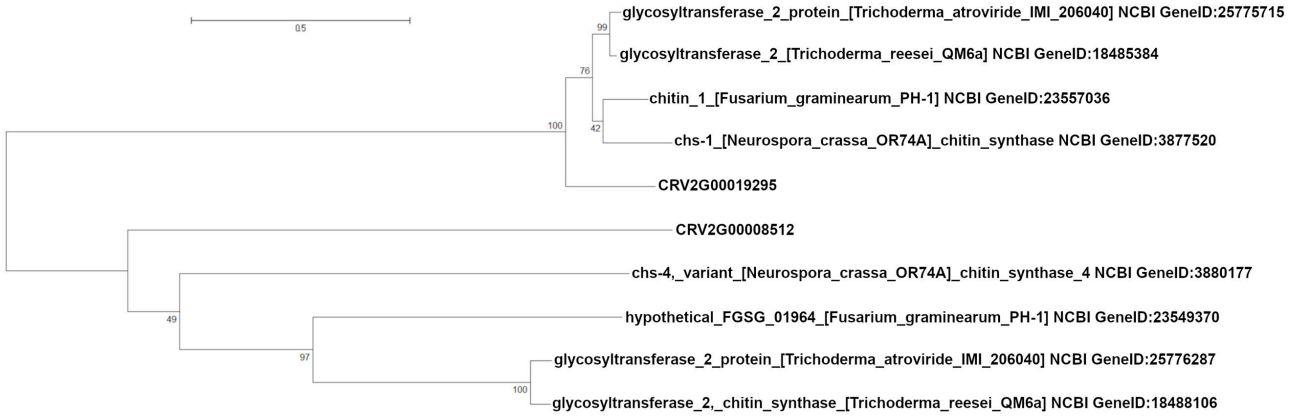

FIGURE 3 | Phylogenetic analysis of *Clonostachys rosea* chitin synthases. Amino acid sequences of selected chitin synthases were aligned using MUSCLE and a phylogenetic analysis conducted using maximum likelihood methods. Bootstrapped branch statistics values are depicted above the branches. The bar indicates mean number of amino acid substitutions per site. Protein identifiers include NCBI Gene ID number.

used both smaller and larger populations to successfully associate SNP markers with virulence in *H. annosum* (23 strains), *Z. tritici* (106 strains), *P. nodorum* (191 strains), with virulence, deoxynivaleol production and azole sensitivity in *F. graminearum* (119 strains) and with azole sensitivity in *Rhynchosporium commune* (120 strains) (Dalman et al., 2013; Gao et al., 2016; Mohd-Assaad et al., 2016; Talas et al., 2016; Hartmann et al., 2017).

Another requirement of successful GWA analyses is the presence of enough recombination events in the population. The homothallic reproductive mode of *C. rosea* (Schroers et al., 1999) may be an obstacle for this type of analysis if repeated selfings between identical genomes results in an essentially clonal population. However, the high genetic variation and rapid LD decay detected in our worldwide *C. rosea* population is a strong indication of reoccurring outcrossing between genetically different strains, showing that *C. rosea* is a facultative homothallic species. Genetically distinct *C. rosea* individuals have been isolated from the same field in Denmark (Bulat et al., 2000), indicating local genetic variation. Another homothallic species, *Aspergillus nidulans*, has been shown to occasionally outcross, resulting in genetic recombination within populations (Kronstad, 2007; López-Villavicencio et al., 2013). Recombination and possible outcrossing has also been reported for *Aspergillus fumigatus* and *Letharia* species (Kroken and Taylor, 2001; Pringle et al., 2005).

High variation in growth rate at 10°C in *C. rosea*, with no connection with the geographic origin of the strains and the lack of genetic population structure indicate that a GWAS of the trait is possible. High growth rate at lower temperature may be an important trait for BCAs, especially for rapid colonization of new substrates with limited amounts of competing microorganisms such as wounds, flowers, and developing roots (Jensen et al., 2016). The connection between cold tolerance and interference competition through mycoparasitism or antibiosis (Jensen et al., 2017) is less well established. In fact, *C. rosea* strain IK726 was among the most slow-growing strains at 10°C in our study, at the same time as it repeatedly has been shown to be a very efficient BCA against several different fungal plant pathogenic species (Jensen et al., 2007).

The normal distribution of the cold tolerance trait in *C. rosea* further suggests a polygenic inheritance that depends on several different genes. Many medically and agriculturally relevant traits are in fact multigenic and it has been notoriously difficult to achieve a reliable estimation of the true effect size of individual loci to genetic variation contributing to polygenic phenotypic differences (Boyle et al., 2017). Thus, the emerging view of the genome as a uniform distribution of contributing, however small, sequence variants to different phenotypes, the "omnigenic" model, highlights the propensity to underestimate the true significance of SNPs and similar genomic variations on a trait (Boyle et al., 2017). So, in line with the omnigenic trait view of the genome, we used the R package ashr that produces SNPs with a true effect size of zero or non-zero (Stephens, 2016). Recently, ashr has been used in some GWASs as an empirical Bayes large scale hypothesis testing alternative to false discovery rate analysis, by using effect size and its standard error, instead of using only one parameter, such as *P*-values (Stephens, 2016; Boyle et al., 2017; Petit et al., 2017). The approach by Stephens (2016) has been proposed to be more robust when dealing with large scale hypothesis testing, producing a local false sign rate (lfsr) as an analogous alternative to false discovery rate. The use of ashr allowed us to identify 1,478 SNPs significantly associated with *C. rosea* growth rate at 10°C, located physically (<1000 bp) close to about 265 genes.

As *C. rosea* is found globally, an evolved ability for cold tolerance would be integral for a generalist lifestyle across climates (Knudsen et al., 1995; Robinson, 2001; Abreu et al., 2014; Karlsson et al., 2015; Moreira et al., 2016). One important reason for wanting to study cold tolerance refers to the survival in temperate and arctic regions, as well as, in cold storage spaces, imperative for the long-term practical function and fitness of BCAs. The mechanisms for adapting to cold are numerous, and may include secretion of proteins with high catalytic efficiency active at low temperatures, transporters, lipid metabolism, secretion of secondary metabolites that counteract freezing damage of the membrane and intracellularly (Robinson, 2001; Blanc et al., 2012). Temperature and day length, depending on the geographical location, have been suggested to be major environmental factors impacting local adaptation of diverging *N. crassa* populations (Ellison et al., 2011). Significant SNPs were identified in or close to three genes encoding putative chaperone proteins. Regulation of mitochondrial chaperone proteins has been identified in association with temperature adaptation in diverse organisms such as the moth *Epiblema scudderiana* and the fungus *S. cerevisiae* (Schmitt, 1996; Lyons et al., 2015; Zhang et al., 2018). As chaperone proteins have also been discussed as important for cold tolerance in plants as well, this result demonstrates an interesting basis for further studies of chaperone importance in cold stress in *C. rosea* (Al-Whaibi, 2011). Several other genes putatively encoding proteins related to the mitochondria were identified by the GWAS, and further emphasize the importance of mitochondrial functioning for abiotic stress tolerance. The importance of mitochondrial activity in response to cold stress has been discussed in both animals and plants (Mollica et al., 2005; Fangue et al., 2009; Karami-Moalem et al., 2018).

Chitin is an important component of the fungal cell wall, and balancing chitin synthesis and degradation provides the appropriate plasticity and rigidity needed for hyphal growth (Specht et al., 1996). Therefore, it was interesting to find two putative chitin synthase genes and the *chiA4* chitinase gene among the genes associated with cold tolerance. The *chiA4* gene was reported to be constitutively expressed in *C. rosea* (Tzelepis et al., 2015), which fits well with a role in cell wall modeling during growth. Chitinases have also been implicated in cold tolerance in plants (Nakamura et al., 2008; Kashyap and Deswal, 2017). Certain fungal chitin synthases have also been associated with adaptation to temperature stress (Lenardon et al., 2009; Liu et al., 2017). The chitin synthase encoded by CRV2G00019295 was found to be most related to chs-1 in *N. crassa*, which has been found to play a major role in cell wall biogenesis (Yarden and Yanofsky, 1991).

Three different putative membrane efflux transporter genes from the MFS drug:H+ antiporter-2 family also contained SNPs associated with cold tolerance. Both the MFS transporter families 2.A.1.3.33 and 2.A.1.3.65 are shown to evolve under selection for increased gene copy numbers in *C. rosea*, emphasizing the importance for membrane transport in the lifestyle of *C. rosea* (Nygren et al., 2018). The connection between membrane transport and cold tolerance is less established. Efflux pumps have been associated with cold stress adaptation in bacteria, specifically by *Moraxella catarrhalis*, where cold stress reportedly

activates transcription and efflux activity the *AcrAB-OprM* system (Spaniol et al., 2015). Furthermore, studies indicate a connection between ions, secondary metabolite production (such as flavonoids) and membrane transport with cold tolerance in animals and plants (Kaplan, 2004; Wei et al., 2006; Storey and Storey, 2012; Wang M. et al., 2013; Wang X. C. et al., 2013). Additionally, secondary metabolites such as melanin have proven to be important in adjustment to temperature for the fungus *R. commune* and *Cryptococcus neoformans* (Rosas and Casadevall, 1997; Zhu et al., 2018). Thus, differences in transporter effectiveness due to differing alleles between strains may impact the ability of fungi to adjust their osmotic equilibrium, concentration of important metabolites for protein stability and membrane stability.

Finally, indications of lipid modifications in *C. rosea* as a response to colder temperatures comes from the association of SNPs situated in several putative lipases. Lipid structure and concentration is important for cold adaptation in many organisms (Arthur and Watson, 1976; Upchurch, 2008; van Dooremalen et al., 2011; Treseder and Lennon, 2015) and further studies of the association between the lipases and cold tolerance *C. rosea* is warranted. Comparative genomics and a growth assay at 10°C of *N. crassa* has suggested that the FRQ protein may be of significance in cold resistance, in part due to the link between lower temperatures and less daylight hours across geographical location (Ellison et al., 2011). From the GWAS we detected four significant SNPs associated with two genes in *C. rosea* encoding predicted FRQ proteins with some homology (∼80–90% cover, 33–36% identities) to *N. crassa* FRQ; CRV2G00020684 (one SNP 6578 bp upstream, two in the UTR5 region) and CRV2G00007803 (one exonic SNP). These results support the link between growth in cold and FRQ (**Table 2**, **Supplementary Table 4**).

We here present an improved genome assembly of *C. rosea* strain IK726 and whole-genome re-sequencing of an additional 52 *C. rosea* strains, thereby establishing *C. rosea* as the premier model species for genomic investigations of fungal BCAs. We further show that GWAS is a powerful tool for studying the genetic basis for phenotypes related with biocontrol activity. We identified an association between cold tolerance and SNPs residing in multiple genes, encoding putative mitochondrial chaperone and abiotic stress proteins, membrane efflux transport proteins, and lipases. These genes are of interest for further studies of cold stress and potential biocontrol efficiency in temperate climates.

AUTHOR CONTRIBUTIONS

All authors were involved in planning the study and writing the manuscript. M-HS, S-DL, and H-JS performed identification of the strains, KI and MD performed fungal growth and maintenance, and KI performed DNA extraction and preparation. MB and MK performed the growth assays. MB, MBD, and MK performed the genome sequencing analysis and GWAS analysis. DJ, MBD, and MK secured the funding.

FUNDING

This study was financially supported by the Swedish Research Council for Environment, Agricultural Sciences and Spatial Planning (FORMAS) (grant number 942-2015-1128) and by the Centre for Biological Control (CBC) at the Swedish University of Agricultural Sciences.

ACKNOWLEDGMENTS

The authors would like to acknowledge support of the National Genomics Infrastructure (NGI)/Uppsala Genome Center and UPPMAX for providing assistance in massive parallel sequencing and computational infrastructure. Work performed at NGI/Uppsala Genome Center has been funded by RFI/VR and Science for Life Laboratory, Sweden. Illumina sequencing was performed by the SNP&SEQ Technology Platform in Uppsala. The facility is part of NGI Sweden and Science for Life Laboratory. The SNP&SEQ Platform is also supported by the Swedish Research Council and the Knut and Alice Wallenberg Foundation.

SUPPLEMENTARY MATERIAL

The Supplementary Material for this article can be found online at: https://www.frontiersin.org/articles/10.3389/fmicb.2018.02844/full#supplementary-material

Supplementary Figure 1 | Origin of strains does not correlate with growth on PDA at 10°C. Using principal component analysis, we compared growth rates on PDA at 10°C, PDA at room temperature, and adjusted growth at 10°C to room temperature. The analysis revealed no correlation to the strains' origin of isolation.

Supplementary Figure 2 | MUMmer alignment output of PacBio long contigs to *Clonostachys rosea* IK726 ver. 1 genome scaffolds.

Supplementary Table 1 | List of all *Clonostachys rosea* isolates sequenced using the Illumina platform in this study, their origin, and Bowtie2 alignment rate.

Supplementary Table 2 | Details of the assembled *Clonostachys rosea* IK726 genome version 2.

Supplementary Table 3 | List of *Clonostachys rosea* genome version 2 scaffolds and their corresponding scaffold numbers in **Figure 2**.

Supplementary Table 4 | Significant GWAS analysis results based on PLINK and ashr.

Supplementary Table 5 | Protein sequences of chitin synthases used in the phylogenetic analysis in **Figure 3**.

REFERENCES

Abreu, L. M., Moreira, G. M., Ferreira, D., Rodrigues-Filho, E., and Pfenning, L. H. (2014). Diversity of Clonostachys species assessed by molecular phylogenetics and MALDI-TOF mass spectrometry. *Fungal Biol.* 118, 1004–1012. doi: 10.1016/j.funbio.2014.10.001

Al-Whaibi, M. H. (2011). Plant heat-shock proteins: a mini review. *J. King Saud Univ. Sci.* 23, 139–150. doi: 10.1016/j.jksus.2010.06.022

Arthur, H., and Watson, K. (1976). Thermal adaptation in yeast: growth temperatures, membrane lipid, and cytochrome composition of psychrophilic, mesophilic, and thermophilic yeasts. *J. Bacteriol.* 128, 56–68.

Blanc, G., Agarkova, I., Grimwood, J., Kuo, A., Brueggeman, A., Dunigan, D. D., et al. (2012). The genome of the polar eukaryotic microalga Coccomyxa subellipsoidea reveals traits of cold adaptation. *Genome Biol.* 13:R39. doi: 10.1186/gb-2012-13-5-r39

Boyle, E. A., Li, Y. I., and Pritchard, J. K. (2017). An expanded view of complex traits: from polygenic to omnigenic. *Cell* 169, 1177–1186. doi: 10.1016/j.cell.2017.05.038

Bulat, S. A., Lübeck, M., Alekhina, I. A., Jensen, D. F., Knudsen, I. M. B., and Lübeck, P. S. (2000). Identification of a universally primed-PCR-derived sequence-characterized amplified region marker for an antagonistic strain of clonostachys rosea and development of a strain-specific PCR detection assay. *Appl. Environ. Microbiol.* 66, 4758–4763. doi: 10.1128/AEM.66.11.4758-4763.2000

Chakraborty, M., Baldwin-Brown, J. G., Long, A. D., and Emerson, J. J. (2016). Contiguous and accurate *de novo* assembly of metazoan genomes with modest long read coverage. *Nucleic Acids Res.* 44:e147. doi: 10.1093/nar/gkw654

Chin, C. S., Alexander, D. H., Marks, P., Klammer, A. A., Drake, J., Heiner, C., et al. (2013). Nonhybrid, finished microbial genome assemblies from long-read SMRT sequencing data. *Nat. Methods* 10, 563–569. doi: 10.1038/nmeth.2474

Coleman, J. J., Rounsley, S. D., Rodriguez-Carres, M., Kuo, A., Wasmann, C. C., Grimwood, J., et al. (2009). The genome of nectria haematococca: contribution of supernumerary chromosomes to gene expansion. *PLoS Genet.* 5:e1000618. doi: 10.1371/journal.pgen.1000618

Dalman, K., Himmelstrand, K., Olson, Å., Lind, M., Brandström-Durling, M., and Stenlid, J. (2013). A genome-wide association study identifies genomic regions for virulence in the non-model organism heterobasidion annosum s.s. *PLoS ONE* 8:e53525. doi: 10.1371/journal.pone.0053525

D'Amico, S., Claverie, P., Collins, T., Georlette, D., Gratia, E., Hoyoux, A., et al. (2002). Molecular basis of cold adaptation. *Philos. Trans. R. Soc. B Biol. Sci.* 357, 917–925. doi: 10.1098/rstb.2002.1105

Danecek, P., Auton, A., Abecasis, G., Albers, C. A., Banks, E., DePristo, M. A., et al. (2011). The variant call format and VCFtools. *Bioinformatics* 27, 2156–2158. doi: 10.1093/bioinformatics/btr330

de Man, T. J., Stajich, J. E., Kubicek, C. P., Teiling, C., Chenthamara, K., Atanasova, L., et al. (2016). Small genome of the fungus *Escovopsis weberi*, a specialized disease agent of ant agriculture. *Proc. Natl. Acad. Sci. U.S.A.* 113, 3567–3572. doi: 10.1073/pnas.1518501113

Delcher, A. L., Salzberg, S. L., and Phillippy, A. M. (2003). Using MUMmer to identify similar regions in large sequence sets. *Curr. Protoc. Bioinform.* 10:10.3. doi: 10.1002/0471250953.bi1003s00

Edgar, R. C. (2004). MUSCLE: multiple sequence alignment with high accuracy and high throughput. *Nucleic Acids Res.* 32, 1792–1797. doi: 10.1093/nar/gkh340

Ellison, C. E., Hall, C., Kowbel, D., Welch, J., Brem, R. B., Glass, N. L., et al. (2011). Population genomics and local adaptation in wild isolates of a model microbial eukaryote. *Proc. Natl. Acad. Sci. U.S.A.* 108, 2831–2836. doi: 10.1073/pnas.1014971108

Fangue, N. A., Richards, J. G., and Schulte, P. M. (2009). Do mitochondrial properties explain intraspecific variation in thermal tolerance? *J. Exp. Biol.* 212, 514–522. doi: 10.1242/jeb.024034

Gao, Y., Liu, Z., Faris, J. D., Richards, J., Brueggeman, R. S., Li, X., et al. (2016). Validation of genome-wide association studies as a tool to identify virulence factors in *Parastagonospora nodorum*. *Phytopathology* 106, 1177–1185. doi: 10.1094/PHYTO-02-16-0113-FI

Garrison, E. (2018). *Bamaddrg: Adds Sample Names and Read-Group (RG) Tags to BAM Alignments*. Available online at: https://github.com/ekg/bamaddrg (Accessed February 7, 2018).

Garrison, E., and Marth, G. (2012). *Haplotype-Based Variant Detection From Short-Read Sequencing*. ArXiv12073907 Q-Bio. Available online at: http://arxiv.org/abs/1207.3907 (Accessed February 7, 2018).

Hartmann, F. E., Sánchez-Vallet, A., McDonald, B. A., and Croll, D. (2017). A fungal wheat pathogen evolved host specialization by extensive chromosomal rearrangements. *ISME J.* 11, 1189–1204. doi: 10.1038/ismej.2016.196

Hubisz, M. J., Falush, D., Stephens, M., and Pritchard, J. K. (2009). Inferring weak population structure with the assistance of sample group information. *Mol. Ecol. Resour.* 9, 1322–1332. doi: 10.1111/j.1755-0998.2009.02591.x

Jayakumar, V., and Sakakibara, Y. (2017). Comprehensive evaluation of non-hybrid genome assembly tools for third-generation PacBio long-read sequence data. *Brief. Bioinformatics*. doi: 10.1093/bib/bbx147

Jensen, D. F., Karlsson, M., and Lindahl, B. D. (2017). "Chapter 38: Fungal–fungal interactions: from natural ecosystems to managed plant production, with emphasis on biological control of plant diseases," in *Mycology*, eds J. Dighton and J. F. White (Boca Raton, FL: CRC Press), 549–562. doi: 10.1201/9781315119496-39

Jensen, D. F., Karlsson, M., Sarrocco, S., and Vannacci, G. (2016). "Biological control using microorganisms as an alternative to disease resistance," in *Plant Pathogen Resistance Biotechnology*, ed D. B. Collinge (Hoboken, NJ: John Wiley & Sons, Inc), 341–363. doi: 10.1002/9781118867716.ch18

Jensen, D. F., Knudsen, I. M. B., Beck, M. L., Mamarabadi, M., Hockenhull, J., and Jensen, B. (2007). Development of a biocontrol agent for plant disease control with special emphasis on the near commercial fungal antagonist *Clonostachys rosea* strain 'IK726.' *Australas. Plant Pathol.* 36, 95–101. doi: 10.1071/AP07009

Kaplan, F. (2004). Exploring the temperature-stress metabolome of arabidopsis. *Plant Physiol.* 136, 4159–4168. doi: 10.1104/pp.104.052142

Karami-Moalem, S., Maali-Amiri, R., and Kazemi-Shahandashti, S. S. (2018). Effect of cold stress on oxidative damage and mitochondrial respiratory properties in chickpea. *Plant Physiol. Biochem.* 122, 31–39. doi: 10.1016/j.plaphy.2017.11.011

Karlsson, M., Atanasova, L., Jensen, D. F., and Zeilinger, S. (2018). "Necrotrophic mycoparasites and their genomes," in *The Fungal Kingdom*, eds Heitman, Howlett, Crous, Stukenbrock, James, and Gow (Washington, DC: ASM Press), 1005–1026.

Karlsson, M., Durling, M. B., Choi, J., Kosawang, C., Lackner, G., Tzelepis, G. D., et al. (2015). Insights on the evolution of mycoparasitism from the genome of Clonostachys rosea. *Genome Biol. Evol.* 7, 465–480. doi: 10.1093/gbe/evu292

Kashyap, P., and Deswal, R. (2017). A novel class I chitinase from *Hippophae rhamnoides*: indications for participating in ICE-CBF cold stress signaling pathway. *Plant Sci.* 259, 62–70. doi: 10.1016/j.plantsci.2017.03.004

Knudsen, I. M. B., Hockenhull, J., and Jensen, D. F. (1995). Biocontrol of seedling diseases of barley and wheat caused by *Fusarium culmorum* and *Bipolaris sorokiniana*: effects of selected fungal antagonists on growth and yield components. *Plant Pathol.* 44, 467–477. doi: 10.1111/j.1365-3059.1995.tb01669.x

Kroken, S., and Taylor, J. W. (2001). Outcrossing and recombination in the lichenized fungus letharia. *Fungal Genet. Biol.* 34, 83–92. doi: 10.1006/fgbi.2001.1291

Kronstad, J. W. (2007). Self-fertility: the genetics of sex in lonely fungi. *Curr. Biol.* 17, R843–R845. doi: 10.1016/j.cub.2007.08.002

Kubicek, C. P., Herrera-Estrella, A., Seidl-Seiboth, V., Martinez, D. A., Druzhinina, I. S., Thon, M., et al. (2011). Comparative genome sequence analysis underscores mycoparasitism as the ancestral life style of Trichoderma. *Genome Biol.* 12:R40. doi: 10.1186/gb-2011-12-4-r40

Langmead, B., and Salzberg, S. L. (2012). Fast gapped-read alignment with Bowtie 2. *Nat. Methods* 9, 357–359. doi: 10.1038/nmeth.1923

Lenardon, M. D., Lesiak, I., Munro, C. A., and Gow, N. A. (2009). Dissection of the *Candida albicans* class I chitin synthase promoters. *Mol. Genet. Genomics* 281, 459–471. doi: 10.1007/s00438-009-0423-0

Li, G. Q., Huang, H. C., Kokko, E. G., and Acharya, S. N. (2002). Ultrastructural study of mycoparasitism of Gliocladium roseum on *Botrytis cinerea*. *Bot. Bull. Acad. Sin.* 43, 211–218. doi: 10.7016/BBAS.200207.0211

Li, H., Handsaker, B., Wysoker, A., Fennell, T., Ruan, J., Homer, N., et al. (2009). The sequence alignment/map format and SAMtools. *Bioinformatics* 25, 2078–2079. doi: 10.1093/bioinformatics/btp352

Li, H.-Y., Shen, M., Zhou, Z.-P., Li, T., Wei, Y., and Lin, L. (2012). Diversity and cold adaptation of endophytic fungi from five dominant plant species collected from the baima snow mountain, southwest China. *Fungal Divers.* 54, 79–86. doi: 10.1007/s13225-012-0153-1

Liu, R., Xu, C., Zhang, Q., Wang, S., and Fang, W. (2017). Evolution of the chitin synthase gene family correlates with fungal morphogenesis and adaption to ecological niches. *Sci. Rep.* 7:44527. doi: 10.1038/srep44527

López-Villavicencio, M., Debets, A. J. M., Slakhorst, M., Giraud, T., and Schoustra, S. E. (2013). Deleterious effects of recombination and possible nonrecombinatorial advantages of sex in a fungal model. *J. Evol. Biol.* 26, 1968–1978. doi: 10.1111/jeb.12196

Lyons, P. J., Crapoulet, N., Storey, K. B., and Morin, P. J. (2015). Identification and profiling of miRNAs in the freeze-avoiding gall moth Epiblema scudderiana via next-generation sequencing. *Mol. Cell. Biochem.* 410, 155–163. doi: 10.1007/s11010-015-2547-3

Ma, L. J., van der Does, H. C., Borkovich, K. A., Coleman, J. J., Daboussi, M. J., Di Pietro, A., et al. (2010). Comparative genomics reveals mobile pathogenicity chromosomes in Fusarium. *Nature* 464, 367–373. doi: 10.1038/nature08850

Marchler-Bauer, A., Bo, Y., Han, L., He, J., Lanczycki, C. J., Lu, S., et al. (2017). CDD/SPARCLE: functional classification of proteins via subfamily domain architectures. *Nucleic Acids Res.* 45, D200–D203. doi: 10.1093/nar/gkw1129

Menkis, A., Marčiulynas, A., Gedminas, A., Lynikien,e, J., and Povilaitien,e, A. (2015). High-throughput sequencing reveals drastic changes in fungal communities in the phyllosphere of norway spruce (*Picea abies*) following invasion of the spruce bud scale (*Physokermes piceae*). *Microb. Ecol.* 70, 904–911. doi: 10.1007/s00248-015-0638-z

Mohd-Assaad, N., McDonald, B. A., and Croll, D. (2016). Multilocus resistance evolution to azole fungicides in fungal plant pathogen populations. *Mol. Ecol.* 25, 6124–6142. doi: 10.1111/mec.13916

Mollica, M. P., Lionetti, L., Crescenzo, R., Tasso, R., Barletta, A., Liverini, G., et al. (2005). Cold exposure differently influences mitochondrial energy efficiency in rat liver and skeletal muscle. *FEBS Lett.* 579, 1978–1982. doi: 10.1016/j.febslet.2005.02.044

Moreira, G. M., Abreu, L. M., Carvalho, V. G., Schroers, H.-J., and Pfenning, L. H. (2016). Multilocus phylogeny of *Clonostachys* subgenus *Bionectria* from Brazil and description of *Clonostachys chloroleuca* sp. nov. *Mycol. Prog.* 15, 1031–1039. doi: 10.1007/s11557-016-1224-6

Nakamura, T., Ishikawa, M., Nakatani, H., and Oda, A. (2008). Characterization of cold-responsive extracellular chitinase in bromegrass cell cultures and its relationship to antifreeze activity. *Plant Physiol.* 147, 391–401. doi: 10.1104/pp.106.081497

Nygren, K., Dubey, M., Zapparata, A., Iqbal, M., Tzelepis, G. D., Durling, M. B., et al. (2018). The mycoparasitic fungus *Clonostachys rosea* responds with both common and specific gene expression during interspecific interactions with fungal prey. *Evol. Appl.* 11, 931–949. doi: 10.1111/eva.12609

Petit, M., Astruc, J. M., Sarry, J., Drouilhet, L., Fabre, S., Moreno, C., et al. (2017). Variation in recombination rate and its genetic determinism in sheep populations. *Genetics* 207, 767–784. doi: 10.1534/genetics.117.300123

Pringle, A., Baker, D. M., Platt, J. L., Wares, J. P., Latgé, J. P., and Taylor, J. W. (2005). Cryptic speciation in the cosmopolitan and clonal human pathogenic fungus *Asperigillus fumigatus*. *Evolution* 59, 1886–1899. doi: 10.1111/j.0014-3820.2005.tb01059.x

Purcell, S., Neale, B., Todd-Brown, K., Thomas, L., Ferreira, M. A., Bender, D., et al. (2007). PLINK: a tool set for whole-genome association and population-based linkage analyses. *Am. J. Hum. Genet.* 81, 559–575. doi: 10.1086/519795

Quandt, C. A., Bushley, K. E., and Spatafora, J. W. (2015). The genome of the truffle-parasite *Tolypocladium ophioglossoides* and the evolution of antifungal peptaibiotics. *BMC Genomics* 16:553. doi: 10.1186/s12864-015-1777-9

Rhoads, A., and Au, K. F. (2015). PacBio sequencing and its applications. *Genomics Proteomics Bioinformatics* 13, 278–289. doi: 10.1016/j.gpb.2015.08.002

Roberts, R. J., Carneiro, M. O., and Schatz, M. C. (2013). The advantages of SMRT sequencing. *Genome Biol.* 14:405. doi: 10.1186/gb-2013-14-6-405

Robinson, C. H. (2001). Cold adaptation in Arctic and Antarctic fungi. *New Phytol.* 151, 341–353. doi: 10.1046/j.1469-8137.2001.00177.x

Rodríguez, M. A., Cabrera, G., Gozzo, F. C., Eberlin, M. N., and Godeas, A. (2011). *Clonostachys rosea* BAFC3874 as a *Sclerotinia sclerotiorum* antagonist: mechanisms involved and potential as a biocontrol agent: *Clonostachys rosea* as a *Sclerotinia sclerotiorum* antagonist. *J. Appl. Microbiol.* 110, 1177–1186. doi: 10.1111/j.1365-2672.2011.04970.x

Rosas, A. L., and Casadevall, A. (1997). Melanization affects susceptibility of *Cryptococcus neoformans* to heat and cold. *FEMS Microbiol. Lett.* 153, 265–272.

Ruisi, S., Barreca, D., Selbmann, L., Zucconi, L., and Onofri, S. (2007). Fungi in Antarctica. *Rev. Environ. Sci. Biotechnol.* 6, 127–141. doi: 10.1007/s11157-006-9107-y

Saier, M. H., Reddy, V. S., Tsu, B. V., Ahmed, M. S., Li, C., and Moreno-Hagelsieb, G. (2016). The Transporter Classification Database (TCDB): recent advances. *Nucleic Acids Res.* 44, D372–D379. doi: 10.1093/nar/gkv1103

Schadt, E. E., Turner, S., and Kasarskis, A. (2010). A window into third-generation sequencing. *Hum. Mol. Genet.* 19, R227–R240. doi: 10.1093/hmg/ddq416

Schmitt, M. (1996). The molecular chaperone Hsp78 confers compartment-specific thermotolerance to mitochondria. *J. Cell Biol.* 134, 1375–1386. doi: 10.1083/jcb.134.6.1375

Schroers, H.-J., Samuels, G. J., Seifert, K. A., and Gams, W. (1999). Classification of the mycoparasite Gliocladium roseum in Clonostachys as *C. rosea*, its relationship to *Bionectria ochroleuca*, and notes on other Gliocladium-like fungi. *Mycologia* 91, 365–385. doi: 10.2307/3761383

Spaniol, V., Bernhard, S., and Aebi, C. (2015). *Moraxella catarrhalis* AcrAB-OprM efflux pump contributes to antimicrobial resistance and is enhanced during cold shock response. *Antimicrob. Agents Chemother.* 59, 1886–1894. doi: 10.1128/AAC.03727-14

Specht, C. A., Liu, Y., Robbins, P. W., Bulawa, C. E., Iartchouk, N., Winter, K. R., et al. (1996). The chsD and chsE genes of *Aspergillus nidulans* and their roles in chitin synthesis. *Fungal Genet. Biol.* 20, 153–167. doi: 10.1006/fgbi.1996.0030

Stephens, M. (2016). False discovery rates: a new deal. *Biostatistics*. 18, 275–294. doi: 10.1093/biostatistics/kxw041

Storey, K. B., and Storey, J. M. (2012). Insect cold hardiness: metabolic, gene, and protein adaptation. *Can. J. Zool.* 90, 456–475. doi: 10.1139/z2012-011

Studholme, D. J., Harris, B., Le Cocq, K., Winsbury, R., Perera, V., Ryder, L., et al. (2013). Investigating the beneficial traits of *Trichoderma hamatum* GD12 for sustainable agriculture—insights from genomics. *Front. Plant Sci.* 4:258. doi: 10.3389/fpls.2013.00258

Sun, Z. B., Sun, M. H., and Li, S. D. (2015). Draft genome sequence of mycoparasite *Clonostachys rosea* strain 67-1. *Genome Announc.* 3, e00546–e00515. doi: 10.1128/genomeA.00546-15

Sutton, J. C., Li, D.-W., Peng, G., Yu, H., Zhang, P., and Valdebenito-Sanhueza, R. M. (1997). *Gliocladium roseum* a versatile adversary of *Botrytis cinera* in crops. *Plant Dis.* 81, 316–328. doi: 10.1094/PDIS.1997.81.4.316

Syed Ab Rahman, S. F., Singh, E., Pieterse, C. M. J., and Schenk, P. M. (2018). Emerging microbial biocontrol strategies for plant pathogens. *Plant Sci.* 267, 102–111. doi: 10.1016/j.plantsci.2017.11.012

Talas, F., Kalih, R., Miedaner, T., and McDonald, B. A. (2016). Genome-wide association study identifies novel candidate genes for aggressiveness, deoxynivalenol production, and azole sensitivity in natural field populations of *Fusarium graminearum*. *Mol. Plant Microbe Interact.* 29, 417–430. doi: 10.1094/MPMI-09-15-0218-R

Tamura, K., Stecher, G., Peterson, D., Filipski, A., and Kumar, S. (2013). MEGA6: molecular evolutionary genetics analysis version 6.0. *Mol. Biol. Evol.* 30, 2725–2729. doi: 10.1093/molbev/mst197

Teperi, E., Keskinen, M., Ketoja, E., and Tahvonen, R. (1998). Screening for fungal antagonists of seed-borne *Fusarium culmorum* on wheat using *in vivo* tests. *Eur. J. Plant Pathol.* 104, 243–251. doi: 10.1023/A:1008647607310

Treseder, K. K., and Lennon, J. T. (2015). Fungal traits that drive ecosystem dynamics on land. *Microbiol. Mol. Biol. Rev.* 79, 243–262. doi: 10.1128/MMBR.00001-15

Tzelepis, G., Dubey, M., Jensen, D. F., and Karlsson, M. (2015). Identifying glycoside hydrolase family 18 genes in the mycoparasitic fungal species *Clonostachys rosea*. *Microbiology* 161, 1407–1419. doi: 10.1099/mic.0.000096

Upchurch, R. G. (2008). Fatty acid unsaturation, mobilization, and regulation in the response of plants to stress. *Biotechnol. Lett.* 30, 967–977. doi: 10.1007/s10529-008-9639-z

van Dooremalen, C., Suring, W., and Ellers, J. (2011). Fatty acid composition and extreme temperature tolerance following exposure to fluctuating temperatures in a soil arthropod. *J. Insect Physiol.* 57, 1267–1273. doi: 10.1016/j.jinsphys.2011.05.017

Wang, K., Li, M., and Hakonarson, H. (2010). ANNOVAR: functional annotation of genetic variants from high-throughput sequencing data. *Nucleic Acids Res.* 38, e164–e164. doi: 10.1093/nar/gkq603

Wang, M., Zheng, Q., Shen, Q., and Guo, S. (2013). The critical role of potassium in plant stress response. *Int. J. Mol. Sci.* 14, 7370–7390. doi: 10.3390/ijms14047370

Wang, X. C., Zhao, Q. Y., Ma, C. L., Zhang, Z. H., Cao, H. L., Kong, Y. M., et al. (2013). Global transcriptome profiles of *Camellia sinensis* during cold acclimation. *BMC Genomics* 14:415. doi: 10.1186/1471-2164-14-415

Wei, H., Dhanaraj, A. L., Arora, R., Rowland, L. J., Fu, Y., and Sun, L. (2006). Identification of cold acclimation-responsive rhododendron genes for lipid metabolism, membrane transport and lignin biosynthesis: importance of moderately abundant ESTs in genomic studies. *Plant Cell Environ.* 29, 558–570. doi: 10.1111/j.1365-3040.2005.01432.x

Xie, B. B., Qin, Q. L., Shi, M., Chen, L. L., Shu, Y. L., Luo, Y., et al. (2014). Comparative genomics provide insights into evolution of trichoderma nutrition style. *Genome Biol. Evol.* 6, 379–390. doi: 10.1093/gbe/evu018

Xue, A. G., Voldeng, H. D., Savard, M. E., Fedak, G., Tian, X., and Hsiang, T. (2009). Biological control of fusarium head blight of wheat with *Clonostachys rosea* strain ACM941. *Can. J. Plant Pathol.* 31, 169–179. doi: 10.1080/07060660909507590

Yarden, O., and Yanofsky, C. (1991). Chitin synthase 1 plays a major role in cell wall biogenesis in *Neurospora crassa*. *Genes Dev.* 5, 2420–2430.

Zhang, G., Storey, J. M., and Storey, K. B. (2018). Elevated chaperone proteins are a feature of winter freeze avoidance by larvae of the goldenrod gall moth, *Epiblema scudderiana*. *J. Insect Physiol.* 106, 106–113. doi: 10.1016/j.jinsphys.2017.04.007

Zhu, W., Zhan, J., and McDonald, B. A. (2018). Evidence for local adaptation and pleiotropic effects associated with melanization in a plant pathogenic fungus. *Fungal Genet. Biol.* 115, 33–40. doi: 10.1016/j.fgb.2018.04.002

Conflict of Interest Statement: The authors declare that the research was conducted in the absence of any commercial or financial relationships that could be construed as a potential conflict of interest.

frontiers in Microbiology

ORIGINAL RESEARCH
published: 04 December 2018
doi: 10.3389/fmicb.2018.02977

Xylem Sap Proteomics Reveals Distinct Differences Between *R* Gene- and Endophyte-Mediated Resistance Against Fusarium Wilt Disease in Tomato

*Francisco J. de Lamo[1], Maria E. Constantin[1], David H. Fresno[1], Sjef Boeren[2], Martijn Rep[1] and Frank L. W. Takken[1]**

[1] Molecular Plant Pathology, Faculty of Science, Swammerdam Institute for Life Sciences, University of Amsterdam, Amsterdam, Netherlands, [2] Laboratory of Biochemistry, Wageningen University, Wageningen, Netherlands

OPEN ACCESS

Edited by:
Alfredo Herrera-Estrella, Centro de Investigación y de Estudios Avanzados del Instituto Politécnico Nacional, Mexico

Reviewed by:
José Díaz, University of A Coruña, Spain
Maria Raffaella Ercolano, Università degli Studi di Napoli Federico II, Italy

***Correspondence:**
Frank L. W. Takken
F.L.W.Takken@uva.nl

Specialty section:
This article was submitted to Plant Microbe Interactions, a section of the journal Frontiers in Microbiology

Received: *12 September 2018*
Accepted: *19 November 2018*
Published: *04 December 2018*

Citation:
de Lamo FJ, Constantin ME, Fresno DH, Boeren S, Rep M and Takken FLW (2018) Xylem Sap Proteomics Reveals Distinct Differences Between R Gene- and Endophyte-Mediated Resistance Against Fusarium Wilt Disease in Tomato. Front. Microbiol. 9:2977. doi: 10.3389/fmicb.2018.02977

Resistance (*R*) genes and endophytic organisms can both protect plants against pathogens. Although the outcome of both processes is the same, little is known about the commonalities and differences between both immune responses. Here we set out to phenotypically characterize both responses in the tomato-Fusarium pathosystem, and to identify markers to distinguish these responses at the molecular level. As endophyte *Fusarium oxysporum* (Fo) strain Fo47 was employed, which confers protection against various pathogens, including the vascular wilt fungus *F. oxysporum* f.sp. *lycopersici* (Fol). As *R*-gene conferring Fol resistance, the *I-2* gene of tomato (*Solanum lycopersicum*) was used. Fol colonizes the xylem vessels of susceptible and *I-2* resistant tomato plants, but only causes disease in the former. Fol was found to colonize the vasculature of endophyte-colonized plants, and could be isolated from stems of non-diseased plants co-inoculated with Fo47 and Fol. Because the xylem vessels form the main interface between plant and pathogen, the xylem sap proteomes during *R* gene- and Endophyte-Mediated Resistance (RMR and EMR) were compared using label-free quantitative nLC-MS/MS. Surprisingly, both proteomes were remarkably similar to the mock, revealing only one or two differentially accumulated proteins in the respective resistant interactions. Whereas in *I-2* plants the accumulation of the pathogenesis-related protein PR-5x was strongly induced by Fol, the endophyte triggered induction of both NP24, another PR-5 isoform, and of a β-glucanase in the presence of Fol. Notably, over 54% of the identified xylem sap proteins have a predicted intracellular localization, which implies that these might be present in exosomes. In conclusion, whereas both resistance mechanisms permit the pathogen to colonize the vasculature, this does not result in disease and this resistance coincides with specific induction of two distinct PR-5 isoforms and a β-glucanase.

Keywords: endophyte, biocontrol, Fusarium wilt disease, proteomics, NP24, PR-5x, exosomes

INTRODUCTION

Fungal plant pathogens form a major threat to food and feed production worldwide (Fisher et al., 2012). Among those, the soil-borne fungal vascular pathogen *Fusarium oxysporum* (Fo) is one of the most devastating (Dean et al., 2012). Fo encompasses more than 100 host-specific strains, so-called *formae speciales* (ff.spp.) that are typically non-pathogenic to other plant species (Gordon, 2017). Fo *forma specialis* (f.sp.) *lycopersici* (Fol) infects tomato and represents one of the best-studied Fo pathogens (Michielse and Rep, 2009). Fol does not make obvious penetration structures (e.g., appressoria), but enters the plant through natural wounds and cracks in the roots surface (Steinkellner et al., 2005). Subsequently, the fungus colonizes the apoplastic spaces of the root cortex after which it enters the stele, colonizes the xylem vasculature, and invades above-ground tissues (Olivain and Alabouvette, 1999). During infection Fol secretes a plethora of effectors to promote colonization (Houterman et al., 2007; Takken and Rep, 2010). Many of these effectors have been isolated from the xylem sap and are named Six proteins, for Secreted in xylem. One of these Six proteins is Avr2 (= Six3), which is internalized into plant cells where it suppresses PAMP-triggered Immunity (PTI) (Di et al., 2016, 2017).

Monogenic resistance to Fol has evolved several times in tomato (Sela-Buurlage et al., 2001). A number of these *Immunity*, or *I* genes, have been cloned (Simons et al., 1998; Catanzariti et al., 2015, 2017; Gonzalez-Cendales et al., 2016) and some are bred into cultivated tomato after which their resistances have been overcome in the ongoing arms race between tomato and the fungus (Takken and Rep, 2010). The best studied *R* gene is *I-2* (van Ooijen et al., 2007), which encodes a nucleotide-binding and leucine-rich repeat (NB-LRR) protein (Simons et al., 1998) that recognizes Avr2 intracellularly to trigger *R*-gene-Mediated Resistance (RMR) (Houterman et al., 2009; Ma et al., 2013). RMR confers resistance to Fol (Houterman et al., 2009), although it permits the pathogen to colonize the vasculature to a limited extent (Mes et al., 2000; van der Does et al., 2018).

In addition to genetic resistance, endophytic microorganisms can confer protection to Fol (Fravel et al., 2003). Within the Fo species complex the vast majority of strains are harmless commensals that can colonize living plant tissues without causing disease. Fo47 represents the best-studied endophytic Fo strain. It colonizes tomato root surfaces and intercellular junctions of the root epidermis (Bolwerk et al., 2005; Olivain et al., 2006), but not the xylem vessels (Alabouvette et al., 2009). Following colonization Fo47 reduces susceptibility of the host to vascular pathogens such as Fol or *Verticillium dahliae* (Veloso and Diaz, 2012; Aime et al., 2013) thereby conferring Endophyte-Mediated Resistance (EMR).

In a compatible interaction the main interface between tomato and Fol is the xylem vessels. In agreement with this, the xylem sap proteome of susceptible plants is dramatically altered following Fol infection, and the abundance of 92% of the proteins is affected (Gawehns et al., 2015). Specifically, the abundance of stress response-related proteins is strongly increased, including Pathogenesis-Related (PR) proteins such as PR-1, PR-2 (β-glucanase), PR-3 (chitinase) and PR-5 (antimicrobial activity), and several peroxidases (Rep et al., 2002; Houterman et al., 2007; Gawehns et al., 2015). Interestingly, ≈25% of the identified xylem sap proteins does not contain a signal peptide, suggesting the non-classical secretion of the protein into the sap. Similar to tomato, a significant change in the xylem sap proteome has been observed in *Brassicca oleracea* inoculated with Fo f.sp. *conglutinans* (Foc) (Pu et al., 2016). Together, these findings show that pathogenic Fo strains affect the xylem sap proteome during infection, which might contribute to their ability to colonize the host and to cause disease.

Notwithstanding that RMR and EMR are well-studied resistance mechanisms to Fol, little is known about molecular commonalities and differences between these phenotypically indistinguishable mechanisms. Whereas it has been reported that RMR permits the pathogenic fungus to colonize the host to a limited extent (Mes et al., 2000; van der Does et al., 2018), it is currently unknown whether EMR similarly constrains the pathogen. Furthermore, it is unknown whether the composition of the xylem sap proteome is altered upon root colonization by the endophyte and/or during RMR or EMR. To obtain a better mechanistic insight in RMR and EMR – and the potential difference between these at the molecular level – the xylem sap proteomes of bi- and tri-partite interactions were determined using label-free quantitative nLC-MS/MS. The proteomes were subsequently compared with each other, and with those of mock- or Fo47-inoculated plants. In addition, the extent of host colonization by the pathogen during EMR and RMR was determined. It was found that, although the pathogen did colonize the xylem vessels, the xylem sap proteome from the disease-free EMR and RMR plants was very similar to that of non-inoculated controls. Interestingly, specific PR-5 isoforms were found to differentially accumulate during either endophyte or genetic resistance, providing excellent markers to distinguish both resistance types at the molecular level.

MATERIALS AND METHODS

Plant and Fungal Materials and Cultivation Conditions

For fungal re-isolation assays tomato cv. KG52201 and cv. KG324 (Simons et al., 1998), respectively susceptible and resistant to Fol race 2 were used (Houterman et al., 2008). KG324 is a transgenic *I-2*-containing derivative of KG52201 (Simons et al., 1998). For plant inoculation *F. oxysporum* Fo47 (endophyte) and a Fol007 (pathogen, Fol race 2) strain carrying the *BLE* gene conferring resistance to zeocin (InvivoGen) were used (van der Does et al., 2008). For xylem sap collection the same Fol007-susceptible tomato cultivar C32 was used as before (Schmidt et al., 2013; Gawehns et al., 2015), while cv. KG324 was used as resistant cultivar. Plant inoculations where done using Fo47 (Alabouvette et al., 1987) and wild-type Fol007 (Mes et al., 1999). Plants were grown in a climate-controlled greenhouse at 24.5°C, 65% relative humidity and a 16 h photoperiod.

Fungal Stem Reisolation Assays

Fo47 and zeocin-resistant Fol007 (FP1930) were cultured in minimal medium (0.17% Yeast Nitrogen Base without amino acids or ammonium sulfate, 3% sucrose and 100 mM KNO3) at 25°C and 150 rpm during 5 days in the dark. Cultures were filtered through Miracloth (Millipore) and diluted to yield a microconidial inoculum of 107 spores/ml (Di et al., 2016). Co-inoculum of both strains was prepared in a 1:1 ratio (10^7 spores/ml each). For the bioassays, 10-days-old tomato seedlings were uprooted and soil was carefully removed. Roots were trimmed, leaving approximately 1 cm of roots, to facilitate fungal infection. Roots were placed for 5 min in an inoculum of Fo47, Fol007, a Fo47:Fol007 mixture, or in water without spores serving as mock control. Directly after inoculation, tomato plants were repotted and gently watered to avoid spore washing. Three weeks-post-inoculation (wpi) Fresh Weight (FW) and Disease Index (DI) were scored as described before (Gawehns et al., 2014), but adding DI = 5 when plants were dead. A statistical test (Mann–Whitney *U*) was applied on the FW and DI data using PRISM 7.0 (GraphPad). In addition, stems were harvested and surface-sterilized (Di et al., 2016). Under sterile conditions stem pieces were sectioned (0.5 cm thick approximately) at the crown- and cotyledon-level and placed on Potato Dextrose Agar (PDA) plates supplemented with 100 mg/l zeocin to specifically allow growth of Fol007. The plates contained 200 mg/l streptomycine and 100 mg/l penicillin to prevent bacterial growth. Plates were incubated in the dark at 25°C for 4 days allowing the fungus to grow out of the stem sections.

Xylem Sap Collection

Inoculum of Fo47 and wild-type Fol007 (0.5×10^7 spores/ml) and co-inoculum of both strains (0.5×10^7 spores/ml each) was used to inoculate 4-weeks-old plants as described before (Schmidt et al., 2013; Gawehns et al., 2015). At two wpi, once wilt disease symptoms appeared, FW and DI were scored and xylem sap was collected from mock-treated, Fo47-, Fol007- and Fo47:Fol007-inoculated C32 plants (Bioassay 1) and mock-treated and Fol007-inoculated KG324 plants (Bioassay 2). Plants were abundantly watered 1 day and 1 h before sap collection. Tomato stems were cut below the second true leaf, and plants were placed horizontally and connected to a 12 ml- polystyrene tube placed on ice. Plants were bleeding for 6 h and the collected sap was stored at −20°C until further use (Rep et al., 2002; Krasikov et al., 2011). Bioassays were performed four times during four subsequent weeks (i.e., every single repetition equals one biological replicate per treatment). Xylem sap from 24 plants was pooled. Bioassay 1 was carried out from January to March 2017 and Bioassay 2 from October to December 2017.

Sample Preparation for nLC-MS/MS

Potential fungal spores were removed from the sap by centrifugation at 800 × *g* for 10 min. Xylem sap proteins were concentrated by passing 12 ml of cleared sap through Amicon Ultra-15 Filter Units (Millipore). After centrifugation at 2500 × *g* for 15–30 min retentates containing the proteins were recovered. A BCA (bicinchoninic acid) assay (ThermoFischer) was performed to determine the protein concentration. Based on BCA quantification, a volume containing 60 µg of protein was trichloroacetic acid/aceton-precipitated and the pellet was resuspended in SDS loading buffer (2% SDS, 10% glycerol, 60 mM TRIS-HCl pH 6.8, 5% β-mercaptoethanol, 0.01% bromophenol blue), heated at 98°C for 5 min and loaded on a 12% SDS-polyacrylamide gel. Following a short electrophoresis, the proteins were stained overnight at 4°C with Commassie PageBlue (ThermoFischer). The bands containing the proteins were excised and cysteine reduction and alkylation of the proteins was performed by adding 10 mM DTT pH 8 (incubation at 60°C for 1 h) and 20 mM iodoacetamide pH 8 (incubation at room temperature in the dark for 30 min). Protein-containing gel slices were chopped into pieces of approximately 1 mm^2 and transferred to 1.5 ml low-binding tubes (Protein LoBind microcentrifuge tubes, Eppendorf). Tryptic in-gel digestion was performed overnight by adding 50 µl of 5 ng/µl Trypsin Sequencing Grade (Sigma-Aldrich). In-house prepared µcolumns were set up by adding C18 Empore disk and LichroprepC18 column material into a 200 µl pipette tip and the tryptic peptides were eluted from the µcolumn with 50 µl of 50% acetonitrile. Acetonitrile content was reduced to <5% by reducing the volume with a concentrator at 45°C during 2 h and readjusting the volume with 1 mL/L HCOOH in water to 50 µl.

nLC-MS/MS and Label-Free Quantification of the Proteome

Peptides were analyzed by nLC-MS/MS as previously described (Gawehns et al., 2015). Raw data from nLC-MS/MS measurements were analyzed using MaxQuant software (Cox and Mann, 2008; Hubner et al., 2010) to identify and label-free quantify the proteins. For identification of the proteins, UniProt proteome databases of tomato (UP000004994), Fo47 (UP000030766), Fol007 (UP000009097) and an in-house made contaminants database (Peng et al., 2012) were included in the Andromeda search engine (Cox et al., 2014). As before both fungal databases were improved by adding non-annotated sequences of effector proteins and predicted putative effectors (Schmidt et al., 2013). The mass spectrometry proteomics data have been deposited to the ProteomeXchange Consortium via the PRIDE (Vizcaino et al., 2016) partner repository with the dataset identifier PXD011072.

Data filtering from the MaxQuant output was carried out with Perseus 1.5.8.5. Proteins not detected by at least two peptides – of which at least one was unique and at least one was unmodified – were filtered out. Log10 transformation was applied to LFQ (Label-Free Quantification) intensities. Subsequent bioinformatics analysis was performed with R version 3.3.2.

Gene Ontology (GO) Analysis

To sequence-annotate the identified xylem sap proteins the online webtool Mercator[1] was used. Mercator performs (i) Blast searches against Arabidopsis TAIR 10, swiss-prot and Uniref90 databases, (ii) RPS-Blast searches against cdd and KOG and (iii) an InterPro scan. As described (Gawehns et al., 2015), specific

[1] http://mapman.gabipd.org

MapMan bin-codes were assigned to each protein by Mercator and proteins were manually sorted into 10 ontology categories.

Secretion Analysis

To determine whether the detected xylem sap proteins were secreted extracellularly, SecretomeP 2.0 and ApoplastP 1.0 web tools were used. SecretomeP (Bendtsen et al., 2004) predicts both classical protein secretion via the endoplasmic reticulum-Golgi pathway (Kehr et al., 2005) and non-classical protein secretion. SecretomeP was trained with mammalian sequences and its accuracy for plant proteomes has been questioned (Lonsdale et al., 2016), therefore ApoplastP was used as well. ApoplastP is a machine learning method that predicts apoplastic localization of proteins. ApoplastP was trained with apoplastic plant and fungal proteins (Sperschneider et al., 2018).

RESULTS

Both Endophyte- and *R*-Gene-Mediated Resistance Reduce Susceptibility to Fol in Tomato Seedlings

Both the fungal endophyte Fo47 (Fuchs et al., 1997) and the *I-2* resistance gene (Simons et al., 1998) have been reported to reduce susceptibility to Fusarium wilt disease in tomato. To test whether Endophyte- or *R*-gene-Mediated Resistance (EMR or RMR) also reduce susceptibility to Fol007 under our conditions, Fol007-susceptible KG52201 tomato and *I-2*-carrying resistant KG324 tomato cultivars were root dip-inoculated with either water (mock), Fol007 or a Fo47:Fol007 spore mixture (**Figure 1A**). Co-inoculation of KG52201 with Fo47 and Fol007 led to reduced susceptibility to Fusarium wilt disease, resulting in

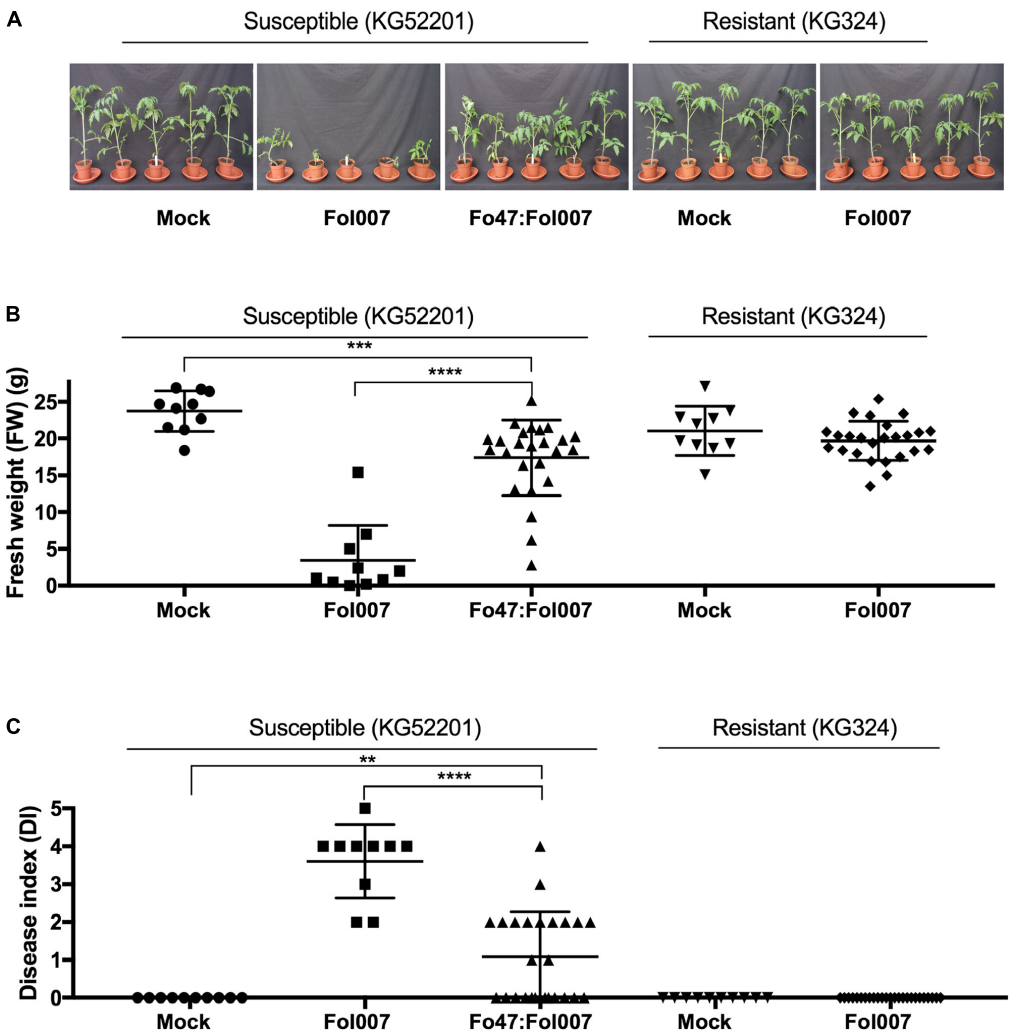

FIGURE 1 | EMR and RMR reduce susceptibility to Fusarium wilt (Fol007). **(A)** Ten-days-old seedlings of Fol007-susceptible KG52201 and Fol007-resistant KG324 were root dip-inoculated with water (mock), Fol007 or a mixture of Fo47:Fol007 (25 replicates for Fo47:Fol007 co-inoculated KG52201 and Fol007-inoculated KG324 seedlings, 10 replicates for the control treatments). Three-weeks-post-inoculation **(B)** FW and **(C)** DI were scored (See Materials and Methods). The experiment was repeated three times yielding similar results (**Supplementary Figures S1**, **S2**). Error bars represent mean ±SD (**$P_{val} < 0.01$, ***$P_{val} < 0.001$, ****$P_{val} < 0.0001$). An unpaired comparison for FW and DI was performed using the non-parametric Mann–Whitney *U* test.

a significantly higher Fresh Weight (FW) than Fol007-inoculated KG52201 plants. In one repetition the FW was indistinguishable to that of the mock (**Supplementary Figure S1**) while in two of the three experiments, co-inoculated plants show a slightly reduced weight as compared to the mock control (**Figure 1B** and **Supplementary Figure S2**). The Disease Index (DI) (i.e., vessel browning, yellowing and wilting) was significantly reduced in co-inoculated plants as compared to Fol007-inoculated plants, but increased when compared to the mock (**Figure 1C**). These findings are in line with the previously reported biocontrol properties of the Fo47 strain (Fuchs et al., 1997). Inoculation of resistant *I-2*-containing KG324 plants with Fol007 revealed a strong resistance, as FW was not affected when compared to the control, and inoculated plants were disease-symptom free (DI = 0) (**Figures 1B,C**). Inoculation with Fo47 alone did not result in disease symptom development or a significant change in the weight of the plants (data not shown). In summary, these data show that both EMR and RMR are effective in dampening Fol007 pathogenicity resulting in a reduction, or even absence, of disease symptoms in Fol007-inoculated plants.

Both EMR and RMR Fail in Constraining Fol Into the Root System

To determine to what extent Fol007 is halted by EMR or RMR, stem sections from the above-mentioned three bioassays (**Figure 1A**) were collected. After surface sterilization, stem slices corresponding to the crown- and cotyledon-level were placed on PDA plates supplemented with zeocin to select for Fol007 growth, and streptomycin and penicillin to prevent bacterial growth (**Figure 2A**).

Stem pieces isolated from control treatments, mock-inoculated KG52201 and KG324 plants did not show any fungal outgrowth. However, fungal outgrowth was observed in all stem slices of Fol007-inoculated KG52201 plants, confirming the suitability of the technique for Fol007 re-isolation (**Figure 2A**). When co-inoculating susceptible KG52201 with Fo47 and Fol007 on average 17% of the plants showed Fol007 colonization only at the crown-level, whereas in 69% the fungus reached both the crown- and cotyledon-level. In 13% of the co-inoculated plants no colonization of any stem piece was observed (**Figure 2B**). In contrast, in Fol007-inoculated KG324 plants the fungus was halted at the crown-level in 53% of the replicates and only in 15% reached also the cotyledon-level, while in 32% no colonization was found. We conclude that RMR (i.e., genetic resistance) is more effective than EMR in restricting fungal growth.

EMR and RMR Reduce Susceptibility to Fol in 4-Weeks-Old Tomato Plants

Next, we tested whether EMR and RMR also reduce susceptibility to Fol007 infection of 4-weeks-old plants that can be used for xylem sap isolation. Four-weeks-old Fol007-susceptible C32 plants were root dip-inoculated with water (mock), Fo47, Fol007 or a mixture of Fo47:Fol007 (**Figure 3A**). This bioassay was repeated four times. Two weeks-post-inoculation (wpi), FW of Fo47:Fol007 co-inoculated C32 plants was higher than that of Fol007-inoculated C32 plants and indistinguishable from the

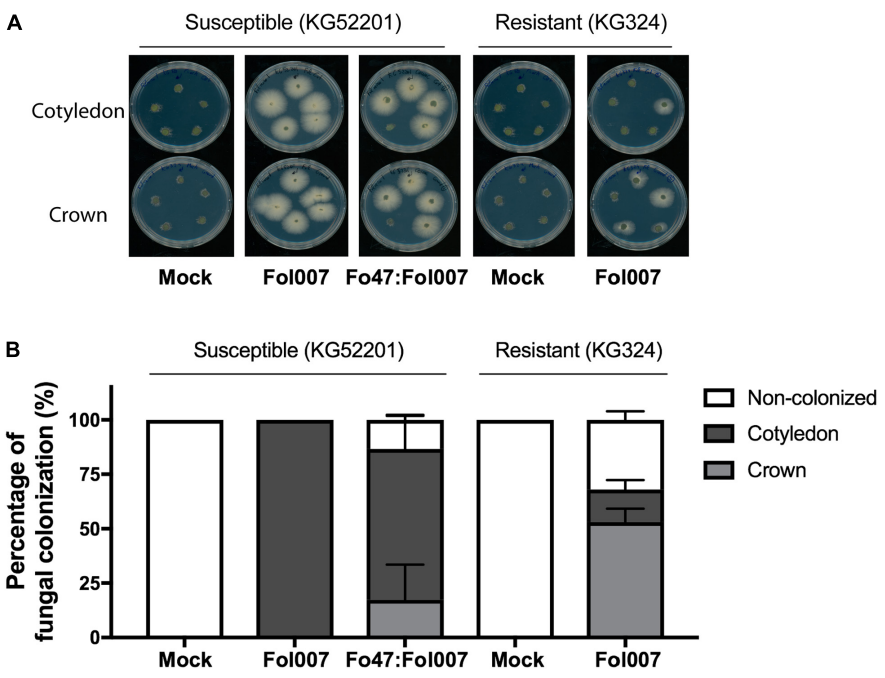

FIGURE 2 | Fol007 colonizes tomato stems despite EMR or RMR. **(A)** To monitor stem colonization by Fol007 3-weeks-post-inoculation, stem sections at the crown and cotyledon-level were placed on PDA plates (25 replicates for Fo47:Fol007 co-inoculated KG52201 and Fol007-inoculated KG324 seedlings, 10 replicates for the control treatments). Plates were scanned after 4 days of incubation. **(B)** Fungal outgrowth of the stem sections plotted as a percentage of infected sections. The graph represents the combined data of three independent bioassays, error bars indicate SD.

mock in two of the four bioassays (**Figure 3B**). In the other two assays, no significant differences in FW were found. Regarding the DI, Fo47:Fol007 co-inoculated C32 plants showed a strongly reduced DI as compared to Fol007-inoculated plants, but an increased DI when compared to the mock (**Figure 1C**). This pattern was consistent in all four repetitions. Hence, EMR is effective in 4-weeks-old tomato plants and results in a strong reduction of the DI as compared to the susceptible control and in no discernible difference in weight in two of the four assays as compared to the mock.

Concerning resistant KG324 plants, 4-weeks-old plants were root dip-inoculated with water (mock) or Fol007 (**Figure 3D**). Scoring the plants two wpi revealed that FW and DI where not significantly altered following Fol007-inoculation as compared to the mock (**Figures 3E,F**). This pattern was consistently observed in four repetitions showing the strong protection conferred by RMR to Fol007. In brief, both EMR and RMR are effective in reducing Fusarium wilt disease in 4-weeks-old plants.

Fo47 Does Not Affect the Tomato Xylem Sap Proteome in Bi-partite Interactions

Infection of susceptible tomato with pathogenic Fol007 strongly affects the tomato xylem sap proteome (Gawehns et al., 2015). To investigate whether Fo47 inoculation also affects the proteome, and whether putative changes correlate with biocontrol abilities of the fungus, nLC-MS/MS analysis was performed on xylem sap collected from Fo47-inoculated tomato plants. The relative abundance of the identified protein was then compared to that of mock-inoculated plants.

As reported before, Fol007 infection causes a major shift in the relative abundance of many xylem sap proteins as compared to the mock (Gawehns et al., 2015). However, fewer

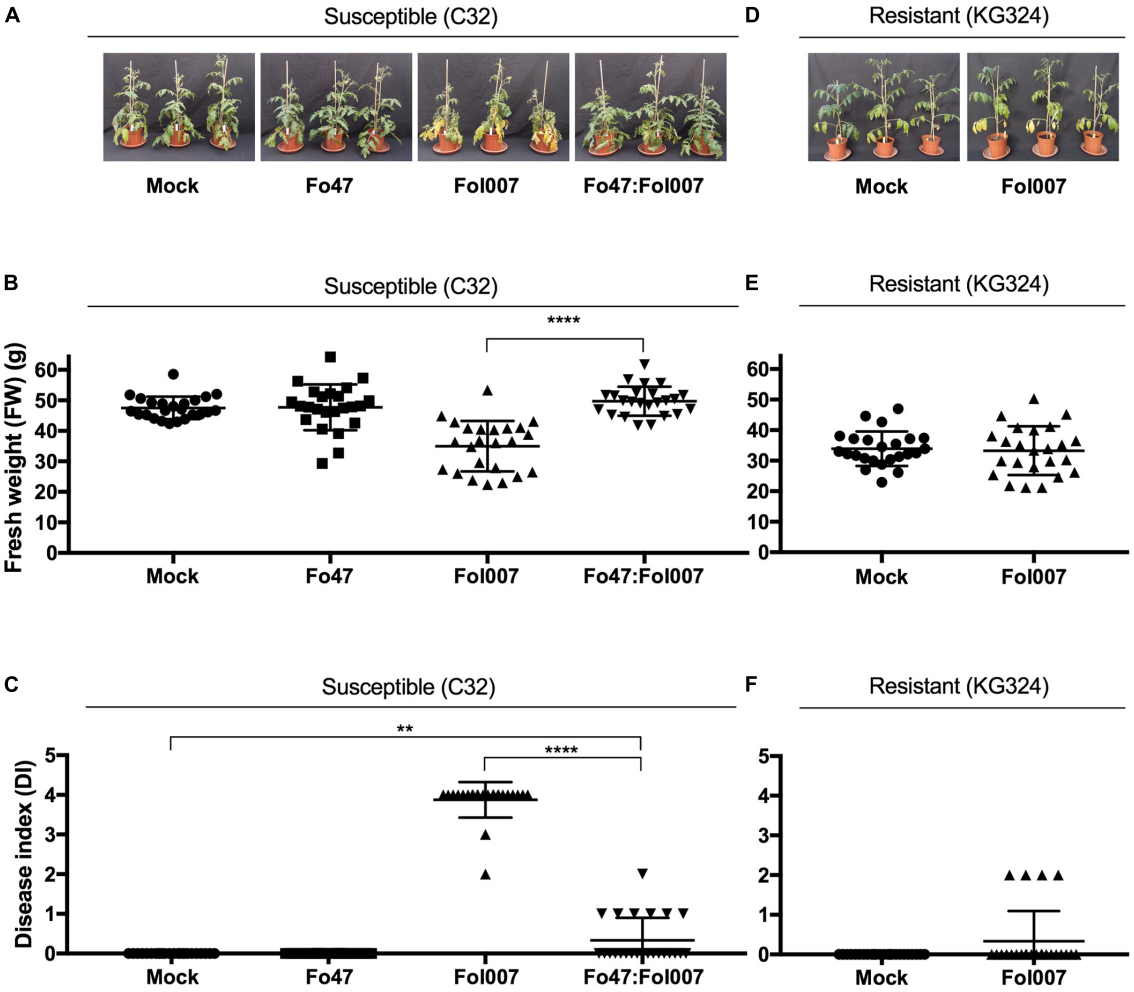

FIGURE 3 | Disease symptoms induced by Fol007 are reduced by EMR or RMR in 4-weeks-old plants. **(A)** 4-weeks-old Fol007-susceptible KG52201 plants were inoculated with water (mock), Fo47, Fol007 or a mixture of Fo47:Fol007 (24 plants/replicate). Two-week-post inoculation **(B)** FW and **(C)** DI were scored (See Materials and Methods). In an independent experiment **(D)** 4-weeks-old Fol007-resistant KG324 plants were inoculated with water (mock) or Fol007. Two-week-post inoculation **(E)** FW and **(F)** DI were scored. **(A–C)** Correspond to the Bioassay 1 and **(D–F)** to Bioassay 2. Error bars represent mean ±SD (**$P_{val} < 0.01$, ****$P_{val} < 0.0001$). An unpaired comparison for FW and DI was performed using the non-parametric Mann–Whitney *U* test.

Differentially Accumulated Proteins (DAPs) were found in the current study due to a more stringent cutoff as a S0 index was used, which besides the *P*-value also takes fold-change into account (**Figure 4A**). Out of the 388 proteins found in xylem sap of mock- and Fol007-infected tomato plants, 71 were DAPs (**Supplementary Table S1**). The protein with the highest fold-change was PR-10 (K4CWC5), which accumulated 246-fold. Six β-glucanases were identified showing distinct accumulation patterns: β-glucanases Q01412 and K4BBH7 accumulated 161-fold and 31-fold respectively, whereas quantities of the other four decreased (K4BZT8 158-fold, K4B3H0 66-fold, K4CF40 24-fold, and K4CMF9 10-fold). A similar pattern was observed for chitinases. Two basic chitinases (K4B667 and P32045) accumulated 131-fold and 84-fold while the quantity of an acidic chitinase (Q05540) decreased 59-fold. Notably, in the xylem sap of Fo47-inoculated plants no DAPs were identified among the 388 proteins, implying that colonization by the endophyte (**Supplementary Figure S4**) does not affect the xylem sap proteome. Furthermore, no Fo47-specific proteins were detected in the sap (**Figure 4B**).

EMR Significantly Affects the Abundance of a Single Tomato Xylem Sap Protein

Fo47 does not affect the xylem sap proteome of tomato in a bi-partite interaction (**Figure 4B**). However, it is not known whether Fo47 is able to do so when EMR is triggered by co-inoculation with Fol007 (**Figure 3**) and the pathogen colonizes the shoot (**Figure 2**). To examine this, xylem sap protein abundance of Fo47:Fol007-coinoculated C32 plants was compared to mock-inoculated plants (**Figure 4C**) and, surprisingly, only a single DAP was identified. This protein, a β-glucanase (K4BBH7), was detected by 11 unique peptides and its abundance was increased 45-fold as compared to the mock. Besides this protein also

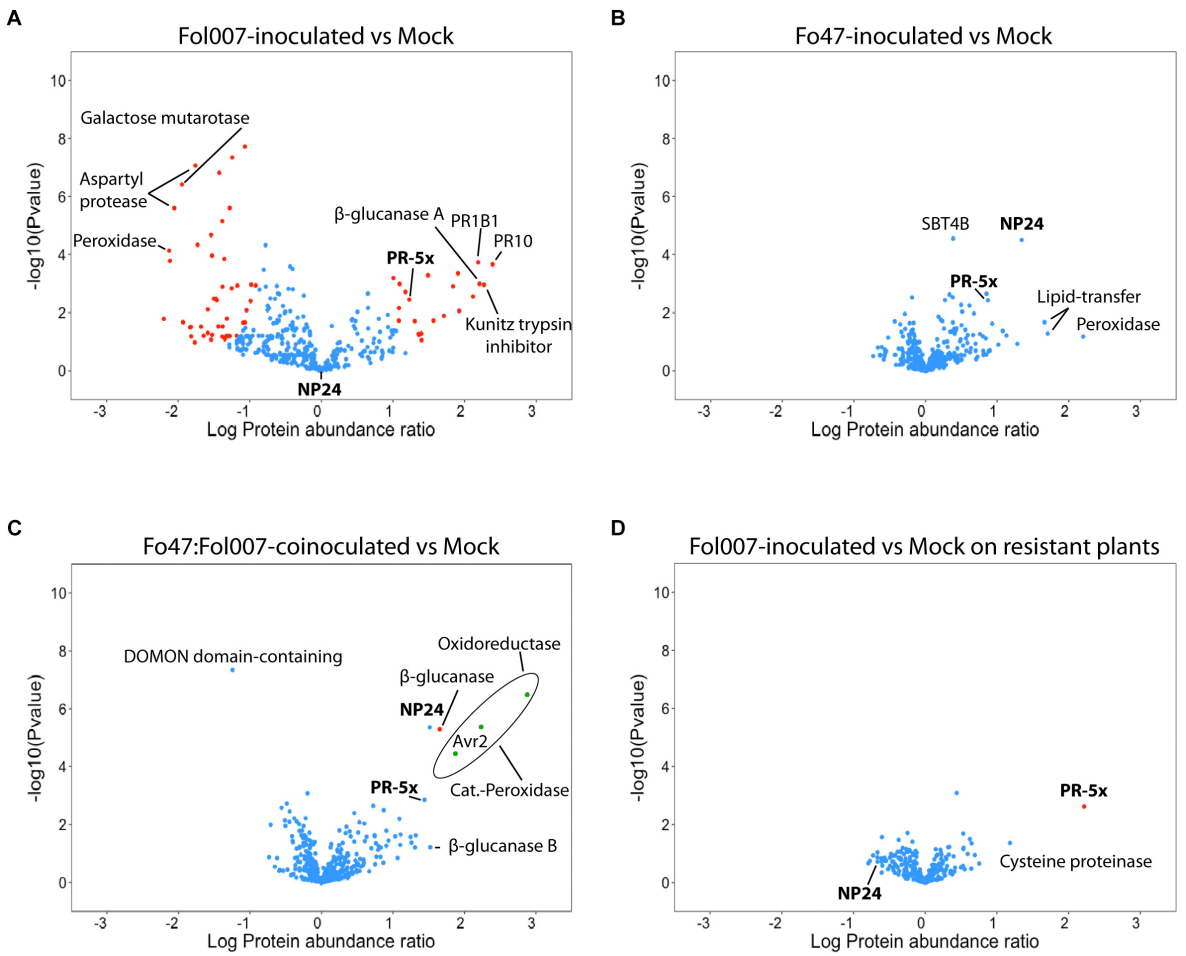

FIGURE 4 | Bi- and tri-partite interactions between tomato, Fo47 and Fol007 differentially affect the xylem sap proteome. Volcano plots showing the comparison between –log10 Pvalue (*y*-axis) and log10 Fold change (*x*-axis) of two different treatments (four biological replicates each). Blue dots represent proteins whose abundance did not change among the compared treatments, whereas red dots are DAPs. Green dots represent fungal DAPs. PR-5 isoforms are marked in bold font and the others correspond to the top up- or down-accumulated proteins (up to eight). **(A)** Xylem sap proteome of susceptible C32 plants inoculated with Fol007, **(B)** Fo47 and **(C)** Fo47:Fol007-coinoculated as compared to mock-inoculated C32. Also, **(D)** xylem sap proteome of resistant KG324 plants inoculated with Fol007 as compared to mock-inoculated KG324. PR1B1 on 4A panel refers to Pathogenesis-related leaf protein 6.

NP24 – a PR-5 isoform – highly accumulated (33-fold), but this protein was not identified as a DAP due to the stringent S0 settings applied. Hence, even though Fol007 dramatically affects the tomato xylem sap proteome in bi-partite interactions, the proteome remained almost unaltered when the pathogen is co-inoculated with Fo47.

When Fol007 was inoculated alone, 39 fungal proteins were found of which 36 were identified as DAPs according to their LFQ intensity values (**Supplementary Table S2**). Upon co-inoculation 13 fungal proteins were identified in the xylem sap of which three were DAPs (**Figure 4C**, green dots). These three proteins were, from lowest to highest abundance, the Fol007 effector Avr2 (A0A0C4DI32), a catalase-peroxidase (A0A0J9W9G5) and an oxidoreductase (A0A0C4DHX8). The LFQ values show a reduced accumulation of these Fol007 proteins upon co-inoculation with Fo47.

Notably, when Fo47 was inoculated alone or co-inoculated with Fol007 nine tomato xylem sap proteins were specifically induced and these were not detected following mock- or Fol007-inoculation (**Supplementary Figure S3A**). These proteins were present in relatively low quantities therefore they were not assigned as DAPs (**Supplementary Table S1**). These proteins represent a β-glucosidase 08 (B5M9E5), Aspartyl protease (K4AXP3), GDSL-like Lipase/Acylhydrolase (K4B1C4), Cysteine proteinase (K4B7P1), Unknown protein (K4BJU1), Zn-dependent exopeptidase (K4BJY1), Aspartyl protease (K4C3U1), aldehyde dehydrogenase (K4C8H3) and a Glycosyltransferase (K4D3D1).

Next, a comparison was made between the xylem sap proteomes of Fo47:Fol007-coinoculated plants versus Fo47-inoculated C32 to identify DAPs that are potentially linked to reduced susceptibility to Fol007 (**Supplementary Figure S3B**). Within this set of 393 proteins eight were identified as DAPs. These are two glucanases (K4BBH7, Q01412), two peroxidases (K4ASJ7, K4C1C1), a Aconitate hydratase (K4CFD4), a FASCICLIN-like arabinogalactan protein (K4C9N8) and a Lipid transfer protein (K4B273). Notably also a Leucine-rich repeat protein kinase (K4BK30) was found, which is typically a plasma membrane localized protein (**Supplementary Table S5**).

Taken together, inoculation with the endophyte alone or in combination with Fol007 pathogen, results in highly similar proteome profiles as those of the mock. Comparison of Fo47:Fol007 with the mock results in a single DAP while comparison to Fo47-inoculated plants reveals eight DAPs.

RMR Significantly Affects the Abundance of a Distinct PR-5 Isoform

To identify proteins indicative for RMR, the xylem sap proteomes of mock- and Fol007-inoculated *I-2*-containing tomato plants were compared. As observed for EMR, the proteome profiles of mock and Fol007-inoculated are highly similar showing only a single DAP. Accumulation of this DAP, PR-5x (Q8LPU1), was strongly induced (158-fold) following pathogen inoculation as compared to the mock (**Figure 4D**).

Identification of two PR-5 family members being strongly induced in either RMR (PR-5x) or EMR (NP24) is intriguing, as it implies an important role for this class of proteins in resistance to Fusarium wilt in tomato. Within the xylem sap proteomes 12 PR-5 proteins were identified: PR-5x (Q8LPU1), NP24 (P12670), five osmotin-like proteins (K4CP63, Q01591, K4CP65, K4CP64, K4CP59) and five thaumatin-like proteins (K4BV68, K4BVN4, K4BAP4, K4DFX0, K4BBQ9) (**Supplementary Table S4**).

In the xylem sap of a compatible interaction between susceptible C32 tomato and Fol007, a 17-fold increase in PR-5x accumulation was observed as compared to the mock (**Figure 4A**). Notably, in these plants accumulation of NP24 is not altered and the absolute quantity of this protein is lower than that of PR-5x. In contrast, when tomato is inoculated with Fo47 NP24 accumulated 22-fold as compared to the mock while PR-5x is only induced to a limited extent (7-fold change vs. mock) (**Figure 4B**). Upon co-inoculation of tomato with Fo47 and Fol007 both PR-5 isoforms are induced to a similar level: PR-5x accumulates 28-fold and NP-24 33-fold compared to the mock control (**Figure 4C**).

Altogether, these results show that PR-5x accumulation is specifically induced upon pathogen infection in both compatible and incompatible interactions of tomato with Fol007. But although induced in both cases, the induction of PR-5x in RMR is much higher than that in a diseased susceptible plant (158- vs. 17-fold). In Fo47 inoculated plants NP24 accumulation was induced 22-fold in the absence-, and 33-fold in the presence of Fol007. The remarkable difference between the relative accumulation between these two PR-5 isoforms in RMR and EMR indicate that they can be used as markers to distinguish both resistances types on the molecular level.

Many Xylem Sap Proteins Have a Predicted Intracellular Localization

It has been reported that ≈75% of the tomato xylem sap proteins carry a signal peptide for extracellular secretion (Gawehns et al., 2015). Of the remaining proteins, ≈10% was predicted to be non-classically secreted (Gawehns et al., 2015) whereas the other ≈15% has a proposed intracellular localization. Here we set out to investigate whether similar ratios of putative extracellular- and cytoplasmic-localized proteins are present in our current datasets (**Supplementary Tables S1**, **S3**). The percentage of predicted extracellular and intracellular proteins in the xylem sap proteins of non-inoculated and Fol007-inoculated susceptible plants was analyzed using two different algorithms: SecretomeP (Bendtsen et al., 2004) and ApoplastP (Sperschneider et al., 2018).

As reported SecretomeP predicted the majority of the proteins to be secreted to extracellular spaces (Gawehns et al., 2015). For both mock- and Fol007-inoculated plants 74% of all proteins identified are predicted as conventionally secreted proteins, 9% as leaderless secreted proteins and 17% as being non-secreted (**Figure 5**). ApoplastP predicted respectively 44 and 46% of the proteins from mock- and Fol007-inoculate to be secreted. Hence, the majority of the xylem sap proteins (>54%) is not identified by the program as a putative extracellular protein. The difference between both programs is remarkable, but nevertheless both predict a large subset of proteins to be localized intracellularly. In conclusion, both SecretomeP and ApoplastP predict an intracellular location for a large population of the xylem sap proteins.

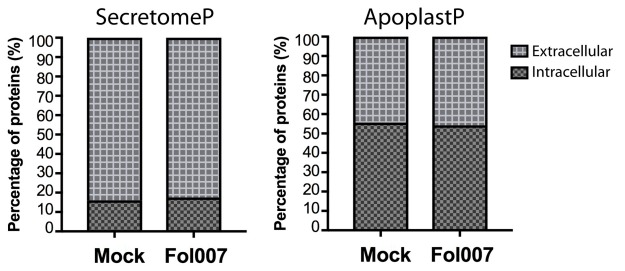

FIGURE 5 | The xylem sap proteome contains predicted intracellular proteins. Bar plots representing the percentage of intracellular or extracellular tomato xylem sap proteins found in mock- and Fol007-inoculated plants. Prediction was carried out by the webtools SecretomeP **(left)** and ApoplastP **(right)**.

DISCUSSION

Here, we show that Endophyte-Mediated Resistance (EMR) and *R*-gene-Mediated Resistance (RMR) have remarkably similar xylem sap proteome profiles. Upon Fol007 inoculation of *I-2*-containing resistant KG324 tomato plants (i.e., RMR) the accumulation of the vast majority of xylem sap proteins was similar to that of the mock. Strikingly, out of 303 tomato proteins identified, PR-5x was the only DAP and its abundance was increased by 158-fold. Contrarily, a different PR-5 isoform (NP24) specifically accumulated upon (co)inoculation of Fo47 on susceptible C32 tomato (i.e., EMR). Upon Fo47 and Fol007 co-inoculation also a β-glucanase, forming the only DAP in this dataset, was specifically induced. Within this tri-partite interaction between Fol007, Fo47 and C32 tomato, several Fol007 proteins were found in the xylem sap showing that EMR does not restrict the ability of Fol007 to colonize the xylem vessels. Furthermore, the major changes in the proteome profile that are observed in susceptible interactions, and are concomitant with disease symptoms, are not observed during EMR.

In compatible interactions with susceptible tomato plants Fol007 dramatically alters the xylem sap proteome (**Figure 4A**). Contrarily, Fo47 inoculation alone did not significantly affect the xylem sap proteome. As shown in **Supplementary Figure S4** the fungus could be re-isolated from stems of Fo47-inoculated tomato plants. However, not a single Fo47 protein was found in the xylem sap from either Fo47-inoculated or Fo47:Fol007-coinoculated tomato plants, which indicates that the endophyte does not colonize the vasculature or at least not in detectable amounts. This conclusion is in correspondence with previous reports describing Fo47 as a colonizer of root surfaces and of intercellular junctions of the root epidermis (Bolwerk et al., 2005; Olivain et al., 2006) and not being able to reach the xylem vessels (Alabouvette et al., 2009). Nine tomato proteins were exclusively detected in low quantities upon inoculation with Fo47 regardless of the presence of Fol007. The specific accumulation of these proteins might be linked to the colonization and concomitant biocontrol conferred by the endophyte (**Supplementary Figure S3A** and **Supplementary Table S1**). The genes encoding these proteins could be targeted in future study to assess their potential involvement in these processes.

When Fo47 is co-inoculated with Fol007 the latter retained its ability to colonize the xylem vessel (**Figure 2** and **Supplementary Table S2**). The identification of 13 Fol007 proteins in the sap upon co-inoculation with Fo47 confirms the presence of Fol007 in the xylem. The number and abundance of identified Fol007 proteins in EMR is, however, lower than that in susceptible plants. Together with a reduced DI, this suggests that Fol007 biomass is reduced by EMR. Since both fungi appear not to co-exist in the xylem vessels, this implies that EMR is mediated by the plant. This idea is supported by the finding that Fo47 induces resistance to Fol in a tomato split-root system (Fuchs et al., 1997). Moreover, it has been demonstrated that Fo47 can prime defense responses and reduce susceptibility to wilt disease when inoculated before Fol inoculation (Aime et al., 2013). Since it takes Fol007 at least 2 days to reach the vasculature (van der Does et al., 2018), it appears that defense priming induced by Fo47 suffices to limit the ability of the pathogen to extensively colonize the vessels and cause disease. The xylem sap proteins involved in this process are unknown, but the eight DAPs obtained in the proteome comparison between Fo47:Fol007-co-inoculated and Fo47-inoculated susceptible plants represent good candidates to be involved in this process (**Supplementary Table S5**). In future studies, the genes for these proteins could be targeted to assess their potential involvement in EMR.

When resistant *I-2*-containing tomato plants where inoculated with Fol007, not a single fungal protein was identified, although the fungus could be isolated from the infected stem pieces (**Figure 2**). A similar strong reduction in the ability of Fo to colonize the vessels of a resistant host was observed in *B. oleracea* cultivars challenged with Foc, and Foc fungal proteins were only detected in xylem sap of susceptible plants (Pu et al., 2016). These observations suggest that the amount of fungal biomass in the vessels is strongly reduced by RMR, which is in agreement with the complete absence of disease symptoms. The absence of symptoms and the presence of the fungus in the vessels led to the proposition that *R* genes switch the lifestyle of a pathogenic *Fusarium* into that of an endophyte (van der Does et al., 2018). Our data support this hypothesis, by showing that not only disease symptoms are absent, but also the proteome is essentially identical to that of non-inoculated- or endophyte-inoculated plants.

β-glucanases are among the most commonly detected proteins within the tomato xylem sap. In fact, 17 β-glucanases were detected in Bioassay 1 and 2, but only a single β-glucanase (K4BBH7) was identified as a DAP upon co-inoculation of Fo47 and Fol007 (**Supplementary Tables S1**, **S3**). These enzymes target β-glucans, which present the most abundant fungal cell wall polysaccharides. Together with chitin glucans form the main structural component of the cell walls. Enzymatic attack of this network by β-glucanases has a direct antimicrobial effect by perturbation of the fungal cell wall integrity (Stintzi et al., 1993). In addition, the subsequent release of β-1,6-glucans, which are specific to fungi and members of the Stramenopiles, can elicit PTI in many plant species (Fesel and Zuccaro, 2016). To avoid glucan degradation and subsequent PTI activation the fungal endophyte *Serendipita indica* (formerly *Piriformospora indica*)

secretes a fungal-specific lectin (FGB1). FGB1 binds β-glucan- and suppresses glucan triggered immunity, thereby facilitating fungal host colonization (Wawra et al., 2016). Whether Fo47 or Fol007 produce secreted lectins is currently unknown. Fungal lectins have not been identified in the xylem sap of infected plants in the current study nor in a former analysis, although LysM-containing proteins have been identified in this former study and these are proposed to sequester released chitin (Gawehns et al., 2015). Whether the identified β-glucanases play a role in biocontrol and/or restriction of disease symptom development during EMR remains to be tested.

Endophytic interactions of Fo47 with tomato resulted in a 22-fold induction of the PR-5 isoform NP24 (**Figure 4B**). This protein accumulated 33-fold higher in a tri-partite interaction with Fol007 (**Figure 4C**), but was not identified as a DAP due to stringent setting of the S0 index. However, when the same settings are applied as used previously (Gawehns et al., 2015) NP24 is identified as a significant DAP and the protein is no longer identified in the mock. In addition, the amount of NP24 might be underestimated in our setup. A limitation of using LFQ values is that identification of a protein relies on the presence of at least two tryptic peptides, of which at least one is unique. When proteins belong to a family sharing high sequence similarity, a non-unique peptide is assigned only to a single member of the family, resulting in the underestimation of the amounts of the other members. For instance, NP24 is detected by five peptides of which three are unique but two are non-unique and are assigned to PR-5x (**Supplementary Table S6**). When only the unique peptides are used for protein quantification, then its absolute amount is underestimated (i.e., LFQ values will be reduced) but the calculated fold change is more precise. When quantification of NP24 is done based on unique peptides only, then the accumulation in the Fo47-inoculated plants differs significantly from the mock as the protein is absent in the latter (**Supplementary Table S7**). NP24 has *in vitro* antimicrobial activity against *Phytophthora infestans* (Woloshuk et al., 1991) and is involved in resistance of ripe pepper fruits to *Colletotrichum gloeosporioides* (King et al., 1988; Oh et al., 2003). The correlation between NP24 protein abundance and reduced disease symptoms during EMR could indicate that the protein might also have antifungal activity *in planta*, thereby reducing the extent of Fol007 colonization of the vasculature.

PR-5x accumulation was specifically induced in the xylem sap of resistant (158-fold) and susceptible (17-fold) tomato plants upon Fol007 infection (**Figure 4A**). PR-5x was identified previously in tomato xylem sap following Fol infection of susceptible and resistant plants, hence its name PR-5xylem (Rep et al., 2002). The protein is distinct from the PR-5 isoforms present in apoplastic fluid of tomato leafs infected by *Cladosporium fulvum* and it is not present in the latter (Joosten and De Wit, 1989; Rep et al., 2002). Compared to other PR-5 isoforms, the gene encoding PR-5x shows a root-specific expression (Rep et al., 2002). A similar xylem sap-specific accumulation of PR-5 isoforms has been observed upon Foc infection of Foc-resistant and -susceptible cultivars of *B. oleracea* (Pu et al., 2016). Colonization of *Arabidopsis thaliana* roots by non-pathogenic fluorescent *Pseudomonas* spp. triggers induction of *AtTLP1,* a PR-5 family member, in the vascular bundle, which is related to a local response to colonization of this non-pathogenic bacterium (Leon-Kloosterziel et al., 2005). It has also been reported that accumulation of PR-5 isoforms in the xylem sap of tomato is strongly induced in plants inoculated with Fol strains in which key effectors, such as Avr2, Six1 and Six6 have been knocked out. These Fol mutants were still capable of causing disease, yet the amount of fungal biomass in the plant was strongly reduced concomitant with a reduction in disease symptoms. Specifically, NP24 accumulated > 200-fold in plants inoculated with a *SIX1* or *SIX6* knockout Fol strain in comparison to inoculation with wild type Fol. Similarly, a Thaumatin (K4DFX0) accumulated strongly when Avr2 was knocked out (Gawehns et al., 2015). Based on these observations it is tempting to speculate that antimicrobial activity of PR-5 isoforms might be the main determinant controlling the amount of *Fusarium* biomass in the xylem vessels. Antimicrobial activity of these small ± 24 kDa cysteine-rich proteins has been described before (Hoffmann-Sommergruber, 2000; Chowdhury et al., 2015). PR-5 proteins disrupt the lipid bi-layer of fungi, resulting in the formation of transmembrane pores that cause a strong permeability of the plasma membrane (Vigers et al., 1992). In addition to its antimicrobial activity, PR-5 proteins may themselves trigger plant defense responses. Transgenic Arabidopsis plants over-expressing *Prunus domestica PR5-1* show induction of the *phenylalanine ammonia-lyase (PAL)* gene and a concomitant increased flux through the phenylpropanoid biosynthesis pathway. Moreover, genes involved in the biosynthesis of camalexin (a phytoalexin), which is an endproduct of the phenylpropanoid pathway, are up-regulated in these transgenic plants. *PdPR5-1* Arabidopsis plants also showed an increased resistance to *Alternaria brassicicola* (El-Kereamy et al., 2011). It is imaginable that that PR-5x and NP24 have a function similar as *PdPR5-1* and confer both direct and indirect resistance to *F. oxysporum* in tomato. The identification of two distinct PR-5 family members, whose induced expression correlates with either RMR and EMR, shows that both resistance mechanisms independently induce the expression of a specific PR-5 isoform to control pathogen proliferation in the plant. The underlying mechanism remains to be elucidated, but the PR-5 isoforms identified provide excellent markers to distinguish both immune responses.

ApoplastP and SecretomeP predicted many of the proteins detected in the xylem sap to be localized intracellularly (**Figure 5** and **Supplementary Tables S1**, **S3**). It is intriguing that predicted cytosolic proteins appear in the xylem sap, which is an extracellular space. A possible explanation is that cellular damage caused by Fol007 releases proteins from xylem adjacent cells. However, these proteins were also present in the mock treatments making this explanation unlikely. In addition, only a relatively small number of intracellular proteins in processes like photosynthesis (2% of all identified proteins) or primary metabolism (2%), or TCA cycle (1%) were found, which is suggestive for a specific secretion mechanism rather than generic loss of cellular integrity. A recently proposed mechanism for this is that these putative 'intracellular' proteins are contained in exosomes. Since long it is known that plant

cells can secrete exosomes into extracellular spaces (Halperin and Jensen, 1967), but little was known about their role in plant-microbe interactions. Recently, exosomes were isolated from the apoplastic fluid of *A. thaliana* and these were found to be enriched in proteins related to stress and plant defense (Rutter and Innes, 2017). In fact, homologues proteins identified in that study were also present in our datasets. Among these are Leucine-rich repeat receptor-like protein kinase (K4D401), Early nodulin-like protein (K4CXN7), Lipase/Lipooxygenase and PLAT/LH2 family protein (K4BIL3). Together with our observation that three proteins involved in vesicle-mediated trafficking (K4B1S4, K4CPC9 and K4D8S6) were identified in the tomato xylem sap, this could imply that exosomes may play a role in the interaction between Fo and tomato.

In this study two different PR-5 isoforms were identified whose abundance correlate with a reduction in pathogen biomass. Furthermore, these PR-5 proteins serve as specific markers for either RMR (PR-5x) or EMR (NP24). Current studies, in which these genes are knocked out or overexpressed in tomato, could address the question whether their specific increase in abundance is causal to Fol007 resistance. It will be interesting to investigate accumulation of extracellular PR-5 members in other Fo-plant pathosystems, such as melon containing the *Fom2* resistance gene and *F. oxysporum f. sp. melonis*, to elucidate whether increased accumulation of PR-5 members is a conserved feature of resistance to Fusarium wilt disease. If so, this finding will yield exciting possibilities for novel strategies for resistance breeding in crop species where dominant resistance genes are unavailable, such as banana, or when use of endophytes is not applicable or feasible.

AUTHOR CONTRIBUTIONS

FT and FL designed the experiments. FL and MC performed the fungal stem re-isolation assays. FL, MC, and DF collected the xylem sap. FL prepared the samples for nLC-MS/MS measurements. SB performed the nLC-MS/MS measurements. FL and SB analyzed the data. MR gave intellectual input and critically revised the manuscript. FL and FT wrote the manuscript.

FUNDING

FT, MC, FL, and MR are partners is the same project. This project is part of the BestPass funded by the European Union's Horizon 2020 research and innovation program under the Marie Skłodowska-Curie grant agreement No 676480 (International Training Network BestPass). FT obtains support from the NWO-Earth and Life Sciences funded VICI project No. 865.14.003.

ACKNOWLEDGMENTS

We are grateful to Petra Houterman for sharing expertise on the xylem sap collection, Ben Cornelissen for critically reviewing the manuscript, Fleur Gawehns for facilitating identification of distinct PR-5 isoforms, and Ludek Tikovsky and Harold Lemereis for plant care.

SUPPLEMENTARY MATERIAL

The Supplementary Material for this article can be found online at: https://www.frontiersin.org/articles/10.3389/fmicb.2018.02977/full#supplementary-material

FIGURE S1 | EMR and RMR reduce susceptibility to Fusarium wilt (Fol007). **(A)** Ten-days-old seedlings of Fol007-susceptible KG52201 and Fol007-resistant KG324 were root dip-inoculated with water (mock), Fol007 or a mixture of Fo47:Fol007 (25 replicates for Fo47:Fol007 co-inoculated KG52201 and Fol007-inoculated KG324 seedlings, 10 replicates for the control treatments). Three-weeks-post-inoculation **(B)** FW and **(C)** DI were scored (See Materials and Methods). The experiment was repeated three times yielding similar results (**Figure 1** and **Supplementary Figure S2**). Error bars represent mean ±SD (**$P_{val} < 0.01$, ***$P_{val} < 0.001$, ****$P_{val} < 0.0001$). An unpaired comparison for FW and DI was performed using the non-parametric Mann–Whitney *U* test.

FIGURE S2 | EMR and RMR reduce susceptibility to Fusarium wilt (Fol007). **(A)** Ten-days-old seedlings of Fol007-susceptible KG52201 and Fol007-resistant KG324 were root dip-inoculated with water (mock), Fol007 or a mixture of Fo47:Fol007 (25 replicates for Fo47:Fol007 co-inoculated KG52201 and Fol007-inoculated KG324 seedlings, 10 replicates for the control treatments). Three-weeks-post-inoculation **(B)** FW and **(C)** DI were scored (See Materials and Methods). The experiment was repeated three times yielding similar results (**Figure 1** and **Supplementary Figure S1**). Error bars represent mean ±SD (**$P_{val} < 0.01$, ***$P_{val} < 0.001$, ****$P_{val} < 0.0001$). An unpaired comparison for FW and DI was performed using the non-parametric Mann–Whitney *U* test.

FIGURE S3 | Fo47 inoculation affects accumulation of specific proteins. **(A)** Proteins that were detected in at least three out of four replicates where labeled as present. Treatments embraced mock-inoculated, Fo47-inoculated, Fo47:Fol007-coinoculated and Fol007-inoculated C32 susceptible tomato plants. The black circle marks proteins that were specifically present in Fo47 inoculated plants. **(B)** Volcano plot showing xylem sap protein abundance difference between Fo47:Fol007-coinoculated compared to Fo47-inoculated on susceptible C32 plants. Names of the DAPs are depicted in **Supplementary Table S5**.

FIGURE S4 | Fo47 colonizes tomato stems **(A)** To monitor stem colonization by Fo47 3-weeks-post-inoculation, stem sections at the crown and cotyledon-level were placed on PDA plates (10 replicates). Plates were scanned after 4 days of incubation. **(B)** Fungal outgrowth of the stem sections plotted as a percentage of infected sections. The experiment was repeated three times showing the same pattern.

TABLE S1 | Tomato proteins identified and label-free quantified in Bioassay 1. Samples labeled as 'Mock' for the water control, and 'Endo,' 'Coinoc' and 'Patho' for Fo47-inoculated, Fo47:Fol007-coinoculated and Fol007-inoculated C32 susceptible tomato plants. DAPs are marked with +. LFQ values are represented in Log10 scale. Sequence coverage (%), molecular weight (KDa), GO description and SecretomeP and ApoplastP outputs are provided for all proteins.

TABLE S2 | Fol007 proteins identified and label-free quantified in Bioassay 1. LFQ values are in Log10 scale and 3,9 represent the LFQ cutoff.

TABLE S3 | Tomato proteins identified and label-free quantified in Bioassay 2. Samples labeled as 'Mock' for the water control, and 'Patho' for Fol007-inoculated KG324 resistant tomato plants. DAPs are marked with +. LFQ values are represented in Log10 scale. Sequence coverage (%), molecular weight (KDa), GO description and SecretomeP and ApoplastP outputs are provided for all the proteins.

TABLE S4 | List of PR-5 proteins found in xylem sap of both bioassays. Uniprot IDs, names of the proteins, average of LFQ intensities for every treatment of the two bioassays, predicted location, GO category, disulphide bonds and length of the proteins are depicted in the table. LFQ values are represented in Log10 scale.

TABLE S5 | List of xylem sap proteins whose relative abundance changes upon co-inoculation of tomato with Fo47:Fol007 comparing to Fo47-inoculated.

TABLE S6 | Overview of the peptides matching NP24 and PR-5x proteins.

TABLE S7 | Overview of the protein groups detected peptides overlapping with NP24 and PR-5x. Filled in green the LFQ intensities obtained by only using unique peptides for the protein quantification. LFQ intensities are represented in Log10 scale.

REFERENCES

Aime, S., Alabouvette, C., Steinberg, C., and Olivain, C. (2013). The endophytic strain *Fusarium oxysporum* Fo47: a good candidate for priming the defense responses in tomato roots. *Mol. Plant Microbe Interact.* 26, 918–926. doi: 10.1094/MPMI-12-12-0290-R

Alabouvette, C., De la Broise, D., Lemanceau, P., Couteaudier, Y., and Louvet, J. (1987). Utilisation de souches non pathogènes de Fusarium pour lutter contre les fusarioses: situation actuelle dans la pratique. *OEPP/EPPO Bull.* 17, 665–674.

Alabouvette, C., Olivain, C., Migheli, Q., and Steinberg, C. (2009). Microbiological control of soil-borne phytopathogenic fungi with special emphasis on wilt-inducing *Fusarium oxysporum*. *New Phytol.* 184, 529–544. doi: 10.1111/j.1469-8137.2009.03014.x

Bendtsen, J. D., Jensen, L. J., Blom, N., von Heijne, G., and Brunak, S. (2004). Feature-based prediction of non-classical and leaderless protein secretion. *Protein Eng. Des. Sel.* 17, 349–356. doi: 10.1093/protein/gzh037

Bolwerk, A., Lagopodi, A. L., Lugtenberg, B. J. J., and Bloemberg, G. V. (2005). Visualization of interactions between a pathogenic and a beneficial Fusarium strain during biocontrol of tomato foot and root rot. *Mol. Plant Microbe Interact.* 18, 710–721. doi: 10.1094/Mpmi-18-0710

Catanzariti, A. M., Do, H. T. T., Bru, P., de Sain, M., Thatcher, L. F., Rep, M., et al. (2017). The tomato I gene for fusarium wilt resistance encodes an atypical leucine-rich repeat receptor-like protein whose function is nevertheless dependent on SOBIR1 and SERK3/BAK1. *Plant J.* 89, 1195–1209. doi: 10.1111/tpj.13458

Catanzariti, A. M., Lim, G. T. T., and Jones, D. A. (2015). The tomato I-3 gene: a novel gene for resistance to fusarium wilt disease. *New Phytol.* 207, 106–118. doi: 10.1111/nph.13348

Chowdhury, S., Basu, A., and Kundu, S. (2015). Cloning, characterization, and bacterial over-expression of an osmotin-like protein gene from *Solanum nigrum* L. with antifungal activity against three necrotrophic fungi. *Mol. Biotechnol.* 57, 371–381. doi: 10.1007/s12033-014-9831-4

Cox, J., Hein, M. Y., Luber, C. A., Paron, I., Nagaraj, N., and Mann, M. (2014). Accurate proteome-wide label-free quantification by delayed normalization and maximal peptide ratio extraction, termed MaxLFQ. *Mol. Cell. Proteom.* 13, 2513–2526. doi: 10.1074/mcp.M113.031591

Cox, J., and Mann, M. (2008). Maxquant enables high peptide identification rates, individualized p.p.b.-range mass accuracies and proteome-wide protein quantification. *Nat. Biotechnol.* 26, 1367–1372. doi: 10.1038/nbt.1511

Dean, R., Van Kan, J. A. L., Pretorius, Z. A., Hammond-Kosack, K. E., Di Pietro, A., Spanu, P. D., et al. (2012). The top 10 fungal pathogens in molecular plant pathology. *Mol. Plant Pathol.* 13, 414–430. doi: 10.1111/j.1364-3703.2011.00783.x

Di, X., Gomila, J., Ma, L., van den Burg, H. A., and Takken, F. L. (2016). Uptake of the fusarium effector avr2 by tomato is not a cell autonomous event. *Front. Plant Sci.* 7:1915. doi: 10.3389/fpls.2016.01915

Di, X. T., Cao, L. X., Hughes, R. K., Tintor, N., Banfield, M. J., and Takken, F. L. W. (2017). Structure-function analysis of the *Fusarium oxysporum* Avr2 effector allows uncoupling of its immune-suppressing activity from recognition. *New Phytol.* 216, 897–914. doi: 10.1111/nph.14733

El-Kereamy, A., El-Sharkawy, I., Ramamoorthy, R., Taheri, A., Errampalli, D., Kumar, P., et al. (2011). Prunus domestica pathogenesis-related protein-5 activates the defense response pathway and enhances the resistance to fungal infection. *PLoS One* 6:e17973. doi: 10.1371/journal.pone.0017973

Fesel, P. H., and Zuccaro, A. (2016). Beta-glucan: crucial component of the fungal cell wall and elusive MAMP in plants. *Fungal Genet. Biol.* 90, 53–60. doi: 10.1016/j.fgb.2015.12.004

Fisher, M. C., Henk, D. A., Briggs, C. J., Brownstein, J. S., Madoff, L. C., McCraw, S. L., et al. (2012). Emerging fungal threats to animal, plant and ecosystem health. *Nature* 484, 186–194. doi: 10.1038/nature10947

Fravel, D., Olivain, C., and Alabouvette, C. (2003). *Fusarium oxysporum* and its biocontrol. *New Phytol.* 157, 493–502. doi: 10.1046/j.1469-8137.2003.00700.x

Fuchs, J. G., Moënne-Loccoz, Y., and Défago, G. (1997). Nonpathogenic *Fusarium oxysporum* strain Fo47 induces resistance to fusarium wilt in tomato. *Plant Dis.* 81, 492–496. doi: 10.1094/Pdis.1997.81.5.492

Gawehns, F., Houterman, P. M., Ichou, F. A., Michielse, C. B., Hijdra, M., Cornelissen, B. J., et al. (2014). The *Fusarium oxysporum* effector Six6 contributes to virulence and suppresses I-2-mediated cell death. *Mol. Plant Microbe Interact.* 27, 336–348. doi: 10.1094/MPMI-11-13-0330-R

Gawehns, F., Ma, L., Bruning, O., Houterman, P. M., Boeren, S., Cornelissen, B. J., et al. (2015). The effector repertoire of *Fusarium oxysporum* determines the tomato xylem proteome composition following infection. *Front. Plant Sci.* 6:967. doi: 10.3389/fpls.2015.00967

Gonzalez-Cendales, Y., Catanzariti, A. M., Baker, B., McGrath, D. J., and Jones, D. A. (2016). Identification of I-7 expands the repertoire of genes for resistance to fusarium wilt in tomato to three resistance gene classes. *Mol. Plant Pathol.* 17, 448–463. doi: 10.1111/mpp.12294

Gordon, T. R. (2017). *Fusarium oxysporum* and the fusarium wilt syndrome. *Ann. Rev. Phytopathol.* 55, 23–39. doi: 10.1146/annurev-phyto-080615095919

Halperin, W., and Jensen, W. A. (1967). Ultrastructural changes during growth and embryogenesis in carrot cell cultures. *J. Ultrastruct. Res.* 18, 428–443.

Hoffmann-Sommergruber, K. (2000). Plant allergens and pathogenesis-related proteins - what do they have in common? *Int. Arch. Allergy Immunol.* 122, 155–166. doi: 10.1159/000024392

Houterman, P. M., Cornelissen, B. J., and Rep, M. (2008). Suppression of plant resistance gene-based immunity by a fungal effector. *PLoS Pathog.* 4:e1000061. doi: 10.1371/journal.ppat.1000061

Houterman, P. M., Ma, L., van Ooijen, G., de Vroomen, M. J., Cornelissen, B. J. C., Takken, F. L. W., et al. (2009). The effector protein Avr2 of the xylem-colonizing fungus *Fusarium oxysporum* activates the tomato resistance protein I-2 intracellularly. *Plant J.* 58, 970–978. doi: 10.1111/j.1365-313X.2009.03838.x

Houterman, P. M., Speijer, D., Dekker, H. L., de Koster, C. G., Cornelissen, B. J. C., and Rep, M. (2007). The mixed xylem sap proteome of *Fusarium oxysporum*-infected tomato plants. *Mol. Plant Pathol.* 8, 215–221. doi: 10.1111/J.1364-3703.2007.00384.X

Hubner, N. C., Bird, A. W., Cox, J., Splettstoesser, B., Bandilla, P., Poser, I., et al. (2010). Quantitative proteomics combined with BAC transgeneomics reveals in vivo protein interactions. *J. Cell Biol.* 189, 739–754. doi: 10.1083/jcb.200911091

Joosten, M. H. A. J., and De Wit, P. J. G. M. (1989). Identification of several pathogenesis-related proteins in tomato leaves inoculated with *Cladosporium fulvum* (syn. *Fulvia fulva*) as 1,3-β-glucanases and chitinases. *Plant Physiol.* 89, 945–951. doi: 10.1104/pp.89.3.945

Kehr, J., Buhtz, A., and Giavalisco, P. (2005). Analysis of xylem sap proteins from *Brassica napus*. *BMC Plant Biol.* 5:11. doi: 10.1186/1471-2229-5-11

King, G. J., Turner, V. A., Hussey, C. E., Wurtele, E. S., and Lee, S. M. (1988). Isolation and characterization of a tomato cdna clone which codes for a salt-induced protein. *Plant Mol. Biol.* 10, 401–412. doi: 10.1007/Bf00014946

Krasikov, V., Dekker, H. L., Rep, M., and Takken, F. L. W. (2011). The tomato xylem sap protein XSP10 is required for full susceptibility to Fusarium wilt disease. *J. Exp. Bot.* 62, 963–973. doi: 10.1093/jxb/erq327

Leon-Kloosterziel, K. M., Verhagen, B. W. M., Keurentjes, J. J. B., VanPelt, J. A., Rep, M., VanLoon, L. C., et al. (2005). Colonization of the arabidopsis rhizosphere by fluorescent *Pseudomonas* spp. activates a root-specific, ethylene-responsive PR-5 gene in the vascular bundle. *Plant Mol. Biol.* 57, 731–748. doi: 10.1007/s11103-005-3097-y

Lonsdale, A., Davis, M. J., Doblin, M. S., and Bacic, A. (2016). Better than nothing? limitations of the prediction tool secretome-P in the search for leaderless secretory proteins (LSPs) in plants. *Front. Plant Sci.* 7:1451. doi: 10.3389/fpls.2016.01451

Ma, L. S., Cornelissen, B. J. C., and Takken, F. L. W. (2013). A nuclear localization for avr2 from *Fusarium oxysporum* is required to activate the tomato resistance protein i-2. *Front. Plant Sci.* 4:94. doi: 10.3389/fpls.2013.00094

Mes, J. J., van Doorn, A. A., Wijbrandi, J., Simons, G., Cornelissen, B. J. C., and Haring, M. A. (2000). Expression of the fusarium resistance gene I-2 colocalizes with the site of fungal containment. *Plant J.* 23, 183–193. doi: 10.1046/j.1365-313x.2000.00765.x

Mes, J. J., Weststeijn, E. A., Herlaar, F., Lambalk, J. J. M., Wijbrandi, J., Haring, M. A., et al. (1999). Biological and molecular characterization of *Fusarium oxysporum* f sp lycopersici divides race 1 isolates into separate virulence groups. *Phytopathology* 89, 156–160. doi: 10.1094/Phyto.1999.89.2.156

Michielse, C. B., and Rep, M. (2009). Pathogen profile update: *Fusarium oxysporum*. *Mol. Plant Pathol.* 10, 311–324. doi: 10.1111/J.1364-3703.2009.00538.X

Oh, B. J., Ko, M. K., Kim, K. S., Kim, Y. S., Lee, H. H., Jeon, W. B., et al. (2003). Isolation of defense-related genes differentially expressed in the resistance interaction between pepper fruits and the anthracnose fungus *Colletotrichum gloeosporioides*. *Mol. Cells* 15, 349–355.

Olivain, C., and Alabouvette, C. (1999). Process of tomato root colonization by a pathogenic strain of *Fusarium oxysporum* f. sp. lycopersici in comparison with a non-pathogenic strain. *New Phytol.* 141, 497–510. doi: 10.1046/j.1469-8137.1999.00365.x

Olivain, C., Humbert, C., Nahalkova, J., Fatehi, J., L'Haridon, F., and Alabouvette, C. (2006). Colonization of tomato root by pathogenic and nonpathogenic *Fusarium oxysporum* strains inoculated together and separately into the soil. *Appl. Environ. Microbiol.* 72, 1523–1531. doi: 10.1128/AEM.72.2.1523-1531.2006

Peng, K., van Lent, J. W., Boeren, S., Fang, M., Theilmann, D. A., Erlandson, M. A., et al. (2012). Characterization of novel components of the baculovirus per os infectivity factor complex. *J. Virol.* 86, 4981–4988. doi: 10.1128/JVI.06801-11

Pu, Z., Ino, Y., Kimura, Y., Tago, A., Shimizu, M., Natsume, S., et al. (2016). Changes in the proteome of xylem sap in *Brassica oleracea* in response to *Fusarium oxysporum* stress. *Front. Plant Sci.* 7:31. doi: 10.3389/fpls.2016.00031

Rep, M., Dekker, H. L., Vossen, J. H., de Boer, A. D., Houterman, P. M., Speijer, D., et al. (2002). Mass spectrometric identification of isoforms of PR proteins in xylem sap of fungus-infected tomato. *Plant Physiol.* 130, 904–917. doi: 10.1104/pp.007427

Rutter, B. D., and Innes, R. W. (2017). Extracellular vesicles isolated from the leaf apoplast carry stress-response proteins. *Plant Physiol.* 173, 728–741. doi: 10.1104/pp.16.01253

Schmidt, S. M., Houterman, P. M., Schreiver, I., Ma, L. S., Amyotte, S., Chellappan, B., et al. (2013). MITEs in the promoters of effector genes allow prediction of novel virulence genes in *Fusarium oxysporum*. *BMC Genomics* 14:119. doi: 10.1186/1471-2164-14-119

Sela-Buurlage, M. B., Budai-Hadrian, O., Pan, Q., Carmel-Goren, L., Vunsch, R., Zamir, D., et al. (2001). Genome-wide dissection of fusarium resistance in tomato reveals multiple complex loci. *Mol. Genet. Genomics* 265, 1104–1111.

Simons, G., Groenendijk, J., Wijbrandi, J., Reijans, M., Groenen, J., Diergaarde, P., et al. (1998). Dissection of the fusarium I2 gene cluster in tomato reveals six homologs and one active gene copy. *Plant Cell* 10, 1055–1068.

Sperschneider, J., Dodds, P. N., Singh, K. B., and Taylor, J. M. (2018). apoplastp: prediction of effectors and plant proteins in the apoplast using machine learning. *New Phytol.* 217, 1764–1778. doi: 10.1111/nph.14946

Steinkellner, S., Mammerler, R., and Vierheilig, H. (2005). Microconidia germination of the tomato pathogen *Fusarium oxysporum* in the presence of root exudates. *J. Plant Interact.* 1, 23–30. doi: 10.1080/17429140500134334

Stintzi, A., Heitz, T., Prasad, V., Wiedemannmerdinoglu, S., Kauffmann, S., Geoffroy, P., et al. (1993). Plant pathogenesis-related proteins and their role in defense against pathogens. *Biochimie* 75, 687–706. doi: 10.1016/0300-9084(93)90100-7

Takken, F. L. W., and Rep, M. (2010). The arms race between tomato and *Fusarium oxysporum*. *Mol. Plant Pathol.* 11, 309–314. doi: 10.1111/j.1364-3703.2009.00605.x

van der Does, H. C., Constantin, M. E., Houterman, P. M., Takken, F. L. W., Cornelissen, B. J. C., Haring, M. A., et al. (2018). *Fusarium oxysporum* colonizes the stem of resistant tomato plants, the extent varying with the R-gene present. *Eur. J. Plant Pathol.* doi: 10.1007/s10658-018-1596-3

van der Does, H. C., Lievens, B., Claes, L., Houterman, P. M., Cornelissen, B. J., and Rep, M. (2008). The presence of a virulence locus discriminates *Fusarium oxysporum* isolates causing tomato wilt from other isolates. *Environ. Microbiol.* 10, 1475–1485. doi: 10.1111/j.1462-2920.2007.01561.x

van Ooijen, G., van den Burg, H. A., Cornelissen, B. J. C., and Takken, F. L. W. (2007). Structure and function of resistance proteins in solanaceous plants. *Annu. Rev. Phytopathol.* 45, 43–72. doi: 10.1146/annurev.phyto.45.062806.094430

Veloso, J., and Diaz, J. (2012). *Fusarium oxysporum* Fo47 confers protection to pepper plants against *Verticillium dahliae* and *Phytophthora capsici*, and induces the expression of defence genes. *Plant Pathol.* 61, 281–288. doi: 10.1111/j.1365-3059.2011.02516.x

Vigers, A. J., Wiedemann, S., Roberts, W. K., Legrand, M., Selitrennikoff, C. P., and Fritig, B. (1992). Thaumatin-like pathogenesis-related proteins are antifungal. *Plant Sci.* 83, 155–161. doi: 10.1016/0168-9452(92)90074-V

Vizcaino, J. A., Csordas, A., Del-Toro, N., Dianes, J. A., Griss, J., Lavidas, I., et al. (2016). 2016 update of the pride database and its related tools. *Nucleic Acids Res.* 44, D447–D456. doi: 10.1093/nar/gkw880

Wawra, S., Fesel, P., Widmer, H., Timm, M., Seibel, J., Leson, L., et al. (2016). The fungal-specific beta-glucan-binding lectin FGB1 alters cell-wall composition and suppresses glucan-triggered immunity in plants. *Nat. Commun.* 7:13188. doi: 10.1038/ncomms13188

Woloshuk, C. P., Meulenhoff, J. S., Sela-Buurlage, M., van den Elzen, P. J., and Cornelissen, B. J. (1991). Pathogen-induced proteins with inhibitory activity toward *Phytophthora infestans*. *Plant Cell* 3, 619–628. doi: 10.1105/tpc.3.6.619

Conflict of Interest Statement: The authors declare that the research was conducted in the absence of any commercial or financial relationships that could be construed as a potential conflict of interest.

frontiers in Microbiology

CORRECTION
published: 13 August 2019
doi: 10.3389/fmicb.2019.01872

Corrigendum: Xylem Sap Proteomics Reveals Distinct Differences Between *R* Gene- and Endophyte-Mediated Resistance Against Fusarium Wilt Disease in Tomato

Francisco J. de Lamo[1], *Maria E. Constantin*[1], *David H. Fresno*[1], *Sjef Boeren*[2], *Martijn Rep*[1] *and Frank L. W. Takken*[1]*

[1] Molecular Plant Pathology, Faculty of Science, Swammerdam Institute for Life Sciences, University of Amsterdam, Amsterdam, Netherlands, [2] Laboratory of Biochemistry, Wageningen University, Wageningen, Netherlands

Keywords: endophyte, biocontrol, Fusarium wilt disease, proteomics, NP24, PR-5x, exosomes

OPEN ACCESS

Edited and reviewed by:
Alfredo Herrera-Estrella, Center for Research and Advanced Studies of the National Polytechnic Institute, Mexico

***Correspondence:**
Frank L. W. Takken
f.l.w.takken@uva.nl

Specialty section:
This article was submitted to Plant Microbe Interactions, a section of the journal Frontiers in Microbiology

Received: *04 July 2019*
Accepted: *29 July 2019*
Published: *13 August 2019*

Citation:
de Lamo FJ, Constantin ME, Fresno DH, Boeren S, Rep M and Takken FLW (2019) Corrigendum: Xylem Sap Proteomics Reveals Distinct Differences Between R Gene- and Endophyte-Mediated Resistance Against Fusarium Wilt Disease in Tomato. Front. Microbiol. 10:1872. doi: 10.3389/fmicb.2019.01872

A Corrigendum on

Xylem Sap Proteomics Reveals Distinct Differences Between *R* Gene- and Endophyte-Mediated Resistance Against Fusarium Wilt Disease in Tomato
by de Lamo, F. J., Constantin, M. E., Fresno, D. H., Boeren, S., Rep, M., and Takken, F. L. W. (2018). Front. Microbiol. 9:2977. doi: 10.3389/fmicb.2018.02977

In the original article, there was an error. The amount of xylem sap protein used for nLC-MS/MS analysis was incorrectly depicted; instead of 540 μg of protein 60 μg of protein was TCA precipitated and used for SDS-polyacrylamide gel electrophoresis.

A correction has been made to the **MATERIALS AND METHODS section, in the sub-section Sample Preparation for nLC-MS/MS**:

Potential fungal spores were removed from the sap by centrifugation at 800 $\times g$ for 10 min. Xylem sap proteins were concentrated by passing 12 ml of cleared sap through Amicon Ultra-15 Filter Units (Millipore). After centrifugation at 2500 $\times g$ for 15–30 min retentates containing the proteins were recovered. A BCA (bicinchoninic acid) assay (ThermoFischer) was performed to determine the protein concentration. Based on BCA quantification, a volume containing 60 μg of protein was trichloroacetic acid/aceton-precipitated and the pellet was resuspended in SDS loading buffer (2% SDS, 10% glycerol, 60 mM TRIS-HCl pH 6.8, 5% β-mercaptoethanol, 0.01% bromophenol blue), heated at 98°C for 5 min and loaded on a 12% SDS-polyacrylamide gel. Following a short electrophoresis, the proteins were stained overnight at 4°C with Commassie PageBlue (ThermoFischer). The bands containing the proteins were excised and cysteine reduction and alkylation of the proteins was performed by adding 10 mM DTT pH 8 (incubation at 60°C for 1 h) and 20 mM iodoacetamide pH 8 (incubation at room temperature in the dark for 30 min). Protein-containing gel slices were chopped into pieces of approximately 1 mm^2 and transferred to 1.5 ml low-binding tubes (Protein LoBind microcentrifuge tubes, Eppendorf). Tryptic in-gel digestion was performed overnight by adding 50 μl of 5 ng/μl Trypsin Sequencing Grade (Sigma-Aldrich). In-house prepared μcolumns were set up by adding C18 Empore disk and LichroprepC18 column material into a 200 μl pipette tip and the tryptic peptides were eluted from the μcolumn

with 50 µl of 50% acetonitrile. Acetonitrile content was reduced to <5% by reducing the volume with a concentrator at 45°C during 2 h and readjusting the volume with 1 mL/L HCOOH in water to 50 µl.

The authors apologize for this error and state that this does not change the scientific conclusions of the article in any way. The original article has been updated.

frontiers in Microbiology

ORIGINAL RESEARCH
published: 16 January 2019
doi: 10.3389/fmicb.2018.03321

A Survey of Culturable Fungal Endophytes From *Festuca rubra* subsp. *pruinosa*, a Grass From Marine Cliffs, Reveals a Core Microbiome

*Eric Pereira[1], Beatriz R. Vázquez de Aldana[1], Leticia San Emeterio[2] and Iñigo Zabalgogeazcoa[1]**

[1] Institute of Natural Resources and Agrobiology of Salamanca, Consejo Superior de Investigaciones Científicas (IRNASA-CSIC), Salamanca, Spain, [2] Research Institute on Innovation & Sustainable Development in Food Chain (ISFood), Universidad Pública de Navarra, Pamplona, Spain

Festuca rubra subsp. *pruinosa* is a perennial grass that inhabits sea cliffs of the Atlantic coasts of Europe. In this unhospitable environment plants grow in rock crevices and are exposed to abiotic stress factors such as low nutrient availability, wind, and salinity. *Festuca rubra* subsp. *pruinosa* is a host of the fungal endophyte *Epichloë festucae*, which colonizes aerial organs, but its root mycobiota is unknown. The culturable endophytic mycobiota of FRP roots was surveyed in a set of 105 plants sampled at five populations in marine cliffs from the northern coast of Spain. In total, 135 different fungal taxa were identified, 17 of them occurred in more than 10% of plants and in two or more populations. Seven taxa belonging to *Fusarium*, *Diaporthe*, Helotiales, *Drechslera*, *Slopeiomyces,* and *Penicillium* appeared to be constituents of the core microbiome of *Festuca rubra* subsp. *pruinosa* roots because they occurred in more than 20% of the plants analyzed, and at three or more populations. Most fungal strains analyzed (71.8%) were halotolerant. The presence of *Epichloë festucae* in aboveground tissue was detected in 65.7% of the plants, but its presence did not seem to significantly affect the structure of the core or other root microbiota, when compared to that of plants free of this endophyte. When plants of the grass *Lolium perenne* were inoculated with fungal strains obtained from *Festuca rubra* subsp. *pruinosa* roots, a *Diaporthe* strain significantly promoted leaf biomass production under normal and saline (200 mM NaCl) watering regimes. These results suggest that the core mycobiome of *Festuca rubra* subsp. *pruinosa* could have a role in host plant adaptation, and might be useful for the improvement of agricultural grasses.

Keywords: mycobiome, *Diaporthe*, *Fusarium oxysporum*, *Epichloë*, salinity, halophyte, grass

OPEN ACCESS

Edited by:
David B. Collinge, University of Copenhagen, Denmark

Reviewed by:
George Newcombe, University of Idaho, United States
Huzefa A. Raja, University of North Carolina at Greensboro, United States

****Correspondence:***
Iñigo Zabalgogeazcoa
i.zabalgo@irnasa.csic.es

Specialty section:
This article was submitted to Plant Microbe Interactions, a section of the journal Frontiers in Microbiology

Received: *17 October 2018*
Accepted: *20 December 2018*
Published: *16 January 2019*

Citation:
Pereira E, Vázquez de Aldana BR, San Emeterio L and Zabalgogeazcoa I (2019) A Survey of Culturable Fungal Endophytes From Festuca rubra subsp. pruinosa, a Grass From Marine Cliffs, Reveals a Core Microbiome. Front. Microbiol. 9:3321. doi: 10.3389/fmicb.2018.03321

INTRODUCTION

The vegetation that inhabits coastal marine cliffs is adapted to environmental conditions that are far from optimal for plant growth and survival. The rock substrate and vertical cliffs makes soil scarce or non-existent. Sea water spray adds salinity to the scenario, and exposure to sea winds favor plant dehydration. Those conditions of low nutrient availability, salinity, and wind exposure

can be persistent in sea cliffs, and as a result, sea cliff vegetation is often endemic, reflecting habitat specialization in order to survive under these unhospitable conditions (Doody, 2001; López-Bedoya and Pérez-Alberti, 2009).

Festuca rubra subsp. *pruinosa* (FRP) is a plant species common in cliffs of the Atlantic coasts of Europe (Markgraf-Dannenberg, 1980; López-Bedoya and Pérez-Alberti, 2009). This perennial grass grows as a chasmophyte in rock fissures, or in very shallow soils formed on cliff cavities and slopes. In nature this species rarely occurs away from sea cliffs, where other vegetation predominates, and its salt tolerance is greater than that of other *F. rubra* subspecies adapted to inland habitats (Humpreys, 1982). Some anatomical characteristics might contribute to the adaptation to cliffs of this plant, for instance, the epithet *pruinosa* refers to the apparent epicuticular wax coat that covers its leaves, possibly having a role in preventing water loss (Ortuñez and de la Fuente, 2010; Martínez Sagarra et al., 2017).

In addition to traits inherent to the plant genome, the plant microbiome can also contribute to adaptation. Studies of some plants adapted to high stress habitats revealed that fungal endophytes confer habitat-specific stress tolerance to their hosts, and without these fungal endophytes plant adaptation is reduced in their native habitats (Rodriguez and Redman, 2008). Examples include improved tolerance to biotic and abiotic stress factors such as disease, herbivory, heat, or salinity mediated by endophytic fungi (Clay and Schardl, 2002; Waller et al., 2005; Rodriguez et al., 2008). Some of the endophytes reported in these studies conferred improved stress tolerance to new host species, highlighting the importance that endophytic fungi could have for the improvement of agricultural crops.

Like other subspecies of *Festuca rubra*, FRP plants maintain associations with the fungal endophyte *Epichloë festucae*. This fungus systemically colonizes the stems and leaves of host plants, but not the roots, and it is transmitted vertically to seeds (Leuchtmann et al., 1994; Zabalgogeazcoa et al., 2006). Endophytic *Epichloë* species can have a mutualistic relationship with their hosts, and increased tolerance of symbiotic plants to biotic and abiotic stress factors have been reported to occur in some situations. For example, *Epichloë festucae* can produce several types of alkaloids that might protect host plants against herbivores (Clay and Schardl, 2002).

In marine cliffs the roots of FRP plants grow in rock fissures or minimal soil, forming a compact fibrous system which holds the plant and captures nutrients. The root mycobiota of FRP is unknown, and some of its components could be useful for the improvement of other plant species of agronomic interest, as it has been demonstrated in other plant-endophyte associations (Rodriguez et al., 2008). Thus, the objectives of this work were: (1) to identify the culturable endophytic mycobiota of FRP roots, (2) to determine if the presence of *Epichloë* affects the structure of the root mycobiota, and (3) to test if some FRP root endophytes affect the performance of another grass, *Lolium perenne*, when exposed to salinity.

MATERIALS AND METHODS

Study Sites and Plant Sampling

Plants of *Festuca rubra* subsp. *pruinosa* (FRP) were collected at five locations in sea cliffs in the North Atlantic coast of Spain. Three locations were in Galicia: Torre de Hércules (TDH), 43°23′09″N 8°24′23″W, Cedeira (CED), 43°40′46″N 8°01′15″W, and Estaca de Bares (EDB), 43°47′25″N 7°41′16″W, and two in Asturias: San Pedro de la Rivera (SPR), 43°34′43″N 6°13′17″W, and Cabo de Peñas (CDP), 43°39′02″N 5°51′00″W. The shortest distance in straight line among these locations is 30 km. The predominant flora in the walls of these sea cliffs mainly consisted of *Festuca rubra* subsp. *pruinosa*, *Armeria* spp. and *Crithmum maritimum*. The climate in the coast of Galicia and Asturias is mild with oceanic influence and abundant rainfall spread over the year; during the 1981–2010 period the mean annual precipitation was 1106 and 1062 mm, and the average annual temperature 13.5 and 13.8°C in Galicia and Asturias, respectively (AEMET, 2012). In the spring of 2016, a total of 105 FRP plants, about 20 plants per location, were collected. Most plants grew in fissures in the rock, where soil was very scarce or absent. The plants were transported in a refrigerated cooler to the laboratory in Salamanca, and processed for the isolation of fungi from roots the day after they were sampled. Afterward the plants were transplanted to pots with a 1:1 (v:v) mixture of peat and perlite and maintained in a wirehouse outdoors.

Isolation of Fungi

To isolate fungi from roots, a sample of about 20 root fragments of 4–5 cm was collected from each plant. Each root sample was surface-disinfected with a solution of 20% commercial bleach (1% active chlorine) containing 0.02% Tween 80 (v:v) for 6 min, followed by treatment with an aqueous solution of 70% ethanol for 30 s. Finally, the roots were rinsed with sterile water and cut into pieces about 5 mm long. Thirty root pieces of each sample were plated in two Petri plates (15 pieces/plate) with potato dextrose agar (PDA) containing 200 mg/L of chloramphenicol. This antibiotic was used to exclude the isolation of endophytic bacteria. A root sample of each of the 105 plants was prepared as outlined above, and kept in the dark at room temperature. As mycelium emerged from a root fragment into the agar, a small piece of the mycelium from the leading edge of the colony was transferred to a new PDA plate and maintained at room temperature. The root fragment and remaining mycelium were taken out of the original plate to avoid overgrowth. The plates with root samples were checked daily for the presence of fungi for about 4 weeks.

The presence of *Epichloë festucae* on each plant was diagnosed by isolation. Several leaf sheaths were collected from each plant, cut into fragments about 5 mm long, and surface disinfected by immersion in a solution of 20% commercial bleach for 10 min. The fragments were then rinsed with sterile water, and about 15 fragments from each plant were placed in a PDA plate containing 200 mg/L of chloramphenicol. The plates were kept at room temperature, and fungi emerging from leaf fragments during the first 2–5 days were discarded together with its leaf sheath

fragment. White *Epichloë* mycelium emerging from the extremes of the leaf fragments about 1 week after plating was transferred to new PDA plates for further identification.

Identification of Fungi

The fungal isolates obtained from roots were first grouped into different morphotypes according to morphological characteristics such as colony color, exudate production, mycelium appearance, and growth rate. One or a few isolates of each morphotype were used for further classification based on rDNA nucleotide sequences. Fungal DNA was extracted from a small amount of mycelium scraped from a PDA culture using the Phire Plant Direct PCR Kit (Thermo Fisher Scientific). A ribosomal DNA region including the internal transcribed spacer 1 (ITS1), 5.8S rDNA, and ITS2 was amplified by PCR using primers ITS1 and ITS4 (White et al., 1990). Amplification conditions were: 98°C for 5 min, followed by 35 cycles of 98°C for 5 s, 54°C for 5 s, and 72°C for 20 s; after that the reaction was kept at 72°C for 1 min. PCR amplicons were cleaned (MSB Spin PCRapace, Stratec biomedical, Germany) and sequenced at the DNA sequencing service of the University of Salamanca (Spain).

All the sequences obtained were grouped into operational taxonomic units (OTU), considering that groups of sequences with a similarity greater than 97% belonged to the same OTU. This clustering operation was done using BlastClust software (NCBI, 2004). Afterward, a sequence representative of each OTU was used to search for similar curated sequences at the UNITE fungal database. A taxonomic identity was assigned to each OTU considering that the species rank of a UNITE database match was accepted when the identity between the OTU and database sequences was greater than 97%, and most UNITE matches corresponded to the same taxon. When the similarity was 97% – 95%, or UNITE matches corresponded to several species of the same genus, only the genus rank was accepted. In other cases the sequences were assigned to orders or families whenever it was reasonable.

Analysis of Root Fungal Diversity

For each location (referred to as population from here on), species accumulation curves showing the relationship between the number of plants sampled and the number of fungal species obtained, were estimated using the 'specaccum' function and the exact method with the Vegan Package in R (Oksanen et al., 2017). Estimations of the maximum number of fungal species at each population were obtained with the Bootstrap and Chao indexes using EstimateS 9.0 software (Colwell, 2005). Shannon's index of diversity (H') was estimated from the relative abundance of each taxon identified. The distribution of the relative abundance of the fungal species was observed with a rank-abundance curve. The similarity of fungal communities between each pair of populations was estimated using Jaccard's index of similarity (J). It is calculated from the equation $J = c/(a + b + c)$, where 'c' is the number of fungal taxa shared between two populations, 'a' the number of fungal taxa unique to the first population and 'b' the number of fungal taxa unique to the second population (Jaccard, 1912).

Effect of *Epichloë* on Root Mycobiota

Species richness (number of different root endophyte species per plant) was analyzed with a two-way ANOVA with *Epichloë* presence (E+) or absence (E−) and plant population (CED, CDP, EDB, SPR, and TDH) as factors. A type III sum of squares was used because the number of E+ and E− plants was unbalanced.

Species accumulation curves and beta diversity index estimations, plus a Canonical Correspondence Analysis (CCA) were made using the Vegan Package in R (Oksanen et al., 2017). Species accumulation curves for E+ and E− plants were estimated using the 'specaccum' function and the exact method. Beta-diversity indexes were estimated using the 'betadiver' function and the z index based on the Arrhenius species-area model (Koleff et al., 2003). Differences in beta diversity among groups were determined by Tukey multiple comparisons. A CCA was made because the gradient length of the detrended correspondence analysis (DCA) was greater than four, which indicated an unimodal response (Lepš and Šmilauer, 2003). Taxa appearing in less than three plants were omitted for this analysis; as a result, 61 taxa remained. A forward selection procedure (ordistep function) was used to determine the subset of explanatory variables (*Epichloë* incidence, population, *Epichloë*: population) explaining most variation in root mycobiome. The statistical power of the analysis was assessed by Monte Carlo permutation tests ($n = 999$).

Salt Tolerance of Fungal Isolates

A set of 46 fungal strains belonging to 20 of the most abundant genera isolated from FRP roots plus nine *Epichloë festucae* strains were analyzed to determine their salt tolerance *in vitro*. For each fungal strain a 6 mm diameter mycelial disk was placed in the center of 9 cm Petri plates with PDA containing three different concentrations of sodium chloride: 600 mM (equivalent to sea water concentration), 300 mM, and a control without NaCl. For each fungal strain and salt treatment three replicate plates were prepared. All plates were incubated at room temperature in the dark. The colony diameter was measured at two perpendicular axes when colonies in the fastest growing medium reached a diameter of 4–6 cm. The effect of salinity treatments on the radial growth of fungal colonies was assessed by means of a one-way ANOVA, and statistical significance of differences among means using Tukey's test ($p < 0.05$).

Extracellular Enzyme Activity

In vitro cellulase and amylase activity was analyzed for 43 strains belonging to some of the most abundant taxa. The production of cellulase was assayed using the method described by Sunitha et al. (2013) adapted to PDA plates. For each fungal strain a 6 mm diameter mycelial disk was placed in the center of a 9 cm. Petri plate and incubated for 5 days at 25°± 1°C in the dark. After incubation the plates were flooded with 0.2% (w/v) aqueous Congo Red, and distained with 1 M NaCl for 15 min. The presence of a clear zone surrounding the colony

indicated cellulase activity. Amylase activity was assessed on PDA containing 2% (w/v) soluble starch. After incubation the plates were flooded for 15 min with a solution of 1% (w/v) iodine in 2% (w/v) potassium iodide. A clear zone surrounding the colony indicated amylase activity (Hankin and Anagnostakis, 1975).

Inoculation of *Lolium perenne* Plants With Root Endophytes From FRP

To test whether FRP endophytes affect the growth of the grass *Lolium perenne* under salinity, plants were inoculated with three fungal strains belonging to some of the core taxa from FRP roots. A greenhouse experiment was conducted with a completely randomized design with 14 plant replicates for each fungal strain (*Periconia* S6, *Penicillium* E7, and *Diaporthe* S69) and salinity treatment (0 and 200 mM NaCl). Seeds of *Lolium perenne* cv. Tivoli (DLF, Denmark) were sown in 200 mL plastic pots filled with a substrate composed of seven parts of peat and perlite (1:1) previously sterilized at 80°C for 24 h, mixed with one part (v:v) of fungal inoculum. The fungal inoculum was a 4 week old culture of each fungus grown in autoclaved sugar beet pulp. Several seeds were sown in each pot, and thinned to four seedlings after emergence. Three weeks after germination, plants were watered with 0 or 200 mM NaCl during 3 weeks. Plants subject to the salinity treatment were watered with 50 and 100 mM NaCl on the first and third day respectively to avoid salt shock, and the 200 mM concentration was applied from day 5 onward. After 3 weeks of salt treatment the plants were harvested.

Five replicates of each treatment (salt and fungal strain) were analyzed for K and Na concentration by inductively coupled plasma atomic emission spectroscopy (ICP-OES, Varian 720-ES). Previously, dried plant samples were calcined at 450°C for 8 h, and ashes dissolved in $HCl:HNO_3:H_2O$ (1:1:8).

A two-way ANOVA was made to determine the effects of salt treatment and fungal strain on shoot biomass, K and Na concentrations, and differences between means were assessed using Tukey's test ($p < 0.05$). The success of the inoculation was determined after harvest by the reisolation of the inoculated fungi from surface disinfected roots, using the method above explained.

RESULTS

Endophyte Isolation

After plating 3150 root fragments on culture media, a total of 2324 fungal isolates were obtained, ranging from 355 to 578 among populations (**Table 1**). Most isolates emerged in the first 5 days after the placement of the roots on plates. Isolates were obtained from 73.8% of the root fragments plated. All sampled plants harbored fungi in their roots, and on average, 21 isolates were obtained from the roots of each plant.

Epichloë festucae was isolated from leaves of 65.7% of the plants. Its incidence among populations ranged from 20.0 to 100.0% (**Table 1**).

Identification of Fungal Isolates and Taxonomic Structure

When the isolates of each population were grouped according to morphotypes, the TDH isolates were classified into 177 morphotypes, CED in 142, EDB in 125, SPR in 137, and those from CDP in 107.

Nucleotide sequences were obtained from one or more isolates of each morphotype. As a result, 502 ITS1-5.8S-ITS2 nucleotide sequences were obtained, and those differing in homology by less than 3% were considered to belong to the same taxon. After this clustering process, 138 different sequences remained. These sequences were used to interrogate the UNITE sequence database, and as a result 135 fungal taxa were identified (**Supplementary Table S1**). Twenty-three taxa were identified to a species rank, 69 to genus rank and the remaining 43 were assigned to an order, class, family or division (**Table 2**). All the taxa could be assigned to 64 different fungal genera, 96% of them within the Ascomycota. Pleosporales, Hypocreales, and Eurotiales were the most representative orders, in terms of the number of taxa (23, 18, and 10%, respectively). The remaining orders were marginally represented (**Figure 1**). Among plant populations the number of fungal taxa ranged from 34 to 59 (**Table 1**).

The distribution of the taxa according to their incidence can be visualized in the rank-abundance curve shown in **Figure 2**. Seven species occurred in more than 20% of the plants at three

TABLE 1 | Incidence of *Epichloë* and fungal species richness in roots of *Festuca rubra* subsp. *pruinosa* at five populations from marine cliffs in Northern Spain.

Population	Number of plants analyzed	Incidence of *Epichloë festucae* (%)	Root mycobiota			
			Number of isolates obtained	Colonization[1]	Number of fungal species	Fungal species per plant
TDH	21	57.1	471	74.8	34	1.62
CED	19	68.4	355	62.3	46	2.42
EDB	22	77.3	473	71.7	47	2.47
CDP	20	20.0	447	74.5	59	2.57
SPR	23	100.0	578	83.8	46	2.19
Total/mean	105	65.7	2324	73.8	135	1.29

[1] *Percentage of root pieces from which fungi emerged into growth medium.*

TABLE 2 | Core and abundant fungal species isolated from surface sterilized roots of *Festuca rubra* subsp. *pruinosa* at five populations from marine cliffs in northern Spain.

Strain	Taxon	Identity to closest match (%)	ITS sequence accession number	Order	Incidence in plants (%)	Number of populations
T150	*Fusarium oxysporum*	100	MH578626	Hypocreales	57.1	5
EB4	*Diaporthe* sp. A	100	MH578627	Diaporthales	54.3	5
C29	*Fusarium* sp. A	100	MH626490	Helotiales	41.0	4
S75	Helotiales sp. A	100	MH626491	Helotiales	37.1	5
T105	*Drechslera* sp.	100	MH626492	Pleosporales	27.6	4
S132	*Slopeiomyces cylindrosporus*	100	MH626493	Magnaporthales	27.6	3
T120	*Penicillium* sp. F	100	MH626494	Eurotiales	20.0	5
S7	*Darksidea* sp.	99	MH628220	Pleosporales	17.1	3
T131	*Periconia macrospinosa*	100	MH628221	Pleosporales	16.2	3
T122	*Penicillium* sp. A	100	MH628222	Eurotiales	14.3	4
T16	*Alternaria* sp. A	99	MH628223	Pleosporales	13.3	3
S38	*Fusarium* sp. B	99	MH628224	Hypocreales	13.3	4
C2	*Dactylonectria alcacerensis*	100	MH628225	Hypocreales	13.3	4
E79	Helotiales sp. B	100	MH628226	Helotiales	11.4	3
T140	*Alternaria* sp. B	100	MH628227	Pleosporales	10.5	4
E74	*Lachnum* sp. A	99	MH628228	Helotiales	10.5	3
CP17	*Trichoderma* sp. B	100	MH628229	Hypocreales	10.5	2

Only the taxa with an incidence in plants greater than 20% are listed. ***Supplementary Table S1*** *contains the complete list of 135 taxa identified.*

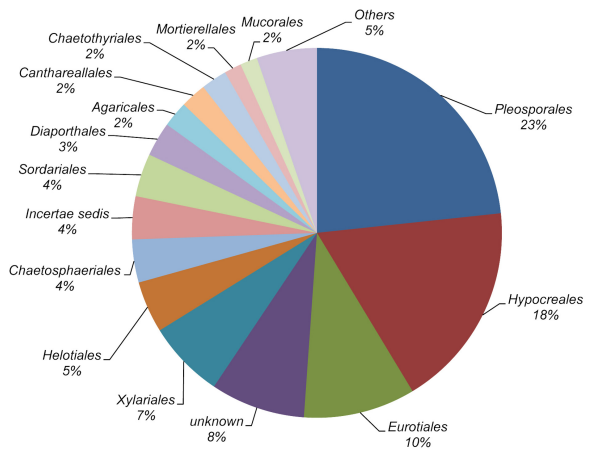

FIGURE 1 | Distribution of fungal taxa from roots of *Festuca rubra* subsp. *pruinosa* plants from marine cliffs in northern Spain according to orders.

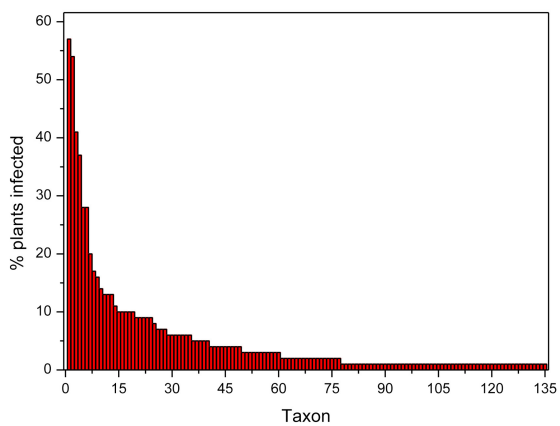

FIGURE 2 | Rank-abundance plot showing the incidence in plants of each taxon identified in roots of *Festuca rubra* subsp. *pruinosa* plants from marine cliffs in northern Spain.

or more populations: *Fusarium oxysporum* (57.1%), *Diaporthe* sp. A (54.3%), *Fusarium* sp. A (40.9%), Helotiales sp. A (37.1%), *Slopeiomyces cylindrosporus* (27.6%), *Drechslera* sp. (27.6%), and *Penicillium* sp. F (20.0%) (**Table 2**). The identification of several *F. oxysporum* strains was confirmed by Martijn Rep and Maria Constantin (University of Amsterdam) by means of an analysis of their EF1α gene sequence. Because of their relatively high incidence within and among populations, these taxa could be considered as part of the core microbiome of FRP.

A second set of relatively abundant taxa were isolated from 10 to 20% of the plants, and at two or more populations (**Table 2**), these were *Darksidea* sp., *Periconia macrospinosa*, *Penicillium* sp. *A*, *Alternaria* sp. A, *Fusarium sp. B*, *Dactylonectria alcacerensis*, Helotiales sp. B, *Alternaria* sp. B, *Lachnum* sp. A and *Trichoderma* sp. B. The remaining 118 taxa were found in less than 10% of the plants and 58 of them were singletons, occurring in a single plant.

Some of most abundant taxa, like *Darksidea* sp., *Periconia macrospinosa, Slopeiomyces cylindrosporus* and *Drechslera* sp., belong to the group of fungi known as dark septate endophytes (DSE). Fungi from the DSE group present some particular morphological characteristics, such as septated and melanized hyphae. These characteristics were observed in hyphae from two strains of Helotiales sp. A under the light microscope. Therefore, Helotiales sp. A also seems to belong to the DSE.

All populations produced non-asymptotic species accumulation curves, suggesting that increased sampling effort would reveal new fungal species (**Figure 3**). The Chao and Bootstrap estimators of the maximum number of species did not approach an horizontal asymptote, what made them unreliable estimators for this particular case.

Effect of *Epichloë festucae* on Root Endophytic Fungal Communities

In the set of 105 plants analyzed, 69 were infected by *Epichloë festucae* (E+) and 36 were not (E−). Out of the 135 fungal species identified in all plants, 52 were exclusive of E+ plants, 29 of E− plants, and 54 occurred in both.

The ANOVA showed that neither the presence of *Epichloë* nor population had a significant effect on species richness ($F = 1.999$; $p = 0.276$ and $F = 1.626$; $p = 0.174$ respectively). The beta diversity index showed a similar trend, no significant differences were found between E+ and E− plants ($p = 0.989$) or among populations ($p = 0.377$ for all pairwise comparisons). The values of the Shannon diversity index (H') were relatively high, but similar for E+ and E− plants (**Table 3**).

Both E+ and E− plants displayed similar species accumulation curves when the data from all five populations were pooled (**Figure 4A**). The species richness accumulated at 36 plants was 80.93 ± 5.24 for E+ plants and 72.03 ± 1.04 for E− plants. Within each population, we found small differences (both positive and negative) between E+ and E− plants (**Figures 4B–F**).

The first two axes of the CCA were statistically significant ($p = 0.001$) and explained 35.18 and 29.36% of the variance. After the forward selection, only the variable population was finally included in the CCA and explained the 5.29% of the variation. The CCA biplot showed no clear separation between E+ and E− plants (**Figure 5**). However, there was a segregation among plant populations: the first axis clustered populations according to regions and separated the Asturian populations (CDP and SPR) from the Galician ones (TDH, CED and EDB); and the second axis segregated both Asturian populations, suggesting that the structure of the root mycobiota of these two populations differ between them and with respect to the Galician populations (**Figure 5**). All the core and the abundant taxa were present in both E+ and E− plants, although some species were more abundant in E+ (*Slopeiomyces cylindrosporus*) or in E− plants (*Drechslera* sp.) (**Figure 6**).

In terms of similarity of the fungal assemblages between pairs of populations, *J* values were higher between populations from the same region, 0.238 to 0.362 among Galician populations and 0.238 between Asturian populations, than between Galician and Asturian populations, which ranged from 0.095 to 0.193 (**Table 4**).

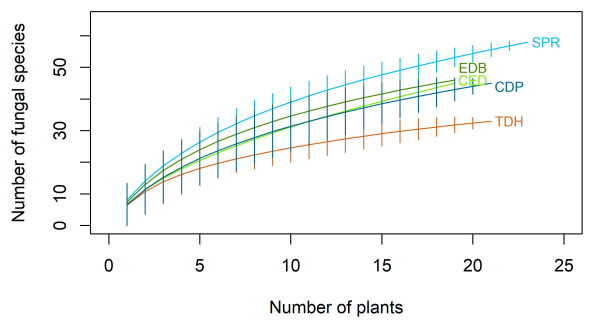

FIGURE 3 | Species accumulation curves for fungal species isolated from roots of *Festuca rubra* subsp. *pruinosa* at five populations from marine cliffs in northern Spain. TDH, Torre de Hércules; CED, Cedeira; EDB, Estaca de Bares; SPR, San Pedro de la Rivera; CDP, Cabo de Peñas.

TABLE 3 | Fungal species richness and diversity in roots of *Festuca rubra* subsp. *pruinosa* plants infected (E+) or not infected (E−) by *Epichloë festucae* at five populations in marine cliffs.

Factor		Number of plants analyzed	Species per plant	ß diversity (Kolleff)	H' Shannon
Epichloë	E+	69	7.19 ± 2.63	0.59 ± 0.07	4.04
	E−	36	7.08 ± 3.11	0.59 ± 0.08	3.90
Population	TDH	21	6.52 ± 1.91	0.51 ± 0.10	3.13
	CED	19	6.84 ± 2.59	0.50 ± 0.10	3.32
	EDB	22	7.47 ± 2.55	0.56 ± 0.10	3.48
	CDP	20	6.67 ± 3.45	0.55 ± 0.10	3.59
	SPR	23	8.17 ± 3.04	0.55 ± 0.05	3.43

Salt Tolerance and Enzymatic Activity of Endophytic Fungi

The salt tolerance assay showed that fungal strains had three different types of response in terms of their radial growth. Most strains analyzed (71.8%) were halophilic, showing a statistically significant increase in radial growth in PDA plates containing NaCl respect to the control (**Supplementary Table S2**). The radial growth of 51.5% of these halophilic strains increased at both NaCl concentrations; that of 21.2% increased only in 600 mM NaCl, and that of 27.3% increased only in 300 mM NaCl. All nine *Fusarium* strains and four of the five *Diaporthe* sp. A strains tested were halophylic.

Some strains (6.5%) were halotolerant, not showing a significant difference in radial growth in 300 mM and 600 mM NaCl with respect to the control. Finally, 21.7% of the strains showed a radial growth decrease in culture media containing NaCl and were classified as halosensitive, 80.0% of these strains decreased only in 600mM NaCl, and the remaining 20.0% did it at both salt concentrations. Within taxa like *Diaporthe* sp. A, *Periconia macrospinosa* or *Penicillium* sp. F, some strains had different responses, i.e., *Diaporthe* strain S129 was halophilic and strain S69 halosensitive (**Supplementary Table S2**).

The nine *E. festucae* strains tested were halosensitive, all decreased in radial growth in the 600 mM medium (**Table 5**). Seven of them did not show a significant difference in radial growth with respect to the control at 300 mM NaCl.

Cellulase and amylase activities were assayed for 43 fungal strains (**Table 6**). Twenty three of these strains, including all tested strains of *Fusarium oxysporum, Penicillium* and Helotiales sp. A, showed cellulase activity *in vitro*. In contrast, none of the

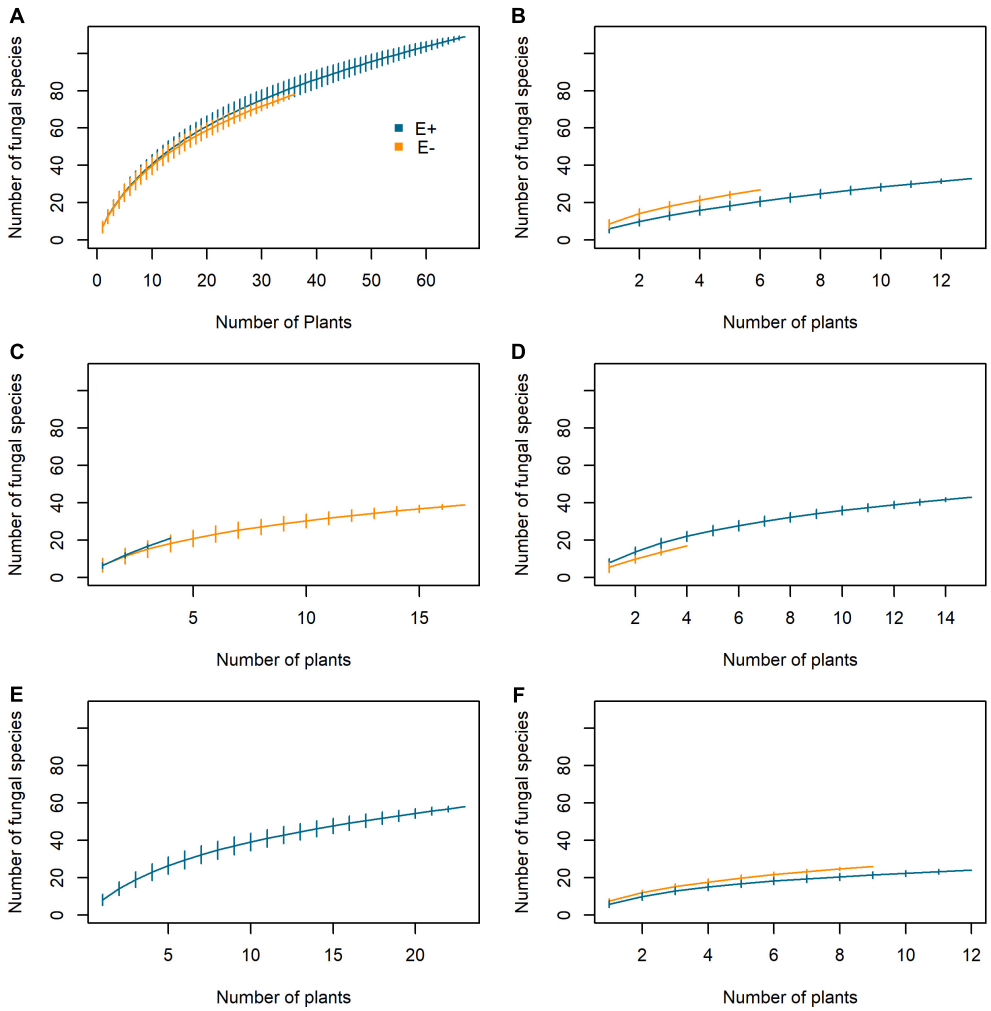

FIGURE 4 | Species accumulation curves of root mycobiota in *Epichloë festucae* infected (E+) and non-infected (E–) plants of *Festuca rubra* subsp. *pruinosa* from five marine cliff populations in northern Spain. **(A)** Whole plant set; **(B)** Cedeira; **(C)** Cabo de Peñas; **(D)** Estaca de Bares; **(E)** San Pedro de la Rivera; **(F)** Torre de Hércules.

six *Diaporthe* sp. A strains tested was positive. Amylase activity was detected in only nine strains, including all four *Penicillium* strains tested.

Effect of FRP Endophytes on Growth of *Lolium perenne*

A two-way ANOVA showed a significant effect of salinity (p = 0.004; $\bar{X}_{control}$ = 0.236 g, $\bar{X}_{NaCl}$ = 0.192 g), endophyte inoculated (p < 0.001; $\bar{X}_{control}$ = 0.194 g, $\bar{X}_{Periconia}$ = 0.231 g, $\bar{X}_{Penicillium}$ = 0.109, $\bar{X}_{Diaporthe}$ = 0.321 g), and their interaction (p = 0.034; **Figure 7**) on dry matter production of *L. perenne*. Plants inoculated with *Diaporthe* S69, a *Diaporthe* sp. A strain, showed a significant increase in biomass production with respect to the uninoculated control plants in both watering treatments: 31.3% in tap water and 48.9% under saline irrigation (**Figure 7**). The plants inoculated with *Periconia* S6 had greater biomass in both watering treatments, but the difference respect to the controls was not significant. In contrast, plants inoculated with *Penicillium* E7 did not show visual symptoms of stress such as dry leaves, but showed a significant decrease in biomass production under the tap water treatment; in the salinity treatment the difference in biomass was not significant with respect to uninoculated plants. In addition, the biomass of plants inoculated with *Penicillium* E7 did not differ between tap water and salinity treatments.

Sodium was significantly affected by salt (p < 0.001), endophyte inoculated (p < 0.001) and their interaction (p = 0.002). Inoculated plants with *Periconia* S6 and *Diaporthe* S69 strains had greater Na than controls under tap water treatment (**Figure 7**). When plants were salt irrigated, the increase in Na was greater in plants inoculated with E7, S6 or S69 strains than in control plants. Potassium content was significantly affected by salt (p = 0.038), endophyte inoculated (p < 0.001) and their interaction (p = 0.003). Inoculated plants with E7, S6 or S69

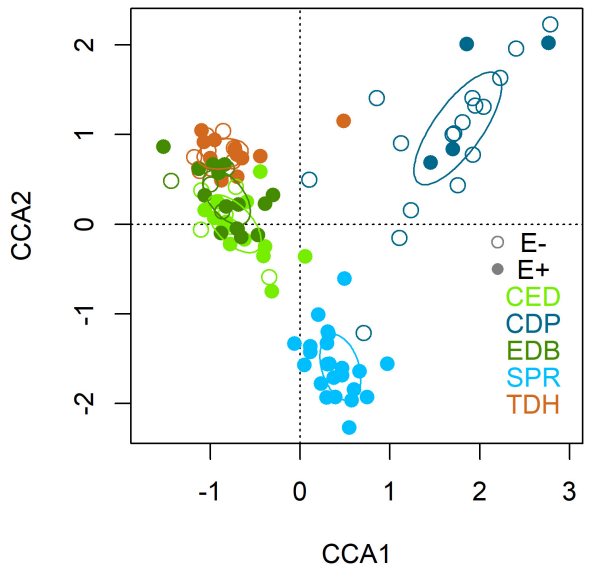

FIGURE 5 | Canonical correspondence analysis (CCA) of the fungal endophyte community composition of roots of *Festuca rubra* subsp. *pruinosa* from marine cliffs according to the presence (E+) or absence (E–) of *Epichloë festucae,* and population (CED, Cedeira; CDP, Cabo de Peñas; EDB, Estaca de Bares; SPR, San Pedro de la Rivera; TDH, Torre de Hércules).

strains had significantly greater K concentration than controls at water treatment (**Figure 7**). At salt treatment, plants inoculated with *Penicillium* E7 had the greatest K content.

After the harvest, root fragments of *Lolium perenne* were plated on culture media and the fungal isolates obtained were identified through morphological characteristics as the endophytes inoculated into the plants. The reisolation of these fungi indicated their compatibility with *L. perenne* and the success of plant inoculation.

DISCUSSION

The Core Microbiome of *Festuca rubra* subsp. *pruinosa*

The roots of *Festuca rubra* subsp. *pruinosa* were found to be a niche containing numerous fungal species, an assemblage of 135 culturable species was identified. This magnitude is not unusual in surveys of the mycobiota of grasses (Sánchez Márquez et al., 2012), but the high incidence of seven species that were present in more than 20% of the plants, and in several populations is remarkable. These species were *Fusarium oxysporum*, *Diaporthe* sp. A, *Fusarium* sp. A, Helotiales sp. A, *Drechslera* sp., *Slopeiomyces cylindrosporus,* and *Penicillium* sp. F. In particular, *Fusarium oxysporum* and *Diaporthe* sp. A occurred in more than 50% of the plants, and at all five populations examined. Those seven fungal species seem to be components of the core microbiome of FRP, because they are shared by a significant number of plants, and occur at different populations (Shade and Handelsman, 2012). It is not common to find a group of fungal species with such high incidence within and among plant populations. Using similar methodology, as well as culture independent methods, no more than two or three species with an incidence greater than 20% were found in surveys of other grasses (Sánchez Márquez et al., 2008, 2010; Ofek-Lalzar et al., 2016; Zhong et al., 2018). In addition, dominant species reported in several taxa of inland grasses, such as *Cladosporium* or *Epicoccum*, were absent from FRP plants (Peláez et al., 1998; Sánchez Márquez et al., 2012; Ofek-Lalzar et al., 2016).

Two of the core taxa of FRP belonged to the genus *Fusarium*. Although this genus is best known due to important pathogens of numerous agricultural species, it is also one of the most commonly isolated genera of endophytes from grasses and other plants (Vázquez de Aldana et al., 2013; Martins et al., 2016; Lofgren et al., 2018). Research on endophytic *Fusarium* has shown that some strains can improve the salinity tolerance of their host plants (Rodriguez and Redman, 2008; Redman et al., 2011). Furthermore, *F. oxysporum* strains obtained from FRP plants in this study were found to protect tomato plants against a pathogenic strain of *F. oxysporum* f.sp. *lycopersici* (Constantin et al., 2017).

The genus *Diaporthe* contains numerous species that behave as endophytes or pathogens, and in some cases as both, depending on the host plant species (Gomes et al., 2013). *Diaporthe* sp. A is a main component of the core microbiome of FRP, and species of this genus have also been reported as dominant components of the microbiome of olive and other plants (Martins et al., 2016; Noriler et al., 2018). Regarding mutualism, *Diaporthe* strains originally isolated from wild plant species promoted the growth of rice and tritordeum (Yang et al., 2015; Zabalgogeazcoa et al., 2018).

Our work revealed that associations between DSE and FRP roots are common in sea cliffs. Some of the core and most abundant taxa, such as *Darksidea* sp., *Periconia macrospinosa, Slopeiomyces cylindrosporus* and *Drechslera* sp., were previously reported as DSE in other grasses (Hornby et al., 1977; Knapp et al., 2012, 2015; Siless et al., 2018). In addition, Helotiales sp. A also seems to be a DSE because its hyphae had characteristics of this group, and other members of the Helotiales (i.e., *Phialocephala fortinii*) are recognized as DSE (Sieber and Grünig, 2013; Ridout et al., 2017). DSE colonize roots of plants communities in different habitats, and some authors hypothesized that these fungi can play an important role in plant adaptation to abiotic stress conditions, especially drought (Porras-Alfaro et al., 2008; Knapp et al., 2015). However, in spite of their abundance in nature, there is still uncertainty about the ecological significance of plant-DSE symbioses (Mandyam and Jumpponen, 2014).

Given the characteristics of the FRP habitat, strains from taxa belonging to the core microbiome of FRP are excellent candidates to test their possible role in host plant adaptation to salinity. Habitat-adapted symbiosis is a phenomenon which occurs when plants establish relationships with symbionts which enhance their adaptation to a particular stress factor present in their habitat (Rodriguez and Redman, 2008). Whether this occurs in the plant-endophyte systems here described would require inoculation of FRP seedlings and evaluation of plant performance

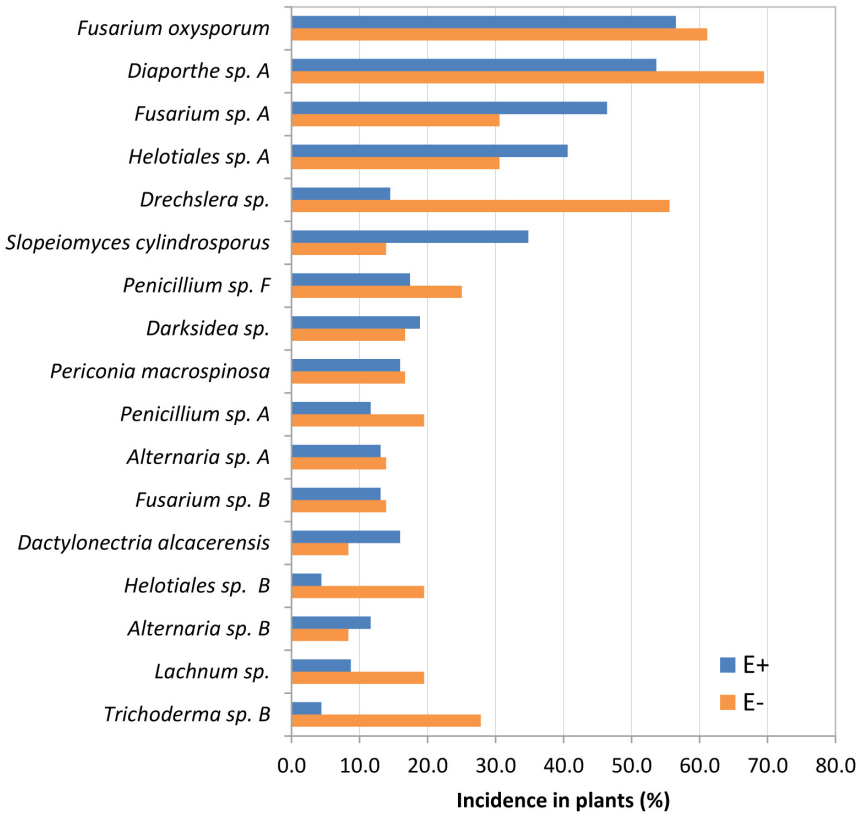

FIGURE 6 | Incidence in plants of *Festuca rubra* subsp. *pruinosa* from marine cliffs infected (E+) and not infected (E–) by *Epichloë festucae* of root species that constitute the core and abundant classes of the culturable mycobiome.

TABLE 4 | Jaccard index of similarity (bold) and number of fungal species identified in roots of each pair of populations (italic) of *Festuca rubra* subsp. *pruinosa* plants from marine cliffs.

Population	TDH	CED	EDB	SPR	CDP
TDH	**1.000**	**0.238**	**0.362**	**0.095**	**0.147**
CED	*63*	**1.000**	**0.300**	**0.182**	**0.154**
EDB	*58*	*70*	**1.000**	**0.193**	**0.182**
SPR	*84*	*88*	*88*	**1.000**	**0.238**
CDP	*68*	*78*	*77*	*84*	**1.000**

parameters under salinity stress. The search for endophytes from the core microbiome of wild plants adapted to unhospitable habitats has produced interesting solutions for the improvement of stress tolerance on agronomic crops (Redman et al., 2011; Ali et al., 2018).

Because of our research interest in culturable fungi, and the isolation methods used, components of the plant microbiome such as bacteria or non-culturable fungi were not identified in this survey. Members of these groups could have an important role in the adaptation of FRP plants to marine cliffs. For instance, symbioses with arbuscular mycorrizal fungi (AMF) can contribute to plant growth and protection under environmental stress (Lenoir et al., 2016). Symbiotic associations with AMF have been reported for some *Festuca* species (i.e., Dalpé and Aiken, 1998; Santos et al., 2006), but their presence and effects in FRP were not studied, and deserve attention.

In this work, about 72% of the fungal strains from FRP roots were classified as halophilic, their radial growth *in vitro* increased in the presence of NaCl. This category included some species of the core microbiome of FRP, like *Diaporthe* sp. A, *Fusarium oxysporum*, *Fusarium* sp. A, and Helotiales sp. A. In contrast, *E. festucae* showed a halosensitive response. The life cycle of this fungus which colonizes the intercellular space of aerial tissues and is seed transmitted, can be completely endophytic. Thus, host plants protect the fungus from the harmful saline environment. However, other fungal species which spend a part of their life cycle outside of their plant hosts might benefit from being halotolerant.

Cellulase or amylase enzymatic activity *in vitro* was detected in some of the core taxa, such as *Fusarium oxysporum,* Helotiales sp. A and *Penicillium* sp. F. These enzymes degrade cellulose and starch to soluble sugars such as glucose, cellobiose, and other oligomers which can be readily absorbed by plant roots (Carroll et al., 1983). Considering that FRP plants grow in rock fissures where soil and nutrients are very scarce, fungi with these enzymatic activities could have a role recycling nutrients from dead roots. However, these two enzymatic activities were not detected in cultures of *Slopeiomyces cylindrosporus*, a fungus with saprobic capability (Hornby et al., 1977), and cellulase activity

TABLE 5 | Radial growth of nine *Epichloë festucae strains* isolated from *Festuca rubra* subsp. *pruinosa* plants from marine cliffs in PDA plates with different NaCl concentrations.

Strain	Radial growth (cm)			Type of response
	0 mM	300 mM	600 mM	
TDH1	2.12 ab	2.40 b	1.60 a	Halosensitive
TDH11	1.97 ab	2.42 a	1.82 b	Halosensitive
TDH3	2.67 a	2.60 a	1.62 b	Halosensitive
CED6	2.67 a	2.17 ab	1.43 b	Halosensitive
CED12	2.43 a	2.37 a	1.55 b	Halosensitive
CED10	2.48 a	2.40 a	1.32 b	Halosensitive
CED1	2.42 a	2.33 a	1.42 b	Halosensitive
EDB9	2.37 a	1.25 b	0.67 c	Halosensitive
EDB11	2.85 a	1.65 b	0.68 c	Halosensitive

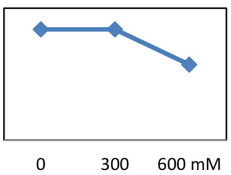

For each row different letters indicate significant differences at $p < 0.05$.

was absent form *Diaporthe* sp. A strains. This result could be due to non-induction of these enzymes in the culture medium used, because both fungal strains grew well as saprobes in a beet pulp medium, rich in carbohydrate and protein, which was used to prepare inoculum for plant inoculations.

Potential of FRP Endophytes for Plant Improvement

Knowledge about the role of endophytic fungi on plant adaptation to salinity stress is important because the world surface of saline soils is increasing, producing economic losses in crops (Munns and Gilliham, 2015). *Diaporthe* sp. A strain S69 improved the growth of plants of *Lolium perenne,* an important forage grass, in the presence and absence of salinity stress. On average, plants inoculated with *Diaporthe* S69 produced 31% more aerial biomass than the uninoculated controls under normal conditions, and 49% more under salinity stress. Similarly, fungal endophytes such as *Piriformospora indica*, *Fusarium culmorum*, or *Penicillium minioluteum* can alter physiological processes and improve tolerance to salt stress in agricultural crop species (Baltruschat et al., 2008; Khan et al., 2011; Redman et al., 2011).

One of the indirect consequences of salinity is an enrichment of Na and deficiency of K in plant cells, caused by the competition between Na and K, that have similar ionic radii and ion hydration energies (Munns and Tester, 2008). We found that *L. perenne* plants inoculated with *Periconia* S6, *Penicillium* E7 and *Diaporthe* S69 strains accumulated significantly more K in aboveground tissues under the tap water treatment than uninoculated plants; this suggests that an enrichment of Na due to salinity might have been prevented by the increased K content present before the stress. Similar results were observed in grasses inoculated with *Aspergillus aculeatus* (Xie et al., 2017) suggesting that the maintenance of a high level of K may contribute the alleviation of the negative effect of sodium. A beneficial effect of K accumulation in plants has also been reported for associations with arbuscular mycorrhiza (Langenfeld-Heyser et al., 2007) and *Epichloë* spp. (Chen et al., 2018). It is important to point out that the increase in biomass of *L. perenne* plants inoculated with *Diaporthe* strain S69 occurred not only during salt treatment but also in the tap water treatment. This implies that the fungal effect improving plant growth was not a specific process induced by salinity. To study the effect of fungal strains on plant parameters which can be altered by endophytes to improve plant performance, such as phytohormones, photosynthetic capacity, nutrient absorption or antioxidant capability (Baltruschat et al., 2008; Redman et al., 2011; Leitão and Enguita, 2016) is a future objective of our research.

Effect of *Epichloë festucae*, an Aboveground Tissue Endophyte, on Root Mycobiota

The incidence of *Epichlöe festucae* in FRP populations was 65.7%, a value very similar to that of 69% observed in a previous survey that included the same populations from Galicia (Zabalgogeazcoa et al., 2006). The relatively high incidence of *E. festucae* suggests that in an unhospitable habitat like sea cliffs, the costs of harboring a systemic symbiont could be compensated by mutualism. However, endophyte incidences closer to 100% could be expected under such circumstances. Whether natural selection favoring E+ plants, the efficiency of seed transmission, or a combination of both processes are involved in the prevalence rates of *Epichloë* observed in FRP populations is unknown, and deserves further study. Imperfect seed transmission (<100%) has been reported in other grass – *Epichloë* systems (Gundel et al., 2009). High incidence of *Epichloë festucae* in *Festuca rubra* populations has been reported in semiarid grasslands (70%) (Zabalgogeazcoa et al., 1999), or in the Scottish islands of St. Kilda (80%) (Bazely et al., 1997). In contrast, in Finland only 9 of 49 infected *F. rubra* populations had frequencies greater than 50% (Wali et al., 2007), and no plants harboring *Epichloë* were found in populations from subarctic regions of Canada (Santangelo and Kotanen, 2016).

In some grass-endophyte associations *Epichloë* species could play a key role in salt tolerance. In pot experiments *Epichloë coenophiala* increased the root biomass of tall fescue (*Schedonorus arundinaceous*) (Sabzalian and Mirlohi, 2010), and another *Epichloë* species increased the shoot and root biomass

TABLE 6 | Cellulase and amylase activity in fungal strains isolated from roots *Festuca rubra* subsp. *pruinosa* plants from marine cliffs.

ID	Endophyte	Cellulase activity	Amylase activity
T16	*Alternaria* sp. *A*	–	++
C115	*Alternaria* sp. *B*	–	+
T90	*Codinaeopsis* sp.	++	–
C2	*Dactylonectria alcacerensis*	–	–
C1	*Darksidea* sp.	+	–
C7	*Darksidea* sp.	+	–
CP36	*Diaporthe* sp. A	–	–
EB4	*Diaporthe* sp. A	–	–
S129	*Diaporthe* sp. A	–	+
S32	*Diaporthe* sp. A	–	–
S69	*Diaporthe* sp. A	–	–
T18	*Diaporthe* sp. A	–	–
CP1	*Drechslera* sp.	–	–
E71	*Drechslera* sp.	–	–
T41	*Drechslera* sp.	–	–
T50	*Drechslera* sp.	–	–
CD8	*Epichloë festucae*	–	–
S13	*Fusarium* sp. A	+	–
T112	*Fusarium* sp. A	+	–
T6	*Fusarium* sp. A	+	–
C70	*Fusarium* sp. B	+	–
S38	*Fusarium* sp. B	+	+
CP3	*Fusarium oxysporum*	++	–
S10	*Fusarium oxysporum*	+	++
SP8	*Fusarium oxysporum*	+	–
T150	*Fusarium oxysporum*	+	–
E79	Helotiales sp. B	+++	–
S74	*Lachnum* sp.	–	–
C44	Helotiales sp. A	++	–
S75	Helotiales sp. A	++	–
T141	Helotiales sp. A	++	–
T29	Helotiales sp. A	+	–
T3	Helotiales sp. A	++	–
T114	*Penicillium* sp. F	++	+++
C13	*Penicillium* sp. A	+	+
E7	*Penicillium* sp. A	+++	+
T59	*Penicillium* sp. A	++	+
S6	*Periconia macrospinosa*	–	–
T131	*Periconia macrospinosa*	–	–
C43	*Slopeiomyces cylindrosporus*	–	–
S5	*Slopeiomyces cylindrosporus*	–	–
T70	*Slopeiomyces cylindrosporus*	–	–
CP17	*Trichoderma* sp. B	++	–

(–) No enzymatic activity; (+) Slight activity; halo < 3 mm. (++) Moderate activity; halo < 5 mm. (+++) High activity; halo > 5 mm.

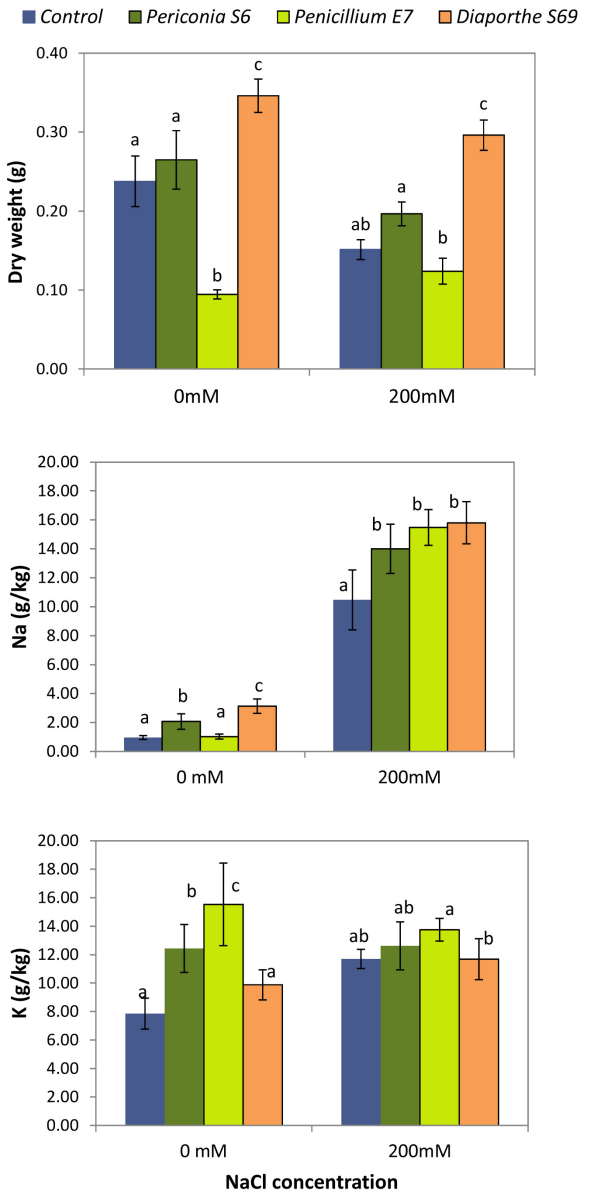

FIGURE 7 | Effect of inoculation with strains *Periconia* S6, *Penicillium* E7 and *Diaporthe* S69, isolated from *Festuca rubra* subsp. *pruinosa,* on dry matter production, and Na and K content of *Lolium perenne* plants watered with 0 mM and 200 mM NaCl. For each NaCl concentration, different letters indicate significantly different means ($p < 0.05$).

of wild barley (*Hordeum brevisubulatum*) under salinity stress (Song et al., 2015; Chen et al., 2018). In contrast, in FRP plants no significant effect of *Epichloë* on shoot dry weight was detected under salt treatment, although root growth or other parameters that could be affected by the presence of *E. festucae* under salinity were not analyzed (Zabalgogeazcoa et al., 2006). Nevertheless, in a stressful habitat like sea cliffs, environmental pressure on a holobiont might not necessarily affect an individual endophyte, but an assemblage where interactions among the plant host and the eukaryotic and prokaryotic microbiome components might be complex.

The presence of *Epichloë* in aboveground tissues of the host plant can affect underground processes by altering rhizospheric conditions that affect the density and activity of soil microorganisms (Omacini et al., 2012). This may result from endophyte effects on root exudates that can act as

chemical attractants or repellents in the rhizosphere (Malinowski et al., 1998). For instance, phenolic compounds are microbial inhibitors, and they increase in roots due to the presence of *Epichloë* (Ponce et al., 2009; Vázquez de Aldana et al., 2011). The effect of *Epichloë* on arbuscular mycorrhizal fungi has been extensively studied, and reduction, promotion, and null effects have been reported (Omacini et al., 2006; Novas et al., 2012; Rojas et al., 2016). Our results indicate that *E. festucae* did not have a clear and significant effect on the composition of the core microbiome or other mycobiota from FRP roots, although changes in the abundance of some species were found. These results are in agreement with other studies where the presence of *Epichloë* did not alter fungal colonization in roots (Vandegrift et al., 2015; Slaughter and McCulley, 2016) or shoots (Zabalgogeazcoa et al., 2013). Nevertheless, Zhong et al. (2018) reported that the presence of *Epichloë* decreased the diversity of root-associated fungi in *Achnatherum inebrians* and changed the community composition. However, such changes were in fungal orders with an abundance lower than 10%, where the number of isolates of these taxa can be low.

CONCLUSION

In conclusion, this study shows that numerous species of culturable fungi are associated to the roots of *Festuca rubra* subsp. *pruinosa* in its sea cliff habitat. Within this fungal assemblage of 135 species, a set of seven species occurred in a relatively high number of plants and locations, and those seem to be components of the core mycobiome of FRP: *Fusarium oxysporum*, *Diaporthe* sp. A, *Fusarium* sp. A, Helotiales sp. A, *Drechslera* sp., *Slopeiomyces cylindrosporus,* and *Penicillium* sp. F. Strains of these species are very promising candidates to study their role in the adaptation of FRP plants to salinity, a characteristic stress factor of their habitat. Furthermore, a *Diaporthe* strain belonging to the core taxa significantly improved the growth of *Lolium perenne* plants under normal and salinity stress conditions, showing the potential of the FRP core microbiome for the improvement of agricultural crops.

AUTHOR CONTRIBUTIONS

EP collected the plants, isolated and identified fungi, made the experiments, and analyzed the data. BA designed the experiments, participated in plant collection, and analyzed the data. LS made the statistical analyses. IZ supervised the research, helped to sample plants, designed the experiments and analyzed the data. EP, BA, and IZ wrote the article.

FUNDING

This study has received funding from the European Union's Horizon 2020 Research and Innovation Program under the Marie Skłodowska-Curie grant agreement no. 676480. LS was funded through a Talent Recruitment grant from "Obra Social La Caixa–Fundación CAN". We acknowledge support of the publication fee by the CSIC Open Access Publication Support Initiative through its Unit of Information Resources for Research (URICI).

ACKNOWLEDGMENTS

Martijn Rep and Maria Constantin, from the University of Amsterdam, helped to identify *Fusarium oxysporum* strains. The technical help of María José Cuesta and César Paredero are acknowledged.

SUPPLEMENTARY MATERIAL

The Supplementary Material for this article can be found online at: https://www.frontiersin.org/articles/10.3389/fmicb.2018.03321/full#supplementary-material

REFERENCES

AEMET (2012). *Guía Resumida del Clima en España 1981–2010. Gobierno de España*. Available at: http://www.aemet.es/es/serviciosclimaticos/datosclimatologicos/valoresclimatologicos

Ali, A. H., Abdelrahman, M., Radwan, U., El-Zayat, S., and El-Sayed, M. A. (2018). Effect of *Thermomyces* fungal endophyte isolated from extreme hot desert-adapted plant on heat stress tolerance of cucumber. *Appl. Soil Ecol.* 124, 155–162. doi: 10.1016/j.apsoil.2017.11.004

Baltruschat, H., Fodor, J., Harrach, B. D., Niemczyk, E., Barna, B., and Gullner, G. (2008). Salt tolerance of barley induced by the root endophyte *Piriformospora indica* is associated with a strong increase in antioxidants. *New Phytol.* 180, 501–510. doi: 10.1111/j.1469-8137.2008.02583.x

Bazely, D. R., Vicari, M., Emmerich, S., Filip, L., Lin, D., and Inman, A. (1997). Interactions between herbivores and endophyte-infected *Festuca rubra* from the Scottish islands of St. Kilda, Benbecula and Rum. *J. Appl. Ecol.* 34, 847–860. doi: 10.2307/2405276

Carroll, G., Petrini, G., and Petrini, O. (1983). Patterns of substrate utilization by some endophytes from coniferous foliage. *Mycologia* 75, 53–63. doi: 10.2307/3792923

Chen, T., Johnson, R., Chen, S., Lu, H., Zhou, J., and Li, C. (2018). Infection by the fungal endophyte *Epichloë bromicola* enhances the tolerance of wild barley (*Hordeum brevisubulatum*) to salt and alkali stresses. *Plant Soil* 428, 353–370. doi: 10.1007/s11104-018-3643-4

Clay, K., and Schardl, C. (2002). Evolutionary origins and ecological consequences of endophyte symbiosis with grasses. *Am. Natur.* 60, S99–S127. doi: 10.1086/342161

Colwell, R. K. (2005). *EstimateS: Statistical Estimation of Species Richness and Shared Species From Samples. Version 7.5.* Available at: http://purl.oclc.org/estimates.

Constantin, M. E., de Lamo, F., Takken, F., and Rep, M. (2017). "*Fusarium oxysporum* and its biocontrol," in *Proceedings of the Book of abstracts of the 29th Fungal Genetics Conference (2017 March14-19)* (Pacific Grove, CA: Genetics Society of America), 238.

Dalpé, Y., and Aiken, S. G. (1998). Arbuscular mycorrhizal fungi associated with *Festuca* species in the Canadian High Artic. *Can. J. Bot.* 76, 1930–1938. doi: 10.1139/b98-165

Doody, J. P. (2001). "Sea cliffs and sea cliff vegetation," in *Coastal Conservation and Management. An Ecological Perspective. Conservation Biology series*, Vol. 13, ed. J. P. Doody (Berlin: Springer Science), 25–52.

Gomes, R. R., Glienke, C., Videira, S. I. R., Lombard, L., Groenewald, J. Z., and Crous, P. W. (2013). Diaporthe: a genus of endophytic, saprobic and plant pathogenic fungi. *Persoonia* 31, 1–41. doi: 10.3767/003158513X666844

Gundel, P. E., Garibaldi, L. A., Tognetti, P. M., Aragon, R., Ghersa, C. M., and Omacini, M. (2009). Imperfect vertical transmission of the endophyte *Neotyphodium* in exotic grasses in grasslands of the flooding Pampa. *Microb. Ecol.* 57, 740–748. doi: 10.1007/s00248-008-9447-y

Hankin, L., and Anagnostakis, S. L. (1975). The use of solid media for detection of enzyme production by fungi. *Mycologia* 67, 597–607. doi: 10.2307/3758395

Hornby, D., Slope, D. B., Gutteridge, R. J., and Sivanesan, A. (1977). Gaeumannomyces cylindrosporus, a new ascomycete from cereal roots. *Trans. Br. Mycol. Soc.* 69, 21–25.

Humpreys, M. O. (1982). The genetic basis of tolerance to salt spry in popultions of *Festuca rubra* L. *New Phytol.* 91, 287–296. doi: 10.1111/j.1469-8137.1982.tb03313.x

Jaccard, P. (1912). The distribution of the flora in the alpine zone. *New Phytol.* 11, 37–50.

Khan, A., Hamayun, M., Ahmad, N., Hussain, J., Kang, S., Kim, Y., et al. (2011). Salinity stress resistance offered by endophytic fungal interaction between *Penicillium minioluteum* LHL09 and *Glycine max*, L. *J. Microbiol. Biotechnol.* 21, 893–902. doi: 10.4014/jmb.1103.03012

Knapp, D., Kovacs, G., Zajta, E., Groenewald, J., and Crous, P. (2015). Dark septate endophytic pleosporalean genera from semiarid areas. *Persoonia* 35, 87–100. doi: 10.3767/003158515X687669

Knapp, D., Pintye, A., and Kovács, G. (2012). The dark side is not fastidious – Dark septate endophytic fungi of native and invasive plants of semiarid sandy areas. *PLoS One* 7:e32570. doi: 10.1371/journal.pone.0032570

Koleff, P., Gaston, K. J., and Lennon, J. J. (2003). Measuring beta diversity for presence-absence data. *J. Anim. Ecol.* 72, 367–382. doi: 10.1046/j.1365-2656.2003.00710.x

Langenfeld-Heyser, R., Gao, J., Ducic, T., Tachd, P., Lu, C. F., Fritz, E., et al. (2007). *Paxillus involutus* mycorrhiza attenuate NaCl-stress responses in the salt-sensitive hybrid poplar *Populus* × *Canescens*. *Mycorrhiza* 17, 121–131. doi: 10.1007/s00572-006-0084-3

Leitão, A. L., and Enguita, F. J. (2016). Gibberellins in *Penicillium* strains: challenges for endophyte-plant host interactions under salinity stress. *Microbiol. Res.* 183, 8–18. doi: 10.1016/j.micres.2015.11.004

Lenoir, I., Fontaine, J., and Sahraoui, A. (2016). Arbuscular mycorrhizal fungal responses to abiotic stresses: a review. *Phytochemistry* 123, 4–15. doi: 10.1016/j.phytochem.2016.01.002

Lepš, J., and Šmilauer, P. (2003). *Multivariate Analysis of Ecological Data Using CANOCO*. Cambridge: Cambridge University Press.

Leuchtmann, A., Schardl, C. L., and Siegel, M. R. (1994). Sexual compatibility and taxonomy of a new species of *Epichloë* symbiotic with fine fescue grasses. *Mycologia* 8, 6802–6812. doi: 10.2307/3760595

Lofgren, L. A., LeBlanc, N. R., Certano, A. K., Nachtigall, J., LaBine, K. M., Riddle, J., et al. (2018). *Fusarium graminearum*: pathogen or endophyte of North American grasses? *New Phytol.* 217, 1203–1212. doi: 10.1111/nph.14894

López-Bedoya, J. L., and Pérez-Alberti, A. (2009). "1230 Acantilados con vegetación de las costas atlánticas y bálticas," in *Bases Ecológicas Preliminares para la Conservación de los Tipos de Hábitat de Interés Comunitario en España* (Madrid: Ministerio de Medio Ambiente, y Medio Rural y Marino), 1–144.

Malinowski, D. P., Alloush, G. A., and Belesky, D. P. (1998). Evidence for chemical changes on the root surface of tall fescue in response to infection with the fungal endophyte *Neotyphodium coenophialum*. *Plant Soil* 205, 1–12. doi: 10.1023/A:1004331932018

Mandyam, K., and Jumpponen, A. (2014). "Unraveling the dark septate endophyte functions: insights from the *Arabidopsis* model," in *Advances in Endophytic Research*, eds V. C. Verma and A. C. Gange (India: Springer), 115–141. doi: 10.1007/978-81-322-1575-2_6

Markgraf-Dannenberg, I. (1980). '*Festuca* L,' in *Flora Europaea*, eds T. G. Tutin, V. H. Heywood, N. A. Burges, D. M. Moore, D. H. Valentine, S. M. Walters et al. (Cambridge: University Press), 125–153.

Martínez Sagarra, G., Abad, P., and Devesa, J. A. (2017). Study of the leaf anatomy in cross-section in the Iberian species of *Festuca* L. (Poaceae) and its systematic significance. *PhytoKeys* 83, 43–74. doi: 10.3897/phytokeys.83.13746

Martins, F., Pereira, J. A., Bota, P., Bento, A., and Baptista, P. (2016). Fungal endophyte communities in above- and belowground olive tree organs and the effect of season and geographic location on their structures. *Fungal Ecol.* 20, 193–201. doi: 10.1016/j.funeco.2016.01.005

Munns, R., and Gilliham, M. (2015). Salinity tolerance of crops – What is the cost? *New Phytol.* 208, 668–673. doi: 10.1111/nph.13519

Munns, R., and Tester, M. (2008). Mechanisms of salinity tolerance. *Ann. Rev. Plant Biol.* 59, 651–681. doi: 10.1146/annurev.arplant.59.032607.092911

NCBI (2004). *Using BLASTClust to Make Non-Redundant Sequence Sets*. NCBI News. Available at: https://www.ncbi.nlm.nih.gov/Web/Newsltr/Spring04/blastlab.html

Noriler, S. A., Savi, D. C., Aluizio, R., Palácio-Cortes, A. M., Possiede, Y. M., and Glienke, C. (2018). Bioprospecting and structure of fungal endophyte communities found in the *Brazilian biomes, Pantanal,* and *Cerrado*. *Front. Microbiol.* 9:1526. doi: 10.3389/fmicb.2018.01526

Novas, M. V., Iannone, L. J., Godeas, A. M., and Scervino, J. M. (2012). Evidence for leaf endophyte regulation of root symbionts: effect of *Neotyphodium endophytes* on the pre-infective state of mycorrhizal fungi. *Symbiosis* 55, 19–28. doi: 10.1007/s13199-011-0140-4

Ofek-Lalzar, M., Gur, Y., Ben-Moshe, S., Sharon, O., Kosman, E., Mochli, E., et al. (2016). Diversity of fungal endophytes in recent and ancient wheat ancestors *Triticum dicoccoides* and *Aegilops sharonensis*. *FEMS Microbiol. Ecol.* 92:fiw152. doi: 10.1093/femsec/fiw152

Oksanen, J., Blanchet, F. G., Friendly, M., Kindt, R., Legendre, P., McGlinn, D., et al. (2017). *Vegan: Community Ecology Package. R package version 2.4-3*. Available at: https://CRAN.R-project.org/package=vegan

Omacini, M., Eggers, T., Bonkowski, M., Gange, A. C., and Jones, T. H. (2006). Leaf endophytes affect mycorrhizal status and growth of co-infected and neighbouring plants. *Funct. Ecol.* 20, 226–232. doi: 10.1111/j.1365-2435.2006.01099.x

Omacini, M., Semmartin, M., Pérez, L. I., and Gundel, P. E. (2012). Grass-endophyte symbiosis: a neglected aboveground interaction with multiple belowground consequences. *Appl. Soil Ecol.* 61, 273–279. doi: 10.1016/j.apsoil.2011.10.012

Ortuñez, E., and de la Fuente, V. (2010). Epidermal micromorphology of the genus *Festuca* L. (Poaceae) in the Iberian Peninsula. *Plant. Syst. Evol.* 284, 201–218. doi: 10.1007/s00606-009-0248-7

Peláez, F., Collado, J., Arenal, F., Basilio, A., Cabello, A., Díez Matas, M. T., et al. (1998). Endophytic fungi from plants living on gypsum soils as a source of secondary metabolites with antimicrobial activity. *Mycol. Res.* 102, 755–761.

Ponce, M. A., Bompadre, M. J., Scervino, J. M., Ocampo, J. A., Chaneton, E. J., and Godeas, A. M. (2009). Flavonoids, benzoic acids and cinnamic acids isolated from shoots and roots of Italian rye grass (*Lolium multiflorum* Lam.) with and without endophyte association and arbuscular mycorrhizal fungus. *Biochem. Syst. Ecol.* 37, 245–253. doi: 10.1016/j.bse.2009.03.010

Porras-Alfaro, A., Herrera, J., Sinsabaugh, R. L., Odenbach, K. J., Lowrey, T., and Natvig, D. O. (2008). Novel root fungal consortium associated with a dominant desert grass. *Appl. Environ. Microbiol.* 74, 2805–2813. doi: 10.1128/AEM.02769-07

Redman, R. S., Kim, Y. O., Woodward, C. J., Greer, C., Espino, L., Doty, S. L., et al. (2011). Increased fitness of rice plants to abiotic stress via habitat adapted symbiosis: a strategy for mitigating impacts of climate change. *PLoS One* 6:e14823. doi: 0.1371/journal.pone.0014823

Ridout, M., Houbraken, J., and Newcome, G. (2017). Xerotolerance of *Penicillium* and *Phialocephala fungi*, dominant taxa of fine lateral roots of woody plants in the intermountain Pacific Northwest, USA. *Rhizosphere* 4, 94–103. doi: 10.1016/j.rhisph.2017.09.004

Rodriguez, R., and Redman, R. (2008). More than 400 million years of evolution and some plants still can't make it on their own: plant stress tolerance via fungal symbiosis. *J. Exp. Bot.* 59, 1109–1114. doi: 10.1093/jxb/erm342

Rodriguez, R. J., Henson, J., Van Volkenburgh, E., Hoy, M., Wright, L., Beckwith, F., et al. (2008). Stress tolerance in plants via habitat-adapted symbiosis. *ISME J.* 2, 404–416. doi: 10.1038/ismej.2007.106

Rojas, X., Guo, J., Leff, J., McNear, D., Fierer, N., and McCulley, R. (2016). Infection with a shoot-specific fungal endophyte (Epichloë) alters tall fescue soil microbial communities. *Microb. Ecol.* 72, 197–206. doi: 10.1007/s00248-016-0750-8

Sabzalian, M., and Mirlohi, A. (2010). Neotyphodium endophytes trigger salt resistance in tall and meadow fescues. *J. Plant Nutur. Soil Sci.* 173, 952–957. doi: 10.1002/jpln.200900345

Sánchez Márquez, S., Bills, G. F., Acuña, L. D., and Zabalgogeazcoa, I. (2010). Endophytic mycobiota of leaves and roots of the grass *Holcus lanatus*. *Fungal Divers.* 41, 115–123.

Sánchez Márquez, S., Bills, G. F., Herrero, N., and Zabalgogeazcoa, I. (2012). Non-systemic fungal endophytes of grasses. *Fungal Ecol.* 5, 289–297. doi: 10.1016/j.funeco.2010.12.001

Sánchez Márquez, S., Bills, G. F., and Zabalgogeazcoa, I. (2008). Diversity and structure of the fungal endophytic assemblages from two sympatric coastal grasses. *Fungal Divers.* 33, 87–100.

Santangelo, J. S., and Kotanen, P. M. (2016). Nonsystemic fungal endophytes increase survival but reduce tolerance to simulated herbivory in subarctic *Festuca rubra*. *Ecosphere* 7:e01260. doi: 10.1002/ecs2.1260

Santos, J. C., Finlay, R. D., and Tehler, A. (2006). Molecular analysis of arbuscular mycorrhizal fungi colonising a seminatural grassland along a fertilisation gradient. *New Phytol.* 172, 159–168. doi: 10.1111/j.1469-8137.2006.01799.x

Shade, A., and Handelsman, J. (2012). Beyond the Venn diagram: the hunt for a core microbiome. *Environ. Microbiol.* 14, 4–12. doi: 10.1111/j.1462-2920.2011.02585.x

Sieber, T. H., and Grünig, C. R. (2013). "Fungal root endophytes," in *The Hidden Half*, eds A. Eshel and T. Beeckman. (Boca Raton: CRC Press). doi: 10.1201/9780203909423.ch49

Siless, G. E., Gallarfo, G. L., Rodriguez, M. J., Rincón, Y. A., Godeas, A. M., and Cabrera, G. M. (2018). Metabolites from the dark septate endophyte *Drechslera* sp. evaluation by LC/MS and principal component analysis of culture extracts with histone deacetylase inhibitors. *Chem. Biodivers.* 15:e1800133. doi: 10.1002/cbdv.201800133

Slaughter, L., and McCulley, R. (2016). Aboveground Epichloë coenophiala–Grass associations do not affect belowground fungal symbionts or associated plant, soil parameters. *Microb. Ecol.* 72, 682–691. doi: 10.1007/s00248-016-0828-3

Song, M., Chai, Q., Li, X., Yao, X., Li, C., Christensen, M., et al. (2015). An asexual Epichloë endophyte modifies the nutrient stoichiometry of wild barley (*Hordeum brevisubulatum*) under salt stress. *Plant Soil* 387, 153–165. doi: 10.1007/s11104-014-2289-0

Sunitha, V. H., Nirmala Devi, D., and Srinivas, C. (2013). Extracellular enzymatic activity of endophytic fungal strains isolated from medicinal plants. *World J. Agric. Sci.* 9, 1–9. doi: 10.5829/idosi.wjas.2013.9.1.72148

Vandegrift, R., Roy, B., Pfeifer-Meister, L., Johnson, B., and Bridgham, S. (2015). The herbaceous landlord: integrating the effects of symbiont consortia within a single host. *Peer J.* 3:e1379. doi: 10.7717/peerj.1379

Vázquez de Aldana, B. R., Bills, G., and Zabalgogeazcoa, I. (2013). Are endophytes an important link between airborne spores and allergen exposure? *Fungal Divers.* 60, 33–42. doi: 10.1007/s13225-013-0223-z

Vázquez de Aldana, B. R., Romo, M., Garcia-Ciudad, A., Petisco, C., and Garcia-Criado, B. (2011). Infection with the fungal endophyte *Epichloe festucae* may alter the allelopathic potential of red fescue. *Ann. Appl. Biol.* 159, 281–290. doi: 10.1111/j.1744-7348.2011.00495.x

Wali, P. R., Ahlholm, J. U., Helander, M., and Saikkonen, K. (2007). Occurrence and genetic structure of the systemic grass endophyte *Epichloe festucae* in fine fescue populations. *Microb. Ecol.* 53, 20–29. doi: 10.1007/s00248-006-9076-2

Waller, F., Achatz, B., Baltruschat, H., Fodor, J., Becker, K., Fischer, M., et al. (2005). The endophytic fungus *Piriformospora indica* reprograms barley to salt-stress tolerance, disease resistance, and higher yield. *Proc. Nat. Acad. Sci. U.S.A.* 102, 13386–13391. doi: 10.1073/pnas.0504423102

White, T. J., Bruns, T., Lee, S., and Taylor, J. (1990). "Amplificacition and direct sequencing of fungal rigosomal RNA genes for phylogenetics," in *PCR Protocols: A guide to Methods and Applications*, ed M. A. Innis (San Diego, CA: Academic Press), 315–322.

Xie, Y., Han, S., Li, X., Amombo, E., and Fu, J. (2017). Amelioration of salt stress on bermudagrass by the fungus *Aspergillus aculeatus*. *Mol. Plant-Microbe Interact.* 30, 245–254. doi: 10.1094/MPMI-12-16-0263-R

Yang, B., Wang, X. M., Ma, H. Y., Yang, T., Jia, Y., Zhou, J., et al. (2015). Fungal endophyte *Phomopsis liquidambari* affects nitrogen transformation processes and related microorganisms in the rice rhizosphere. *Front. Microbiol.* 6:982. doi: 10.3389/fmicb.2015.00982

Zabalgogeazcoa, I., Cuesta, M. J., Arellano, J. B., Mellado-Ortega, E., Oiz, L. F., Oiz, L., et al. (2018). "A *Diaporthe endophyte* improves the field performance of tritordeum," in *Proceedings of the Book of Abstracts of the 10th International Symposium on Fungal Endophytes of Grasses*, eds B. R. Vázquez de Aldana and I. Zabalgogeazcoa (Salamanca: Universidad de Salamanca), 121.

Zabalgogeazcoa, I., Gundel, P., Helander, M., and Saikkonen, K. (2013). Non-systemic fungal endophytes in *Festuca rubra* plants infected by *Epichloë festucae* in subarctic habitats. *Fungal Divers.* 60, 25–32. doi: 10.1007/s13225-013-0233-x

Zabalgogeazcoa, I., Romo, M., Keck, E., Vázquez de Aldana, B., García Ciudad, A., García Criado, B., et al. (2006). The infection of *Festuca rubra* subsp. pruinosa by *Epichloë festucae*. *Grass Forage Sci.* 61, 71–76. doi: 10.1111/j.1365-2494.2006.00509.x

Zabalgogeazcoa, I., Vázquez de Aldana, B. R., García Criado, B., and García Ciudad, A. (1999). The infection of *Festuca rubra* by the fungal endophyte *Epichloë festucae* in Mediterranean permanent grasslands. *Grass Forage Sci.* 54, 91–95. doi: 10.1046/j.1365-2494.1999.00155.x

Zhong, R., Xia, C., Ju, Y., Li, N., Zhang, X., Nan, Z., et al. (2018). Effects of *Epichloë gansuensis* on root-associated fungal communities of *Achnatherum inebrians* under different growth conditions. *Fungal Ecol.* 31, 29–36. doi: 10.1016/j.funeco.2017.10.005

Conflict of Interest Statement: The authors declare that the research was conducted in the absence of any commercial or financial relationships that could be construed as a potential conflict of interest.

frontiers in Plant Science

OPINION
published: 15 February 2019
doi: 10.3389/fpls.2019.00135

CRISPR-Cas for Fungal Genome Editing: A New Tool for the Management of Plant Diseases

Isabel Vicente Muñoz[1], *Sabrina Sarrocco*[1]*, *Luca Malfatti*[1], *Riccardo Baroncelli*[2] and *Giovanni Vannacci*[1]

[1] Department of Agriculture, Food and Environment, University of Pisa, Pisa, Italy, [2] Spanish-Portuguese Center for Agricultural Research (CIALE), Department of Microbiology and Genetics, University of Salamanca, Villamayor, Spain

Keywords: genome editing, CRISPR-Cas9, filamentous fungi, biocontrol, plant diseases management, fungal pathogens, beneficial fungi

BACKGROUND

Fungal pathogens are the main factors responsible for the most severe diseases affecting plants, leading to significant reduction in yield and crop quality and causing enormous economic losses worldwide. It is estimated that around 30% of the emerging diseases are caused by fungi (Giraud et al., 2010) thus requiring new strategies to improve their management. Biological control approach, frequently referred to the use of non-pathogenic microbial antagonists or products derived from their metabolism, represents a valid and promising alternative under a more ecological perspective to reduce the activities and to control populations of target pathogens (Singh, 2016). However, although the use of antagonists belonging to species different from that of the pathogen has been successfully reported, the use of competitors belonging to the same species of the pathogen is not widespread. A biocontrol strategy based on competition for space and nutrients and/or the induction of plant defenses against virulent pathogens performed by attenuated or avirulent pathogens (Ghorbanpour et al., 2018) could, therefore, be considered a valid alternative.

THE RESULTS SO FAR

Veloso et al. (2015) reported the use of an avirulent isolate of *Fusarium oxysporum* to reduce Verticillium wilt severity in pepper, through competition and induction of the plant defense responses. A similar approach was described by Salazar et al. (2012) for the management of anthracnose in strawberries. The avirulent isolate F7 of *Colletotrichum fragariae* conferred full protection from the infection caused by *C. acutatum* and also enhanced plant resistance against *Botrytis cinerea* through the induction of plant defense responses. Similarly, the use of an attenuated *Verticillium nigrescens* isolate reduced cotton wilt caused by a virulent isolate of *V. dahliae* (Vagelas and Leontopoulos, 2015).

(Aimé et al., 2013) used an avirulent isolate of *F. oxysporum* to combat *F. oxysporum* f. sp. *lycopersici* to reduce Fusarium wilt by priming a Salicylic-dependant signaling defense on tomato plants. The use of an avirulent strain of *Valsa mali* var. *mali* reduced the infection rate of apple tree canker caused by the virulent strain LXS080601 from 97 to 41% (Zhang et al., 2014) on apple callus. In 1993 as regards the mycotoxigenic fungi, Cotty and Bayman (1993) suggested the use of a non-aflatoxigenic isolate of *Aspergillus flavus* to control the development of aflatoxigenic strains in maize kernels by competitive exclusion and this strategy today is commercially applied in several countries (Ojiambo et al., 2018).

OPEN ACCESS

Edited by:
Ivan Baccelli, Istituto per la Protezione sostenibile delle Piante, Italy

Reviewed by:
Kemal Kazan, Commonwealth Scientific and Industrial Research Organization (CSIRO), Australia

***Correspondence:**
Sabrina Sarrocco
sabrina.sarrocco@unipi.it

Specialty section:
This article was submitted to Plant Microbe Interactions, a section of the journal Frontiers in Plant Science

Received: *29 November 2018*
Accepted: *28 January 2019*
Published: *15 February 2019*

Citation:
Muñoz IV, Sarrocco S, Malfatti L, Baroncelli R and Vannacci G (2019) CRISPR-Cas for Fungal Genome Editing: A New Tool for the Management of Plant Diseases. Front. Plant Sci. 10:135. doi: 10.3389/fpls.2019.00135

However, the selection of suitable isolates to be used as potential antagonists from the local fungal community often takes (long) time for identification and screening. Selection within a great number of isolates based on morphological, physiological and genetic features is usually required, followed by an *in vivo* screening against the pathogen on a real disease scenario. An interesting alternative to easily and quickly obtain new genotypes able to act as biocontrol agents, could be the induction of genetic mutations in the virulent genotypes, providing new avirulent strains that can compete directly with the virulent ones or induce plant defense responses (Ghorbanpour et al., 2018). The application of genetic transformation techniques to silencing genes putatively involved in pathogenicity has been widely used to uncoil the role of these genes in the establishment and development of the infection processes (Johnson et al., 2018). However, the disruption of a gene function usually involves the integration in the genome of foreign DNA sequences used as reporter genes in order to select transformants, leading to the generation of antibiotic-resistant or fluorescent strains. These genetic modifications represent a major constraint for their use in field.

THE GENOME-EDITING ERA: STATE OF THE ART AND PERSPECTIVES FOR THE MANAGEMENT OF PLANT DISEASES

The arrival of the CRISPR-Cas9 (Clustered Regularly Interspaced Short Palindromic Repeats – CRISPR Associated protein 9) genome-editing technique enabled researchers to modify genomic sequences in a more precise way (Knott and Doudna, 2018). CRISPR-Cas9 Type II system uses two principal components for gene targeting and cleavage: the RNA guide (sgRNA) and the Cas9 endonuclease. The sgRNA consists of a simple chimeric strand of RNA, which leads Cas9 up to the localization in the genome of the target gene, whose expression has to be blocked. Cas9 is able to bind the DNA and to produce a double strand break (DSB) in the target gene. The DSB then induces the activation of one of the DNA cellular reparation systems, the Non-Homologous End-Joining (NHEJ) system, that can re-join the ends of the DSB without introducing errors or, unlikely, giving rise to insertions or deletions of nucleotides during the repair. These InDels led to changes in the gene reading frame producing non-sense sequences or causing the appearance of premature stop codons, thus blocking the transcription of the target gene (Bono et al., 2015). In most cases the application of the technique in filamentous fungi consisted of a proof of concept of its feasibility (see **Table 1**). The system has the advantage that once implemented in the organism, it is possible to change the target gene by changing the sgRNA spacer sequence, as well as silencing several genes simultaneously by transforming the cell with different sgRNAs along with Cas9 (Hsu et al., 2015). Nevertheless, the most interesting advantage is that it allows to perform marker-free deletions by using transient expression plasmids that can self-replicate only under antibiotic pressure (Katayama et al., 2015, Nødvig et al., 2015; Schuster et al., 2016; Zhang et al., 2016; Liu et al., 2017; Wenderoth et al., 2017; Weyda et al., 2017; Wang et al., 2018). The use of CRISPR-Cas not only provides a time-saving path to perform genomic functional analyses, but also could provide new fungal genotypes, that can be used as potential competitors of plant pathogens and/or in the priming of plant defense responses.

One possible scenario for the application of CRISPR-Cas9 silenced mutants could be Fusarium Head Blight (FHB), one of the most destructive diseases of grain cereal crops worldwide caused by different *Fusarium* spp., with *F. graminearum* and *F. culmorum* as the most common and aggressive agents. In FHB, while yield loss derives from sterility of infected florets, grain quality reduction is mainly due to the accumulation of trichothecenes—coded by the fungal *tri* genes cluster—highly toxic for humans and animals. Previous studies reported that iRNA (interference RNA) Δ*tri6* mutants of *F. culmorum* showed reduced disease indices ranging from 40 to 80% on durum wheat (Scherm et al., 2011). In addition, classic knocked-out Δ*tri5* and Δ*tri6* mutants of *F. graminearum* were unable to spread the disease to the adjacent spikelets and grains on wheat and corn, respectively, and also induced plant defense responses (Ravensdale et al., 2014). Likewise, Δ*map1* mutants of *F. graminearum* showed two-fold reduction of mycotoxin production and were unable to produce perithecia as well as to penetrate in wheat tissues, while the ability to colonize the straw was not affected (Urban et al., 2003). Considering that competition for space and nutrients between virulent and non-virulent strains could reduce the disease, the field release of non-virulent CRISPR-mutant strains of *F. graminearum* and *F. culmorum* might help to control the incidence of FHB

Another contribution of CRISPR-Cas9 is the production of well-known antagonists with enhanced biocontrol aptitudes achieved through genome-editing (Vicente Muñoz et al., 2017). For example, species belonging to genus *Trichoderma* have been considered outstanding biocontrol agents able to reduce the disease severity (Sarrocco et al., 2013), not only by constraining the growth of the phytopathogens (Sarrocco et al., 2009), even killing them, but also by eliciting the plant defense responses (Fiorini et al., 2016; Sarrocco et al., 2017). One of the mechanisms through which these fungi can antagonize phytopathogenic fungi is the release of a wide arsenal of cell-wall degrading enzymes and secondary metabolites such as antibiotics, among others (Khalid, 2017).

Genetic engineering of the metabolic pathways that trigger the biosynthesis of secreted proteins and secondary compounds could provide new fungal strains with enhanced biocontrol activity. Previous studies reported that it is possible to achieve the same effect through the silencing of negative regulatory elements, signal-transduction components or genes belonging to contiguous metabolic networks, thus, redirecting metabolite flow and biosynthesis or supressing the feedback inhibition by which its production could be regulated (Bailey, 1991). For example, Δ*tvk1* mutants of *T. virens* displayed enhanced biocontrol activity against *R. solani,* in addition to an increased expression of mycoparasitism-related genes and overproduction of lytic enzymes (Mendoza-Mendoza et al., 2003). Likewise, four knockout mutants in SSCPs (small secreted cysteine rich proteins)-encoding genes of *T. virens* showed greater

TABLE 1 | Application of CRISPR-Cas9 for gene-silencing in filamentous fungi.

Fungal species	Edited gene	Aim	References
Alternaria alternata	Polyketide synthase A (*pksA*) 1,3,8-THN reductase (*bmr2*)	Proof of concept	Wenderoth et al., 2017
Aspergillus aculeatus *Aspergillus brasilensis* *Aspergillus carbonarius* *Aspergillus luchuensis* *Aspergillus nidulans* *Aspergillus niger*	Polyketide synthase (albA) Laccase (yA)	Proof of concept	Nødvig et al., 2015
Aspergillus carbonarius	Pigment biosynthetic gene (*ayg1*)	Proof of concept	Weyda et al., 2017
Aspergillus fumigatus	Polyketide synthase P (*pksP*)	Proof of concept	Zhang et al., 2016
Aspergillus nidulans *Aspergillus niger* *Aspergillus oryzae*	Laccase (*yA*) Polyketide synthase (*albA*) Polyketide synthase (*wA*)	Proof of concept	Nødvig et al., 2018
Aspergillus niger	AMP-dependent synthetase and ligase α-aminoadipate-semialdehyde dehydrogenase Aldo/keto reductase Alcohol dehydrogenase, zinc-binding Short-chain dehydrogenase/reductase FAD-dependent oxidoreductase Mandelate racemase/muconate lactonizing enzyme d-isomer specific 2-hydroxyacid dehydrogenase	Production of galactaric acid	Kuivanen et al., 2016
Aspergillus niger	Polyketide synthase (*albA*)	Proof of concept	Zheng et al., 2018
Aspergillus oryzae	Polyketide synthase (*wA*) Conidial laccase (*yA*) Orotidine 5-phosphate decarboxylase (*pyrG*)	Proof of concept	Katayama et al., 2015
Fusarium graminearum	Histidine kinase 1 (*os1*) Trichodiene synthase (*tri5*)	Proof of concept	Gardiner and Kazan, 2018
Fusarium oxysporum	Orotate phosphoribosiltransferase (*ura3, ura5*) Polyketide synthase 4 (*pks4*)	Proof of concept	Wang et al., 2018
Ganoderma lucidum *Ganoderma lingzhi*	Orotate phosphoribosyltransferase (ura3)	Proof of concept	Qin et al., 2017
Myceliopthora thermophila *Myceliopthora heterotalica*	Carbon catabolite repression transcription factor (*cre-1*) Endoplasmic reticulum stress regulator (*res-1*) β-glucosidase (*gh1-1*) Alkaline protease (*alp-1*)	Enhancement of lignocellulase production	Liu et al., 2017
Neurospora crassa	Carbon catabolism repressor (*cre-1)*	Enhancement of cellulase production	Matsu-ura et al., 2018
Penicillium chrysogenum	Polyketide synthase (*pks17*)	Proof of concept	Pohl et al., 2016, 2018
Pyricularia oryzae	Scytalone dehydratase (*sdh*) suppressor of RAD six (*sdr2*)	Proof of concept	Arazoe et al., 2015
Trichoderma reesei	Transcription factor in cellulase biosynthesis (*clr2*) Orotate phosphoribosyltransferase (*ura5*) Gene putatively involved in glucose signaling and carbon catabolism repression (*vib1*) Methyltransferase (*lae1*)	Proof of concept	Liu et al., 2015
Sclerotinia sclerotiorum	Oxaloacetate acetylhydrolase (*Ssoah1*) Polyketide synthase (*Sspks13*)	Proof of concept Pathogenicity test	Li et al., 2018
Ustilago maydis	Central regulator of pathogenic development (*bW2*) (*bE1*)	Proof of concept	Schuster et al., 2016

ability to induce ISR (Induced Systemic Resistance) on corn against *Cochliobolus heterostrophus* than the wild type (Lamdan et al., 2015). Another example of biocontrol enhanced ability was described by Reithner et al. (2005) in *T. atroviride*, in which the Δ*tga1* mutants exhibited an overproduction of antifungal secondary metabolites. Similarly, the Δ*tmk1* mutants of *T. atroviride* showed overproduction of 6-pentyl-pyrone and peptaibols, resulting in an enhanced antifungal activity and increased protection of bean plants against *Rhizoctonia solani* (Reithner et al., 2007). On the other hand, biosynthesis of secondary metabolites is often carried out by clustered genes whose expression could be induced by environmental conditions.

However, in many cases these clusters are silent and their activation cannot be achieved (Osbourn, 2010). Bok et al. (2009) demonstrated that the silencing of a transcription factor involved in the methylation of lysine 4 of the histone H3 in *Aspergillus nidulans* activated the expression of cryptic clusters and yielded novel secondary metabolites. The silencing of *ace1* gene induces the up-regulation of four polyketide biosynthetic gene clusters in *T. atroviride*, leading to an increase in the production of antibiotics and other secondary metabolites that clearly enhanced its potential as biocontrol agent against *F. oxysporum* and *R. solani* (Fang and Chen, 2018). Following this approach, it is possible to induce the activation of unknown clusters in beneficial fungi by using CRISPR-Cas9, allowing the discovery of new secondary metabolites that could interact with plants or phytopathogens. This could result in new interesting biocontrol strains to be released in field avoiding the introduction of transgenes in the environment.

CONCLUSIONS

The availability of novel or the improvement of known techniques that are safer for people and the environment is of outmost importance to guarantee food safety and security especially in those countries where famine is still an important issue (Vurro et al., 2010). A novel technique that allows the production of precise knock-out mutants without the insertion of foreign DNA in a saprotrophic/pathogenic fungus opens new possibilities of controlling plant pathogens. The use of such edited fungal strains needs a correct strategy to minimize possible risks. The major risk related to the release of a mutant strain is the rise, in the field, of novel combinations of pathogenesis/fitness related genes following the sexual or parasexual cycle. The genetic background of an edited isolate and its wild type is exactly the same, except for the edited gene, thus novel combinations of genes are not conceivable. Anyway, to further reduce such possibility, we can imagine a strategy of deployment that includes 1) the gene edit of the most prevalent genotype of the pathogen/saprotroph in the release area; 2) the editing of more than one gene in the same metabolic pathway and 3) the editing also of the idiomorphs and /or the HET genes, to make sexual or parasexual recombination (including the re-gain of virulence) even less likely.

Anyway, the application of novel techniques and the release of new products need, as usual, to be evaluated for their safety and to be accepted by populations. A recent sentence of the Court of Justice of the EU stated that edited organisms, even if they do not contain alien DNA, have to be subjected to the rules set up for Genetically Modified Organisms. This is not the place to discuss this issue, but it is high time, in EU at least, to reconsider the whole GMO legislation.

AUTHOR CONTRIBUTIONS

All authors listed have made a substantial, direct and intellectual contribution to the work, and approved it for publication.

REFERENCES

Aimé, S., Alabouvette, C., Steinberg, C., and Olivain, C. (2013). The endophytic strain *Fusarium oxysporum* Fo47: a good candidate for priming the defense responses in tomato roots. *Mol. Plant Microbe Interact.* 26, 918–926. doi: 10.1094/MPMI-12-12-0290-R

Arazoe, T., Miyoshi, K., Yamato, T., Ogawa, T., Ohsato, S., Arie, T., et al. (2015). Tailor-made CRISPR/Cas system for highly efficient targeted gene replacement in the rice blast fungus. *Biotech. Bioeng.* 112, 2543–2549. doi: 10.1002/bit.25662

Bailey, J. (1991). Toward a science of metabolic engineering. *Science* 252, 1668–1675. doi: 10.1126/science.2047876

Bok, J. W., Chiang, Y. M., Szewczyk, E., Reyes-Dominguez, Y., Davidson, A. D., Sanchez, J. F., et al. (2009). Chromatin-level regulation of biosynthetic gene clusters. *Nat. Chem. Biol.* 5, 462–464. doi: 10.1038/nchembio.177

Bono, J. M., Olesniky, E. C., Matzkin, L. M. (2015). Connecting genotypes, phenotypes and fitness: harnessing the power of CRISPR/Cas9 genome editing. *Mol. Ecol.* 24, 3810–3822. doi: 10.1111/mec.13252

Cotty, P. J., Bayman, P. (1993). Competitive exclusion of a toxigenic strain of *Aspergillus flavus* by an atoxigenic strain. *Phytopathology* 83, 1283–1287. doi: 10.1094/Phyto-83-1283

Fang, C., and Chen, X. (2018). Potential biocontrol efficacy of *Trichoderma atroviride* with cellulase expression regulator ace1 gene knock-out. *Biotechnology* 8:302. doi: 10.1007/s13205-018-1314-z

Fiorini, L., Guglielminetti, L., Mariotti, L., Curadi, M., Picciarelli, P., Scartazza, A., et al. (2016). *Trichoderma harzianum* T6776 modulates a complex metabolic network to stimulate tomato *cv* Micro-Tom growth. *Plant Soil* 400, 351–366. doi: 10.1007/s11104-015-2736-6

Gardiner, D. M., and Kazan, K. (2018). Selection is required for efficient Cas9-mediated genome editing in *Fusarium graminearum*. *Fungal Biol.* 122, 131–137. doi: 10.1016/j.funbio.2017.11.006

Ghorbanpour, M., Omidvari, M., Abbaszadeh-Dahaji, P., Omidvar, R., Kariman, K. (2018). Mechanisms underlying the protective effects of beneficial fungi against plant diseases. *Biol. Cont.* 117, 147–157. doi: 10.1016/j.biocontrol.2017.11.006

Giraud, T., Gladieux, P., Gavrilets, S. (2010). Linking the emergence of fungal plant diseases with ecological speciation. *Trends Ecol. Evol.* 25, 387–395. doi: 10.1016/j.tree.2010.03.006

Hsu, P. D., Lander, E. S., Zhang, F. (2015). Development and applications of CRISPR-Cas9 for genome engineering. *Cell* 157, 1262–1278. doi: 10.1016/j.cell.2014.05.010

Johnson, E. T., Proctor, R. H., Dunlap, C. A., Busman, M. (2018). Reducing production of fumonisin mycotoxins in *Fusarium verticillioides* by RNA interference. *Myc. Res.* 34, 29–37. doi: 10.1007/s12550-017-0296-8

Katayama, T., Tanaka, Y., Okabe, T., Nakamura, H., Fuji, W., Kitamoto, K., et al. (2015). Development of a genome editing technique using the CRISPR/Cas9 system in the industrial filamentous fungus *Aspergillus oryzae*. *Biotech. Lett.* 38, 637–642. doi: 10.1007/s10529-015-2015-x

Khalid, S. A. (2017). *Trichoderma* as biological control weapon against soil borne plant pathogens. *Afr. J. Biotech.* 16, 2299–2306. doi: 10.5897/AJB2017.16270

Knott, G. J., and Doudna, J. A. (2018). CRISPR-Cas guides the future of genetic engineering. *Science*. 361, 866–869. doi: 10.1126/science.aat5011

Kuivanen, J., Wang, Y. M. J., Richard, P. (2016). Engineering *Aspergillus niger* for galactaric acid production: elimination of galactaric acid catabolism by using RNA sequencing and CRISPR/Cas9. *Micr. Cell Fact.* 15:210.. doi: 10.1186/s12934-016-0613-5

Lamdan, N. L., Shalaby, S., Ziv, T., Kenerley, C. M., Horwitz, B. A. (2015). Secretome of *Trichoderma* interacting with maize roots: role in induced systemic resistance. *Mol. Cell. Prot.* 14, 1054–1063. doi: 10.1074/mcp.M114.046607

Li, J., Zhang, Y., Zhang, Y., Yu, P. L., Pan, H., and Rollins, J. A. (2018). Introduction of large sequence inserts by CRISPR-Cas9 to create pathogenicity mutants in the multinucleate filamentous pathogen *Sclerotinia sclerotiorum*. *mBio* 9:e00567–18. doi: 10.1128/mBio.00567-18

Liu, Q., Gao, R., Li, J., Lin, L., Zhao, J., Sun, W., et al. (2017). Development of a genome-editing CRISPR/Cas9 system in thermophilic fungal *Myceliophthora* species and its application to hyper-cellulase production strain engineering. *Biotech. Biofuels* 10:1. doi: 10.1186/s13068-016-0693-9

Liu, R., Chen, L., Jiang, Y., Zhou, Z., Zou, G. (2015). Efficient genome editing in filamentous fungus *Trichoderma reesei* using the CRISPR/Cas9 system. *Cell Disc.* 1:15007. doi: 10.1038/celldisc.2015.7

Matsu-ura, T., Dovzhenok, A. A., Coradetti, S. T., Subramanian, K. R., Meyer, D. R., Kwon, J. J., et al. (2018). Synthetic gene network with positive feedback loop amplifies cellulase gene expression in *Neurospora crassa*. *ACS Synth. Biol.* 7, 1395–1405. doi: 10.1021/acssynbio.8b00011

Mendoza-Mendoza, A., Pozo, M. J., Grzegorski, D., Martinez, P., Garcia, J. M., Olmedo-Monfil, V., et al. (2003). Enhanced biocontrol activity of *Trichoderma* through inactivation of a mitogen-activated protein kinase. *Proc Natl Acad Sci U.S.A.* 100, 15965–15970. doi: 10.1073/pnas.2136716100

Nødvig, C. S., Hoof, J. B., Kogle, M. E., Jarczynska, Z. D., Lehmbeck, J., Klitgaard, D. K., et al. (2018). Efficient oligo nucleotide mediated CRISPR-Cas9 gene editing in Aspergilli. *Fung. Gen. Biol.* 115, 78–89. doi: 10.1016/j.fgb.2018.01.004

Nødvig, C. S., Nielsen, J. B., Kogle, M. E., Mortensen, U. H. (2015). A CRISPR-Cas9 system for genetic engineering of filamentous fungi. *PLoS ONE* 10:e0133085. doi: 10.1371/journal.pone.0133085

Ojiambo, P. S., Battilani, P., Cary, J. W., Blum, B. H., Carbone, I. (2018). Cultural and genetic approaches to manage aflatoxin contamination: recent insights provide opportunities for improved control. *Phytopath* 108, 1024–1037. doi: 10.1094/PHYTO-04-18-0134-RVW

Osbourn, A. (2010). Secondary metabolic gene clusters: evolutionary toolkits for chemical innovation. *Trends Gen.* 26, 449–457. doi: 10.1016/j.tig.2010.07.001

Pohl, C., Kiel, J. A. K. W., Driessen, A. J. M., Bovenberg, R. A. L., Nygård,Y. (2016). CRISPR/Cas9 based genome editing of *Penicillium chrysogenum*. *Synth. Biol.* 5, 754–764. doi: 10.1021/acssynbio.6b00082

Pohl, C., Mózsik, L., Driessen, A. J. M., Bovenberg, R. A. L., Nygård, Y. I. (2018). Genome editing in *Penicillium chrysogenum* using Cas9 ribonucleoprotein particles. *Synth. Biol.* 1772, 213–232. doi: 10.1007/978-1-4939-7795-6_12

Qin, H., Xiao, H., Zou, G., Zhou, Z., Zhong, J. J. (2017). CRISPR-Cas9 assisted gene disruption in the higher fungus Ganoderma species. *Proc. Biochem.* 56, 57–61. doi: 10.1016/j.procbio.2017.02.012

Ravensdale, M., Rocheleau, H., Wang, L., Nasmith, C., Ouellet, T., Subramaniam, R. (2014). Components of priming-induced resistance to fusarium head blight in wheat revealed by two distinct mutants of *Fusarium graminearum*. *Mol. Plant Path.* 5, 948–956. doi: 10.1111/mpp.12145

Reithner, B., Brunner, K., Schuhmacher, R., Peissl, I., Seidl, V., Krska, R., et al. (2005). The G protein α subunit Tga1 of *Trichoderma atroviride* is involved in chitinase formation and differential production of antifungal metabolites. *Fung. Gen. Biol.*42, 749–760. doi: 10.1016/j.fgb.2005.04.009

Reithner, B., Schuhmacher, R., Stoppacher, N., Pucher, M., Brunner, K., Zeilinger, S. (2007). Signaling via the *Trichoderma atroviride* mitogen-activated protein kinase Tmk1 differentially affects mycoparasitism and plant protection. *Fung. Gen. Biol.* 44, 1123–1133. doi: 10.1016/j.fgb.2007.04.001

Salazar, S. M., Grellet, C. F., Chalfoun, N. R., Castagnaro, A. P., Díaz Ricci, J. C. (2012). Avirulent strain of Colletotrichum induces a systemic resistance in strawberry. *Eur. J. Plant Path.* 135, 877–888. doi: 10.1007/s10658-012-0134-y

Sarrocco, S., Guidi, L., Fambrini, S., Degl'Innocenti, E., Vannacci, G. (2009). Competition for cellulose exploitation between *Rhizoctonia solani* and two *Trichoderma* isolates in the decomposition of wheat straw. *J. Plant Path.* 91, 331–338.. doi: 10.4454/jpp.v91i2.962

Sarrocco, S., Matarese, F., Baroncelli, R., Seidl-Seiboth, V., Kubicek, C. P., Vannacci, G., et al. (2017). The constitutive endopolygalacturonase TvPG2 regulates the induction of plant systemic resistance by *Trichoderma virens*. *Phytopath ology* 107, 537–544. doi: 10.1094/PHYTO-03-16-0139-R

Sarrocco, S., Matarese, F., Moncini, L., Pachetti, G., Ritieni, A., Moretti, et al. (2013). Biocontrol of fusarium head blight by spike application of *Trichoderma gamsii*. *J. Plant Pathol.* S1, 19–27.

Scherm, B., Orr,ú, M., Balmas, V., Spanu, F., Azara, E., Delogu, G., et al. (2011). Altered trichothecene biosynthesis in TRI6-silenced transformants of *Fusarium culmorum* influences the severity of crown and foot rot on durum wheat seedlings. *Mol. Plant Pathol.* 12, 759–771. doi: 10.1111/j.1364-3703.2011.00709.x

Schuster, M., Schweizer, G., Reissmann, S., Kahmann, R. (2016). Genome editing in *Ustilago maydis* using the CRISPR–Cas system. *Fung. Gen. Biol.* 89, 3–9. doi: 10.1016/j.fgb.2015.09.001

Singh, S. (2016). Role of nonpathogenic fungi in inducing systemic resistance in crop plants against phytopathogens. *Micr. Inoc. Sust. Agric. Prod.* 69–83. doi: 10.1007/978-81-322-2644-4_5

Urban, M., Mott, E., Farley, T., Hammond-Kosack, K. (2003). The *Fusarium graminearum* MAP1 gene is essential for pathogenicity and development of perithecia. *Mol. Plant Pathol.* 4, 347–359. doi: 10.1046/j.1364-3703.2003.00183.x

Vagelas, J., and Leontopoulos, S. (2015). Cross-protection of cotton against *Verticillium* wilt by *Verticillium nigrescens*. *Emir. J. Food Agric.* 27, 687–691. doi: 10.9755/ejfa.2015-04-047

Veloso, J., Alabouvette, C., Olivain, C., Flors, V., Pastor, V., García, et al. (2015). Modes of action of the protective strain Fo47 in controlling Verticillium wilt of pepper. *Plant Pathol.* 65, 997–1007. doi: 10.1111/ppa.12477

Vicente Muñoz, I., Sarrocco, S., Vannacci, G. (2017). CRISPR-CAS for the genome editing of two *Trichoderma* spp. beneficial isolates. *J. Plant Pathol.* 99:S63. doi: 10.1038/srep45763

Vurro, M., Bonciani, B., Vannacci, G. (2010). Emerging infectious diseases of crop plants in developing countries: impact on agriculture and socio-economic consequences. *Food Sec.* 2, 113–132. doi: 10.1007/s12571-010-0062-7

Wang, Q., Cobine, P. A., Coleman, J. J. (2018). Efficient genome editing in *Fusarium oxysporum* based on CRISPR/Cas9 ribonucleoprotein complexes. *Fung. Gen. Biol.* 117, 21–29. doi: 10.1016/j.fgb.2018.05.003

Wenderoth, M., Pinecker, C., Vo,ß, B., Fischer, R. (2017). Establishment of CRISPR/Cas9 in *Alternaria alternata*. *Fung. Gen. Biol.* 101, 55–60. doi: 10.1016/j.fgb.2017.03.001

Weyda, I., Yang, L., Vang, J., Ahring, B. K., Lübeck, M., Lübeck, P. S. (2017). A comparison of Agrobacterium-mediated transformation and protoplast-mediated transformation with CRISPR-Cas9 and bipartite gene targeting substrates, as effective gene targeting tools for *Aspergillus carbonarius*. *J. Micrbiol. Methods* 135, 26–34. doi: 10.1016/j.mimet.2017.01.015

Zhang, C., Meng, X., Wei, X., Lu, L. (2016). Highly efficient CRISPR mutagenesis by microhomology-mediated end joining in *Aspergillus fumigatus*. *Fungal Gen. Biol.* 86, 47–57. doi: 10.1016/j.fgb.2015.12.007

Zhang, Q., Wang, C., Yong, D., Li, G., Dong, X., Li, B. (2014). Induction of resistance mediated by an attenuated strain of *Valsa mali* var.*mali* using pathogen-apple callus interaction system. *Sci. World J.* 2014:201382. doi: 10.1155/2014/201382

Zheng, X., Zheng, P., Sun, J., Kun, Z., Ma, Y. (2018). Heterologous and endogenous U6 snRNA promoters enable CRISPR/Cas9 mediated genome editing in *Aspergillus niger*. *Fung. Biol. Biotech.* 5:2. doi: 10.1186/s40694-018-0047-4

Conflict of Interest Statement: The authors declare that the research was conducted in the absence of any commercial or financial relationships that could be construed as a potential conflict of interest.

frontiers in Microbiology

ORIGINAL RESEARCH
published: 18 February 2019
doi: 10.3389/fmicb.2019.00261

Combined Metabarcoding and Co-occurrence Network Analysis to Profile the Bacterial, Fungal and *Fusarium* Communities and Their Interactions in Maize Stalks

*José Francisco Cobo-Díaz[1], Riccardo Baroncelli[2], Gaétan Le Floch[1] and Adeline Picot[1]**

[1] Laboratoire Universitaire de Biodiversité et Ecologie Microbienne, IBSAM, ESIAB, Université de Bretagne Occidentale, Plouzané, France, [2] Instituto Hispano-Luso de Investigaciones Agrarias (CIALE), University of Salamanca, Salamanca, Spain

OPEN ACCESS

Edited by:
David B. Collinge, University of Copenhagen, Denmark

Reviewed by:
Javier Plasencia, National Autonomous University of Mexico, Mexico
Tuan Duong, University of Pretoria, South Africa

***Correspondence:**
Adeline Picot
adeline.picot@univ-brest.fr

Specialty section:
This article was submitted to Plant Microbe Interactions, a section of the journal Frontiers in Microbiology

Received: *13 June 2018*
Accepted: *31 January 2019*
Published: *18 February 2019*

Citation:
Cobo-Díaz JF, Baroncelli R, Le Floch G and Picot A (2019) Combined Metabarcoding and Co-occurrence Network Analysis to Profile the Bacterial, Fungal and Fusarium Communities and Their Interactions in Maize Stalks. Front. Microbiol. 10:261. doi: 10.3389/fmicb.2019.00261

Fusarium Head Blight (FHB) is one of the most devastating diseases of cereals worldwide, threatening both crop production by affecting cereal grain development, and human and animal health by contaminating grains with mycotoxins. Despite that maize residues constitute the primary source of inoculum for *Fusarium* pathogenic species, the structure and diversity of *Fusarium* spp. and microbial communities in maize residues have received much less attention than in grains. In this study, a metabarcoding approach was used to study the bacterial, fungal and *Fusarium* communities encountered in maize stalks collected from 8 fields in Brittany, France, after maize harvest during fall 2015. Some predominant genera found in maize residues were cereal or maize pathogens, such as the fungal *Fusarium*, *Acremonium*, and *Phoma* genera, and the bacterial *Pseudomonas* and *Erwinia* genera. Furthermore, a high predominance of genera with previously reported biocontrol activity was found, including the bacterial *Sphingomonas*, *Pedobacter*, *Flavobacterium, Pseudomonas,* and *Janthinobacterium* genera; and the fungal *Epicoccum*, *Articulospora*, *Exophiala*, and *Sarocladium* genera. Among *Fusarium* spp., *F. graminearum* and *F. avenaceum* were dominant. We also found that the maize cultivar and previous crop could influence the structure of microbial communities. Using SparCC co-occurrence network analysis, significant negative correlations were obtained between *Fusarium* spp. responsible for FHB (including *F. graminearum* and *F. avenaceum*) and bacterial OTUs classified as *Sphingomonas* and fungal OTUs classified as *Sarocladium* and *Epicoccum*. Considering that isolates belonging to these taxa have already been associated with antagonist effect against different *Fusarium* spp. and/or other pathogenic microorganisms and due to their predominance and negative associations with *Fusarium* spp., they may be good candidates as biocontrol agents. Combining the use of *Fusarium*-specific primers with universal primers for bacteria and fungi allowed us to study the microbial communities,

but also to track correlations between *Fusarium* spp. and other bacterial and fungal genera, using co-occurrence network analysis. Such approach could be a useful tool as part of a screening strategy for novel antagonist candidates against toxigenic *Fusarium* spp., allowing the selection of taxa of interest.

Keywords: maize residues, bacterial communities, fungal communities, *Fusarium* communities, biocontrol agents, co-occurrence network

INTRODUCTION

Fusarium Head Blight (FHB) of cereals (Nazari et al., 2014) is caused by several *Fusarium* species among which *F. graminearum*, *F. culmorum*, *F. avenaceum,* and *F. poae* are the main causal agents in Europe (Xu et al., 2005; Hellin et al., 2016). FHB is one of the most important diseases affecting cereals worldwide (Ramirez et al., 2006; Bateman et al., 2007; Gong et al., 2015) and represents a threat to human and animal health due to the possible production of mycotoxins by *Fusarium* species (Desjardins and Proctor, 2007). Crop rotation, and in particular maize as previous crop, can increase the risk of FHB incidence as previous crop infected residues are the primary source of pathogenic species (Shaner, 2003; Bateman et al., 2007; Fernandez et al., 2008). A high incidence of *Fusarium* species was found in the first internode-stalk of maize plants (Scauflaire et al., 2011), which is usually left in the field, turning into a main inoculum source for the following crop (Maiorano et al., 2008). Current crop, cropping history and tillage system have a significant influence on *Fusarium* and fungal communities of crop residues (Fernandez et al., 2008), on maize rhizospheric microbiome (Benitez et al., 2017) and on bulk soil microbial communities (Legrand et al., 2018). Although the plant genotype affects the rhizosphere microbial communities in maize (Aira et al., 2010), no studies have focused on how maize genotype affect the phyllosphere or the crop residue microbiome.

The low efficacy of current control strategies, mainly based on agricultural practices including tillage and the use of less sensitive cultivars, is prompting the scientific community to seek alternatives. Among them, the application of biocontrol agent against *Fusarium* species has been one of the major focuses of current research due to their compliance with environmental standards. Several candidate antagonists have been developed after isolation of microbial strains from different parts of cereals, such as root rhizosphere from maize (Abiala et al., 2015) and barley (Abd El Daim et al., 2015), wheat anthers (Palazzini et al., 2007), seed endophytes from wheat (Díaz Herrera et al., 2016), endophytes from maize (Mousa et al., 2015), or even from maize residues (Luongo et al., 2005; Singh et al., 2009), agricultural soils (He et al., 2009), silages and forest soils (Baffoni et al., 2015). Generally, the isolation of antagonistic candidates is empirical and needs confrontation tests under laboratory conditions which are used to screen a high number of candidates before field evaluations (He et al., 2009; Schöneberg et al., 2015). The efficacy of antagonists is usually reduced under field conditions compared to laboratory conditions (Luongo et al., 2005; Crane et al., 2013; Schisler et al., 2015; Legrand et al., 2017), mainly because of the complex interactions of antagonists with their biotic and abiotic environment in the field. Alternatively, this stepwise approach may also result in the possible loss of isolates that does not pass laboratory selection step but have good efficacy under field conditions (Schöneberg et al., 2015). In the latter study, they found that *Clonostachys rosea*, a weak competitor in *in vitro* co-culture with two *F. graminearum* and one *F. crookwellense* strains, showed the best antagonist potential of the total 12 strains screened in the field and was the only one able to reduce FHB incidence when inoculated after the pathogen. To increase the efficacy, recent studies demonstrated a synergistic/antagonistic activity of cocktail strains, such as the use of seven species isolated from maize roots to increase the efficacy of protection against *F. verticillioides* in maize kernels (Niu et al., 2017); similar results have been reached using a consortium of individually non-antagonistic bacteria of *F. oxysporum* in *Arabidopsis thaliana* (Fujiwara et al., 2016). Such isolation approach, however, is time-consuming, and still lack of efficacy. Despite some promising results, only a limited number of FHB biocontrol agents are commercially available (Legrand et al., 2017).

These approaches could undoubtedly benefit from the use of -omics technologies to better describe the microbial community functioning and improve the screening of antagonist organisms. Indeed, we must first gain a deeper understanding of the microbiota to which pathogens are confronted, and study the diversity and structure of pathogens themselves, especially for complex pathosystems such as FHB. Such knowledge may help select more appropriate biocontrol strategies, adapted to the *Fusarium* and microbial communities, which may vary according to the pedo-climatic environment of the agroecosystem. Specific primers designed to track *Fusarium* communities in soils and in wheat kernels using Next Generation Sequencing (NGS) approaches have already been developed (Edel-Hermann et al., 2015; Karlsson et al., 2016) but no studies combined this approach with the use of universal primers for fungal and/or bacterial species. A few metabarcoding studies aimed at describing the microbial communities in maize crop bulk soils and/or rhizospheric soils (Peiffer et al., 2013; Li et al., 2014; Zhao et al., 2016), while other focused on the influence of the presence of maize residues on soil microbiota (Chen et al., 2015; De la Cruz-Barrón et al., 2017) but none were dedicated to the microbial communities found on maize crop residues. Yet, since the primary source of *Fusarium* spp. inoculum originates from infected maize crop residues, it is important to deepen the knowledge of microbial communities associated with maize stalks. Those communities may contribute to soil suppressiveness against *Fusarium* pathogenic species and may be a good source of potential antagonists. Such approaches have already been undertaken in suppressive soils to vanilla and banana Fusarium

wilt disease (Fu et al., 2017; Xiong et al., 2017) and in suppressive maize stalks to Fusarium ear rot (Köhl et al., 2015).

In this context, the aims of the present study were to (i) describe the bacterial, fungal and *Fusarium* communities found in maize stalks collected from fields after harvest in Brittany, France, using a metabarcoding approach; (ii) determine whether agronomic factors including the cultivar and/or the previous crop influence the microbial community structure and diversity; (iii) correlate the abundance of *Fusarium* pathogenic species with other bacterial and fungal taxa, using SparCC co-occurrence network analysis, as a preliminary step to identify potential antagonist microorganisms.

MATERIALS AND METHODS

Maize Stalk Sampling

Maize stalks were collected from eight agricultural fields across Brittany, France in November 2015. In total, seven fields were surveyed in Finistère (Gouesnou, Saint-Renan, Locmaria-Plouzané and Plouzané) and one in Ille-Et-Vilaine (Gennes sur Seiche) located approximately 300 km away from the other fields (**Figure 1**). Field characteristics including the maize types and varieties, the previous crop and tillage practices were recorded (**Figure 1**). In each field, the above-ground parts of 15 maize stalks with nodal region were randomly sampled. Stalks were sampled within 3 days after maize harvest and were stored at −80°C until DNA extraction, except the one in Ille-Et-Vilaine, which was sampled within a month after maize harvest. P1 was chosen as an outgroup to help interpret the degree of variability observed within the maize kernel silage fields from Finistère.

DNA Extraction

For each field, 15 stalks were randomly chosen and 3 groups of 3 stalks were randomly selected at laboratory with each group corresponding to a biological replicate. For each replicate, four different portions of approximately 1 cm (nodal, internodal without leave, internodal with leave, and the external part) were cut with a sterilized scalpel from each stalk, mixed altogether and ground with liquid nitrogen in an autoclaved mortar and pestle. The pulverized tissues were stored in 1.5 mL Eppendorf tubes at 4°C until DNA extraction, performed within 4 h. DNA was extracted from 200 mg of pulverized maize stalks using FastDNA®SPIN kit (MP Biomedicals, Santa Ana, CA, United States) following the manufacturer's instructions. Quality and concentration of purified DNA were determined using a UV spectrophotometer (NanoDrop 1000, Thermo Scientific, United States), and dilutions of at least 10 ng/μl were prepared for each DNA sample.

PCR Amplification and MiSeq Sequencing

A total of 24 samples (8 fields × 3 replicates) were selected for amplicon PCRs and high-throughput sequencing. Preparation of 16S rRNA, ITS and TEF1 libraries, and Illumina MiSeq 300 PE sequencing were performed at the McGill University and Génome Québec Innovation Centre, Montreal, Canada. Primers 341F (5′-CCTACGGGNGGCWGCAG-3′) and 805R (5′-GACTACHVGGGTATCTAATCC-3′) (Herlemann et al., 2011) were used to amplify the variable regions V3 and V4 of the 16S rRNA gene; primers ITS1F (5′-CTTGGTCATTTAGAGGAAGTAA-3′) and ITS4 (5′-TCCTCCGCTTATTGATATGC-3′) (White et al., 1990; Gardes and Bruns, 1993) to amplify the internal transcribed spacer; and primers TEF_FUS_F6

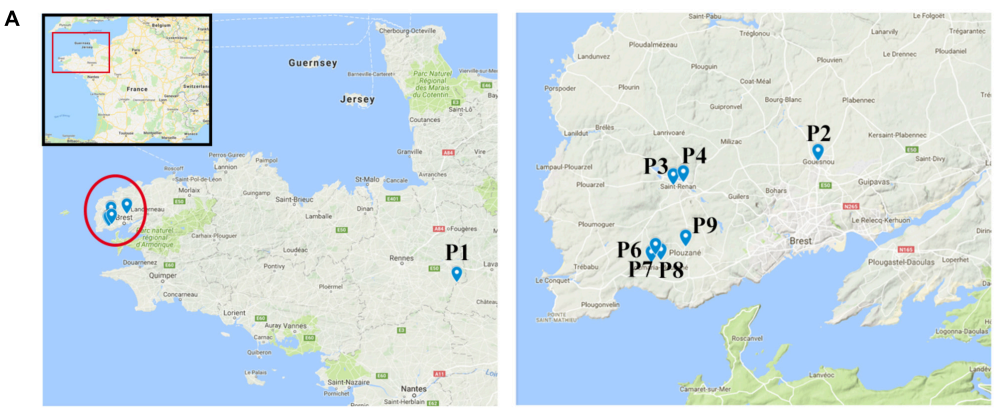

B

Code	Location (City)	GPS Coordinates	Maize type *	Soil preparation **	Variety	Previous crop	Sowing Date	Harvest date	Collection Date
P1	Gennes sur seiche	47.98 N 1.12 W	Maize forage silage	No	Belicio	Maize "feed"	21/04/15	15/09/15	16/10/15
P2	Gouesnou	48.48 N 4.46 W	Maize kernel silage	Yes	Telexx	Wheat	22/04/15	02/11/15	05/11/15
P3	Saint Renan	48.43 N 4.62 W	Maize kernel silage	Yes	Luigi	Mustard	20-22/04/15	08/11/15	09/11/15
P4	Saint Renan	48.43 N 4.62 W	Maize kernel silage	Yes	Zoé	Mustard	20-22/04/15	08/11/15	09/11/15
P6	Locmaria Plouzané	48.37 N 4.65 W	Maize kernel silage	Yes	Telexx	Herbs	10/04/15	09/11/15	10/11/15
P7	Locmaria Plouzané	48.37 N 4.65 W	Maize kernel silage	Yes	P8400	Forage rapeseed	20/04/15	09/11/15	10/11/15
P8	Locmaria Plouzané	48.37 N 4.65 W	Maize kernel silage	Yes	P8400	Forage rapeseed	20/04/15	09/11/15	10/11/15
P9	Plouzané	48.38 N 4.62 W	Maize kernel silage	Yes	Telexx	Wheat	24/04/15	14-15/11/5	16/11/15

* Maize forage silage = whole plant is used for silage, Maize kernel silage = only kernels are used as silage.
** No = for the last 4 years, Yes = end November

FIGURE 1 | Field characteristics. **(A)** Location of the sampled fields; **(B)** agronomic characteristics of the fields.

(5′-CCGGTCACTTGATCTACCAG-3′) and TEF_FUS_R7 (5′-ATGACGGTGACATAGTAGCG-3′) (Cobo-Diaz, Baroncelli, Le Floch, Picot, unpublished) to amplify a 430 bp region of the translation elongation factor (TEF1) of *Fusarium* species.

16S rRNA Read Filtering

The raw sequences were processed and analyzed with QIIME v1.9.1 (Quantitative Insights Into Microbial Ecology) (Caporaso et al., 2010). After joining the paired-end reads using the *multiple_join_paired_ends.py* and *multiple_split_libraries_fastq.py* scripts with default parameters, the chimeric sequences were then removed using UCHIME algorithm (Edgar et al., 2011) implemented in VSEARCH v1.1.3[1] against the ChimeraSlayer reference database (Haas et al., 2011). UCLUST algorithm (Edgar, 2010) was used for OTU picking and taxonomic assignment, which was made against GreenGenes v13.5 database (McDonald et al., 2012). To minimize the inflation of rare OTUs in the community analysis, we include only OTUs with sequence count greater than 10 (Brown et al., 2015; Oliver et al., 2015). Also, chloroplast, mitochondria and "No assigned" OTUs were discarded.

ITS Read Filtering

Although expected, a low level of joined paired-end reads was obtained for the ITS dataset, leading us to choose a different approach using QIIME v1.9.1 (Caporaso et al., 2010). The forward and reverse files were merged independently, using *multiple_split_libraries_fastq.py*. ITS1 and ITS2 regions were first extracted separately from forward and reverse non-chimera-fasta files, respectively, using ITSx v1.0.11 (Bengtsson-Palme et al., 2013) before being concatenated in a new file. A chimera filtering was made on concatenated file using the UCHIME algorithm (Edgar et al., 2011) with VSEARCH v1.1.3 see text footnote[1] and a modified version of the UNITE/INSDC representative/reference sequences version 7.2 (UNITE Community, 2017) as reference database. The modification consisted in extracting ITS1 and ITS2 regions by ITSx software and concatenated them in the modified version of the database.

The ITS1-ITS2 concatenated file of non-chimeric sequences was used for OTU picking running the QIIME script *pick_open_reference_otus.py*, with BLAST (Altschul et al., 1990) as taxonomic assignment method and a modified version of UNITE plus INSD non-redundant ITS database version 7.1 (Kõljalg et al., 2013). Again, the modified version consisted in concatenating ITS1 and ITS2 regions after extracting them using ITSx software.

To minimize the overestimation of rare OTUs in the community analysis, we include only OTUs with sequence count greater than 10 (Brown et al., 2015; Oliver et al., 2015). Only OTUs assigned to kingdom Fungi were used for further analysis. The taxonomy for fungi known to have both sexual and asexual stages was replaced by accepted names according to Chen et al. (2018).

[1]https://github.com/torognes/vsearch

TEF1 Read Filtering

Paired-end reads were processed with QIIME (Caporaso et al., 2010), using the *multiple_join_paired_ends.py* and *multiple_split_libraries_fastq.py* scripts with default parameters. Pick *de novo* strategy was then employed to cluster the sequences into OTUs using *pick_de_novo_otus.py*, at 97% similarity cutoff. A first taxonomic assignment was performed using BLAST (Altschul et al., 1990) against NCBI non-redundant nucleotide database (nt)[2]. Only sequences assigned to *Fusarium* or the teleomorph name (*Gibberella* and *Nectria*), longer than 360 bp and with a percentage of identity higher than 97% were selected for further analysis, and only OTUs with sequence count greater than 10 were selected to minimize the inflation of rare OTUs in the community analysis (Brown et al., 2015; Oliver et al., 2015).

A second step of taxonomic assignment was done using the Fusarium MLST database web[3], with the "pairse DNA alignments" tool, and compared with that provided by nt database. TEF1 sequences obtained along with references were aligned using MAFFT v7.304 (Katoh et al., 2017). Multiple sequence alignments were exported to MEGA7 (Kumar et al., 2016) and the best-fit substitution model was calculated for each separate sequence dataset. Using MrBayes 3.2.6 (Ronquist et al., 2012), the Markov chain Monte Carlo (MCMC) algorithm was performed to generate phylogenetic trees with Bayesian posterior probabilities for combined sequence datasets using the nucleotide substitution models determined by MEGA7 (Kimura 2-parameter with gamma distributed rate variation among sites [K2-G]). Four MCMC chains were run simultaneously for random trees for 2,000,000 generations (standard deviation of split frequencies between runs reached <0.01). Samples were taken every 500 generations. The first 25% of trees were discarded as burn-in phase of each analysis and posterior probabilities were determined from the remaining trees.

Alpha and Beta-Diversity Analysis

Metabarcoding datasets obtained after filtering (V3-V4 region of 16S rRNA, ITS1-ITS2 concatenated regions and *Fusarium* TEF1 sequences) were processed equally. A single rarefaction, based on the sample with the lowest number of reads, was used for alpha-diversity analysis using *single_rarefaction.py* QIIME script. OTUs richness (observed_otus) and evenness (equitability or Pielou's index) were calculated with *alpha_diversity.py* QIIME script. The statistical software R v2.9.10 was used to perform one-way ANOVA with Tukey HSD *post hoc* test, for statistical analysis. Differences with $p < 0.05$ were regarded as statistically significant.

Taxa relative abundances across samples were compared with STAMP (Statistical Analysis of Metagenomic Profiles) bioinformatics software v 2.1.3 (Parks et al., 2014), using the OTU table from QIIME pipeline without any rarefaction. Statistical significance of the differences between multiple group-samples were calculated using ANOVA test, Tukey-Kramer *post hoc* test at 0.95 confidence interval, and corresponding *p*-values

[2]ftp://ftp.ncbi.nlm.nih.gov/../blast/db/

[3]http://www.westerdijkinstitute.nl/fusarium/

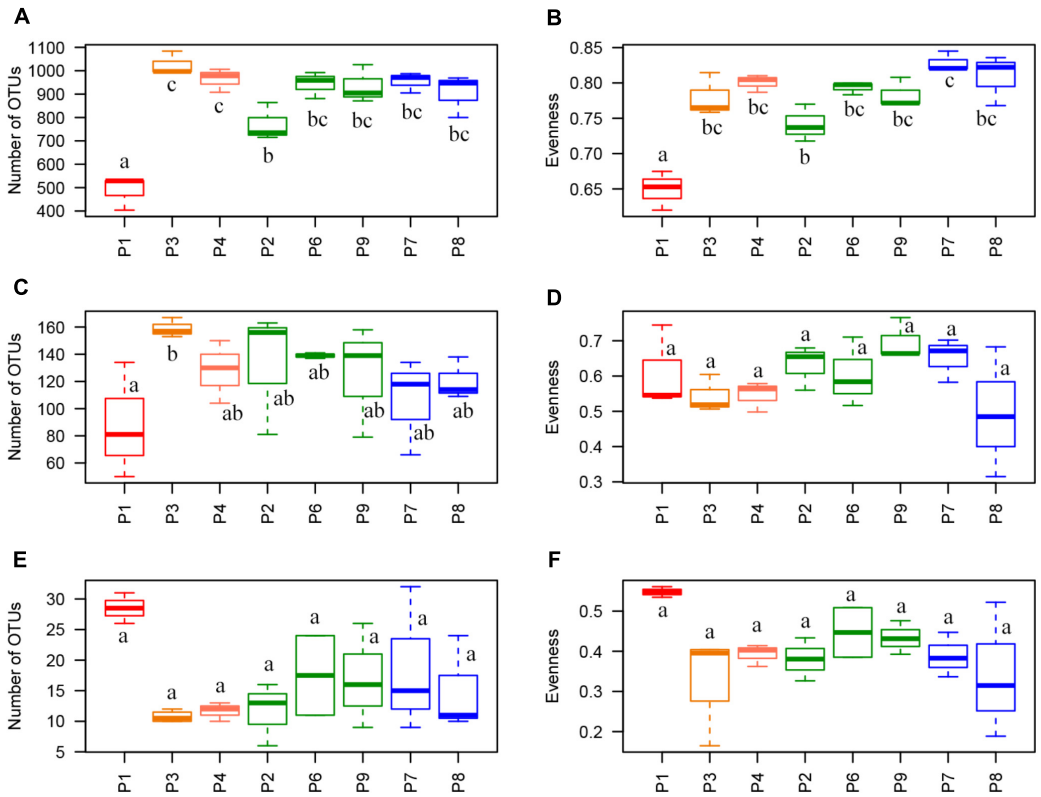

FIGURE 2 | Alpha-diversity indices. Richness index (Observed OTUs) and evenness index (equitability or Pielou's index) per sample for **(A,B)** 16S rRNA data, **(C,D)** ITS data, and **(E,F)** TEF1 data. Letters indicate statistical differences between samples ($p < 0.05$). Telexx variety samples are plotted in green and P8600 variety samples are plotted in blue.

were corrected by Benjamini-Hochberg FDR (Benjamini and Hochberg, 2000).

Canonical Correspondence Analysis (CCA) were made at OTU level using four different datasets: (i) grouping the replicates by field samples, (ii) removing sample P1, (iii) grouping only maize varieties Telexx and P8400, and (iv) grouping previous crop forage rapeseed, wheat and mustard; using R package Vegan. Analyses of variance (ANOVA) were made between fields, variety or previous crop.

Significant correlations between the relative abundance of bacterial, fungal and *Fusarium* OTUs were made using Sparse Correlations for Compositional data algorithm implemented in SparCC python module (Friedman and Alm, 2012) and corresponding networks were plotted using the R package qgraph (Epskamp et al., 2012). Only correlations with a R-corr absolute value greater than 0.3 and *p*-value less than 0.05 were plotted. For correlation analysis, the relative abundance per bacterial, fungal or *Fusarium* OTUs was calculated by dividing the number of sequences per OTU by the total number of amplicon sequences for each sample. Additionally, relative abundance of *Fusarium* OTUs obtained with TEF1 primers, was also divided by the percentage of ITS sequences assigned to *Fusarium* genus, in order to have an estimated relative abundance (percentage) of each *Fusarium* species (determined by TEF1) in the total fungal community (determined by ITS).

Accession Numbers

All the raw reads have been deposited at the NCBI and are available under the Bioproject ID PRJNA394063[4], with BioSample accession numbers from SAMN07348271 to SAMN07348278.

RESULTS

Microbial Community Structure

A total of 1,041,456 sequences of 16S rRNA gene were clustered into 2,334 OTUs after filtering raw reads from 24 maize residue samples (8 fields × 3 biological replicates) and 12,936 sequences per sample were randomly extracted for alpha-diversity analysis. Only 1.98 and 4.54 % of the sequences were assigned to mitochondria and chloroplast, respectively, and removed along filtering step. Richness and evenness indices were significantly found the lowest in P1, with 488 observed OTUs, vs. 771 to 1,025 in the other samples, and with evenness value of 0.65 vs. 0.74 to 0.83. P2 also had significantly lower values compared to P3 and P4 for richness (771 OTUs vs. 964 OTUs in P4 and 1,025 in P3) and compared to P7 for evenness (0.74 vs. 0.83 in P7) (**Figures 2A,B**).

[4]http://www.ncbi.nlm.nih.gov/

For ITS, 1,129,203 sequences were clustered into 455 OTUs and 29,319 sequences per sample were randomly extracted for alpha-diversity analysis. No sequences belonging to plants were detected. There were no significant differences for alpha-diversity indices between fields, with average values of richness between 88 and 159 OTUs, and 0.49 to 0.70 for equitability, except for the significantly higher values of observed richness found in P3 compared to P1 (159 vs. 88 OTUs, respectively) (**Figures 2C,D**).

In the case of TEF1 sequences assigned to *Fusarium*, a total of 1,023,229 sequences were clustered into 48 OTUs after raw read filtering. The percentage of sequences not assigned to the *Fusarium* genus was very low and only represented 0.039 % of the total sequences after removing those corresponding to phage phiX174, used for quality controls in Illumina sequencing. Between 33,688 and 56,829 sequences per sample (except replicate 1 from P1, which was removed for further analysis because it only had 15 sequences) were obtained, and 33,693 sequences per sample were randomly extracted for alpha-diversity analysis. Although P1 showed a higher value of evenness (0.55) and richness (28 OTUs) than other fields (evenness from 0.34 to 0.43 and richness from 11 to 19 OTUs), these differences were not statistically significant (**Figures 2E,F**).

Bacterial Community Composition

A total of 17 phyla and 143 genera were detected based on 16S rRNA sequences. The most abundant phyla were Proteobacteria (50.5–80.6%), Bacteroidetes (13.6–31.9%), Verrucomicrobia (0.8–8.0%), Actinobacteria (2.7–5.1%), and TM7 (0.2–4.4%), with Alphaproteobacteria (23.4–42.8%), Gammaproteobacteria (7.7–32.2%), and Betaproteobacteria (6.6–14.8%) as the main proteobacteria classes (**Figure 3A**). P1 had a significantly higher abundance of Proteobacteria (80.6% vs. 50.5 to 67.7%) and a lower abundance of Betaproteobacteria (6.6% vs. 11.4 to 31.9%), Bacteroidetes (13.6% vs. 21.9 to 31.9%), and Verrucomicrobia (1.3 and 0.8, vs. 4.1 to 5.1%) compared to the other fields. Alpha and Gamma-proteobacteria were also found to be higher in P1 although differences were not significant. Other significant differences were found in P3, where a higher abundance of Proteobacteria (67.7% vs. 50.5 to 62.8%) and Gammaproteobacteria (28.8% vs. 7.7 to 18.3%) and a lower abundance of Bacteroidetes (21.9% vs. 24.1 to 31.9%) were observed compared to the other samples, except P1 (**Figure 3A**).

The most abundant genera were 4 proteobacteria: *Sphingomonas* (9.6–27.9%), *Pseudomonas* (1.1–6.2%), *Janthinobacterium* (0.1–5.2%) and *Sphingobium* (1.3–2.4%); and 2 bacteroidetes: *Pedobacter* (2.1–9.8%) and *Flavobacterium* (0.6–7.7%) (**Figure 3B**). In total, the abundance of 18 genera was found to be significantly different between samples, with some genera more abundant in P1, such as *Adhaeribacter*, *Phormidium*, *Stenotrophomonas*, and *Skermanella* (**Figure 4**). Some genera were also found to be significantly more abundant in field P3 (*Rodhoferax*, *Sporocytophaga*, *Buchnera*, and *Sediminibacterium*), P4 (*Segetibacter* and *Paracoccus*), P6 (*Paenibacillus* and *Mycobacterium*), P7 (*Polaromonas*, *Bdellovibrio*, and *Gemmatimonas*), and P9 (*Kaistia*) (**Figure 4**).

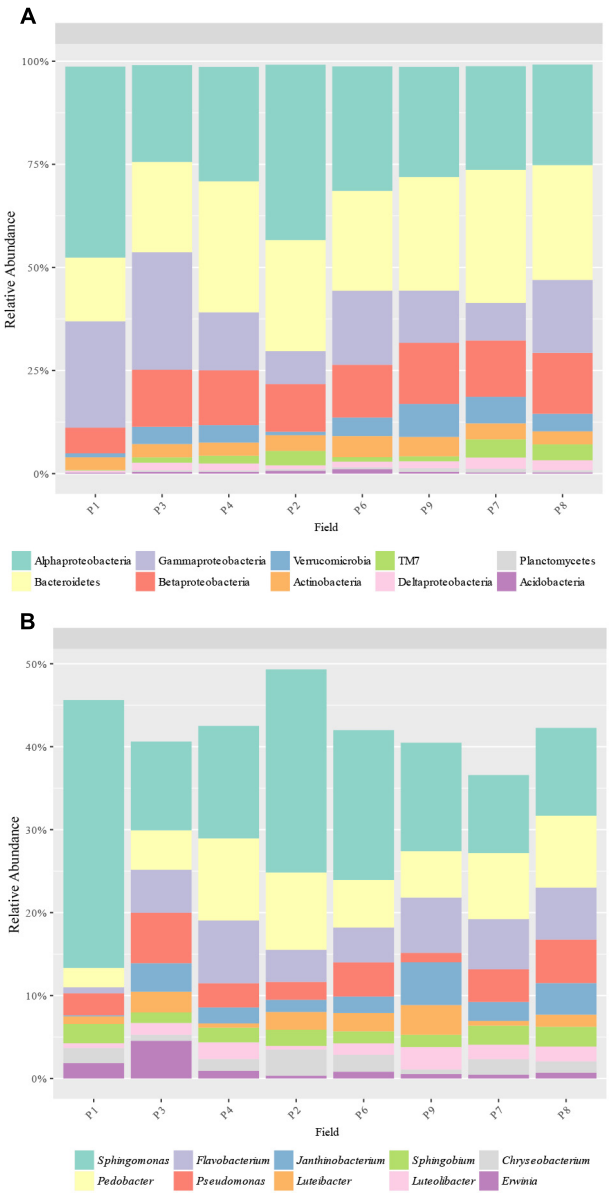

FIGURE 3 | Bacterial taxa distribution. Relative abundance of the predominant **(A)** bacterial phyla (and Proteobacteria classes) and **(B)** genera obtained by 16S rRNA amplicons.

Fungal Community Composition

A total of 16 classes and 124 genera were detected from ITS sequences. The most abundant classes were Sordariomycetes (20.3–63.1%), Dothideomycetes (12.5–39.6%), Leotiomycetes (3.6–18.0%), Eurotiomycetes (1.8–13.8%), Tremellomycetes (2.4–9.9%), and Saccharomycetes (0.0–33.0%), with Sordariomycetes being the most abundant class in all samples except in P1, which had Saccharomycetes as the main class (**Figure 5A**). In addition, Saccharomycetes was the unique class with different relative abundances between samples, which was more abundant in P1 than the others (33.0%

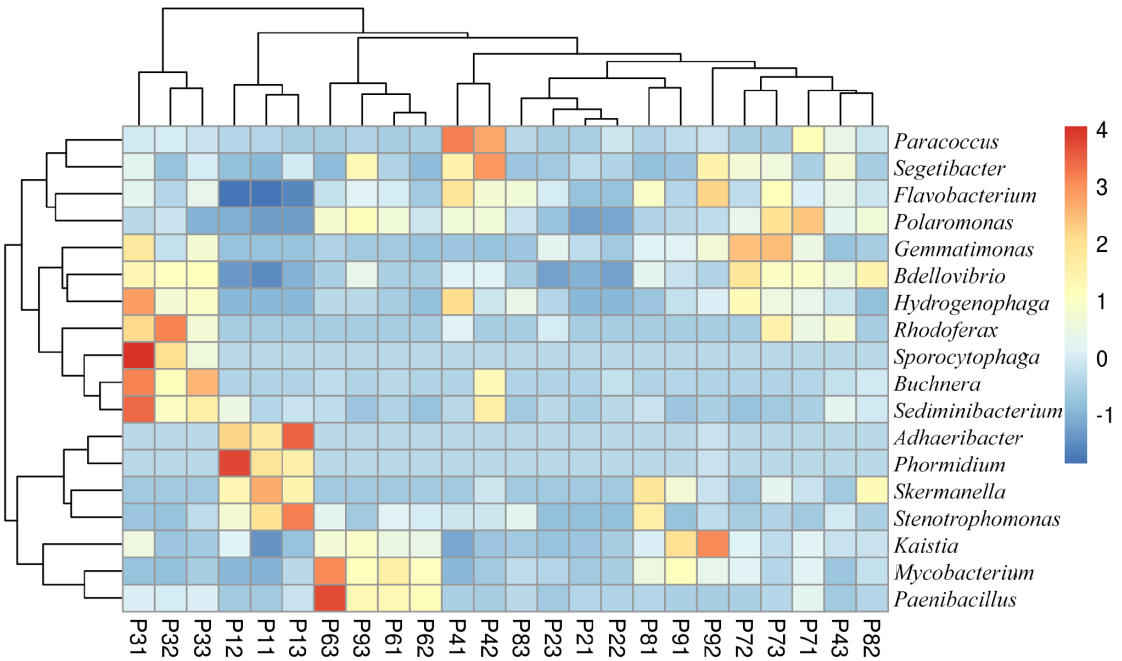

FIGURE 4 | Heatmap of bacterial genera with significant differences ($p < 0.05$) between samples. Relative abundance data were z-scored normalized by row. Plot was made using *pheatmap* R package with the default parameters. Sample names have the format Pij, where i refers to the field site (i = 1–8) and j refers to the replicate within the field (j = 1–3).

vs. up to 2.3%). The most abundant genera obtained were *Fusarium* (6.1–44.8%), *Epicoccum* (1.4–27.1%), *Articulospora* (3.5–16.6%), *Microdochium* (0.3–24.6%), *Exophiala* (1.0–12.9%), *Sarocladium* (0.4–14.5%), *Cryptococcus* (2.1–7.7%), *Candida* (0.0–30.0%), *Acremonium* (0.1–11.5%), and *Phoma* (0.0–9.2%) (**Figure 5B**). Only 2 genera had significant different abundances between fields: *Candida* (class Saccharomycetes) and *Phoma* (class Dothideomycetes) were more abundant in P1 than other fields (30.0% vs. up to 2.4% and 9.2 vs. up to 5.4%, respectively) (**Figure 5B**).

Fusarium Community Composition

A total of 15 *Fusarium* species were detected according to taxonomic assignment performed by phylogenetic tree, although 5 OTUs were not clearly assigned to species level (**Figure 6** and **Supplementary Table S1**). Three of them (denovo419, denovo339, and denovo314) were named as *Fusarium* sp. for further analysis, while denovo380 and denovo779 were grouped with the 2 OTUs assigned to *F. equiseti* (denovo921 and denovo438) inside *Fusarium* sp. FIESC (*Fusarium incarnatum-equiseti* species complex) for further analysis.

Major species were *F. graminearum* (18.9–71.9%), *F. avenaceum* (15.7–53.8%), *F. poae* (0.0–18.6%), *F. oxysporum* (0.002–12.5%), *F. verticillioides* (0.0–13.4%), *F. temperatum* (0–10.1%), and *F. sporotrichioides* (0.0–11.1%), which covered between 80.2 to 100% of the total *Fusarium* sequences per field (**Figure 7**). The abundance of these species was unevenly distributed across fields. However, whatever the field, the most abundant species were *F. graminearum* and *F. avenaceum*, which sum accounted for 68.9 to 90.1% of the total *Fusarium* sequences per field, except in P1 (46.6%), and they were also the 2 *Fusarium* species present in all the fields. It is noteworthy that *F. avenaceum* outnumbered *F. graminearum* only in the three fields that had Telexx as maize variety (P2, P6, and P9). Moreover, other species were also subdominant depending on the field: *F. poae* in P4, P6, P7, and P8 (from 9.2 to 18.6%); *F. oxysporum* in P1 and P8 (15.4 and 11.8%, respectively); *F. sporotrichioides* and *F. temperatum* in P1 (16.6 and 15.2%, respectively); and *F. verticillioides* in P9 (13.4%); although there were not significant differences in relative abundance of *Fusarium* species between samples (**Figure 7**).

Canonical Correspondence Analysis

Unsurprisingly, Canonical Correspondence Analysis (CCA) showed that the composition and distribution of microbial communities in the outgroup P1 was different from the others samples. Bacterial, fungal and *Fusarium* communities presented significant differences between fields (ANOVA: $F = 1.6308$, $Pr < 0.001$ for bacteria; $F = 2.0422$, $Pr < 0.001$ for fungi; $F = 1.7723$, $Pr < 0.001$ for *Fusarium*), with P1 as the most different field in all 3 cases; and also P2, P3, and P9 for bacteria, and P9 for *Fusarium* communities (**Figures 8A–C**). The CCA excluding P1 showed similar degree of significance between samples ($F = 1.4219$ and 1.6738, for bacterial and fungal, respectively, $Pr < 0.001$), except for *Fusarium* ($F = 1.3428$, $Pr = 0.038$). A clear separation of almost all fields was observed for bacterial communities; P4 and P6 for fungal communities; and P6 and P9 for *Fusarium* communities (**Figures 8D–F**). The same analysis was done selecting the fields which had Telexx

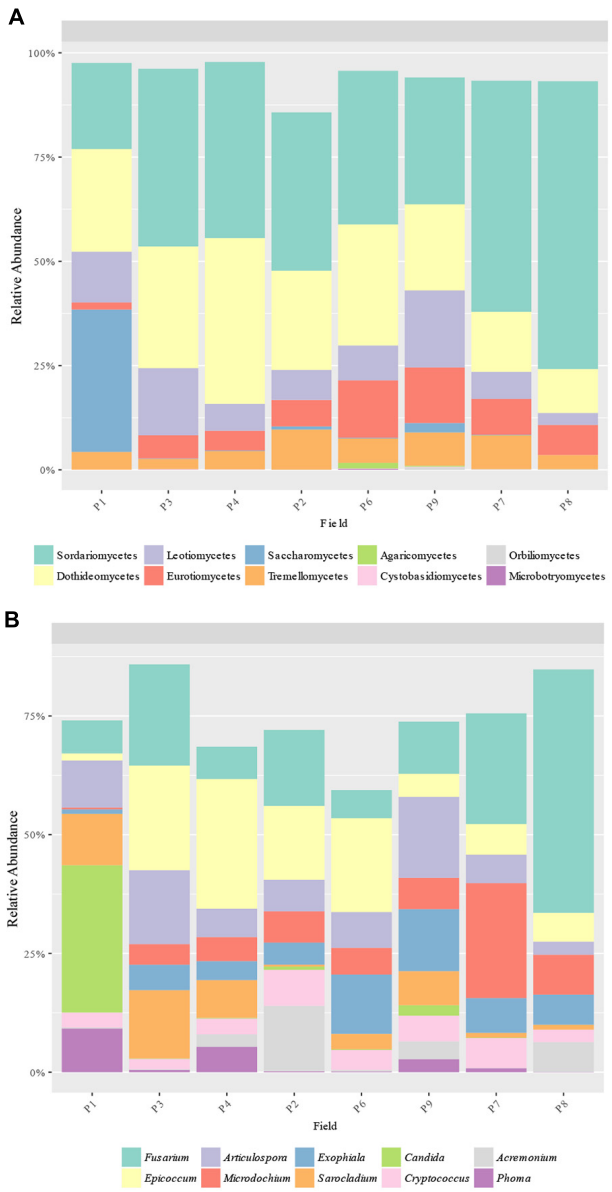

FIGURE 5 | Fungal taxa distribution. Relative abundance of the predominant fungal **(A)** classes and **(B)** genera obtained by ITS amplicons.

and P8400 as maize varieties, obtaining significant differences between varieties in bacterial (F = 1.5128, Pr = 0.002) and fungal (F = 1.7022, Pr = 0.015) communities but not in *Fusarium* communities (F = 1.2672, Pr = 0.214) (**Figures 8G–I**). Regarding the previous crop, only forage rapeseed, mustard and wheat were analyzed, resulting in significant differences between groups in bacterial (F = 1.4201, Pr = 0.001), fungal (F = 1.7673, Pr = 0.001) and *Fusarium* communities (F = 1.716, Pr = 0.01) (**Figures 8J–L**).

SparCC Correlation Network

In total, 26 positive and 13 negative significant correlations (|coefficient correlation (=corr)|>0.3 and p-value < 0.05) were found between 27 OTUs: 6 from 16SrRNA, 19 from ITS and 4 from TEF1 (**Figure 9A**). The highest positive correlations were obviously found between F01 and Fs01, both assigned to *F. graminearum* by ITS and TEF1 sequencing, respectively (corr = 0.82); and between F02 and Fs02, both assigned to *F. avenaceum* by ITS and TEF1 sequencing (corr = 0.51). There were also significant positive correlations between Fs02 and the 2 *F. graminearum* OTUs (F01 and Fs01, corr = 0.40 for both) (**Figure 9A**). One fungal and one bacteria OTUs presented negative correlations with some *Fusarium* OTU(s): F04, assigned to *Sarocladium strictum*, against Fs03, assigned to *F. oxysporum* (corr = −0.30); and B01, assigned to *Sphingomonas*, against F01, Fs01, and Fs04, assigned to *F. graminearum* by ITS and TEF1, and to *F. poae* by TEF1 (corr = −0.36, −032 and −0.32, respectively). Moreover, B01 also presented negative correlations with B02, B03, B04, F06, and F07, assigned to *Pseudomonas*, *Luteolibacter*, family Xanthomonadaceae, *Monographella cucumerina*, and *F. poae*, respectively (**Figure 9A**).

The same SparCC correlation analysis was done excluding the results from the outgroup field P1, which fungal and bacterial communities and distribution greatly varied from the other fields. In total 28 OTUs (7 from 16SrRNA, 18 from ITS and 3 from TEF1) presented 20 positive and 16 negative significant correlations between them (**Figure 9B**). As happened in the previous network analysis, the highest positive correlations were between F01 and Fs01 (corr = 0.83), assigned to *F. graminearum* by ITS and TEF1, respectively; between F02 and Fs02 (corr = 0.53), assigned to *F. avenaceum* by ITS and TEF, respectively; and between F02 and the two OTUs assigned to *F. graminearum* (corr = 0.41 for both TEF1 and ITS). Two fungal OTUs had negative correlations vs. some *Fusarium* OTU: the same *Sarocladium* OTU identified before (F04) vs. Fs03 and F08, assigned to *F. oxysporum* by TEF1 and ITS sequences (corr = −0.31 and −0.35, respectively); and F05, assigned to *Epicoccum nigrum*, vs. Fs04 and F10, assigned to *F. temperatum* and *Candida sake* (corr = −0.34 and −0.35, respectively) (**Figure 9B**).

DISCUSSION

By sequencing three different amplicons from 24 maize samples, a total of 2,334 bacterial OTUs, 1,428 fungal OTUs and 48 *Fusarium* OTUs were obtained. This study is one of the first metabarcoding studies on maize residues, resulting in a higher diversity than previously found in other NGS studies of the maize rhizosphere (Peiffer et al., 2013; Li et al., 2014).

Proteobacteria (mainly alpha and gamma-proteobacteria), Bacteroidetes and Actinobacteria were found as the most abundant phyla in maize stalk surface, the first two of which have already been reported as the most abundant in the maize rhizosphere (Peiffer et al., 2013; Li et al., 2014), in soil samples after maize harvesting (Chen et al., 2015) and in the first stages of maize straw decomposition (Sun et al., 2013). Although maize residues can be considered as a separate compartment and a particular ecological niche compared to soil samples, some of the more abundant bacterial genera in the present study had

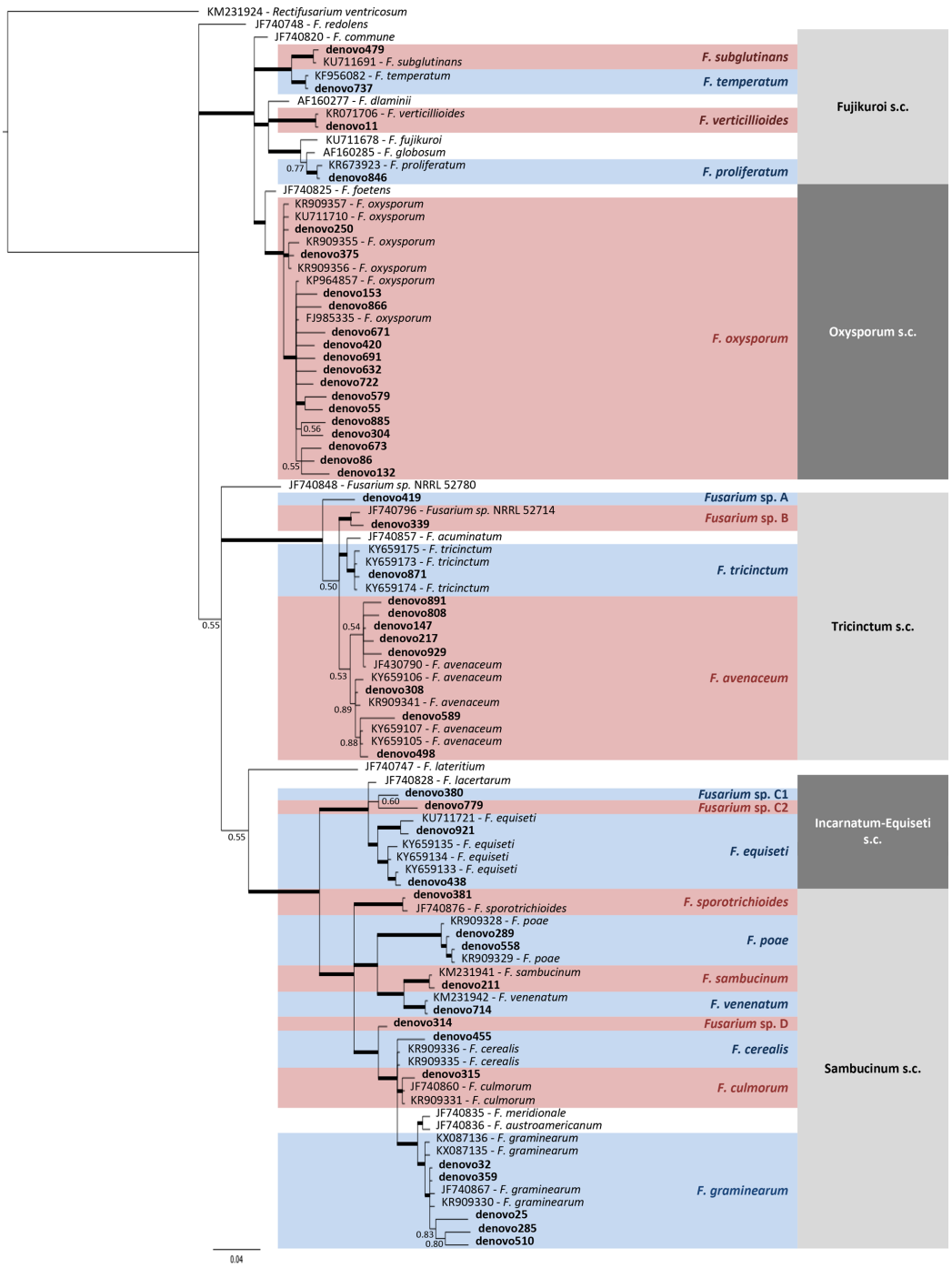

FIGURE 6 | Phylogenetic tree of TEF1 sequences from *Fusarium* OTUs and reference isolates, which accession number was indicated. Bayesian posterior probability (BPP) values (above 0.50) are shown at the nodes. The thickened nodes represent BPP values higher than 0.9.

also been found as predominant in maize rhizospheric soils, including *Sphingobium* (Peiffer et al., 2013; Li et al., 2014), *Flavobacterium* (Li et al., 2014; Yang et al., 2017; Correa-Galeote et al., 2016) and *Sphingomonas* (Correa-Galeote et al., 2018). Apart from these genera, the diversity of bacterial communities found in our maize residues generally differed from that of maize rhizospheric soils found in other studies (Peiffer et al., 2013; Li et al., 2014; Correa-Galeote et al., 2016; Yang et al., 2017). It should also be underlined that 2 of the over-represented genera in P1, *Adhaeribacter* and *Stenotrophomonas*, were also significantly more abundant in Fusarium wilt suppressive soils (Siegel-Hertz et al., 2018).

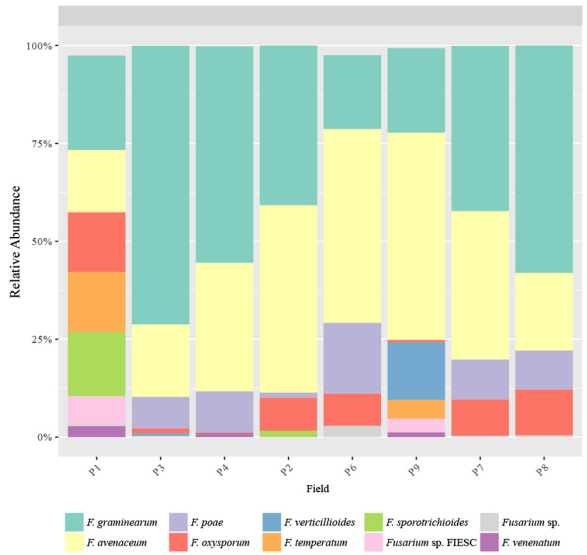

FIGURE 7 | *Fusarium* species distribution. Relative abundance of the predominant *Fusarium* species obtained by TEF1 amplicons.

Some of the most abundant fungal genera found in the present study, including *Fusarium*, *Epicoccum*, *Acremonium*, *Sarocladium*, and *Phoma* had been reported as endophytes isolated from maize (Pan and May, 2009; Amin, 2013; Xing et al., 2018). In particular, *Fusarium*, *Epicoccum*, and *Phoma* were reported as the most abundant endophytes isolated from maize leaves, using two different lineages (Szilagyi-Zecchin et al., 2016), while *Acremonium* was detected exclusively in Fusarium wilt suppressive soils, but not in conducive soils (Siegel-Hertz et al., 2018). It is important to highlight that, in our maize samples, genera with reported biocontrol activity (**Table 1**) were predominant and included several bacterial genera such as *Sphingomonas*, *Pedobacter*, *Flavobacterium*, *Pseudomonas*, *Janthinobacterium*, *Sphingobium*, *Chryseobacterium*, *Luteibacter*, *Dyadobacter*, and *Rhizobium;* and fungal genera such as *Epicoccum*, *Articulospora*, *Exophiala*, *Sarocladium*, *Cryptococcus*, *Candida*, *Acremonium*, and *Metschnikowia*. On the other hand, only two bacterial genera, *Pseudomonas* and *Erwinia*, and three fungal genera, *Fusarium*, *Acremonium*, and *Phoma*, within the most abundant ones are known to include maize or cereal pathogens. *A priori*, although maize residues have been reported as the primary source of pathogenic species (Shaner, 2003; Bateman et al., 2007; Fernandez et al., 2008), microbial communities obtained from maize crop residues presented an important amount of organisms that could increase the protection of future rhizospheric complexes against pathogens. This hypothesis was corroborated with the presence of one bacterial and two fungal OTUs, assigned to *Sphingomonas, Epicoccum nigrum*, and *Sarocladium strictum*, negatively correlated to some *Fusarium* OTUs; these three genera were within the most abundant ones in the microbial communities studied. Likewise, a lower increase of *Fusarium* spp. colonization of maize stalks has also been reported when *Sphingomonas* species were more abundant (Köhl et al., 2015) and a strain of *Sphingomonas* was found to be antagonistic against *F. avenaceum*, *F. culmorum*, *F. tricinctum*, and *F. graminearum* (Wachowska et al., 2013). *Acremonium* spp. (basionym of *Sarocladium*) (Summerbell et al., 2011) were also found to be more abundant in maize stalks characterized by a lower increase in *Fusarium* colonization, rendering it as a potential antagonist of *Fusarium* spp. (Köhl et al., 2015). A better taxonomic classification of the *Acremonium* species present in our samples might be necessary as some species belonging to this genera have been reported to be pathogenic on maize (Tagne et al., 2002). Several *Acremonium* strains isolated from maize were able to inhibit the growth of some pathogens, such as *Pythium ultimum*, *Sclerotium oryzae*, *Rhizoctonia solani*, and *Pyricularia oryzae* (Potshangbam et al., 2017) or produce pyrrocidines A and B, which induce host defense mechanisms against microbial pathogens (Wicklow and Poling, 2009). Some *Sarocladium* endophytes isolated from wheat were also reported to inhibit *F. graminearum* and *F. culmorum* growth (Comby et al., 2017). It was also found that some strains of *Epicoccum nigrum* were able to reduce the mycelial growth of *F. graminearum*, *F. avenaceum*, and *F. oxysporum* on PDA (Ogórek and Plaskowska, 2011) and also in sterile wheat grain assays with *F. graminearum* (Jensen et al., 2016); or to reduce the sporulation of *F. culmorum* and *F. graminearum* on wheat straw (Luongo et al., 2005). Furthermore, *E. nigrum* has been used as a biological control on peaches and nectarines orchards against *Monilinia* spp. (De Cal et al., 2009) and against *Pythium debaryanum* and *P. ultimum* on cotton seedlings (Hashem and Ali, 2004). Overall, the high presence of these genera, previously reported as antagonists and negatively correlated to toxigenic *Fusarium* species or other pathogenic organisms, suggests that such taxa may be of interest as part of biocontrol strategies against toxigenic *Fusarium* spp.

The most abundant *Fusarium* species found in our maize residues were *F. graminearum*, *F. avenaceum*, and *F. poae*, with 41.3, 35.4, and 7.1% of the total sequences, respectively, which are one of the main causal agents responsible for FHB (Parry et al., 1995; Bottalico and Perrone, 2002). Likewise, *F. graminearum* and *F. avenaceum* were also described as the predominant species on maize stalks after a 6-month exposure period in the field, as evaluated by qPCR (Köhl et al., 2015) and are commonly found as the main *Fusarium* species in wheat, using TEF1 as well as *Fusarium* spp. specific primers (Karlsson et al., 2016, 2017) or using culture-dependent approaches (Xu et al., 2005; Nicolaisen et al., 2014; Basler, 2016). *F. avenaceum* was also found as the dominant *Fusarium* species in some soil samples associated to perennial plants (LeBlanc et al., 2017). In opposite to our findings, *F. culmorum* is commonly described as a dominant *Fusarium* species in maize or cereals (Scauflaire et al., 2011; Basler, 2016; Hellin et al., 2016). Mutual exclusion between strains of *F. graminearum* and *F. culmorum* had been previously demonstrated (Siou et al., 2015). This competition could account for the low abundance of *F. culmorum* (0.05%) in maize stalks in our present study. In addition, shifts from *F. culmorum* to *F. graminearum* on wheat have been described in different European

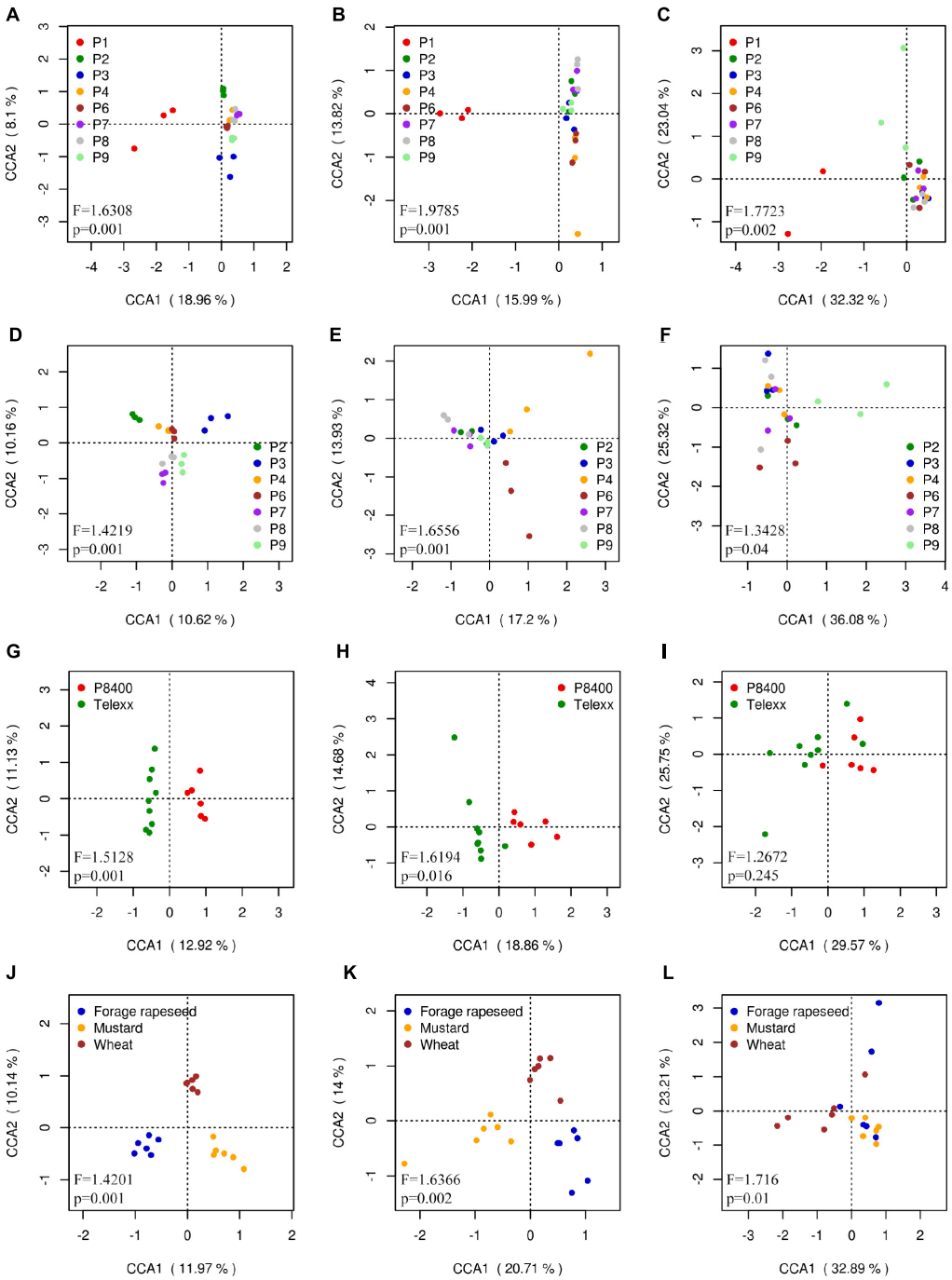

FIGURE 8 | Canonical correspondence analysis (CCA) calculated using OTUs relative abundance. Each dot represents a sample replicate for **(A,D,G,J)** bacterial, **(B,E,H,K)** fungal, and **(C,F,I,L)** *Fusarium* communities, using **(A,B,C)** all sites, **(D,E,F)** all sites except P1, **(G,H,I)** samples grouped by maize variety and **(J,K,L)** by previous crop.

countries, such as England and Wales (Jennings et al., 2004), Netherlands (Waalwijk et al., 2003), Denmark (Nielsen et al., 2011), and Belgium for maize ears and stalks (Scauflaire et al., 2011). Climatic changes were the main hypothesis put forward, although the increase in maize-wheat rotation crops may also contribute to this increase in *F. graminearum* and decrease in *F. culmorum* (Dill-Macky and Jones, 2000; Cromey et al., 2002). The distribution of the *Fusarium* communities also strongly depends on the environmental conditions which would favor some species over the others. For instance, Dorn et al. (2011) found that *F. graminearum*, *F. verticillioides*, and *F. proliferatum* were

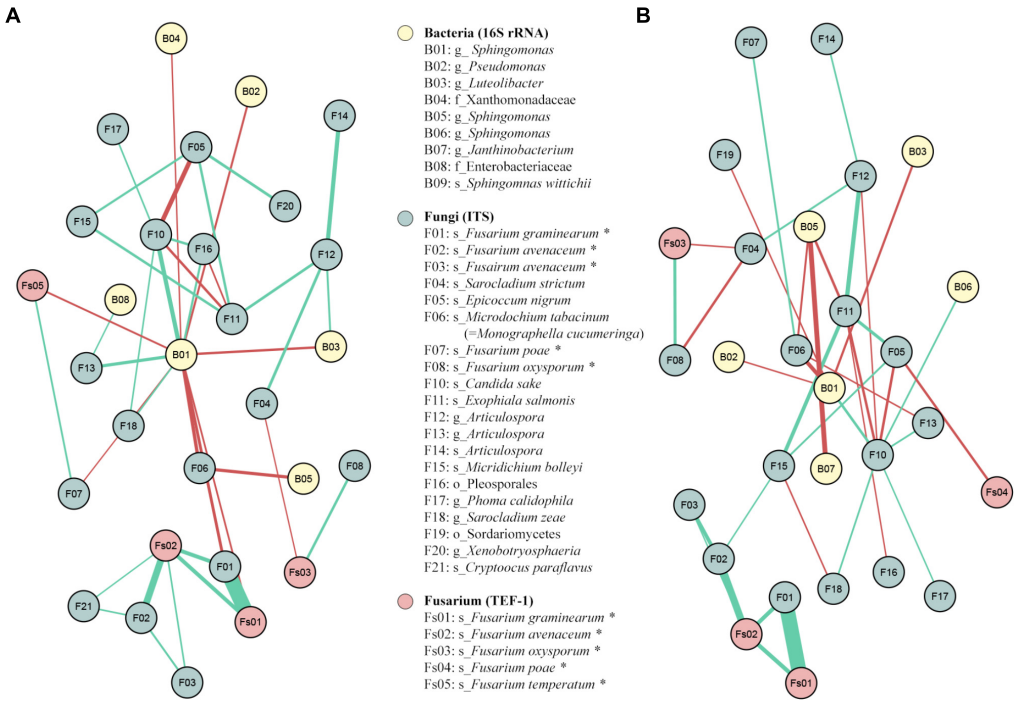

FIGURE 9 | SparCC correlation networks observed between OTUs, obtained with 16S rRNA gene (Bacteria), ITS (Fungi), and TEF1 (*Fusarium*) sequences. Nodes correspond to OTUs, and connecting edges indicate correlations between them. Only nodes with negative or positive correlations, with values less than –0.30 (red) or larger than 0.30 (green), were represented. **(A)** SparCC correlation network using all the samples; **(B)** SparCC correlation network without the outgroup P1. OTUs marked with asterisk had been reassigned taxonomically using blastn against nr/nt-NCBI database and *Fusarium* MLST web database (**Supplementary Table S2**).

the most dominant *Fusarium* species isolated from maize kernels in Switzerland (22.3–81.6, 2.5–41.8, and 0.6–22.0% of occurrence in kernels, respectively), while *F. equiseti*, *F. proliferatum*, and *F. verticillioides* were the main *Fusarium* species in stalks (43.6, 16.3, and 11.5% of occurrence in nodes, and 27.6, 41.5, and 15.5% in internodes, respectively). In our study, *F. graminearum* and *F. avenaceum* seem to be more adapted than species from the *Fusarium fujikuroi* species complex (FFSC), including *F. verticillioides* and *F. temperatum*, which were dominant in maize kernels in Poland (Czembor et al., 2015) and in maize kernels from Southern to Central Europe (Logrieco et al., 2002). The mild and humid climatic conditions found in Brittany, which are known to be favorable to *F. graminearum* and *F. avenaceum* (Xu et al., 2008) may account for such observations. In contrast, higher prevalence of Fusarium ear rot caused by FFSC including *F. verticillioides* occurs under hot and dry conditions. For instance, *F. verticillioides* incidence was found negatively correlated to rainfall values in maize fields in Argentina (Pereira et al., 2011) and to kernel moisture in maize fields in United States (Bush et al., 2004). Moreover, we found that Telexx maize variety had highest abundance of *F. avenaceum* than *F. graminearum*, while the opposite was found for the other varieties used in the study. These differences in *Fusarium* composition could also induce differences in mycotoxin concentrations, as deoxynivalenol and zearalenone are produced by *F. graminearum* while moniliformin, enniatins and beauvericin can be produced by *F. avenaceum* (Ferrigo et al., 2016).

Microbial communities found in the maize residues on field P1 was the most different compared to the other fields. In general, this field was characterized by both significant lower bacterial and a higher *Fusarium* alpha-diversity indices, with a higher abundance of the fungal *Candida*. Several factors differed from the outgroup P1 compared to the other fields (**Table 1**) including the maize type and cultivar, the agricultural practices, the previous crop and the location. In addition, these samples were collected 1 month after harvest, suggesting that maize residues were already in the process of degradation. Maize genotype has already been reported to influence the microbial communities in rhizospheric samples (Li et al., 2014), it could also have a strong influence in the microbial communities on others parts of the plant including the residues. But due to bias in the sampling design (because this study was rather designed to estimate the diversity found in maize residues from various fields in Brittany), we cannot conclude which factor(s) contributed mainly to these differences between P1 and the other fields. Additional sampling will be undertaken to further clarify which factor(s) has(have) the higher influence on microbial communities, with an emphasis to maize microbial dynamics over the course of maize residue degradation.

The significance of this study first lies in its design of a new specific pair of primers to identify *Fusarium* species with metabarcoding approach. This new culture-independent approach for *Fusarium* species identification could be adapted to other genera, by the design of specific primers for Illumina

TABLE 1 | Pathogen and antagonistic characteristics of species or strains belonging to the most abundant genus obtained in maize residues.

	% of total sequences	Plant pathogen	Wheat pathogen	Maize pathogen	Biocontrol activity	Reference for biocontrol activity
Bacterial genus						
Sphingomonas	16.0	Yes	No	No	Yes	Wachowska et al., 2013
Pedobacter	6.7	No	No	No	Yes	De Boer et al., 2007; Song et al., 2017
Flavobacterium	5.1	No	No	No	Yes	Gunasinghe et al., 2004
Pseudomonas	3.6	Yes	Yes	Yes	Yes	Hennessy et al., 2017
Janthinobacterium	2.5	No	No	No	Yes	Berg et al., 2001
Sphingobium	1.9	Yes	No	No	Yes	van Bruggen et al., 2014; Fu et al., 2017
Chryseobacterium	1.7	Yes	No	No	Yes	Yin et al., 2013; Sang et al., 2018
Luteibacter	1.7	No	No	No	Yes	De Boer et al., 2007
Luteolibacter	1.5	No	No	No	No	
Erwinia	1.3	Yes	Yes	Yes	No	
Agrobacterium	1.3	Yes	No	No	(1)	
Hymenobacter	1.2	No	No	No	No	
Dyadobacter	1.0	No	No	No	Yes (2)	Fu et al., 2017
Rhizobium	0.8	No	No	No	Yes (3)	Al-Ani et al., 2012
Fungal genus						
Fusarium	17.1	Yes	Yes	Yes	Yes (3,4)	Ghini et al., 2000; Boari and Vurro, 2004
Epicoccum	13.1	Yes	No	No	Yes	Luongo et al., 2005
Articulospora	9.1	No	No	No	Yes	Sugahara et al., 2008
Microdochium	7.6	Yes	Yes	No	No	
Exophiala	7.0	No	No	No	Yes	Duvick et al., 1998
Sarocladium	5.7	Yes	No	No	Yes	Comby et al., 2017
Cryptococcus	4.4	Yes	No	No	Yes	Schisler et al., 2015
Candida	4.2	No	No	No	Yes	Calvo-Garrido et al., 2013
Acremonium	3.1	Yes	Yes	Yes	Yes (3)	Rajakumar et al., 2005
Phoma	2.4	Yes	Yes	Yes	No	
Xenobotryosphaeria	2.2	No	No	No	No	
Pyrenochaetopsis	2.2	No	No	No	No	
Ramularia	0.6	Yes	No	No	No	
Hannaella	0.5	Yes	No	No	No	
Metschnikowia	0.4	No	No	No	Yes	Manso and Nunes, 2011

(1) Used for Agrobacterium-mediated plant transformation (Genetically Modified Organisms).
(2) Associated to disease suppressiveness.
(3) Over-represented in Fusarium wilt suppressive soils (Siegel-Hertz et al., 2018).
(4) Non-pathogenic strains.

metabarcoding. In addition, the combined used of these primers with universal primers for fungi and bacteria allowed, not only to provide an accurate description of the microbiota as well as the pathogenic *Fusarium* spp. under various agronomic practices (maize cultivar, previous crop), but also to assess the potential relationships between microorganisms using co-occurrence network analysis. More particularly, we could identify predominant taxa negatively correlated to toxigenic *Fusarium* spp. Therefore, such approach could be used as a pre-filtering for the selection of potential antagonists as part of biocontrol strategies. Following this investigation, culture-dependent approaches must be done to determine the antagonistic potential of species identified by the co-occurrence network analysis, both in laboratory and field experiments. Illumina technology allows putting more than one amplicon type and dozens of samples in only one run (Herbold et al., 2015). This approach is time-saving compared to the empirical BCA isolation strategies, and could have more importance in the screening of antagonists.

Based on the results of this preliminary study, we also suggest focusing on the microbial dynamics throughout the plant cultivation cycle in maize-wheat rotations, taking also into account the influence of plant cultivar on microbial communities.

AUTHOR CONTRIBUTIONS

AP and GLF contributed to the conception and design of the study. AP performed sampling. JC-D performed DNA extraction and shipping, read filtering and OTU table filtering, and wrote the first draft of the manuscript. JC-D and GLF performed statistical analysis. RB performed phylogenetic tree. All authors contributed to manuscript revision, read and approved the submitted version.

FUNDING

This work was supported by the Brittany Region (Grant #9097 MycoRes) and the Institut Brestois Santé-Agro-Matière (IBSAM).

ACKNOWLEDGMENTS

We gratefully thank the farmers for kindly giving us access to their field and providing information about their field management.

SUPPLEMENTARY MATERIAL

The Supplementary Material for this article can be found online at: https://www.frontiersin.org/articles/10.3389/fmicb.2019.00261/full#supplementary-material

TABLE S1 | Taxonomic assignment of representative TEF1 sequences for each *Fusarium* OTU obtained, using phylogenetic tree, blastn vs. nt-NCBI database, and pairse alignment vs. FUSARIUM-MLST database.

TABLE S2 | Taxonomic assignment of representative TEF1 and ITS sequences for each *Fusarium* and unclassified genus OTUs plotted in network analysis, using blastn vs. nt-NCBI database, and pairse alignment vs. FUSARIUM-MLST database.

REFERENCES

Abd El Daim, I. A., Häggblom, P., Karlsson, M., Stenström, E., and Timmusk, S. (2015). Paenibacillus polymyxa A26 Sfp-type PPTase inactivation limits bacterial antagonism against *Fusarium graminearum* but not of *F. culmorum in kernel assay. Front. Plant Sci.* 6:368. doi: 10.3389/fpls.2015.00368

Abiala, M. A., Odebode, A. C., Hsu, S. F., and Blackwood, C. B. (2015). Phytobeneficial properties of bacteria isolated from the rhizosphere of maize in Southwestern Nigerian soils. *Appl. Environ. Microbiol.* 81, 4736–4743. doi: 10.1128/AEM.00570-15

Aira, M., Gómez-Brandón, M., Lazcano, C., Bååth, E., and Domínguez, J. (2010). Plant genotype strongly modifies the structure and growth of maize rhizosphere microbial communities. *Soil Biol. Biochem.* 42, 2276–2281. doi: 10.1016/j.soilbio.2010.08.029

Al-Ani, R. A., Adhab, M. A., Mahdi, M. H., and Abood, H. M. (2012). Rhizobium japonicum as a biocontrol agent of soybean root rot disease caused by *Fusarium solani* and *Macrophomina phaseolina. Plant Protect. Sci.* 4, 149–1155. doi: 10.17221/16/2012-PPS

Altschul, S. F., Gish, W., Miller, W., Myers, E. W., and Lipman, D. J. (1990). Basic local alignment search tool. *J. Mol. Biol.* 215, 403–410. doi: 10.1016/S0022-2836(05)80360-2

Amin, N. (2013). Diversity of endophytic fungi from root of maize var. pulut (waxy corn local variety of South Sulawesi, Indonesia). *Int. J. Curr. Microbiol. Appl. Sci.* 2, 148–154.

Baffoni, L., Gaggia, F., Dalanaj, N., Prodi, A., Nipoti, P., Pisi, A., et al. (2015). Microbial inoculants for the biocontrol of *Fusarium* spp. in durum wheat. *BMC Microbiol.* 15:242. doi: 10.1186/s12866-015-0573-7

Basler, R. (2016). Diversity of *Fusarium* species isolated from UK forage maize and the population structure of *F. graminearum* from maize and wheat. *PeerJ* 4:e2143. doi: 10.7717/peerj.2143

Bateman, G. L., Gutteridge, R. J., Gherbawy, Y., Thomsett, M. A., and Nicholson, P. (2007). Infection of stem bases and grains of winter wheat by *Fusarium culmorum* and *F. graminearum* and effects of tillage method and maize-stalk residues. *Plant Pathol.* 56, 604–615. doi: 10.1111/j.1365-3059.2007.01577.x

Bengtsson-Palme, J., Ryberg, M., Hartmann, M., Branco, S., Wang, Z., Godhe, A., et al. (2013). Improved software detection and extraction of ITS1 and ITS2 from ribosomal ITS sequences of fungi and other eukaryotes for analysis of environmental sequencing data. *Methods Ecol. Evol.* 4, 914–919. doi: 10.1111/2041-210X.12073

Benitez, M.-S., Osborne, S. L., and Lehman, R. M. (2017). Previous crop and rotation history effects on maize seedling health and associated rhizosphere microbiome. *Sci. Rep.* 7:15709. doi: 10.1038/s41598-017-15955-9

Benjamini, Y., and Hochberg, Y. (2000). On the adaptive control of the false discovery rate in multiple testing with independent statistics. *J. Educ. Behav. Statist.* 25, 60–83. doi: 10.3102/10769986025001060

Berg, G., Fritze, A., Roskot, N., and Smalla, K. (2001). Evaluation of potential biocontrol rhizobacteria from different host plants of *Verticillium dahliae* Kleb. *J. Appl. Microbiol.* 91, 963–971. doi: 10.1046/j.1365-2672.2001.01462.x

Boari, A., and Vurro, M. (2004). Evaluation of *Fusarium* spp. and other fungi as biological control agents of broomrape (*Orobanche ramosa*). *Biol. Control* 30, 212–219. doi: 10.1016/j.biocontrol.2003.12.003

Bottalico, A., and Perrone, G. (2002). Toxigenic *Fusarium* species and mycotoxins associated with head blight in small-grain cereals in Europe. *Eur. J. Plant Pathol.* 108, 611–624. doi: 10.1023/A:1020635214971

Brown, S. P., Veach, A. M., Rigdon-Huss, A. R., Grond, K., Lickteig, S. K., Lothamer, K., et al. (2015). Scraping the bottom of the barrel: are rare high throughput sequences artifacts? *Fungal Ecol.* 13, 221–225. doi: 10.1016/j.funeco.2014.08.006

Bush, B. J., Carson, M. L., Cubeta, M. A., Hagler, W. M., and Payne, G. A. (2004). Infection and fumonisin production by *Fusarium verticillioides* in developing maize kernels. *Phytopathology* 94, 88–93. doi: 10.1094/PHYTO.2004.94.1.88

Calvo-Garrido, C., Elmer, P. A. G., Viñas, I., Usall, J., Bartra, E., and Teixidó, N. (2013). Biological control of Botrytis bunch rot in organic wine grapes with the yeast antagonist *Candida sake* CPA-1. *Plant Pathol.* 62, 510–519. doi: 10.1111/j.1365-3059.2012.02684.x

Caporaso, J. G., Kuczynski, J., Stombaugh, J., Bittinger, K., Bushman, F. D., Costello, E. K., et al. (2010). QIIME allows analysis of high-throughput community sequencing data. *Nature Methods* 7, 335–336. doi: 10.1038/nmeth.f.303

Chen, L., Zhang, J., Zhao, B., Zhou, G., and Ruan, L. (2015). Bacterial community structure in maize stubble-amended soils with different moisture levels estimated by bar-coded pyrosequencing. *Appl. Soil Ecol.* 86, 62–70. doi: 10.1016/j.apsoil.2014.09.011

Chen, W., Hambleton, S., Seifert, K. A., Carisse, O., Diarra, M. S., Peters, R. D., et al. (2018). Assessing performance of spore samplers in monitoring aeromycobiota and fungal plant pathogen diversity in Canada. *Appl. Environ. Microbiol.* 84, e2601–e2617. doi: 10.1128/AEM.02601-17

Comby, M., Gacoin, M., Robineau, M., Rabenoelina, F., Ptas, S., Dupont, J., et al. (2017). Screening of wheat endophytes as biological control agents against *Fusarium* head blight using two different in vitro tests. *Microbiol. Res.* 202, 11–20. doi: 10.1016/j.micres.2017.04.014

Correa-Galeote, D., Bedmar, E. J., and Arone, G. J. (2018). Maize endophytic bacterial diversity as affected by soil cultivation history. *Front. Microbiol.* 9:484. doi: 10.3389/fmicb.2018.00484

Correa-Galeote, D., Bedmar, E. J., Fernández-González, A. J., Fernández-López, M., and Arone, G. J. (2016). Bacterial communities in the rhizosphere of amilaceous maize (*Zea mays* L.) as assessed by pyrosequencing. *Front. Plant Sci.* 7:1016. doi: 10.3389/fpls.2016.01016

Crane, J. M., Gibson, D. M., Vaughan, R. H., and Bergstrom, G. C. (2013). Iturin levels on wheat spikes linked to biological control of *Fusarium* head blight by *Bacillus amyloliquefaciens*. *Phytopathology* 103, 146–155. doi: 10.1094/PHYTO-07-12-0154-R

Cromey, M. G., Shorter, S. C., Lauren, D. R., and Sinclair, K. I. (2002). Cultivar and crop management influences on *Fusarium* head blight and mycotoxins in spring wheat *(Triticum aestivum)* in New Zealand. *N. Z. J. Crop Hortic. Sci.* 30, 235–247. doi: 10.1080/01140671.2002.9514220

Czembor, E., Stępień, Ł., and Waśkiewicz, A. (2015). Effect of environmental factors on *Fusarium* species and associated mycotoxins in maize grain grown in Poland. *PLoS One* 10:e0133644. doi: 10.1371/journal.pone.0133644

De Boer, W., Wagenaar, A.-M., Klein Gunnewiek, P. J. A., and Van Veen, J. A. (2007). In vitro suppression of fungi caused by combinations of apparently non-antagonistic soil bacteria: suppression of fungi by non-antagonistic soil bacteria. *FEMS Microbiol. Ecol.* 59, 177–185. doi: 10.1111/j.1574-6941.2006.00197.x

De Cal, A., Larena, I., Liñán, M., Torres, R., Lamarca, N., Usall, J., et al. (2009). Population dynamics of *Epicoccum nigrum*, a biocontrol agent against brown rot in stone fruit. *J. Appl. Microbiol.* 106, 592–605. doi: 10.1111/j.1365-2672.2008.04030.x

De la Cruz-Barrón, M., Cruz-Mendoza, A., Navarro–Noya, Y. E., Ruiz-Valdiviezo, V. M., Ortíz-Gutiérrez, D., Ramírez-Villanueva, D. A., et al. (2017). The bacterial community structure and dynamics of carbon and nitrogen when maize (*Zea mays* L.) and its neutral detergent fibre were added to soil from Zimbabwe with contrasting management practices. *Microb. Ecol.* 73, 135–152. doi: 10.1007/s00248-016-0807-8

Desjardins, A. E., and Proctor, R. H. (2007). Molecular biology of *Fusarium* mycotoxins. *Int. J. Food Microbiol.* 119, 47–50. doi: 10.1016/j.ijfoodmicro.2007.07.024

Díaz Herrera, S., Grossi, C., Zawoznik, M., and Groppa, M. D. (2016). Wheat seeds harbour bacterial endophytes with potential as plant growth promoters and biocontrol agents of *Fusarium graminearum*. *Microbiol. Res.* 18, 37–43. doi: 10.1016/j.micres.2016.03.002

Dill-Macky, R., and Jones, R. K. (2000). The effect of previous crop residues and tillage on *Fusarium* head blight of wheat. *Plant Dis.* 84, 71–76. doi: 10.1094/PDIS.2000.84.1.71

Dorn, B., Forrer, H. R., Jenny, E., Wettstein, F. E., Bucheli, T. D., and Vogelgsang, S. (2011). *Fusarium* species complex and mycotoxins in grain maize from maize hybrid trials and from grower's fields. *J. Appl. Microbiol.* 111, 693–706. doi: 10.1111/j.1365-2672.2011.05091.x

Duvick, J., Rood, T., Maddox, J., and Gilliam, J. (1998). "Detoxification of mycotoxins in planta as a strategy for improving grain quality and disease resistance: identification of fumonisin-degrading microbes from maize," in *Molecular Genetics of Host-Specific Toxins in Plant Disease*, eds K. Kohmoto and O. C. Yoder (Dordrecht: Springer), 369–381. doi: 10.1007/978-94-011-5218-1_41

Edel-Hermann, V., Gautheron, N., Mounier, A., and Steinberg, C. (2015). *Fusarium* diversity in soil using a specific molecular approach and a cultural approach. *J. Microbiol. Methods* 111, 64–71. doi: 10.1016/j.mimet.2015.01.026

Edgar, R. C. (2010). Search and clustering orders of magnitude faster than BLAST. *Bioinformatics* 26, 2460–2461. doi: 10.1093/bioinformatics/btq461

Edgar, R. C., Haas, B. J., Clemente, J. C., Quince, C., and Knight, R. (2011). UCHIME improves sensitivity and speed of chimera detection. *Bioinformatics* 27, 2194–2200. doi: 10.1093/bioinformatics/btr381

Epskamp, S., Cramer, A. O. J., Waldorp, L. J., Schmittmann, V. D., and Borsboom, D. (2012). qgraph: network visualizations of relationships in psychometric data. *J. Statist. Softw.* 48. doi: 10.18637/jss.v048.i04

Fernandez, M., Huber, D., Basnyat, P., and Zentner, R. (2008). Impact of agronomic practices on populations of *Fusarium* and other fungi in cereal and noncereal crop residues on the Canadian Prairies. *Soil Tillage Res.* 100, 60–71. doi: 10.1016/j.still.2008.04.008

Ferrigo, D., Raiola, A., and Causin, R. (2016). *Fusarium* toxins in cereals: occurrence, legislation, factors promoting the appearance and their management. *Molecules* 21:627. doi: 10.3390/molecules21050627

Friedman, J., and Alm, E. J. (2012). Inferring correlation networks from genomic survey data. *PLoS Comput. Biol.* 8:e1002687. doi: 10.1371/journal.pcbi.1002687

Fu, L., Penton, C. R., Ruan, Y., Shen, Z., Xue, C., Li, R., et al. (2017). Inducing the rhizosphere microbiome by biofertilizer application to suppress banana *Fusarium* wilt disease. *Soil Biol. Biochem.* 104, 39–48. doi: 10.1016/j.soilbio.2016.10.008

Fujiwara, K., Iida, Y., Someya, N., Takano, M., Ohnishi, J., Terami, F., et al. (2016). Emergence of antagonism against the pathogenic fungus *Fusarium oxysporum* by interplay among non-antagonistic bacteria in a hydroponics using multiple parallel mineralization. *J. Phytopathol.* 164, 853–862. doi: 10.1111/jph.12504

Gardes, M., and Bruns, T. D. (1993). ITS primers with enhanced specificity for basidiomycetes – Application to the identification of mycorrhizae and rusts. *Mol. Ecol.* 2, 113–118. doi: 10.1111/j.1365-294X.1993.tb00005.x

Ghini, R., Mezzalama, M., Ambrosoli, R., Barberis, E., Garibaldi, A., and Piedade, S. M. S. (2000). *Fusarium oxysporum* strains as biocontrol agents against *Fusarium* wilt: effects on soil microbial biomass and activity. *Pesquisa Agropecuária Brasileira* 35, 93–101. doi: 10.1590/S0100-204X2000000100012

Gong, A.-D., Li, H.-P., Yuan, Q.-S., Song, X.-S., Yao, W., He, W.-J., et al. (2015). Antagonistic mechanism of iturin A and plipastatin A from *Bacillus amyloliquefaciens* S76-3 from wheat spikes against *Fusarium graminearum*. *PLoS One* 10:e0116871. doi: 10.1371/journal.pone.0116871

Gunasinghe, R. N., Ikiriwatte, C. J., and Karunaratne, A. M. (2004). The use of *Pantoea agglomerans* and *Flavobacterium* sp. to control banana pathogens. *J. Hortic. Sci. Biotechnol.* 79, 1002–1006. doi: 10.1080/14620316.2004.11511852

Haas, B. J., Gevers, D., Earl, A. M., Feldgarden, M., Ward, D. V., Giannoukos, G., et al. (2011). Chimeric 16S rRNA sequence formation and detection in sanger and 454-pyrosequenced PCR amplicons. *Genome Res.* 21, 494–504. doi: 10.1101/gr.112730.110

Hashem, M., and Ali, E. (2004). *Epicoccum Nigrum* as biocontrol agent of *Pythium* damping-off and root-rot of cotton seedlings. *Arch. Phytopathol. Plant Protect.* 37, 283–297. doi: 10.1080/03235400310001612955

He, J., Boland, G. J., and Zhou, T. (2009). Concurrent selection for microbial suppression of *Fusarium graminearum*, *Fusarium* head blight and deoxynivalenol in wheat. *J. Appl. Microbiol.* 106, 1805–1817. doi: 10.1111/j.1365-2672.2009.04147.x

Hellin, P., Dedeurwaerder, G., Duvivier, M., Scauflaire, J., Huybrechts, B., Callebaut, A., et al. (2016). Relationship between *Fusarium* spp. diversity and mycotoxin contents of mature grains in southern Belgium. *Food Addit. Contam. Part A* 33, 1228–1240. doi: 10.1080/19440049.2016.1185900

Hennessy, R. C., Glaring, M. A., Olsson, S., and Stougaard, P. (2017). Transcriptomic profiling of microbe–microbe interactions reveals the specific response of the biocontrol strain *P. fluorescens* In5 to the phytopathogen *Rhizoctonia solani*. *BMC Res. Notes* 10:376. doi: 10.1186/s13104-017-2704-8

Herbold, C. W., Pelikan, C., Kuzyk, O., Hausmann, B., Angel, R., Berry, D., et al. (2015). A flexible and economical barcoding approach for highly multiplexed amplicon sequencing of diverse target genes. *Front. Microbiol.* 6:731. doi: 10.3389/fmicb.2015.00731

Herlemann, D. P., Labrenz, M., Jürgens, K., Bertilsson, S., Waniek, J. J., and Andersson, A. F. (2011). Transitions in bacterial communities along the 2000 km salinity gradient of the Baltic Sea. *ISME J.* 5, 1571–1579. doi: 10.1038/ismej.2011.41

Jennings, P., Coates, M. E., Walsh, K., Turner, J. A., and Nicholson, P. (2004). Determination of deoxynivalenol- and nivalenol-producing chemotypes of *Fusarium graminearum* isolated from wheat crops in England and Wales. *Plant Pathol.* 53, 643–652. doi: 10.1111/j.0032-0862.2004.01061.x

Jensen, B. D., Knorr, K., and Nicolaisen, M. (2016). In vitro competition between *Fusarium graminearum* and *Epicoccum nigrum* on media and wheat grains. *Eur. J. Plant Pathol.* 146, 657–670. doi: 10.1007/s10658-016-0950-6

Karlsson, I., Edel-Hermann, V., Gautheron, N., Durling, M. B., Kolseth, A.-K., Steinberg, C., et al. (2016). Genus-specific primers for study of *Fusarium* communities in field samples. *Appl. Environ. Microbiol.* 82, 491–501. doi: 10.1128/AEM.02748-15

Karlsson, I., Friberg, H., Kolseth, A.-K., Steinberg, C., and Persson, P. (2017). Agricultural factors affecting *Fusarium* communities in wheat kernels. *Int. J. Food Microbiol.* 252, 53–60. doi: 10.1016/j.ijfoodmicro.2017.04.011

Katoh, K., Rozewicki, J., and Yamada, K. D. (2017). MAFFT online service: multiple sequence alignment, interactive sequence choice and visualization. *Briefings Bioinform. bbx*108. doi: 10.1093/bib/bbx108

Köhl, J., Lombaers, C., Moretti, A., Bandyopadhyay, R., Somma, S., and Kastelein, P. (2015). Analysis of microbial taxonomical groups present in maize stalks suppressive to colonization by toxigenic *Fusarium* spp.: a strategy for the identification of potential antagonists. *Biol. Control* 83, 20–28. doi: 10.1016/j.biocontrol.2014.12.007

Kõljalg, U., Nilsson, R. H., Abarenkov, K., Tedersoo, L., Taylor, A. F. S., Bahram, M., et al. (2013). Towards a unified paradigm for sequence-based identification of fungi. *Mol. Ecol.* 22, 5271–5277. doi: 10.1111/mec.12481

Kumar, S., Stecher, G., and Tamura, K. (2016). MEGA7: molecular evolutionary genetics analysis version 7.0 for bigger datasets. *Mol. Biol. Evol.* 33, 1870–1874. doi: 10.1093/molbev/msw054

LeBlanc, N., Kinkel, L., and Kistler, H. C. (2017). Plant diversity and plant identity influence *Fusarium* communities in soil. *Mycologia* 109, 128–139. doi: 10.1080/00275514.2017.1281697

Legrand, F., Picot, A., Cobo-Díaz, J. F., Chen, W., and Le Floch, G. (2017). Challenges facing the biological control strategies for the management of *Fusarium* head blight of cereals caused by *F. graminearum*. *Biol. Control* 113, 26–38. doi: 10.1016/j.biocontrol.2017.06.011

Legrand, F., Picot, A., Cobo-Díaz, J. F., Carof, M., Chen, W., and Le Floch, G. (2018). Effect of tillage and static abiotic soil properties on microbial diversity. *Appl. Soil Ecol.* 132, 135–145. doi: 10.1016/j.apsoil.2018.08.016

Li, X., Rui, J., Mao, Y., Yannarell, A., and Mackie, R. (2014). Dynamics of the bacterial community structure in the rhizosphere of a maize cultivar. *Soil Biol. Biochem.* 68, 392–401. doi: 10.1016/j.soilbio.2013.10.017

Logrieco, A., Mulè, G., Moretti, A., and Bottalico, A. (2002). Toxigenic *Fusarium* species and mycotoxins associated with maize ear rot in Europe. *Eur. J. Plant Pathol.* 108:597. doi: 10.1023/A:1020679029993

Luongo, L., Galli, M., Corazza, L., Meekes, E., Haas, L. D., Van Der Plas, C. L., et al. (2005). Potential of fungal antagonists for biocontrol of *Fusarium* spp. in wheat and maize through competition in crop debris. *Biocontrol Sci. Technol.* 15, 229–242. doi: 10.1080/09583150400016852

Maiorano, A., Blandino, M., Reyneri, A., and Vanara, F. (2008). Effects of maize residues on the *Fusarium* spp. infection and deoxynivalenol (DON) contamination of wheat grain. *Crop Protect.* 27, 182–188. doi: 10.1016/j.cropro.2007.05.004

Manso, T., and Nunes, C. (2011). *Metschnikowia andauensis* as a new biocontrol agent of fruit postharvest diseases. *Postharv. Biol. Technol.* 61, 64–71. doi: 10.1016/j.postharvbio.2011.02.004

McDonald, D., Price, M. N., Goodrich, J., Nawrocki, E. P., DeSantis, T. Z., Probst, A., et al. (2012). An improved Greengenes taxonomy with explicit ranks for ecological and evolutionary analyses of bacteria and archaea. *ISME J.* 6, 610–618. doi: 10.1038/ismej.2011.139

Mousa, W. K., Shearer, C. R., Limay-Rios, V., Zhou, T., and Raizada, M. N. (2015). Bacterial endophytes from wild maize suppress *Fusarium graminearum* in modern maize and inhibit mycotoxin accumulation. *Front. Plant Sci.* 6:805. doi: 10.3389/fpls.2015.00805

Nazari, L., Pattori, E., Terzi, V., Morcia, C., and Rossi, V. (2014). Influence of temperature on infection, growth, and mycotoxin production by *Fusarium langsethiae* and *F. sporotrichioides* in durum wheat. *Food Microbiol.* 39, 19–26. doi: 10.1016/j.fm.2013.10.009

Nicolaisen, M., Justesen, A. F., Knorr, K., Wang, J., and Pinnschmidt, H. O. (2014). Fungal communities in wheat grain show significant co-existence patterns among species. *Fungal Ecol.* 11, 145–153. doi: 10.1016/j.funeco.2014.06.002

Nielsen, L. K., Jensen, J. D., Nielsen, G. C., Jensen, J. E., Spliid, N. H., Thomsen, I. K., et al. (2011). *Fusarium* head blight of cereals in Denmark: species complex and related mycotoxins. *Phytopathology* 101, 960–969. doi: 10.1094/PHYTO-07-10-0188

Niu, B., Paulson, J. N., Zheng, X., and Kolter, R. (2017). Simplified and representative bacterial community of maize roots. *Proc. Natl. Acad. Sci. U.S.A.* 114, E2450–E2459. doi: 10.1073/pnas.1616148114

Ogórek, R., and Plaskowska, E. (2011). *Epicoccum nigrum* for biocontrol agents in vitro of plant fungal pathogens. *Commun. Agric. Appl. Biol. Sci.* 76, 691–697.

Oliver, A. K., Brown, S. P., Callaham, M. A., and Jumpponen, A. (2015). Polymerase matters: non-proofreading enzymes inflate fungal community richness estimates by up to 15 %. *Fungal Ecol.* 15, 86–89. doi: 10.1016/j.funeco.2015.03.003

Palazzini, J. M., Ramirez, M. L., Torres, A. M., and Chulze, S. N. (2007). Potential biocontrol agents for *Fusarium* head blight and deoxynivalenol production in wheat. *Crop Protect.* 26, 1702–1710. doi: 10.1016/j.cropro.2007.03.004

Pan, J. J., and May, G. (2009). Fungal-fungal associations affect the assembly of endophyte communities in maize (*Zea mays*). *Microb. Ecol.* 58, 668–678. doi: 10.1007/s00248-009-9543-7

Parks, D. H., Tyson, G. W., Hugenholtz, P., and Beiko, R. G. (2014). STAMP: statistical analysis of taxonomic and functional profiles. *Bioinformatics* 30, 3123–3124. doi: 10.1093/bioinformatics/btu494

Parry, D. W., Jenkinson, P., and McLEOD, L. (1995). *Fusarium* ear blight (scab) in small grain cereals? – A review. *Plant Pathol.* 44, 207–238. doi: 10.1111/j.1365-3059.1995.tb02773.x

Peiffer, J. A., Spor, A., Koren, O., Jin, Z., Tringe, S. G., Dangl, J. L., et al. (2013). Diversity and heritability of the maize rhizosphere microbiome under field conditions. *Proc. Natl. Acad. Sci. U.S.A.* 110, 6548–6553. doi: 10.1073/pnas.1302837110

Pereira, P., Nesci, A., Castillo, C., and Etcheverry, M. (2011). Field studies on the relationship between *Fusarium verticillioides* and maize (*Zea mays* L.): effect of biocontrol agents on fungal infection and toxin content of grains at harvest. *Int. J. Agron.* 2011:486914. doi: 10.1155/2011/486914

Potshangbam, M., Devi, S. I., Sahoo, D., and Strobel, G. A. (2017). Functional characterization of endophytic fungal community associated with *Oryza sativa* L. and *Zea mays* L. *Front. Microbiol.* 8:325. doi: 10.3389/fmicb.2017.00325

Rajakumar, E., Aggarwal, R., and Singh, B. (2005). Fungal antagonists for the biological control of *Ascochyta* blight of chickpea. *Acta Phytopathol. Entomol. Hungarica* 40, 35–42. doi: 10.1556/APhyt.40.2005.1-2.5

Ramirez, M. L., Chulze, S., and Magan, N. (2006). Temperature and water activity effects on growth and temporal deoxynivalenol production by two Argentinean strains of *Fusarium graminearum* on irradiated wheat grain. *Int. J. Food Microbiol.* 106, 291–296. doi: 10.1016/j.ijfoodmicro.2005.09.004

Ronquist, F., Teslenko, M., van der Mark, P., Ayres, D. L., Darling, A., Höhna, S., et al. (2012). MrBayes 3.2: efficient bayesian phylogenetic inference and model choice across a large model space. *Syst. Biol.* 61, 539–542. doi: 10.1093/sysbio/sys029

Sang, M. K., Jeong, J.-J., Kim, J., and Kim, K. D. (2018). Growth promotion and root colonisation in pepper plants by phosphate-solubilising *Chryseobacterium* sp. strain ISE14 that suppresses *Phytophthora* blight: biocontrol and plant growth by phosphate-solubilising *Chryseobacterium*. *Ann. Appl. Biol.* 172, 208–223. doi: 10.1111/aab.12413

Scauflaire, J., Mahieu, O., Louvieaux, J., Foucart, G., Renard, F., and Munaut, F. (2011). Biodiversity of *Fusarium* species in ears and stalks of maize plants in Belgium. *Eur. J. Plant Pathol.* 131, 59–66. doi: 10.1007/s10658-011-9787-1

Schisler, D. A., Boehm, M. J., Paul, P. A., Rooney, A. P., and Dunlap, C. A. (2015). Reduction of *Fusarium* head blight using prothioconazole and prothioconazole-tolerant variants of the *Fusarium* head blight antagonist *Cryptococcus flavescens* OH 182.9. *Biol. Control* 86, 36–45. doi: 10.1016/j.biocontrol.2015.04.002

Schöneberg, A., Musa, T., Voegele, R. T., and Vogelgsang, S. (2015). The potential of antagonistic fungi for control of *Fusarium graminearum* and *Fusarium crookwellense* varies depending on the experimental approach. *J. Appl. Microbiol.* 118, 1165–1179. doi: 10.1111/jam.12775

Shaner, G. (2003). "Epidemiology of *Fusarium* head blight of small grain cereals in North America", in *Fusarium Head Blight of Wheat and Barley,* eds K. J. Leonard and W. R. Bushnell (St. Paul, MN: The American Phytopathological Society), 84–119.

Siegel-Hertz, K., Edel-Hermann, V., Chapelle, E., Terrat, S., Raaijmakers, J. M., and Steinberg, C. (2018). Comparative microbiome analysis of a *Fusarium* wilt suppressive soil and a *Fusarium* wilt conducive soil from the Châteaurenard Region. *Front. Microbiol.* 9:568. doi: 10.3389/fmicb.2018.00568

Singh, D. P., Backhouse, D., and Kristiansen, P. (2009). Interactions of temperature and water potential in displacement of *Fusarium pseudograminearum* from cereal residues by fungal antagonists. *Biol. Control* 48, 188–195. doi: 10.1016/j.biocontrol.2008.10.015

Siou, D., Gélisse, S., Laval, V., Suffert, F., and Lannou, C. (2015). Mutual exclusion between fungal species of the *Fusarium* head blight complex in a wheat spike. *Appl. Environ. Microbiol.* 81, 4682–4689. doi: 10.1128/AEM.00525-15

Song, Y.-S., Seo, D.-J., and Jung, W.-J. (2017). Identification, purification, and expression patterns of chitinase from psychrotolerant *Pedobacter* sp. PR-M6 and antifungal activity in vitro. *Microb. Pathogen.* 107, 62–68. doi: 10.1016/j.micpath.2017.03.018

Sugahara, H., Kondo, T., Okada, M., Ikeda, Y., Kaida, K., Fudou, R., et al. (2008). *Articulospora* sp. produces Art1, an inhibitor of bacterial histidine kinase. *Biosci. Biotechnol. Biochem.* 72, 2521–2525. doi: 10.1271/bbb.80021

Summerbell, R. C., Gueidan, C., Schroers, H.-J., de Hoog, G. S., Starink, M., Rosete, Y. A., et al. (2011). Acremonium phylogenetic overview and revision of *Gliomastix*, *Sarocladium*, and *Trichothecium*. *Stud. Mycol.* 68, 139–162. doi: 10.3114/sim.2011.68.06

Sun, B., Wang, X., Wang, F., Jiang, Y., and Zhang, X.-X. (2013). Assessing the relative effects of geographic location and soil type on microbial communities associated with straw decomposition. *Appl. Environ. Microbiol.* 79, 3327–3335. doi: 10.1128/AEM.00083-13

Szilagyi-Zecchin, V. J., Adamoski, D., Gomes, R. R., Hungria, M., Ikeda, A. C., Kava-Cordeiro, V., et al. (2016). Composition of endophytic fungal community associated with leaves of maize cultivated in south Brazilian field. *Acta Microbiol. Immunol. Hungar.* 63, 449–466. doi: 10.1556/030.63.2016.020

Tagne, A., Neergaard, E., Hansen, H. J., and The, C. (2002). Studies of host–pathogen interaction between maize and *Acremonium strictum* from Cameroon. *Eur. J. Plant Pathol.* 108, 93–102. doi: 10.1023/A:1015092030874

UNITE Community (2017). *UNITE USEARCH/UTAX Release*. Available at: https://search.datacite.org/works/10.15156/bio/587476

van Bruggen, A. H. C., Francis, I. M., and Jochimsen, K. N. (2014). Non-pathogenic rhizosphere bacteria belonging to the genera *Rhizorhapis* and *Sphingobium* provide specific control of lettuce corky root disease caused by species of the same bacterial genera. *Plant Pathol.* 63, 1384–1394. doi: 10.1111/ppa.12212

Waalwijk, C., Kastekein, P., de Vries, I., Kerényi, Z., Van Der Lee, T., Hesselink, T., et al. (2003). Major changes in *Fusarium* spp. in wheat in the Netherlands. *Eur. J. Plant Pathol.* 109, 743–754. doi: 10.1023/A:1026086510156

Wachowska, U., Kucharska, K., Jędryczka, M., and Łobik, N. (2013). Microorganisms as biological control agents against *Fusarium* pathogens in winter wheat. *Polish J. Environ. Stud.* 22, 591–597.

White, T. J., Bruns, T. D., Lee, S. B., and Taylor, J. (1990). "Amplification and direct sequencing of fungal ribosomal RNA genes for phylogenetics," in *PCR Protocols – A Guide to Methods and Applications*, eds M. A. Innis, D. H. Gelfand, J. J. Sninsky, and T. J. White (San Diego, CA: Academic Press), 315–322.

Wicklow, D. T., and Poling, S. M. (2009). Antimicrobial activity of pyrrocidines from *Acremonium zeae* against endophytes and pathogens of maize. *Phytopathology* 99, 109–115. doi: 10.1094/PHYTO-99-1-0109

Xing, H.-Q., Ma, J.-C., Xu, B.-L., Zhang, S.-W., Wang, J., Cao, L., et al. (2018). Mycobiota of maize seeds revealed by rDNA-ITS sequence analysis of samples with varying storage times. *Microbiology Open* 7:e00609. doi: 10.1002/mbo3.609

Xiong, W., Li, R., Ren, Y., Liu, C., Zhao, Q., Wu, H., et al. (2017). Distinct roles for soil fungal and bacterial communities associated with the suppression of vanilla *Fusarium* wilt disease. *Soil Biol. Biochem.* 107, 198–207. doi: 10.1016/j.soilbio.2017.01.010

Xu, X.-M., Nicholson, P., Thomsett, M. A., Simpson, D., Cooke, B. M., Doohan, F. M., et al. (2008). Relationship between the fungal complex causing *Fusarium* head blight of wheat and environmental conditions. *Phytopathology* 98, 69–78. doi: 10.1094/PHYTO-98-1-0069

Xu, X.-M., Parry, D. W., Nicholson, P., Thomsett, M. A., Simpson, D., Edwards, S. G., et al. (2005). Predominance and association of pathogenic fungi causing *Fusarium* ear blightin wheat in four European countries. *Eur. J. Plant Pathol.* 112, 143–154. doi: 10.1007/s10658-005-2446-7

Yang, Y., Wang, N., Guo, X., Zhang, Y., and Ye, B. (2017). Comparative analysis of bacterial community structure in the rhizosphere of maize by high-throughput pyrosequencing. *PLoS One* 12:e0178425. doi: 10.1371/journal.pone.0178425

Yin, C., Hulbert, S. H., Schroeder, K. L., Mavrodi, O., Mavrodi, D., Dhingra, A., et al. (2013). Role of bacterial communities in the natural suppression of *Rhizoctonia solani* bare patch disease of wheat (*Triticum aestivum* L.). *Appl. Environ. Microbiol.* 79, 7428–7438. doi: 10.1128/AEM.01610-13

Zhao, M., Sun, B., Wu, L., Gao, Q., Wang, F., Wen, C., et al. (2016). Zonal soil type determines soil microbial responses to maize cropping and fertilization. *mSystems* 1:e00075-16. doi: 10.1128/mSystems.00075-16

Conflict of Interest Statement: The authors declare that the research was conducted in the absence of any commercial or financial relationships that could be construed as a potential conflict of interest.

frontiers in Microbiology

ORIGINAL RESEARCH
published: 15 March 2019
doi: 10.3389/fmicb.2019.00506

Prediction of Host-Specific Genes by Pan-Genome Analyses of the Korean *Ralstonia solanacearum* Species Complex

Heejung Cho[1], Eun-Sung Song[1], Sunggi Heu[2], JeongHo Baek[1], Young Kee Lee[1], Seungdon Lee[1], Seon-Woo Lee[3], Dong Suk Park[1], Tae-Ho Lee[1], Jeong-Gu Kim[1] and Ingyu Hwang[4]*

[1] National Institute of Agricultural Sciences, Rural Development Administration, Jeonju, South Korea, [2] National Institute of Crop Science, Rural Development Administration, Jeonju, South Korea, [3] Department of Applied Biology, Dong-A University, Busan, South Korea, [4] Department of Agricultural Biotechnology, Seoul National University, Seoul, South Korea

OPEN ACCESS

Edited by:
David B. Collinge, University of Copenhagen, Denmark

Reviewed by:
Brian H. Kvitko, University of Georgia, United States
Maria Raffaella Ercolano, University of Naples Federico II, Italy

***Correspondence:**
Heejung Cho
chohj78@korea.kr

Specialty section:
This article was submitted to Plant Microbe Interactions, a section of the journal Frontiers in Microbiology

Received: *21 November 2018*
Accepted: *27 February 2019*
Published: *15 March 2019*

Citation:
Cho H, Song E-S, Heu S, Baek J, Lee YK, Lee S, Lee S-W, Park DS, Lee T-H, Kim J-G and Hwang I (2019) Prediction of Host-Specific Genes by Pan-Genome Analyses of the Korean Ralstonia solanacearum Species Complex. Front. Microbiol. 10:506. doi: 10.3389/fmicb.2019.00506

The soil-borne pathogenic *Ralstonia solanacearum* species complex (RSSC) is a group of plant pathogens that is economically destructive worldwide and has a broad host range, including various solanaceae plants, banana, ginger, sesame, and clove. Previously, Korean RSSC strains isolated from samples of potato bacterial wilt were grouped into four pathotypes based on virulence tests against potato, tomato, eggplant, and pepper. In this study, we sequenced the genomes of 25 Korean RSSC strains selected based on these pathotypes. The newly sequenced genomes were analyzed to determine the phylogenetic relationships between the strains with average nucleotide identity values, and structurally compared via multiple genome alignment using Mauve software. To identify candidate genes responsible for the host specificity of the pathotypes, functional genome comparisons were conducted by analyzing pan-genome orthologous group (POG) and type III secretion system effectors (T3es). POG analyses revealed that a total of 128 genes were shared only in tomato-non-pathogenic strains, 8 genes in tomato-pathogenic strains, 5 genes in eggplant-non-pathogenic strains, 7 genes in eggplant-pathogenic strains, 1 gene in pepper-non-pathogenic strains, and 34 genes in pepper-pathogenic strains. When we analyzed T3es, three host-specific effectors were predicted: RipS3 (SKWP3) and RipH3 (HLK3) were found only in tomato-pathogenic strains, and RipAC (PopC) were found only in eggplant-pathogenic strains. Overall, we identified host-specific genes and effectors that may be responsible for virulence functions in RSSC *in silico*. The expected characters of those genes suggest that the host range of RSSC is determined by the comprehensive actions of various virulence factors, including effectors, secretion systems, and metabolic enzymes.

Keywords: *Ralstonia solanacearum* species complex, bacterial wilt, host specificity, genome, pan-genome, type III secretion system effectors

INTRODUCTION

The *Ralstonia solanacearum* species complex (RSSC) is a group of rod-shaped Gram-negative bacteria with polar flagella belonging to the Burkholderiaceae family of the Betaproteobacteria class. RSSC are soil-borne pathogens and can live for several years without a host. The bacteria invade host vascular tissues through injured roots or natural openings. Then, colonization and production of exopolysaccharide (EPS) in the stem block water transport in the xylem, resulting in wilting and death of the host plant (Denny, 2006).

Ralstonia solanacearum has an uncommonly broad host range, infecting more than 450 plant species that belong to more than 50 families, encompassing monocots and dicots and herbaceous and woody plants (Hayward, 1991; Wicker et al., 2007; Jiang et al., 2017). *R. solanacearum* are found in distinct geographical regions, which include tropical, subtropical, and warm and cool temperate areas across the six continents of Asia, Africa, Europe, and North and South America, and Oceania (Hayward, 1991; Denny, 2006). With their broad host range and wide geographical distribution, *R. solanacearum* have demonstrated great diversity in their genetic and phenotypic properties, and thus strains of this species have been designated as a species complex, the RSSC (Fegan and Prior, 2005; Genin and Denny, 2012). The RSSC group has been expanded to include *Ralstonia syzygii* and blood disease bacteria (BDB), which are closely related organisms (Taghavi et al., 1996).

The investigation of the genome of *R. solanacearum* began with the complete genome sequencing of strain GMI1000, which significantly advanced the study of pathogenicity by characterizing the molecular complexity of the organism (Salanoubat et al., 2002). Subsequently, the complete or draft genomes of many *R. solanacearum* strains with various host ranges became available. To date, there are 86 genomes of RSSC deposited in the National Center for Biotechnology Information (NCBI database in Aug 2018[1]). RSSC usually have a bipartite genome, with one chromosome and one megaplasmid; however, some strains (i.e., CMR15 and PSI07) carry an additional plasmid (Remenant et al., 2010). Whole-genome comparisons of sequenced genomes have confirmed the phylotype classification scheme of RSSC: phylotype I (GMI1000, FQY_4, EP1, and Y45), phylotype II (CFBP2957, IPO1609, K60, MolK2, Po82, and UW551), phylotype III (CMR15), and phylotype IV (PSI07, *R. syzygii* R24 and BDB R229). RSSC have been reclassified into three species, based on analyses of various biochemical properties and genomic comparisons, as follows: *R. solanacearum* (phylotype II strains), *Ralstonia pseudosolanacearum* (phylotype I and III strains), and *R. syzygii* (phylotype IV strains, including *R. syzygii* R24 and BDB R229) (Safni et al., 2014). RSSC is also divided into five biovars based on carbohydrate utilization, i.e. the ability to oxidize 3 disaccharides (lactose, maltose, and cellobiose) and 3 hexose alcohols (mannitol, dulcitol, and sorbitol) (Hayward, 1991).

[1]https://www.ncbi.nlm.nih.gov

A number of factors are responsible for the pathogenesis of RSSC: global regulatory transcription factors, EPS, plant hormones, host cell wall-degrading enzymes, adhesion/surface proteins, toxins, and oxidative stress resistance. Many of them are secreted in RSSC, and the bacterial pathogen mainly use type II (T2SS) and type III secretion systems (T3SS). Three types of T2SS, one orthodox system and two unorthodox systems, have been found in seven reference genomes, including those of phylotypes I, II, III, and IV (Li et al., 2016). T3SS is also crucial for bacterial virulence as the plant-inducible secretion machinery, which is encoded by the highly conserved *hrp* gene cluster in strains of phylotypes I, II, III, and IV (Li et al., 2016).

Type III secretion systems exports virulence factors directly into the host cells, and these injected proteins are called type III effector proteins (T3e) (Cunnac et al., 2004; Mukaihara et al., 2010). T3es of RSSC have been designated as Rip (*Ralstonia*-injected proteins), which include the Pop/AWR/Gala families (Peeters et al., 2013). These proteins have various functions in the invasion of host plants. For instance, the GALA family has F-box and leucine-rich repeat (LRR) domains that are required for full virulence (Angot et al., 2006; Kajava et al., 2008; Remigi et al., 2011). PopP family proteins work as avirulence proteins with acetyl transferase activity (PopP2) (Deslandes et al., 2003), and some AWR family effectors induce necrotic cell death in host plants (Sole et al., 2012). Likewise, T3e disrupts the homeostasis of host plants by disturbing signal transduction. Their defense system falters, leading to bacterial infection and death by wilting (Poueymiro and Genin, 2009). In a previous study, pan-genome analyses of 11 representative RSSC strains identified 94 Rips (Peeters et al., 2013). Individual RSSC strains possess around 60–75 effectors, and effector repertoire comparisons have revealed 32 core effectors in 10 strains. Most *rip* genes have a feature in their promoter region called a plant-inducible promoter (PIP) box, which is responsive to the T3SS transcriptional regulator HrpB (Cunnac et al., 2004).

A number of studies have investigated the host specificity of this highly vulnerable pathogen; however, because of the indefinite host range and bacterial nomenclature related to virulence, few systematic studies have clearly defined host specificity (Guidot et al., 2007; Cellier et al., 2012; Peeters et al., 2013; Ailloud et al., 2015). Nonetheless, the *rsa1* gene from strain SL2029 (phylotype IV biovar 2) has been described as a pepper-specific avirulence gene. The Rsa1 protein from strain SL2029 is specifically avirulent for pepper infection, and when this gene is introduced into the pepper pathogenic strain SL341 (phylotype I biovar 4), the SL341 with the *rsa1* gene becomes avirulent for pepper (Jeong et al., 2011).

In our previous study of the pathogenicity against potato, tomato, eggplant, and pepper, Korean RSSC were divided into four pathotypes. Since pathotypes reflect genetic traits of RSSC, we attempted to identify bacterial genes for host specificity of RSSC by adopting pan-genome analysis. In this study, we sequenced whole genome of 25 Korean RSSC strains and performed comparative genome analyses to present the candidate genes responsible for host specificity including T3es and pathogenesis related genes.

MATERIALS AND METHODS

Strain Selection

We previously analyzed the genetic and pathogenic diversity of Korean RSSC using 93 strains isolated from samples of potato bacterial wilt throughout the country. To conduct in-depth analyses of the genetic relationships between RSSC and hosts, 25 isolates were selected based on their host range on solanaceous crop plants, with typical representative characters for each of the individual phylotypes (Cho et al., 2018).

Genome Sequencing

For genomic DNA preparation, high-molecular-weight genomic DNA was prepared as previously described (Cho et al., 2018). Each bacterial genome was sequenced using the Pacific Biosciences' Single Molecule Real Time (SMRT) Sequencing Technology with a 20 kb library, P6/C4 chemistry, and one SMRT cell running ([2]DNAlink, South Korea). *De novo* assembly was conducted using the hierarchical genome assembly process (HGAP ver. 2.3) workflow (Chin et al., 2013), including consensus polishing with Quiver, and the default parameters (Minimum Subread Length 500 bp, Minimum Polymerase Read Quality 0.8, and Minimum Polymerase Read Length 100 bp). After error correction based on the longest seed reads with shorter reads, sequences were assembled with error-corrected reads. Gene prediction was carried out using the Glimmer3 to predict coding sequences (CDSs), and RNAmmer-1.2 and tRNAscan-SE were used to identify rRNA and tRNA sequences in the assembled genome. The annotation of each CDS was performed using homology search against Blastall ver. 2.2.26.

Genome Comparisons

For comparison with reference strains, the genome sequences of GMI1000, FQY_4, CMR15, PO82, and PSI07 were retrieved from the National Center for Biotechnology Information (NCBI) database and those of *R. syzygii* R24 and BDB R229 were obtained from the EMBL database (**Table 1**). To analyze the overall genome sequence similarity, the Orthologous Average Nucleotide Identity (OrthoANI) tool was used (Lee et al., 2016). Multiple genome alignments were performed using the Mauve software[3].

Analysis of Clusters of Orthologous Groups and Pan-Genome Orthologous Groups

For comparative genome analyses, clusters of orthologous group (COG) and pan-genome orthologous group (POG) analyses were performed using the Chunlab pipeline ([4]South Korea) (Chun et al., 2009). Gene prediction and annotation were analyzed using the Server for Rapid Annotations using Subsystem Technology (RAST) (Aziz et al., 2008). The annotation of each CDS was conducted by homology search against the Swiss-Prot, EggNOG 4.1, SEED (the database and infrastructure for comparative genomics), and Kyoto Encyclopedia of Genes and Genomes (KEGG) databases.

Effectors Prediction

The effectors of T3es of the Korean RSSC strains were identified using the RalstoT3E server[5] (Peeters et al., 2013).

Genome Submission

The genome sequences of 25 Korean RSSC strains were deposited in the NCBI database and the accession numbers are listed in **Table 1**.

RESULTS

General Genomic Features of the RSSC Strains

High-quality genomes of the Korean RSSC strains were constructed using PacBio long read sequencing data. The general genomic features of the RSSC strains used in this study are summarized in **Table 1**. The newly sequenced 25 Korean RSSC genomes were complete and contained two contigs: one for the chromosome and another for a megaplasmid, except for T78 strain, which contained one chromosome, one megaplasmid, and one small plasmid.

All 25 strains analyzed in this study belong to phylotype I and IV, the assembled genome sizes were 5.4–6.15 Mbp and the GC contents were 66.4–66.9%. The number of predicted genes was 5,071–6,811, that of rRNA genes was 9 or 12, and that of tRNA genes was 54–59. The genome comparison revealed several differences between the genomes of phylotype I and phylotype IV, as follows: the average genome sizes of phylotype I and IV were 5.8 and 5.5 Mbp, the average GC contents were 66.91 and 66.39%, the average number of predicted CDSs was 5,551 and 5,152, the number of rRNA genes was 12 and 9, and the average number of tRNA genes was 58 and 55, respectively. All genomic features (genome size, GC content, and number of CDSs, rRNAs, and tRNAs) of the phylotype I strains were larger than those of the phylotype IV strains, except for the T42 strain, which was similar in genome size and CDS number to the phylotype IV strains.

Comparative Genomics: OrthoANI Analyses and Multiple Genome Alignments

To compare the overall similarity of the 25 Korean genomes and 9 reference genomes, the OrthoANI values were calculated (**Supplementary Table S1**) and are presented with the phylogenetic tree in **Figure 1**. In this tree, all Korean phylotype I strains clustered with the phylotype I reference strains GMI1000 (biovar 3, isolated from tomato in French Guyana) and FQY_4 (biovar 4, isolated from bacterial wilt in a nursery in China) (Salanoubat et al., 2002; Cao et al., 2013). Among the Korean phylotype I strains, four biovar 3 isolates (SL2330, SL3755, T25, and T110) clustered more closely with GMI1000, and

[2]www.dnalink.com

[3]http://darlinglab.org/mauve/mauve.html

[4]http://www.chunlab.com

[5]https://iant.toulouse.inra.fr/bacteria/annotation/site/prj/T3Ev3

ten other biovar 4 isolates (SL2729, SL3103, SL3300, SL3730, SL3822, SL3882, T42, T60, T78, and T117) clustered more closely with FQY_4. Eleven Korean phylotype IV strains (SL2064, SL2312, SL3022, SL3175, T11, T12, T51, T82, T95, T98, and T101) clustered with the phylotype IV strains of PSI07 (from tomato in Indonesia), BDB R229 (from banana in Indonesia), and *R. syzygii* R24 (from clove in Indonesia), which originated from the Indonesian region. Among the Korean phylotype IV strains, SL3175 and T98 were closer to reference strains PSI07 and BDB R229.

To demonstrate the consistency or variation among the Korean RSSC genomes, multiple genome alignment was performed using the Mauve tool (**Figure 2**). This alignment revealed that eleven phylotype IV-biovar 2 (hereafter, IV-2) strains were co-linear along the chromosomes and the megaplasmids. For phylotype I strains, the phylotype I-biovar 3 (I-3) and phylotype I-biovar 4 (I-4) strains were generally similar to each other with respect to their genome organization; however, some strains had a genetic inversion, i.e., SL3300 and T117 had an inversion in the middle of the chromosome, and T25 and SL3822 had a large inversion in the megaplasmid. Between the phylotype I and IV strains, the gene organization revealed many rearrangements, particularly in the megaplasmid.

COG Distribution Between RSSC Strains

To compare the distribution of functional genes between the RSSC strains in relation to bacterial virulence and potential host specificity, the functional categories of COG were analyzed (**Figure 3** and **Supplementary Table S2**). Among the predicted CDSs, about 70% of the genes were classified into one of the 22 COG categories and about 30% were of unknown function. Aside from the genes of unknown function (S), the largest

TABLE 1 | General genome features of the RSSC strains used in this study.

Strain[a]	Phyl-bv[b]	Contigs	Size (bp)	GC (%)	CDSs	rRNA	tRNA	Genome accession[c]
SL2312	IV-2	2	5,521,456	66.4	5,079	9	56	CP022796, CP022797
SL2064	IV-2	2	5,473,607	66.4	5,169	9	55	CP022798, CP022799
SL3022	IV-2	2	5,605,251	66.3	5,376	9	55	CP023016, CP023017
SL3175	IV-2	2	5,555,993	66.4	5,170	9	54	CP022788, CP022789
T11	IV-2	2	5,450,627	66.4	5,143	9	56	CP022776, CP022777
T12	IV-2	2	5,520,985	66.4	5,189	9	56	CP022774, CP022775
T51	IV-2	2	5,400,849	66.4	5,074	9	55	CP022770, CP022771
T82	IV-2	2	5,521,457	66.4	5,071	9	56	CP022763, CP022764
T95	IV-2	2	5,474,514	66.4	5,146	9	55	CP022761, CP022762
T98	IV-2	2	5,555,978	66.4	5,172	9	54	CP022759, CP022760
T101	IV-2	2	5,521,368	66.4	5,086	9	56	CP022757, CP022758
SL2330	I-3	2	5,674,600	67	5,242	12	58	CP022794, CP022795
SL3755	I-3	2	5,792,854	66.9	5,413	12	58	CP022782, CP022783
T25	I-3	2	5,715,510	67	5,805	12	58	CP023014, CP023015
T110	I-3	2	5,642,243	67.1	6,811	12	57	CP023012, CP023013
SL2729	I-4	2	5,703,338	67	5,304	12	58	CP022792, CP022793
SL3103	I-4	2	5,618,133	67	5,257	12	58	CP022790, CP022791
SL3300	I-4	2	5,903,911	66.8	5,482	12	58	CP022786, CP022787
SL3730	I-4	2	5,686,064	67	5,348	12	58	CP022784, CP022785
SL3822	I-4	2	5,971,831	66.8	5,558	12	59	CP022780, CP022781
SL3882	I-4	2	6,025,869	66.8	5,594	12	59	CP022778, CP022779
T42	I-4	2	5,497,698	67	5,133	12	57	CP022772, CP022773
T60	I-4	2	6,015,554	66.8	5,588	12	59	CP022768, CP022769
T78	I-4	3	6,147,432	66.7	5,807	12	59	CP022765, CP022766,CP022767
T117	I-4	2	5,807,463	66.9	5,378	12	59	CP022755,CP022756
PSI07	IV-2	3	5,605,618	66.32	4,810	9	54	FP885906.2, FP885891.2
R. syzygii R24	IV	7	5,423,991	65.87	4,865	6	50	EMBL FR854086 – FR854092
BDB R229	IV	27	5,158,998	66.44	4,614	8	67	EMBL FR854059 – FR854085
CMR15	III	3	5,590,372	66.79	4,890	12	59	FP885895.1, FP885896.1, FP885893.1
CFBP2957	IIA-2	1	3,417,386	66.44	3,158	9	53	FP885897.1
Po82	IIB-2	2	5,430,263	66.67	4,745	9	54	CP002819.1, CP002820.1
IPO1609	IIB-2	10	5,318,522	64.85	4,659	6	31	NZ_CDGL000000000.1
GMI1000	I-3	2	5,810,922	66.98	5,055	12	57	AL646052.1, AL646053.1
FQY_4	I-4	2	5,805,250	66.81	5,068	12	51	CP004012.1, CP004013.1

[a]*Strain T78 had third circular plasmid of 128,742 bp, 156 CDSs, and no rRNA and tRNA.* [b]*Phylotype-biovar.* [c]*NCBI genome accession numbers, except R. syzygii R24 and Blood Disease Bacterium (BDB) R229 genome, which were EMBL genome accession numbers.*

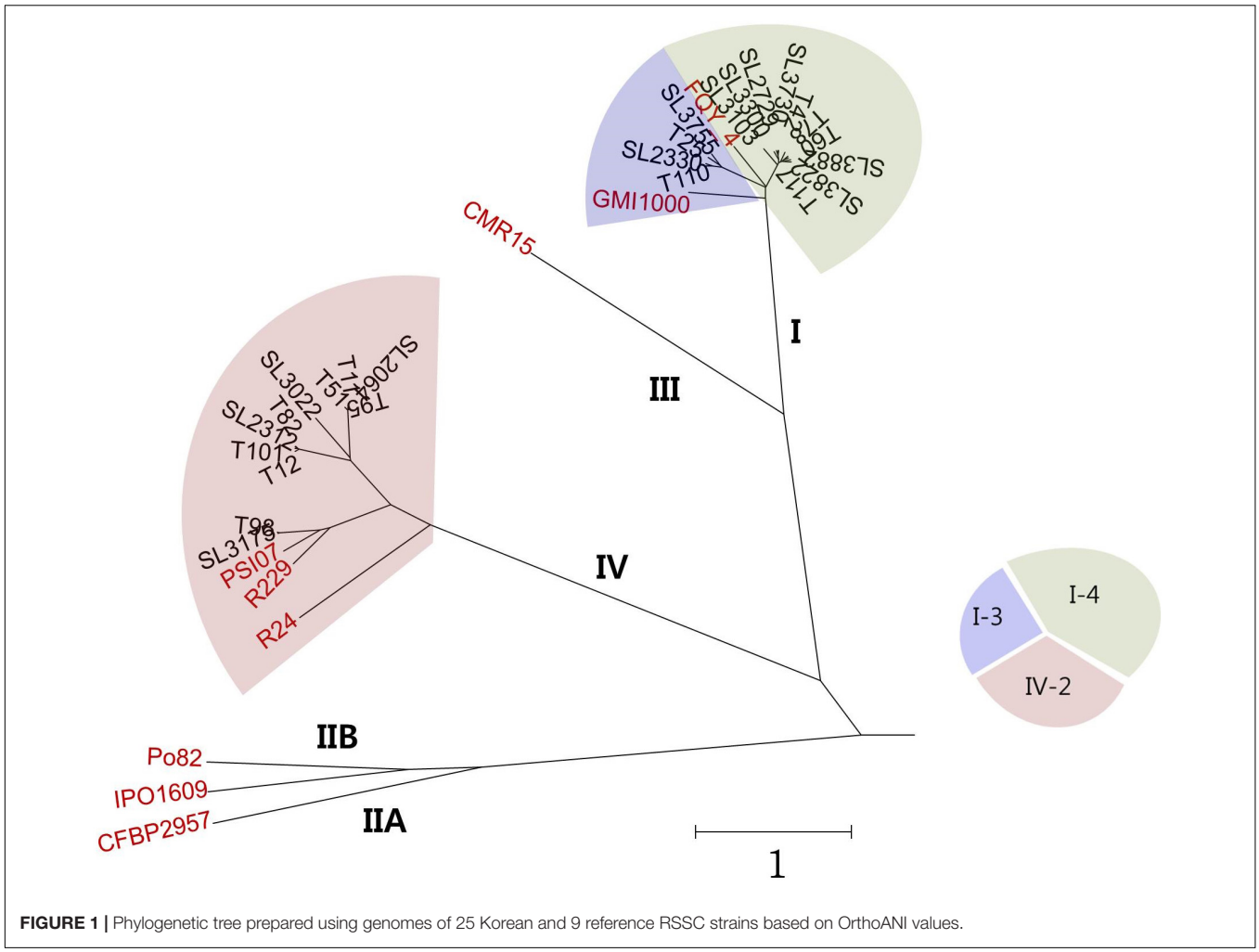

FIGURE 1 | Phylogenetic tree prepared using genomes of 25 Korean and 9 reference RSSC strains based on OrthoANI values.

functional group was the amino acid transport and metabolism group (E), which contained an average of 367 genes, followed by the transcription group (K), which contained an average of 330 genes, and the energy production and conversion group (C), which contained an average of 286 genes. COGs were distributed differently between the phylotype I and IV strains. The phylotype I strains had more genes than the phylotype IV strains in the categories of transcription (K); replication; recombination and repair (L); intracellular trafficking, secretion, and vesicular transport (U); carbohydrate transport and metabolism (G); and secondary metabolite biosynthesis, transport, and catabolism (Q). The phylotype IV strains had more genes than the phylotype I strains in the categories of signal transduction mechanisms (T) and inorganic ion transport and metabolism (P).

Candidate Host-Specific Genes for Bacterial Virulence

To identify genes responsible for host specificity, comparative genome analyses were performed by comparing functional genes among the four pathotypes. Previously, Korean RSSC strains isolated from samples of potato bacterial wilt were divided into four different pathotypes based on tests against four *solanaceae* plants: potato, tomato, eggplant, and pepper. The classifications were only pathogenic on potato (P); pathogenic on potato and tomato (PT); pathogenic on potato, tomato, and eggplant (PTE); and pathogenic on potato, tomato, eggplant, and pepper (PTEPe) (Cho et al., 2018).

Using pan-genome analyses of the Korean isolates, we identified a number of candidate genes expected to contribute to host specificity (**Table 2**) and the POGs are listed in **Supplementary Tables S3–S5**. A total of 128 genes were only found in four tomato-non-pathogenic strains. Most of these genes encoded proteins with hypothetical functions and a few of the functionally designated genes were related to mobile elements, such as bacteriophage infection or insertional elements (**Supplementary Table S3**). Three genes revealed homology with a gene encoding the clustered regularly interspaced short palindromic repeat (CRISPR) proteins, Cas9, Cas1, and Cas2 (**Supplementary Figure S1A**). CRISPR is an adaptive immune system in prokaryotes that provides protection against mobile genetic elements (viruses, transposable elements, and conjugative plasmids). Four genes showed homology with a gene encoding Mu-like prophage proteins (**Supplementary Figure S1B**), and

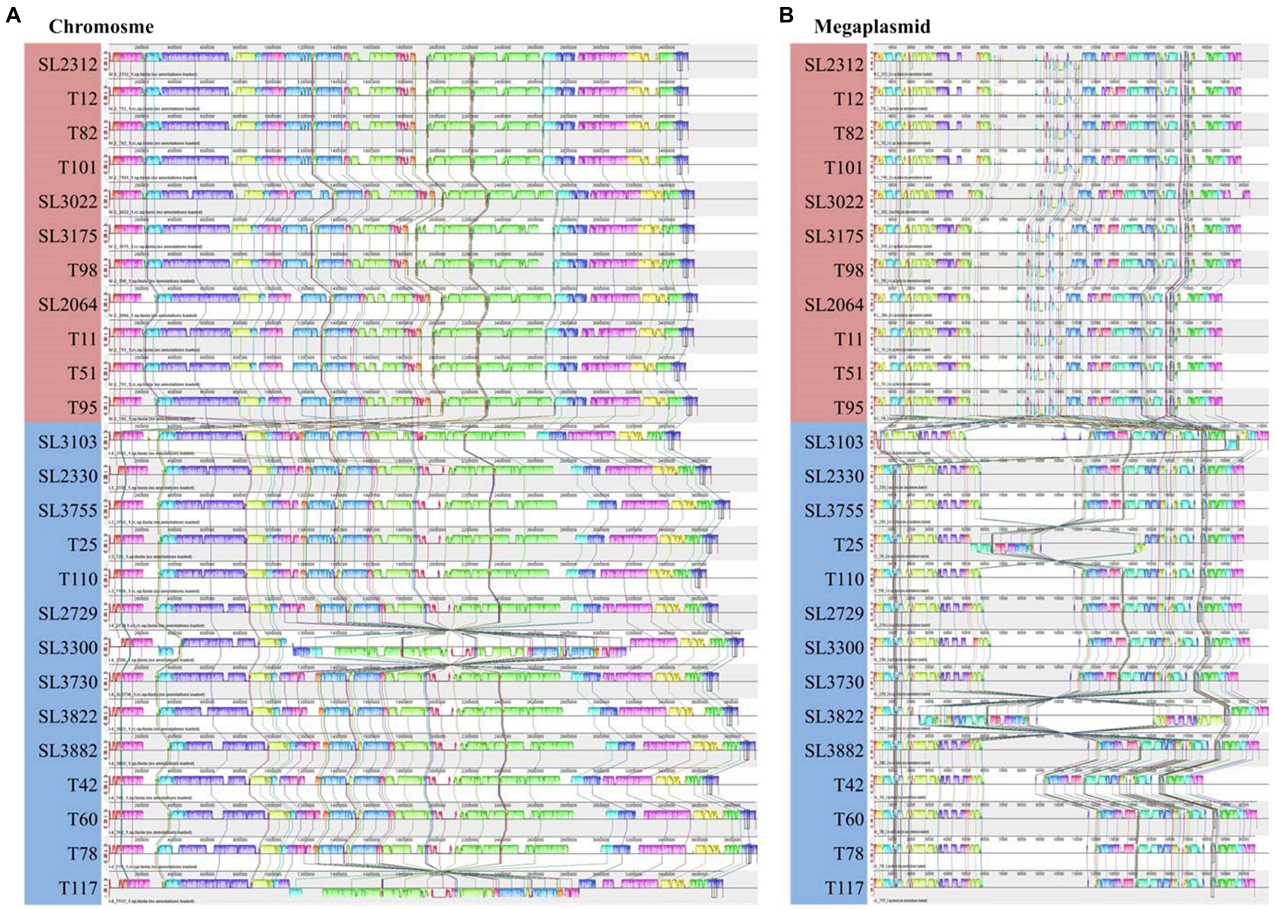

FIGURE 2 | Multiple genome alignment for 25 Korean RSSC strains produce using Mauve software. The sequences of chromosome **(A)** and megaplasmid **(B)** were aligned. The red and blue boxes represent phylotype IV and I, respectively. Colored lines between genomes represent rearrangements or inversions.

one capsid protein and another Mu-like virus tape-measure protein were identified by the analyses. In addition, two copies of insertional element IS476 were also identified in the analyses (**Supplementary Figure S1C**). In the tomato-pathogenic group, these bacteria shared 8 genes. Among them, three genes encoded components of the type II secretion system (T2SS) and next one gene encoded RhsB (rearrangement hotspot), which is a probable deoxyribonuclease (**Table 2**, **Supplementary Figure S2**, and **Supplementary Table S3**).

Regarding eggplant, seven eggplant-non-pathogenic strains shared 5 genes (**Supplementary Table S4**). Four of them encoded hypothetical proteins and one was similar to a gene encoding a putative RipA, which is a transcriptional regulator for type III secretion with a helix-turn-helix DNA binding motif (**Supplementary Figure S3**). For eggplant infection, it was predicted that 7 genes were shared. None of these genes were similar to genes of known function.

For pepper, the phylotype I strain SL3103 belonged to the pepper-non-pathogenic group, unlike other phylotype I strains, all of which were pathogenic on pepper plants. As a result, we were able to determine the candidate genes related to organic metabolisms rather than effectors. Twelve pepper-non-pathogenic strains (eleven phylotype IV and one phylotype I strains) shared 1 gene, whose function was unknown, and thirteen pepper-pathogenic strains (all phylotype I strains) shared 34 genes, including genes involved in aromatic compound metabolism (**Supplementary Figure S4** and **Supplementary Table S5**). Among them, 12 genes (from POG_2330_01480 to POG_2330_01491) produced a cluster related to aromatic compound metabolism (**Supplementary Table S5**). This cluster was highly homologous with the *dhb* gene cluster from *Pseudomonas reinekei* MT1: *dhbA* (67% identity with POG_2330_01480), *dhbB* (64% identity with POG_2330_01481), *dhbC* (65% identity with POG_2330_01482), *dhbD* (47% identity with POG_2330_01483), *dhbE* (42% identity with POG_2330_01484), *dhbF* (60% identity with POG_2330_01485), *dhbG* (66% identity with POG_2330_01486), *dhbH* (83% identity with POG_2330_01487). This *dhb* cluster encodes genes that participate in 2,3-dihyroxybenzoate (2,3-DHB) aromatic ring degradation via the *meta*-cleavage pathway (Marin et al., 2012).

T3SS Effectors

Type III secretion systems is deeply involved in pathogenicity and RSSC carries abundant T3es that are secreted through the

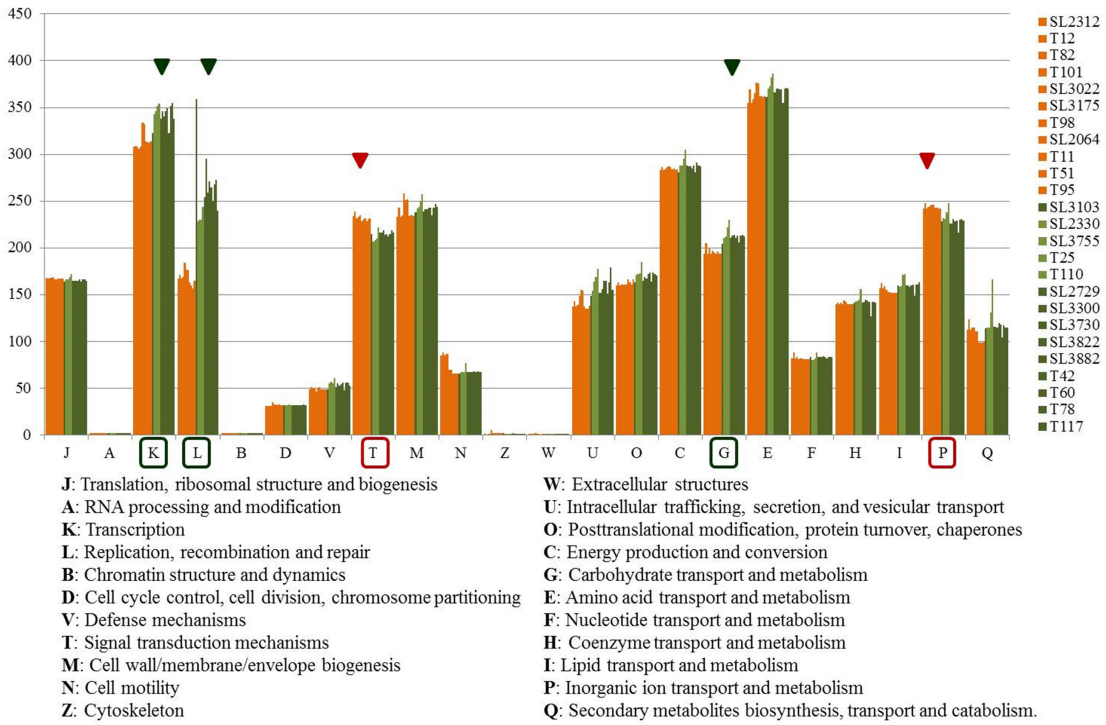

FIGURE 3 | Graph of COG functional categories of 25 Korean strains. Orange color represents phylotype IV-biovar 2 strains, and olive and green colors represent the phylotype I-biovar 3 and phylotype I-biovar 4 strains. The red triangle and box indicate the category with more genes in phylotype IV than in phylotype I, and the green triangle and box indicate the category with more genes in phylotype I than phyloytpe IV. Category S, genes of unknown function, is excluded from the graph.

T3SS (Peeters et al., 2013). Therefore, we predicted the T3es of the Korean RSSC using the RalstoT3E annotation server and analyzed effectors related to host range on four Solanaceae plants (**Figure 4**). Of a total of 94 T3e repertoires of RSSC, 82 effectors were identified as full or partial forms and 12 effectors were absent (**Figure 4A**). While a total of 30 effectors were present in all sequenced Korean strains, 8 were present only in phylotype I and 6 were found only in phylotype IV (**Figure 4B**). Regarding the sharing of effectors, it was shared 68 effectors in four I-3 strains, 70 in ten I-4 strains, and 70 in eleven IV-2 strains. In general, phylotype I strains had more effectors than phylotype IV strains and the distributions of each effector revealed a more conserved patterns in phylotype I strains than in phylotype IV strains. In the case of SL3175 and T98 of phylotype IV, revealed different distribution pattern compared to the other phylotype IV strains, which this clustering was consistent with the genomic phylogenetic tree (**Figure 1**).

Next, we investigated the presence of effectors related to host specificity for tomato, eggplant, or pepper plant infections. Among them, we identified three host-specific effectors: two for tomato (RipH3 and RipS3) and one for eggplant (RipAC). The genetic loci of the genes encoding these proteins are depicted in **Figure 5**. The gene *ripS3* (also known as SKWP3) was present in all 21 tomato-pathogenic strains, but was absent in the four tomato-non-pathogenic strains (SL2312, T12, T82, and T101). The function of RipS3 is unknown; however, it contains the nucleotidyl transferase (NT) domain of the RelA- and Spo-like protein (**Supplementary Figure S5A**). The gene *ripH3* (HLK3) was present as a partial form with a truncated N-terminal or C-terminal region in the tomato-non-pathogenic strains, whereas it was present in a complete form in tomato-pathogenic strains. The *ripH3* gene contained a PIP box in the promoter region, but did not exhibit any known functional domain. In the case of RipAC (PopC) in strains pathogenic for eggplant, the gene was different from that of non-pathogenic strains, which had another type of *ripAC* (**Supplementary Figure S5B**). In the *ripAC* gene, it was difficult to find DNA sequence similarity between eggplant-pathogenic and non-pathogenic strains; however, there was 34% homology in the amino acid sequences, which had 17 LRR motifs and 10 LRRs in common with each other.

DISCUSSION

Ralstonia solanacearum species complex is a sophisticated complex of plant pathogens with an unusually broad host range and wide geographical distribution. We identified genes that are relevant to host specificity by analyzing whole genomes of 25 Korean RSSC strains isolated from potato bacterial wilt and performing *in silico* genome-wide comparison of four different pathotypes of RSSC strains.

The isolated Korean potato bacterial wilt strains belonged to phylotypes I or IV, and phylotype I strains showed destructive pathogenicity, not only on potato, but also on tomato, eggplant,

TABLE 2 | Specific gene numbers of RSSC strains that are pathogenic and nonpathogenic toward tomato, eggplant, and pepper.

Strains	Phylotype-biovar	Original Host	Pathotype[a]	Specific genes		
				Tomato	Eggplant	Pepper
SL2312	IV-2	Potato	P	128	5	1
T12	IV-2	Potato	P			
T82	IV-2	Potato	P			
T101	IV-2	Potato	P			
SL3022	IV-2	Potato	PT	8	7	34
SL3175	IV-2	Potato	PT			
T98	IV-2	Potato	PT			
SL2064	IV-2	Potato	PTE			
T11	IV-2	Potato	PTE			
T51	IV-2	Potato	PTE			
T95	IV-2	Potato	PTE			
SL3103	I-4	Potato	PTE			
SL2330	I-3	Potato	PTEPe			
SL3755	I-3	Potato	PTEPe			
T25	I-3	Potato	PTEPe			
T110	I-3	Potato	PTEPe			
SL2729	I-4	Potato	PTEPe			
SL3300	I-4	Potato	PTEPe			
SL3730	I-4	Potato	PTEPe			
SL3822	I-4	Potato	PTEPe			
SL3882	I-4	Potato	PTEPe			
T42	I-4	Potato	PTEPe			
T60	I-4	Potato	PTEPe			
T78	I-4	Potato	PTEPe			
T117	I-4	Potato	PTEPe			

[a] *Pathotype: (P) only pathogenic on potato, (PT) pathogenic on potato and tomato, (PTE) pathogenic on potato, tomato, and eggplant, and (PTEPe) pathogenic on all tested crops – potato, tomato, eggplant, and pepper.*

and pepper plants (Cho et al., 2018). Previously, it had been suggested that phylotype I strains may have evolved from phylotype IV strains (Wicker et al., 2012; Li et al., 2016). The genomes of phylotype I strains possess distinctive features compared to those of the other representative phylotype II (Po82, IPO1609), III (CMR15), and IV strains (PSI07, R24, and R229): large genome size, high GC content, and larger numbers of rRNA and tRNA genes. From these genomic features, we suppose the possibility that phylotype I strains have accepted foreign DNA fragments to adapt to various environments resulting in increased GC content and genome size, and among the imported fragments, there might be various virulence factors that enable these strains to infect new hosts.

When we compared the genomes to identify genes responsible for host specificity, we found specific genes from the tomato pathogenic strains: two T3es (*ripS3* and *ripH3*), a set of T2SS, and an adjacent *rhsB* (**Figure 6**). The function of RipS3 has not been reported; however, RipS3 has the nucleotidyl transferase domain of RelA- and SpoT-like ppGpp synthetases and hydrolases, and belongs to the PRK09169 superfamily (**Supplementary Figure S5A**). The ppGpp works as an alarmone, which integrates general stress responses, such as starvation, heat shock, and oxidative stress in bacteria and plants (Van der Biezen et al., 2000; Braeken et al., 2006; Wang et al., 2016). We speculate that effector RipS3 is translocated into host plant cells and may disturb the host stress response mediated by the ppGpp. The other effector, RipH3, possesses a PIP box but no known functional motif. The *ripH3* gene was partially present in the tomato-non-pathogenic strains (**Figure 5**), and this feature is consistent with a previous report that a triple deletion mutant of *ripH1-H3* (HLK1–3) was significantly impaired with respect to tomato infection (Chen et al., 2014).

Type II secretion systems (T2SSs) have been identified in bacteria belonging to the alpha, beta, gamma, and delta-proteobacteria, and are encoded by 12 to 16 genes, of which the core components are named as *gsp* (general secretory proteins) (Abby et al., 2016). Substrates of T2SS are recruited and transported as fully folded and often oligomeric proteins (Gu et al., 2017). It has been reported that RSSC possessed three types of T2SS: one is the orthodox system constructed out of 12 components, and the others are the unorthodox systems, possessing 7 core genes (Li et al., 2016). In our study,

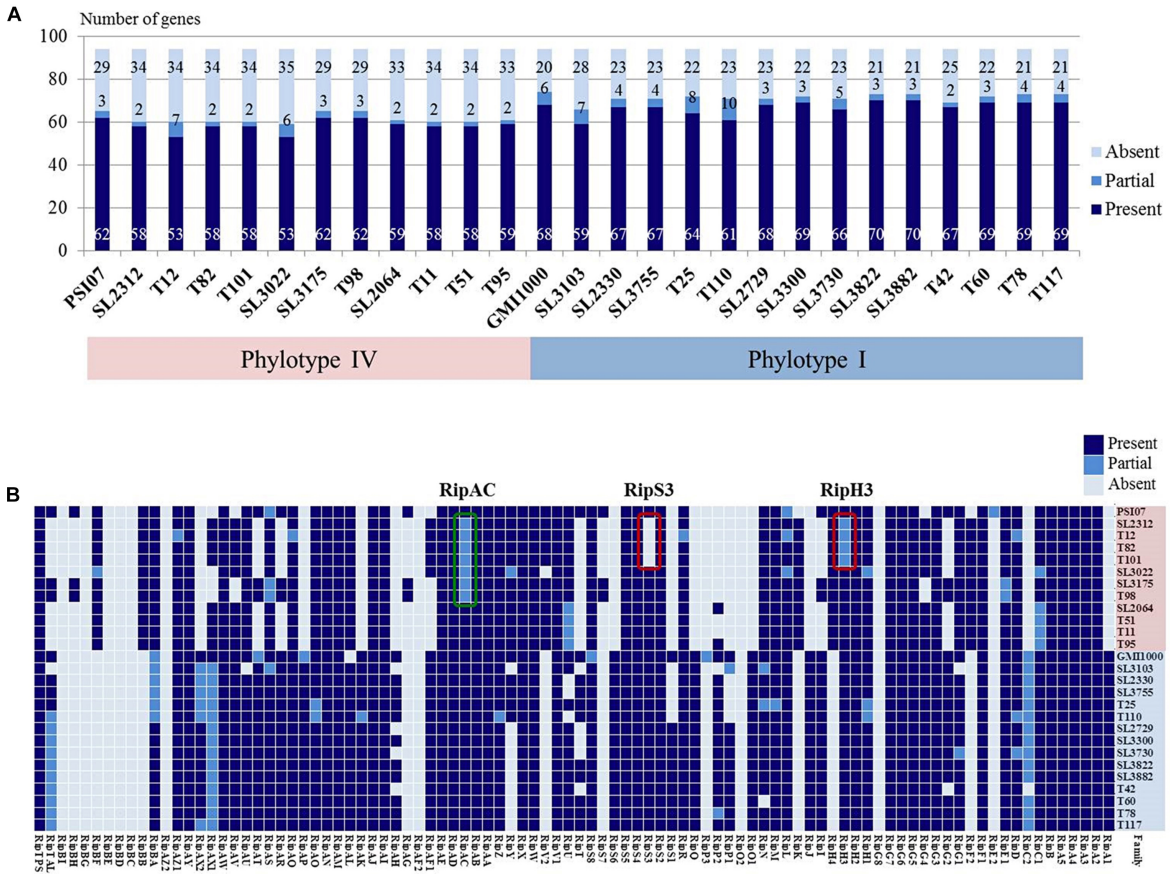

FIGURE 4 | (A) Graph of predicted effector gene numbers. The colors represent as follows: dark blue, presence of a gene; blue, partial gene; light blue, absence of a gene. **(B)** Distribution of the T3e genes in 25 Korean strains and the reference GMI1000 and PSI07 strains. Red boxes represent tomato-non-pathogenic strains and green box represent eggplant-non-pathogenic strains.

the tomato-non-pathogenic strains were lacking one set of unorthodox T2SS and the adjacent *rhsB* gene (**Figure 6**). Because T2SS mutants were impaired in colonization and proliferation *in planta* (Kang et al., 1994), this feature appears to relate one set of the T2SS deficiency with the tomato-non-pathogenic trait. In addition, the *rhsB* gene, which was located next to the T2SS-encoding gene cluster, was also absent in the tomato-non-pathogenic strains. Rhs protein possesses YD-peptide repeats, which play a role in the bacterial-eukaryotic host cell interaction, and it also carries nuclease domain to degrade target cell DNA (Koskiniemi et al., 2013). In *Dickeya dadantii* 3937, Rhs protein worked as a DNase toxin to inhibit neighboring cell growth in a contact-dependent manner, and its translocation to host cells provided evidence that Rhs may be exported through a type VI secretion system (T6SS) (Koskiniemi et al., 2013). Although it is a distinctive genetic feature of tomato-pathogenic strains, further experiments are required to define the mechanisms of T2SS and RhsB in tomato infection.

Our pan-genome analyses to identify host-specific genes for bacterial virulence revealed that a number of genes encoding hypothetical protein with unknown function and mobile element or phage-related genes are present in four pathotypes of Korean RSSC (**Supplementary Tables S3–S5**). Functional studies of each gene identified by *in silico* analysis should be performed to define their involvement in bacterial virulence in a host-specific infection and virulence. It would be also interesting to investigate if mobile element or prophages can contribute to host specific virulence of each pathotypes by disrupting certain avirulence- or virulence-related function of RSSC strains.

In analyses using the RalstoT3E prediction system, we identified the RipAC for eggplant-specific effector. RipAC was previously called as PopC and has LRR motifs, which are expected to interact with some host proteins (Peeters et al., 2013). The *popC* (*ripAC*) gene constitutes an operon with *popA* (*ripX*) and *popB* (*ripAB*) expressed by a promoter containing a PIP box (Guéneron et al., 2000). This *popABC* operon was located next to the *hrp* gene cluster, and the encoded PopA (harpin), PopB (NLS motif), and PopC (LRR motifs) proteins were secreted by T3SS. In the RalstoT3E database, the names of these effectors were assigned as RipX (PopA), RipAB (PopB), and RipAC (PopC) (Peeters et al., 2013). Interestingly, the RNA expressions of these genes were upregulated in tomato plants (Ailloud et al., 2016), but Tn5-B20-inserted mutants of these genes were still pathogenic on tomato (Marenda et al., 1998). In general, the

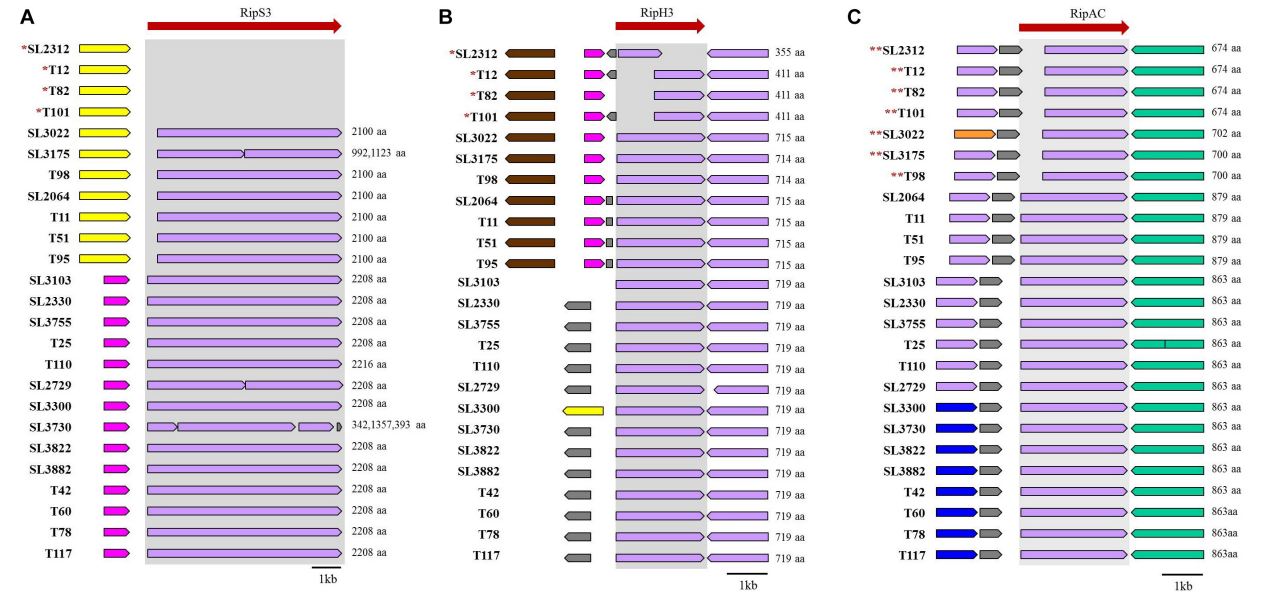

FIGURE 5 | Genetic regions of RipS3 **(A)**, RipH3 **(B)**, and RipAC **(C)**. *non-pathogenic strains for tomato. **non-pathogenic strains for eggplant.

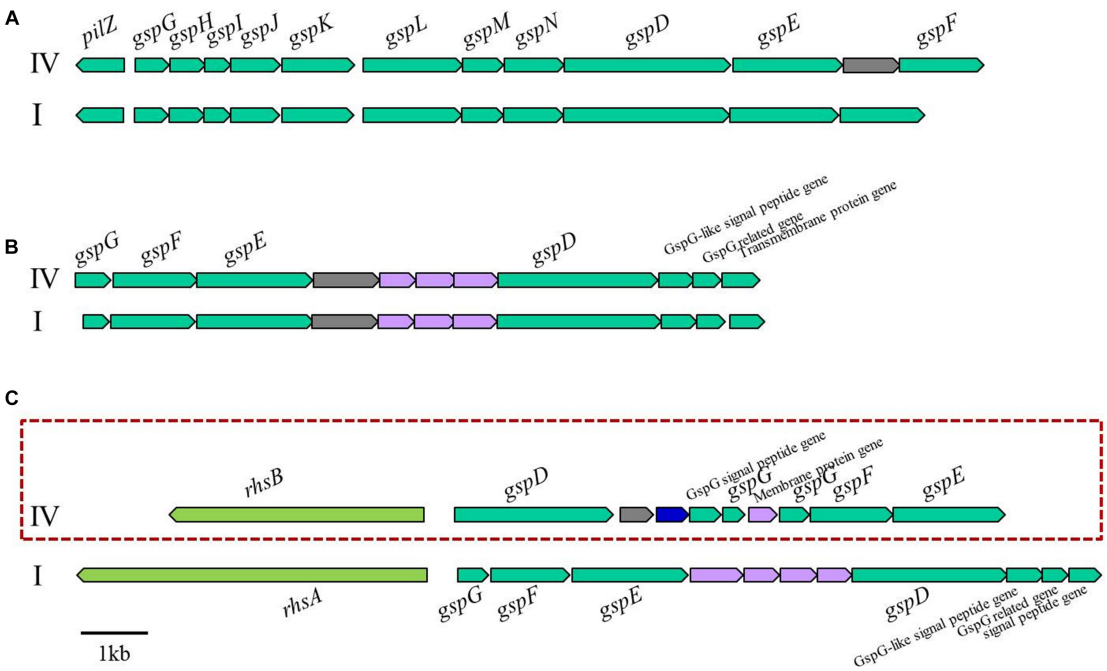

FIGURE 6 | Genetic organization of three T2SS gene clusters in phylotype IV and I strains of RSSC **(A)** orthodox T2SS cluster, **(B)** and **(C)** unorthodox T2SS cluster. IV, phylotype IV; I, phylotype I. The T2SS gene cluster in the red box did not exist in the strains of tomato non-pathogens (SL2312, T12, T82, and T101).

Korean RSSC strains carried the similar gene organization with previously reported RSSC strains for *popABC* operon driven by a promoter with a PIP box and adjacent *hrp* cluster. However, while *popA* (*ripX*) and *popB* (*ripAB*) were present in all strains, *popC* (*ripAC*) was not; the *popC* gene of most strains encoded a protein with 17 LRR motifs, like that of the GMI1000 strain, but 7 eggplant-non-pathogenic strains carried a smaller *popC* gene encoding 10 LRR motifs, like that of R24 and BDB 225 (**Supplementary Figure S5B**). These results suggest that *popC* (*ripAC*) may be involved in eggplant-infection of RSSC.

The *dhb* gene cluster homologs were identified as pepper-specific candidate virulence genes. The metabolite

2,3-dihydroxybenzoate (DHB) works as an isochorismate-derived secondary metabolite in plants (Bartsch et al., 2010), or a key intermediate of several siderophores: enterobactin (*Salmonella enterica* and *Escherichia coli*), anguibactin, and vanchrobacin (*Vibrio anguillarum*) (Raymond et al., 2003; Li and Ma, 2017). Siderophores are low molecular weight iron-chelating molecules that facilitates iron uptake in many gram-negative bacteria. Iron uptake systems are critical for the function of some pathogens to infect host plants to lead to disease (Wolf and Crosa, 1986). In the pepper-non-pathogenic RSSC strains, the *dhb* gene cluster homologs and other related genes were absent. This deficiency appeared to affect the ability of the bacteria to infect pepper.

A previous study identified a pepper-specific avirulence gene *rsa1,* which confers avirulence to a pepper-pathogenic strain, from a potato pathogenic SL2029 (Jeong et al., 2011). In our study, this *rsa1* gene was present in the genome of all pepper non-pathogenic phylotype IV strains of Korean RSSC as expected. However, the *rsa1* gene was not identified as a host-specific avirulence gene in comparative analysis. This was because one of phylotype I strains, SL3103, does not carry *rsa1* gene in its genome while this strain was pepper non-pathogenic unlike to other phylotype I strains. It is likely that the strain SL3103 is pepper non-pathogenic due to the absence of *dhb* gene cluster (**Supplementary Figure S4** and **Supplementary Table S5**), while other phylotype I strains carry *dhb* gene cluster.

Our extensive comparative genomic analyses uncovered several genes associated with the pathogenicity of RSSC on different crops. It is likely that the host-specificity of RSSC will be a function of the comprehensive actions of various virulence factors, effectors, secretion systems, and metabolic enzymes. Although further biological functions of these genes should be determined, these data contribute to expand our understanding on the host specificity of RSSC.

DATA AVAILABILITY

The whole genome sequences of 25 Korean RSSC strains can be found in the NCBI GenBank and the accession numbers are listed in **Table 1**.

AUTHOR CONTRIBUTIONS

HC, E-SS, DP, J-GK, and IH conceived and designed the study. YL, SL, and S-WL provided the RSSC isolates and related information. HC and E-SS carried out the experiments. JB and T-HL assembled and analyzed the genomes. HC and IH analyzed and interpreted the data. HC, SH, and S-WL prepared the manuscript.

FUNDING

This work was supported by a grant from the National Institute of Agricultural Sciences, Rural Development Administration (PJ01008502 and PJ01246601), South Korea.

SUPPLEMENTARY MATERIAL

The Supplementary Material for this article can be found online at: https://www.frontiersin.org/articles/10.3389/fmicb.2019.00506/full#supplementary-material

REFERENCES

Abby, S. S., Cury, J., Guglielmini, J., Neron, B., Touchon, M., and Rocha, E. P. (2016). Identification of protein secretion systems in bacterial genomes. *Sci. Rep.* 6:23080. doi: 10.1038/srep23080

Ailloud, F., Lowe, T., Cellier, G., Roche, D., Allen, C., and Prior, P. (2015). Comparative genomic analysis of *Ralstonia solanacearum* reveals candidate genes for host specificity. *BMC Genomics* 16:270. doi: 10.1186/s12864-015-1474-8

Ailloud, F., Lowe, T. M., Robene, I., Cruveiller, S., Allen, C., and Prior, P. (2016). In planta comparative transcriptomics of host-adapted strains of *Ralstonia solanacearum*. *PeerJ.* 4:e1549. doi: 10.7717/peerj.1549

Angot, A., Peeters, N., Lechner, E., Vailleau, F., Baud, C., Gentzbittel, L., et al. (2006). *Ralstonia solanacearum* requires F-box-like domain-containing type III effectors to promote disease on several host plants. *Proc. Natl. Acad. Sci. U.S.A.* 103, 14620–14625. doi: 10.1073/pnas.0509393103

Aziz, R. K., Bartels, D., Best, A. A., DeJongh, M., Disz, T., Edwards, R. A., et al. (2008). The RAST server: rapid annotations using subsystems technology. *BMC Genomics* 9:75. doi: 10.1186/1471-2164-9-75

Bartsch, M., Bednarek, P., Vivancos, P. D., Schneider, B., von Roepenack-Lahaye, E., Foyer, C. H., et al. (2010). Accumulation of isochorismate-derived 2,3-dihydroxybenzoic 3-O-beta-D-xyloside in arabidopsis resistance to pathogens and ageing of leaves. *J. Biol. Chem.* 285, 25654–25665. doi: 10.1074/jbc.M109.092569

Braeken, K., Moris, M., Daniels, R., Vanderleyden, J., and Michiels, J. (2006). New horizons for (p) ppGpp in bacterial and plant physiology. *Trends Microbiol.* 14, 45–54. doi: 10.1016/j.tim.2005.11.006

Cao, Y., Tian, B., Liu, Y., Cai, L., Wang, H., Lu, N., et al. (2013). Genome sequencing of *Ralstonia solanacearum* FQY_4, isolated from a bacterial wilt nursery used for breeding crop resistance. *Genome Announc.* 1:e125–13. doi: 10.1128/genomeA.00125-13

Cellier, G., Remenant, B., Chiroleu, F., Lefeuvre, P., and Prior, P. (2012). Phylogeny and population structure of brown rot- and Moko disease-causing strains of *Ralstonia solanacearum* phylotype II. *Appl. Environ. Microbiol.* 78, 2367–2375. doi: 10.1128/AEM.06123-11

Chen, L., Shirota, M., Zhang, Y., Kiba, A., Hikichi, Y., and Ohnishi, K. (2014). Involvement of HLK effectors in *Ralstonia solanacearum* disease development in tomato. *J. Gen. Plant Pathol.* 80, 79–84. doi: 10.1007/s10327-013-0490-2

Chin, C. S., Alexander, D. H., Marks, P., Klammer, A. A., Drake, J., Heiner, C., et al. (2013). Nonhybrid, finished microbial genome assemblies from long-read SMRT sequencing data. *Nat. Methods* 10, 563–569. doi: 10.1038/nmeth.2474

Cho, H., Song, E. S., Lee, Y. K., Lee, S., Lee, S. W., Jo, A., et al. (2018). Analysis of genetic and pathogenic diversity of *Ralstonia solanacearum* causing potato bacterial wilt in Korea. *Plant Pathol. J.* 34, 23–34. doi: 10.5423/PPJ.FT.09.2017.0203

Chun, J., Grim, C. J., Hasan, N. A., Lee, J. H., Choi, S. Y., Haley, B. J., et al. (2009). Comparative genomics reveals mechanism for short-term and long-term clonal transitions in pandemic *Vibrio cholerae*. *Proc. Natl. Acad. Sci. U.S.A.* 106, 15442–15447. doi: 10.1073/pnas.0907787106

Cunnac, S., Occhialini, A., Barberis, P., Boucher, C., and Genin, S. (2004). Inventory and functional analysis of the large Hrp regulon in *Ralstonia solanacearum*: identification of novel effector proteins translocated to plant host cells through the type III secretion system. *Mol. Microbiol.* 53, 115–128. doi: 10.1111/j.1365-2958.2004.04118.x

Denny, T. (2006). *Plant Pathogenic Ralstonia species. Plant-Associated Bacteria*. New York, NY: Springer, 573–644. doi: 10.1007/978-1-4020-4538-7_16

Deslandes, L., Olivier, J., Peeters, N., Feng, D. X., Khounlotham, M., Boucher, C., et al. (2003). Physical interaction between RRS1-R, a protein conferring resistance to bacterial wilt, and PopP2, a type III effector targeted to the plant nucleus. *Proc. Natl. Acad. Sci. U.S.A.* 100, 8024–8029. doi: 10.1073/pnas.1230660100

Fegan, M., and Prior, P. (2005). "How complex is the *Ralstonia solanacearum* species complex," in *Bacterial Wilt Disease and the Ralstonia Solanacearum Species Complex*, eds C. Allen, P. Prior, and A. C. Hayward (Saint Paul, MN: American Phytopathological Society), 449–462.

Genin, S., and Denny, T. P. (2012). Pathogenomics of the *Ralstonia solanacearum* species complex. *Ann. Rev. Phytopathol.* 50, 67–89. doi: 10.1146/annurev-phyto-081211-173000

Gu, S., Shevchik, V. E., Shaw, R., Pickersgill, R. W., and Garnett, J. A. (2017). The role of intrinsic disorder and dynamics in the assembly and function of the type II secretion system. *Biochim. Biophys. Acta* 1865, 1255–1266. doi: 10.1016/j.bbapap.2017.07.006

Guéneron, M., Timmers, A. C., Boucher, C., and Arlat, M. (2000). Two novel proteins, PopB, which has functional nuclear localization signals, and PopC, which has a large leucine-rich repeat domain, are secreted through the hrp-secretion apparatus of *Ralstonia solanacearum*. *Mol. Microbiol.* 36, 261–277. doi: 10.1046/j.1365-2958.2000.01870.x

Guidot, A., Prior, P., Schoenfeld, J., Carrere, S., Genin, S., and Boucher, C. (2007). Genomic structure and phylogeny of the plant pathogen *Ralstonia solanacearum* inferred from gene distribution analysis. *J. Bacteriol.* 189, 377–387. doi: 10.1128/JB.00999-06

Hayward, A. C. (1991). Biology and epidemiology of bacterial wilt caused by *Pseudomonas solanacearum*. *Ann. Rev. Phytopathol.* 29, 65–87. doi: 10.1146/annurev.py.29.090191.000433

Jeong, Y., Cheong, H., Choi, O., Kim, J. K., Kang, Y., Kim, J., et al. (2011). An HrpB-dependent but type III-independent extracellular aspartic protease is a virulence factor of *Ralstonia solanacearum*. *Mol. Plant Pathol.* 12, 373–380. doi: 10.1111/j.1364-3703.2010.00679.x

Jiang, G., Wei, Z., Xu, J., Chen, H., Zhang, Y., She, X., et al. (2017). Bacterial wilt in china: history, current status, and future perspectives. *Front. Plant Sci.* 8:1549. doi: 10.3389/fpls.2017.01549

Kajava, A. V., Anisimova, M., and Peeters, N. (2008). Origin and evolution of GALA-LRR, a new member of the CC-LRR subfamily: from plants to bacteria? *PLoS One* 3:e1694. doi: 10.1371/journal.pone.0001694

Kang, Y., Huang, J., Mao, G., He, L., and Schell, M. (1994). Dramatically reduced virulence of mutants of *Pseudomonas solanacearum* defective in export of extracellular proteins across the outer membrane. *Mol. Plant Microbe Interact.* 7, 370–377. doi: 10.1094/MPMI-7-0370

Koskiniemi, S., Lamoureux, J. G., Nikolakakis, K. C., t'Kint de Roodenbeke, C., Kaplan, M. D., Low, D. A., et al. (2013). Rhs proteins from diverse bacteria mediate intercellular competition. *Proc. Natl. Acad. Sci. U.S.A.* 110, 7032–7037. doi: 10.1073/pnas.1300627110

Lee, I., Ouk Kim, Y., Park, S. C., and Chun, J. (2016). OrthoANI: an improved algorithm and software for calculating average nucleotide identity. *Int. J. Syst. Evol. Microbiol.* 66, 1100–1103. doi: 10.1099/ijsem.0.000760

Li, P., Wang, D., Yan, J., Zhou, J., Deng, Y., Jiang, Z., et al. (2016). Genomic analysis of phylotype I strain EP1 reveals substantial divergence from other strains in the *Ralstonia solanacearum* species complex. *Front. Microbiol.* 7:1719. doi: 10.3389/fmicb.2016.01719

Li, Y., and Ma, Q. (2017). Iron acquisition strategies of *Vibrio anguillarum*. *Front. Cell Infect. Microbiol.* 7:342. doi: 10.3389/fcimb.2017.00342

Marenda, M., Brito, B., Callard, D., Genin, S., Barberis, P., Boucher, C., et al. (1998). PrhA controls a novel regulatory pathway required for the specific induction of *Ralstonia solanacearum hrp* genes in the presence of plant cells. *Mol. Microbiol.* 27, 437–453. doi: 10.1046/j.1365-2958.1998.00692.x

Marin, M., Plumeier, I., and Pieper, D. H. (2012). Degradation of 2,3-dihydroxybenzoate by a novel meta-cleavage pathway. *J. Bacteriol.* 194, 3851–3860. doi: 10.1128/JB.00430-12

Mukaihara, T., Tamura, N., and Iwabuchi, M. (2010). Genome-wide identification of a large repertoire of *Ralstonia solanacearum* type III effector proteins by a new functional screen. *Mol. Plant Microbe Interact.* 23, 251–262. doi: 10.1094/MPMI-23-3-0251

Peeters, N., Carrere, S., Anisimova, M., Plener, L., Cazale, A. C., and Genin, S. (2013). Repertoire, unified nomenclature and evolution of the Type III effector gene set in the *Ralstonia solanacearum* species complex. *BMC Genomics* 14:859. doi: 10.1186/1471-2164-14-859

Poueymiro, M., and Genin, S. (2009). Secreted proteins from *Ralstonia solanacearum*: a hundred tricks to kill a plant. *Curr. Opin. Microbiol.* 12, 44–52. doi: 10.1016/j.mib.2008.11.008

Raymond, K. N., Dertz, E. A., and Kim, S. S. (2003). Enterobactin: an archetype for microbial iron transport. *Proc. Natl. Acad. Sci. U.S.A.* 100, 3584–3588. doi: 10.1073/pnas.0630018100

Remenant, B., Coupat-Goutaland, B., Guidot, A., Cellier, G., Wicker, E., Allen, C., et al. (2010). Genomes of three tomato pathogens within the *Ralstonia solanacearum* species complex reveal significant evolutionary divergence. *BMC Genomics* 11:379. doi: 10.1186/1471-2164-11-379

Remigi, P., Anisimova, M., Guidot, A., Genin, S., and Peeters, N. (2011). Functional diversification of the GALA type III effector family contributes to *Ralstonia solanacearum* adaptation on different plant hosts. *New Phytol.* 192, 976–987. doi: 10.1111/j.1469-8137.2011.03854.x

Safni, I., Cleenwerck, I., De Vos, P., Fegan, M., Sly, L., and Kappler, U. (2014). Polyphasic taxonomic revision of the *Ralstonia solanacearum* species complex: proposal to emend the descriptions of *Ralstonia solanacearum* and *Ralstonia syzygii* and reclassify current R. syzygii strains as *Ralstonia syzygii* subsp syzygii subsp nov., R. solanacearum phylotype IV strains as *Ralstonia syzygii* subsp indonesiensis subsp nov., banana blood disease bacterium strains as *Ralstonia syzygii* subsp celebesensis subsp nov and R. solanacearum phylotype I and III strains as Ralstonia pseudosolanacearum sp nov. *Int. J. Syst. Evol. Microbiol.* 64, 3087–3103. doi: 10.1099/ijs.0.066712-0

Salanoubat, M., Genin, S., Artiguenave, F., Gouzy, J., Mangenot, S., Arlat, M., et al. (2002). Genome sequence of the plant pathogen *Ralstonia solanacearum*. *Nature* 415, 497–502. doi: 10.1038/415497a

Sole, M., Popa, C., Mith, O., Sohn, K. H., Jones, J. D., Deslandes, L., et al. (2012). The awr gene family encodes a novel class of *Ralstonia solanacearum* type III effectors displaying virulence and avirulence activities. *Mol. Plant Microbe Interact.* 25, 941–953. doi: 10.1094/MPMI-12-11-0321

Taghavi, M., Hayward, C., Sly, L. I., and Fegan, M. (1996). Analysis of the phylogenetic relationships of strains of *Burkholderia solanacearum*, *Pseudomonas syzygii*, and the blood disease bacterium of banana based on 16S rRNA gene sequences. *Int. J. Syst. Bacteriol.* 46, 10–15. doi: 10.1099/00207713-46-1-10

Van der Biezen, E. A., Sun, J., Coleman, M. J., Bibb, M. J., and Jones, J. D. G. (2000). Arabidopsis RelA/SpoT homologs implicate (p)ppGpp in plant signaling. *Proc. Natl. Acad. Sci. U.S.A.* 97, 3747–3752. doi: 10.1073/pnas.97.7.3747

Wang, J., Tian, Y., Zhou, Z., Zhang, L., Zhang, W., Lin, M., et al. (2016). Identification and functional analysis of RelA/SpoT Homolog (RSH) genes in *Deinococcus radiodurans*. *J. Microbiol. Biotechnol.* 26, 2106–2115. doi: 10.4014/jmb.1601.01017

Wicker, E., Grassart, L., Coranson-Beaudu, R., Mian, D., Guilbaud, C., Fegan, M., et al. (2007). *Ralstonia solanacearum* strains from Martinique (French west indies) exhibiting a new pathogenic potential. *Appl. Environ. Microbiol.* 73, 6790–6801. doi: 10.1128/AEM.00841-07

Wicker, E., Lefeuvre, P., de Cambiaire, J. C., Lemaire, C., Poussier, S., and Prior, P. (2012). Contrasting recombination patterns and demographic histories of the plant pathogen *Ralstonia solanacearum* inferred from MLSA. *ISME J.* 6, 961–974. doi: 10.1038/ismej.2011.160

Wolf, M. K., and Crosa, J. H. (1986). Evidence for the role of a siderophore in promoting *Vibrio anguillarum* infections. *J. Gen. Microbiol.* 132, 2949–2952. doi: 10.1099/00221287-132-10-2949

Conflict of Interest Statement: The authors declare that the research was conducted in the absence of any commercial or financial relationships that could be construed as a potential conflict of interest.

frontiers in Microbiology

REVIEW
published: 15 May 2019
doi: 10.3389/fmicb.2019.01030

Trichoderma as a Model to Study Effector-Like Molecules

*Claudia A. Ramírez-Valdespino[1,2], Sergio Casas-Flores[3] and Vianey Olmedo-Monfil[1]**

[1] División de Ciencias Naturales y Exactas, Departamento de Biología, Universidad de Guanajuato, Guanajuato, Mexico, [2] Laboratorio de Biohidrometalurgia, Departamento de Medio Ambiente y Energía, Centro de Investigación en Materiales Avanzados, Chihuahua, Mexico, [3] Laboratorio de Genómica Funcional y Comparativa, División de Biología Molecular, Instituto Potosino de Investigación Científica y Tecnológica, San Luis Potosí, Mexico

Plants are capable of perceiving microorganisms by coordinating processes to establish different forms of plant–microbe relationships. Plant colonization is governed in fungal and bacterial systems by secreted effector molecules, suppressing plant defense responses and modulating plant physiology to promote either virulence or compatibility. Proteins, secondary metabolites, and small RNAs have been described as effector molecules that use different mechanisms to establish the interaction. Effector molecules have been studied in more detail due to their involvement in harmful interactions, leading to a negative impact on agriculture. Recently, research groups have started to study the effectors in symbiotic interactions. Interestingly, most symbiotic effectors are members of the same families present in phytopathogens. Nevertheless, the quantity and ratio of secreted effectors depends on the microorganism and the host, suggesting a complex mechanism of recognition between the plant and their associated microorganisms. Fungi belonging to *Trichoderma* genus interact with plants by inducing their defense system and promoting plant growth. Research suggests that some of these effects are associated with effector molecules that *Trichoderma* delivers during the association with the plant. In this review, we will focus on the main findings concerning the effector molecules reported in *Trichoderma* spp. and their role during the interaction with plants, mainly in the molecular dialogue that takes place between them.

Keywords: *Trichoderma*, effector molecules, plant–microbe interactions, secondary metabolites, effector proteins, small RNA

OPEN ACCESS

Edited by:
Sabrina Sarrocco, University of Pisa, Italy

Reviewed by:
Paul Dean, Teesside University, United Kingdom
Francesco Vinale, Istituto per la Protezione Sostenibile delle Piante (CNR), Italy

***Correspondence:**
Vianey Olmedo-Monfil
vg.olmedo@ugto.mx

Specialty section:
This article was submitted to Plant Microbe Interactions, a section of the journal Frontiers in Microbiology

Received: *30 November 2018*
Accepted: *24 April 2019*
Published: *15 May 2019*

Citation:
Ramírez-Valdespino CA, Casas-Flores S and Olmedo-Monfil V (2019) Trichoderma as a Model to Study Effector-Like Molecules. Front. Microbiol. 10:1030. doi: 10.3389/fmicb.2019.01030

INTRODUCTION

One of the main challenges that agriculture production encounters today is to supply the demands of quality and quantity for the producer and consumer without affecting the environment. Various pathogenic agents attack the crops, among which filamentous fungi are the most destructive, causing important economic losses (Singh, 2014). To implement strategies to control plant diseases, it is necessary to understand the pathogenic process, determining how these fungi are established in plants and how they generate tissue damage and bypass plant defenses. In this sense, one of the main events currently under scrutiny corresponds to the early stages of the pathogen–plant interaction.

Now it is known that successful pathogens deliver a wide range of molecules to the plant, which allows them to overcome the obstacles presented by the plant, regarding perception, signaling, or active defense response (Di et al., 2016; Shen et al., 2018). Also, there is ambiguity about the

classification of the molecules released by the pathogens, depending on the degree of response generated by the plant immune system and their impact on the pathogenic process (Thomma et al., 2011). Initially, the gene-for-gene model proposed that the interaction of an avirulent protein (Avr) from the pathogen with a plant counterpart, a resistant plant protein (R), triggers the plant defense response, avoiding disease progression. However, it has been determined that this interaction could also lead to the pathogenic processes, so it was redefined that avirulence factors can also be virulence factors (Flor, 1942; Bent and Mackey, 2007; Boller and Felix, 2009). For these pathogen-derived molecules, the term "effector" was proposed, defined as any given molecule that can alter the physiology, structure or function of another organism, facilitating the infection and/or triggering defense responses (Kamoun, 2006). This definition does not imply a positive or negative impact on the outcome of the host–pathogen interaction and therefore, can be applied to non-pathogenic interactions as well (Thomma et al., 2011).

In the plant–pathogen interaction, the participation of elicitors has also been reported, and those are described as a diverse group of molecules that induce plant defense in a weak and non-specific fashion and independent of races or cultivars (Alba et al., 2011). Additionally, it has been proposed that the participation of highly conserved pathogen-derived molecules, with essential functions in the pathogens, for example chitin and flagellin, are needed for the establishment of the interaction with the host. Overall, these molecules are termed Pathogen-Associated Molecular Patterns (PAMPs) and, since they have been described in non-pathogenic microorganisms, the more general concept of Microorganism-Associated Molecular Patterns (MAMPs) is also used (Jones and Dangl, 2006). Because of the wide distribution showed by elicitors, as well as their functional features, it was recently proposed to refer to them as PAMPs/MAMPs. In some cases, the distinction between PAMPs/MAMPs and effectors is not sufficiently defined, which is mainly related to the fact that PAMPs/MAMPs are highly conserved among genera, while effectors tend to be related to a single or few related species. However, new studies have uncovered that certain molecules classified as effectors are also widely distributed among several species (Thomma et al., 2011; Pazzagli et al., 2014). The debate about the functional classification of the molecules released by microorganisms remains open, and new evidence is necessary to clearly classify them and assign distinctive features for them. In order to avoid conceptual confusion, in this review, we will refer to effectors as those non-structural molecules derived from microorganisms that have a function modulating the plant defense pathways and/or participating in the establishment of associations with plants.

Plant defense response is based on the perception of PAMPs/MAMPs inducing primary PAMP- or MAMP-immunity (PTI/MTI), to counteract invading microorganisms (Jones and Dangl, 2006). The 'effector-triggered immunity' (ETI) is a second layer of defense, providing systemic resistance by sensing effectors from microorganisms to activate the induced systemic resistance (ISR), mediated by jasmonic acid (JA) and ethylene (ET). In this layer of defense, *PDF1.2* (Plant defensin 1.2), *Thi2.1* (Thionin) or *Chib* (Chitinase B) are commonly used as marker genes (Van Loon et al., 2006). Also, the systemic acquired resistance (SAR), regulated by salicylic acid (SA), leads to the expression of Pathogenesis-Related genes (PR) (Bari and Jones, 2009). Pathogens suppress the PTI producing a wide number of effectors with different functions, such as the prevention of the plant recognition or in the formation of infective structures (Kulkarni et al., 2005; de Jonge et al., 2010).

Traditionally, agriculture techniques to counteract phytopathogens involve the use of chemical formulations that have secondary effects such as toxicity and soil pollution. Safer agricultural strategies imply the use of biocontrol agents, displacing and eliminating phytopathogens. Among these agents, fungi classified in the *Trichoderma* genus are predominant. The antagonistic capacity of *Trichoderma* has been widely studied, and the mechanisms associated with it include competition for space and nutrients against its adversaries, antibiosis and mycoparasitism (Mukherjee et al., 2013).

Some *Trichoderma* species can effectively colonize plant roots and shoots and establish a molecular dialogue, having a positive effect in plants (Macías-Rodríguez et al., 2018; Manganiello et al., 2018). Mostafa and Gayed (1952) made the first observations in this regard, reporting that *Trichoderma* improves fresh and dry weight in cotton plants. More than 20 years later, Catska et al. (1975) reported that exudates from lettuce have a beneficial effect in conidia germination of *Trichoderma viride*, indicating that the fungus and plants obtain mutual benefits.

Moreover, an increasing amount of reports demonstrate that *Trichoderma* is an important plant endophyte that can interact with plants such as maize, cucumber, cotton, tomato, and *Arabidopsis thaliana* (Contreras-Cornejo et al., 2009; Vishnevetsky et al., 2010; Lopes et al., 2012; Mastouri et al., 2012; Reithner et al., 2014; Zhang et al., 2014; Lamdan et al., 2015). *Trichoderma* penetrates the first or second layers of cells of the epidermis in the root tissue or even colonizes intracellular spaces and grows between the plasma membrane and the plant cell wall (Yedidia et al., 1999; Nogueira-Lopez et al., 2018). Colonization by *Trichoderma* promotes plant growth, biomass gaining, higher seed germination, increased plant height, root development, shoot dry mass and leaf number, increased crop yield and improved plant vigor (Harman et al., 2004; Salas-Marina et al., 2015; Chagas et al., 2017). One of the most evident morphologic changes in plants triggered by *Trichoderma* is the increase of lateral roots, thus modifying root architecture. In this process, previous observations have demonstrated the participation of auxins (Contreras-Cornejo et al., 2009) as well as a cross-talk between ET and auxins through the signaling pathways mediated by MAP-kinases (Contreras-Cornejo et al., 2015). Also, the presence of *Trichoderma* not only modulates the levels of the hormones produced by the plant but *Trichoderma* itself can contribute with its own hormones or could provide intermediates for the synthesis of some phytohormones, as a part of the benefits reported in the *Trichoderma*–plant interaction (Guzmán-Guzmán et al., 2019).

Recent research has confirmed that these fungi activate plant defense pathways. However, how *Trichoderma* modulates the

plant immune response to establish a beneficial interaction is one of the main challenges to be addressed. In the establishment of the beneficial association between *Trichoderma* and plants, the effectors may play key roles, as demonstrated in mycorrhizal systems such as *Laccaria bicolor* and *Glomus intraradices* (Kloppholz et al., 2011; Plett et al., 2011).

Here, we will focus on the filamentous fungi *Trichoderma* spp. and the efforts of the scientific community has done to identify their effector molecules, as well as their role in the establishment of a beneficial relationship with plants that promote growth and immune response activation.

PLANT DEFENSE RESPONSE AND ITS ACTIVATION BY *Trichoderma*

One of the first observations related with the *Trichoderma*-induced ISR in plants was the induction of the hypersensitive response (HR) and synthesis of phytoalexins in grapevine cell cultures after the application of a cellulase from *T. viride* (Calderón et al., 1994). *Trichoderma harzianum* also increases the resistance of *Phaseolus vulgaris* against *Botrytis cinerea* and *Colletotrichum lindemuthianum* (Bigirimana et al., 1997). *Arabidopsis* mutants, impaired in JA biosynthesis, showed a similar level of root colonization to wild-type plants (Martínez-Medina et al., 2017). The opposite effect was observed when impaired plants in the SA synthesis were analyzed. These plants were unable to restrict the colonization by the fungus, indicating that SA-mediated response is implicated in the regulation of the *Trichoderma*–plant colonization, thus preventing vascular system invasion (Alonso-Ramírez et al., 2014). These two results suggested that ISR does not play a relevant role during *Trichoderma* plant colonization, while SAR pathway modulates the root colonization extend.

Moreover, other studies indicate that ISR induced by *Trichoderma asperellum* in cucumber was associated with an increase in chitinase and peroxidase activity, as well as the modulation of genes that are implicated in the JA/ET signaling pathways (Yedidia et al., 2000; Yedidia et al., 2003; Shoresh et al., 2005).

Trichoderma can also induce SAR defense even when ISR defense is activated and they can improve the plant resistance against phytopathogens, such as *Sclerotinia sclerotiorum*, where the effect of *Trichoderma* strains correlates with the production of cell-wall degrading enzymes by the plant (Contreras-Cornejo et al., 2011; Salas-Marina et al., 2011; Lopes et al., 2012). In pepper, *Trichoderma stilbohypoxyli*, *Trichoderma Caribbaeum*, and *Trichoderma theobromicola* altered the expression of the genes involved in the hypersensitive response and sesquiterpene phytoalexins biosynthesis (Bae et al., 2010). In a tripartite system, involving pathogenic nematodes, *T. harzianum* T-79 and tomato plants, the presence of T-79 differentially primes the responses related to SA and JA in the plant. T-79 initially primes the SA pathway leading to a faster defense response, protecting the plant from the invasion. Later, the nematode suppresses the JA-mediated defense pathway, but T-79 initiates its priming activity on this pathway, antagonizing the pathogen and reducing its development and reproduction. Finally, when the infection by nematodes has already been established, T-79 intensely activates the SA pathway, increasing the defense against subsequent attacks by juvenile nematodes. These results show that the effects of T-79 over the plants are a dynamic phenomenon, which can be adapted to signals from other organisms in the near environment (Martínez-Medina et al., 2016).

PROTEINS AS EFFECTORS IN *Trichoderma*–PLANT INTERACTIONS

Proteins were the first molecules proposed as effectors and have been widely studied in pathogenic systems. There is not much information about *Trichoderma* effector proteins, less than 20 effectors have been experimentally analyzed during the interaction with plant systems (**Table 1**), among them the following:

Cerato-Platanins

These are non-catalytic secreted proteins, which contribute to virulence in pathogens, acting as expansin-like proteins weakening cellulose aggregates from the cell wall (Baccelli et al., 2013). The Small Proteins (Sm) Sm1/2/3 from *Trichoderma virens* and their orthologs in *Trichoderma atroviride* Eliciting plant-response (Epl) Epl1/2/3 are produced in the association with plants, playing different roles. Transcripts and proteins corresponding to Sm1/Epl1 are detected as the most abundant in cultures supplemented with glucose or during the interaction with tomato or maize plants (Djonovic et al., 2006; Seidl et al., 2006; Gaderer et al., 2015). In maize, only the monomeric form of Sm1 or Epl1 proteins can induce the plant defense response and the dimeric form blocks the activation of ISR. When *T. virens* and *T. atroviride* strains were cultured in the presence of maize seedlings, Sm1 and Epl1 were produced as a glycosylated monomer and as a non-glycosylated dimer, respectively. These results suggest that the signals released by the plant influence the state of glycosylation and multimerization of Sm1/Epl1 proteins that may control the *Trichoderma*–plant molecular dialogue (Vargas et al., 2008). However, Sm2/Epl2 proteins are quantitatively fewer present that Sm1/Epl1 during the interaction with maize, there is evidence showing that Sm2 and Epl2 are more relevant in the activation of defense and root colonization in maize. The mechanism employed by Sm2/Epl2 to induce plant defense is unknown, but a strong reduction of the protection level of maize seedlings against *Cochliobolus heterostrophus* was observed when plants were treated with the *sm2*/*epl2* knockout strains in contrast with *sm1*/*epl1* knockout strains (Crutcher et al., 2015; Gaderer et al., 2015).

Hydrophobins

These are small surface-active proteins, which are only found in fungi. The genomes from *T. virens* and *T. atroviride* contain 17 sequences encoding for hydrophobins (Kubicek et al., 2011), and the upregulation of some of them has been reported during *Trichoderma*–plant interactions. The expression of the hydrophobin-encoding gene *HFB2-6* was down-regulated in the

TABLE 1 | Protein effectors from *Trichoderma* functionally validated during the interaction with plants.

Family	Protein	*Trichoderma* strain	Function in interaction with plants	References
Cerato-platanins	Sm1 (small protein 1)	*T. virens*	Induction of defense-related genes, production of ROS and phenolic compounds.	Djonovic et al., 2006, Djonovic et al., 2007; Salas-Marina et al., 2015
	Sm2 (small protein 2)	*T. virens*	Involved in root colonization and plant protection.	Crutcher et al., 2015
	Epl1 (eliciting plant response-like)	*T. atroviride*	Induction of defense-related genes.	Salas-Marina et al., 2015
		T. harzianum	Induction of defense-related genes.	Gomes et al., 2015
		T. formosa	Triggered of plant immune system.	Cheng et al., 2018
		T. asperellum	Induction of defense-related genes.	Yu et al., 2018
	Swollenin (expansin-like protein)	*T. asperellum*	Involved in root colonization and induction of plant defense.	Brotman et al., 2008
Glycoside-hydrolases	Thph1 and Thph2 (cellulase-like protein)	*T. harzianum*	Induction of defense-related genes.	Saravanakumar et al., 2016
	Cellulases	*T. longibrachiatum*	Activation of plant defense pathways.	Martínez et al., 2001
	ThPG1	*T. harzianum*	Involved on colonization of plant roots.	Morán-Diez et al., 2009
	Eix (xylanase)	*T. viride*	Triggers ET biosynthesis and hypersensitive response.	Rotblat et al., 2002
Hydrophobins	HYTLO1	*T. longibrachiatum*	Activate defense-related responses and growth promotion.	Ruocco et al., 2015; Moscatiello et al., 2018
	TVHYDII1	*T. virens*	Involved in colonization of plant roots.	Guzmán-Guzmán et al., 2017
	HBF2-6	*T. asperellum*	Involved in root colonization and induction of JA and SA pathways.	Huang et al., 2015
	TasHyd1	*T. asperellum*	Involved in root colonization.	Viterbo and Chet, 2010

The effectors are divided by families, we indicate the strain from Trichoderma that produce the protein effector and their function in plants.

presence of 1% poplar leaves powder, whilst the gene upregulated under 1% poplar root powder, suggesting that HFB2-6 has a function in root colonization. Moreover, the recombinant hydrophobin purified from *E. coli* activated the JA and SA signal transduction pathways when used on poplar seedling. Also, the upregulation of two genes related to auxin signaling was observed. Therefore, this protein seems to be involved in the promotion of growth and defense of poplar plants (Huang et al., 2015). TVHYDII1, from *T. virens*, participates in the colonization of tomato roots; this was demonstrated by using null and overexpressing *tvhydii1* strains (Guzmán-Guzmán et al., 2017). Likewise, the *TasHyd1* from *T. asperellum* participates in the colonization of cucumber plants (Viterbo and Chet, 2010). The purified hydrophobin HYTLO1 from *Trichoderma longibrachiatum* activates the defense response and promotes plant growth. Moreover, knockout strains significantly decreased their antagonistic activity and their capability to promote plant growth (Ruocco et al., 2015). Therefore, HYTLO1 has a dual role in the process of interaction with plants.

Glycoside-Hydrolases

This is a wider group of proteins with enzymatic activity that are secreted by *Trichoderma*; some of them have been characterized and implicated in the *Trichoderma*–plant interaction. The xylanase Eix (ethylene induced xylanase) from *T. viride* triggers ET biosynthesis and the hypersensitive response in tobacco plants, highlighting that the elicitation of ET biosynthesis is not related with Eix enzymatic activity (Sharon et al., 1993; Rotblat et al., 2002). The cellulases, Thph1 and Thph2 from *T. harzianum*, were applied on maize leaves and this treatment led to the transient elevation of free cytosolic calcium and the production of reactive oxygen species (ROS). The Δ*Thph1*- or Δ*Thph2* null mutants were not able to upregulate the expression of genes related to the jasmonate/ET signaling pathway in maize. By using the yeast two-hybrid system, Thph1 and Thph2 can bind to the autophagocytosis associated protein (ZmATG3) and germin-like protein (ZmGL) of the plant, respectively. The identification of this molecular interaction opens the possibility to analyze the cellular localization of these targets as well as their participation in the ISR (Saravanakumar et al., 2016, 2018).

CFEM and Small Secreted Cysteine-Rich Proteins (SSCPs)

In *Trichoderma* spp., one of the most abundant groups of secreted proteins corresponds to small proteins containing four or more cysteine residues. The SSCPs could be grouped into protein families with functions such as hydrophobins, some glycosyl hydrolases, cerato-platanins, CFEM proteins (Common in several Fungal Extracellular Membrane) as well as proteins with unknown function (Druzhinina et al., 2012).

Lamdan et al. (2015) reported a secretome analysis from the interaction between *T. virens* and maize, detecting 13 SSCPs negatively regulated by the presence of the roots. Plant inoculation with independent knockouts strains, for four of these genes encoding the SSCPs (ID 92810, ID 71692, ID 111486, and ID 77560), showed an improvement in ISR activity compared

with the wild-type strain, without affecting root colonization. SSCPs could act as negative effectors reducing the defense levels in the plant and may be important for the fine-tuning of ISR by *Trichoderma*. Bioinformatic predictions indicated the abundant presence of SSCPs in *T. atroviride* and *T. virens* genomes, some of them containing CFEM domains, which are present in cell surface proteins with important roles in the interaction with other organisms (Pérez et al., 2011; Druzhinina et al., 2012). Possibly, but not in all cases, CFEM proteins participate as negative regulators of plant defense. In the bioinformatic analysis reported by Guzmán-Guzmán et al. (2017), there are 32 sequences grouped as CFEM; among them the *tacfem1* gene, which was upregulated when the fungus was co-cultivated with *A. thaliana*, suggesting a possible role during the establishment of the interaction. Also, in *T. virens*, the SSCP gene ID 19757 was upregulated in the interaction with both maize and tomato, while the ID 17705 gene was upregulated only by the presence of maize plants, rendering it a promising candidate for further analysis during the *T. virens*-maize interaction (Morán-Diez et al., 2015).

Hunting for New *Trichoderma* Protein Effectors

One of the main strategies to identify effector proteins is to analyze their upregulation in the presence of plants (Djonovic et al., 2006; Plett et al., 2011; Guzmán-Guzmán et al., 2017). *Trichoderma* transcriptome and secretome analyses under different culture conditions led to describe that cellulases, small proteins, and cytochrome p450, among others, are highly represented (Lamdan et al., 2015; Morán-Diez et al., 2015; Rocha et al., 2016). Recently, a catalog of 233 putative effector proteins was reported from *T. virens*, *T. atroviride*, and *Trichoderma reesei*, identified and grouped in 18 families. The expression pattern of some of these genes was analyzed during the *Trichoderma–Arabidopsis* interaction, observing the upregulation of genes grouped in LysM proteins, Serine-proteases, Thioredoxins, Hydrophobins, CFEM, and Cerato-platanin families. Down-regulation was also observed, as in the case of the *Tvmp1* gene, encoding for a Metalloprotease (Guzmán-Guzmán et al., 2017), and for the *Tvcyt2* gene, which encodes a p450-cytochrome (Ramírez-Valdespino et al., 2018). However, more than 200 sequences from this *in silico* analysis were not studied further and their possible function during *Trichoderma*–plants interaction remains unknown.

The LysM effectors play relevant roles in the establishment of pathogenic interactions: they protect the fungal mycelium by either covering the surface of the hypha, thereby interfering with the enzymatic activity of the plant delivered chitinases or hijacking fungal cell wall derived chitin fragments, thereby avoiding the stimulation of the immune response (de Jonge et al., 2010; Kombrink et al., 2017). LysM encoding genes are present in *Trichoderma* genomes, but they are not characterized as well (Mendoza-Mendoza et al., 2018). In the catalog of putative effector proteins, there are 15 LysM encoding genes, six belonging to *T. atroviride* and nine to *T. virens*. Additionally, the *tvlysm1* gene was upregulated in co-culture of *T. virens* with *Arabidopsis*, suggesting a role during *Trichoderma* interaction with the plant (Guzmán-Guzmán et al., 2017). Additionally, the Tal6 protein from *T. atroviride*, was reported as an inhibitor of conidia germination (Seidl et al., 2013); however, their direct participation with plants has not been determined.

The differences in the experimental design in each case, where *Trichoderma*–Plant transcriptome/secretome are analyzed, makes it difficult to compare among all data sets to determine the functional relevance of these genes. In the case of *T. virens*, two secretomes obtained from hydroponic cultures, were analyzed looking for proteins differentially expressed during their interaction with maize seedlings. One of them analyzed the soluble proteins, while the other focused only on the proteins found in the plant apoplast. The main differences between both studies are related to the culture medium used and the time length of interaction. Lamdan et al. (2015) obtained the secretome from hydroponic cultures in sucrose-supplemented MS media after 96 h of interaction, a total of 280 soluble proteins were detected, of which 86% (241 proteins) contained a predicted signal peptide, identifying members of glycoside hydrolases (GH), LysM proteins, CFEM, lipases, and SSCPs, including Sm1 as the most abundant protein. From all secreted proteins, 66 were identified as differentially expressed, 32 were increased, while the remaining 34 showed a decrease when maize seedlings were present. Nogueira-Lopez et al. (2018) reported 43 secreted proteins, obtained from apoplastic space of maize roots cultured in Hoagland's solution after 60 h of interaction with *T. virens*, and using a filtered-pipeline, nine of them were classified as putative effector proteins. Both secretomes share 13 putative candidates, being the GH group; the most representative proteins with five protein family members (**Supplementary Table S1**). The low number of common sequences could be due to the filtered-pipeline used in each study or due to the differences in growth conditions and sample collection times; without leaving aside the possibility that the roots could retain some proteins limiting their detection in the media (Lamdan et al., 2015).

The comparison between each secretome with the proposed *T. virens* effectors from the *in silico* analysis showed differences related to the number of effector candidates, which is expected given that the predicted secretome includes all sequences with the potential of being effectors.

Considering the full list of the apoplastic secretome (43 proteins), the proteins found with differential expression in the complete soluble secretome (66 proteins) and the effector candidates from the *in silico* prediction (84 proteins), we only found the CFEM member (ID 92810) and the GH member (ID 42143) in the three research works, while 22 common sequences were found between the soluble secretome (Lamdan et al., 2015) with the predicted effectors (Guzmán-Guzmán et al., 2017). Whereas, five sequences from the *in silico* analysis are present among the apoplastic secretome proteins, but they were not considered as effectors.

The differences observed among the experimental strategies to identify new protein effectors in the association of *Trichoderma* with plants suggests that there is still no consensus to consider products with the potential to participate as effectors, which represents a relevant topic to analyze further. The *in silico* analysis can be less precise when identifying effector molecules, but

they provide a wide range of candidates to determine biological functions and the best way to know the function of a putative effector is to perform a wide and specialized characterization. Understanding and identifying the effector proteins will provide tools to deepen our understanding on how plant-beneficial fungi interaction is established and which could be the differences between a beneficial and a pathogenic system.

SECONDARY METABOLITES AS EFFECTORS IN *Trichoderma*–PLANT INTERACTIONS

One of the main characteristics of fungi is the production of a huge diversity of secondary metabolites (SMs); compounds with potential application in food, pharmaceutical and agricultural industries (Brakhage, 2013). It is generally assumed that SMs are not essential for growth and development in fungi but play important functions in the sensing, signaling and counteracting processes for the organisms present in their environment (Macheleidt et al., 2016). SMs comprise compounds of low molecular weight, diffusible in the culture medium or volatile, which are synthesized through a great variety of pathways (Brakhage, 2013). The synthesis of SMs is usually different between strains, and is influenced by growth conditions (Yu and Keller, 2005). At the molecular level, this environmental influence is related to the availability of regulatory elements. In *T. reesei*, the SOR cluster contains two genes encoding for transcription factors involved in biosynthesis of sorbecillinoids, a group of yellow pigments with antimicrobial activities. YPR2, one of those transcription factors, carries out its major function in constant darkness and in the presence of cellulose as a carbon source. The function of YPR is positively related to the levels of alamethicin and to the production of orsellinic acid in darkness (Hitzenhammer et al., 2019). In *T. atroviride* and *T. virens*, it has been shown that heterotrimeric G proteins, mitogen-activated protein kinases (MAPK) and transcription factors are involved in the signaling pathway leading to SMs synthesis, which also respond to environmental conditions as a type of nutrients, pH, light or temperature (Reithner et al., 2005; Mukherjee and Kenerley, 2010). Antibiotic activity has been reported for SMs produced by *Trichoderma* species against various yeast, filamentous fungi and bacteria, causing growth inhibition or cell death. These SMs, acting synergistically with hydrolytic enzymes, are more likely to be implicated in the effectiveness of the strain producing them as a biological control agent (Reino et al., 2008).

Although the metabolites produced by plants could also affect the association with microorganisms, either by favoring it or by restricting it, in this section we will focus on those SMs produced by *Trichoderma* species that have shown impact in their capacity as plant symbionts.

Lactones

These are generally very pleasant, potent, flavor materials, which are widely distributed in nature (Kapfer et al., 1989). The best-known SM for *Trichoderma* species is 6-pentyl-2H-pyran-2-one (6-PP), derived from linoleic acid and the pathway of its formation has been elucidated by metabolization of [U-14C] and of [1-14C] linoleic acid in *T. harzianum* (Serrano-Carreon et al., 1993). In plants, 6-PP interferes with the signaling pathway involving auxins and ET, promotes plant growth, and regulates root architecture by inhibiting the growth of the primary root and inducing the formation of lateral shoots, by modulating the expression of genes encoding for auxin transporters. The modification related to the lateral shoots is mediated by the TIR1, AFB2, and AFB3 receptors and the ARF7 and ARF19 transcription factors, while the sensitization in the main root is mediated by EIN2 (Garnica-Vergara et al., 2016). In field, the application of 6PP (1 μM) or a spore suspension of *T. harzianum* T22 (10^8 spore/liter) in *Vitis vinifera*, increased polyphenol content, antioxidant activity and weight in fruits (Pascale et al., 2017). Cremenolide is a 10-member lactone isolated from *Trichoderma cremeum*, that improved the root length and fresh weight in tomato seedlings, but changes in plant height were not observed (Vinale et al., 2016).

Peptaibols

These are small linear peptides of non-ribosomal synthesis, which usually have a high content of 2-amino-isobutyric acid (Aib) bound to unconventional amino acids, such as ethyl-valine, isovaline, and hydroxyproline. There are at least 190 compounds of this type synthesized by *Trichoderma* species[1].

In *T. virens*, 18-mer peptaibols are produced through the activity of the Non-Ribosomal Peptide Synthase (NRPS) encoded by the gene *Tex1*. This kind of peptaibols activates the plant defense in *Cucumis sativus* against *Pseudomonas syringae*. Cucumber plants growing in contact with *T. virens* increase the expression of three genes involved in the synthesis of phytoalexins, *hpl*, *pal1*, and *prx*, which encode for a hydroxy peroxide lyase, phenylalanine ammonia lyase, and peroxidase, respectively. The *tex1* null mutants lose their ability to produce 18-mer peptaibols, leading to a lower expression of *hpl*, *pal1*, and *prx* genes in plants. The use of two synthetic peptaibols TvBI and TvBII on cucumber seedlings activated systemic protection against bacteria and induced the expression of *hpl*, *pal1*, and *prx* (Viterbo et al., 2007). Null mutants in *ppt1* gene, which codes for a 4-phosphopantetheinyl transferase in *T. virens*, are affected in the synthesis of 11, 14, and 18-mer peptaibols, although their capability to colonize roots is not affected. Furthermore, antibiosis on phytopathogens, as well as the ability to induce the synthesis of SA and of camalexin in *Arabidopsis* plants, is compromised in these strains (Velázquez-Robledo et al., 2011).

Alamethicin is one of the most studied peptaibols due to its ability to induce defense responses in plants such as callose deposition, expression of genes related to plant defense, production of SMs, and accumulation of phenolic compounds, that together can improve the vigor of plants and their response to stressing conditions (Rippa et al., 2010). In *A. thaliana*, the presence of alamethicin interferes with the synthesis of methy farnesoate (MeFA), an SM related to herbivory, by altering the presence of the *miRNA163*, which targets genes

[1]http://peptaibol.cryst.bbk.ac.uk/home.shtml

encoding methyltransferases relevant in the synthetic pathway of the MeFA (Ng et al., 2011). It is proposed that alamethicin increases ion permeability in the cell membrane (Duclohier and Wróblewski, 2001). Trichokonin VI (TK VI) is produced by *T. longibrachiatum* SMF2, and it has been shown that this peptaibol interferes with the GORK channel, a rectifying K+ channel gated outwardly, which alters the root structure by inhibiting cell division and elongation in the main root. TK VI increases the auxin content and interrupts its gradient at the tips of the roots, interfering with the local synthesis and its polar transport (Shi et al., 2016).

Polyketides

These are one of the most abundant groups of SMs in nature, which includes macrolides, polyenes, and polyphenols. They have been studied in detail because the group includes compounds with an impact on human health such as sterigmatocystin, aflatoxin B1 and lovastatin. They are produced by polyketide synthases (PKSs), multi-domain proteins similar to fatty acid synthases, which condense acetyl coenzyme A or malonyl coenzyme A units, to form carbon chains of variable length (Chiang et al., 2010). In *Trichoderma arundinaceum*, the production of 4 aspinolides has been reported, in particular, aspinolide C participates in the induction of genes *PR1b1*, *PR-P2* involved in the signaling pathway mediated by SA. During the interaction of *T. virens* with maize plants, the expression of the defense-related genes *pal1* and *aos* (allene oxide synthase) is increased. This upregulation is related to SMs produced by *T. virens* through the activity of the PKS/NPRS encoded by the *Tex 13* gene. Strains affected in *Tex13* retained their ability to increase the expression of the gene *aos* in plant, but they could not upregulate the *pal1* gene (Mukherjee et al., 2012).

Terpenes

These are a highly diverse family of SMs at the structural and stereochemical level. These molecules are derived from long polyisoprenoid diphosphates that can be cyclized to generate single or multiple ring products. The cyclization reactions are carried out by high-affinity terpene cyclase enzymes, which generate a single product or by promiscuous enzymes that can generate up to 52 different products (Christianson, 2008). Cytochrome p450 enzymes are involved in the reactions of synthesis and/or modification of terpenes. Recently 477 cytochrome P450s have been identified from seven *Trichoderma* species (Chadha et al., 2018). Cytochrome p450 activity is needed for the synthesis of SMs, which are related to the mycoparasitic capacity and/or its association with plants. The enzyme encoded by the *G3* gene in *Trichoderma hamatum* is activated in response to *Sclerotinia* and *Sclerotium* species (Carpenter et al., 2008). Through the generation of mutant and overexpressing strains of the *Tvcyt2* gene of *T. virens*, five terpene-like compounds were identified as involved in the antagonistic activity against *Rhizoctonia solani*, in the activation of genes related to the JA pathway in *Arabidopsis* plants as well as in the promotion of growth in *Arabidopsis* and tomato seedlings (Ramírez-Valdespino et al., 2018).

Trichothecenes

Trichoderma brevicompactum produces trichodermin through a pathway involving the activity of p450 enzyme, encoded by *Tri5* gene. The overexpressing strains of this gene had a negative effect in tomato plants, decreasing the root length and plant size (Malmierca et al., 2015). Harzianum A (HA), isolated from *T. arundinaceum*, did not show any effect over growth of tomato seedlings. However, mutant strains that do not produce HA were impaired to upregulate the expression of genes involved in plant defense at the same level. HA could be sensitizing the plant cell to induce those genes faster and at higher levels (Malmierca et al., 2012).

Volatile Organic Compounds (VOCs)

The VOCs group includes several small compounds with different chemical natures, playing relevant roles as essential signals in interactions among plant roots, microbes, and insects (Schenkel et al., 2015). The effect by the VOCs produced by 25 different *Trichoderma* strains on the plants were analyzed using *A. thaliana* as a host, in two independent research works. The general results showed that one of the strains produced VOCs with a negative impact on plant growth, 10 of the strains did not have any obvious effect on the plants, while fourteen of them had a positive effect on total biomass and on chlorophyll content. The analysis of the VOCs produced by each strain determined the presence of great diversity of compounds, suggesting the participation of several mechanisms to generate the final effect on plants (Lee et al., 2016; Nieto-Jacobo et al., 2017). This blend of compounds present in VOCs makes it difficult to determine which of the metabolites is responsible for the effects observed on the plants. Some strategies that could help to define their biological role are based on genetic manipulation in order to generate strains affected in key elements of the VOCs biosynthesis. Trichodiene (TD) is a VOC used as a substrate by the sesquiterpene synthase Tri5 to produce the compound Harzianum A (HA) in *T. arundinaceum*. The heterologous expression of the gene *Tri5* in *T. harzianum* led to the production of TD. VOCs released by this *Tri5*-transformant and TD itself induced the expression of tomato defense genes related to SA (Malmierca et al., 2015). In *T. atroviride*, the mutation of genes encoding membrane-bound NADPH oxidases (Nox), leads to the alteration of VOCs profiles. Loss of function of Nox1 or the regulator NoxR, in the presence of a functional Nox2 enzyme leads to the production of VOCs with inhibitory effects on plant growth (Cruz-Magalhães et al., 2019).

Phytohormones

Phytohormones are important growth regulators with relevant roles on metabolism and plant defense responses. Several root-associated microbes are able to produce phytohormones that have an effect in plants (Egamberdieva et al., 2017). *T. virens* produces Indole-3-acetic acid (IAA) and indole-3-acetaldehyde (IAAId), which promotes plant growth and development in *A. thaliana* (Contreras-Cornejo et al., 2009).

Cytokinins (CKs) are essential molecules that regulate plant growth and development (Osugi and Sakakibara, 2015). ET is a volatile hormone that regulates a range of processes, from seed germination, organ senescence, among others (Bleecker and Kende, 2000). CKs promote hyphal branching and help in oxidative stress tolerance in *Magnaporthe oryzae* (Chanclud et al., 2016), whilst in mycorrhizal fungi, ET affects spore germination and growth (Barker and Tagu, 2000). There are no reports in *Trichoderma* about CKs or ET production, though in the genome of *T. atroviride*, the genes necessary to synthesize both compounds are present, suggesting that it could produce these phytohormones, with a potential impact in the association with plants (Guzmán-Guzmán et al., 2019). Abscisic acid (ABA) is involved in seed dormancy and development, abiotic stress response, among other roles in plants, and there is evidence of its production by several fungi on which ABA was proposed as a factor promoting plant colonization (Charpenter et al., 2014; Chanclud and Morel, 2016). There were six genes related to the ABA biosynthesis pathway identified in *T. atroviride*. However, no homolog to *bcaba3/ataba3*, a gene encoding a key enzyme in last steps of the biosynthesis of ABA was found, suggesting that *T. virens* is unlikely to produce this phytohormone and that it could only provide an ABA intermediary (Guzmán-Guzmán et al., 2019). Additionally, it was proposed that *T. virens* and *T. atroviride* modulate ABA-regulated responses, such as stomatal aperture and leaf transpiration in *A. thaliana* (Contreras-Cornejo et al., 2015).

Factors That Influence the Effect of SMs on Plants

Three relevant factors related to the positive effect generated on the plants by SMs are, the dose used of each SM, the physiological state, as well as the genetic background of the plants tested (Vinale et al., 2009; Li et al., 2019). The effect of alamethicin over plants has been tested at high doses such as 10 and 50 mM. When these are applied to *Arabidopsis* seedlings, they generate plant death and this toxicity is related to cleavage of ribosomal RNA and cellular lysis. The use of alamethicin at lower doses (5 μM) suggest that a threshold in the concentration of this SM is required to trigger only plant-cell permeabilization and induce programed cell death as a hypersensitive response, showing similarities with the response elicited by avirulent pathogens or by compounds that mimic a pathogen attack (Rippa et al., 2007; Rippa et al., 2010). Koninginins A, B, C, E, and G tested at 10^{-3} M, inhibited growth of etiolated wheat coleoptiles at different rates, varying between 54 and 65% and up to 100% (Reino et al., 2008). Treatments of 6-PP over *A. thaliana* seedlings in doses from 50 to 175 μM increased shoot, root and total plant biomass while at 200 μM, no increase in biomass was observed. 6-PP also raised both lateral root number and density in a dose- dependent manner, showing an inhibition of primary root growth from 125 μM onwards, without cell damage (Garnica-Vergara et al., 2016).

The plant genetic background is a determinant in the response generated by specific strains of *Trichoderma*. In maize, the use of *T. harzianum* T22, one of the most widely used commercial strains, induced strong positive growth over eight maize hybrids tested, it had little effect on growth over eight other hybrids and it even negatively affected growth of two other maize hybrids (Harman, 2006). While in tomato, independent symbiotic interactions between *T. harzianum* T22 or *T. atroviride* P1 with four *Solanum lycopersicum* lines or the wild *Solanum habrochaites* accession demonstrated that genetic variability is a determinant in the response shown by plants related to growth, weight, resistance against *B. cinerea* and the expression of genes involved in plant defense (Tucci et al., 2011).

We propose that many SMs can be classified as effectors and the different *Trichoderma*–plant systems developed by different work groups make evident the utility of using them as a biological model. Metabolomic analysis, involving the study of the concentrations, structures and interactions of thousands of SMs represents a useful tool to identify molecules with potential biotechnological application in the improvement of plant yield and vigor.

Trichoderma's SMALL RNAs AS PUTATIVE EFFECTORS

Thus far, plant analysis has focused on the identification of proteins involved in the plant immune response. However, several lines of evidence have shown that plants also use non-coding RNAs against pathogens (Pumplin and Voinnet, 2013) and symbionts (Pieterse et al., 2014). Small RNAs (sRNAs) play important roles in plant immune responses against virus, bacteria, fungi, and oomycetes (Pumplin and Voinnet, 2013). sRNAs are 20–30 nucleotide long non-coding, sequence specific regulatory RNA molecules that mediate gene silencing to regulate physiological and developmental processes (Chang et al., 2012; Pumplin and Voinnet, 2013). In plants, sRNAs are processed from double-stranded or single-stranded RNA with hairpin structures by Dicer-like (DCL) proteins, which release RNA duplexes. After processing, sRNAs are loaded into RNA-induced silencing complexes (RISC), which contains one member of the ARGONAUTE (AGO) protein family, leading to transcriptional gene silencing by guiding heterochromatin formation, inhibiting mRNA translation or inducing mRNA degradation. Several members of the sRNA biogenesis machinery are involved in plant immunity, including DCL, AGO, DCL associated proteins and RNA dependent RNA polymerases (RDRs). Mutants in such genes show defects in sRNAs accumulation and are impaired in pathogen response (Seo et al., 2013).

During the last decade, cross-kingdom RNA interference (RNAi) between host and phytopathogens has demonstrated its role in the successful colonization of plant tissues by the phytopathogens or in their avoidance by the plant. For instance, host-induced gene silencing (HIGS), a technology developed to protect crops from fungal infections by expressing dsRNA *in planta* to silence virulence genes, enhances plant resistance to *Fusarium verticillioides* or *Blumeria* spp. upon infection of

the host plant (Nowara et al., 2010; Tinoco et al., 2010). HIGS technology is also effective against *Puccinia* spp. (Yin et al., 2011, 2014), *Fusarium* spp. (Koch et al., 2013; Hu et al., 2015) and *S. sclerotiorum* (Andrade et al., 2016).

B. cinerea, produces complementary sRNAs against plant immunity related genes in *Arabidopsis* and *Lycopersicum esculentum* (Weiberg et al., 2013). Upon infection of *Arabidopsis* by *B. cinerea*, the fungal sRNAs associate with *Arabidopsis* AGO1 protein, interfering with plant target mRNAs, for example, those encoding MAPKs. These findings indicate that the fungus hijacks the host RNAi machinery to silence the host own genes (Weiberg et al., 2013; Wang M. et al., 2017). Moreover, *Arabidopsis ago1-27* mutants are more resistant to *B. cinerea* infection, supporting that the fungus uses the plant RNAi machinery to silence host genes. Transferred fungal sRNAs into the plant cell are detected in *B. cinerea dcl1* or *dcl2* single mutants, but not in a *dcl1/dcl2* double mutant, leading to a diminished fungal virulence, indicating that the biogenesis of sRNAs is required for pathogenesis (Weiberg et al., 2013). Transgenic plants expressing one of these sRNAs (Bc-siR37) silence *Arabidopsis* genes encoding a pectin lyase, a WRKY transcription factor, and a receptor-like kinase (Wang M. et al., 2017). The causal agent of wheat stripe rust disease, *Puccinia striiformis*, silences the mRNA that encodes for the PR-2 protein, through Pst-milR1, a miRNA-like sRNA (Wang B. et al., 2017). In *Verticillium dahliae*, it was shown that AGO2 does not play a role in the infection of *Arabidopsis*. This pathogen infected *Arabidopsis ago2*-1 normally, whereas in *ago1-27* mutant, the rate of infection was reduced (Wang et al., 2016).

Successful establishment of the *Trichoderma*–plant interaction during early stages of root colonization implies the activation of cell detoxification and protection mechanisms in the fungi (Ruocco et al., 2009; Estrada-Rivera et al., 2019). Therefore, these fungi possess effective systems that efficiently scavenge harmful compounds from the cell. This has been partially shown with the suppression of phytoalexin and plant genes related to the defense mechanisms in *Lotus japonicus* and *Arabidopsis* during its interaction with *Trichoderma koningii* and *T. atroviride*. Application of these fungi to plant roots induced a rapid accumulation of host transcripts that encode key enzymes of SAR and ISR and those involved in phytoalexin synthesis. The expression of these genes is transient and decreased to levels of the control plants. *Trichoderma* resembles mycorrhizal fungi in the establishment of symbiotic associations rather than fungal pathogens (Masunaka et al., 2011; Estrada-Rivera et al., 2019). Production of sRNAs by filamentous fungi, including *Trichoderma* species, has been documented. Although analysis of mutants in the biogenesis components of sRNAs in fungi have shown their role on their biology (Chang et al., 2012; Carreras-Villaseñor et al., 2013), much is yet to be explored regarding the roles of sRNAs in this kingdom. There is no direct evidence for the role of beneficial microorganisms sRNAs on the suppression of plant immunity to establish a symbiotic relationship. In our group, we sequenced sRNAs libraries during *Arabidopsis–T. atroviride* interaction at different interaction times. Mapping the sRNAs over the *T. atroviride* genome revealed that 37 sRNAs of the fungus matched with genes of the host plant. Interestingly, target genes encode lytic enzymes, MAPKs putatively involved in plant immunity, proteins with a domain of unknown function, disease resistance protein, NBS-LRR class family proteins, and *S*-Adenosyl-L-Methionine-dependent methyltransferases superfamily proteins, among others. This indicates that *T. atroviride* could be using sRNAs as effector molecules, similarly to *B. cinerea* and *V. dahliae*, to establish a symbiotic relationship with *Arabidopsis* through interfering mRNAs involved in plant immunity, chromatin modifications and cell wall degrading enzymes, among others that remain to be determined. However, more research is needed to unravel the molecular mechanisms mediated by the fungal sRNAs that allows us to better understand the mechanisms that lead to the establishment of this beneficial association.

CONCLUSION

The consequence in the field of the presence of *Trichoderma* on plants can be indirect, for example by exerting antagonistic activity on potential phytopathogens, by attacking them, and

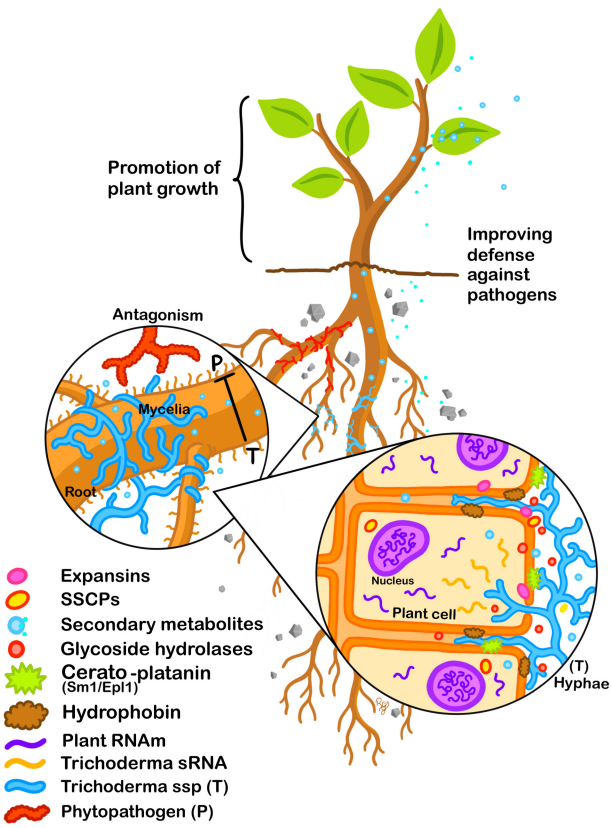

FIGURE 1 | Effectors participate during *Trichoderma*–plant interaction. Antagonist activity of *Trichoderma* against phytopathogenic fungi. The release of molecules from *Trichoderma* with activity as effectors is highlighted. These molecules will modulate the plant hormonal balance as well as its defense response, allowing colonization. The beneficial association will result in the improvement of plant growth and in the resistance against phytopathogens.

by colonizing the rhizosphere, so they can avoid the contact of the pathogen with plant tissue. Direct beneficial effects on plants by *Trichoderma* are related to root colonization, although in many cases it has been shown that direct contact may not be necessary. Effectors of *Trichoderma* may play a key role in the success of colonization of the plant, first by establishing the initial contact and subsequently maintaining the fungus–plant interaction (**Figure 1**). Many of the effectors that have been identified in *Trichoderma*, and in other fungal symbionts, have reported activities described in their pathogenic counterparts. Therefore, the success of the interaction must not only rely on molecules playing these functions. The physiological state of both participants, as well as their threshold of perception toward the molecular signals exchanged are also important factors. This regulation does not depend solely on the genetic background of the fungus, the signals generated by the plant are also important. The study of effectors in *Trichoderma* is a relatively recent topic; however, thanks to technological advances to detect, identify and quantify molecules (proteins, secondary metabolites, and RNAs), the scientific community already has an extensive catalog of effector candidates. In most cases, it is necessary to carry out biological validation and determine the spectrum of action of these effectors on different plants at the level of cultivars, species and even genera. Moreover, the analysis of the interaction, considering longer times, may indicate how *Trichoderma* can change the plant physiology, during its complete life cycle. Due to the versatility shown by *Trichoderma* to associate with a wide variety of plants, it would be possible to determine the relevance of those candidates in different plant systems. In this review, we have focused mainly on the participation of the effectors in the interaction with plants, but its relevance in fungus–fungus associations is still pending, highlighting the idea of a multidirectional molecular exchange in the rhizosphere.

AUTHOR CONTRIBUTIONS

CR-V, SC-F, and VO-M contributed equally with ideas and discussion material. VO-M coordinated the work. CR-V wrote the review.

FUNDING

Research conducted by the groups, related to the topics of this review was supported by CONACyT grants CB-286709 and FC-2016-1538 conferred to VO-M and SC-F, respectively.

ACKNOWLEDGMENTS

We would like to thank Bernardo Franco-Bárcenas Ph.D. for his useful suggestions and corrections and Roberto Gámez-Ramírez for his support to make the drawing in **Figure 1**.

SUPPLEMENTARY MATERIAL

The Supplementary Material for this article can be found online at: https://www.frontiersin.org/articles/10.3389/fmicb.2019.01030/full#supplementary-material

REFERENCES

Alba, J. M., Glas, J. J., Schimmel, B. C., and Kant, M. R. (2011). Avoidance and suppression of plant defenses by herbivores. *J. Plant Interact.* 6, 221–227. doi: 10.1080/17429145.2010.551670

Alonso-Ramírez, A., Poveda, J., Martín, I., Hermosa, R., Monte, E., and Nicolás, C. (2014). Salicylic acid prevents *Trichoderma harzianum* from entering the vascular system of roots. *Mol. Plant Pathol.* 15, 823–831. doi: 10.1111/mpp.12141

Andrade, C. M., Tinoco, M. L. P., Rieth, A. F., Maia, F. C. O., and Aragao, F. J. L. (2016). Host-induced gene silencing in the necrotrophic fungal pathogen *Sclerotinia Sclerotiorum*. *Plant Pathol.* 65, 626–632. doi: 10.1111/ppa.12447

Baccelli, I., Luti, S., Bernardi, R., Scala, A., and Pazzagli, L. (2013). Cerato-platanin shows expansin-like activity on cellulosic materials. *Appl. Microbiol. Biotechnol.* 98, 175–184. doi: 10.1007/s00253-013-4822-0

Bae, H., Roberts, D. P., Lim, H. S., Strem, M. D., Park, S. C., Ryu, C. M., et al. (2010). Endophytic *Trichoderma* isolates from tropical environments delay disease onset and induce resistance against *Phytophthora capsica* in hot pepper using multiple mechanisms. *Mol. Plant Microbe Interact.* 24, 336–351. doi: 10.1094/MPMI-09-10-0221

Bari, R., and Jones, J. D. (2009). Role of plant hormones in plant defense responses. *Plant Mol. Biol.* 69, 473–488. doi: 10.1007/s11103-008-9435-0

Barker, S. J., and Tagu, D. (2000). The roles of auxins and cytokinins in mycorrhizal symbionses. *J. Plant Growth Regul.* 19, 144–154.

Bent, A. F., and Mackey, D. (2007). Elicitors, effectors, and R genes: the new paradigm and a lifetime supply of questions. *Annu. Rev. Phytopathol.* 45, 399–436. doi: 10.1146/annurev.phyto.45.062806.094427

Bigirimana, J., De Mejer, G., Poppe, J., Elad, Y., and Hofte, M. (1997). Induction of systemic resistance on bean (*Phaseolus vulgaris*) by *Trichoderma harzianum*. mededelingen van de faculteit landbouwkundige en toegepaste biologische wetenschappen, universiteit. *Gent* 62, 1001–1007.

Bleecker, A. B., and Kende, H. (2000). Ethylene: a gaseous signal molecule in plants. *Annu. Rev. Cell Dev. Biol.* 16, 1–18. doi: 10.1146/annurev.cellbio.16.1.1

Boller, T., and Felix, G. (2009). A renaissance of elicitors: perception of microbe-associated molecular patterns and danger signals by pattern-recognition receptors. *Annu. Rev. Plant Biol.* 60, 379–406. doi: 10.1146/annurev.arplant.57.032905.105346

Brakhage, A. (2013). Regulation of fungal secondary metabolism. *Nat. Rev. Microbiol.* 11, 21–32. doi: 10.1038/nrmicro2916

Brotman, Y., Briff, E., Viterbo, A., and Chet, I. (2008). Role of swollenin, an expansin-like protein from *Trichoderma*, in plant root colonization. *Plant Physiol.* 147, 779–789. doi: 10.1104/pp.108.116293

Calderón, A. A., Zapata, J. M., and Barceló, R. (1994). Peroxidase-mediated formation of resveratrol oxidation products during the hypersensitive-like reaction of grapevine cells to an elicitor from *Trichoderma viride*. *Physiol. Mol. Plant Pathol.* 44, 289–299. doi: 10.1016/s0885-5765(05)80031-1

Carpenter, M. A., Ridgway, H. J., Stringer, A. M., Hay, A. J., and Stewart, A. (2008). Characterisation of a *Trichoderma hamatum* monooxygenase gene involved in antagonistic activity against fungal plant pathogens. *Curr. Genet.* 53, 193–205. doi: 10.1007/s00294-007-0175-5

Carreras-Villaseñor, N., Esquivel-Naranjo, E. U., Villalobos-Escobedo, J. M., Abreu-Goodger, C., and Herrera-Estrella, A. (2013). The RNAi machinery regulates growth and development in the filamentous fungus *T richoderma atroviride*. *Mol. Microbiol.* 89, 96–112. doi: 10.1111/mmi.12261

Catska, V., Afifi, A. F., and Vancura, V. (1975). The effect of volatile and gaseous metabolites of swealling seeds on germination of fungal spores. *Folia Microbiol.* 20, 152–156. doi: 10.1007/bf02876772

Chadha, S., Mehetre, S. T., Bansal, R., Kuo, A., Aerts, A., Grigoriev, I. V., et al. (2018). Genome-wide analysis of the cytochrome p450 of *Trichoderma* spp.: annotation and evolutionary relationships. *Fungal Biol. Biotechnol.* 4:12. doi: 10.1186/s40694-018-0056-3

Chagas, L. F., Orozco, B. S., and Rodrigues, G. (2017). Rice growth influence by *Trichoderma* spp. with natural phosphate fertilization under greenhouse conditions. *IJDR* 7, 13147–13152.

Chanclud, E., Kisiala, A., Emery, N. R., Chalvon, V., Ducasse, A., Romiti-Michel, C., et al. (2016). Cytokinin production by the rice blast fungus is a pivotal requirement for full virulence. *PLoS Pathog.* 12:e1005457. doi: 10.1371/journal.ppat.1005457

Chanclud, E., and Morel, J. B. (2016). Plant hormones: a fungal point of view. *Mol. Plant Pathol.* 17, 1289–1297. doi: 10.1111/mpp.12393

Chang, S., Zhang, Z., and Liu, Y. (2012). RNA interference pathway in fungi: mechanisms and functions. *Annu. Rev. Microbiol.* 66, 305–323. doi: 10.1146/annurev-micro-092611-150138

Charpenter, M., Sun, J., Wen, J., Mysore, K. S., and Oldroyd, G. E. (2014). Abscisic acid promotion of arbuscular mycorrhizal colonization requires a component of the protein phosphatase 2A complex. *Plant Physiol.* 166, 2077–2090. doi: 10.1104/pp.114.246371

Cheng, C. H., Shen, B. N., Shang, Q. W., Liu, L. D., Peng, K. C., Chen, Y. H., et al. (2018). Gene-to-gene network análisis of the mediation of plant innate immunity by the eliciting plant response-like 1 (Epl1) elicitor of *Thicoderma formosa*. *Mol. Plant Microbe Interact.* 31, 683–691. doi: 10.1094/MPMI-01-18-0002-TA

Chiang, Y. M., Oakley, B. R., Keller, N. P., and Wang, C. C. (2010). Unraveling polyketide synthesis in members of the genus *Aspergillus*. *Appl. Microbiol. Biothechnol.* 86, 1719–1736. doi: 10.1007/s00253-010-2525-3

Christianson, D. W. (2008). Unearthing the roots of the terpenome. *Curr. Opin. Chem. Biol.* 12, 141–150. doi: 10.1016/j.cbpa.2007.12.008

Contreras-Cornejo, H. A., López-Bucio, J., Méndez-Bravo, A., Macías-Rodríguez, L., Ramos-Vega, M., Guevara-García, A. A., et al. (2015). Mitogen-Activated Protein Kinase 6 and ethylene and auxin signaling pathways are involved in *Arabidopsis* root-system architecture alteratios by *Trichoderma atroviride*. *Mol. Plant Microbe Interact.* 28, 701–710. doi: 10.1094/MPMI-01-15-0005-R

Contreras-Cornejo, H. A., Macías-Rodríguez, L., Beltrán-Peña, E., Herrera-Estrella, A., and López-Bucio, J. (2011). Trichoderma-induced plant immunity likely involves both hormonal- and camalexin-dependent mechanisms in *Arabidopsis thaliana* and confers resistance against necrotrophic fungi *Botrytis cinerea*. *Plant Signal. Behav.* 6, 1554–1563. doi: 10.4161/psb.6.10.17443

Contreras-Cornejo, H. A., Macías-Rodríguez, L., Cortés-Penagos, C., and López-Bucio, J. (2009). Trichoderma virens, a plant beneficial fungus, enhances biomass production and promotes lateral root growth through an auxin-dependent mechanism in *Arabidopsis*. *Plant Physiol.* 149, 1579–1592. doi: 10.1104/pp.108.130369

Crutcher, F. K., Moran-Diez, M. E., Ding, S. L., Liu, J., Horwitz, B., Mukherjee, P. K., et al. (2015). A paralog of the proteinaceous elicitor SM1 is involved in colonization of maize roots by *Trichoderma virens*. *Fungal Biol.* 119, 476–486. doi: 10.1016/j.funbio.2015.01.004

Cruz-Magalhães, V., Nieto-Jacobo, M. F., van Zijll de Jong, E., Rostás, M., Padilla-Arizmendi, F., Kandula, D., et al. (2019). The NADPH oxidases Nox1 and Nox2 differentially regulate volatile organic compounds, fungistatic activity, plant growth promotion and nutrient assimilation in *Trichoderma atroviride*. *Front. Microbiol.* 23:3271. doi: 10.3389/fmicb.2018.03271

de Jonge, R., van Esse, H. P., Kombrink, A., Shinya, T., Desaki, Y., Bours, R., et al. (2010). Conserved fungal LysM effector Ecp6 prevents chitin-triggered immunity in plants. *Science* 329, 953–955. doi: 10.1126/science.1190859

Di, X., Takken, F. L. W., and Tintor, N. (2016). How phytohormones shape interactions between plants and the soil-borne fungus *Fusarium oxysporum*. *Front. Plant Sci.* 7:170. doi: 10.3389/fpls.2016.00170

Djonovic, S., Pozo, M. J., Dangott, L. J., Howell, C. R., and Kenerley, C. M. (2006). Sm1, a proteinaceous elicitor secreted by the biocontrol fungus *Trichoderma virens* induces plant defense responses and systemic resistance. *Mol. Plant Microbe Interact.* 19, 838–853. doi: 10.1094/mpmi-19-0838

Djonovic, S., Vargas, W. A., Kolomiets, M. V., Horndeski, M., Wiest, A., and Kenerley, C. M. (2007). A proteinaceous elicitor Sm1 from the beneficial fungus *Trichoderma virens* is required for induced systemic resistance in maize. *Plant Physiol.* 145, 875–889. doi: 10.1104/pp.107.103689

Druzhinina, I. S., Shelest, E., and Kubicek, C. P. (2012). Novel traits of *Trichoderma* predicted through the analysis of its secretome. *FEMS Microbiol. Lett.* 337, 1–9. doi: 10.1111/j.1574-6968.2012.02665.x

Duclohier, H., and Wróblewski, H. (2001). Voltage-dependent pore formation and antimicrobial activity by alamethicin and analogues. *J. Membr. Biol.* 184, 1–12. doi: 10.1007/s00232-001-0077-2

Egamberdieva, D., Wirth, S. J., Alqarawi, A. A., Abd Allah, E. F., and Hashem, A. (2017). Phytohormones and beneficial microbes: essential components for plants to balance stress and fitness. *Front. Microbiol.* 31:2104. doi: 10.3389/fmicb.2017.02104

Estrada-Rivera, M., Rebolledo-Prudencio, O. G., Pérez-Robles, D. A., Rocha-Medina, M. C., González-López, M. C., and Casas-Flores, S. (2019). Histone deacetylase HDA-2 is essential in *Trichoderma* to modulate multiple responses in *Arabidopsis*. *Plant Physiol.* 179, 1343–1361. doi: 10.1104/pp.18.01092

Flor, H. H. (1942). Inheritance of pathogenicity in *Melampsora lini*. *Phytopathology* 32, 653–669.

Gaderer, R., Lamdan, N., Frischmann, A., Sulyok, M., Krska, R., Horwitz, B. A., et al. (2015). Sm2, a paralog of the *Trichoderma* cerato-platanin elicitor Sm1, is also highly important for plant protection conferred by the fungal-root interaction of *Trichoderma* with maize. *BMC Microbiol.* 15:2. doi: 10.1186/s12866-014-0333-0

Garnica-Vergara, A., Barrera-Ortiz, S., Muñoz-Parra, E., Raya-González, J., Méndez-Bravo, A., Macías-Rodríguez, L., et al. (2016). The volatile 6-pentyl-2H-pyran-2-one from *Trichoderma atroviride* regulates *Arabidopsis thaliana* root morphogenesis via auxin signaling and ETHYLENE INSENSITIVE 2 functioning. *New Phytol.* 209, 1496–1512. doi: 10.1111/nph.13725

Gomes, E. V., Costa, N., de Paula, R. G., de Azevedo, R. R., da Silva, F. L., Noronha, E. F., et al. (2015). The cerato-platanin protein Epl-1 from *Trichoderma harzianum* is involved in mycoparasitism, plant resistance induction and self wall protection. *Sci. Rep.* 5:17998. doi: 10.1038/srep17998

Guzmán-Guzmán, P., Alemán-Duarte, M. I., Delaye, L., Herrera-Estrella, A., and Olmedo-Monfil, V. (2017). Identification of effector-like proteins in *Trichoderma* spp. and role of hydrophobin in the plant-fungus interaction and mycoparasitism. *BMC Genet.* 18:16. doi: 10.1186/s12863-017-0481-y

Guzmán-Guzmán, P., Porras-Troncoso, M. D., Olmedo-Monfil, V., and Herrera-Estrella, A. (2019). *Trichoderma* species: versatile plant symbionts. *Phytopathology* 109, 6–16. doi: 10.1094/PHYTO-07-18-0218-RVW

Harman, G. E. (2006). Overwiew of mechanisms and uses of *Trichoderma* spp. *Phytopathology* 96, 190–194. doi: 10.1094/PHYTO-96-0190

Harman, G. E., Petzoldt, R., Comis, A., and Chen, J. (2004). Interactions between *Trichoderma harzianum* strain T22 and maize inbred line Mo17 and effects of these interactions on diseases caused by *Pythium ultimum* and *Colletotrichum graminicola*. *Phytopathology* 94, 147–153. doi: 10.1094/PHYTO.2004.94.2.147

Hitzenhammer, E., Büschl, C., Sulyok, M., Schuhmacher, R., Kluger, B., Wischnitzki, E., et al. (2019). YPR2 is a regulator of light modulated carbon and secondary metabolism in *Trichoderma reesei*. *BMC Genomics* 20:211. doi: 10.1186/s12864-019-5574-8

Hu, Z., Parekh, U., Maruta, N., Trusov, Y., and Botella, J. R. (2015). Down-regulation of *Fusarium oxysporum* endogenous genes by host-delivered RNA interference enhances disease resistance. *Front. Chem.* 3:1. doi: 10.3389/fchem.2015.00001

Huang, Y., Mijiti, G., Wang, Z., Yu, W., Fan, H., Zhang, R., et al. (2015). Functional analysis of the class II hydrophobins gene HFB2-6 from the biocontrol agent *Trichoderma asperellum* ACCC30536. *Microbiol. Res.* 171, 8–20. doi: 10.1016/j.micres.2014.12.004

Jones, J. D., and Dangl, J. L. (2006). The plant immune system. *Nature* 444, 323–329.

Kamoun, S. (2006). A catalogue of the effector secretome of plant pathogenic oomycets. *Annu. Rev. Phytopathol.* 44, 41–60. doi: 10.1146/annurev.phyto.44.070505.143436

Kapfer, G. F., Berger, R. G., and Drawert, F. (1989). Production of 4-decanolid by semi-continuous fermentation of *Tyromyces sambuceus*. *Biotechnol. Lett.* 11, 561–566. doi: 10.1007/bf01040036

Kloppholz, S., Kuhn, H., and Requena, N. (2011). A secreted fungal effector of *Glomus intrarradices* promotes symbiotic biotrophy. *Curr. Biol.* 21, 1204–1209. doi: 10.1016/j.cub.2011.06.044

Koch, A., Kumar, N., Weber, L., Keller, H., Imani, J., and Kogel, K. H. (2013). Host-induced gene silencing of cytochrome P450 lanosterol C14α-demethylase–encoding genes confers strong resistance to *Fusarium* species. *Proc. Natl. Acad. Sci. U.S.A.* 110, 19324–19329. doi: 10.1073/pnas.1306373110

Kombrink, A., Rovenich, H., Shi-Kunne, X., Rojas-Padilla, E., van den Berg, G. C., Domazakis, E., et al. (2017). *Verticillium dahliae* LysM effectors differentially contribute to virulence on plants hosts. *Mol. Plant Pathol.* 18, 596–608. doi: 10.1111/mpp.12520

Kubicek, C. P., Herrera, A., Seidl, V., Martinez, D., Druzhinina, I. S., Thon, M., et al. (2011). Comparative genome sequence analysis underscores mycoparasitism as the ancestral life style of *Trichoderma*. *Genome Biol.* 12, R40. doi: 10.1186/gb-2011-12-4-r40

Kulkarni, R. D., Thon, M. R., Pan, H., and Dean, R. A. (2005). Novel G-protein-coupled receptor-like proteins in the plant pathogenic fungus *Magnaporthe grisea*. *Genome Biol.* 6, R24.

Lamdan, N., Shalaby, S., Ziv, T., Kenerley, C. M., and Horwitz, B. A. (2015). Secretome of the biocontrol fungus *Trichoderma virens* co-cultured with maize roots: tole in induced systemic resistance. *Mol. Cell Proteomics* 14, 1054–1063. doi: 10.1074/mcp.m114.046607

Lee, S., Yap, M., Behringer, G., Hung, R., and Bennett, J. W. (2016). Volatile organic compounds emitted by *Trichoderma* species mediate plant growth. *Fungal Biol. Biotechnol.* 29:7. doi: 10.1186/s40694-016-0025-7

Li, M., Li, G., and Zhang, K. (2019). Non-volatile metabolites from *Trichoderma* spp. *Metabolites* 9:58. doi: 10.3390/metabo9030058

Lopes, F. A., Steindorff, A. S., Geraldine, A. M., Brandao, R. S., Monteiro, V. N., Lobo, M. Jr., et al. (2012). Biochemical and metabolic profiles of *Trichoderma* strains isolated from common bean crops in the Brazilian Cerrado, and potential antagonism against *Sclerotinia sclerotiorum*. *Fungal Biol.* 116, 815–824. doi: 10.1016/j.funbio.2012.04.015

Macheleidt, J., Mattern, D. J., Fischer, J., Netzker, T., Weber, J., Schroeckh, V., et al. (2016). Regulation and role of fungal secondary metabolites. *Annu. Rev. Genet.* 23, 371–392.

Macías-Rodríguez, L., Guzmán-Gómez, A., García-Juárez, P., and Contreras-Cornejo, H. A. (2018). *Trichoderma atroviride* promotes tomato development and alters the root exudation of carbohydrates, which stimulates fungal growth and the biocontrol of the phytopathogen *Phytophtora cinnamomic* in a tripartite interaction system. *FEMS Microbiol. Ecol.* 94,

Malmierca, M. G., Cardoza, R. E., Alexander, N. J., McCormick, S. P., Hermosa, R., Monte, E., et al. (2012). Involvement of *Trichoderma* trichothecenes in the biocontrol activity and induction of plant defense-related genes. *Appl. Environ. Microbiol.* 78, 4856–4868. doi: 10.1128/AEM.00385-12

Malmierca, M. G., McCormick, S. P., Cardoza, R. E., Alexander, N. J., Monte, E., and Gutiérrez, S. (2015). Production of trichodiene by *Trichoderma harzianum* alters the perception of this biocontrol strain by plants and antagonized fungi. *Environ. Microbiol.* 17, 2628–2646. doi: 10.1111/1462-2920.12506

Manganiello, G., Sacco, A., Ercolano, M. R., Vinale, F., Lanzuise, S., Pascale, A., et al. (2018). Modulation of tomato response to *Rhizoctonia solani* by *Trichoderma harzianum* and its secondary metabolite harzianic acid. *Front. Microbiol.* 9:1966. doi: 10.3389/fmicb.2018.01966

Martínez, C., Blanc, F., Le Claire, E., Besnard, O., Nicole, M., and Baccou, J. C. (2001). Salicylic acid and ethylene pathways are differentially activated in melon cotyledons by active or heat-denatured cellulase from *Trichoderma lingibrachiatum*. *Plant Physiol.* 127, 334–344. doi: 10.1104/pp.127.1.334

Martínez-Medina, A., Appels, F. V. W., and van Wees, S. C. M. (2017). Impact of salycilic acid- and jasmonic acid-regulated defenses on root colonization by *Trichoderma harzianum* T-78. *Plant Signal. Behav.* 12, e1345404. doi: 10.1080/15592324.2017.1345404

Martínez-Medina, A., Fernández, I., Lok, G. B., Pozo, M. J., Pieterse, C. M., and Van Wees, S. C. (2016). Shifting from priming of salicylic acid- to jasmonic acid-regulated defences by *Trichoderma* protects tomato against the root knot nematode *Meloidogyne incognita*. *New Phytol.* 13, 1363–1377. doi: 10.1111/nph.14251

Mastouri, F., Björkman, T., and Harman, G. E. (2012). *Trichoderma harzianum* enhances antioxidant defense of tomato seedlings and resistance to water deficit. *Mol. Plant Microbe Interact.* 25, 1264–1271. doi: 10.1094/MPMI-09-11-0240

Masunaka, A., Hyakumachi, M., and Takenaka, S. (2011). Plant growthpromoting fungus. Trichoderma koningi suppresses isoflavonoid phytoalexin vestitol production for colonization on/in the roots of Lotus japonicus. *Microbes Environ.* 26, 128–134. doi: 10.1264/jsme2.me10176

Mendoza-Mendoza, A., Zaid, R., Lawry, R., Hermosa, R., Monte, E., Horwitz, A., et al. (2018). Molecular dialogues between *Trichoderma* and roots: role of the fungal secretome. *Fungal Biol. Rev.* 32, 62–85. doi: 10.1016/j.fbr.2017.12.001

Morán-Diez, E., Hermosa, R., Ambrosino, P., Cardoza, R. E., Gutiérrez, S., Lorito, M., et al. (2009). The ThPG1 endopolygalacturonase is required for the *Trichoderma harzianum*-plant beneficial interaction. *Mol. Plant Microbe Interact.* 22, 1021–1031. doi: 10.1094/MPMI-22-8-1021

Morán-Diez, M. E., Trushina, N., Lamdan, N. L., Rosenfelder, L., Mukherjee, P. K., Kenerley, C. M., et al. (2015). Host-specific transcriptomic pattern of *Trichoderma virens* during interaction with maize or tomato roots. *BMC Genomics* 16:8. doi: 10.1186/s12864-014-1208-3

Moscatiello, R., Sello, S., Ruocco, M., Barbulova, A., Cortese, E., Nigris, S., et al. (2018). The hydrophobin HYTLO1 secreted by the biocontrol fungus *Trichoderma longibrachiatum* triggers a NAADP-mediated calcium signaling pathway in *Lotus japonicus*. *Int. J. Mol. Sci.* 19, E2596. doi: 10.3390/ijms19092596

Mostafa, M. A., and Gayed, S. K. (1952). Effect of *Trichoderma* metabolites on growth of cotton plants. *Nature* 169, 359–360. doi: 10.1038/169359a0

Mukherjee, P. K., Buensanteai, N., Morán-Diez, M. E., and Druzhinina, I. S. (2012). Functional analysis of non-ribosomal peptide synthetases (NRPSs) in *Trichoderma virens* reveals a polyketide synthase (PKS)/NRPS hybrid enzyme involved in the induced systemic resistance response in maize. *Microbiology* 158(Pt 1), 155–165. doi: 10.1099/mic.0.052159-0

Mukherjee, P. K., Horwitz, B., Herrera-Estrella, A., Schmoll, M., and Kenerley, C. M. (2013). *Trichoderma* research in the genome era. *Annu. Rev. Phytopathol.* 51, 105–129. doi: 10.1146/annurev-phyto-082712-102353

Mukherjee, P. K., and Kenerley, C. M. (2010). Regulation of morphogenesis and biocontrol properties in *Trichoderma virens* by a VELVET protein. Vel1. *Appl. Environ. Microbiol.* 76, 2345–2352. doi: 10.1128/AEM.02391-09

Ng, D. W., Zhang, C., Miller, M., Palmer, G., Whiteley, M., Tholl, D., et al. (2011). Cis- and trans-regulation of miR163 and target genes confers natural variation of secondary metabolites in two *Arabidopsis* species and their allopolyploids. *Plant Cell* 23, 1729–1740. doi: 10.1105/tpc.111.083915

Nieto-Jacobo, M. F., Steyaert, J. M., Salazar-Badillo, F. B., Nguyen, D. V., Rostás, M., Braithwaite, M., et al. (2017). Environmental growth conditions of Trichoderma spp. affects indole acetic acid derivatives, volatile organic compounds, and plant growth promotion. *Front. Plant Sci.* 8:102. doi: 10.3389/fpls.2017.00102

Nogueira-Lopez, G., Greenwood, D. R., Middleditch, M., Winefield, C., Eaton, C., Steyaert, J. M., et al. (2018). The apoplastic secretome of *Trichoderma virens* during interaction with maize roots shows an inhibition of plant defense and scavenging oxidative stress secreted proteins. *Front. Plant Sci.* 5:409. doi: 10.3389/fpls.2018.00409

Nowara, D., Gay, A., Lacomme, C., Shaw, J., Ridout, C., Douchkov, D., et al. (2010). HIGS: host-induced gene silencing in the obligate biotrophic fungal pathogen *Blumeria graminis*. *Plant Cell* 22, 3130–3141. doi: 10.1105/tpc.110.077040

Osugi, A., and Sakakibara, H. (2015). Q&A: how do plants respond to cytokinins and what is their importance? *BMC Biol.* 27:102. doi: 10.1186/s12915-015-0214-5

Pascale, A., Vinale, F., Manganiello, G., Nigro, M., Lanzuise, S., Ruocco, M., et al. (2017). Trichoderma and its secondary metabolites improve yield and quality of grapes. *Crop Prot.* 92, 176–181. doi: 10.1016/j.cropro.2016.11.010

Pazzagli, L., Seidl-Seiboth, V., Barsottini, M., Vargas, W. A., Scala, A., and Mukherjee, P. K. (2014). Cerato-platanins: elicitors and effectors. *Plant Sci.* 228, 79–87. doi: 10.1016/j.plantsci.2014.02.009

Pérez, A., Ramage, G., Blanes, R., Murgui, A., Casanova, M., and Martínez, J. P. (2011). Some biological features of *Candida albicans* mutants for genes coding fungal proteins containing the CFEM domain. *FEMS Yest Res.* 11, 273–284. doi: 10.1111/j.1567-1364.2010.00714.x

Pieterse, C. M., Zamioudis, C., Berendsen, R. L., Weller, D. M., Van Wees, S. C., and Bakker, P. A. (2014). Induced systemic resistance by beneficial microbes. *Annu. Rev. Phytopathol.* 52, 347–375. doi: 10.1146/annurev-phyto-082712-102340

Plett, J. M. M., Kemppainen, M., Kale, S. D. D., Kohler, A., Legué, V., Brun, A., et al. (2011). A secreted effector protein of *Laccaria bicolor* is required for symbiosis development. *Curr. Biol.* 21, 1197–1203. doi: 10.1016/j.cub.2011.05.033

Pumplin, N., and Voinnet, O. (2013). RNA silencing suppression by plant pathogens: defence, counter-defence and counter-counter-defence. *Nat. Rev. Microbiol.* 11:745. doi: 10.1038/nrmicro3120

Ramírez-Valdespino, C. A., Porras-Troncoso, M. D., Corrales-Escobosa, A. R., Wrobel, K., Martínez-Hernández, P., and Olmedo-Monfil, V. (2018). Functional characterization of TvCyt2, a member of the p450 monooxygenases from *Trichoderma virens* relevant during the association with plants and mycoparasitism. *Mol. Plant Microbe Interact.* 31, 289–298. doi: 10.1094/MPMI-01-17-0015-R

Reino, J. L., Guerrero, R. F., Hernández-Galan, R., and Collado, I. G. (2008). Secondary metabolites from species of the biocontrol agent *Trichoderma*. *Phytochem. Rev.* 7, 89–123. doi: 10.1007/s11101-006-9032-2

Reithner, B., Brunner, K., Schuhmacher, R., Peissl, I., Seidl, V., Krska, R., et al. (2005). The G protein alpha subunit Tga1 of *Trichoderma atroviride* is involved in chitinase formation and differential production of antifungal metabolites. *Fungal Genet. Biol.* 42, 749–760. doi: 10.1016/j.fgb.2005.04.009

Reithner, B., Mach-Aigner, A. R., Herrera-Estrella, A., and Mach, R. L. (2014). *Trichoderma atroviride* transcriptional regulator Xyr1 supports the induction of systemic resistance in plants. *Appl. Environ. Microbiol.* 80, 5274–5281. doi: 10.1128/AEM.00930-14

Rippa, S., Adenier, H., Derbaly, M., and Béven, L. (2007). The Peptaibol Alamethicin Induces an rRNA-Cleavage-Associated Death in *Arabidopsis thaliana*. *Chem. Biodivers.* 4, 1360–1373. doi: 10.1002/cbdv.200790116

Rippa, S., Eid, M., Formaggio, F., Toníolo, C., and Béven, L. (2010). Hypersensitive-like response to the pore-former peptaibol alamethicin in *Arabidopsis thaliana*. *ChemBioChem* 11, 2042–2049. doi: 10.1002/cbic.201000262

Rocha, A. L., Maeda, N., Pereira, N., Kern, F., Elias, L., Simister, R., et al. (2016). Characterization of the cellulolytic secretome of *Trichoderma harzianum* during growth on sugarcane bagasse and analysis of the activity boosting effects of swwollenin. *Biothechnol. Prog.* 32, 327–336. doi: 10.1002/btpr.2217

Rotblat, B., Enshell-Seijffers, D., Gershoni, J. M., Schuster, S., and Avni, A. (2002). Identification of an essential component of the elicitation active site of the EIX protein elicitor. *Plant J.* 32, 1049–1055. doi: 10.1046/j.1365-313x.2002.01490.x

Ruocco, M., Lanzuise, S., Vinale, F., Marra, R., Turrà, D., Woo, S. L., et al. (2009). Identification of a new biocontrol gene in *Trichoderma atroviride*: the role of an ABC transporter membrane pump in the interaction with different plant-pathogenic fungi. *Mol. Plant Microbe Interact.* 22, 291–301. doi: 10.1094/MPMI-22-3-0291

Ruocco, M., Lanzuise, S., Woo, S. L., Vinale, F., Marra, R., Varlese, R., et al. (2015). Multiple roles and effects of a novel *Trichoderma* hydrophobin. *Mol. Plant Microbe Interact.* 28, 167–179. doi: 10.1094/MPMI-07-14-0194-R

Salas-Marina, M. A., Isordia-Jasso, M. I., Islas-Osuna, M. A., Delgado-Sánchez, P., Jiménez-Bremont, J. F., Rodríguez-Kessler, M., et al. (2015). The Epl1 and Sm1 proteins from *Trichoderma atroviride* and *Trichoderma virens* differentially modulate systemic disease resistance against different life style pathogens in *Solanum lycopersicum*. *Front. Plant Sci.* 23:77. doi: 10.3389/fpls.2015.00077

Salas-Marina, M. A., Silva-Flores, M. A., Uresti-Rivera, E. E., Castro-Longoria, E., Herrera-Estrella, A., and Casas-Flores, S. (2011). Colonization of *Arabidopsis* roots by *Trichoderma atroviride* promotes growth and enhances systemic disease resistance through jasmonic acid/ethylene and salicylic acid pathways. *Eur. J. Plant Pathol.* 131, 15–26. doi: 10.1007/s10658-011-9782-6

Saravanakumar, K., Fan, L., Fu, K., Yu, C., Wang, M., Xia, H., et al. (2016). Cellulase from *Trichoderma harzianum* interacts with roots and triggers induced systemic resistence to foliar disease in maize. *Sci. Rep.* 10:35543. doi: 10.1038/srep35543

Saravanakumar, K., Wang, S., Dou, K., Lu, Z., and Chen, J. (2018). Yest two-hybrid and label-free proteomics-based screening of maize root receptor to cellulase of *Trichoderma harzianum*. *Physiol. Mol. Plant Pathol.* 104, 86–94. doi: 10.1016/j.pmpp.2018.10.002

Schenkel, D., Lemfack, M. C., Piechulla, B., and Splivallo, R. (2015). A meta-analysis approach for assessing the diversity and specificity of belowground root and microbial volatiles. *Front. Plant Sci.* 14:707. doi: 10.3389/fpls.2015.00707

Seidl, V., Marchetti, M., Schandl, R., Kubicek, C. P., Allmaier, G., and Kubicek, C. P. (2006). Epl1, the major secreted protein of *Hypocrea atroviridis* on glucose, is a member of a strongly conserved protein family comprising plant defense response elicitors. *FEBS J.* 273, 4346–4359. doi: 10.1111/j.1742-4658.2006.05435.x

Seidl, V., Zach, S., Frischmann, A., Spadiut, O., Dietzsch, C., Herwig, C., et al. (2013). Spore germination of *Trichoderma atroviride* is inhibited by its LysM protein TAL6. *FEBS J.* 280, 1226–1236. doi: 10.1111/febs.12113

Seo, J., Wu, J., Lii, Y., Li, Y., and Jin, H. (2013). Contribution of Small RNA Pathway Components in Plant Immunity. *Mol. Plant Microbe Interact.* 26, 617–625. doi: 10.1094/MPMI-10-12-0255-IA

Serrano-Carreon, L., Hathout, Y., Bensoussan, M., and Belin, J. M. (1993). Metabolism of linoleic acid or mevalonate and 6-pentyl-alpha-pyrone biosynthesis by *Trichoderma* species. *Appl. Environ. Microbiol.* 59, 2945–2950.

Sharon, A., Fuchs, Y., and Anderson, J. D. (1993). The elicitation of ethylene biosynthesis by a *Trichoderma* xylanase is not related to the cell wall degradation activity of the enzyme. *Plant Physiol.* 102, 1325–1329. doi: 10.1104/pp.102.4.1325

Shen, Q., Liu, L., Wang, L., and Wang, Q. (2018). Indole primes plant defense against necrotrophic fungal pathogen infection. *PLoS One* 13:e0207607. doi: 10.1371/journal.pone.0207607

Shi, W. L., Chen, X. L., Wang, L. X., Gong, Z. T., Li, S., Li, C. L., et al. (2016). Cellular and molecular insight into the inhibition of primary root growth of *Arabidopsis* induced by peptaibols, a class of linear peptide antibiotics mainly produced by *Trichoderma* spp. *J. Exp. Bot.* 67, 2191–2205. doi: 10.1093/jxb/erw023

Shoresh, M., Yedida, I., and Chet, I. (2005). Involvement of jasmonic acid/ethylene signaling pathway in the systemic resistance induced in cucumber by *Trichoderma asperellum* T203. *Phytopathology* 96, 76–84. doi: 10.1094/PHYTO-95-0076

Singh, H. B. (2014). Management of plant pathogens with microorganisms. *Nat. Sci. Acad.* 80, 443–454.

Thomma, B. P., Nürnberger, T., and Joosten, M. H. (2011). Of PAMPs and effectors: the blurred PTI-ETI dichotomy. *Plant Cell* 23, 4–15. doi: 10.1105/tpc.110.082602

Tinoco, M. L., Dias, B. B., Dall'Astta, R. C., Pamphile, J. A., and Aragao, F. J. (2010). In vivo trans-specific gene silencing in fungal cells by in planta expression of a double-stranded RNA. *BMC Biol.* 31:27. doi: 10.1186/1741-7007-8-27

Tucci, M., Roucco, M., De Masi, L., De Palma, M., and Lorito, M. (2011). The beneficial effect of *Trichoderma* spp. *on tomato is modulated by the plant genotype*. *Mol. Plant Pathol.* 12, 341–354. doi: 10.1111/j.1364-3703.2010.00674.x

Van Loon, L. C., Rep, M., and Pieterse, C. M. (2006). Significance of inducible defense-related proteins in infected plants. *Annu. Rev. Phytopathol.* 44, 135–162. doi: 10.1146/annurev.phyto.44.070505.143425

Vargas, W. A., Djonovic, S., Sukno, S. A., and Kenerley, C. M. (2008). Dimerization controls the activity of fungal elicitors that trigger systemic resistance in plants. *J. Biol. Chem.* 283, 19804–19815. doi: 10.1074/jbc.M802724200

Velázquez-Robledo, R., Contreras-Cornejo, H. A., Macías-Rodrígez, L., Hernández-Morales, A., Aguirre, J., Casas-Flores, S., et al. (2011). Role of the 4-phosphopantetheinyl transferase of *Trichoderma virens* in secondary metabolism and induction of plant defense response. *Mol. Plant Microbe Interact.* 24, 1459–1471. doi: 10.1094/mpmi-02-11-0045

Vinale, F., Flematti, G., Sivasithamparam, K., Lorito, M., Marra, R., Skelton, B. W., et al. (2009). Harzianic acid, an antifungal and plant growth promoting metabolite from *Trichoderma harzianum*. *J. Nat. Prod.* 72, 2032–2035. doi: 10.1021/np900548p

Vinale, F., Strakowska, J., Mazzei, P., Piccolo, A., Marra, R., Lombardi, N., et al. (2016). Cremenolide, a new antifungal, 10-member lactone from *Trichoderma cremeum* with plant growth promotion activity. *Nat. Prod. Res.* 30, 2575–2581. doi: 10.1080/14786419.2015.1131985

Vishnevetsky, J., White, T. L. Jr., Palmateer, A. J., Flaishman, M., Cohen, Y., Elad, Y., et al. (2010). Improved tolerance toward fungal diseases in transgenic *Cavendish banana* (Musa spp AAA group) cv. grand nain. *Transgenic Res.* 20, 61–72. doi: 10.1007/s11248-010-9392-7

Viterbo, A., and Chet, I. (2010). *TasHyd1,* a new hydrophobin gene from the biocontrol agent *Trichoderma asperellum,* is involved in plant root colonization. *Mol Plant Pathol.* 7:4. doi: 10.1111/j.1364-3703.2006.00335.x

Viterbo, A., Wiest, A., Brotman, Y., Chet, I., and Kenerley, C. (2007). The 18mer peptaibols from *Trichoderma virens* elicit plant defense responses. *Mol. Plant Pathol.* 8, 737–746. doi: 10.1111/j.1364-3703.2007.00430.x

Wang, M., Weiberg, A., Dellota, E. Jr., Yamane, D., and Jin, H. (2017). *Botrytis* small RNA Bc-siR37 suppresses plant defense genes by cross-kingdom RNAi. *RNA Biol.* 14, 421–428. doi: 10.1080/15476286.2017.1291112

Wang, B., Sun, Y., Song, N., Zhao, M., Liu, R., Feng, H., et al. (2017). *Puccinia striiformis* f. *sp. tritici microRNA-like RNA* 1 (Pst-milR1), an important pathogenicity factor of Pst, impairs wheat resistance to Pst by suppressing the wheat pathogenesis-related 2 gene. *New Phytol.* 215, 338–350. doi: 10.1111/nph.14577

Wang, M., Weiberg, A., Lin, F. M., Thomma, B. P., Huang, H. D., and Jin, H. (2016). Bidirectional cross-kingdom RNAi and fungal uptake of external RNAs confer plant protection. *Nat. Plants.* 2, 16151. doi: 10.1038/nplants.2016.151

Weiberg, A., Wang, M., Lin, F. M., Zhao, H., Zhao, Z., Kaloshian, I., et al. (2013). Fungal small RNAs suppress plant immunity by hijacking host RNA interference pathways. *Science* 342, 118–123. doi: 10.1126/science.1239705

Yedidia, I., Benhamou, N., and Chet, I. (1999). Induction of defense responses in cucumber plants (*Cucumis sativus* L.) *by the biocontrol agent Trichoderma harzianum*. *Appl. Environ. Microbiol.* 65, 1061–1070.

Yedidia, I., Benhamou, N., Kapulnik, Y., and Chet, I. (2000). Induction and accumulation of PR proteins activity during early stages of root colonization by the mycoparasite *Trichoderma harzianum* strain T-203. *Plant Physiol. Biochem.* 38, 863–873. doi: 10.1016/s0981-9428(00)01198-0

Yedidia, I., Shoresh, M., Kerem, Z., Benhamou, N., Kapulnik, Y., and Chet, I. (2003). Concomitant induction of systemic resistance to *Pseudomonas syringae* pv. *Lachrymans* in cucumber by *Trichoderma asperellum* (T-203) and acumulation of phytoalexins. *Am. Soc. Microbiol.* 69, 7343–7353. doi: 10.1128/aem.69.12.7343-7353.2003

Yin, C., Jurgenson, J. E., and Hulbert, S. H. (2011). Development of a host-induced RNAi system in the wheat stripe rust fungus *Puccinia striiformis* f. sp. *tritici*. *Mol. Plant-Microbe Interact.* 24, 554–561. doi: 10.1094/MPMI-10-10-0229

Yin, C., Park, J. J., Gang, D. R., and Hulbert, S. H. (2014). Characterization of a tryptophan 2-monooxygenase gene from *Puccinia graminis* f. sp. tritici involved in auxin biosynthesis and rust pathogenicity. *Mol. Plant-Microbe Interact.* 27, 227–235. doi: 10.1094/MPMI-09-13-0289-FI

Yu, J. H., and Keller, N. (2005). Regulation of secondary metabolism in filamentous fungi. *Annu. Rev. Phytopathol.* 43, 437–458. doi: 10.1146/annurev.phyto.43.040204.140214

Yu, W., Mijiti, G., Huang, Y., Fan, H., Wang, Y., and Liu, Z. (2018). Functional analysis of eliciting plant response protein Epl1-Tas from *Trichoderma asperellum* ACCC30536. *Sci. Rep.* 8:7974. doi: 10.1038/s41598-018-26328-1

Zhang, F., Meng, X., Yang, X., Ran, W., and Shen, Q. (2014). Quantification and role of organic acids in cucumber root exudates in *Trichoderma harzianum* T-E5 colonization. *Plant Physiol. Biochem.* 83, 250–257. doi: 10.1016/j.plaphy.2014.08.011

Conflict of Interest Statement: The authors declare that the research was conducted in the absence of any commercial or financial relationships that could be construed as a potential conflict of interest.

frontiers in Microbiology

ORIGINAL RESEARCH
published: 07 August 2019
doi: 10.3389/fmicb.2019.01662

Different Components of the RNA Interference Machinery Are Required for Conidiation, Ascosporogenesis, Virulence, Deoxynivalenol Production, and Fungal Inhibition by Exogenous Double-Stranded RNA in the Head Blight Pathogen *Fusarium graminearum*

Fatima Yousif Gaffar[1†], Jafargholi Imani[1†], Petr Karlovsky[2], Aline Koch[1] and Karl-Heinz Kogel[1]*

[1]Department of Phytopathology, Centre for BioSystems, Land Use and Nutrition, Justus Liebig University, Giessen, Germany, [2]Department of Crop Sciences, Molecular Phytopathology and Mycotoxin Research, University of Göttingen, Göttingen, Germany

OPEN ACCESS

Edited by:
David B. Collinge,
University of Copenhagen, Denmark

Reviewed by:
Liao Yucai,
Huazhong Agricultural University, China
Li-Jun Ma,
University of Massachusetts Amherst, United States

***Correspondence:**
Karl-Heinz Kogel
karl-heinz.kogel@agrar.uni-giessen.de

[†]These authors have contributed equally to this work

Specialty section:
This article was submitted to Plant Microbe Interactions, a section of the journal Frontiers in Microbiology

Received: 16 November 2018
Accepted: 04 July 2019
Published: 07 August 2019

Citation:
Gaffar FY, Imani J, Karlovsky P, Koch A and Kogel K-H (2019) Different Components of the RNA Interference Machinery Are Required for Conidiation, Ascosporogenesis, Virulence, Deoxynivalenol Production, and Fungal Inhibition by Exogenous Double-Stranded RNA in the Head Blight Pathogen Fusarium graminearum. Front. Microbiol. 10:1662. doi: 10.3389/fmicb.2019.01662

In filamentous fungi, gene silencing through RNA interference (RNAi) shapes many biological processes, including pathogenicity. We explored the requirement of key components of fungal RNAi machineries, including DICER-like 1 and 2 (*Fg*DCL1, *Fg*DCL2), ARGONAUTE 1 and 2 (*Fg*AGO1, *Fg*AGO2), AGO-interacting protein *Fg*QIP (QDE2-interacting protein), RecQ helicase (*Fg*QDE3), and four RNA-dependent RNA polymerases (*Fg*RdRP1, *Fg*RdRP2, *Fg*RdRP3, *Fg*RdRP4), in the ascomycete mycotoxin-producing fungal pathogen *Fusarium graminearum* (*Fg*) for sexual and asexual multiplication, pathogenicity, and its sensitivity to double-stranded (ds)RNA. We corroborate and extend earlier findings that conidiation, ascosporogenesis, and Fusarium head blight (FHB) symptom development require an operable RNAi machinery. The involvement of RNAi in conidiation is dependent on environmental conditions as it is detectable only under low light (<2 μmol m^{-2} s^{-1}). Although both DCLs and AGOs partially share their functions, the sexual ascosporogenesis is mediated primarily by *Fg*DCL1 and *Fg*AGO2, while *Fg*DCL2 and *Fg*AGO1 contribute to asexual conidia formation and germination. *Fg*DCL1 and *Fg*AGO2 also account for pathogenesis as their knockout (KO) results in reduced FHB development. Apart from KO mutants *Δdcl2* and *Δago1*, mutants *Δrdrp2*, *Δrdrp3*, *Δrdrp4*, *Δqde3*, and *Δqip* are strongly compromised for conidiation, while KO mutations in all *RdPRs*, *QDE3*, and *QIP* strongly affect ascosporogenesis. Analysis of trichothecenes mycotoxins in wheat kernels showed that the relative amount of deoxynivalenol (DON), calculated as [DON] per amount of fungal genomic DNA was reduced in all spikes infected with RNAi mutants, suggesting the possibility that the fungal RNAi pathways affect *Fg*'s

DON production. Moreover, silencing of fungal genes by exogenous target gene-specific double-stranded RNA (dsRNA) (spray-induced gene silencing, SIGS) is dependent on DCLs, AGOs, and QIP, but not on QDE3. Together these data show that in *F. graminearum*, different key components of the RNAi machinery are crucial in different steps of fungal development and pathogenicity.

Keywords: Argonaute, double-stranded RNA, small RNA, *Fusarium graminearum*, spray-induced gene silencing, wheat

INTRODUCTION

RNA interference (RNAi) is a conserved mechanism triggered by double-stranded (ds)RNA that mediates resistance to exogenous nucleic acids, regulates the expression of protein-coding genes on the transcriptional and post-transcriptional level, and preserves genome stability by transposon silencing (Fire et al., 1998; Mello and Conte, 2004; Hammond, 2005; Baulcombe, 2013). Many reports have demonstrated that this natural mechanism for sequence-specific gene silencing also holds promise for experimental biology and offers practical applications in functional genomics, therapeutic intervention, and agriculture (Nowara et al., 2010; Koch and Kogel, 2014; Cai et al., 2018; Zanini et al., 2018). Core RNAi pathway components are conserved in eukaryotes, including most parasitic and beneficial fungi (Cogoni and Macino, 1999; Dang et al., 2011; Carreras-Villaseñor et al., 2013; Torres-Martínez and Ruiz-Vázquez, 2017): DICER-like (DCL) enzymes, which belong to the RNase III superfamily, generate double-stranded small interfering (si)RNAs and micro (mi)RNAs (Meng et al., 2017; Song and Rossi, 2017); ARGONAUTE (AGO) superfamily proteins bind small RNA duplexes to form an RNA-induced silencing complex (RISC) for transcriptional and post-transcriptional gene silencing (PTGS) (Zhang et al., 2015; Nguyen et al., 2018); and RNA-dependent RNA polymerases (RdRPs) are involved in the production of double-stranded RNA (dsRNA) that initiate the silencing mechanism as well as in the amplification of the silencing signals through the generation of secondary siRNAs (Calo et al., 2012).

Fungal RNAi pathways contribute to genome protection (Meng et al., 2017), pathogenicity (Weiberg et al., 2013; Kusch et al., 2018; Zanini et al., 2019), development (Carreras-Villaseñor et al., 2013), and antiviral defense (Segers et al., 2007; Campo et al., 2016; Wang et al., 2016a). In *Aspergillus flavus* (Bai et al., 2015), *Magnaporthe oryzae* (Raman et al., 2017), and *Penicillium marneffei* (Lau et al., 2013), sRNAs were shown to be responsive to environmental stress. In *Trichoderma atroviride*, both light-dependent asexual reproduction and light-independent hyphal growth require an operational RNAi machinery (Carreras-Villaseñor et al., 2013). Similarly, in *Mucor circinelloides,* defects in the RNAi machinery resulted in various developmental defects such as dysfunction during sexual and asexual reproduction (Torres-Martínez and Ruiz-Vázquez, 2017).

Neurospora crassa, a model organism for studying RNAi in filamentous fungi, has different silencing pathways, including quelling (Romano and Macino, 1992) and meiotic silencing by unpaired DNA (MSUD) (Shiu et al., 2001). In the vegetative stage, the introduction of transgenes results in PTGS of the transgenes and cognate endogenous mRNAs, an RNAi silencing phenomenon known as quelling. The process requires *QDE3* (*Quelling defective 3*), which encodes a RecQ helicase, and RPA (subunit of replication protein A), which recognizes aberrant DNA structures. Interaction of these proteins recruits Quelling defective 1 (QDE1), a protein with dual function as DNA-dependent RNA polymerase (DdRP) and RdPR, to the single-stranded (ss)DNA locus, resulting in production of aberrant ssRNAs and its conversion to dsRNAs. Subsequently, the dsRNA is processed into small RNAs by DCL1. sRNAs duplexes are loaded onto QDE2 (Quelling defective 2), which encodes an AGO homolog. QDE2 cleaves the passenger strand and the exonuclease QIP (QDE2-interacting protein) assists to remove it to form an active RISC that targets complementary mRNA for degradation (Chang et al., 2012). MSUD occurs during sexual development in prophase I of meiosis, when unpaired homologous DNA sequences have been detected during the pairing of the homologous chromosomes, which then also leads to the production of aberrant RNA transcripts (Chang et al., 2012). Genes required for MSUD are *SAD1* (*Suppressor of ascus dominance 1*), a paralog of *QDE-1*, and *SAD2*. SAD2 recruits SAD1 to the perinuclear region, where aberrant RNA is converted to dsRNA. Upon silencing by DCL1, the small RNA duplexes are loaded onto SMS2 (Suppressor of meiotic silencing 2), an AGO homolog in *Neurospora*, which also is assisted by QIP. In contrast, QDE-2 and DCL2 are not required for MSUD in *Neurospora*, indicating that there are two parallel RNAi pathways functioning separately in the vegetative and meiotic stages.

Fusarium graminearum (*Fg*) is one of the devastating pathogens of cereals causing Fusarium head blight (FHB) and Crown Rot (FCR) (Dean et al., 2012; Harris et al., 2016). The pathogen belongs to the filamentous ascomycetes. Ascospores are the primary inoculum for FHB epidemics as these spores are forcibly shot into the environment and also can pass long distances (Maldonado-Ramirez et al., 2005). Moreover, the sexual

Abbreviations: AGO, ARGONAUTE; CYP51, *Cytochrome P450 lanosterol C-14α-demethylase*; DCL, DICER-like l; DON, deoxynivalenol; *Fg*, *Fusarium graminearum*; FHB, Fusarium head blight; HIGS, host-induced gene silencing; hpRNA, hairpin RNA; MSUD, meiotic silencing by unpaired DNA; NIV, nivalenol; PEG, potato extract glucose; QDE 2,3, Quelling defective 2,3; QIP, QDE-interacting protein; RdRp, RNA-dependent RNA polymerase; RISC, RNA-dependent silencing complex; RNAi, RNA interference; RPA, subunit of replication protein A; siRNA, small interfering RNA; SN, synthetic nutrient agar; ssDNA, single-stranded DNA; TGW, thousand grain weight.

development ensures the formation of survival structures necessary for overwintering (Dill-Macky and Jones, 2000) and the genetic diversity of the population (Cuomo et al., 2007). Of note, spike infections can be symptomless or symptomatic (Urban et al., 2015; Brown et al., 2017). In both cases, *Fusarium* fungi contaminate the grain with mycotoxins and thus decrease grain quality. Among the mycotoxins, the B group trichothecenes, including deoxynivalenol (DON), nivalenol (NIV), and their acetylated derivatives (3A-DON, 15A-DON, and 4A-NIV) influence the virulence of the fungus (Desjardins et al., 1993; Jansen et al., 2005; Ilgen et al., 2009). Mycotoxins such as DON trigger an oxidative burst in the host plants, resulting in cell necrosis and disintegration of the defense system, which then favors colonization of the plant tissues by a necrotrophic fungus (Audenaert et al., 2014). Importantly, *Fg* possesses a functional MSUD mechanism (Son et al., 2011) and *AGO* genes *FgSMS2* or *FgAGO2* are necessary for sexual reproduction (Kim et al., 2015). A recent work discovered that the sex-induced RNAi mechanism has important roles in sexual reproduction (Son et al., 2017). siRNAs produced from exonic gene regions (ex-siRNAs) participate in PTGS at a genome-wide level in the late stages of sexual reproduction. The sex-specific RNAi pathway is primarily governed by *Fg*DCL1 and *Fg*AGO2. Thus, *Fg* primarily utilizes ex-siRNA-mediated RNAi for ascospore formation. Consistent with the key role of *Fg*DCL1 in generative development, the combination of sRNA and transcriptome sequencing predicted 143 novel microRNA-like RNAs (milRNAs) in wild-type perithecia, of which most were dependent on *Fg*DCL1. Given that 117 potential target genes were predicted, these perithecium-specific milRNAs may play roles in sexual development (Zeng et al., 2018).

To develop RNAi-based plant protection strategies such as host-induced gene silencing (HIGS) (Koch et al., 2013) and spray-induced gene silencing (SIGS) (Koch et al., 2016, 2018) against *Fusarium* species, it is required to bank on knowledge about the RNAi components involved in *Fusarium* development and pathogenicity. A report of Chen and colleagues (Chen et al., 2015) demonstrated that, in *Fg*, a hairpin RNA (hpRNA) can efficiently silence the expression of a target gene, and that the RNAi components *Fg*DCL2 and *Fg*AGO1 are required for silencing. This finding is consistent with reports showing that a *Fg* wild-type (WT) strain, but not *Fg* RNAi mutants, is amenable to SIGS-mediated target gene silencing, when it grows on a plant sprayed with exogenous dsRNA directed against the fungal *Cytochrome P450 lanosterol C-14α-demethylase* (*CYP51*) genes (Koch et al., 2016). In the present study study, we expanded previous studies to address the requirement of an extended set of *Fg* RNAi genes in growth, reproduction, virulence, toxin production, and SIGS-mediated inhibition of fungal infection cereal hosts.

MATERIALS AND METHODS

Fungal Material, Generation of Gene Deletion Mutants in *Fusarium graminearum*

The *Fg* strain PH1 and the PH1 *dcl1 dcl2* double mutant were a gift of Dr. Martin Urban, Rothamsted Research, England. RNAi gene deletion mutants were generated in the *Fg* strain IFA65 (IFA, Department for Agrobiotechnology, Tulln, Austria), hereafter termed IFA WT. They were generated by homolog recombination using the pPK2 binary vector. *Fg* RNAi genes were identified by blasting *Neurospora crassa* genes against the Fusarium genome sequence in the Broad institute database. Disruption vectors were constructed by inserting two flanking fragments (~1,000 bp) upstream and downstream of the corresponding genes in the pPK2 vector as follows: *RdRP1*, *AGO1*, *QDE3*, *QIP*, *AGO2*, *DCL1*, *RdRP2*, *RdRP3*, *RdRP4*, and *DCL2* upstream flanking sequences were inserted in the plasmid between PacI-KpnI restriction sites, and the downstream flanking sequences were inserted between XbaI-HindIII restriction sites, except the *AGO2* downstream flanking sequence which was inserted in XbaI restriction site (primers used in disruption plasmid construction are listed in **Supplementary Table S1**). Disruption vectors were introduced into *Agrobacterium tumefaciens* (LBA440 and AGL1 strains) by electroporation. A single colony of Agrobacterium containing the pPK2 plasmid was grown in 10 ml of YEB medium (Vervliet et al., 1975) containing the appropriate antibiotics (5 μg/ml tetracycline +25 μg/ml rifampicin +50 μg/ml kanamycin for LBA440, and 25 μg/ml carbenicillin +25 μg/ml rifampicin +50 μg/ml kanamycin for AGL1) and incubated at 28°C till OD_{600nm} 0.7 was reached. T-DNA was mobilized in Agrobacterium with 200 μM acetosyringone, and Agrobacterium and fungal recipient IFA WT were co-cultivated on black filter paper (DP 551070, Albert LabScience, Hahnemühle, Dassel, Germany), respectively. Putative fungal mutants were selected on potato extract glucose (PEG, Roth, Germany) medium containing 150 μg/ml hygromycin +150 μg/ml ticarcillin and grown for 5 days. For genotyping, genomic DNA of putative Fusarium mutants was extracted from mycelia.

Genotyping of *Fusarium* Mutants

Fg IFA mutants were confirmed by genotyping using primers located in hygromycin and corresponding gene flanking sequences (located after the cloned flanking sequence in the genome) (**Supplementary Table S2**). Upon amplification, the samples were sequenced. Additionally, mRNA expression levels in mutants vs. levels in IFA WT were measured by quantitative real-time PCR (qRT-PCR) using primers pairs listed in (**Supplementary Table S3**). The mRNA transcripts were measured using 1 × SYBR Green JumpStart Taq Ready Mix (Sigma-Aldrich, Germany) according to manufacturer's instructions and assayed in 7500 Fast Real-Time PCR cycler (Applied Biosystems Inc., CA, USA) under the following thermal cycling conditions: initial activation step at 95°C for 5 min, 40 cycles (95°C for 30 s, 53°C for 30 s, and 72°C for 30 s). The Ct values were determined with the software in the qRT-PCR instrument and the transcript levels of the genes were determined according to the $2^{-\Delta\Delta Ct}$ method (Livak and Schmittgen, 2001).

Colony Morphology

The RNAi mutants were cultured on PEG, starch agar (SA) and synthetic nutrient agar (SNA) (Leslie and Summerell, 2006). The cultures were incubated at 25°C in 12-h light/12-h dark (52 μmol m^{-2} s^{-1}, Philips Master TL-D HF 16 W/840). The growth was documented after 5 days. For growth in liquid

cultures, agar blocks (1 cm in diameter) from 2-week-old fungal cultures were incubated in liquid PEG for 5 days at room temperature (RT) under light (2 μmol m^{-2} s^{-1}) with shaking. Each mutant was grown in flask containing medium supplemented with hygromycin (100 μg/ml) and flask containing medium without hygromycin. Photos were taken to document the growth pattern after 5 days of incubation.

Production of Fungal Biomass

Fifty milligram mycelia (fresh mycelia from 4-day-old fungal cultures grown on Aspergillus complete medium (CM) plates in the dark; Leslie and Summerell, 2006) were incubated in a 100-ml flask containing 20 ml of PEG medium incubated at RT with shaking under 12-h light (2 μmol m^{-2} s^{-1}). Fungal mycelium was harvested after 3 days by filtration through filter paper (Munktell, Germany), washed with distilled water twice, and dried at 75°C overnight. The dry weight was calculated by using the following formula: Dry weight = (weight of filter paper + mycelium) − (weight of filter paper).

Conidiation Assay

Production of conidia was done according to Yun et al. (2015) with slight modification. Four-day-old cultures of each mutant and IFA WT growing in CM agar plates in the dark at 25°C were used for fresh mycelia preparation. The mycelia were scraped from the plate surface using a sterile toothpick; then, 50 mg mycelia were inoculated in a 100-ml flask containing 20 ml of SN medium. The flasks were incubated at RT for 5 days in light (2 μmol m^{-2} s^{-1}) on a shaker (100 rpm). Subsequently, the conidia produced from each mutant and WT were counted using a hemocytometer (Fuchs Rosenthal, Superior Marienfeld, Germany).

Viability Test of Conidia

Fourteen milliliters from the same cultures used in conidiation assay were centrifuged at 4,000 rpm for 10 min to precipitate conidia. The conidia were resuspended in 5 ml 2% sucrose water and incubated in dark for 2 days at 23°C. Germinated and non-germinated conidia were visualized and counted under an inverse microscope. Conidia germination rate was determined as percentage of germinated conidia of the total conidia number.

Perithecia Production and Ascospore Discharge Assay

Fungi were grown on carrot agar prepared under bright fluorescent light at RT (18–24°C) for 5 days (Klittich and Leslie, 1988). Aerial mycelia were removed with a sterile toothpick. To stimulate sexual reproduction and perithecia formation, 1 ml of 2.5% Tween 60 was applied to the plates with a sterile glass rod after scraping the mycelia (Cavinder et al., 2012). The plates were incubated under fluorescent light at RT for 9 days. Subsequently, agar blocks (1.5 cm in diameter) were cut from the plates containing the mature perithecia using a cork borer. Agar blocks were sliced in half, placed on glass microscope slides, and incubated in boxes under high humidity for 2 days under 24 h of light (52 μmol m^{-2} s^{-1} Philips Master TL-D HF 16 W/840). During this time, ascospores discharged from the perithecia accumulated on the slide. For the quantification of discharged ascospores, slides were washed off by 2 ml of an aqueous Tween 20 (0.002%) solution and counted using a hemocytometer.

Viability Test of the Discharged Ascospores

Mycelia with mature perithecia (13 days after sexual induction) on carrot agar were incubated in a humid box at RT under light for 4 days according to Son et al. (2017). The discharged ascospores were washed from the plate cover using SN liquid medium and incubated in the dark for 24 h in a humid box. The germinated and non-germinated ascospores were visualized under an inverse microscope and counted.

Pathogenicity Assay on Wheat Ears

The susceptible wheat cultivar Apogee was used. Plants were grown in an environmentally controlled growth chamber (24°C, 16 h light, 180 μmol m^{-2} s^{-1} photon flux density, 60% rel. humidity) till anthesis. Point inoculations to the second single floret of each spike were performed at mid-anthesis with 5 μl of a 40,000 conidia/ml suspension amended with 0.002% v/v Tween 20 (Gosman et al., 2010). Control plants were treated with sterile Tween 20. For each *Fg* genotype, 10 wheat heads were inoculated and incubated in plastic boxes misted with water to maintain high humidity for 2 days. Incubation continued at 22°C in 60% rel. humidity. Infected wheat heads were observed nine and 13 dpi and infection percentage was determined as the ratio of infected spikelets to the total spikelet number per ear.

Thousand Grain Weight of Infected Wheat Kernels

One hundred kernels from two biological experiments with 10 wheat heads point-inoculated with IFA WT and mutants were counted and weighed. TGW was calculated in grams per 1,000 kernels of cleaned wheat seeds.

Quantification of Fungal DNA in Infected Wheat Kernels

Fungal genomic DNA in kernels was quantified using qPCR as described (Brandfass and Karlovsky, 2008). Dried grains were ground and DNA was extracted from 30 mg of flour and dissolved in 50 μl of TE buffer. One microliter of 50x diluted DNA was used as template for RT-PCR with primers amplifying a 280-bp fragment specific for *Fg*. The PCR mix consisted of reaction buffer [16 mM $(NH_4)_2SO_4$, 67 mM Tris-HCl, 0.01% Tween-20, pH 8.8 at 25°C; 3 mM $MgCl_2$, 0.3 μM of each primer, 0.2 mM of each dATP, dTTP, dCTP and dGTP (Bioline), 0.03 U/μl Taq DNA polymerase (Bioline, Luckenwalde, Germany) and 0.1x SYBR Green I solution (Invitrogen, Karlsruhe, Germany)]. The PCR was performed in CFX384 thermocycler (BioRad, Hercules, CA, USA) according to the following cycling condition: initial denaturation for 2 min at 95°C, 35 cycles with 30 s at 94°C, 30 s at 61°C, 30 s at 68°C, and final elongation for 5 min at 68°C. No matrix effects were detectable with 50-fold diluted DNA extracted from grains. Standards were prepared from pure *Fg* DNA in 3-fold dilution steps from 100 pg to 0.4 pg/well.

Analysis of Mycotoxins in Infected Wheat Kernels

The content of mycotoxins in wheat kernels infected with *Fg* RNAi mutants and IFA WT was determined using high-performance liquid chromatography coupled to tandem mass spectrometry (HPLC-MS/MS). Mycotoxins were extracted from ground grains with mixture containing 84% acetonitrile, 15% water, and 1% acetic acid and the extracts were defatted with cyclohexane. Chromatographic separation was carried out on a C18 column eluted with a water/methanol gradient and the analytes were ionized by electrospray and detected by MS/MS in multiple reaction monitoring (MRM) mode essentially as described (Sulyok et al., 2006).

Spray Application of Double-Stranded RNA on Barley Leaves

Second leaves of 3-week-old barley cultivar Golden Promise were detached and transferred to square Petri plates containing 1% agar. dsRNA spray applications and leaf inoculation were done as described (Koch et al., 2016). For the TE control, TE buffer was diluted in 500 µl of water corresponding to the amount used for dilution of the dsRNA. Typical RNA concentration after elution was 500 ng μl^{-1}, representing a buffer concentration of 400 µM Tris-HCL and 40 µM EDTA (TE buffer) in the final dilution. TE buffer was indistinguishable from treatments with control dsRNA generated from the GFP or GUS gene, respectively (Koch et al., 2016, 2018). Thus, we used TE buffer as control to save costs. Spraying of the leaves was carried out in the semi-systemic design (Koch et al., 2016), where the lower parts of the detached leaf segments were covered by a tinfoil to avoid direct contact of dsRNA with the leaf surface that was subsequently inoculated.

STATISTICS AND ANALYSIS

Data obtained from two or three repetitions were subjected to the Student's *t* test in Microsoft office Excel 2010. Significance was determined as $p \leq 0.05$, 0.01, or 0.001 and indicated by *, **, or ***, respectively. Unless specified otherwise, data are presented as mean ± standard error or mean ± standard deviation of the mean. Sequence analysis was performed on the ApE plasmid editor free tool. Basic Local Alignment Search Tool (BLAST) NCBI BLAST[1] was used for sequence search and alignment.

RESULTS

Requirement of RNA Interference Pathway Core Components Under Different Light Regimes

The *Fg* genome obtained from the Broad Institute[2] contains many functional RNAi machinery components (Chen et al., 2015; Son et al., 2017). We generated *Fg* gene replacement mutants for several major RNAi genes by homolog recombination using the pPK2 binary vector (**Table 1**). Disruption vectors for *FgDCL1*, *FgDCL2*, *FgAGO1*, *FgAGO2*, *FgRdRP1*, *FgRdRP2*, *FgRdRP3*, *FgRdRP4*, *FgQDE3*, and *FgQIP* were constructed by inserting two flanking fragments (~1,000 bp) upstream and downstream of the corresponding genes in pPK2 vector (**Supplementary Table S1; Supplementary Figure S1**). The vectors were introduced into *Agrobacterium tumefaciens*, followed by agro-transformation of the *Fg* strain IFA. Transformants were transferred to Petri dishes of PEG medium, containing 150 µg/ml hygromycin and 150 µg/ml ticarcillin. Mutants were verified by PCR analysis with genomic DNA as template (**Figure 1**) and by expression analysis of the respective RNAi gene (**Supplementary Figure S2**). Colony morphology of PCR-verified mutants (12 h light, see section "Methods") was inspected in axenic cultures of three different media, PEG, SNA, and SA. In the PEG agar medium, all mutants showed slightly reduced radial growth, while there were no clear differences as compared with the IFA WT strain in SN and SA media (**Supplementary Figures S3A–C**). In liquid PEG medium under day light conditions, all mutants produced comparable amounts of mycelium biomass, though different amounts of the red pigment aurofusarin (Frandsen et al., 2006): *Δdcl1*, *Δdcl2*, *Δrdrp1*, *Δqde3,* and *Δqip1* showed reduced pigmentation, while *Δago1*, *Δrdrp2*, *Δrdrp3*, and *Δrdrp4* showed higher pigmentation compared to IFA WT (**Supplementary Figure S3D; Table 2**). Under light induction conditions (12-h light; 52 µmol m^{-2} s^{-1}), conidia grown in 96-well plate liquid SN cultures showed normal germ tube emergence (not shown). All RNAi mutants formed an elongated hyphal cell type, producing abundant conidia on conidiophores and directly from hyphae. Conidia were moderately curved with clear septations.

When grown continuously under dimmed light (2 µmol m^{-2} s^{-1}), liquid SN cultures of RNAi mutants showed significantly reduced conidiation compared to IFA WT, except *Δago2* and *Δrdrp1*, which were only slightly affected (**Figure 2A**). Under this non-inductive condition, some RNAi mutants also were compromised in conidial germination: *Δago1*, *Δago2*, and *Δrdrp4* showed significantly reduced germination, while *Δrdrp3*, *Δdcl1*, *Δrdrp1*, and *Δdcl2* showed a slight reduction, and *rdrp2, Δqip*, and *Δqde3* showed normal conidial germination (**Figure 2B**; see **Table 2**). All RNAi mutants had a normal germ tube morphology, except *Δrdrp4*, which tends to develop multiple germ tubes (**Figure 2C**). These results suggest a requirement for *Fg* RNAi genes in the control of asexual development depending on the environmental conditions.

F. graminearum RNA Interference Components Are Required for Sexual Development

Because there were contrasting data in the literature, we resumed asking the question of whether RNAi components are required for sexual reproduction of *Fg*. To this end perithecia (fruiting bodies) formation was induced in axenic cultures on carrot agar (Cavinder et al., 2012). All RNAi mutants produced

[1]http://blast.ncbi.nlm.nih.gov/Blast.cgi
[2]www.broadinstitute.org

TABLE 1 | RNAi pathway genes of *Fusarium graminearum* (*Fg*) used in this study.

RNAi proteins in *Neurospora crassa*	Homologs in *Fg*	Amino acid identity (%)	Fusarium gene ID	Gene function in *Fg*
DICER 1	*Fg*DCL1	43	FGSG_09025	Antiviral defense (Wang et al., 2016a).
				Minor role in processing of exogenous dsRNA, hpRNA, or pre-milRNA in mycelium (Chen et al., 2015).
				Major role in sex-specific RNAi pathway: production of regulatory sRNAs. Required for ascospore production (Son et al., 2017).
DICER 2	*Fg*DCL2	35%	FGSG_04408	Processing of exogenous dsRNA, hpRNA and pre-milRNA in mycelium (Chen et al., 2015).
				Partially shared DCL-1 role in production of regulatory sRNAs in the sexual stage (Son et al., 2017).
ARGONAUTE 1 (syn. Quelling defective 2)	*Fg*AGO1	59	FGSG_08752	Major component in the RISC during quelling (Chen et al., 2015).
ARGONAUTE 2 (syn. Suppressor of meiotic silencing 2, SMS2)	*Fg*AGO2	43	FGSG_00348	Minor role in binding siRNA derived from exogenous dsRNA, hpRNA or pre-milRNA in mycelium (Chen et al., 2015).
				Major role in sex-specific RNAi pathway; required for ascospore production (Son et al., 2017).
RNA-DEPENDENT RNA	*Fg*RdRP1	38	FGSG_06504	Maybe associated with secondary sRNA production (Chen et al., 2015).
POLYMERASE (syn. Quelling defective 1)	*Fg*RdRP4	33	FGSG_04619	Maybe associated with secondary sRNA production (Chen et al., 2015).
RNA-DEPENDENT RNA	*Fg*RdRp2	42	FGSG_08716	Maybe associated with secondary sRNA production (Chen et al., 2015).
POLYMERASE (syn. Suppressor of ascus dominance, SAD1)	*Fg*RdRp5	29	FGSG_09076	Roles in the antiviral defense.
				Maybe associated with secondary sRNA production (Chen et al., 2015).
RNA-DEPENDENT RNA POLYMERASE (RRP3)	*Fg*RdRP3	47	FGSG_01582	Maybe associated with secondary sRNA production (Chen et al., 2015).
QDE2-INTERACTING PROTEIN	*Fg*QIP	32	FGSG_06722	The homolog has been identified in Chen et al. (2015), but not yet studied in depth.
RecQ HELICASE QDE3	*Fg*QDE3	46	FGSG_00551	Not studied.

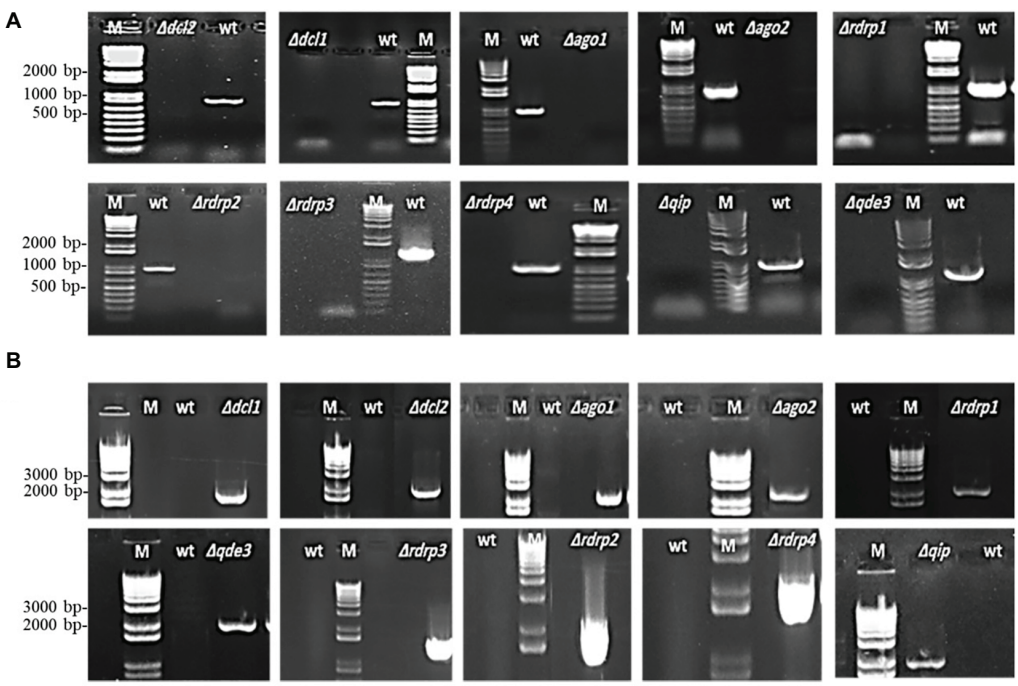

FIGURE 1 | PCR verification of targeted gene replacement in *Fusarium graminearum*. **(A)** Amplification of an internal part of the targeted genes *DCL1*, *DCL2*, *AGO1*, *AGO2*, *RdRP1*, *RdRP4*, *RdRP2*, *RdRP3*, *QIP*, and *QDE3* is positive in IFA WT and negative in corresponding mutants. **(B)** PCR with primer pairs in the right recombination sequence and hygromycin, showing that the antibiotic resistance gene had integrated into the target gene locus. PCR products were analyzed on 1.5% agarose gel electrophoresis. M, DNA marker; WT, wild type.

TABLE 2 | Function of *Fusarium graminearum* RNAi mutants in various developmental and pathogenic processes.

Fungal strain	Aurofusarin pigment[1]	Conidiation[2]	Conidial germination[2]	Ascospore discharge	Ascospore germination	Spike infection[3]	rDON	SIGS[4]
IFA WT	+	+	+	+	+	+	+	+
Δdcl1	–	–	(–)	–	(+)	–	(–)	–
Δdcl2	–	–	(–)	–	+	++	(–)	–
Δago1	++	–	–	–	(+)	+	–	(+)
Δago2	+	(+)	–	–	+	–	–	(+)
Δrdrp1	–	(+)	(–)	–	+	+	+	(+)
Δrdrp2	++	–	+	–	+	+	–	nd
Δrdrp3	++	–	(–)	+	–	+	–	nd
Δrdrp4	++	–	–	+	–	+	–	nd
Δqde3	–	–	+	–	+	+	+	+
Δqip	–	–	+	–	(+)	+	+	–
Δdcl1 Δdcl2	nd	nd	nd	nd	nd	nd	nd	–
PH1	nd	nd	nd	nd	nd	nd	nd	+

[1]*In liquid PEG medium under day light conditions.*
[2]*Dimmed light (2 µmol m^{-2} s^{-1}), liquid SN cultures.*
[3]*At 9 dpi (not at 13 dpi).*
[4]*On barley leaves, 20 ng $µl^{-1}$ CYP3RNA; conclusion from two independent validation assays.*

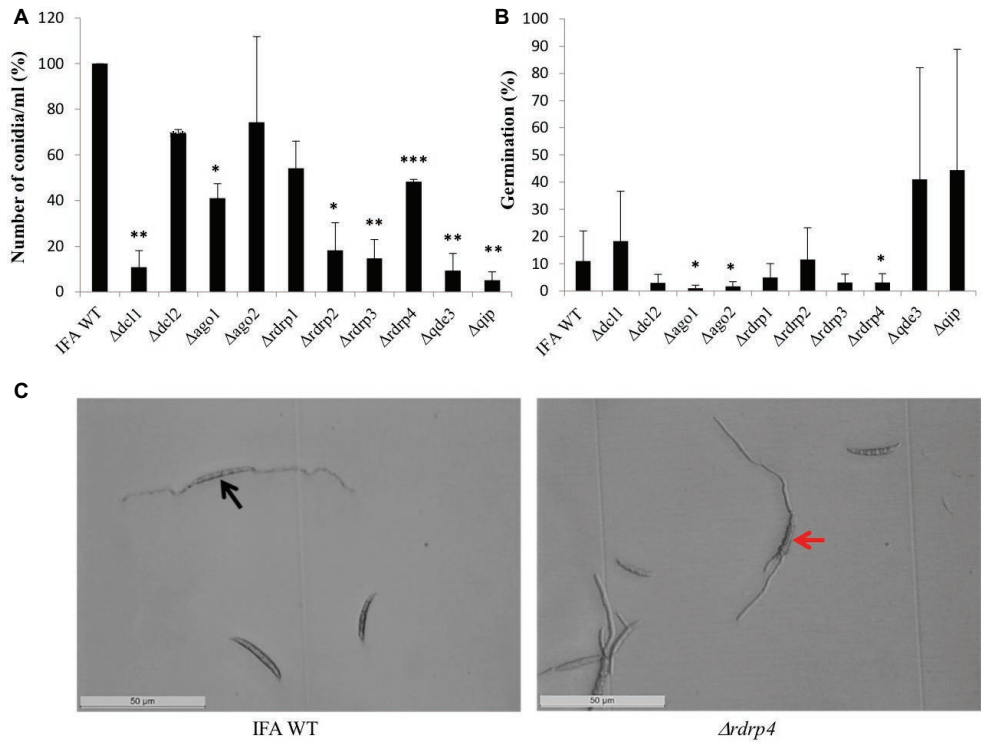

FIGURE 2 | The RNAi pathway is required for asexual development of *Fusarium graminearum* in the absence of inductive light. **(A)** Number of conidia produced: means ± SEs of the percentage of conidia numbers from three repeated experiments. Significant differences are marked: *$p < 0.05$; **$p < 0.01$; ***$p < 0.001$ (Student's *t* test). **(B)** Percent of conidial germination: means± SEs of the percentage of germinated spores from three biological repetitions. Significant differences are marked: *$p < 0.05$ (Student's *t* test). **(C)** Microscopic observation of germinated and non-germinated conidia of IFA WT and *Δrdrp4*. Imaging after 48 h of incubation in the dark, scale bar: 50 µm. Black arrow, conidia forming a bipolar germ tube. Red arrow, conidia forming multiple germ tubes.

melanized mature perithecia to the same extent as compared to IFA WT (not shown). Next, we assessed the forcible discharge of ascospores by a spore discharge assay (**Figure 3**). Discharge of ascospores from perithecia into the environment results from turgor pressure within the asci; the dispersal of ascospores by forcible discharge is a proxy for fungal fitness as it is important for dissemination of the disease. To this end, half circular agar blocks covered with mature perithecia were placed on glass slides and images from forcibly fired ascospores (white cloudy) were taken after 48 h of incubation in boxes under high humidity and fluorescent light. We found that the forcible discharge of ascospores was severely

compromised in *Δdcl1*, *Δago2*, *Δrdrp1*, *Δrdrp2*, *Δqde3*, and less severe in *Δdcl2*, *Δago1, Δqip1,* while *Δrdrp3* and *Δrdrp4* were indistinguishable from IFA WT (**Figures 3A,B**). Microscopic observation of the discharged ascospores revealed that their morphology was not affected (not shown). However, the percentage of discharged ascospores that retained the ability to germinate varied in the mutants with *Δrdrp3* and *Δrdrp4*, showing strong reduction in the ascospore germination (**Figure 3C**; see **Table 2**). Together, these results confirm that the RNAi pathway is involved in sexual reproduction, though the requirement of individual RNAi components greatly varies in the different developmental stages.

F. graminearum RNA Interference Mutants Show Variation in Kernel Infection

It has been reported that *Fg* mutants defective in DCL, AGO, or RdRP were not compromised in virulence on wheat spikes (Chen et al., 2015). We extended this previous study by testing additional *Fg* RNAi mutants. Conidia were point-inoculated to a single spikelet at the bottom of a spike of the susceptible wheat cultivar Apogee. Fungal colonization was quantified 9 and 13 days post inoculation (dpi) by determining the infection strength. Infected parts of a spike bleached out, whereas the non-inoculated spikes remained greenish. At late infection stages (13 dpi), all RNAi mutants caused strong FHB symptoms comparable with IFA WT. However, we found differences in the severity of infections at earlier time points (9 dpi), with *Δdcl1* and *Δago2* showing most compromised FHB development (**Figure 4A**; see **Table 2**). At 13 dpi, RNAi mutants also showed considerable variation in *Fg*-infected kernel morphology (**Supplementary Figure S4A**). Thousand-grain-weight (TGW) of kernels infected with RNAi mutants showed slight, though not significant. Differences in the total weights compared to IFA WT infection (**Supplementary Figure S4B**).

Deoxynivalenol Production Is Compromised in *F. graminearum* Mutants That Show Reduced Pathogenicity on Wheat Kernels

We quantified the amount of DON in *Fg*-infected wheat spikes at 13 dpi (point inoculation using 5 µl of 0.002% Tween 20 water containing 40,000 conidia/ml) at mid-anthesis. Of note, the relative amount of DON [rDON], calculated as [DON] relative to the amount of fungal genomic DNA, was reduced in virtually all spikes infected with RNAi mutants, whereby spikes infected by *Δqip* and *Δdcl2* showed the lowest toxin reduction as compared with the other mutants (**Table 3**). The data suggest that fungal RNAi pathways affect *Fg*'s DON production in wheat spikes. Moreover, while [rDON] changed, the ratio of [DON] and [A-DON] (comprising 3A-DON and 15A-DON) remained constant in all mutants vs. IFA WT, suggesting that the fungal RNAi pathways do not affect the trichothecene metabolism.

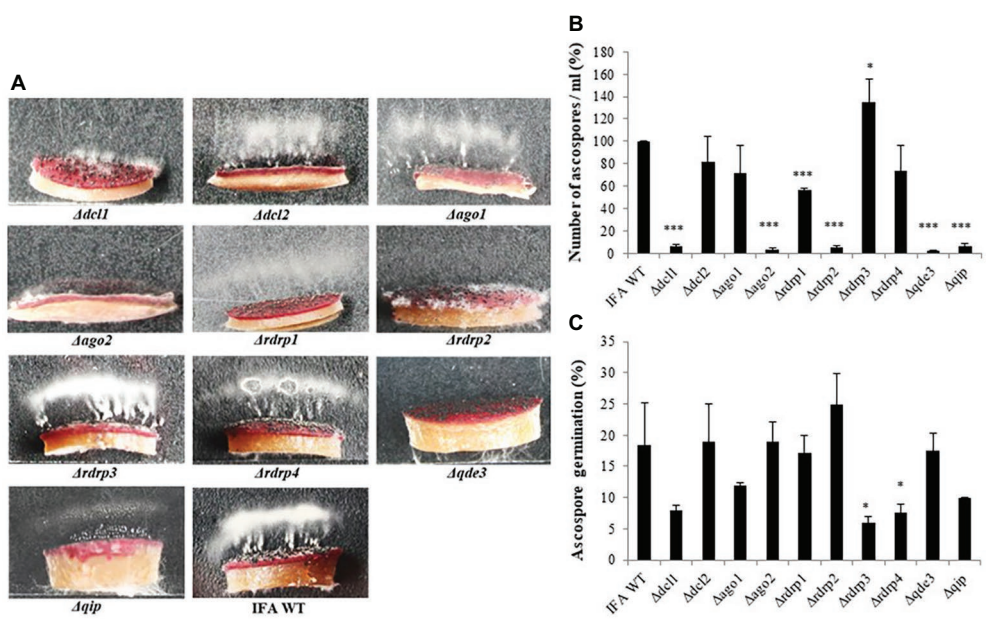

FIGURE 3 | Forcible ascospore discharge in *Fusarium graminearum* RNAi mutants and IFA WT. **(A)** Forcible ascospore firing. Half circular carrot agar blocks covered with mature perithecia were placed on glass slides. Photos from forcibly fired ascospores (white cloudy) were taken after 48 h of incubation in boxes under high humidity and fluorescent light. **(B)** Fired ascospores were washed off and counted. Means± SDs of the counted spores is presented from three biological repetitions. Significant differences are marked: *$p < 0.05$; ***$p < 0.001$ (Student's *t* test). **(C)** Ascospore germination. Discharged ascospores were incubated at 100% RT in the dark for 24 h at 23°C in SN liquid medium. The percentage of germination was assessed by examining the ascospore number in three random squares in the counting chamber. Means ± SEs of the percentage of germinated spores from three biological repetitions. Significant differences are marked: *$p < 0.05$ (Student's *t* test).

FIGURE 4 | Infection of Apogee wheat spikes with *Fusarium graminearum* RNAi mutants and IFA WT. **(A)** Representative samples of spikes at 9 dpi. One spikelet at the bottom of each spike (red arrow) was point-inoculated with 5 µl of 0.002% Tween 20 water containing 40,000 conidia/ml. The assay was repeated two times with 10 spikes per fungal genotype and experiment. **(B)** Wheat spikes at 13 dpi.

TABLE 3 | Trichothecenes produced by RNAi mutants in infected wheat kernels at 13 dpi.

Samples	ng *Fg* DNA/ mg seed d.w.	DON (mg/kg seed)	DON/ DNA	A-DON (mg/kg seed)[1]	A-DON/ DON × 1,000[2]
Mock (without *Fg*)	0	0.00	0	0	0
Δago1	0.84	12.7	15.2	0.45	36
Δago2	1.28	32.3	25.2	1.04	32
Δdcl1	2.86	61.9	21.6	1.87	30
Δdcl2	2.03	56.6	27.9	1.89	33
Δrdrp1	4.84	86.7	17.9	3.51	40
Δrdrp2	0.95	16.9	17.8	0.43	25
Δrdrp3	0.78	12.3	15.6	0.35	29
Δrdrp4	0.47	4.90	10.3	0.15	31
Δqip	2.53	68.7	27.2	2.87	42
Δqde3	4.33	82.3	19.0	3.91	47
IFA WT	2.18	78.3	35.9	2.58	33

DON, deoxynivalenol; A-DON, acetyldeoxynivalenol.

[1]3A-DON (3-acetyldeoxynivalenol) and 15A-DON (15-acetyldeoxynivalenol) were measured.

[2]Ratio of concentrations of A-DON and DON, multiplied by 1,000.

F. graminearum RecQ Helicase Mutant *Δqde3* Is Insensitive to Double-Stranded RNA

Spraying plant leaves or fruits with dsRNA targeting essential fungal genes can reduce fungal infections by a mechanism called spray-induced gene silencing (SIGS) (Dalakouras et al., 2016; Koch et al., 2016; Wang et al., 2016b; McLoughlin et al., 2018). We addressed the question which RNAi mutants of our set are compromised in SIGS upon treatment with dsRNA. To this end, we conducted a SIGS experiment on detached barley leaves that were sprayed with 20 ng µl^{-1} CYP3RNA, a 791 nt-long dsRNA that targets the three fungal genes *FgCYP51A*, *FgCYP51B*, and *FgCYP51C* (Koch et al., 2016). By 48 h after spraying, leaves were drop inoculated with 5 × 10^4 conidia ml^{-1} of *Fg* RNAi mutants and IFA WT. Five days later, infected leaves were scored for disease symptoms and harvested to measure the expression of the fungal target genes by qRT-PCR (**Figure 5**). As revealed by reduced disease symptoms, leaves sprayed with CYP3RNA vs. TE (buffer control), only *Δqde3* was equally sensitive to dsRNA like the IFA WT, while all other mutants tested in this experiment were slightly or strongly compromised in SIGS and less sensitive to CYP3RNA (**Figure 5A**, see **Table 2**). Consistent with this, strong down-regulation of all three *CYP51* target genes was observed only in IFA WT and *Δqde3*. In *Δdcl1*, *Δdcl2*, and *Δqip1*, the inhibitory effect of CYP3RNA on *FgCYP51A*, *FgCYP51B*, and *FgCYP51C* expression was completely abolished (**Figure 5B**). To further substantiate this finding, we tested a *dcl1/dcl2* double mutant in *Fg* strain PH1. As anticipated from the experiments with IFA WT, the PH1 *dcl1/dcl2* mutant was fully compromised in SIGS (**Figures 5A,B**).

DISCUSSION

We generated a broad collection of knockout mutants for RNAi genes in the necrotrophic, mycotoxin-producing pathogen *Fusarium graminearum* to demonstrate their involvement in vegetative and generative growth, disease development, mycotoxin production, and sensitivity to environmental RNAi. A summary of the mutants' performance in the various processes is shown in **Table 2**. While all RNAi mutants show normal vegetative development in axenic cultures, there were differences in pigments production in liquid potato extract glucose cultures. This suggests that in *Fg*, an RNAi pathway regulates the gene cluster responsible for the biosynthesis of pigments, including aurofusarin. Aurofusarin is a secondary metabolite belonging to the naphthoquinone group of polyketides that shows antibiotic properties against filamentous fungi and yeast (Medentsev et al., 1993). The function of the compound in the fungus is unknown because white mutants have even higher growth rates and are equally pathogenic than a WT fungus on wheat and barley (Malz et al., 2005).

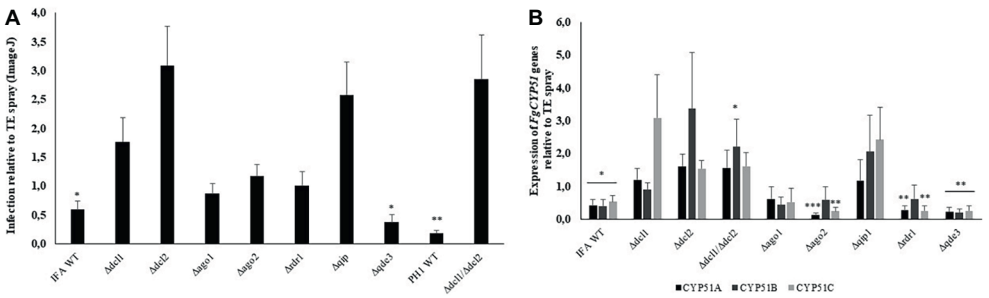

FIGURE 5 | Infection symptoms of *Fg* RNAi mutants on barley leaves sprayed with the dsRNA CYP3RNA. **(A)** Detached leaves of 3-week-old barley plants were sprayed with 20 ng µl^{-1} CYP3RNA or TE buffer, respectively. After 48 h, leaves were drop-inoculated with 5 × 10^4 conidia ml^{-1} of indicated *Fg* RNAi mutants and evaluated for infection symptoms at 5 dpi. Values show relative infection area as calculated from TE- vs. CYP3RNA-treated plants for each RNAi mutant with 10 leaves and three biological repetitions. Asterisks indicate statistical significant reduction of the infection area on CYP3RNA- vs. TE-treated plants measured by ImageJ for each mutant (*$p <$ 0.05; **$p < 0.01$; Student's *t* test). The *dcl1 dcl2* double mutant is generated in *Fg* strain PH1. **(B)** Down-regulation of the three *CYP51* genes in *Fg* mutants upon colonization of CYP3RNA- vs. TE-treated barley leaves. Asterisks indicate statistically significant down-regulation of *CYP51* genes on CYP3RNA vs. TE-treated plants. (*$p <$ 0.05; **$p < 0.01$; ***$p < 0.001$; Student's *t* test). Error bars indicate SE of three independent experiments in **(A)** and **(B)**.

Overall, the contribution of the RNAi pathways to vegetative fungal development and conidiation varies among different fungi and must be considered case by case. Under low light (<2 µmol m^{-2} s^{-1}), all *Fg* RNAi mutants showed reduced conidia production and some showed aberrant germination compared to IFA WT. This suggests that in the absence of light induction, the RNAi pathway is required for conidiation. RNAi may play a role in regulation of light-responsive genes affecting conidiation as shown for *T. atroviride*, where DCL2 and RdRP3 control conidia production under light induction (Carreras-Villaseñor et al., 2013). The authors claimed that *Δdcl2* and *Δrdrp3* are impaired in perception and/or transduction of the light signal affecting the transcriptional response of light-responsive genes. Similarly, *Metarhizium robertsii dcl* and *ago* mutants show reduced abilities to produce conidia under light, though the light quantity was not described (Meng et al., 2017).

Perithecia development has been used to study sexual development and transcription of genes related to sexual development (Trail and Common, 2000; Qi et al., 2006; Hallen et al., 2007). In field situations, ascospores serve as the primary inoculum for FHB epidemics because these spores are shot into the environment and can spread over long distances (Maldonado-Ramirez et al., 2005). We found that all RNAi mutants could produce mature perithecia. However, corroborating and extending the exemplary work of Son et al. (2017), we also found that, besides *FgDCL1* and *FgAGO2*, other RNAi genes such as *RdRP1*, *RdRP2*, *RdRP3*, *RdRP4*, *QDE3, QIP* contribute to the sexual reproduction. Mutations in these genes either showed severe defect in forcible ascospore discharge or significantly reduced germination. The Son et al. (2017) study showed that *Fgdcl1* and *Fgago2* are severely defective in forcible ascospore discharge, while *Fgdcl2* and *Fgago1* show indistinguishable phenotypes compared to the WT. Active roles for *Fg*DCL1 and *Fg*AGO2 are supported by the finding that expression levels of many genes, including those closely related to the mating-type (*MAT*)-mediated regulatory mechanism during the late stages of sexual development, was compromised in the respective mutants after sexual induction (Kim et al., 2015). Moreover, *Fg*DCL1 and *Fg*AGO2 participate in the biogenesis of sRNAs and perithecia-specific miRNA-like RNAs (milRNAs) also are dependent on *Fg*DCL1 (Zeng et al., 2018). Most of the produced sRNA originated from gene transcript regions and affected expression of the corresponding genes at a post-transcriptional level (Son et al., 2017).

While our data show that, in addition to *Fg*DCL1 and *Fg*AGO2, more *Fg* RNAi-related proteins are required for sex-specific RNAi, further transcriptomic analysis and sRNA characterization are needed for a mechanistic explanation. Of note, ex-siRNA functions are important for various developmental stages and stress responses in the fungus *M. circinelloides*, while *Fg* utilizes ex-siRNAs for a specific developmental stage. Thus, ex-siRNA-mediated RNAi might occur in various fungal developmental stages and stress responses depending on the fungal species.

We investigated the involvement of RNAi in pathogenicity and FHB development by infecting wheat spikes of the susceptible cultivar Apogee with fungal conidia. At earlier time points of infection (9 dpi), clear differences in virulence between RNAi mutants were observed, though all mutants could spread within a spike and caused typical FHB symptoms at later time points (13 dpi). Despite full FHB symptom development in all mutants at 13 dpi, we observed various effects of fungal infection on the kernel morphology, corresponding to the different aggressiveness of mutants at early time points. Since this phenomenon may account for differences in producing mycotoxins during infection, we quantified mycotoxins in the kernels. Of note, [rDON] was reduced in virtually all spikes infected with RNAi mutants, though most strongly in spikes colonized with mutants *Δago1*, *Δrdrp1*, *Δrdrp2*, *Δrdrp3*, *Δrdrp4*, and *Δqde3* as compared with IFA WT (see **Tables 2** and **3**). The data suggest that fungal RNAi pathways affect *Fg*'s DON production in wheat spikes. Interestingly, while [rDON] changed, the ratio of [DON] and [3A-DON] remained constant in all mutants vs. IFA WT, suggesting that the fungal RNAi pathways do not affect the trichothecene chemotype.

Our work also identifies additional *Fg* RNAi proteins associated with sensitivity to dsRNA treatments. For the validation of

dsRNA effects, we used two independent tests: infection phenotyping and qRT-PCR analysis of fungal target genes. *Δdcl1* and *Δdcl2* as well as *Δqip* showed compromised SIGS phenotypes in either test, strongly suggesting that these proteins are required for environmental RNAi in *Fg*. Further substantiating our finding, the fungal *dcl1/dcl2* double mutant of *Fg* strain PH1 also showed complete insensitivity to dsRNA and thus is fully compromised to environmental RNAi.

Taken together, our results further substantiate the involvement of RNAi pathways in conidiation, ascosporogenesis, and pathogenicity of *Fg*. Nevertheless, further studies must explore the mechanistic roles of *Fg* RNAi genes in these processes.

AUTHOR CONTRIBUTIONS

FG generated the *Fusarium* mutants and conducted the experiments related to **Figures 1–4**. K-HK and JI designed the research, analyzed the data, and wrote the manuscript. PK oversaw the DON experiments. AK oversaw the experiments related to **Figure 5**.

FUNDING

This research was supported by the German Research Council (DFG) to K-HK and AK in the project GRK2355. FG was supported by the German Academic Exchange Service (DAAD).

ACKNOWLEDGMENTS

The authors thank Mrs. E. Stein for excellent technical assistance, Dr. A. Rathgeb for mycotoxin analysis, and Ms. C. Birkenstock for taking care of the plants. They also thank Dr. Martin Urban, Rothamsted Research, England for providing the *Fg* strains PH1 and PH1 *dcl1 dcl2*.

SUPPLEMENTARY MATERIAL

The Supplementary Material for this article can be found online at: https://www.frontiersin.org/articles/10.3389/fmicb.2019.01662/full#supplementary-material

REFERENCES

Audenaert, K., Vanheule, A., Höfte, M., and Haesaert, G. (2014). Deoxynivalenol: a major player in the multifaceted response of Fusarium to its environment. *Toxins* 6, 1–19. doi: 10.3390/toxins6010001

Bai, Y., Lan, F., Yang, W., Zhang, F., Yang, K., Li, Z., et al. (2015). sRNA profiling in *Aspergillus flavus* reveals differentially expressed miRNA-like RNAs response to water activity and temperature. *Fungal Genet. Biol.* 81, 113–119. doi: 10.1016/j.fgb.2015.03.004

Baulcombe, D. C. (2013). Small RNA-the secret of noble rot. *Science* 342, 45–46. doi: 10.1126/science.1245010

Brandfass, C., and Karlovsky, P. (2008). Upscaled CTAB-based DNA extraction and real-time PCR assays for *Fusarium culmorum* and *F. graminearum* DNA in plant material with reduced sampling error. *Int. J. Mol. Sci.* 9, 2306–2321. doi: 10.3390/ijms9112306

Brown, N., Evans, A. J., Mead, A., and Hammond-Kosack, K. E. (2017). A spatial temporal analysis of the *Fusarium graminearum* transcriptome during symptomless and symptomatic wheat infection. *Mol. Plant Pathol.* 18, 1295–1312. doi: 10.1111/mpp.12564

Cai, Q., He, B., Kogel, K. H., and Jin, H. (2018). Cross-kingdom RNA trafficking and environmental RNAi – nature's blueprint for modern crop protection strategies. *Curr. Opin. Microbiol.* 46, 58–64. doi: 10.1016/j.mib.2018.02.003

Calo, S., Nicolás, F. E., Vila, A., Torres-Martínez, S., and Ruiz-Vázquez, R. M. (2012). Two distinct RNA-dependent RNA polymerases are required for initiation and amplification of RNA silencing in the basal fungus Mucor circinelloides. *Mol. Microbiol.* 83, 379–394. doi: 10.1111/j.1365-2958.2011.07939.x

Campo, S., Gilbert, K. B., and Carrington, J. C. (2016). Small RNA-based antiviral defense in the phytopathogenic fungus *Colletotrichum higginsianum*. *PLoS Pathog.* 12:e1005640. doi: 10.1371/journal.ppat.1005640

Carreras-Villaseñor, N., Esquivel-Naranjo, E. U., Villalobos-Escobedo, J. M., Abreu-Goodger, C., and Herrera-Estrella, A. (2013). The RNAi machinery regulates growth and development in the filamentous fungus *Trichoderma atroviride*. *Mol. Microbiol.* 89, 96–112. doi: 10.1111/mmi.12261

Cavinder, B., Sikhakolli, U., Fellows, K. M., and Trail, F. (2012). Sexual development and ascospore discharge in *Fusarium graminearum*. *J. Vis. Exp.* pii: 3895 doi: 10.3791/3895

Chang, S. S., Zhang, Z., and Liu, Y. (2012). RNA interference pathways in fungi: mechanisms and functions. *Annu. Rev. Microbiol.* 66, 305–323. doi: 10.1146/annurev-micro-092611-150138

Chen, Y., Gao, Q., Huang, M., Liu, Y., Liu, Z., Liu, X., et al. (2015). Characterization of RNA silencing components in the plant pathogenic fungus *Fusarium graminearum*. *Sci. Rep.* 5:12500. doi: 10.1038/srep12500

Cogoni, C., and Macino, G. (1999). Gene silencing in *Neurospora crassa* requires a protein homologous to RNA-dependent RNA polymerase. *Nature* 399, 166–169.

Cuomo, C. A., Güldener, U., Xu, J. R., Trail, F., Turgeon, B. G., Di Pietro, A., et al. (2007). The *Fusarium graminearum* genome reveals a link between localized polymorphism and pathogen specialization. *Science* 317, 1400–1402. doi: 10.1126/science.1143708

Dalakouras, A., Wassenegger, M., McMillan, J. N., Cardoza, V., Maegele, I., Dadami, E., et al. (2016). Induction of silencing in plants by high-pressure spraying of *in vitro*-synthesized small RNAs. *Front. Plant Sci.* 7:1327. doi: 10.3389/fpls.2016.01327

Dang, Y., Yang, Q., Xue, Z., and Liu, Y. (2011). RNA interference in fungi: pathways, functions, and applications. *Eukaryot. Cell* 10, 1148–1155. doi: 10.1128/EC.05109-11

Dean, R., Van Kan, J. A., Pretorius, Z. A., Hammond-Kosack, K. E., Di Pietro, A., Spanu, P. D., et al. (2012). The top 10 fungal pathogens in molecular plant pathology. *Mol. Plant Pathol.* 13, 414–430. doi: 10.1111/j.1364-3703.2011.00783.x

Desjardins, A. E., Hohn, T. M., and McCormick, S. P. (1993). Trichothecene biosynthesis in *Fusarium* species: chemistry, genetics and significance. *Microbiol. Rev.* 57, 595–604.

Dill-Macky, R., and Jones, R. K. (2000). The effect of previous crop residues and tillage on *Fusarium* head blight of wheat. *Plant Dis.* 84, 71–76. doi: 10.1094/PDIS.2000.84.1.71

Fire, A., Xu, S., Montgomery, M. K., Kostas, S. A., Driver, S. E., and Mello, C. C. (1998). Potent and specific genetic interference by double-stranded RNA in *Caenorhabditis elegans*. *Nature* 391, 806–811. doi: 10.1038/35888

Frandsen, R. J., Nielsen, N. J., Maolanon, N., Sørensen, J. C., Olsson, S., Nielsen, J., et al. (2006). The biosynthetic pathway for aurofusarin in *Fusarium graminearum* reveals a close link between the naphthoquinones and naphthopyrones. *Mol. Microbiol.* 61, 1069–1080. doi: 10.1111/j.1365-2958.2006.05295.x

Gosman, N., Steed, A., Chandler, E., Thomsett, M., and Nicholson, P. (2010). Evaluation of type I *Fusarium* head blight resistance of wheat using non-deoxynivalenol-producing fungi. *Plant Pathol.* 59, 147–157. doi: 10.1111/j.1365-3059.2009.02202.x

Hallen, H., Huebner, M., Shiu, S. H., Guldener, U., and Trail, F. (2007). Gene expression shifts during perithecium development in *Gibberella zeae* (anamorph

Fusarium graminearum), with particular emphasis on ion transport proteins. *Fungal Genet. Biol.* 44, 1146–1156. doi: 10.1016/j.fgb.2007.04.007

Hammond, S. M. (2005). Dicing and slicing: the core machinery of the RNA interference pathway. *FEBS Lett.* 579, 5822–5829. doi: 10.1016/j.febslet.2005.08.079

Harris, L. J., Balcerzak, M., Johnston, A., Schneiderman, D., and Ouellet, T. (2016). Host-preferential *Fusarium graminearum* gene expression during infection of wheat, barley, and maize. *Fungal Biol.* 120, 111–123. doi: 10.1016/j.funbio.2015.10.010

Ilgen, P., Hadeler, B., Maier, F. J., and Schäfer, W. (2009). Developing kernel and rachis node induce the trichothecene pathway of *Fusarium graminearum* during wheat head infection. *Mol. Plant Microbe Interact.* 22, 899–908. doi: 10.1094/MPMI-22-8-0899

Jansen, C., von Wettstein, D., Schäfer, W., Kogel, K. H., Felk, F., and Maier, F. J. (2005). Infection patterns in barley and wheat spikes inoculated with wild type and trichodiene synthase gene disrupted *Fusarium graminearum*. *Proc. Natl. Acad. Sci. USA* 102, 16892–16897. doi: 10.1073/pnas.0508467102

Kim, H. K., Jo, S. M., Kim, G. Y., Kim, D. W., Kim, Y. K., and Yun, S. H. (2015). A large-scale functional analysis of putative target genes of mating-type loci provides insight into the regulation of sexual development of the cereal pathogen *Fusarium graminearum*. *PLoS Genet.* 11:e1005486. doi: 10.1371/journal.pgen.1005486

Klittich, C. J. R., and Leslie, J. F. (1988). Nitrate reduction mutants of *Fusarium moniliforme* (*Gibberella fujikuroi*). *Genetics* 118, 417–423.

Koch, A., Biedenkopf, D., Furch, A., Weber, L., Rossbach, O., Abdellatef, E., et al. (2016). An RNAi-Based Control of *Fusarium graminearum* infections through spraying of Long dsRNAs involves a plant passage and is controlled by the fungal silencing machinery. *PLoS Pathog.* 12:e1005901. doi: 10.1371/journal.ppat.1005901

Koch, A., and Kogel, K. H. (2014). New wind in the sails: improving the agronomic value of crop plants through RNAi-mediated gene silencing. *Plant Biotechnol. J.* 12, 821–831. doi: 10.1111/pbi.12226

Koch, A., Kumar, N., Weber, L., Keller, H., Imani, J., and Kogel, K. H. (2013). Host-induced gene silencing of cytochrome P450 lanosterol C14α-demethylase–encoding genes confers strong resistance to *Fusarium* species. *Proc. Natl. Acad. Sci. USA* 110, 19324–19329. doi: 10.1073/pnas.1306373110

Koch, A., Stein, E., and Kogel, K.-H. (2018). RNA-based disease control as a complementary measure to fight Fusarium fungi through silencing of the Azole target cytochrome P450 lanosterol C-14 α-demethylase. *Eu. J. Plant Pathol.* 152, 1003–1010. doi: 10.1007/s10658-018-1518-4

Kusch, S., Frantzeskakis, L., Thieron, H., and Panstruga, R. (2018). Small RNAs from cereal powdery mildew pathogens may target host plant genes. *Fungal Biol.* 122, 1050–1063. doi: 10.1016/j.funbio.2018.08.008

Lau, S. K., Tse, H., Chan, J. S., Zhou, A. C., Curreem, S. O., Lau, C. C., et al. (2013). Proteome profiling of the dimorphic fungus *Penicillium marneffei* extracellular proteins and identification of glyceraldehyde-3-phosphate dehydrogenase as an important adhesion factor for conidial attachment. *FEBS J.* 280, 6613–6626. doi: 10.1111/febs.12566

Leslie, J. F., and Summerell, B. A. (2006). *The Fusarium laboratory manual*. Ames, IA, USA: Blackwell Professional. ISBN: 978-0-813-81919-8.

Livak, K. J., and Schmittgen, T. D. (2001). Analysis of relative gene expression data using real-time quantitative PCR and the 2ΔΔC(T). *Methods* 25, 402–408. doi: 10.1006/meth.2001.1262

Maldonado-Ramirez, S. L., Schmale, D. G. Jr., Shields, E. J., and Bergstrom, G. C. (2005). The relative abundance of viable spores of *Gibberella zeae* in the planetary boundary layer suggests the role of long-distance transport in regional epidemics of Fusarium head blight. *Agric. For. Meteorol.* 132, 20–27. doi: 10.1016/j.agrformet.2005.06.007

Malz, S., Grell, M. N., Thrane, C., Maier, F. J., Rosager, P., Felk, A., et al. (2005). Identification of a gene cluster responsible for the biosynthesis of aurofusarin in the *Fusarium graminearum* species complex. *Fungal Genet. Biol.* 42, 420–433. doi: 10.1016/j.fgb.2005.01.010

McLoughlin, A. G., Wytinck, N., Walker, P. L., Girard, I. J., Rashid, K. Y., de Kievit, T., et al. (2018). Identification and application of exogenous dsRNA confers plant protection against *Sclerotinia sclerotiorum* and *Botrytis cinerea*. *Sci. Rep.* 8:7320. doi: 10.1038/s41598-018-25434-4

Medentsev, A. G., Kotik, A. N., Trufanova, V. A., and Akimenko, V. K. (1993). Identification of aurofusarin in *Fusarium graminearum* isolates, causing a syndrome of worsening of egg quality in chickens. *Prikl. Biokhim. Mikrobiol.* 29, 542–546.

Mello, C. C., and Conte, D. Jr. (2004). Revealing the world of RNA interference. *Nature* 431, 338–342. doi: 10.1038/nature02872

Meng, H., Wang, Z., Wang, Y., Zhu, H., and Huang, B. (2017). Dicer and Argonaute genes involved in RNA interference in the entomopathogenic fungus Metarhizium robertsii. *Appl. Environ. Microbiol.* 83:e03230-16. doi: 10.1128/AEM.03230-16

Nguyen, Q., Iritani, A., Ohkita, S., Vu, B. V., Yokoya, K., Matsubara, A., et al. (2018). A fungal Argonaute interferes with RNA interference. *Nucleic Acids Res.* 46, 2495–2508. doi: 10.1093/nar/gkx1301

Nowara, D., Gay, A., Lacomme, C., Shaw, J., Ridout, C., Douchkov, D., et al. (2010). HIGS: host-induced gene silencing in the obligate biotrophic fungal pathogen *Blumeria graminis*. *Plant Cell* 22, 3130–3141. doi: 10.1105/tpc.110.077040

Qi, W., Kwon, C., and Trail, F. (2006). Microarray analysis of transcript accumulation during perithecium development in *Gibberella zeae* (anamorph *Fusarium graminearum*). *Mol. Gen. Genomics.* 276, 87–100. doi: 10.1007/s00438-006-0125-9

Raman, V., Simon, S. A., Demirci, F., Nakano, M., Meyers, B. C., and Donofrio, N. M. (2017). Small RNA functions are required for growth and development of *Magnaporthe oryzae*. *Mol. Plant Microbe Interact.* 30, 517–530. doi: 10.1094/MPMI-11-16-0236-R

Romano, N., and Macino, G. (1992). Quelling: transient inactivation of gene expression in *Neurospora crassa* by transformation with homologous sequences. *Mol. Microbiol.* 6, 3343–3353. doi: 10.1111/j.1365-2958.1992.tb02202.x

Segers, G. C., Zhang, X., Deng, F., Sun, Q., and Nuss, D. L. (2007). Evidence that RNA silencing functions as an antiviral defense mechanism in fungi. *Proc. Natl. Acad. Sci. USA* 104, 12902–12906. doi: 10.1073/pnas.0702500104

Shiu, P. K., Raju, N. B., Zickler, D., and Metzenberg, R. L. (2001). Meiotic silencing by unpaired DNA. *Cell* 107, 905–916. doi: 10.1016/S0092-8674(01)00609-2

Son, H., Min, K., Lee, J., Raju, N. B., and Lee, Y. W. (2011). Meiotic silencing in the homothallic fungus *Gibberella zeae*. *Fungal Biol.* 115, 1290–1302. doi: 10.1016/j.funbio.2011.09.006

Son, H., Park, A. R., Lim, J. Y., Shin, C., and Lee, Y. W. (2017). Genome-wide exonic small interference RNA-mediated gene silencing regulates sexual reproduction in the homothallic fungus *Fusarium graminearum*. *PLoS Genet.* 13:e1006595. doi: 10.1371/journal.pgen.1006595

Song, M. S., and Rossi, J. J. (2017). Molecular mechanisms of Dicer: endonuclease and enzymatic activity. *Biochem. J.* 474, 1603–1618. doi: 10.1042/BCJ20160759

Sulyok, M., Berthiller, F., Krska, R., and Schuhmacher, R. (2006). Development and validation of a liquid chromatography/tandem mass spectrometric method for the determination of 39 mycotoxins in wheat and maize. *Rapid Commun. Mass Spectrom.* 20, 2649–2659. doi: 10.1002/rcm.2640

Torres-Martínez, S., and Ruiz-Vázquez, R. M. (2017). The RNAi universe in fungi: a varied landscape of small RNAs and biological functions. *Annu. Rev. Microbiol.* 71, 371–391. doi: 10.1146/annurev-micro-090816-093352

Trail, F., and Common, R. (2000). Perithecial development by *Gibberella zeae*: a light microscopy study. *Mycologia* 92, 130–138. doi: 10.2307/3761457

Urban, M., King, R., Hassani-Pak, K., and Hammond-Kosack, K. E. (2015). Whole-genome analysis of *Fusarium graminearum* insertional mutants identifies virulence associated genes and unmasks untagged chromosomal deletions. *BMC Genomics* 16:261. doi: 10.1186/s12864-015-1412-9

Vervliet, G., Holsters, M., Teuchy, H., Van Montagu, M., and Schell, J. (1975). Characterization of different plaque-forming and defective temperate phages in *Agrobacterium* strains. *J. Gen. Virol.* 26, 33–48. doi: 10.1099/0022-1317-26-1-33

Wang, S., Li, P., Zhang, J., Qiu, D., and Guoa, L. (2016a). Generation of a high resolution map of sRNAs from *Fusarium graminearum* and analysis of responses to viral infection. *Sci. Rep.* 6:26151. doi: 10.1038/srep26151

Wang, M., Weiberg, A., Lin, F. M., Thomma, B. P., Huang, H. D., and Jin, H. (2016b). Bidirectional cross-kingdom RNAi and fungal uptake of external RNAs confer plant protection. *Nature Plants* 2:16151. doi: 10.1038/nplants.2016.151

Weiberg, A., Wang, M., Lin, F.-M., Zhao, H., Zhang, Z., Kaloshian, I., et al. (2013). Fungal small RNAs suppress plant immunity by hijacking host RNA interference pathways. *Science* 342, 118–123. doi: 10.1126/science.1239705

Yun, Y., Liu, Z., Yin, Y., Jiang, J., Chen, Y., Xu, J. R., et al. (2015). Functional analysis of the *Fusarium graminearum* phosphatome. *New Phytol.* 207, 119–134. doi: 10.1111/nph.13374

Zanini, S., Šečić, E., Busche, T., Kalinowski, T., and Kogel, K.- H. (2019). Discovery of interaction-related sRNAs and their targets in the *Brachypodium distachyon* and *Magnaporthe oryzae* pathosystem. *BioRxiv [Preprint]*. doi: 10.1101/631945

Zanini, S., Šečić, E., Jelonek, L., and Kogel, K.-H. (2018). A bioinformatics pipeline for the analysis and target prediction of RNA effectors in bidirectional communication during plant-microbe interactions. *Front. Plant Sci.* 9:1212. doi: 10.3389/fpls.2018.01212

Zeng, W., Wang, J., Wang, Y., Lin, J., Fu, Y., Xie, J., et al. (2018). Dicer-like proteins regulate sexual development via the biogenesis of perithecium-specific microRNAs in a plant pathogenic fungus *Fusarium graminearum*. *Front. Microb.* 9:818. doi: 10.3389/fmicb.2018.00818

Zhang, H., Xia, R., Meyers, B. C., and Walbot, V. (2015). Evolution, functions, and mysteries of plant ARGONAUTE proteins. *Curr. Opin. Plant Biol.* 27, 84–90. doi: 10.1016/j.pbi.2015.06.011

Conflict of Interest Statement: The authors declare that the research was conducted in the absence of any commercial or financial relationships that could be construed as a potential conflict of interest.

Advantages of publishing in Frontiers

OPEN ACCESS
Articles are free to read for greatest visibility and readership

FAST PUBLICATION
Around 90 days from submission to decision

HIGH QUALITY PEER-REVIEW
Rigorous, collaborative, and constructive peer-review

TRANSPARENT PEER-REVIEW
Editors and reviewers acknowledged by name on published articles

Frontiers
Avenue du Tribunal-Fédéral 34
1005 Lausanne | Switzerland

Visit us: www.frontiersin.org
Contact us: info@frontiersin.org | +41 21 510 17 00

REPRODUCIBILITY OF RESEARCH
Support open data and methods to enhance research reproducibility

DIGITAL PUBLISHING
Articles designed for optimal readership across devices

FOLLOW US
@frontiersin

IMPACT METRICS
Advanced article metrics track visibility across digital media

EXTENSIVE PROMOTION
Marketing and promotion of impactful research

LOOP RESEARCH NETWORK
Our network increases your article's readership